

STEREOCHEMISTRY OF HEXENYL RADICAL CYCLIZATIONS WITH *TERT*-BUTYL
AND RELATED LARGE GROUPS: SUBSTITUENT AND TEMPERATURE EFFECTS

by

Jonathan C. Tripp

B. Sc., Worcester Polytechnic Institute, 2000

Submitted to the Graduate Faculty of

Arts and Sciences in partial fulfillment

of the requirements for the degree of

Doctor of Philosophy

University of Pittsburgh

2005

UNIVERSITY OF PITTSBURGH
FACULTY OF ARTS AND SCIENCES

This dissertation was presented

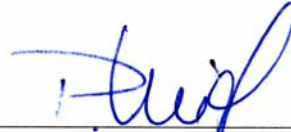
by

Jonathan C. Tripp

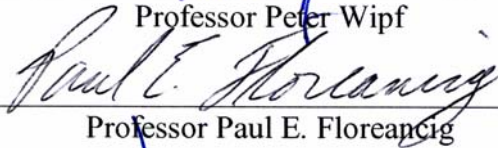
It was defended on

October, 19 2005

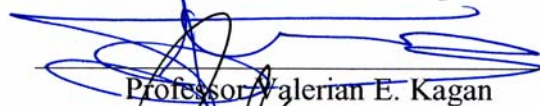
and approved by



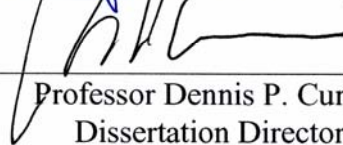
Professor Peter Wipf



Professor Paul E. Floreancig



Professor Valerian E. Kagan



Professor Dennis P. Curran
Dissertation Director

STEREOCHEMISTRY OF HEXENYL RADICAL CYCLIZATIONS WITH *TERT*-BUTYL
AND RELATED LARGE GROUPS: SUBSTITUENT AND TEMPERATURE EFFECTS

Jonathan C. Tripp, Ph. D.

University of Pittsburgh, 2005

The long held notion that hexenyl radicals bearing large substituents on the radical carbon cyclize to give 1,2-*trans*-substituted cyclopentanes is experimentally disproved by study of the radical cyclization of an assortment of simple and complex substrates coupled with careful product analysis and rigorous assignment of configurations. X-ray studies and syntheses of authentic samples establish that the published assignments for *cis*- and *trans*-1-*tert*-butyl-2-methylcyclopentane must be reversed. The original assignment based on catalytic hydrogenation of 1-*tert*-butyl-2-methylenecyclopentane was compromised by migration of the double bond prior to hydrogenation. The cyclization of 1-*tert*-butylhexenyl radical is moderately *cis* selective, and the selectivity is increased by geminal substitution on carbon 3. This selectivity trend is general and extends to relatively complex substrates. It has allowed Ihara to reduce the complexity of an important class of round trip radical cyclizations to make linear triquinanes to the point where two tricyclic products, *cis-syn-cis* and *cis-anti-cis*, account for about 80% of the products. However, the further increase in selectivity that was proposed by lowering the temperature is shown to be an artifact of the analysis methods and is not correct. This work solidifies “1,2-*cis* selectivity” in cyclizations of 1-substituted hexenyl radicals as one of the most general stereochemical trends in radical cyclizations.

TABLE OF CONTENTS

TITLE PAGE.....	i
ABSTRACT.....	iii
TABLE OF CONTENTS.....	iv
LIST OF TABLES.....	vii
LIST OF FIGURES.....	viii
LIST OF SCHEMES.....	ix
LIST OF ABBREVIATIONS.....	xi
PREFACE.....	xiii
Chapter 1 Introduction.....	1
1.1 Chain Mechanisms for the Generation of Carbon Centered Radicals.....	2
1.1.1 Chain Initiation.....	2
1.1.2 Chain Propagation and Termination.....	3
1.2 General Considerations for Running Radical Reactions.....	4
1.3 Common Types of Radical Reactions.....	5
1.3.1 1,5 Hydrogen Atom Transfer Reactions.....	5
1.3.2 The Barton Decarboxylation Reaction.....	7
1.3.3 5- <i>Exo</i> Cyclizations of Hexenyl Radicals.....	8
1.4 Synthesis of Linear Triquinanes by Tandem Radical 5- <i>Exo</i> Cyclization Reactions.....	11
1.4.1 Total Synthesis of Linear Triquinane Natural Products.....	12
1.4.2 Synthesis of Linear Triquinanes from Acyclic Precursors.....	14
1.4.3 Temperature Effects in the Synthesis of Linear Triquinanes.....	19
1.5 Goals.....	23
Chapter 2 Stereochemistry of Hexenyl Radical Cyclizations with <i>tert</i> -Butyl and Related Large Groups in the 1 Position.....	24
2.1 Substrate Design and Synthesis.....	24
2.1.1 Synthesis of Cyclization Precursor 2.4	26
2.1.2 Synthesis of Cyclization Precursors 2.5a,b	26
2.1.3 Synthesis of Cyclization Precursor 2.10	28
2.2 Cyclization Results.....	29
2.3 Configuration Assignment of the Cyclization Products 2.7 , 2.8a,b and 2.12	31
2.3.1 1D NOE Analysis Approach to Configurational Assignment.....	31
2.3.2 Configuration Assignment by Synthesis of an Authentic Sample.....	32
2.3.3 Configuration Assignment by X-Ray Crystallography.....	35
2.4 Stereochemical Relay from Product Mixture 2.7 to 2.8a and 2.8b	36
2.5 Structural Correlation to Beckwith's Work.....	37
2.6 Revisiting Beckwith's Analysis.....	40
2.6.1 Hydrogenation Experiments.....	41
2.6.2 Explaining the NOE Analysis Results.....	44
2.7 Additional Verification of the Reversed <i>Cis/Trans</i> Assignment of 2.45	45

2.8	Transition State Analysis for the Cyclization of 2.2a	48
2.9	Calculations.....	49
2.10	Conclusions.....	51
Chapter 3	Round-Trip Radical Cyclizations	52
3.1	Substrate Design and Rationale	52
3.2	Substrate Synthesis	55
3.2.1	Synthesis of 1.65 , 3.2 and 3.3	55
3.2.2	Synthesis of Z-Unsaturated Ester Cyclization Substrate 3.1	57
3.2.3	Synthesis of the Alkyne Cyclization Substrate 3.4	58
3.3	Cyclization Results	59
3.3.1	Cyclization of Vinyl Iodide 1.65	59
3.3.2	Cyclization Results for Substrates 1.65 , 3.1 and 3.2	63
3.3.3	Cyclization of Allyl Precursor 3.3	66
3.3.4	Cyclization of the Alkynyl Precursor 3.4	69
3.4	Stereochemical Relay Between Systems 1.65 , 3.2 and 3.3	72
3.5	Uncovering the Origin of the Temperature Effect.....	75
3.6	Transition State Analysis for 1.65 and 3.3	78
3.6.1	Transition State Analysis for the Cyclization of 1.65	79
3.6.2	Transition State Analysis for the Cyclization of 3.1	82
3.7	Kinetics of Cyclization	84
3.8	Conclusions.....	88
Chapter 4	Conclusions.....	89
Chapter 5	Experimental Procedures	92
5.1	General Experimental	92
5.2	General Cyclization Procedures.....	93
5.3	Experimental Procedures and Characterization Data for Chapter 2	94
5.3.1	Synthesis of Cyclization Precursor 2.4	94
5.3.2	Synthesis of Cyclization Precursors 2.5a and 2.5b	96
5.3.3	Synthesis of Cyclization Precursor 2.10	99
5.3.4	Cyclization Reactions of Precursors 2.4 , 2.5a,b and 2.10	104
5.3.5	Synthesis of 2.7trans	106
5.3.6	Synthesis of Diol 2.43	110
5.3.7	Monocyclic Relay Experiments.....	110
5.3.8	Full Decarboxylation Experiments	112
5.3.9	Hydrogenation Experiments	113
5.3.10	Deoxygenation Experiments.....	114
5.3.11	Synthesis of 2.62	115
5.4	Experimental Procedures and Characterization Data for Chapter 3	116
5.4.1	Synthesis of Cyclization Precursors 1.65 , 3.2 and 3.3	116
5.4.2	Synthesis of Cyclization Precursor 3.1	125
5.4.3	Synthesis of Precursor 3.4	129
5.4.4	Cyclization Reactions with Precursors 1.65 , 3.1 , 3.3 and 3.4	131
5.4.5	Tricyclic Relay Experiments.....	135
APPENDIX A:	Spectra.....	137
APPENDIX B:	Crystallographic Data Tables	249
	Crystallographic Tables for Diol 2.43	250

Crystallographic Tables for Cyclopentane 2.62	256
APPENDIX C: Gaussian Entry Archives	262
<i>Chair-Equatorial</i> 2.63	263
<i>Chair-Axial</i> 2.64	266
<i>Boat-Equatorial</i> 2.65	270
<i>Boat-Axial</i> 2.66	273
APPENDIX D: The Dioxin and Silicon-Tethered Cyclization Precursor	278
D.1: Cyclization Mechanisms.....	279
D.2: Synthesis of the Dioxin Precursor.....	281
D.2.1: First Retrosynthetic Analysis of Vinyl Iodide D.1	281
D.2.2: Progress Towards the Synthesis of D.1 and D.11 by the Alkylation Route	282
D.2.3: Second Retrosynthetic Analysis of Vinyl Iodide D.1	284
D.2.4: Progress Towards the Synthesis of D.1 by the β -Hydroxy Acid Route	285
D.3: Synthesis of the Silicon Tethered Precursor D.6	286
D.3.1: Forward Synthesis of the Silicon Tethered Precursor D.6	287
D.4: Cyclization Results of the Silicon Tethered Precursors.....	290
D.5: Conclusions and Outlook.....	291
BIBLIOGRAPHY.....	292

LIST OF TABLES

Table 2-1: Cyclization data for precursors 2.4 , 2.5a,b and 2.9	30
Table 2-2: Reduction of 2.50 under various conditions.....	44
Table 2-3: Transition States and Relative Energies for the Cyclization of Radical 2.48	50
Table 3-1: Cyclization data for the cyclization of substrates 1.65 , 3.1 and 3.2	64
Table 3-2: Cyclization data for the cyclization of substrate 3.3	69
Table 3-3: Cyclization data for 3.4 and subsequent hydrogenation.....	72
Table 3-4: Data for the cyclization of 1.65 at 25 °C.....	85
Table 3-5: Data for the cyclization of 1.65 at 80 °C.....	87

LIST OF FIGURES

Figure 1-1: Homolytic versus heterolytic bond dissociation of a molecule A-B	1
Figure 1-2: Common radical initiators and their derived radicals	3
Figure 1-3: Transition state structures for hexenyl radical cyclizations	9
Figure 1-4: Transition states for a 3 substituted hexenyl radical	10
Figure 1-5: Triquinane geometries and natural products	11
Figure 1-6: Strategies for the synthesis of linear triquinanes from acyclic precursors.....	15
Figure 1-7: Comparison of the key hexenyl radicals from the second cyclization.....	21
Figure 1-8: Literature benchmarks for related hexenyl radical cyclizations	21
Figure 2-1: New cyclization benchmarks	24
Figure 2-2: NOE analysis of the four product mixtures 2.7 , 2.8a,b and 2.12	32
Figure 2-3: GC analysis of 2.7trans	33
Figure 2-4: GC analysis of 2.7'	37
Figure 2-5: Comparison of selected ¹ H NMR spectral data for 2.45 and 2.7	38
Figure 2-6: GC analysis of decarboxylation mixture 2.45	40
Figure 2-7: GC analysis of the hydrogenation of 2.42	42
Figure 2-8: Nominal syn pentane interactions in 2.45cis and <i>trans</i>	45
Figure 2-9: GC analysis of the deoxygenation of 2.60	47
Figure 3-1: Tandem round-trip radical cyclization substrates	52
Figure 3-2: GC analysis of the radical cyclization of precursor 1.65	61
Figure 3-3: Potential products from the cyclization of 1.65	61
Figure 3-4: NOSEY correlations for 3.9 and 3.10	62
Figure 3-5: GC analysis of the radical cyclization of precursor 3.2	66
Figure 3-6: Potential products from the cyclization of 3.2	66
Figure 3-7: GC analysis of the radical cyclization of precursor 3.3	67
Figure 3-8: Potential products from the cyclization of 3.3	68
Figure 3-9: ¹ H NMR analysis of the cyclization mixture of precursor 3.4	70
Figure 3-10: GC analysis of the hydrogenation of the cyclization mixture from 3.4	71
Figure 3-11: GC analysis of the transesterified mixture 3.9-3.12	74
Figure 3-12: GC analysis of the decarboxylated tricycle mixture 3.44-3.47	75
Figure 3-13: Comparative ¹ H NMR analysis	77
Figure 3-14: Plot used for determining the rate constant for the cyclization of 1.65 at 25 °C	86
Figure 3-15: Plot used for determining the rate constant for the cyclization of 1.65 at 80 °C	87
Figure 4-1: Reaction coordinate diagram for the cyclization of hexenyl radical 2.2a	90

LIST OF SCHEMES

Scheme 1-1: Propagation and termination steps in a radical chain mechanism	4
Scheme 1-2: 1,5 Hydrogen atom transfer reaction	6
Scheme 1-3: Mechanism for a Barton decarboxylation reaction.....	8
Scheme 1-4: Selectivity in an unsubstituted and 2-substituted hexenyl radical cyclization.....	9
Scheme 1-5: Total synthesis of hirsutene	12
Scheme 1-6: Total synthesis of hirsutene and $\Delta^{9(12)}$ capnellene.....	13
Scheme 1-7: Total synthesis of hypnophilin.....	14
Scheme 1-8: Beckwith's synthesis of linear triquinanes from an acyclic precursor	16
Scheme 1-9: Synthesis of linear triquinanes using a round-trip radical cyclization strategy	17
Scheme 1-10: Malacria's diastereoselective synthesis of a <i>cis-anti-cis</i> triquinane	19
Scheme 1-11: Temperature dependent cyclization of vinyl iodide 1.65	20
Scheme 1-12: Transition state analysis for the cyclization of 1.71 and 1.72	22
Scheme 2-1: Cyclization precursors and pathways for generation of radicals 2.1 and 2.2 a,b ...	25
Scheme 2-2: Cyclization precursor and pathway for the generation of radical 2.3	25
Scheme 2-3: Synthesis of cyclization precursor 2.4	26
Scheme 2-4: Synthesis of cyclization precursors 2.5a,b	27
Scheme 2-5: Attempted approaches towards relay precursor 2.22	28
Scheme 2-6: Synthesis of iodide 2.10	29
Scheme 2-7: Independent synthesis of directly reduced product 2.13	31
Scheme 2-8: Synthesis of 2.7trans	32
Scheme 2-9: Stereoselectivity in the radical addition to diethylmesaconoate 2.33	34
Scheme 2-10: Proposed mechanism for the bis alkylation reaction of dimethyl malonate	35
Scheme 2-11: Synthesis and ORTEP diagram of diol 2.43	36
Scheme 2-12: Stereochemical relay between the three cyclization mixtures	37
Scheme 2-13: Direct comparison of our cyclization mixture of precursor 2.47	39
Scheme 2-14: Isomerization of exo-methylene compound 2.50	41
Scheme 2-15: Synthesis of alkene 2.51	43
Scheme 2-16: Hydrogenation of tetrasubstituted alkene 2.45	43
Scheme 2-17: Confirmation of Beckwith's reversed assignments	46
Scheme 2-18: Derivatization of alcohol 2.58 and ORTEP of cyclopentane 2.62	48
Scheme 2-19: Beckwith Houk transition state analysis for the cyclization of 2.2a	49
Scheme 3-1: Mechanism for the round-trip radical cyclization reaction.....	53
Scheme 3-2: Mechanism for the cyclization of 3.4	54
Scheme 3-3: Synthesis of cyclization precursors 1.65 , 3.2 and 3.3	56
Scheme 3-4: Synthesis of cyclization precursor 3.1	58
Scheme 3-5: Synthesis of alkynyl precursor 3.4	59
Scheme 3-6: Stereochemical relay experiments	73
Scheme 3-7: Summary of the round-trip radical cyclization	79
Scheme 3-8: Transition states and products for the cyclization of radical 3.6E	80

Scheme 3-9: Transition states and products for the cyclization of radical 3.6	82
Scheme 3-10: Transition state analysis for the second radical cyclization of vinyl iodide 3.1 ...	83
Scheme 3-11: Rate determining step in the cyclization of 1.65	85

LIST OF ABBREVIATIONS

Ac	acetyl
AIBN	azobisisobutyronitrile
APCI	atmospheric pressure chemical ionization mass spectrometry
Bu	butyl
Bn	benzyl
COSY	correlation spectroscopy
DCC	<i>N, N'</i> -dicyclohexylcarbodiimide
DBU	1,8-diazabicyclo[5.4.0]undec-7-ene
DMAP	4-dimethylaminopyridine
DMSO	dimethylsulfoxide
DIBAL-H	di-isobutylaluminum hydride
E	methyl ester (CO ₂ Me)
equiv	equivalent
Et	ethyl
GC	gas chromatography
GC-MS	gas chromatography-mass spectrometry
HAT	hydrogen atom transfer
HMPA	hexamethyl phosphoramidate
HPLC	high performance liquid chromatography
HRMS	high resolution mass spectrometry
IR	infrared spectrometry
<i>J</i>	coupling constant (Hz)
LDA	lithium diisopropylamide
M	molar
<i>m</i>-CPBA	<i>meta</i> -chloroperoxybenzoic acid
Me	methyl

MeO	methoxy
MS	low resolution mass spectrometry
NaHMDS	sodium hexamethyldisilazide
NMR	nuclear magnetic resonance
NOE	nuclear Overhauser effect
Ph	phenyl
ppm	parts per million
Pr	propyl
R_f	retention factor
R_t	retention time
rt	room temperature
<i>t</i>	tert
THF	tetrahydrofuran
TLC	thin layer chromatography
TMS	trimethylsilyl
UV	ultraviolet

PREFACE

I would like to take this opportunity to thank a number of people who have helped and supported me throughout my five years at the University of Pittsburgh. First and foremost I would like to thank Dr. Curran for allowing me to work under his guidance and benefit from his teaching. I have learned so much from him not only about chemistry, but also on how to conduct myself professionally as a scientist and a person. I have always appreciated the freedom that he has given me to explore my own ideas and the respect that he has shown me. I would especially like to thank him for his help and patience in preparing this and my proposal documents. In addition I would like to thank all of the Curran group members past and present for their friendship, helpfulness and many good times. Special thanks go out to Andre Lapierre and Tiffany Turner for their support not only on the academic front, but also on the personal front which in many ways has been equally challenging.

I would also like to acknowledge Professors Wipf, Floreancig and Kagan for serving on my dissertation committee and Professors Day and Schafmeister for helping me with my proposal. I would also like to thank Professors Nelson, Koide, Walker and Sheperd for their patience and teaching while I was a student in their classes. Combined everyone has made my time at Pitt incredibly educational and enjoyable. I am sure that my experiences here will serve me well throughout my career and I will always look back upon them very favorably.

I also wish to thank Maiko Ezawa for the incredibly important role that she has played in my life over the past years. She has been an inexhaustible source of support and love and there is no way I would be where I am today without her. We have certainly had our ups and our downs, but we have come out of it happier and stronger. One thing that I want to thank her for is always challenging me to be a better person. I look forward to our future together wherever it decides to take us and that just leaves me to say that we made it!

Last but certainly not least I would like to thank my parents for their love and support no matter how crazy my ideas may sound. They have provided for me in ways too numerous to mention; I will never forget that and am forever grateful. I can not thank you both enough for

helping me realize my dreams by providing me with a warm and loving atmosphere to grow up in. You have both certainly challenged me to think about life in new ways and I am better person because of this. Thanks again for everything and please know that no matter what, I love you both very much. Although I may be far away you are close to my heart and in my thoughts all the time.

To all of my friends and family that I have not mentioned, you have certainly not been forgotten. I cherish your love, friendship and support over the years tremendously. Each and every one of you has contributed in a special way to me reaching this milestone in my life. Thank you all so much.

Chapter 1 Introduction

In the eighteenth century, Lavoisier was the first chemist to use the word “radical” to describe the portion of a molecule that remains unchanged during a chemical reaction. The modern definition of a radical reaction is a chemical process that involves molecules having unpaired electrons. This new definition was born in 1900 when Professor M. Gomberg mixed triphenylchloride and mercury to get the triphenylmethyl radical.^{1,2} Gomberg’s experiment challenged the “fact” that carbon could only be tetravalent and so was met with due skepticism. Gomberg, however, was quite correct that his experiment had produced, albeit briefly, a trivalent carbon atom with an unpaired electron.

Between 1900 and about 1980, radicals were perceived as interesting reactive intermediates with limited synthetic potential. In no small part, this was due to the notion that something so reactive could not possibly be selective, and selectivity is after all the key to a high yielding process. Fortunately the physical organic chemists persevered and forged a great understanding of the structure and reactivity of radicals.³ Based on their work, synthetic organic chemists realized the enormous potential of radical chemistry. It is this realization that has led to the widespread use of radical reactions in synthesis throughout the 1980’s and into the present day.⁴

Radical reactions are ordinarily initiated by a homolytic bond cleavage, Figure 1-1, where atoms A and B each receive one of the electrons from the broken bond. The two products of this homolytic bond cleavage are electronically neutral, but at the same time they are reactive because of the unpaired electron. Ionic reactions on the other hand involve a heterolytic bond dissociation where one atom gets both of the electrons to give reactive cation and anion products.

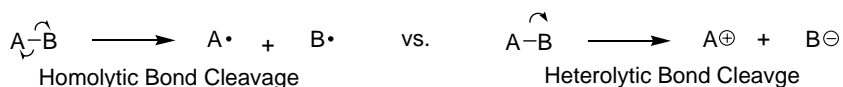


Figure 1-1: Homolytic versus heterolytic bond dissociation of a molecule A-B.

The fact that most radicals are neutral provides them with some nice advantages over their ionic counterparts. For instance, because of this neutrality, radical reactions occur under mild conditions resulting in high functional group tolerance. The elaborate protecting group chemistry often seen in ionic reactions is therefore not necessary. Fortunately, nearly all of the

popular classes of protecting groups are tolerated by radical reactions should they be necessary for other steps in the synthetic sequence. Another advantage of radical over ionic chemistry is that a much wider variety of solvents, including water, can be used to carry out transformations. Furthermore radicals are less sensitive to steric encumbrance than ions are. This means that radicals can be used for transformations that are otherwise difficult to accomplish.⁵ For the reasons mentioned above and many others, radicals have found widespread use in the deoxygenation of alcohols, ketones and aldehydes, as well as desulfurization, deamination, decarboxylation, dehalogenation and carbon-carbon bond forming reactions.

The reactive nature of radicals means that they often react in chains, because the product of one radical reaction is another radical. This radical product then serves as the starting material for another reaction and so on.^{3b} The chain ends with a termination step when two radicals react together to give non-radical products. This work focuses on the chemistry of carbon centered radicals and their involvement in carbon-carbon bond forming reactions.

1.1 Chain Mechanisms for the Generation of Carbon Centered Radicals

Direct formation of the desired carbon centered radical C• from a C-X precursor, would require the homolytic cleavage of the C-X bond. Effecting this cleavage under reasonable conditions is not a trivial task because homolytic bond dissociation energies are high. For instance, the homolytic bond dissociation energy for the carbon-carbon bond in ethane⁶ is 88 kcal mol⁻¹, whereas the “weaker” carbon iodine bond of iodomethane is still 56 kcal mol⁻¹. For this reason, carbon-centered radicals are frequently generated through chain mechanisms that consist of initiation, propagation and termination steps. The initial radical in a chain mechanism is formed by the homolytic cleavage of a weak bond and then transferred by a series of propagation steps to the carbon atom of interest.

1.1.1 Chain Initiation

The compound containing the requisite weak bond to start the chain is known as a radical initiator, and some of the most common initiators are shown in Figure 1-2. When 2,2-azobisisobutyronitrile (AIBN)⁷ **1.1** is heated or irradiated, a molecule of N₂ is extruded giving tertiary radical **1.2**. Unfortunately, the need for heat or light in AIBN initiation precludes its use with some substrates or functional groups. Triethylborane⁸ **1.3** addresses this compatibility

problem by readily reacting with molecular oxygen to give peroxy radical **1.4** and an ethyl radical **1.5** at temperatures as low as $-78\text{ }^{\circ}\text{C}$. Finally, another popular radical initiator is benzoyl peroxide **1.6**. Upon heating, peroxy compound **1.6** decomposes to give two benzoyl radicals **1.7**. The benzoyl radicals **1.7** can initiate chains directly or decompose further to give two phenyl radicals **1.8** and two molecules of carbon dioxide.

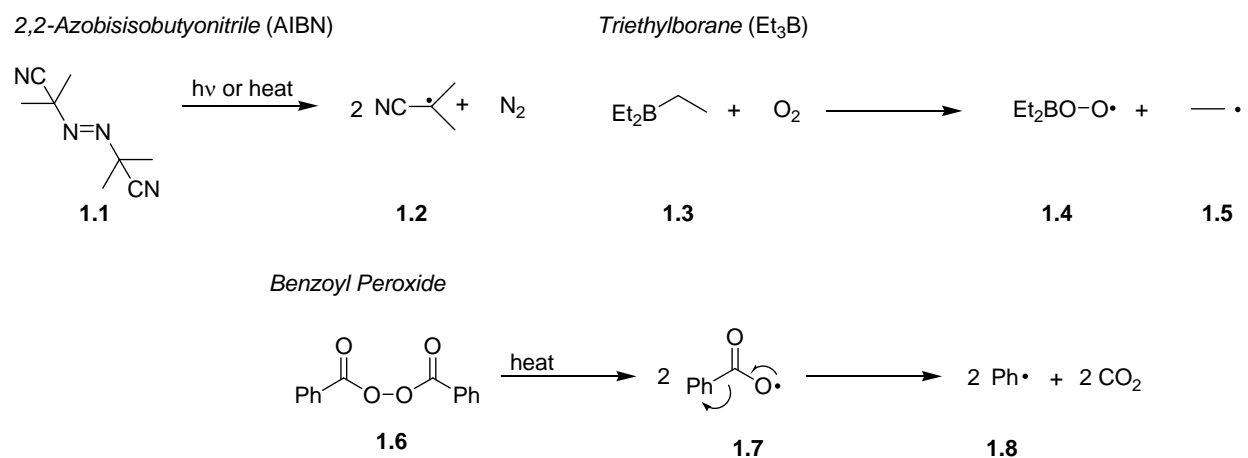


Figure 1-2: Common radical initiators and their derived radicals.

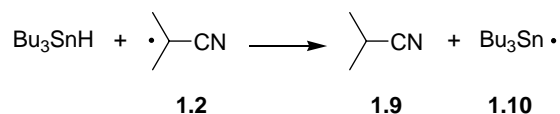
1.1.2 Chain Propagation and Termination

In the propagation steps of a chain mechanism, the desired radical $\text{R}^{\text{A}} \cdot$ **1.11** is formed by the homolytic cleavage of the $\text{R}^{\text{A}}\text{-X}$ bond, Scheme 1-1. $\text{R}^{\text{A}}\text{-X}$ is called a radical precursor and X can be a number of different atoms or groups, some of which are shown in Scheme 1-1. The key to propagation is that one radical is consumed and another one is formed that is used in a subsequent step. The propagation steps are often mediated by a reducing agent such as Bu_3SnH , Ph_3SnH or $(\text{TMS})_3\text{SiH}$. In Scheme 1-1, typical propagation steps are summarized using radical **1.2** from AIBN initiation and Bu_3SnH as the reducing agent.

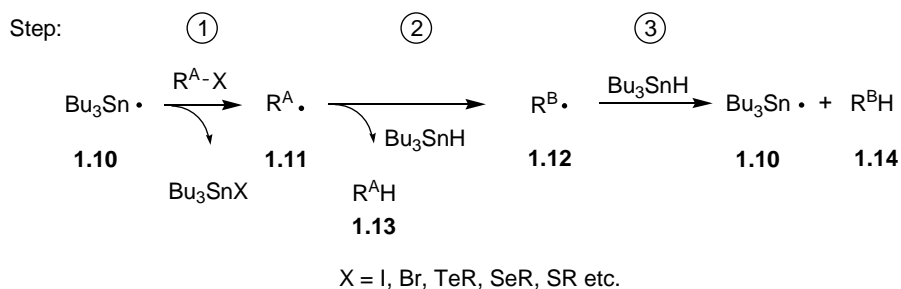
Following from the initiation reaction, radical **1.2** reacts with the Bu_3SnH to give stannyl radical **1.10** and 2-cyanopropane **1.9**. In the first propagation step, the stannyl radical reacts with the radical precursor $\text{R}^{\text{A}}\text{-X}$ to give the desired radical $\text{R}^{\text{A}} \cdot$ **1.11** and Bu_3SnX . Compound **1.11** then undergoes the desired reaction in step 2, be it intra- or intermolecular, to give radical $\text{R}^{\text{B}} \cdot$ **1.12**. Finally, in step 3, **1.12** abstracts a hydrogen from Bu_3SnH to give the desired product $\text{R}^{\text{B}}\text{H}$ **1.14** and the stannyl radical **1.10**. The stannyl radical produced in step 3 then re-enters the chain at step 1.⁹ The regeneration of the stannyl radical in the final step means that the initiator can be

used in substoichiometric amounts. An undesirable side reaction is where radical $R^{\cdot A}$ **1.11** abstracts a hydrogen from the reducing agent to give product $R^A H$ **1.13** before the desired reaction can occur.

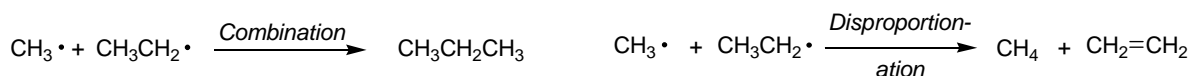
Chain Initiation Step:



Chain Propagation Steps:



Chain Termination Steps:



Scheme 1-1: Propagation and termination steps in a radical chain mechanism.

The chain mechanism can be interrupted when two radicals react together to give non-radical products. This interruption can occur through either a combination or a disproportionation reaction, Scheme 1-1. An example of a combination reaction is where a methyl and an ethyl radical produce a molecule of propane. A disproportionation reaction is where these same two radicals give a molecule of methane and ethene. Such reactions are called termination steps.

1.2 General Considerations for Running Radical Reactions

Radicals are highly reactive species and they will react with each other by combination or disproportionation at rates approaching the diffusion controlled limit (about 10^9 - $10^{10} \text{ M}^{-1} \text{ sec}^{-1}$). Therefore, low concentrations of radical species are generally desirable and can be achieved by controlling the rates of initiation and termination. Furthermore, low concentrations of the

reducing agent are desirable to minimize the reduction of radical $R^A\cdot$ before it undergoes the conversion to $R^B\cdot$.

The easiest way to minimize the undesired side reactions is to use a dilute solution of Bu_3SnH and substrate $R-X$. This however requires a large volume of solvent that is not easy to handle on larger scale. Another way to keep reducing agent concentrations low is to add it to the reaction mixture by syringe pump over a long period of time.^{9,10} It is also possible to regenerate the Bu_3SnH from the Bu_3SnX by using sodium cyanoborohydride¹¹ or sodium borohydride.¹² This allows sub-stoichiometric amounts of reducing agent to be used ensuring that concentrations remain low during the reaction.

While a dilute reaction medium helps in the formation of the desired product R^BH , it is possible for the reducing agent to be too dilute. In order for the chain to propagate, radical **1.12** must abstract a hydrogen from Bu_3SnH to generate **1.10** so that it can re-enter the cycle. Due to the limited lifetime of radicals, $R^B\cdot$ **1.12** could undergo termination or an undesirable reaction instead of abstracting a hydrogen. For example, a common solvent for radical reactions is benzene and the rate constant for radical additions to this solvent is about $10^2 M^{-1} sec^{-1}$. Therefore, if the concentration of Bu_3SnH is low enough, this undesired addition to benzene can compete with hydrogen abstraction from the reducing agent.

1.3 Common Types of Radical Reactions

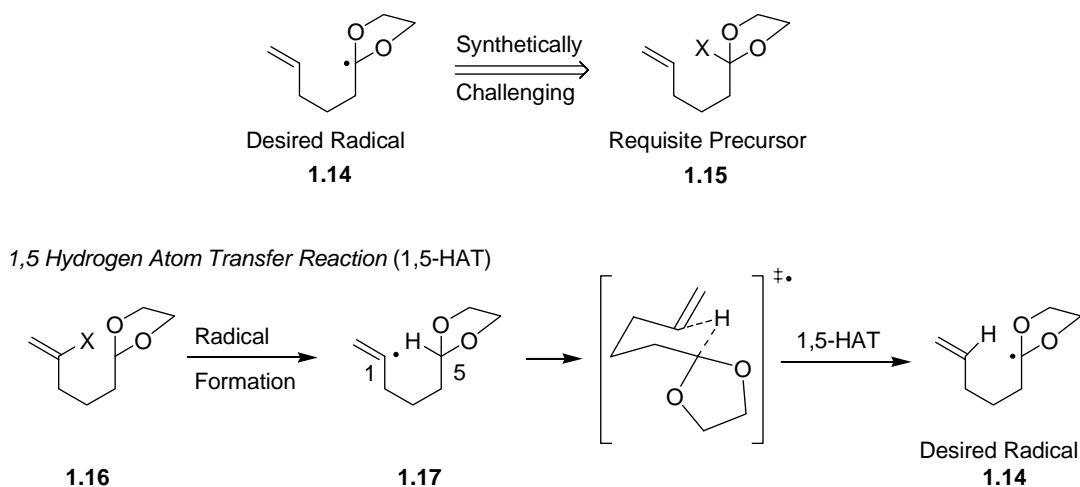
There are a vast number of reactions that are known to proceed through a radical mechanism, but three are of particular relevance to this work, namely the 1,5 hydrogen atom transfer process (1,5 HAT), the Barton decarboxylation and the 5-*exo* cyclization of a hexenyl radical. After a brief overview of the 1,5 HAT process and the Barton decarboxylation reaction, the 5-*exo* cyclization of a hexenyl radical will be discussed in more detail.

1.3.1 1,5 Hydrogen Atom Transfer Reactions

The tin hydride method for generating radicals by homolysis of C-X bonds ($X = I, Br, Cl, SePh$, etc) continues to be one of the most convenient and widely used procedures. In certain instances, however, the desired radical may result from the homolysis of a C-H bond, but this brings with it a number of challenges. The first problem is the thermodynamics of homolytic C-H bond cleavage. With homolytic dissociation energies around $95 kcal mol^{-1}$, C-H bonds are

rather strong in comparison to Sn-H bonds that have bond dissociation energies¹³ around 74 kcal mol⁻¹. The result is that a carbon-centered radical can abstract hydrogen from a Sn-H bond, but the reverse process of a tin radical abstracting hydrogen from C-H bond is thermodynamically unfavorable. A second hurdle is that the C-H bond is the most common bond in organic molecules and so abstraction of a specific hydrogen poses significant challenges.

Nevertheless, using the C-H bond as a radical precursor is desirable because synthesis of a C-X precursor can be challenging, especially when the carbon atom has heteroatomic substituents. A convenient strategy to use the C-H bond as a precursor is to generate the radical at a remote site and then translocate it to the desired position through a 1,5 hydrogen atom transfer (1,5 HAT) process. Generating new carbon-centered radicals from heteroatomic radicals (oxygen or nitrogen) by a 1,5 HAT process is well known and forms the basis for the Barton,¹⁴ Hoffman-Löffler-Freytag¹⁵ and the Fraser-Reid¹⁶ reactions. As a nice complement to the heteroatomic variants, Curran and Shen¹⁷ developed a process where both of the radicals in the 1,5 HAT process are carbon-centered as shown in Scheme 1-2. For example, if the desired radical is acetal **1.14**, then compound **1.15** would serve as the requisite precursor. However, formation of the necessary C-X bond in **1.15** on the same carbon as the acetal functionality may be synthetically challenging. The bottom half of Scheme 1-2 shows radical **1.14** can still be reached from precursor **1.16**. Homolytic cleavage of the C-X bond in **1.16** gives **1.17** with the radical in the 1 position and a hydrogen atom in the 5 position. This hydrogen atom can be readily transferred to give the desired radical **1.14** as shown in Scheme 1-2.

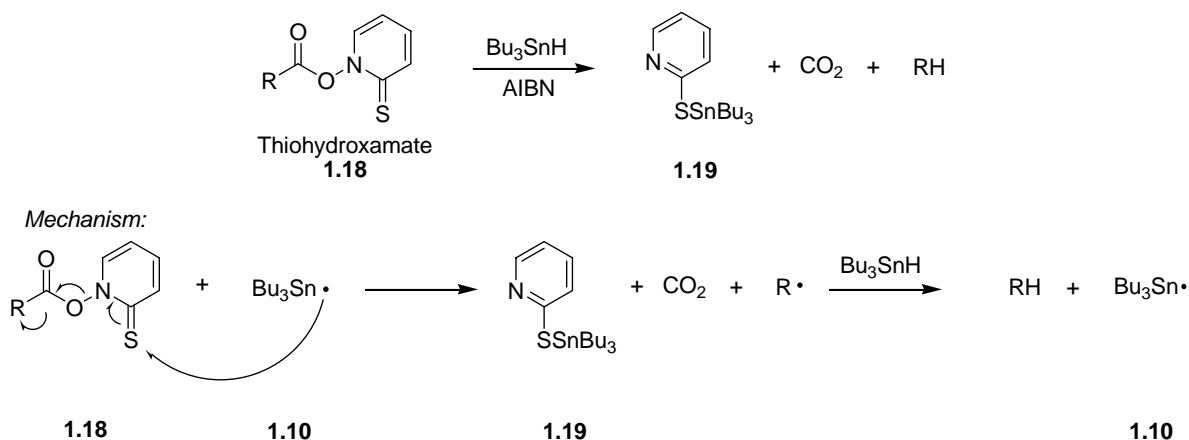


Scheme 1-2: 1,5 Hydrogen atom transfer reaction.

The process of 1,5-HAT is also favorable because it goes through a chair-like transition state,¹⁸ Scheme 1-2, that has minimal strain. While 1,4-, 1,6-, and 1,7-HAT processes are known,¹⁹ it is difficult for them to compete with the 1,5 process. In the case of a 1,4-HAT the chain is too short to allow for the proper alignment of the hydrogen and the radical. For the 1,6- and 1,7-HAT process the entropic cost of reaching the necessary 7 and 8 membered transition states is significantly higher than the 6-membered transition state needed for the 1,5 process. Clearly, the 1,5-HAT method of obtaining carbon centered radicals is an extremely useful and powerful tool in radical chemistry.

1.3.2 The Barton Decarboxylation Reaction

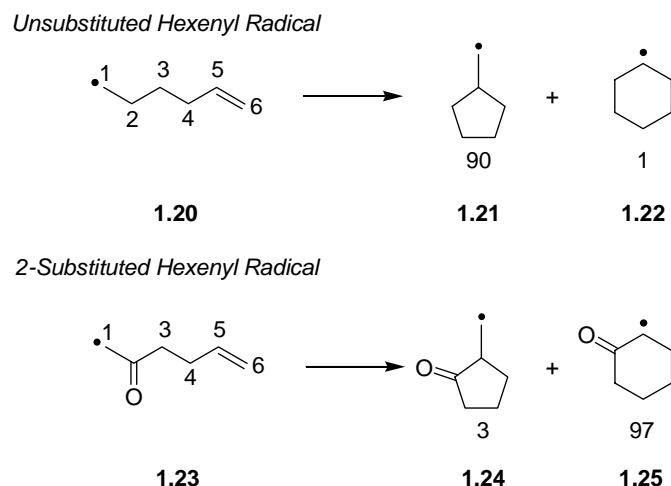
The Barton decarboxylation reaction uses a thiohydroxamate as a radical precursor. In a typical reductive decarboxylation, thiohydroxamate **1.18** is treated with Bu_3SnH to give thiopyridyl compound **1.19**, CO_2 , and the reduced product RH as shown in Scheme 1-3. The fragmentation of the R-C(O) and the N-O bond is initiated by addition of the $\text{Bu}_3\text{Sn}\cdot$ radical **1.10** into the C-S double bond also shown in Scheme 1-3. This fragmentation process is driven by the aromatization of the thiohydroxamate to give thiopyridine **1.19** and the formation of the stable molecule CO_2 . The resulting radical $\text{R}\cdot$ then abstracts a hydrogen from Bu_3SnH to give the reduced product RH and the stannyl radical starting material, thereby propagating the chain. While the Barton decarboxylation is frequently used to remove carboxyl groups from molecules to give the corresponding alkane, the intermediate radical $\text{R}\cdot$ can also be trapped in either an inter- or an intramolecular process.²⁰



Scheme 1-3: Mechanism for a Barton decarboxylation reaction.

1.3.3 5-*Exo* Cyclizations of Hexenyl Radicals

Arguably the most well studied of all radical reactions is the cyclization of a 5-hexenyl radical **1.20**. This radical can cyclize either through a 5-*exo* pathway to give the methyl cyclopentyl radical **1.21**, or in a 6-*endo* manner to give the cyclohexyl radical **1.22** as shown in Scheme 1-4. Stereoelectronic effects dictate that this cyclization favors the 5-*exo* pathway and indeed the 5-*exo* and 6-*endo* products are obtained in a 90/1 ratio.²¹ Substitution of the hexenyl radical normally does not affect the 5-*exo* selectivity of the cyclization. However, with certain substituents the selectivity can be overturned. For instance, placement of a carbonyl group in the 2 position, compound **1.23**, provides the 5-*exo* product **1.24** and the 6-*endo* product **1.25** in a 3/97 ratio.²²



Scheme 1-4: Selectivity in an unsubstituted and 2-substituted hexenyl radical cyclization.

While it is evident that hexenyl radical cyclizations can be regioselective, their widespread use in synthesis also depends on the levels of stereoselectivity that can be obtained. In an effort to understand the factors that affect the stereoselectivity of the cyclization, the Beckwith-Houk transition state model was developed.²³ This model provides a convenient way to predict and rationalize the stereoselectivity of the 5-*exo* hexenyl radical cyclization by providing a clear picture of the transition state. In the addition of a radical to an alkene, a tetrahedral-like approach is preferred and this can be accommodated by either a “chair”^{23a,b} or a “boat”^{23d} transition state, as shown in Figure 1-1. The names of the transition states are derived from the two analogous conformations of cyclohexane.

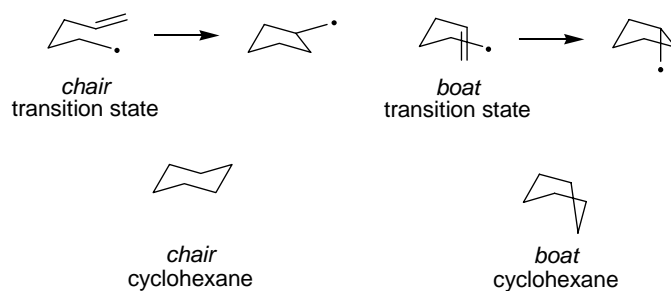


Figure 1-3: Transition state structures for hexenyl radical cyclizations.

Once the various transition states for the radical cyclization have been located, either computationally or conceptually, they can be evaluated using many of the same principles of cyclohexane conformational analysis. For instance, similar to cyclohexane, substituents in the

radical cyclization transition states prefer to adopt an equatorial as opposed to an axial orientation. In this manner, it is possible to decide which of the competing transition states is lowest in energy and thereby most favored. However the analogy does have limits. The boat conformation of cyclohexane is 6.4 kcal mol⁻¹ higher²⁴ in energy than that of the chair, but the boat transition state for a hexenyl radical is only about 1.0 kcal mol⁻¹ higher^{23d} in energy than the hexenyl radical chair. Therefore in the transition state analysis of hexenyl radical cyclizations, a boat is often invoked, whereas the boat conformation of cyclohexane is rarely considered in reactions.²⁵

Adding a substituent to the hexenyl radical in the 2, 3, or 4 position introduces a stereocenter and results in four possible transition states: *chair-equatorial*, *chair-axial*, *boat-equatorial* and *boat-axial*. As an example, the four possible transition states for a 3-substituted hexenyl radical are shown in Figure 1-4. In this case, the *chair-equatorial* and the *boat-axial* transition states lead to the *cis* cyclopentyl radical whereas the *chair-axial* and the *boat-equatorial* both proceed to the *trans* product. It is possible to predict the major product of a cyclization by determining which transition state has the lowest energy. For this reaction, the *cis* product is predicted to be the major isomer, because the *chair-equatorial* transition state is void of axial substituents and therefore the lowest in energy. The *chair-axial* and *boat-equatorial* transition states are destabilized by the axial placement of the R group or the alkene respectively. Although the *boat-axial* transition state also leads to the major product, it is not a major contributor because with two axial substituents it is too high in energy and is thus often ignored.²⁶

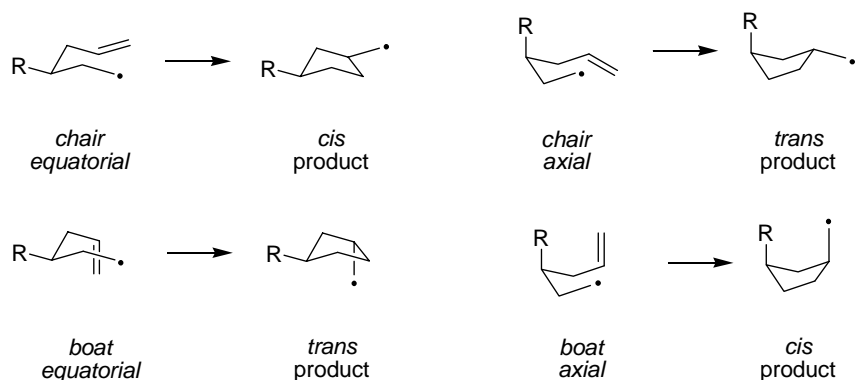


Figure 1-4: Transition states for a 3 substituted hexenyl radical.

1.4 Synthesis of Linear Triquinanes by Tandem Radical 5-Exo Cyclization Reactions

Some of the most powerful reactions in organic synthesis are those where several bond forming steps occur in a single synthetic operation. Such processes are known as tandem reactions. Tietze concisely defined a tandem reaction as a process that involves two or more bond-forming transformations, which take place under the same reaction conditions without additional reagents or catalysts and in which the subsequent reaction is the direct result of the functionality formed in the previous step.²⁷ Tandem reactions are particularly useful because they can quickly build up molecular complexity from relatively simple starting materials. Employing sequential 5-*exo* hexenyl radical cyclizations in a tandem sequence makes polycyclopentanoid molecules or polyquinanes ideal targets.^{4,5b,28}

A number of triquinane natural products, compounds with three cyclopentane rings, have been isolated with a variety of geometries as shown in Figure 1-5. Modhephene contains a propellane geometry in which all three rings have two carbon atoms in common. Silphiperfol-6-ene has an angular triquinane geometry where all three rings share a central carbon atom. Finally hirsutene contains a linear triquinane in which two of the cyclopentane rings surround a central ring. Additionally, a particularly interesting natural product is crinipellin A that contains both a linear and an angular triquinane. For the synthesis of crinipellin A, a tandem radical cyclization approach is ideal and efforts towards constructing the angular triquinane portion by a tandem cyclization sequence have been reported.^{4b,29} As a different approach, we wanted to explore the construction of the linear triquinane portion of crinipellin A using a tandem radical cyclization.

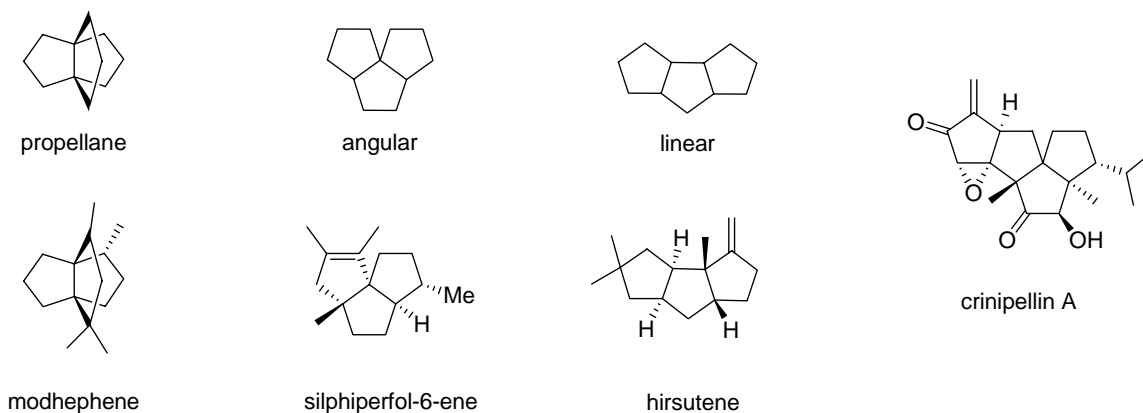
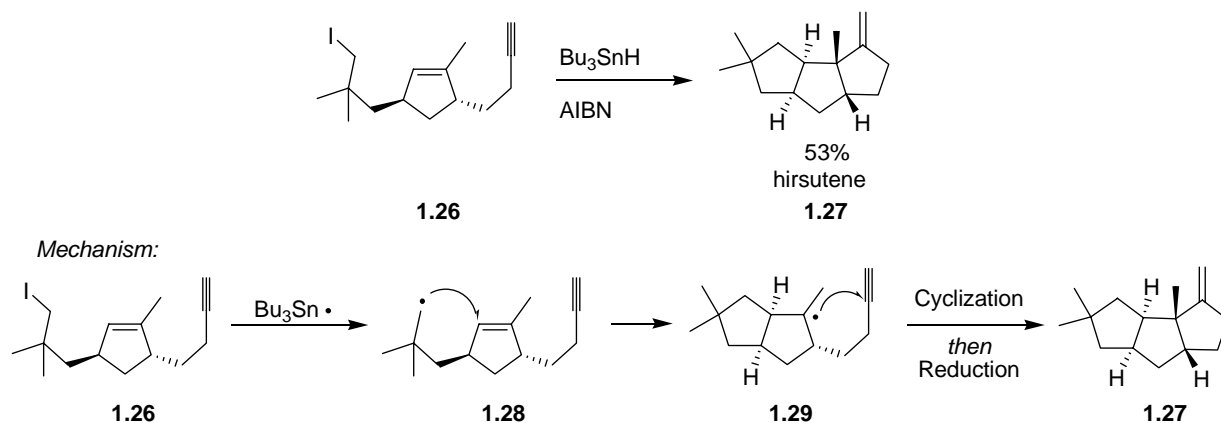


Figure 1-5: Triquinane geometries and natural products.

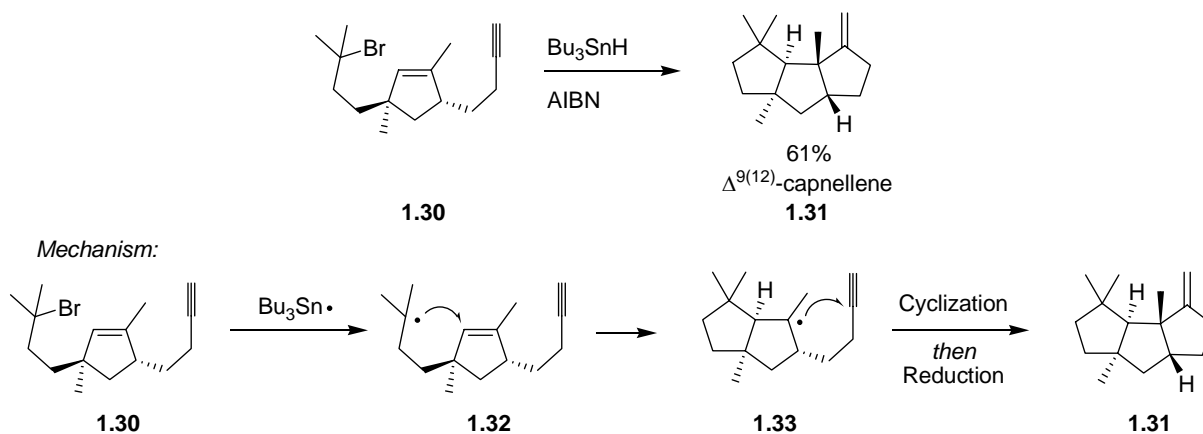
1.4.1 Total Synthesis of Linear Triquinane Natural Products

Tandem radical cyclizations have been employed in the synthesis of several linear triquinane natural products. The synthesis of (\pm)-hirsutene³⁰ by Curran and Rakiewicz was the first report of a total synthesis using this approach, and is shown in Scheme 1-5. The radical precursor in this case is iodide **1.26** and upon treatment with AIBN and Bu₃SnH gives (\pm)-hirsutene **1.27** in 53% yield. The cascade cyclization is initiated by a stannyl radical abstracting iodine from precursor **1.26** to give primary radical **1.28**. This radical then undergoes a 5-*exo trig* cyclization to give tertiary radical **1.29**. Intermediate **1.29** is now perfectly arranged to undergo a 5-*exo dig* cyclization with the pendant alkyne to give (\pm)-hirsutene **1.27** upon reduction.



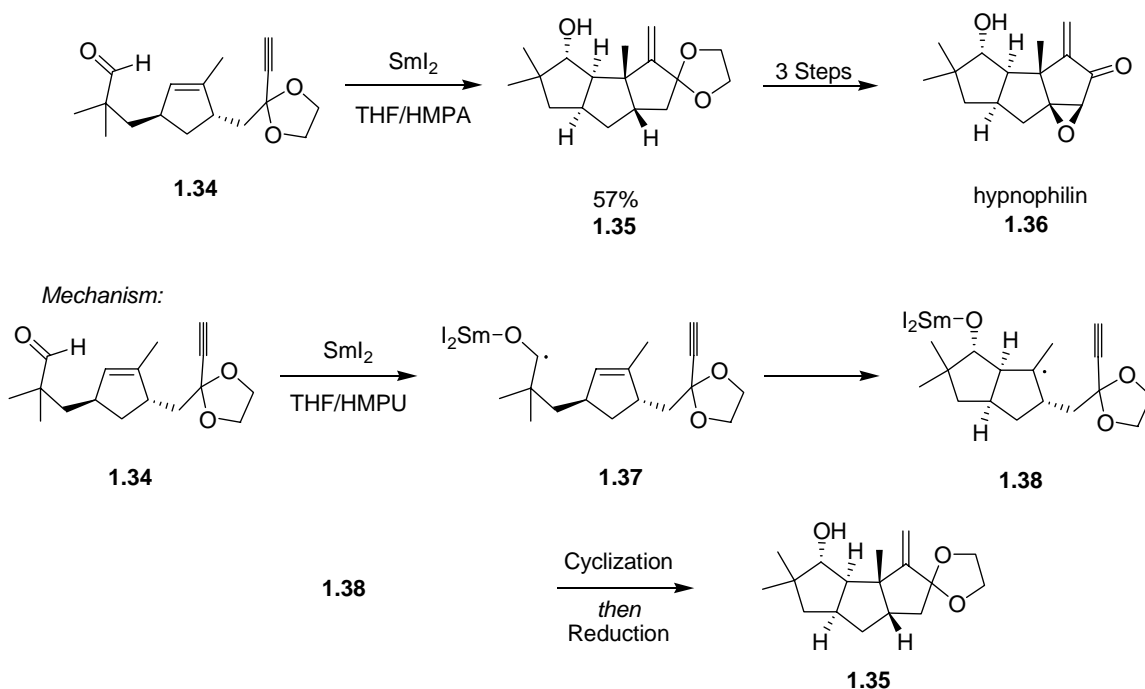
Scheme 1-5: Total synthesis of hirsutene.

A similar strategy was used in the total synthesis of $\Delta^{9(12)}$ -capnellene³¹ starting from bromide **1.30**, Scheme 1-6. Treatment of radical precursor **1.30** with Bu₃SnH and AIBN furnishes $\Delta^{9(12)}$ -capnellene **1.31** in 61% yield. The first step in the cascade is abstraction of the bromide from **1.30** by a stannyl radical to give tertiary radical **1.32**. Radical **1.32** then cyclizes in a 5-*exo trig* fashion to give bicyclic radical **1.33**, that undergoes a 5-*exo dig* cyclization to give $\Delta^{9(12)}$ -capnellene upon reduction. These two total syntheses are good examples of how tandem radical cyclizations can rapidly build up molecular complexity from relatively simple starting materials.



Scheme 1-6: Total synthesis of hirsutene and $\Delta^{9(12)}$ capnellene.

The total synthesis of hypnophilin,³² a more oxygenated member of the hirsutene family, has also been accomplished using a tandem radical cyclization, Scheme 1-7. In this synthesis treatment of radical precursor **1.34** with SmI_2 in a THF/HMPA solvent mixture yields linear triquinane **1.35** in 57% yield. From compound **1.35**, the total synthesis of hypnophilin **1.36** is completed in three steps. The cascade cyclization is initiated by treatment of aldehyde **1.34** with SmI_2 to give ketyl radical **1.37**. Radical cyclization of **1.37** gives compound **1.38** that undergoes a 5-*exo dig* cyclization with the alkyne to give acetal **1.35** after reduction. This synthesis nicely demonstrates how the mild reaction conditions of radical cyclizations can tolerate dense oxygenation and the sensitive acetal functionality. This functional group tolerance is important to consider because crinipellin A is also densely oxygenated.



Scheme 1-7: Total synthesis of hypnophilin.

1.4.2 Synthesis of Linear Triquinanes from Acyclic Precursors

It is clear that a tandem radical cyclization approach to linear triquinane synthesis is efficient. In the three examples presented above, the diastereoselectivity of the cyclization is dictated by the stereochemistry of the cyclopentene ring present in the radical precursor. While using the pre-existing ring as a stereochemical template is successful, it can make the synthesis of the precursors somewhat tedious. An attractive and more direct approach to linear triquinanes would be to use a tandem radical cyclization approach starting from an acyclic precursor.

A number of strategies have been developed for the synthesis of linear triquinanes from acyclic precursors, some of which are summarized in Figure 1-6.^{29d, 33} In the zipper strategy, the radical is generated in the middle of the chain and the cascade then brings the two ends together. In a macrocyclization, strategy the radical is generated at one end of the chain and the first cyclization forms a large ring which then closes down to make the linear triquinane. Finally, a round-trip approach is unique in that the site of the last radical attack is also the carbon where the radical was initially generated. The round-trip strategy further distinguishes itself by being the only one where the formation of geminal bonds is possible.

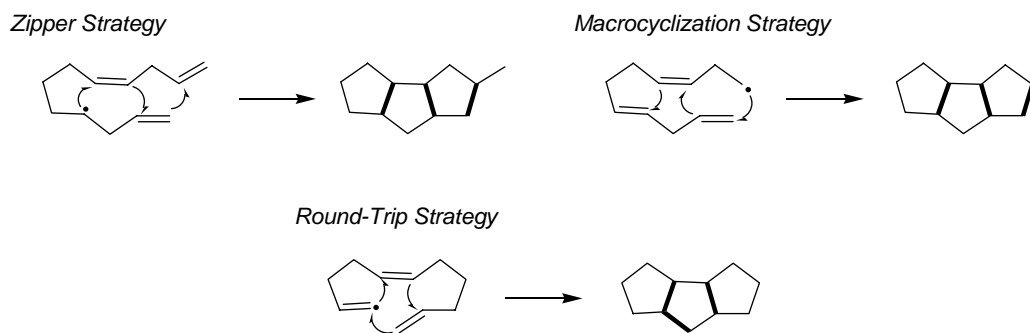
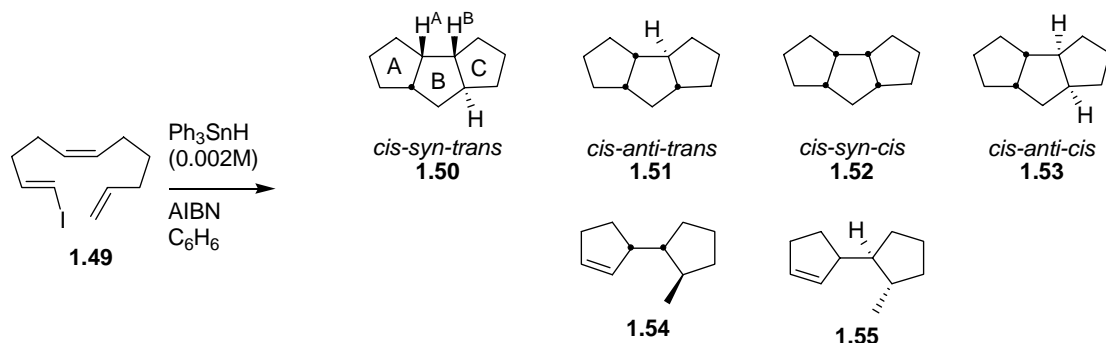


Figure 1-6: Strategies for the synthesis of linear triquinanes from acyclic precursors. Bolded bonds indicate those that are formed during the cascade.

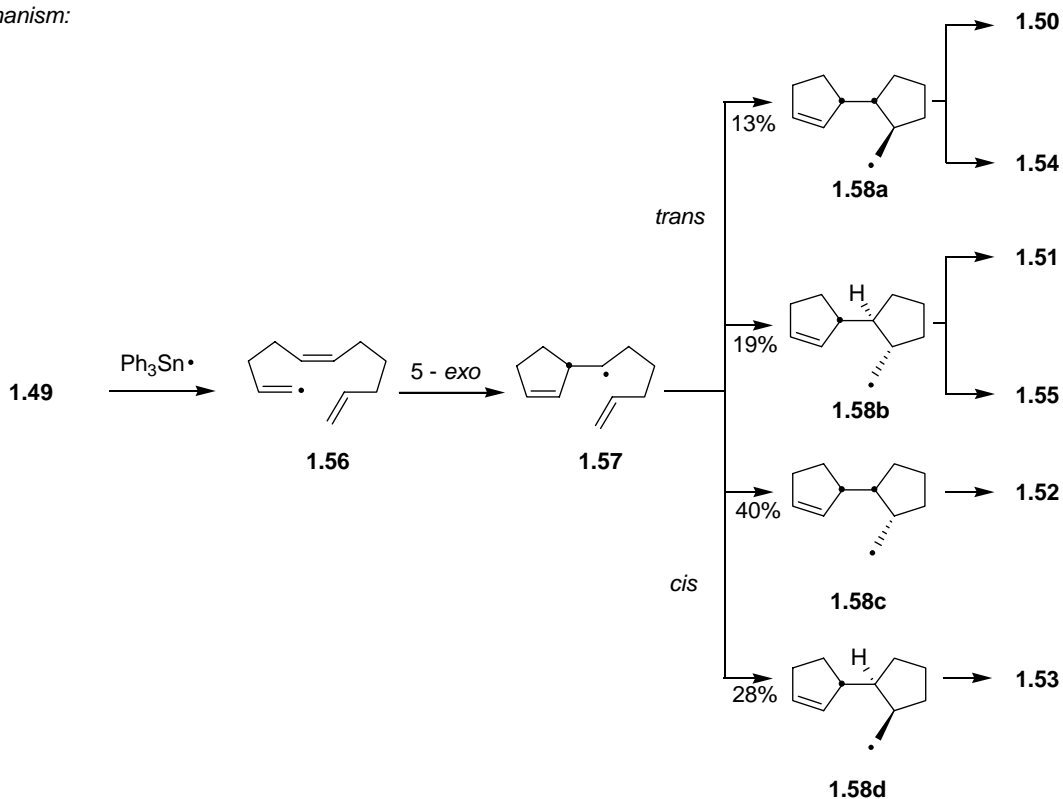
In early work, Beckwith and co-workers³⁴ demonstrated both the power and problems of synthesizing linear triquinanes from an acyclic precursor through a tandem radical cyclization, as shown in Scheme 1-8. They employed a zipper strategy starting from bromide **1.39**. Reduction of radical precursor **1.39** with AIBN and Bu_3GeH gave a complex mixture of linear triquinanes **1.40-1.43** and two cyclohexane containing products **1.44** and **1.45**. The nomenclature of the linear triquinane products is either *cis* or *trans* based on the ring fusion of the A and B rings and then *syn* or *anti* based on the relationship of protons H^{A} and H^{B} shown in **1.40**. The final *cis* or *trans* depends on the ring fusion between the B and C rings.

The cascade cyclization is initiated with abstraction of the bromide in precursor **1.39** by a $\text{Bu}_3\text{Ge}\cdot$ to give acyclic radical **1.46**. Radical **1.46** then cyclizes selectively to give *cis* substituted cyclopentane **1.47**. The problems in this cascade arise in the second cyclization because radical **1.47** can cyclize in a *cis* fashion to give radical **1.48a** or **1.48b**. However **1.47** can also cyclize in a *trans* fashion to give products **1.48c** or **1.48d**. Finally, each diastereomer of **1.48** cyclizes to give a single linear triquinane **1.40** through **1.43** upon reduction. Furthermore the final 5-*exo* cyclization of the two *trans* substituted products **1.48c** and **1.48d** is slow allowing the 6-*endo* pathway to compete giving cyclohexanes **1.44** and **1.45**.

bicyclic radicals, **1.58a** and **1.58b** the final cyclization is slow because it is forming the more strained *trans* triquinanes. This slow cyclization allows reduction by Ph_3SnH to compete giving rise to the bicyclic products **1.54** and **1.55**. Similar to Beckwith's work with precursor **1.39**, the diastereodiversity in the cyclization of **1.49** can be attributed to a lack of selectivity in the second of the three cyclizations.



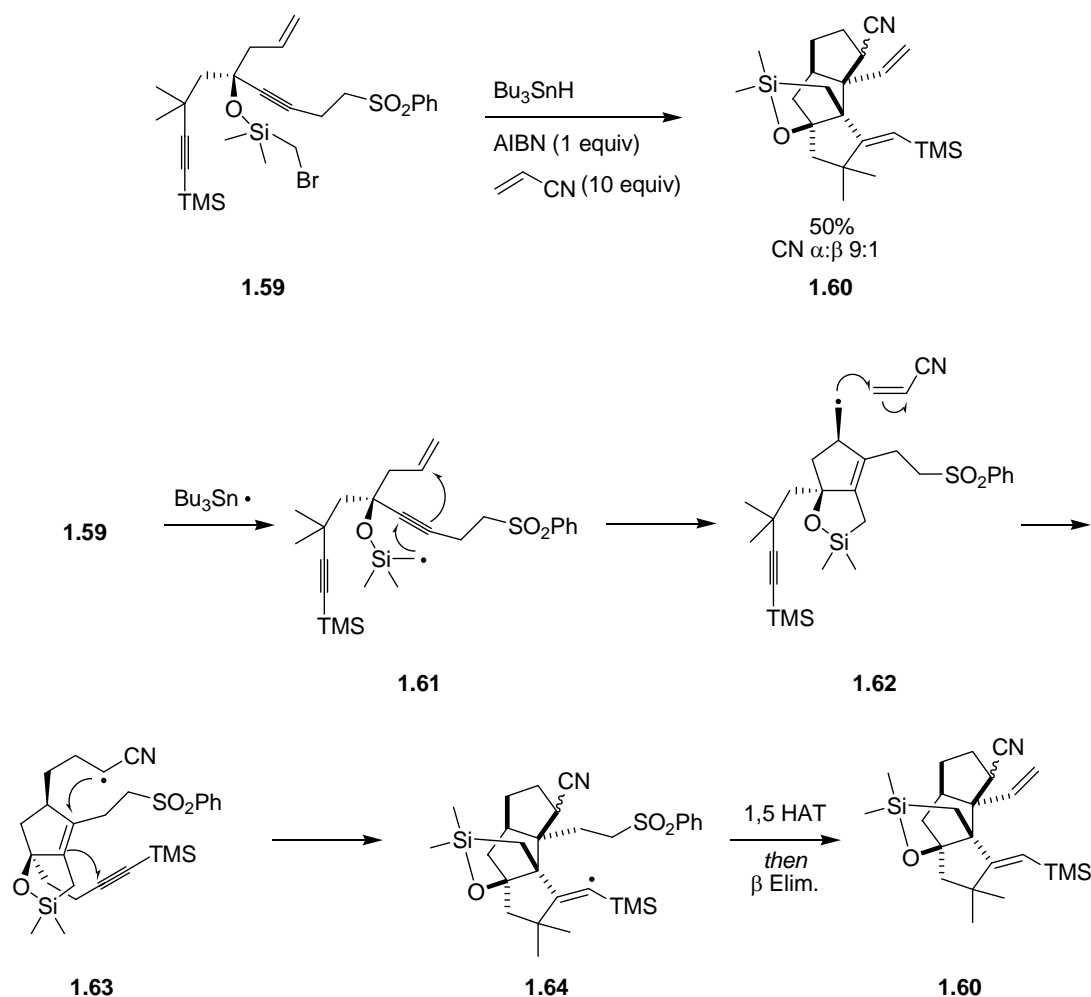
Mechanism:



Scheme 1-9: Synthesis of linear triquinanes using a round-trip radical cyclization strategy.

Diastereoselectivity is clearly the main obstacle for the synthesis of triquinanes from acyclic precursors. Malacria and co-workers,³⁷ however, have had success as shown in Scheme 1-10. Treatment of bromide **1.59** with Bu₃SnH, AIBN and acrylonitrile provides tetracyclic compound **1.60** in 50% yield. This is an impressive result because the triquinane portion of compound **1.50** is obtained diastereomerically pure. They do, however, obtain a 9/1 mixture of epimers at the cyano stereocenter.

The cascade cyclization starts with the abstraction of bromide by Bu₃Sn• from **1.59** to give radical **1.61**. This radical then undergoes a *5-exo dig* followed by a *5-exo trig* cyclization to give bicycle **1.62**. Homoallylic radical **1.62** then reacts intermolecularly with acrylonitrile to give stabilized radical **1.63**. The cascade continues with a *5-exo trig* followed by a *5-exo dig* cyclization onto the pendant alkyne to give tetracyclic compound **1.64**. The sequence is completed by a 1,5-hydrogen atom transfer and subsequent β elimination of the sulfone to give a single *cis-anti-cis* triquinane **1.60**. The diastereoselectivity of this cascade is controlled by the formation of the oxasilolane ring in the first cyclization. While the selectivity in this cascade is impressive, the synthesis of precursor **1.59** is somewhat lengthy.



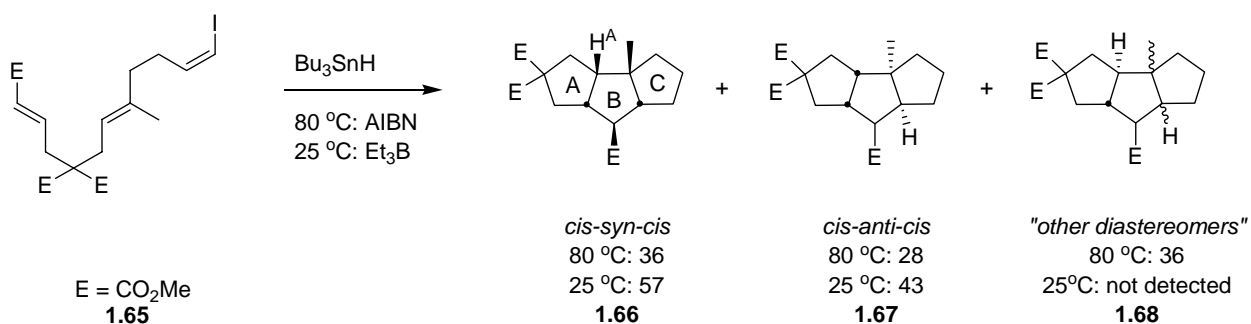
Scheme 1-10: Malacria's diastereoselective synthesis of a *cis-anti-cis* triquinane.

1.4.3 Temperature Effects in the Synthesis of Linear Triquinanes

The examples presented above expose the crux of linear triquinane synthesis from acyclic precursors. If the precursor is easy to synthesize, then it does not cyclize diastereoselectively. On the other hand, if the cyclization is diastereoselective then the precursor is difficult to prepare. Controlling the diastereoselectivity of simple acyclic precursors is therefore particularly attractive, but also challenging because the stereochemical issues must be addressed by control of the reaction conditions.

In 2001, Ihara and co-workers³⁸ reported that reaction temperature had a dramatic effect on the diastereoselectivity of a round-trip cascade radical cyclization as shown in Scheme 1-11. Cyclization of vinyl iodide **1.65** under standard AIBN and Bu_3SnH conditions at 80 °C resulted

in a mixture of the *cis-syn-cis* tricycle **1.66**, the *cis-anti-cis* tricycle **1.67**, and “other diastereomers” in a ratio of 36/28/36. Intriguingly, when the reaction was run at 25 °C using Et₃B/O₂ as the initiator, the “other diastereomers” **1.68** were not detected and the cyclization only provided tricycles **1.66** and **1.67** in a 57/43 ratio. The nomenclature of these isomers is either *cis* or *trans* depending on the A/B ring fusion and *syn* or *anti* based on the relationship between the methyl group and H^A. The final *cis* or *trans* is determined by the geometry of the of the B/C ring fusion.



Scheme 1-11: Temperature dependent cyclization of vinyl iodide **1.65**.

In this report, the structure of the *cis-syn-cis* isomer was fully assigned, but the configuration of the ester-bearing stereocenter in triquinane **1.67** was not. There was also no discussion of the identity of the “other diastereomers” **1.68**. We considered two possibilities for the “other diastereomers.” They might be the epimers at the ester stereocenter of tricycles **1.66** and **1.67** or by analogy to the cyclization of iodide **1.49**, they could be the *trans* isomers at the A/B ring junction as shown for **1.68**. These *trans* isomers would arise in the second of the three cyclizations and the corresponding hexenyl radical is shown in Figure 1-7. If the other diastereomers are indeed the *trans* cyclization products, this report implies that radical **1.69** cyclizes with a 64/37 *cis/trans* selectivity at 80 °C. This selectivity, however, improves to 100/0 when the cyclization is carried out at 25 °C as shown in Figure 1-7. To better understand this selectivity we compared the cyclization of Ihara’s hexenyl radical **1.69** to the second hexenyl radical **1.51** from Curran and Sun’s round-trip cyclization of iodide **1.49**. The cyclization of **1.49** was never run at 25 °C, but we see that the selectivity for both of these cyclizations at 80 °C is about 68/32 *cis/trans*.

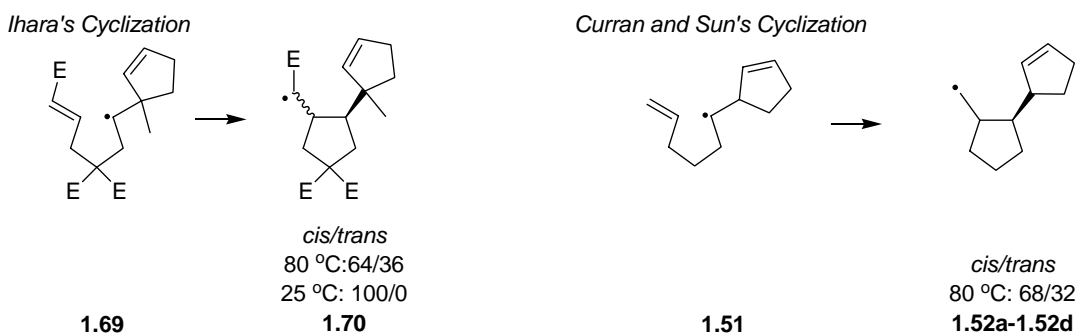


Figure 1-7: Comparison of the key hexenyl radicals from the second cyclization.

Direct comparison of these two results is difficult because the hexenyl radicals **1.51** and **1.69** are materially different in three ways, all of which could affect the selectivity of the key second cyclization. First, the 1-substituent of radical **1.69** is tertiary whereas in radical **1.51**, it is secondary. Second, hexenyl radical **1.69** has a geminal ester substitution in the 3 position where **1.51** only has two hydrogens. Third, the acceptor olefin in **1.69** is an α,β -unsaturated ester whereas in **1.51** it is terminal. While the combined effects of all of these differences is hard to predict, there are a number of literature benchmarks that provide some indication as to what the individual effects might be, as shown in Figure 1-8.

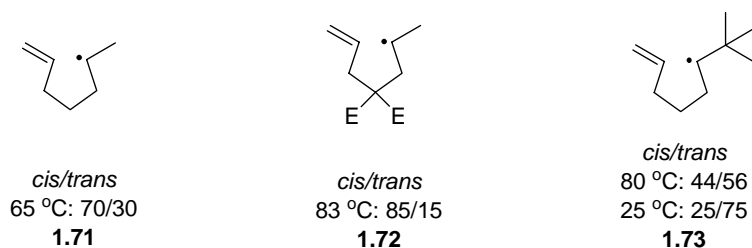
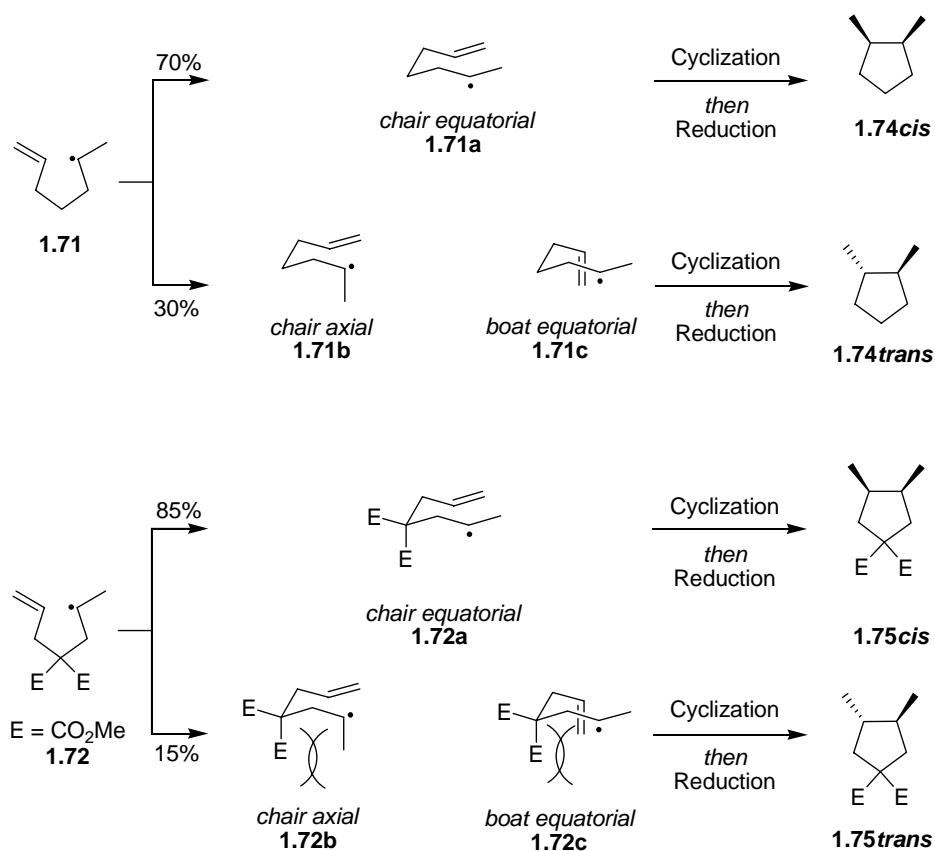


Figure 1-8: Literature benchmarks for related hexenyl radical cyclizations.

The results from the cyclization of **1.71** and **1.72** show that by placing a geminal ester group in the 3 position of the hexenyl radical the *cis* selectivity improves from 70/30 to 85/15 *cis/trans*. In hexenyl radical cyclizations, malonates are well known to not only accelerate the reaction by virtue of the Thorpe-Ingold effect,³⁹ but also to improve the *cis* selectivity.⁴⁰ The improvement to the selectivity can be nicely understood using the Beckwith-Houk transition state model, as shown in Scheme 1-12. Radical **1.71** can adopt three transition states: *chair-equatorial* **1.71a**, *chair-axial* **1.71b**, and *boat-equatorial* **1.71c**. A fourth *boat-axial* transition state (not shown) is also possible, but will be ignored because it is too high in energy to be a

significant contributor. If the cyclization goes through transition state **1.71a**, then the *cis* product **1.74cis** is formed upon reduction of the radical. If, however, the cyclization goes through transition states **1.71b** or **1.71c**, then the product **1.74trans** results upon reduction. For the cyclization of **1.71**, a 70/30 *cis* preference was observed, showing that transition state **1.71a** was favored over **1.71b** and **1.71c**.

For the cyclization of **1.72**, three analogous transition states are possible, **1.72a-c**, with **1.72a** leading to the *cis* product **1.75cis** and **1.72b/c** proceeding to **1.75trans**. The latter two transition states, however, are disfavored over **1.72a** because of the indicated diaxial interaction between the methyl group or the olefin and one of the esters in the 3 position. The 1,3 diaxial interactions that are caused by the introduction of the malonate group explains why the *cis* selectivity improves from 70/30 to 85/15 when comparing the cyclizations of **1.71** and **1.72**.



Scheme 1-12: Top: Transition state analysis for the cyclization of **1.71**. Bottom: Transition state analysis for the cyclization of **1.72**.

The cyclization of hexenyl radical **1.73** reported by Beckwith⁴¹ is an important benchmark because of the *t*-butyl group in the 1 position. The *t*-butyl group in **1.73** is comparable in size to the 1-(1-methylcyclopent-2-enyl) group from radical **1.69**. However, this benchmark hexenyl radical cyclizes with a *trans* preference. This is an exception to the rule because the *cis* selectivity of 1-substituted hexenyl radicals is one of the firmest stereochemical trends in radical cyclization reactions. Interestingly, the stereoselectivity for the cyclization of radical **1.73** also exhibits a dramatic temperature effect improving from 44/56 *cis/trans* at 80 °C to 24/76 at 25 °C. So Ihara and Beckwith's cyclizations both exhibit a dramatic temperature effect, but for the opposite stereoisomer! Given the presence of the malonate in Ihara's hexenyl radical, this result is not entirely inconceivable. Still it is striking that the selectivity in the cyclization of **1.73** could be completely overturned from *trans* to *cis* by the placement of the malonate group in the 3 position.

Finally, the α,β -unsaturated ester that is present in radical **1.69** will accelerate the rate of the cyclization,^{36a} but is not expected to affect the stereochemical outcome. This acceleration is due to the electron withdrawing effect of the ester making the olefin more electrophilic towards the radical.

1.5 Goals

In an attempt to unravel these puzzling temperature and substituent effects, we wanted to extend the number of benchmark substrates to more accurately represent the hexenyl radical for the second cyclization in Ihara's cascade. We also wanted to gain more insight into Ihara's cyclization by getting a better idea of what the "other diastereomers" are. These endeavors are intended to provide a more comprehensive understanding of how very large substituents in the 1 position affect the stereoselectivity in hexenyl radical cyclizations, both alone and in combination with other substituents.

Chapter 2 Stereochemistry of Hexenyl Radical Cyclizations with *tert*-Butyl and Related Large Groups in the 1 Position

To assess the stereochemical outcome of a 3,3 geminally di-substituted hexenyl radical cyclization with a large group in the 1 position, we choose to study the four radicals shown in Figure 2-1. These four radicals serve to extend the number of benchmarks needed to better understand Ihara's cyclization results. Hexenyl radicals **2.1** and **2.2a**, are benchmarks to determine the effect of an α,β -unsaturated ester on the cyclization and radical **2.2b** serves as a relay between the products of the previous two cyclizations for a rigorous assignment of configuration. Radical **2.3** is structurally very close to Ihara's system; it only lacks an olefin in the cyclopentane ring, preventing the round-trip cascade from being completed. However, this modification greatly simplifies product analysis because only two products, *cis* and *trans* cyclopentane isomers, are now possible.

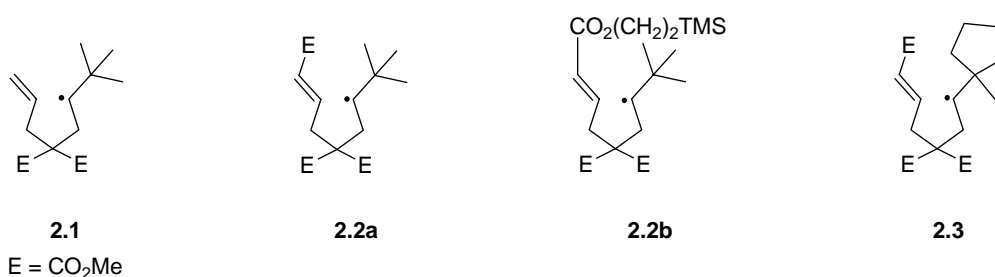
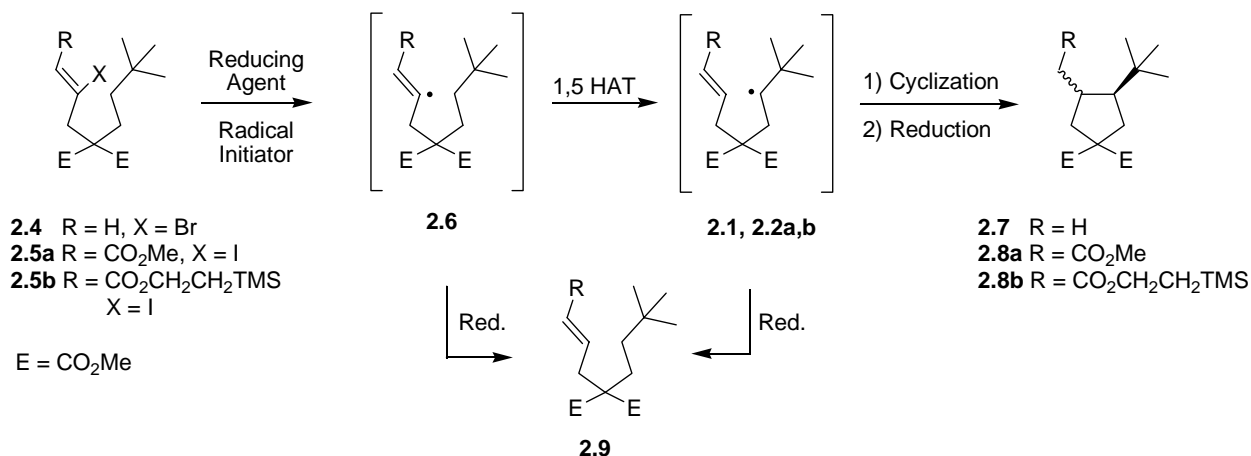


Figure 2-1: New cyclization benchmarks.

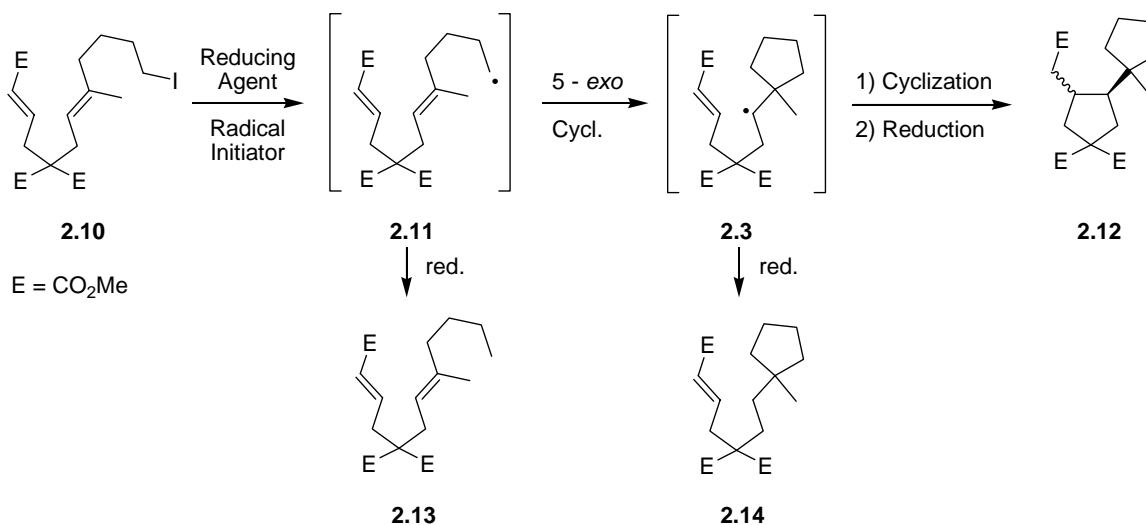
2.1 Substrate Design and Synthesis

For convenience of precursor synthesis, we decided to generate radicals **2.1** and **2.2a,b** by a 1,5 hydrogen atom transfer (1,5 HAT), as shown in Scheme 2-1. Treatment of vinyl halides **2.4** and **2.5a,b** with a suitable reducing agent and radical initiator gives vinyl radicals **2.6**, which undergo a 1,5 HAT to give the hexenyl radicals of interest **2.1** and **2.2a,b**. These radicals, after cyclization and reduction, give cyclopentanes **2.7** and **2.8a,b** as mixtures of the *cis* and *trans* isomers. A potential side reaction for this cascade is the direct reduction of **2.1**, **2.2a,b**, or **2.6** to give **2.9**.

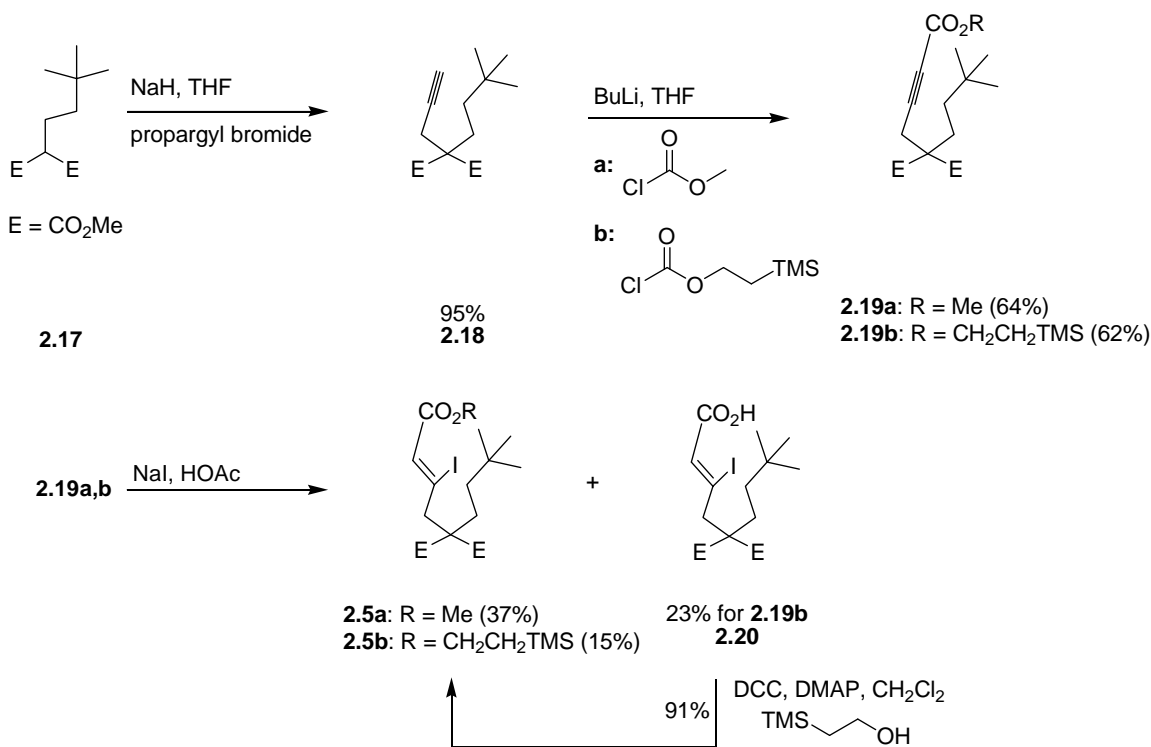


Scheme 2-1: Cyclization precursors and pathways for generation of radicals **2.1** and **2.2 a,b**.

For generation of hexenyl radical **2.3**, we relied on a cascade sequence starting from alkyl iodide **2.10**, as shown in Scheme 2-2. Radical **2.11**, formed by abstraction of iodine from **2.10**, cyclizes in a 5-*exo* fashion to give the desired hexenyl radical **2.3**. After cyclization and reduction, adduct **2.12** is formed as a mixture of *cis* and *trans* isomers. For this cascade, the prematurely reduced products are **2.13** and **2.14** arising from the reduction of **2.11** and **2.3**, respectively.



Scheme 2-2: Cyclization precursor and pathway for the generation of radical **2.3**.

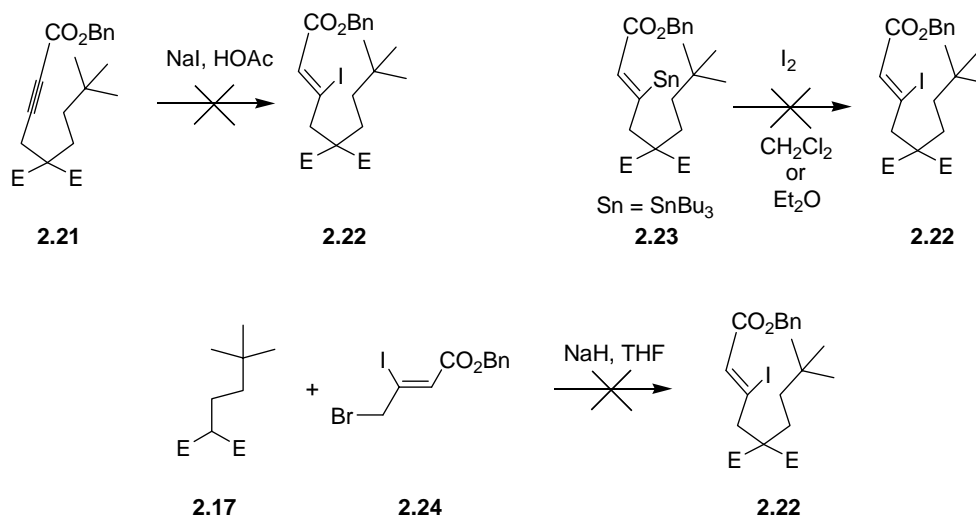


Scheme 2-4: Synthesis of cyclization precursors **2.5a,b**.

The low yield in the hydroiodination of alkyne **2.19b** to give **2.5b** is attributed to hydrolysis of the ethyl TMS ester functionality to give the corresponding acid **2.20**, which accounted for 23% of the material. Acid **2.20** could be isolated and recycled in a DCC-mediated coupling with 2-trimethylsilylethanol to give back **2.5b** in 91% yield.⁴⁷ The *Z*-stereochemistry of the final vinyl iodides was assigned based on literature precedent.⁴⁸ Regardless, the *Z* and *E* isomers give the same rapidly interconverting vinyl radical **2.6** upon treatment with AIBN and Bu₃SnH.⁴⁹

Initially we envisioned using a benzyl ester **2.22** instead of the ethyl TMS ester for the structural relay substrate. However, the synthesis of this precursor was unsuccessful despite a variety of approaches as shown in Scheme 2-5. Hydroiodination of alkyne **2.21** simply led to decomposition, presumably due to iodination at the benzylic position. Surprisingly the iododestannylation of **2.23** in either CH₂Cl₂ or Et₂O also failed, probably for the same reason. As a final approach, an alkylation of malonate **2.17** was attempted with allylic bromide **2.24**, but no desired compound **2.22** could be isolated. The most likely reason for the failure of this

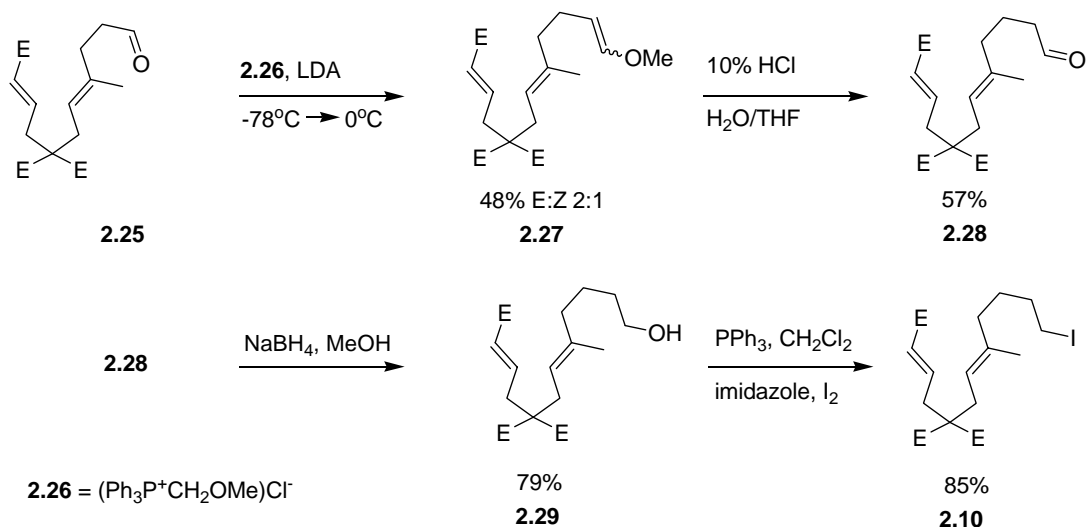
reaction is that either NaH or the malonate anion deprotonated one of the activated allylic protons of **2.24** before an S_N2 displacement of the bromide could occur.



Scheme 2-5: Attempted approaches towards relay precursor **2.22**.

2.1.3 Synthesis of Cyclization Precursor **2.10**

The synthesis of cyclization precursor **2.10** is outlined in Scheme 2-6. Treatment of aldehyde **2.25**, the synthesis of which is discussed in Chapter 3, with LDA and Wittig salt **2.26**⁵⁰ gave a 2:1 *E:Z* mixture of enol ether **2.27** in 48% yield. Stirring this enol ether in dilute hydrochloric acid quickly converted it to the homologated aldehyde **2.28** in 57% yield. Sodium borohydride reduction⁵¹ of aldehyde **2.28** gave alcohol **2.29** in 79% yield. Alcohol **2.29** was then converted to the corresponding iodide **2.10** in 85% yield by treating it with PPh₃, imidazole and I₂.⁵²

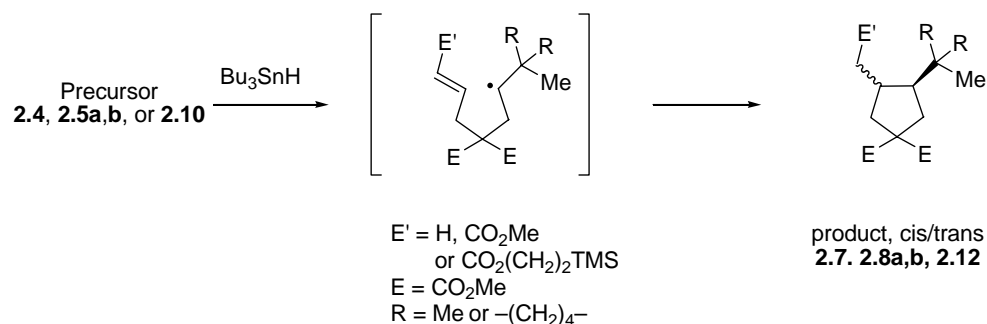


Scheme 2-6: Synthesis of iodide **2.10**.

2.2 Cyclization Results

The cyclizations of the benchmark substrates were all carried out under similar conditions and the results are summarized in Table 2-1. For reactions at 80 °C, the precursor (0.1 mmol) was dissolved in benzene (50 mL, 2 mM with respect to the precursor) and then AIBN (0.05 mmol) and Bu₃SnH (0.12 mmol) were added sequentially. The resulting solution was then refluxed for 4 h, cooled to room temperature and the solvent was removed *in vacuo*. The residue was purified by column chromatography over silica gel to remove the tin by-products and obtain an isolated yield. The mixture was then analyzed by NMR spectroscopy and GC to determine the ratio of *cis* and *trans* products. Both techniques gave very similar results, so only the GC ratio is recorded in the table. For the reactions run at 25 °C, the procedure was similar to the one described above, but the radical initiator was changed from AIBN to Et₃B/O₂. Furthermore, the initiator was the last component to be added to the reaction mixture.

The data in Table 2-1 show that, all four of the precursors exhibit a modest *cis* preference (78/22) when cyclized at 80 °C (entries 2, 4, 6 and 8). The *cis* preference of the cyclization improves marginally to 81/19 when the reaction temperature is lowered to 25 °C (entries 3, 5 and 7). In the reaction of vinyl bromide **2.4** at room temperature, entry 1, all of the starting material was recovered indicating that chain propagation failed under these conditions.

Table 2-1: Cyclization data for precursors **2.4**, **2.5a,b** and **2.9**.

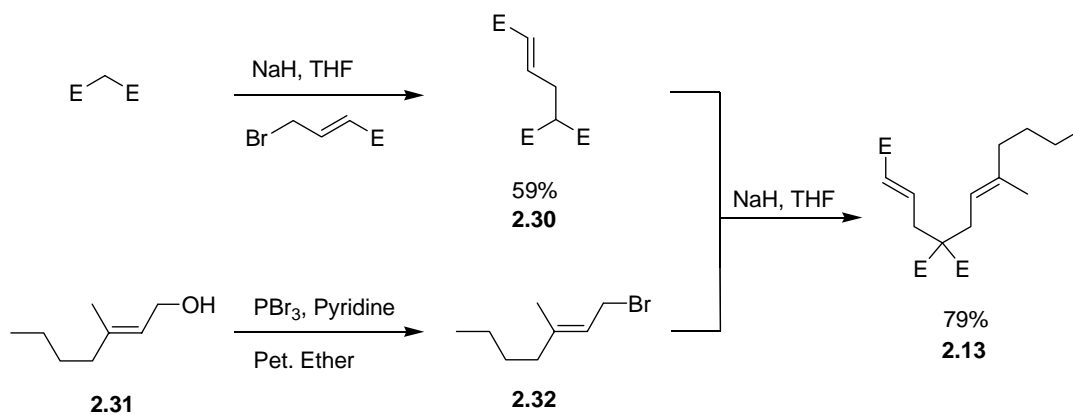
Entry	Precursor	R	E'	Cyclization Method ^a	T (°C)	Product	Selectivity <i>cis/trans</i> ^b	Yield ^c (%)
1	2.4	Me	H	A	25	2.7	-	-
2	2.4	Me	H	B	80	2.7	75/25	50%
3	2.5a	Me	CO ₂ Me	A	25	2.8a	83/17	45%
4	2.5a	Me	CO ₂ Me	B	80	2.8a	78/22	52%
5	2.5b	Me	CO ₂ (CH ₂) ₂ TMS	A	25	2.8b	79/21	35%
6	2.5b	Me	CO ₂ (CH ₂) ₂ TMS	B	80	2.8b	77/23	67%
7	2.9	(CH ₂) ₄	CO ₂ Me	A	25	2.12	81/19	62%
8	2.9	(CH ₂) ₄	CO ₂ Me	B	80	2.12	80/20	60%

^a Initiation at 80 °C with AIBN and at 25 °C with Et₃B/O₂ see chapter 5 for details.

^b Raw GC ratio

^c Isolated yield of a *cis/trans* mixture after flash chromatography

In all of the cyclizations with precursors **2.4** and **2.5a,b**, entries 2-6, prematurely reduced product **2.9** was not observed by GC or NMR. However, in the cyclization of iodide **2.10** about 5% of the crude reaction mixture was directly reduced product **2.13**. This was verified by an independent synthesis of compound **2.13**, as shown in Scheme 2-7, and subsequent GC co-injection with the crude cyclization mixture. Synthesis of the authentic sample of **2.13** started with the deprotonation of dimethyl malonate with sodium hydride and alkylation of the resulting anion with *E*-methyl-4-bromocrotonate to give malonate **2.30** in 59% yield. The next step was to treat known allylic alcohol **2.31**⁵³ with PBr₃ to give allylic bromide **2.32**.⁵⁴ The final step was deprotonation of malonate **2.30** with NaH in THF and quenching of the anion with bromide **2.32**, to give malonate **2.13** in 79% yield.



Scheme 2-7: Independent synthesis of directly reduced product **2.13**.

2.3 Configuration Assignment of the Cyclization Products **2.7**, **2.8a,b** and **2.12**

A key aspect of this work is to unequivocally establish the configuration of the cycloadducts. Unfortunately, we were not able to preparatively separate any of the *cis* and *trans* isomers of **2.7**, **2.8a,b** or **2.12** by column chromatography or HPLC. This led us to pursue a threefold approach to assigning the configuration of the cyclopentanes: 1) 1D NOE analysis of the cyclization mixtures, 2) synthesis of an authentic sample of **2.7trans**, and 3) rigorous assignment of configuration by x-ray diffraction analysis.

2.3.1 1D NOE Analysis Approach to Configurational Assignment

After extensive 1D and 2D NMR analysis of each product mixture **2.7**, **2.8a,b** and **2.12**, it was possible to assign all of the resonances for the major isomer in the ^1H NMR spectrum. With these assignments, a series of 1D NOE experiments were carried out and the key enhancements indicated in Figure 2-2 were observed. For product mixtures **2.8a,b** and **2.12**, the NOE enhancement between the two methine protons led us to tentatively assign the major product from each mixture as the *cis* isomer. Unfortunately, for product **2.7** protons H^{A} and H^{B} are accidentally chemical shift equivalent, making NOE analysis impossible. Additionally, in product **2.7** we observed an NOE enhancement between the methyl group and proton H^{C} . This was unexpected for the *cis* isomer, leading us to conclude that NOE analysis was not a reliable method for assigning the configuration of such compounds anyway.

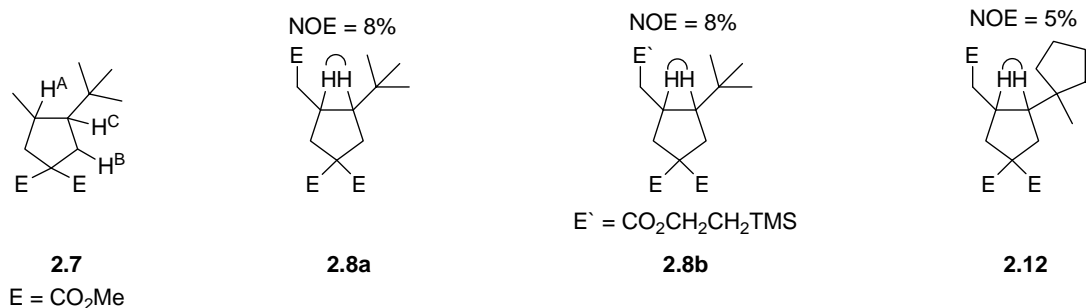
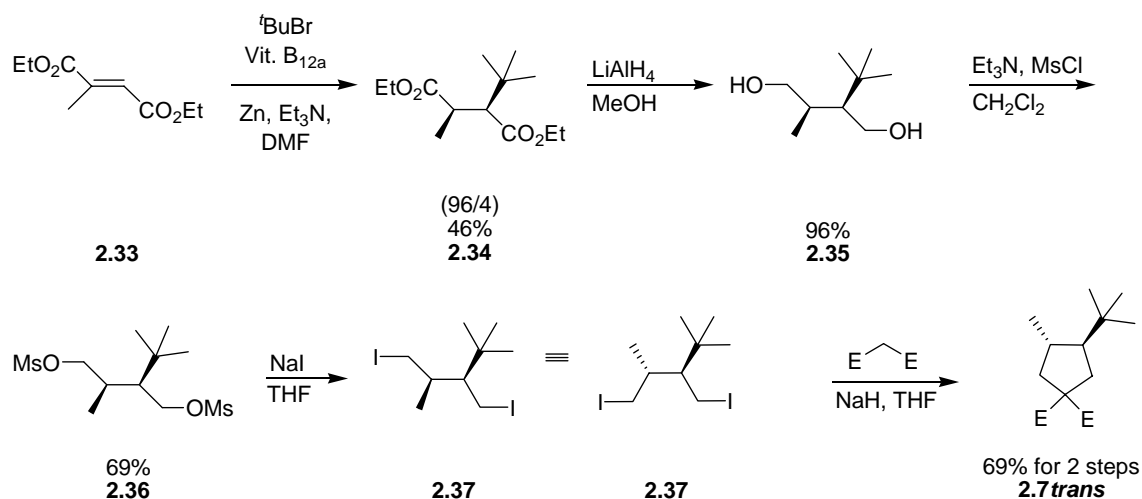


Figure 2-2: NOE analysis of the four product mixtures **2.7**, **2.8a,b** and **2.12**,

2.3.2 Configuration Assignment by Synthesis of an Authentic Sample

For rigorous structural assignment, we synthesized an authentic sample of **2.7trans** by the pathway shown in Scheme 2-8. Starting from diethyl mesaconoate **2.33**,⁵⁵ a vitamin B_{12a} mediated reduction gave *tert*-butyl compound **2.34** as a 96/4 *syn/anti* mixture of diastereomers in 46% yield.⁵⁶ Subsequent LiAlH₄ reduction of the diester gave diol **2.35** in 96% yield as a single diastereomer after chromatography.⁵⁷ Mesylation of the diol gave *bis*-mesylated compound **2.36** in 69% yield. By treatment of the *bis*-mesylate with NaI, the *bis*-iodide **2.37** was obtained. This was used immediately in the alkylation of the dimethylmalonate anion to give **2.7trans** in 69% yield as a single isomer, free of any **2.7cis**.⁵⁸



Scheme 2-8: Synthesis of **2.7trans**.

With authentic **2.7trans** in hand, we were able to verify that the major product from the cyclization of **2.4** has the *cis* configuration by a series of GC injections. Figure 2-3a shows the GC trace when **2.7trans** is injected in pure form. Figure 2-3b is the trace obtained when the cyclization mixture **2.7** is injected, and finally Figure 2-3c is a co-injection of **2.7trans** and mixture **2.7**. These results show that the *trans* isomer is indeed the minor component of the cyclization.

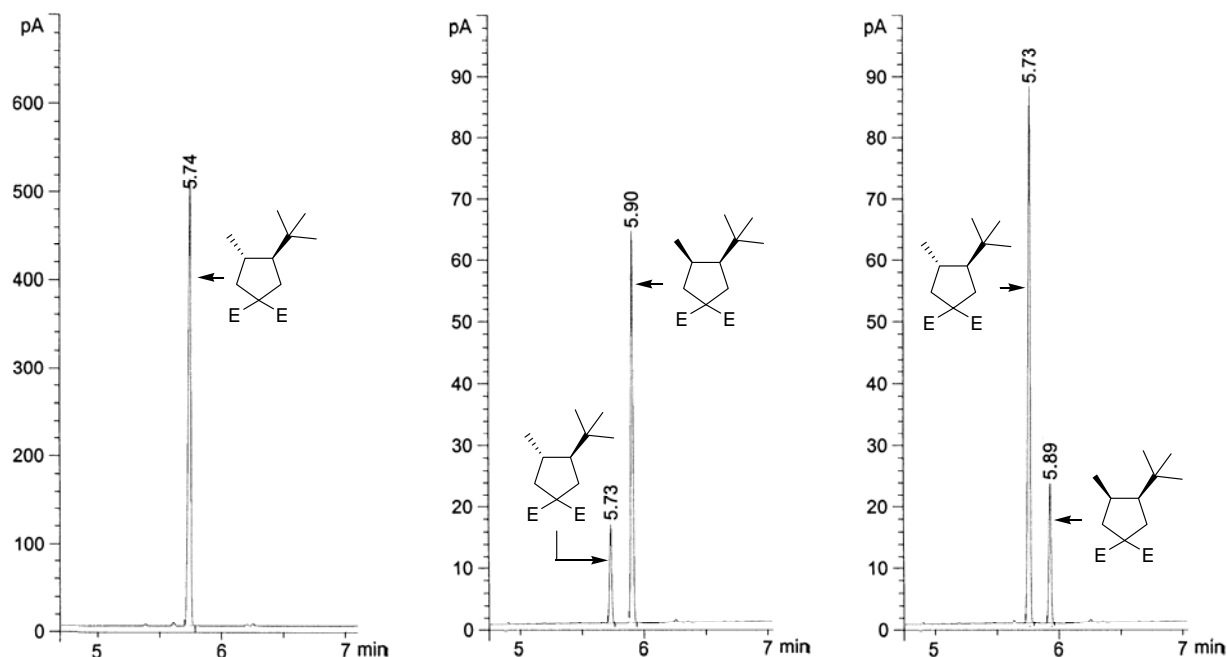
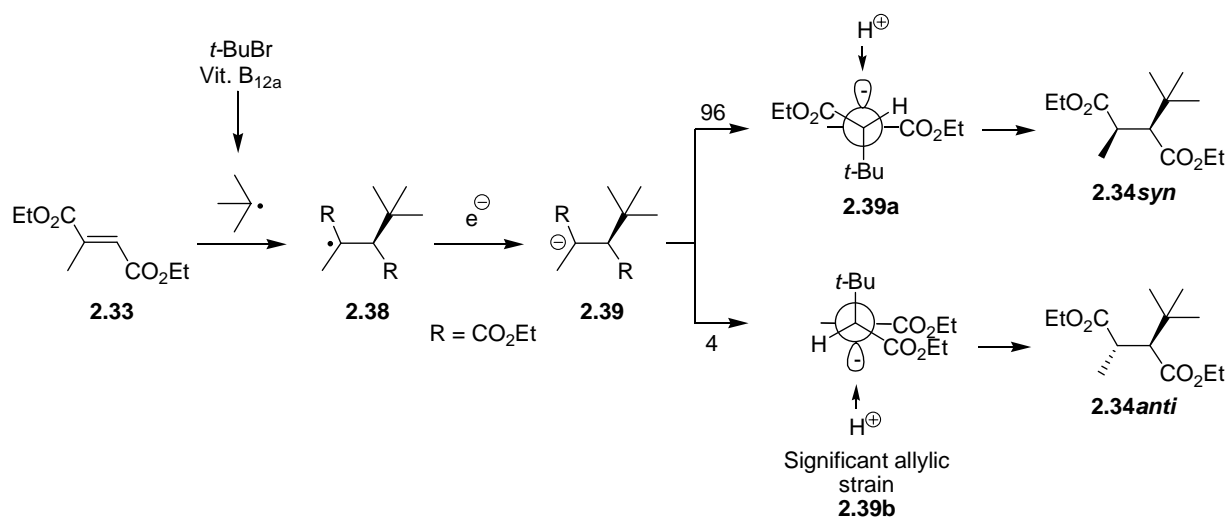


Figure 2-3: a) Left: injection of authentic **2.7trans**, b) Middle: injection of **2.7** from the cyclization of **2.4** and c) Right: co-injection of the two. All three GC injections were performed on an Agilent 6850 gas chromatograph equipped with an HP-1 column: dimethylpolysiloxane, 30m x 0.32mm, and a 0.25 μm film thickness. The initial temperature of 100 $^{\circ}\text{C}$ was then increased by 10 $^{\circ}\text{C}/\text{min}$ to 250 $^{\circ}\text{C}$ and then by 15 $^{\circ}\text{C}/\text{min}$ to 315 $^{\circ}\text{C}$.

The stereoselectivity in the addition of *tert*-butyl bromide to diethyl mesaconoate **2.33** in the synthesis of compound **2.34** is dictated by the minimization of $A^{1,3}$ strain as shown in Scheme 2-9. A *tert*-butyl radical, generated from *tert*-butyl bromide and vitamin B12_a, adds into diethylmesaconoate **2.33** at the less substituted carbon to give radical **2.38**. Radical **2.38** is then reduced by the zinc metal to give anion **2.39**. Upon aqueous workup, the protonation of anion **2.39** must occur from the face opposite to the large *tert*-butyl group, which can be achieved by the two conformations shown in either **2.39a** or **2.39b**. If configuration **2.39a** is favored then the *syn* diester **2.34syn** is formed upon protonation. If however, the protonation occurs to anion

2.39b, the *anti* diester **2.34anti** results. The orientation depicted in **2.39b**, however, is greatly disfavored because of the allylic strain that is introduced between the two ester groups. In **2.39a** this allylic strain is not present. This difference in strain between **2.39a** and **2.39b** explains the observed 96/4 ratio of *syn/anti* adducts.

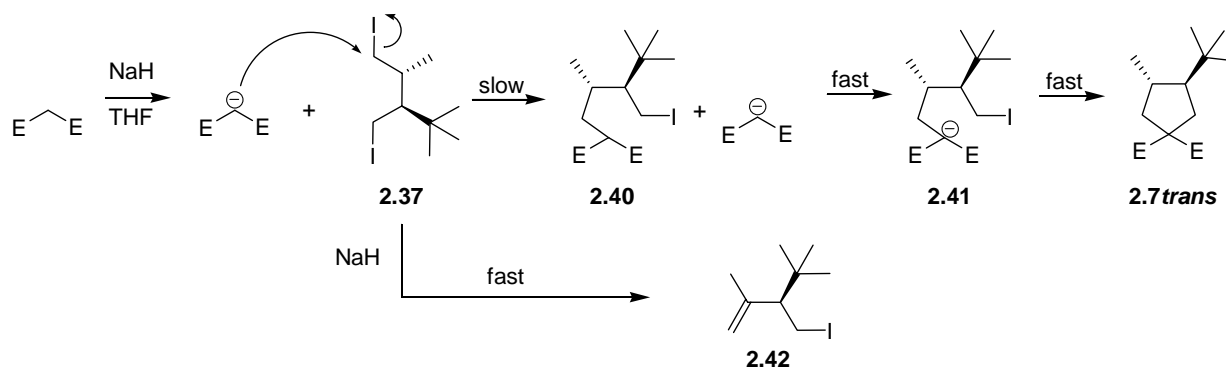


Scheme 2-9: Stereoselectivity in the radical addition of *tert*-butylbromide to diethylmesaconoate **2.33**.

The *bis*-alkylation of dimethyl malonate with *bis*-iodide **2.37** was an interesting reaction because of an unexpected observation. When dimethylmalonate was treated with 1 equiv of NaH followed by the addition of *bis*-iodide **2.37** and the resulting mixture was stirred, we observed a 1/1 mixture of starting iodide **2.37** and product malonate **2.7trans**. Adding more NaH at this point simply lead to the decomposition of iodo compound **2.37** without producing any additional product **2.7trans**. However, if more dimethylmalonate anion was added, the iodide was smoothly consumed, pushing the reaction to completion.

Based on these observations, we propose a mechanism for this double alkylation reaction shown in Scheme 2-10. The first alkylation of dimethylmalonate anion by iodide **2.37** to give malonate **2.40** is the rate determining step. Once intermediate **2.40** has been formed, it reacts with another equivalent of dimethylmalonate anion to give intermediate **2.41**. Anion **2.41** rapidly undergoes the second alkylation step to give **2.7trans**. By invoking the malonate anion as the base in the second deprotonation, we can explain why a 1/1 mixture of starting material to product was initially observed even though only 1 equiv of NaH had been added. Using the malonate base for the second deprotonation is further supported by the observation that more

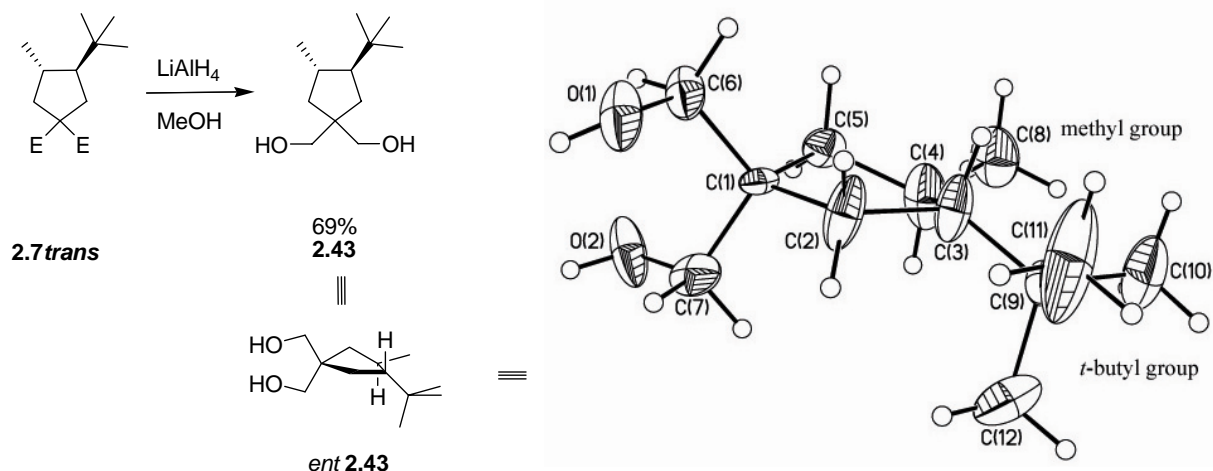
malonate anion drives the reaction to completion. That additional NaH is detrimental to the reaction is explained by the elimination of HI from **2.37** to give **2.42** being faster than the first alkylation of the anion. Fortunately the malonate anion is not a strong enough base to effect this elimination.



Scheme 2-10: Proposed mechanism for the bis alkylation reaction of dimethyl malonate.

2.3.3 Configuration Assignment by X-Ray Crystallography

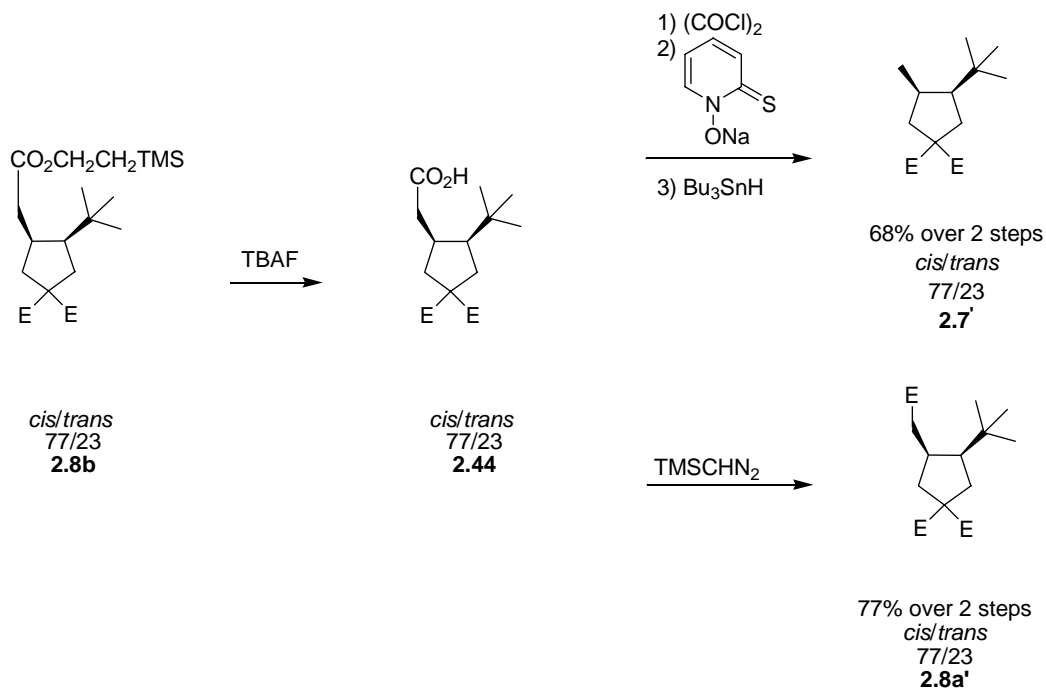
The GC analysis in Chapter 2.3.2 relies on the product of the vitamin B12_a mediated reduction being compound **2.34_{syn}**, Scheme 2-8. So as definitive proof that the minor component in the cyclization of **2.4** is indeed cyclopentane **2.7_{trans}**, we treated pure **2.7_{trans}** with LiAlH₄ to give diol **2.36** in 69% yield as a white solid. By slow vapor phase diffusion of hexanes into a solution of diol **2.43** in ethyl acetate, a single crystal was grown and the x-ray structure solved as shown in Scheme 2-11. With this crystal structure, we are able to unambiguously assign the stereochemical preference for the cyclization of **2.1** as *cis*.



Scheme 2-11: Synthesis and ORTEP diagram of diol **2.43**.

2.4 Stereochemical Relay from Product Mixture **2.7** to **2.8a** and **2.8b**

With the major product of mixture **2.7** firmly assigned as *cis*, we relayed this assignment to the methyl ester product mixture **2.8a** through the TMS ethyl ester mixture **2.8b** as shown in Scheme 2-12. Desilylation⁵⁹ of a 77/23 *cis/trans* mixture of **2.8b** with TBAF gave acid **2.44**. The acid was then split with a portion being treated with oxallyl chloride to give the corresponding acid chloride. The crude acid chloride was treated with 2-mercaptopyridine N-oxide sodium salt to provide the corresponding Barton ester. Finally a Bu_3SnH mediated Barton decarboxylation gave a 77/23 *cis/trans* mixture of **2.7'** in 68% yield from **2.8b**. The other portion of acid **2.44** was treated with (trimethylsilyl)diazomethane⁶⁰ to give a 77/23 *cis/trans* mixture of **2.8a'** in 77% yield over the two steps. Comparative GC analysis of **2.7** with **2.7'**, Figure 2-4a and b, and **2.8a** with **2.8a'**, Figure 2-4c and d, showed that in each case the major and the minor products had identical retention times. This proves that precursors **2.4** and **2.5a,b** all cyclize to give the *cis* adducts as the major products. By analogy, we concluded that the bicyclic system **2.3** also cyclizes with a *cis* preference.



Scheme 2-12: Stereochemical relay between the three cyclization mixtures.

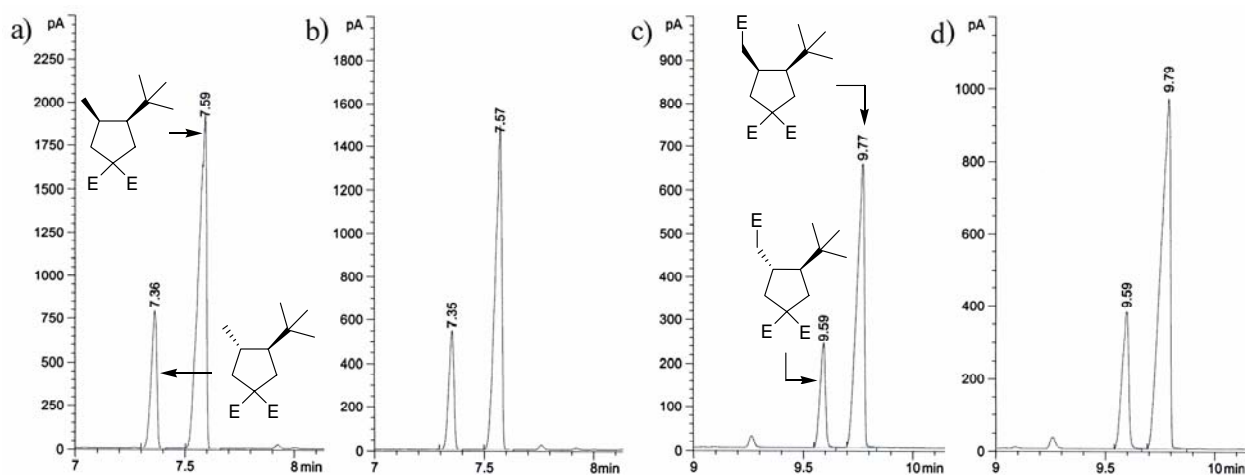


Figure 2-4: a) GC chromatogram of the decarboxylation products **2.7'**, b) GC chromatogram from a co-injection of the cyclization mixture of **2.7** and the decarboxylated products **2.7'**, c) GC chromatogram of the transesterified products **2.8a'**, and d) GC chromatogram from a co-injection of the cyclization mixture **2.8a** and the transesterified products **2.8a'**. All four of the GC injections were performed under the same conditions as described for Figure 2-3.

2.5 Structural Correlation to Beckwith's Work

Comparing the results from the cyclization of **2.4** (*cis* selective) to those of the parent 1-*t*-butyl hexenyl radical **2.48** (*trans* selective), Figure 1-8 and Scheme 2-13, suggests that the

malonate group in the 3 position reverses the stereochemistry of the cyclization. This in itself is not inconsistent with the literature because malonates in the 3 position of a hexenyl radical are known to favor *cis* cyclization. However, a comparison of our spectral data to that of the products from the original cyclization of **1.73**, Figure 2-5, was disconcerting because the resonances assigned to **2.45cis** correlated with those of **2.7trans** and the data for **2.45trans** matched that of compound **2.7cis**. This lack of pattern matching forced us to consider that Beckwith's assignments for cyclopentanes **2.45** may be reversed.

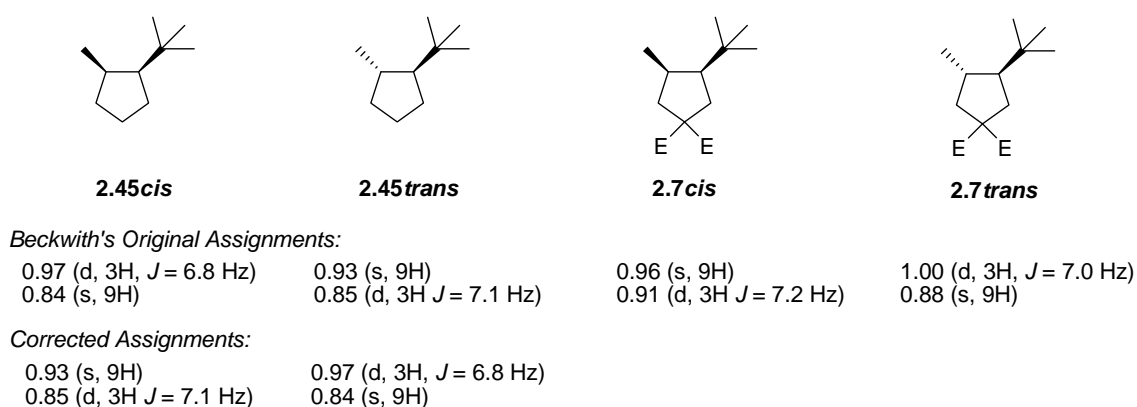
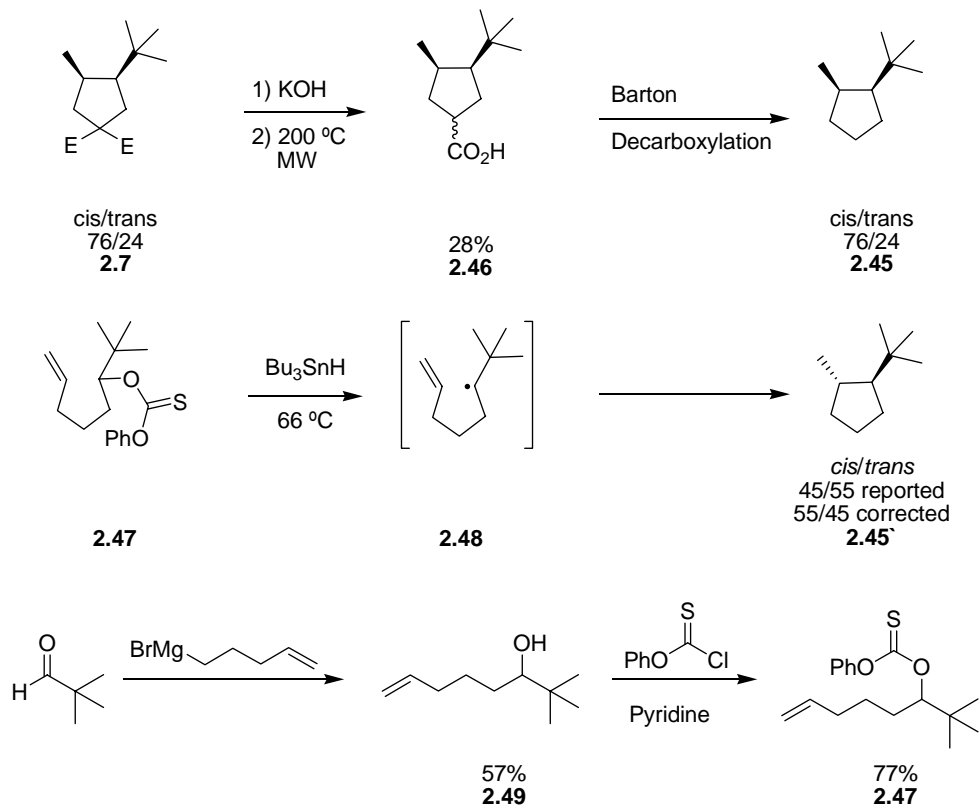


Figure 2-5: Comparison of selected ¹H NMR spectral data for **2.45** and **2.7**.

To resolve this discrepancy, we converted product mixture **2.7** to mixture **2.45** by the sequence outlined in Scheme 2-13. Treatment of a 76/24 *cis/trans* mixture of malonate **2.7** in refluxing potassium hydroxide hydrolyzed the malonic ester to a malonic acid (not shown).⁶¹ The malonic acid was subjected to a microwave mediated decarboxylation⁶² to give mono acid **2.46** in 28% isolated yield over the two steps. This mixture of products was then fully decarboxylated by using a Barton decarboxylation to give a 76/24 *cis/trans* mixture of cyclopentane **2.45**, which was not isolated due to its volatility. For direct comparison, we simultaneously synthesized known compound **2.47**, which upon treatment with AIBN and Bu₃SnH gives hexenyl radical **2.48**. This radical, then cyclizes to give a 45/55 *cis/trans* mixture of cyclopentanes **2.45'**.

The synthesis of cyclization precursor **2.47** is also shown in Scheme 2-13 and starts with the addition of 4-pentenylmagnesium bromide to pivaldehyde to give alcohol **2.49** in 57% yield. The alcohol is then treated with pyridine and phenylchlorothionocarbonate to give precursor **2.47** in 77% yield.



Scheme 2-13: Direct comparison of our cyclization mixture with that of Beckwith's cyclization and synthesis of precursor **2.47**.

If Beckwith's assignments are correct, then the major product of **2.45** should be the minor product of **2.45'** and vice versa. Unfortunately, as shown by the GC chromatograms in Figure 2-6, this was not the case. The major and the minor products from the decarboxylation of **2.46** and the cyclization of **2.47** match with retention times of 6.10 and 6.71 min, respectively. This means that Beckwith's assignments for *cis* and *trans* **2.45** are backwards because the crystal structure confirms that our assignments are correct. How though could Beckwith have mis-assigned the *cis* and *trans* isomers?

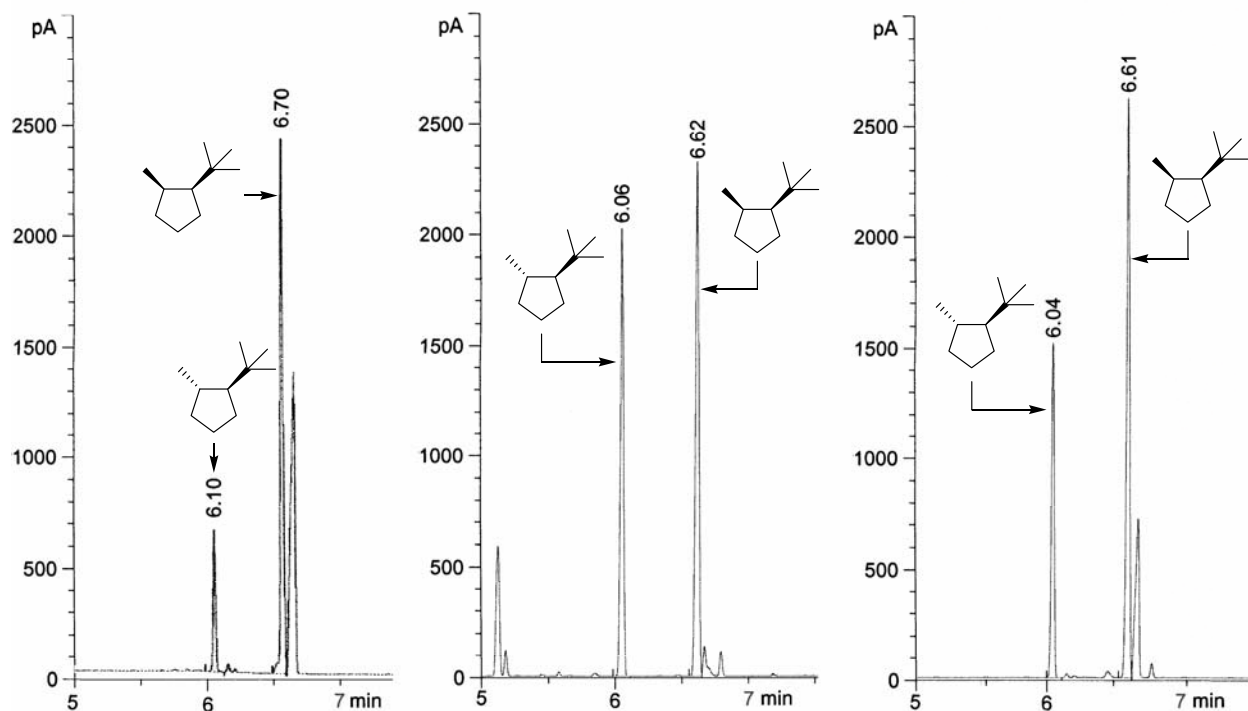


Figure 2-6: a) Left: GC injection of the decarboxylation mixture **2.45** and b) Middle: GC injection of the cyclization mixture **2.45'** and c) Right: co-injection of the two. All three GC injections were performed on an Agilent 6850 gas chromatograph equipped with an HP-1 column: dimethylpolysiloxane, 30m x 0.32mm, and a 0.25 μm film thickness. The temperature profile of the injection has an initial temperature of 30 $^{\circ}\text{C}$ which then increases by 10 $^{\circ}\text{C}/\text{min}$ to a final temperature of 315 $^{\circ}\text{C}$.

2.6 Revisiting Beckwith's Analysis

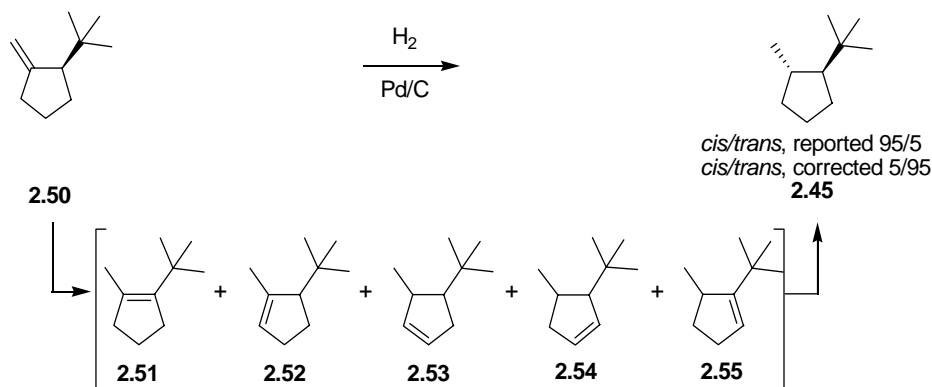
Beckwith assigned the *cis* and *trans* isomers of **2.45** by carrying out a palladium mediated catalytic hydrogenation of *exo*-methylene compound **2.50**, shown in Scheme 2-14. GC analysis of this reaction after 3 h revealed consumption of the starting material and the formation of two products in a 95/5 ratio. Beckwith assumed that hydrogenation occurred opposite to the bulky *tert*-butyl group giving the *cis* substituted cyclopentane as the major product. Molander and Winterfeld have also posited *cis* selectivities in related systems.⁶³ Beckwith was then able to separate the two products from the hydrogenation reaction by a preparative GC experiment. NOE analysis of the major product of the hydrogenation reaction showed a 10% enhancement of the *tert*-butyl singlet when the methyl doublet was irradiated. Beckwith took this enhancement as evidence that the major product was indeed the *cis* isomer of **2.45**. There was no discussion of an NOE analysis for the minor isomer. A likely reason for this is that the small chemical shift

difference of 0.08 ppm between the methyl doublet and the *tert*-butyl singlet of the minor product makes accurate NOE determinations difficult.

We know that Beckwith's assignments are backwards and so how is it that hydrogenation of compound **2.50** gives cyclopentane **2.45***trans* as the major product? Also, how is it possible for compound **2.45***trans* to exhibit such a large NOE enhancement? To answer these two questions, we repeated Beckwith's hydrogenation experiments on olefin **2.50**.

2.6.1 Hydrogenation Experiments

In the palladium on carbon mediated hydrogenation of compound **2.50**, we also observed the 5/95 ratio of products. So the literature ratio for the hydrogenation is correct, but the assumption of *cis* selectivity is not. When we closely monitored the hydrogenation reaction by GC, we observed rapid consumption of alkene **2.50** and the appearance of three product peaks. As will be shown later, these three peaks actually correspond to four products where two products accidentally have the same retention time. A representative GC chromatogram of the four product mixture is shown in Figure 2-7. Two of these products were immediately identified as the *cis* and *trans* isomers of **2.45**. The other two products were tentatively assigned as isomerized products **2.51** and **2.52**, because hindered double bonds are known to undergo palladium catalyzed isomerizations.⁶⁴ Upon continued hydrogenation, the two additional peaks disappeared and the 5/95 ratio of **2.45***cis/trans* resulted, as shown in the second GC chromatogram in Figure 2-7.



Scheme 2-14: Isomerization of exo-methylene compound **2.50** under the hydrogenation conditions.

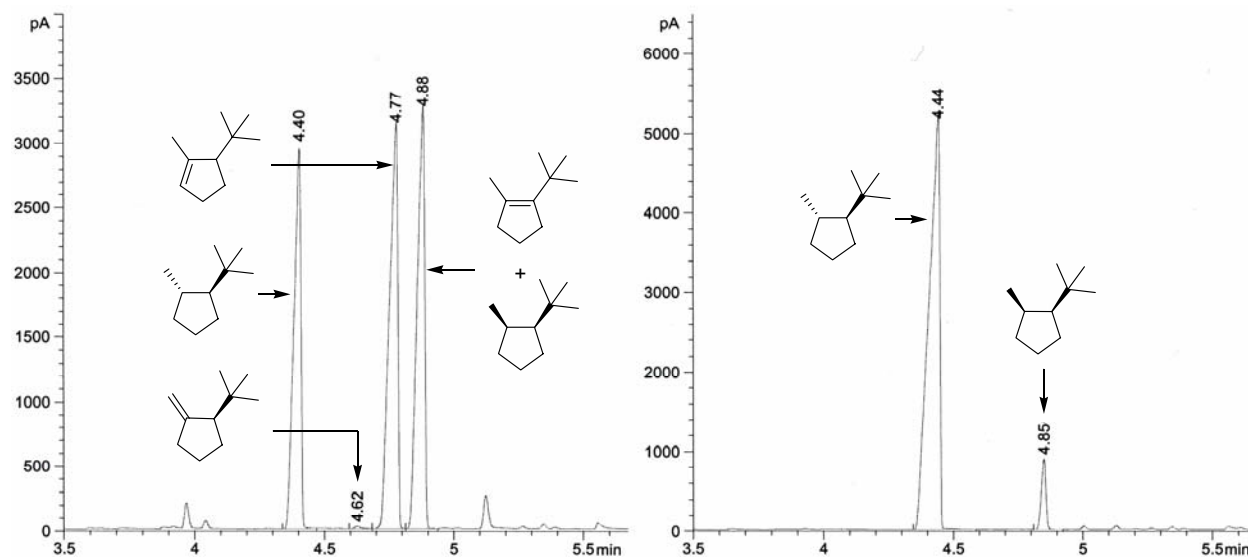
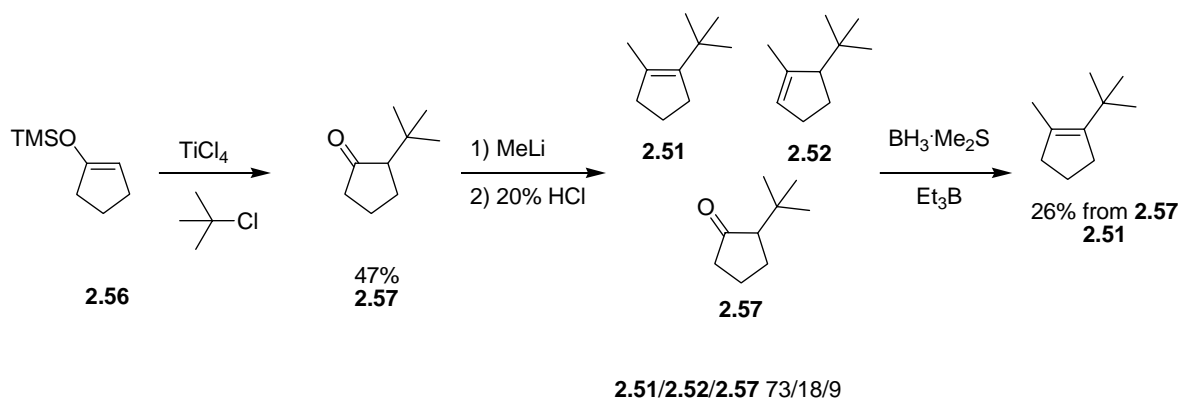


Figure 2-7: a) Left: GC chromatogram of the hydrogenation of **2.42** after 1 h and b) Right: GC chromatogram of the same hydrogenation after 3 h. Both of the GC injections were carried out under the same conditions as described for Figure 2-6.

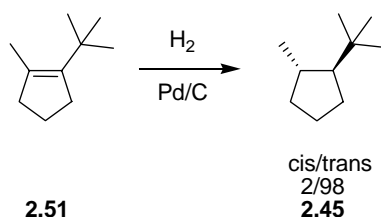
We were able to independently synthesize tetrasubstituted alkene **2.51** by the synthetic sequence shown in Scheme 2-15. The synthesis of **2.51** starts with the commercially available silyl enol ether **2.56**, that is treated with TiCl_4 and *tert*-butyl chloride to give ketone **2.57** in 47% yield.⁶⁵ The addition of MeLi to ketone **2.57** gives a tertiary alcohol (not shown). The alcohol is then eliminated using a 20% aqueous solution of HCl to give an inseparable 73/18/9 mixture of **2.51**, **2.52**, and **2.57**. Treatment of this mixture with $\text{BH}_3 \cdot \text{Me}_2\text{S}$ and Et_3B provided alkene **2.57** as a single product in 26% yield from ketone **2.57**.⁶⁶

Upon GC co-injection of the four compound mixture from the hydrogenation with authentically prepared alkene **2.51** we learned that the peak with a retention time of 4.88 min is compound **2.51**. Unfortunately, the retention times of alkene **2.51** and product **2.45_{cis}** are accidentally identical. By co-injecting the mixture containing **2.51**, **2.52**, and **2.57** with the four compound hydrogenation mixture, we were able to identify the peak at 4.77 min as coming from alkene **2.52** by a process of elimination.



Scheme 2-15: Synthesis of alkene **2.51**.

Interestingly, independent hydrogenation of **2.51**, Scheme 2-16, resulted in a 2/98 *cis/trans* mixture of **2.45**. Direct hydrogenation of cyclopentene **2.51** cannot possibly give **2.45trans** because such hydrogenations are well-known to be stereospecific for the *cis* isomer.⁶⁷ Taken together, all of the hydrogenation results suggest that **2.50** (exclusively), **2.51** (to a large extent) and possibly also **2.52** isomerize prior to hydrogenation and that the isomerization process determines the final *cis/trans* ratio. We speculate that disubstituted olefins **2.53** and **2.54**, resulting from further isomerizations of **2.51** and **2.52**, are the species actually undergoing the hydrogenation and that the *trans* selectivity is the result of a thermodynamically controlled isomerization. Regardless, compound **2.50** is not directly hydrogenated and so any assumptions about its *cis* hydrogenation selectivity, although probably correct, are certainly not relevant given the isomerization problem.



Scheme 2-16: Hydrogenation of tetrasubstituted alkene **2.45**.

We attempted to show that Beckwith's assumption of hydrogenation opposite to the *tert*-butyl group was actually correct. We screened a number of conditions that should not isomerize the *exo*-methylene compound **2.50** prior to hydrogenation and the results are summarized in

Table 2-2. Raney Nickel, entry 1, is reported⁶⁸ to isomerize olefins less than palladium, but significant isomerization products were observed in the GC chromatogram, all of which eventually disappeared to give a 4/96 *cis/trans* mixture of **2.45**. Hydrogenation over platinum, entry 3, is also reported⁶⁹ to significantly reduce the amount of isomerization and although we observed clean conversion of the starting material to the product, we still ended up with a 56/44 *cis/trans* mixture of the products. Finally a diimide reduction was attempted, entry 4, and while again no isomerization was observed an 84/16 *cis/trans* mixture was obtained.⁷⁰

Table 2-2: Reduction of **2.50** under various conditions.

Entry	Reducing Conditions	Selectivity (<i>cis/trans</i>)	Isomerization Intermediates in the GC?
1	Raney Nickel under H ₂	4/96	Yes
2	Pd/C under H ₂	5/95	Yes
3	Pt/C under H ₂	56/44	No
4	Hydrazine/CuSO ₄	84/16	No

The results from the platinum and the diimide reductions, entries 3 and 4, prove that the *trans* isomer can be obtained without the exocyclic olefin isomerizing into the ring. This indicates that both faces of the olefin in compound **2.50** are accessible enough to be hydrogenated. Furthermore the results from these two experiments support Beckwith's assumption that the *tert*-butyl group directs the hydrogenation to the opposite face because the *cis* isomer of **2.45** is the major product in these cases.

2.6.2 Explaining the NOE Analysis Results

The envelope conformations of compounds **2.45cis** and **2.45trans** are shown in Figure 2-8. These representations show that both the *cis* and the *trans* isomer have nominal syn pentane interactions that are known to give strong NOE enhancements.⁷¹ This explains why Beckwith observed the 10% NOE enhancement in the *tert*-butyl singlet when the methyl doublet was irradiated even though he was analyzing the *trans* isomer of **2.45**.

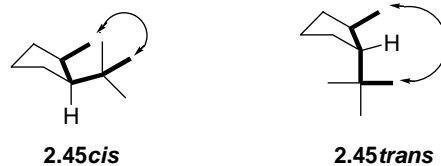
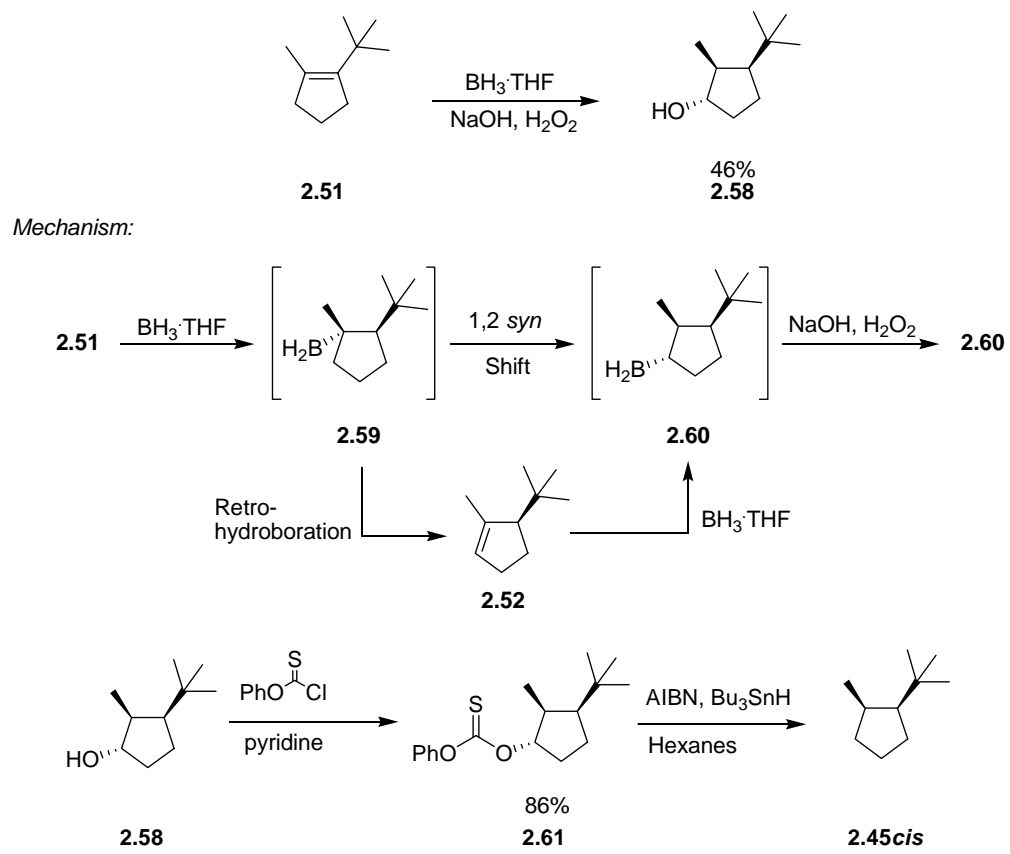


Figure 2-8: Nominal syn pentane interactions in **2.45cis** and *trans*.

2.7 Additional Verification of the Reversed *Cis/Trans* Assignment of **2.45**

As another way to show that Beckwith's assignments for the *cis* and *trans* isomers of **2.45** were backwards, alkene **2.51** was hydroborated to give alcohol **2.58** in 46% yield upon reductive workup, Scheme 2-19. Mechanistically, hydroboration of alkene **2.51** provides borane **2.59**. The regioselectivity of this addition is determined by the large *tert*-butyl group that drives the boron towards the less hindered carbon. Borane **2.59** then undergoes a 1,2 *syn* shift to give compound **2.60**. It is conceivable that borane **2.60** is not formed by this 1,2 *syn* shift, but rather that **2.59** undergoes a retro-hydroboration to give alkene **2.52** which is then hydroborated to give borane **2.59**. In any event intermediate **2.60** gives known alcohol **2.50** upon reductive workup with sodium hydroxide and hydrogen peroxide. We then converted alcohol **2.58** to thionoformate **2.61** in 86% yield. Barton-McCombie deoxygenation⁷² of **2.61** provides **2.45cis** as a single isomer. GC injection of a pure sample of **2.45cis** provides the GC trace shown in Figure 2-9a. Figure 2-9b shows the GC trace from the cyclization mixture **2.48** and finally Figure 2-9c is the GC trace from a co-injection of **2.45cis** from the deoxygenation reaction with the cyclization mixture from **2.47**. This series of injections proves that the major isomer in Beckwith's cyclization of **2.47** is indeed compound **2.45cis** and confirms that the original configurational assignments are reversed.



Scheme 2-17: Confirmation of Beckwith's reversed assignments.

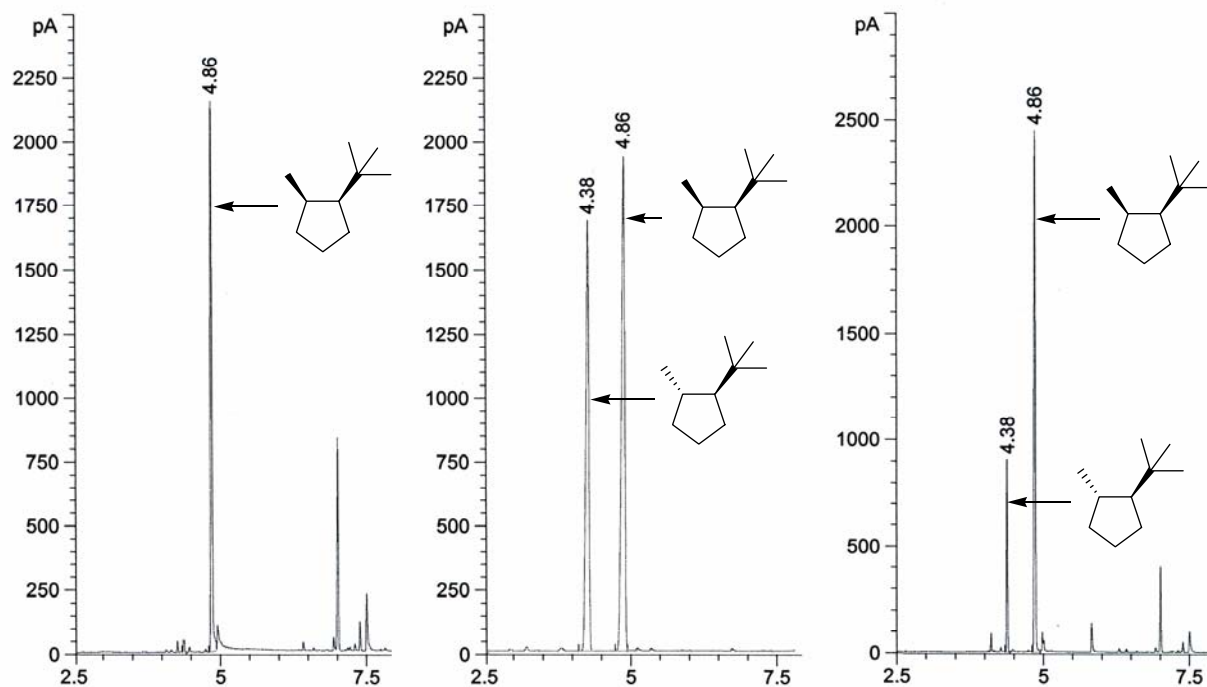
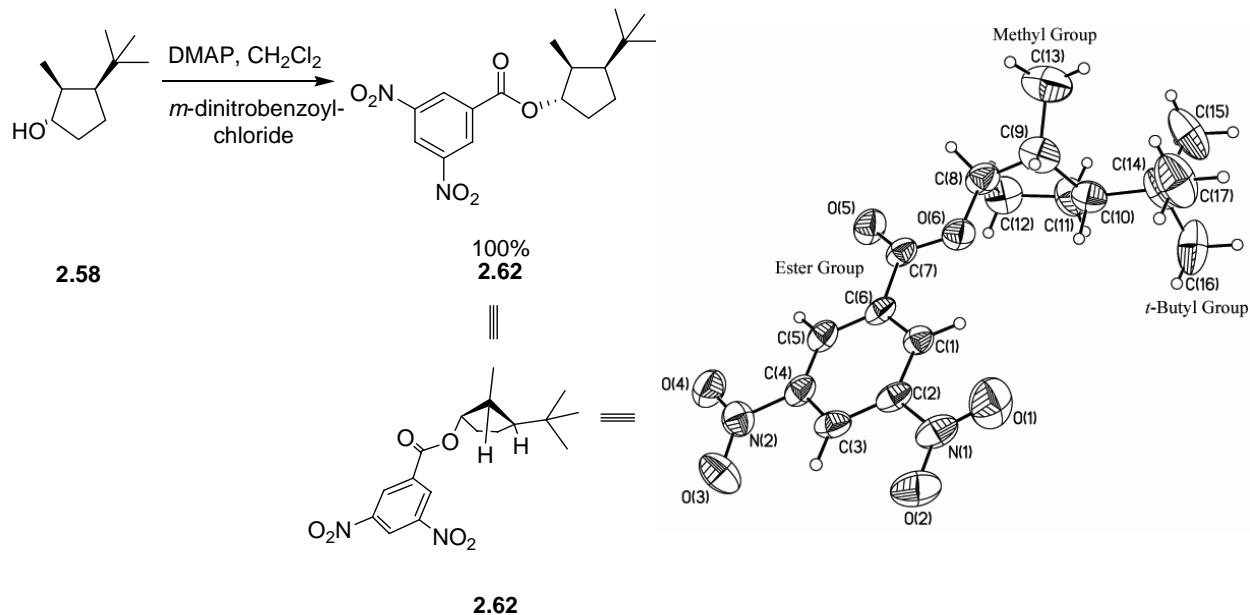


Figure 2-9: a) Left: **2.45** from the deoxygenation of **2.60**, b) Middle: Radical cyclization mixture **2.45** and c) Right: co-injection of a and b. All three of the GC injections were carried out under the same conditions as described for Figure 2-6.

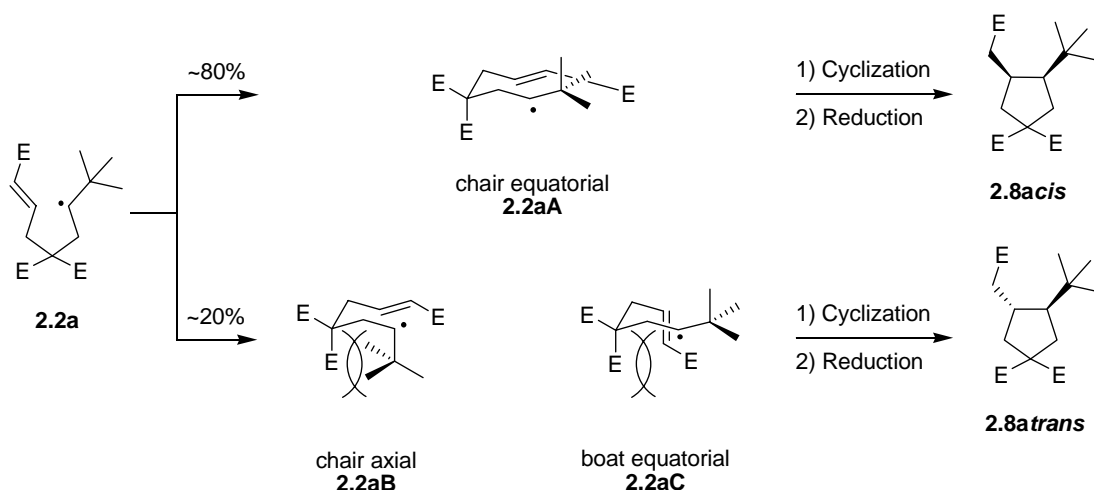
The above proof relies on Knochel's stereochemical assignment of **2.58**, which was made based on 1 and 2D NMR experiments. To verify the assignment of **2.58**, we derivatized the alcohol with *meta*-di-nitrobenzoyl chloride to give ester **2.62** in 100% yield, Scheme 2-18. A single crystal of **2.62** was grown by slow evaporation of a methanol solution and the x-ray diffraction pattern was solved to provide the ORTEP diagram shown in Scheme 2-18.



Scheme 2-18: Derivatization of alcohol **2.58** and ORTEP of cyclopentane **2.62**.

2.8 Transition State Analysis for the Cyclization of 2.2a

We have shown that hexenyl radicals with a large group in the 1 position and a geminal ester substitution in the 3 position cyclize with *cis* selectivity. This result can be nicely rationalized using a Beckwith/Houk transition state analysis as shown in Scheme 2-19. The analysis for radical **2.2a** is representative for all of the cyclizations examined in this work. Radical **2.2a** can adopt three low energy transition states, Scheme 2-19, namely *chair-equatorial 2.2aA*, *chair-axial 2.2aB*, and *boat-equatorial 2.2aC*. A fourth *boat-axial* transition state (not shown) is also possible, but will be ignored because it is too high in energy to be a significant contributor. If radical **2.2a** adopts the *chair-equatorial* transition state, then it will cyclize to give product **2.8a_{cis}** upon reduction. However, if radical **2.2a** cyclized through the *chair-axial* or *boat-equatorial* transition states, then **2.8a_{trans}** results upon reduction. The *chair-axial 2.2aB* and boat equatorial **2.2aC** transition states are disfavored in comparison to the *chair-equatorial 2.2aA* due to the diaxial interactions indicated in Scheme 2-19. These interactions explain the approximate 80/20 partitioning of the *cis/trans* products that we observe.



Scheme 2-19: Beckwith Houk transition state analysis for the cyclization of **2.2a**.

2.9 Calculations

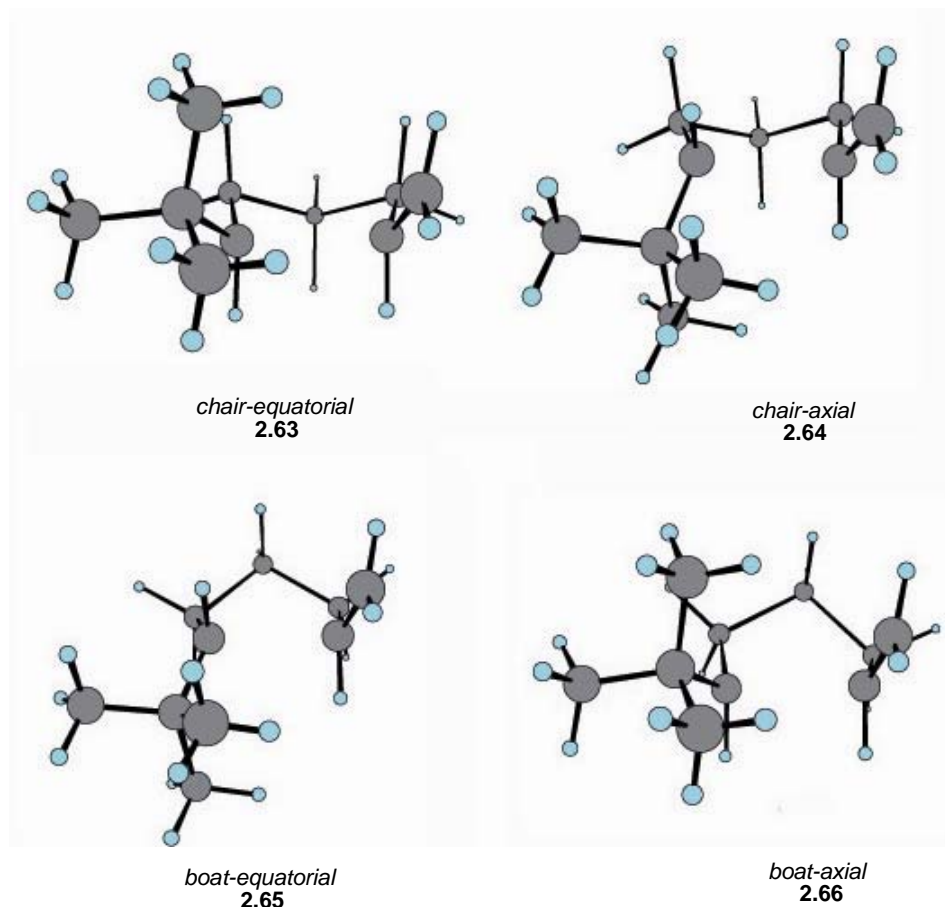
In the original publication, Beckwith discusses two sets of force field calculations that were carried out by Houk/Spellmeyer and by Beckwith/Schiesser. Both sets of calculations independently found that a *chair axial* type of transition was the lowest in energy. This led them both to predict that **2.45trans** would be the major isomer from the cyclization mixture of precursor **2.47**. These calculations nicely supported the experimental results that were obtained at the time. The important caveat with force field calculations is that they only consider the steric and not the electronic interactions of a compound.

Now that we have corrected the *cis* and *trans* assignments from the experimental work, the calculations carried out in 1992 no longer predict the correct stereochemistry for the cyclization of **2.47**. Moreover, these calculations will likely also fail for other hexenyl radicals with bulky substituents in the 1 position. Clearly taking sterics alone into consideration, as the force field calculations did, is inadequate for such radicals. For this reason the calculations were revisited by Professor Carl Schiesser, using *ab initio* and density functional quantum techniques. These techniques consider both the sterics and electronics of a molecule when calculating the potential energy surface.

Upon examining this potential energy surface for radical **2.48**, C₁₀H₁₉, at various levels of theory,⁷³ four transition states were located: *chair-equatorial* **2.63**, *chair-axial* **2.64**, *boat-equatorial* **2.65** and *boat-axial* **2.66**, shown in Table 2-3. These are the same four transition

states that were found in the original force field calculations. If radical **2.48** proceeds through transition states **2.63** or **2.66** then it will cyclize to give **2.45_{cis}**. If on the other hand radical **2.48** adopts transition state **2.64** or **2.65**, then **2.45_{trans}** results upon cyclization. The relative energies of these four transition states, in KJ/mol, were determined using ten different theory data sets and are tabulated Table 2-3.

Table 2-3: Transition States and Relative Energies for the Cyclization of Radical **2.48**.



Entry	Calculation Method	Relative Energy (KJ mol ⁻¹)			
		<i>chair equatorial</i> 2.63	<i>chair axial</i> 2.64	<i>boat equatorial</i> 2.65	<i>boat axial</i> 2.66
1	(UHF/6-31G*)	0	1.1	2.1	12.6
2	(UHF/6-31G* + ZPE)	0	0.8	1.0	12.5
3	(UHF/6-311G**)	0	0.5	1.3	12.6
4	(UHF/6-311G** + ZPE)	0	0.3	0.3	12.4
5	(BHandHLYP/6-311G**)	0	2.2	4.5	12.5
6	(BHandHLYP/6-311G** + ZPE)	0	2.5	3.8	12.8
7	(MP2/6-311G**)	0	1.1	4.6	9.0
8	(BHandHLYP/cc-pVDZ)	0	2.7	5.0	13.4
9	(BHandHLYP/cc-pVDZ + ZPE)	0	3.0	4.3	13.5
10	(BHandHLYP/aug-cc-pVDZ)	0	1.5	4.2	12.6

The above results show that the higher quantum level calculations do indeed predict the correct stereochemical outcome for the cyclization of **2.48**. At all levels of theory, the *chair-equatorial* transition state is the lowest in energy by about 1.2 KJ mol⁻¹. These calculations thereby predict that the *cis* product will be the major isomer of the cyclization. This supports the findings for all of our experiments. These results also indicate that hexenyl radical cyclizations with bulky substituents in the 1 position are strongly influenced by electronic phenomena because quantum mechanical calculations were necessary to correctly predict the experimental outcome. The data also justifies us ignoring the *boat-axial* transition state in the analysis because at all levels of theory it is about 12.4 KJ mol⁻¹ higher in energy than the *chair-equatorial* transition state.

2.10 Conclusions

We have definitively shown that hexenyl radical cyclizations with a large group in the 1 position and a geminal ester substitution in the 3 position cyclize with a modest 80/20 *cis* preference. We have also shown that carrying out the reaction at 25 °C instead of 80 °C gives a small improvement in the *cis* selectivity for this type of hexenyl radical cyclization. In addition, we have investigated the effect that an α,β -unsaturated ester group has on the cyclization of these types of radicals and shown that it has little to no bearing on the outcome of the reaction.

During the course of our investigations, we uncovered an error with the *cis* and *trans* assignments of a key literature benchmark and shown that they are actually reversed. There are very few exceptions to the rule 1 substituted hexenyl radicals cyclize with a *cis* preference, but now there is even one fewer.

Chapter 3 Round-Trip Radical Cyclizations

Having shown that hexenyl radicals with a large *tert*-butyl or other tertiary groups in the 1 position cyclize with a *cis* preference regardless of temperature or additional substitutions at position 3, we turned our attention to Ihara's temperature effect.³⁸ We initially wanted to see whether the temperature effect was reproducible and whether it was substrate dependent. To answer these questions, five tricyclization substrates were chosen all shown in Figure 3-1.

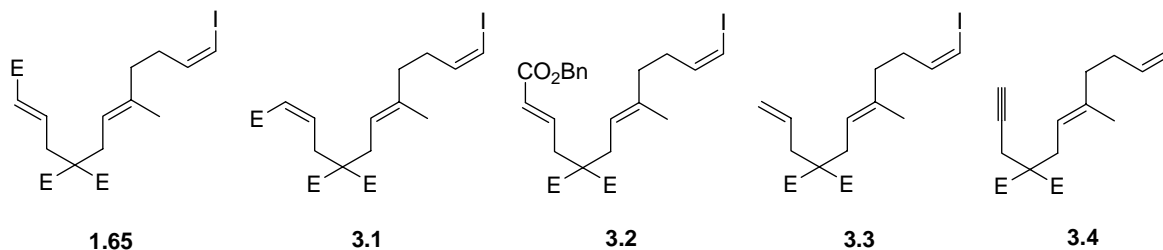


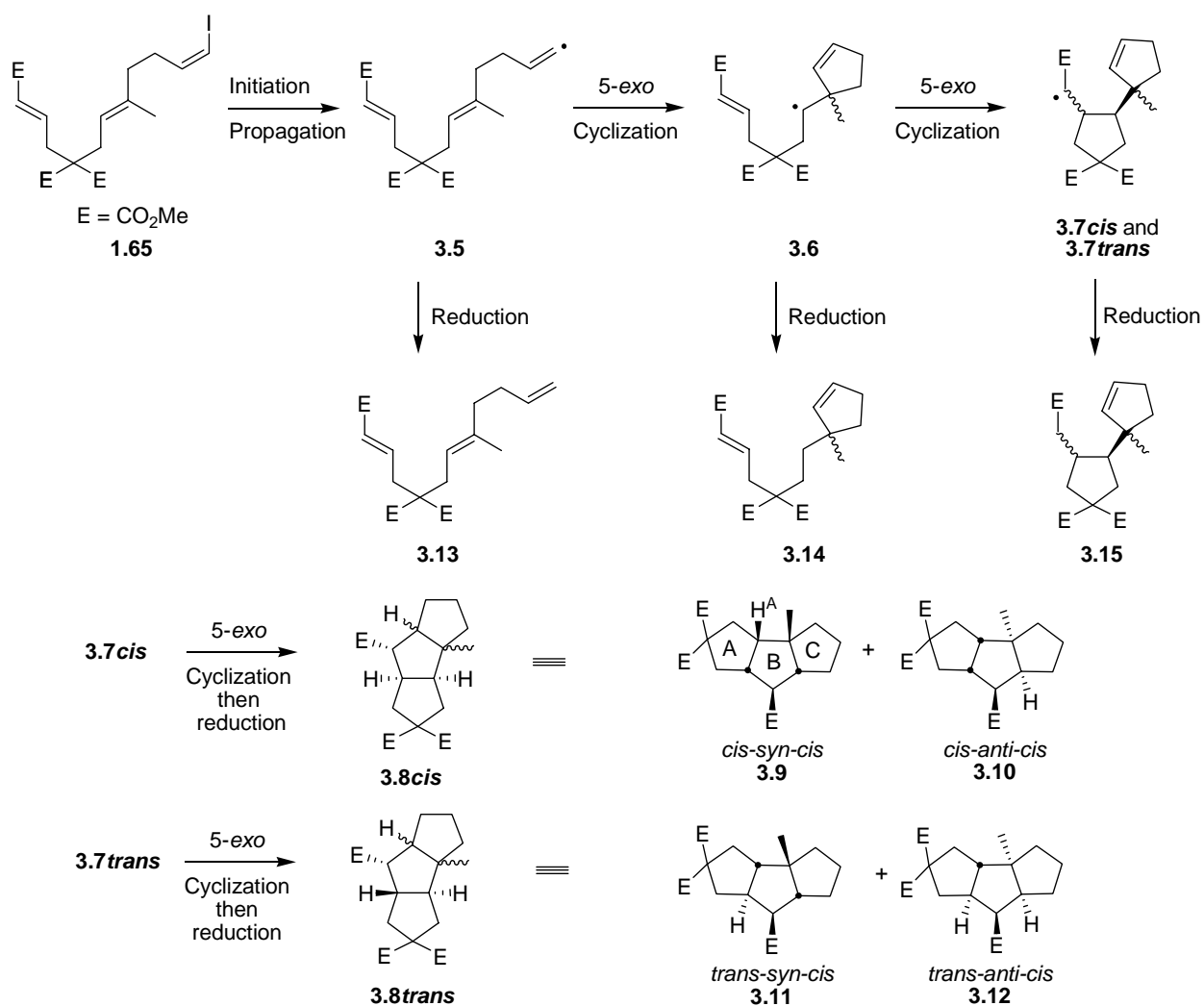
Figure 3-1: Tandem round-trip radical cyclization substrates.

3.1 Substrate Design and Rationale

Vinyl iodide **1.65** is Ihara's cyclization substrate. To assess the effect of the unsaturated ester geometry on the cyclization selectivity, we selected substrate **3.1**, the *Z* isomer of **1.65**, because *Z* unsaturated esters are reported^{26,74} to give higher stereoselectivities in radical cyclizations. Substrate **3.2**, which is the benzyl ester analogue of **1.65**, will serve as the structural relay substrate in this series, like the TMS ethyl ester did previously. Malonate **3.3** lacks the ester in the radical acceptor of the second cyclization and will serve to assess what effect this functionality has on the selectivity. Finally, in vinyl iodide **3.4**, the α,β -unsaturated ester of **1.65** has been replaced with a terminal alkyne, making the second cyclization a *5-exo dig* instead of a *5-exo trig* process.

The mechanism for the round-trip radical cyclization of **1.65** is shown in Scheme 3-1 and it is identical to that for precursors **3.1-3.3**. Treatment of vinyl iodide **1.65** with a suitable initiator (AIBN at 80 °C or Et₃B/O₂ at 25 °C) and a reducing agent gives vinyl radical **3.5**. Radical **3.5** cyclizes in a *5-exo* fashion to give monocyclic radical **3.6**. Hexenyl radical **3.6** then cyclizes again in either a *cis* or *trans* fashion to give **3.7** as a mixture of four diastereomers. Hexenyl radical **3.6** is similar to the systems studied in Chapter 2, and so we expect it to cyclize with an 80/20 *cis* preference. Radicals **3.7_{cis}** then cyclize a third time to give tricycles **3.8_{cis}**

upon reduction, as a mixture of the *cis-syn-cis* **3.9** and the *cis-anti-cis* **3.10** linear triquinane. Likewise, radicals **3.7trans** cyclize to give products **3.8trans**, which are the *trans-syn-cis* **3.11** and the *trans-anti-cis* **3.12** tricyclic isomers. Fortunately each radical in **3.7** cyclizes to give a single triquinane because the formation of a 5,5 fused system gives exclusively the *cis* product.³⁶ The complete cascade can be interrupted by reduction of radicals **3.5**, **3.6**, or **3.7** to give prematurely reduced products **3.13**, **3.14**, and **3.15** respectively. The nomenclature of the linear triquinanes is either *cis* or *trans* depending on the ring fusion of the A/B rings as denoted in **3.9**. The name is then either *syn* or *anti* depending on the relationship between H^A and the methyl group and finally it is either *cis* or *trans* depending on the geometry of the B/C ring fusion.



Scheme 3-1: Mechanism for the round-trip radical cyclization reaction.

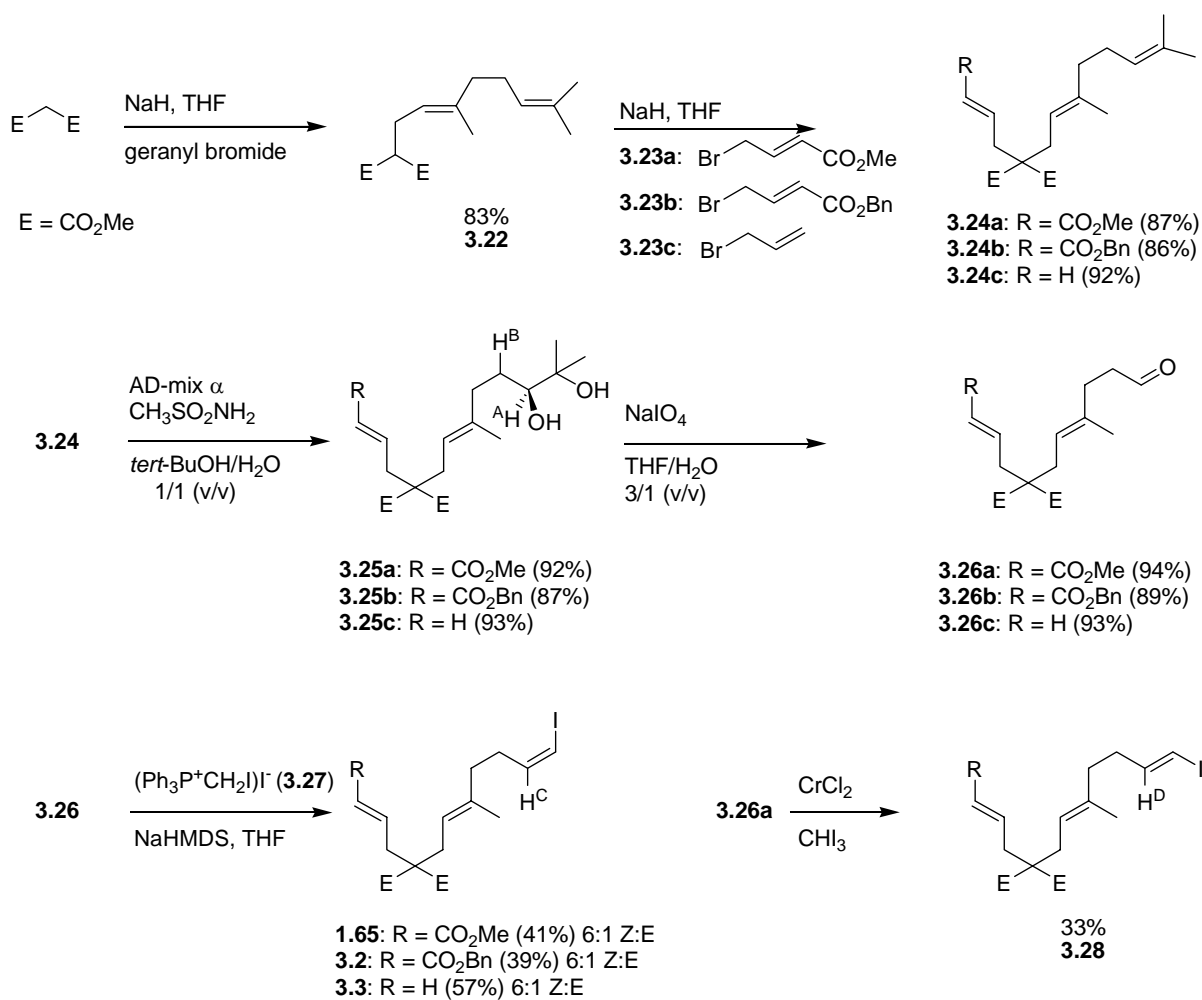
3.2 Substrate Synthesis

The synthesis of all five precursors was readily accomplished through straightforward malonate alkylations. The synthesis of **1.65**, **3.2**, and **3.3** closely followed Ihara's five step synthesis,³⁸ and the synthesis of **3.1** and **3.4** required only appropriate deviations from this.

3.2.1 Synthesis of 1.65, 3.2 and 3.3

The general synthesis of the triene cyclization precursors is outlined in Scheme 3-3. The synthesis of **1.65** is representative for all three substrates and the first step is the deprotonation of dimethyl malonate with sodium hydride. Subsequent alkylation of the anion with geranyl bromide gave alkylated malonate **3.22** in 83% yield.⁴⁴ A second alkylation step with methyl-4-bromocrotonate **3.23a** afforded *bis*-alkylated malonate **3.24a** in 87% yield.⁴⁴

For the dihydroxylation step, Ihara successfully used catalytic OsO₄ with NMO as the oxidant, but in the synthesis of **3.3**, we worried that OsO₄ would preferentially dihydroxylate the mono- over the desired tri-substituted olefin. We chose to use a Sharpless dihydroxylation instead because the addition of CH₃SO₂NH₂ shuts down the reaction for terminal olefins.⁷⁵ Treating triene **3.24a** with AD-mix α and CH₃SO₂NH₂ in *tert*-BuOH/H₂O (1/1) afforded diol **3.25a** in 92% yield. The regioselectivity of this reaction was determined by ¹H-¹H COSY analysis of diol product **3.25a**, which showed a cross peak between H^A (δ 3.27 ppm, dd, J = 2.0, 10.2 Hz) and H^B (δ 1.39–1.34 ppm, m). This proves that the correct olefin was dihydroxylated. The Sharpless' mnemonic⁷⁵ predicts that AD-Mix α dihydroxylation of the desired olefin will give the *S* enantiomer as shown in **3.25a**, but this was not verified because the stereocenter was destroyed in the subsequent step.



Scheme 3-3: Synthesis of cyclization precursors **1.65**, **3.2** and **3.3**.

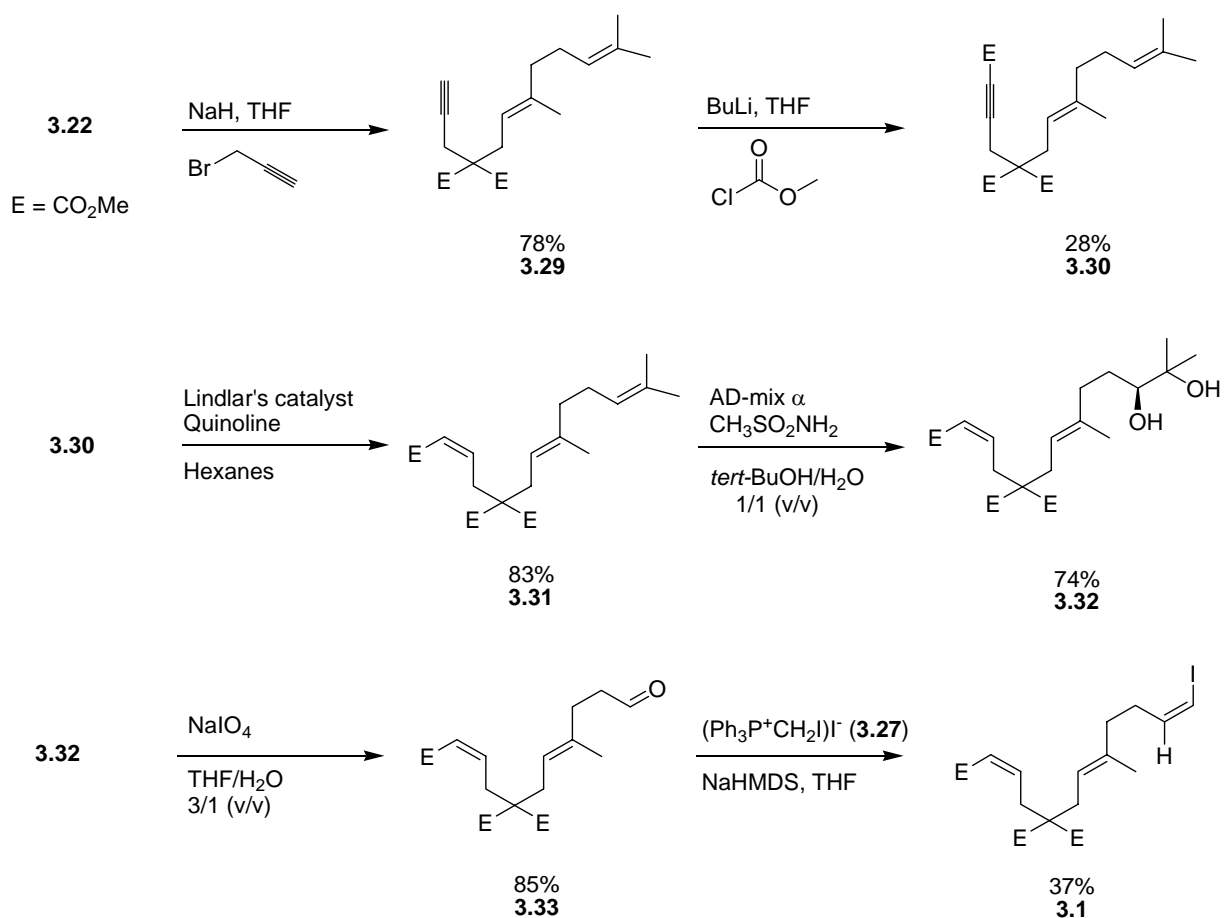
Cleavage of diol **3.25a** with NaIO_4 in $\text{THF}/\text{H}_2\text{O}$ yielded aldehyde **3.26a** in 94% yield.⁷⁶ Wittig olefination using $(\text{Ph}_3\text{P}^+\text{CH}_2\text{I})^-$ **3.27**,⁷⁷ NaHMDS and aldehyde **3.20a** gave vinyl iodide **1.65** in 57% yield as a 6/1 Z:E ratio.⁷⁸ The overall yield of this sequence was 31 % starting from malonate **3.22**. An authentic sample of the *E* isomer was prepared by subjecting aldehyde **3.26a** to a Takai reaction to give iodide **3.28** in 33% yield as a single stereoisomer.⁷⁹ Subsequent integration of the diagnostic H^{C} and H^{D} protons in the ^1H NMR spectrum of the mixture provided the reported ratio. The key proton H^{C} in the *Z* isomer appeared as a doublet of triplets, at δ 6.04 ppm with *J* values of 6.4 and 7.2 Hz. For the *E* isomer, H^{D} appeared as a doublet of triplets at δ 6.46 ppm with *J* values of 6.2 and 14.4 Hz. Although chromatographically separable, the *E* and *Z* isomers were collected together for cyclization purposes. This can be done because the homolysis of the carbon-iodine bond in either the *E* or the *Z* isomer gives the same rapidly

interconverting vinyl radical.⁴⁹ Substrates **3.2** and **3.3** were prepared in 26% and 45% overall yield, respectively, starting from **3.22** following the same synthetic sequence as for **1.65**.

3.2.2 Synthesis of *Z*-Unsaturated Ester Cyclization Substrate **3.1**

We synthesized cyclization precursor **3.1** by the sequence of reactions laid out in Scheme 3-4. Deprotonation of malonate **3.22** with sodium hydride and quenching the subsequent anion with propargyl bromide gave alkyne **3.29** in 78% yield.⁴⁴ Treatment of malonate **3.29** with BuLi and subsequent addition of methyl chloroformate furnished trimethyl ester **3.30** in 28% yield.⁴⁵ This reaction, although low yielding, was very clean and the starting material could be recovered and resubjected to give more of the desired product. Interestingly, the reaction stalled after about 2 h and adding more BuLi and methyl chloroformate did not complete the conversion.

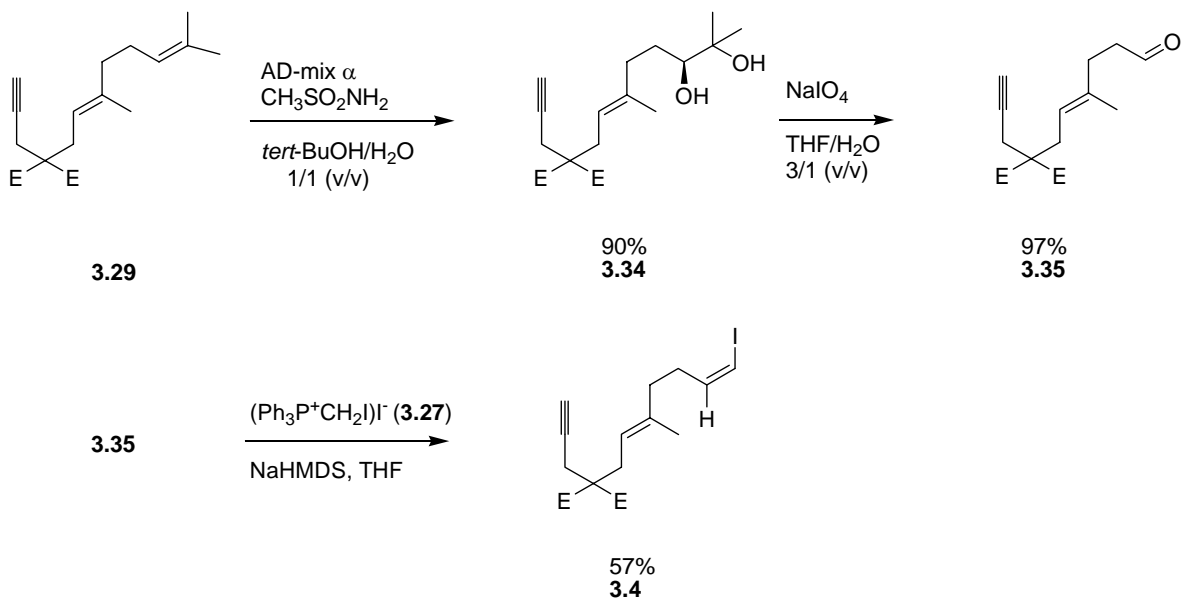
Hydrogenation of malonate **3.30** with Lindlar's catalyst gave the *Z*-olefin **3.31** in 83% yield.⁸⁰ Treatment of alkene **3.31** with AD-Mix α and CH₃SO₂NH₂ gave diol **3.32** in 74% yield.⁷⁵ Cleavage of diol **3.32** with NaIO₄ provided aldehyde **3.33** in 85% yield.⁷⁶ Wittig olefination of aldehyde **3.33** with the phosphorous ylide derived from salt **3.28** furnished *Z*-vinyl iodide **3.1** in 37% yield.⁷⁸ Although our previous experience with this Wittig reaction in the synthesis of **1.65** provided the final vinyl iodide as a 6/1 *Z/E* mixture, the same reaction with aldehyde **3.33**, furnished only the *Z* isomer as observed by TLC or crude NMR analysis.



Scheme 3-4: Synthesis of cyclization precursor **3.1**.

3.2.3 Synthesis of the Alkyne Cyclization Substrate **3.4**

The synthesis of cyclization precursor **3.4** is outlined in Scheme 3-5 and starts by a dihydroxylation of compound **3.22** with AD-mix α and CH₃SO₂NH₂ to give diol **3.27** in 90% yield.⁷⁵ Subsequent cleavage of the diol with NaIO₄ gave aldehyde **3.28** in 97% yield.⁷⁶ Wittig olefination of aldehyde **3.28** with salt **3.27** gave vinyl iodide **3.4** in 57% yield as a single *Z*-stereoisomer.⁷⁸



Scheme 3-5: Synthesis of alkynyl precursor **3.4**.

3.3 Cyclization Results

With the cyclization precursors in hand, we studied the cascade reactions at different temperatures and with a number of reducing agents. The results from the cyclizations of **1.65**, **3.1** and **3.2** are summarized in Table 3-1, while the results from the cyclization of **3.3** and **3.4** are given in Table 3-2 and Table 3-3, respectively.

3.3.1 Cyclization of Vinyl Iodide **1.65**

In a repetition of one of Ihara's key experiments, we reduced **1.65** (0.10 mmol) with Bu_3SnH (0.12 mmol) and AIBN (0.05 mmol) in benzene (55 mL, 2 mM with respect to the reducing agent) at 80 °C, Figure 3-2 and Table 3-1 Entry 2. A relatively complex mixture resulted from this cyclization and column chromatography or HPLC was not helpful for separating out any of the components. Once again, GC analysis proved to be a useful tool. After subjecting the crude reaction mixture to a DBU workup⁸¹ to remove most of the tin containing by-products, the mixture was analyzed by GC to provide the chromatogram shown in Figure 3-2a. In addition to the major peaks at 8.10 min and 8.39 min (44% and 34% of the mixture respectively), there were at least 4 minor peaks. The minor peak with a retention time of 7.66

min was readily identified as directly reduced product **3.13** (Figure 3-3). This was accomplished by an independent synthesis of **3.13** by a Wittig reaction between aldehyde **3.26a** and methyl triphenylphosphonium bromide⁸² to give the triene in 58% yield. GC co-injection of authentically prepared **3.13** and the crude reaction mixture enabled us to identify the peak at 7.66 min as the directly reduced product.

We tentatively assigned the major products of the cyclization as the *cis-syn-cis* isomer **3.9** and the *cis-anti-cis* isomer **3.10** on the basis of Ihara's work.³⁸ We later confirmed this assignment and were able to show that the peak with the shorter retention time corresponded to the *cis-syn-cis* isomer **3.9**. ¹H NMR spectra of the crude cyclization mixture showed small resonances in the alkene region (δ 4.5-6.0 ppm) in addition to those assigned to triene **3.13**. We tentatively assigned those resonances as coming from the mono-cyclized product **3.14** and the *trans* substituted bicyclic product **3.15trans** where the round-trip cyclization was interrupted by reduction with Bu₃SnH. Although it is possible that some of the resonances can be attributed to *cis* bicycles **3.15cis**, it is unlikely that they are present because the corresponding radical **3.7cis** is known to cyclize rapidly to give the linear triquinane.³⁵

To remove the minor alkene containing products from the alkene free tricyclic products, we treated the product mixture with *m*-CPBA with the expectation that the alkene containing products would be epoxidized and thereby rendered more polar. Indeed TLC analysis of the reaction mixture revealed two spots; one with the same R_f as before and a new more polar spot. Flash chromatography of the resulting mixture allowed for isolation of the less polar fraction whose ¹H NMR spectra showed no epoxide or alkene resonances. The GC chromatogram of this purified mixture is shown in Figure 3-2b. The peak from triene **3.13** and several of the other minor peaks have been removed, leaving four products, two major and two minor. In a GC-MS experiment, all four peaks exhibited almost identical fragmentation patterns strongly suggesting that they are all tricyclic and isomeric.

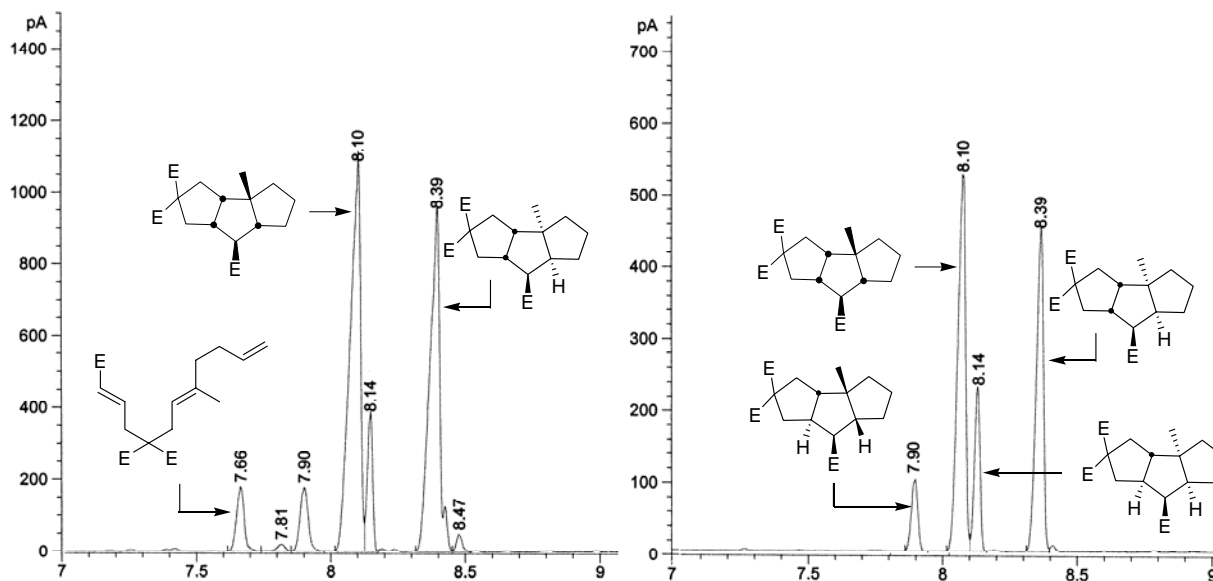


Figure 3-2: a) Left: GC chromatogram of the cyclization reaction of **1.65** after a DBU workup. b) Right: GC chromatogram of the cyclization of **1.65** after DBU workup and *m*-CPBA treatment of the reaction mixture. Both GC injections were performed on an Agilent 6850 gas chromatograph equipped with an HP-1 column: dimethylpolysiloxane, 30m x 0.32mm, and a 0.25 μ m film thickness. The temperature profile of the injection has an initial temperature of 150 $^{\circ}$ C which then increases by 10 $^{\circ}$ C/min to a final temperature of 315 $^{\circ}$ C.

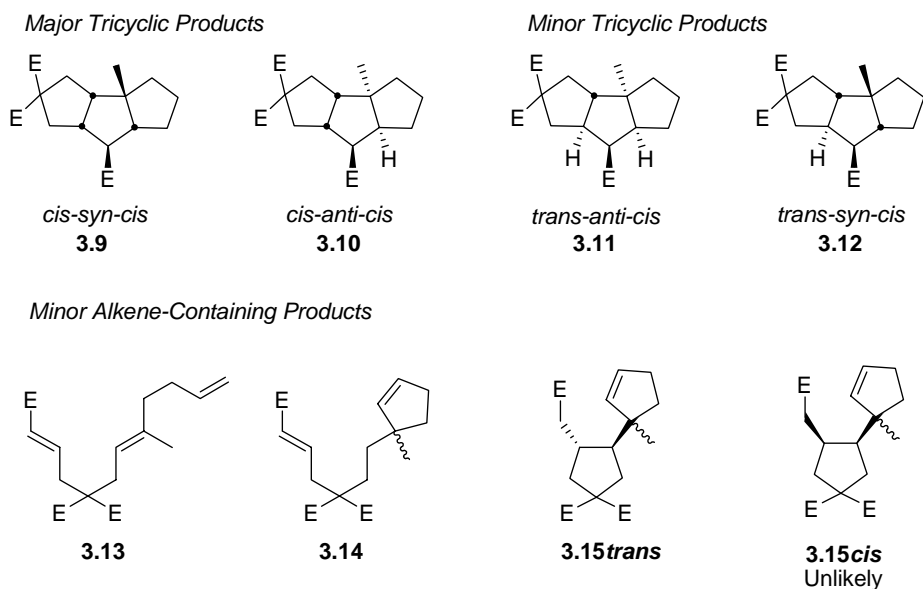


Figure 3-3: Potential products from the cyclization of **1.65**.

Having developed a way to isolate only the tricyclic products of this cyclization, we proceeded to more rigorously assign which peak in the GC chromatogram arose from which tricyclic. Although Ihara reports that compound **3.9** was separated from the other components of

the mixture by flash chromatography, we were unable to do this even when using a Biotage™ purification system. Fortunately, we were able to obtain a 93% enriched sample of **3.9**, with **3.10** being the sole contaminant, through a preparative GC experiment carried out by Prof. M. Newcomb and R. E. P. Chandrasena at the University of Illinois at Chicago. Likewise we obtained a 75% enriched sample of **3.10** with **3.9** as the contaminant. This enabled us to fully assign all of the ^1H NMR resonances for both compounds and acquire NOSEY spectra. From the NOSEY spectra, we assigned the configuration of the second eluting compound as the *cis-syn-cis* isomer and the fourth eluting compound as the *cis-anti-cis* isomer based on the correlations shown in Figure 3-4. Unfortunately, we were unable to assign the configuration of the ester stereocenter in tricycle **3.10**.

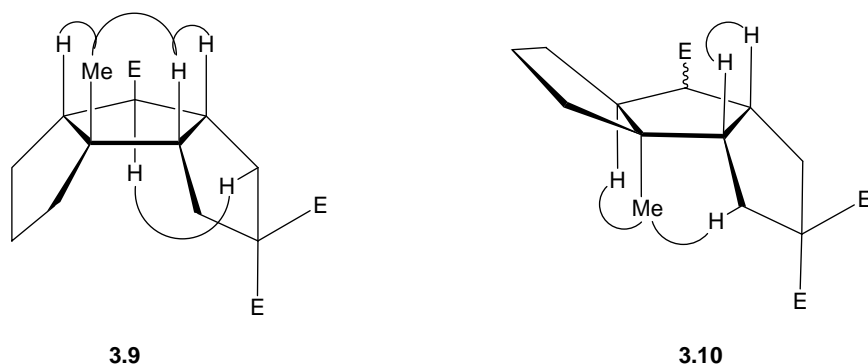


Figure 3-4: a) Left: NOSEY correlations observed for the *cis-syn-cis* isomer **3.9** and b) Right: NOSEY correlations for the *cis-anti-cis* isomer **3.10**.

We assume that the minor peaks in the GC after *m*-CPBA treatment are the *trans* tricyclic products **3.11** and **3.12**. We assigned the peak at 8.14 min as the *trans-anti-cis* isomer **3.11** and the peak at 7.90 min as the *trans-syn-cis* isomer **3.12**. These assignments were made by analogy to the cyclization of **1.49** where the minor *trans* product was the *trans-syn-cis* isomer. However, these assignments are tentative because we could not obtain the compounds in pure enough form for detailed characterization. We considered the possibility that the minor products might be epimers of **3.33** and **3.34** at the ester bearing stereocenter. However, our relay experiments with **3.2**, Chapter 3.4, suggest that this is not the case because the cyclization of **3.3**, without this ester, also gives four tricyclic products.

We have now identified which peaks in the GC chromatogram correspond to the tricyclic products, and we have firmly assigned the configuration of the two major products. Additionally

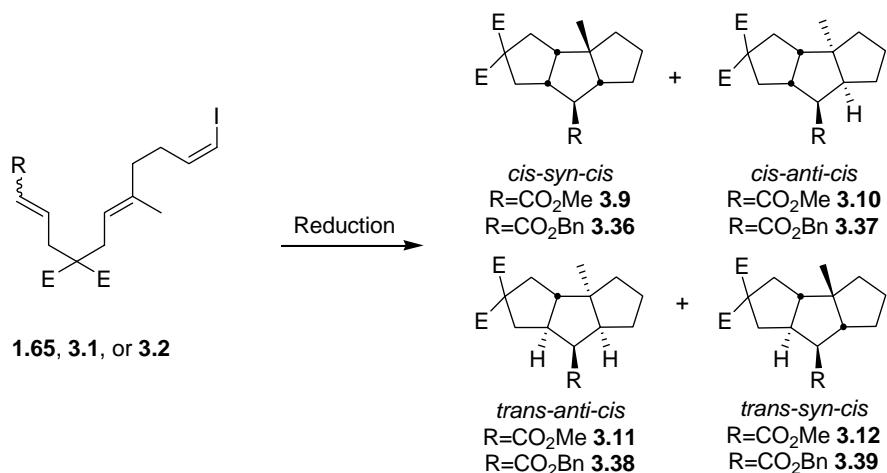
the above analysis for the cyclization of **1.65** allowed us to assign the configuration of the tricycles from the cyclization of *Z*-unsaturated ester **3.1** (see below) because it gives the same set of products.

3.3.2 Cyclization Results for Substrates **1.65**, **3.1** and **3.2**

With a good analysis method in hand, we conducted a series of cyclizations with substrate **1.65** with Bu₃SnH and Ph₃SnH at 80 °C and 25 °C, Table 3-1 entries 1-4. We also varied the reducing agent concentration by adding a 24 mM solution of Bu₃SnH in benzene to the reaction by syringe pump over 3 h, entries 11 and 12. Each reaction was treated with *m*-CPBA and chromatographed to remove any alkene containing products and then subjected to GC analysis to determine the cyclization selectivity reported in Table 3-1. The same analysis procedure was carried out for the two cyclizations of the *Z*-unsaturated ester **3.1**, where we ran one cyclization at 80 °C and the other at 25 °C, Table 3-1 entries 5 and 6. Finally we also performed the cyclization of the benzyl ester substrate **3.2** at 25 °C and 80 °C using Bu₃SnH and Ph₃SnH as the reducing agent entries 7-10.

For the cyclization of vinyl iodide **1.65**, entries 1-4, 11 and 12, the ratio of the four tricyclic products hardly varied at all as shown in Table 3-1. Of special interest is the *cis/trans* selectivity of the second 5-*exo* cyclization. This selectivity was calculated by dividing the sum of the major two *cis/cis* products **3.9** and **3.10** by the sum of the minor two *trans/cis* isomers **3.11** and **3.12**. The temperature dependence of selectivities in the second cyclization are very consistent with those obtained for the benchmark substrates in Chapter 2, but inconsistent with the results reported by Ihara. We only observe a minor improvement in the selectivity from about 77/23 *cis/trans* at 80 °C to 84/16 at 25 °C. The *cis/trans* ratios may be slightly overstated because the minor products removed in the *m*-CPBA treatment are likely to result predominantly from *trans* cyclization in the second step. However, we believe that this error is small because the selectivities in the tricyclization reactions are very similar to those found for the benchmark substrates.

Table 3-1: Cyclization data for the cyclization of substrates **1.65**, **3.1** and **3.2**.



Entry	Substrate	R	Olefin Geometry	Red. Agent ^b	T (°C)	% Composition				Selectivity (<i>cis/trans</i>) ^c	Yield (%)
						3.9 -or- 3.36	3.10 -or- 3.37	3.11 -or- 3.38	3.12 -or- 3.39		
2 mM fixed reducing agent concentration											
1	1.65	CO ₂ Me	<i>E</i>	Bu ₃ SnH	25	47	39	8	6	86/14	52, 69 ^c
2	1.65	CO ₂ Me	<i>E</i>	Bu ₃ SnH	80	44	34	9	13	78/22	50, 70 ^c
3	1.65	CO ₂ Me	<i>E</i>	Ph ₃ SnH	25	44	35	7	14	79/21	48
4	1.65	CO ₂ Me	<i>E</i>	Ph ₃ SnH	80	47	37	9	7	77/23	46
5	3.1	CO ₂ Me	<i>Z</i>	Bu ₃ SnH	25	51	40	8	1	91/09	62
6	3.1	CO ₂ Me	<i>Z</i>	Bu ₃ SnH	80	48	40	5	7	88/12	N.D. ^d
7	3.2	CO ₂ Bn	<i>E</i>	Bu ₃ SnH	25	47	40	6	7	87/13	50
8	3.2	CO ₂ Bn	<i>E</i>	Bu ₃ SnH	80	47	37	7	8	84/16	50
9	3.2	CO ₂ Bn	<i>E</i>	Ph ₃ SnH	25	44	39	10	7	83/17	44
10	3.2	CO ₂ Bn	<i>E</i>	Ph ₃ SnH	80	42	35	15	8	77/23	35
Reducing agent added by syringe pump											
11 ^a	1.65	CO ₂ Me	<i>E</i>	Bu ₃ SnH	25	48	38	8	6	86/14	N.D. ^d
12 ^a	1.65	CO ₂ Me	<i>E</i>	Bu ₃ SnH	80	42	35	9	14	77/23	N.D. ^d

^a Ihara's protocol

^b Cyclization procedures are detailed in Chapter 5

^c Refers to the selectivity of the second 5-*exo* radical cyclization

^d N.D.: isolated yield not determined; the selectivity was determined from a GC of the crude reaction mixture

^e Yield determined using octadecane as an internal GC standard

We noted the moderate (42-50%) isolated yields of our cyclization reactions and worried that we may be selectively removing some products during purification. To see if this was the case, we used octadecane as an internal standard in the reaction, entries 1 and 2, and were able to show that the chemical yield of the cyclization is about 20% higher than the isolated yield. The use of the internal standard, along with the observation that the tricyclic product ratios were the

same before and after purification, assures us that the ratios reported in Table 3-1 are accurate measures of the selectivity.

The cyclization of the *Z*-unsaturated ester **3.1**, entries 5 and 6, shows an improved selectivity in the second cyclization of 90/10 *cis/trans* in comparison to the 80/20 obtained for the *E*-unsaturated ester. The selectivities of the cyclization were also consistent at about 90/10 when the reaction was run at either 80 °C or 25 °C.

Finally, the cyclization of the benzyl ester substrate **3.2** entries 7-10, gave results very similar to those obtained for the methyl ester cyclizations. The product ratios and selectivities were very similar to each other and also showed no temperature dependence. GC chromatograms for a cyclization of substrate **3.2** before (left) and after (right) *m*-CPBA treatment are shown in Figure 3-5. Similar to the cyclization of **1.65**, substrate **3.2** gave a relatively complex mixture of products with two major product peaks at 10.78 min and 11.11 min. We were able to readily identify the directly reduced product **3.40**, Figure 3-6, as the peak at 10.57 min by an independent synthesis and GC co-injection. We once again tentatively assigned the major products as the *cis-syn-cis* isomer **3.36** and the *cis-anti-cis* triquinane **3.37**. Treatment of the cyclization mixture with *m*-CPBA and isolation of the less polar fraction provided a mixture whose ¹H NMR spectra was void of alkene resonances. Analysis of this mixture by GC provided the chromatogram shown in Figure 3-5b that clearly shows four products. All four of these products displayed similar fragmentation patterns in a GC-MS experiment. This indicates that they are all tricyclic and isomeric and so we tentatively assigned the peak at 10.59 min as the *trans-anti-cis* isomer **3.38** and the peak at 10.84 min as the *trans-syn-cis* isomer **3.39**.

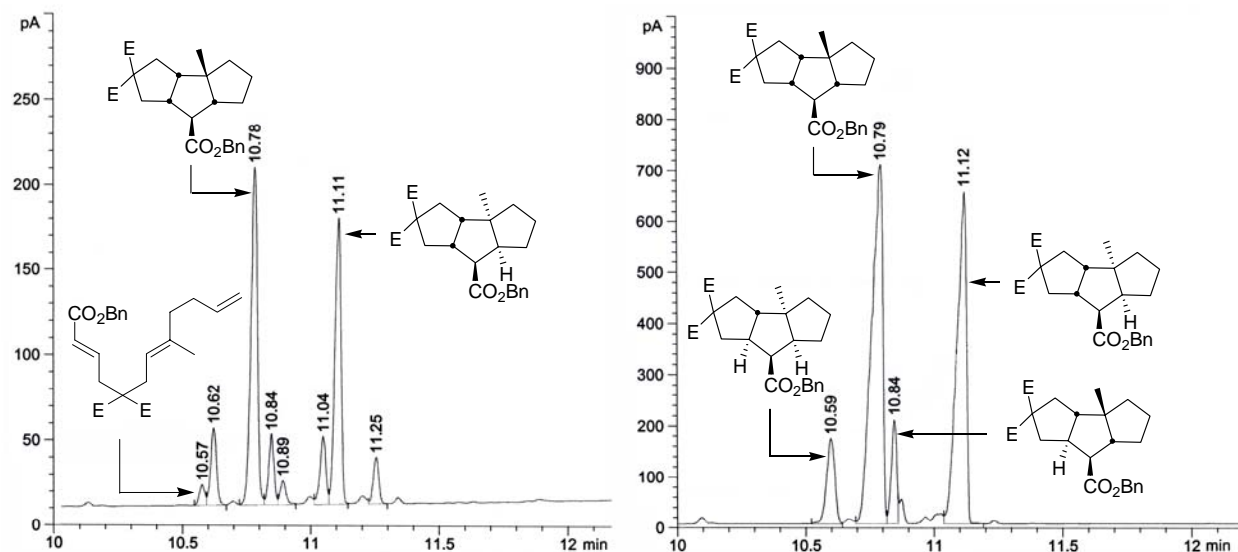


Figure 3-5: a) Left: GC chromatogram of the cyclization reaction of **3.2** after a DBU workup. b) Right: GC chromatogram of the cyclization of **3.2** after DBU workup and *m*-CPBA treatment of the reaction mixture. Both of the GC injections were carried out under the same conditions as described for Figure 3-2.

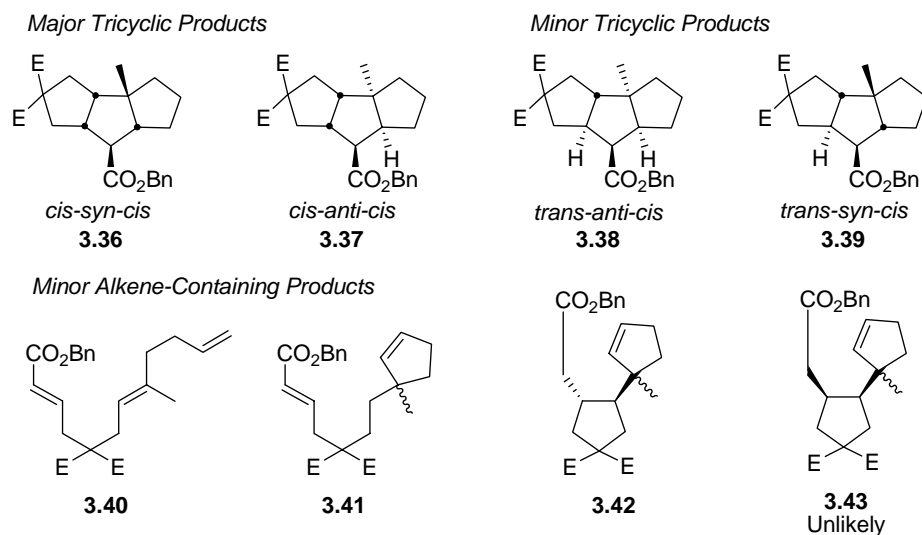


Figure 3-6: Potential products from the cyclization of **3.2**.

3.3.3 Cyclization of Allyl Precursor **3.3**

We next turned our attention to the cyclization of precursor **3.3** to study the effect of the ester on the radical acceptor of the second cyclization. We conducted a series of cyclizations in a manner similar to that for precursors **1.65**, **3.1** and **3.2**. As before, when we reduced **3.3** with Bu_3SnH at $80\text{ }^\circ\text{C}$, a relatively complex mixture resulted with two major and a number of minor

products. GC analysis of this mixture after DBU workup provided the left chromatogram shown in Figure 3-7. We readily identified the peak with a retention time of 5.16 min as coming from the directly reduced product **3.48**, Figure 3-8, and tentatively assigned the peak at 5.74 min as the *cis-syn-cis* triquinane **3.44** and the peak at 5.95 min as the *cis-anti-cis* triquinane **3.45**. After treating the crude cyclization mixture with *m*-CPBA and removing the more polar products by column chromatography, we obtained a mixture that upon GC analysis gave the chromatogram shown in Figure 3-7b. Several of the minor products were removed and we were left with a mixture containing two major and two minor products. All four of the products exhibited similar fragmentation patterns suggesting that they are all tricyclic compounds. We then assigned the peak at 5.51 min as the *trans-anti-cis* isomer **3.46** and the peak at 5.64 min as *trans-syn-cis* isomer **3.47**, but these assignments are tentative.

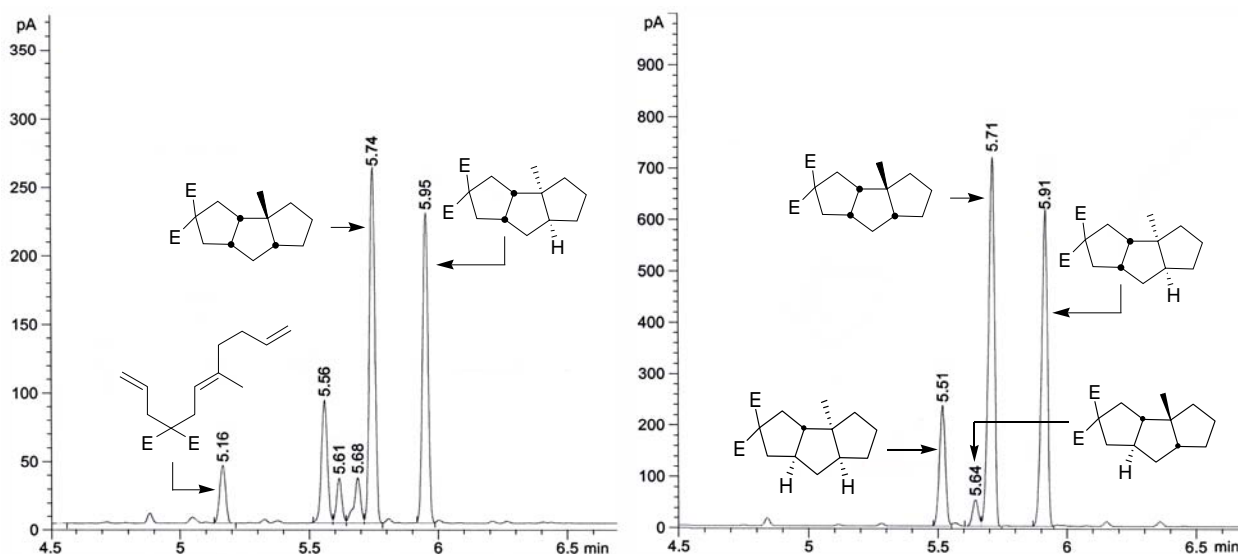


Figure 3-7: a) Left: GC chromatogram of the cyclization reaction of **3.3** after a DBU workup. b) Right: GC chromatogram of the cyclization of **3.3** after DBU workup and *m*-CPBA treatment of the reaction mixture. Both of the GC injections were carried out under the same conditions as described for Figure 3-2.

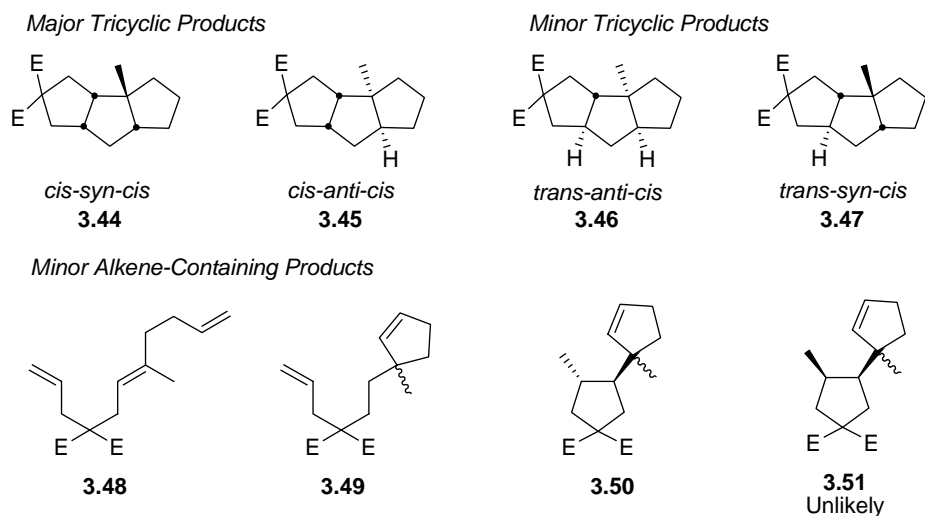
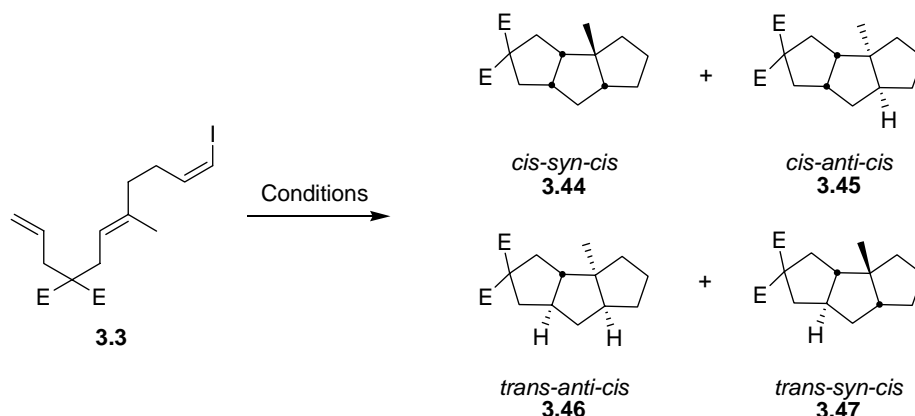


Figure 3-8: Potential products from the cyclization of **3.3**.

Having identified the GC retention times of the four tricyclic products, the cyclization conditions for **3.3** were varied extensively and the results are all summarized in Table 3-2. In total 10 cyclizations were carried out where the reducing agent was changed from Bu_3SnH (entries 1, 2, 7, and 8) to Ph_3SnH (entries 5, 6, 9, and 10) and also $(\text{TMS})_3\text{SiH}$ (entries 3 and 4). The cyclizations were also performed at either 25 °C (entries 1, 3, 5, 7, and 9) or 80 °C (entries 2, 4, 6, 8, and 10) and finally the concentration of the reducing agent was varied between a 2 mM fixed concentration, entries 1-6, and slow addition of the reducing agent by syringe pump over 3 h (entries 7-10).

The results in Table 3-2 show that despite variation of the reaction conditions, the tricyclic product ratios and selectivities in the second cyclization remain virtually unchanged. The selectivity of the second cyclization is once again about 80/20 *cis/trans* regardless of the reaction conditions. Furthermore the ratios of the tricyclic products are also close to those obtained for the cyclizations of precursors **1.65** and **3.2**, proving the the α,β -unsaturated ester has very little bearing on the course of this reaction. The selectivity in the second cyclization is not only close to that of the other tricyclization substrates, but also close to the selectivities observed in the cyclization of all of the benchmark cyclizations. Taken together, the results from this substrate and those found previously question whether the temperature effect exists.

Table 3-2: Cyclization data for the cyclization of substrate **3.3**

Entry	Cyclization Method ^a	Reducing Agent	T (°C)	%Composition				Selectivity ^d (cis/trans)	Yield ^e (%)
				3.44	3.45	3.46	3.47		
2 mM fixed reducing agent concentration									
1	A ^b	Bu ₃ SnH	25	40	42	13	5	82/18	N.D.
2	B	Bu ₃ SnH	80	40	37	19	4	77/23	N.D.
3	A	(TMS) ₃ SiH	25	43	38	12	7	81/19	N.D.
4	B	(TMS) ₃ SiH	80	41	41	11	7	82/18	N.D.
5	A	Ph ₃ SnH	25	47	36	13	4	83/17	N.D.
6	B	Ph ₃ SnH	80	45	38	14	3	83/17	N.D.
Reducing agent added by syringe pump									
7	C ^{b,c}	Bu ₃ SnH	25	44	39	11	6	83/17	51
8	D ^c	Bu ₃ SnH	80	42	38	14	6	80/20	52
9	C ^{b,c}	Ph ₃ SnH	25	43	39	15	3	82/18	N.D.
10	D ^{b,c}	Ph ₃ SnH	80	40	36	19	5	76/24	N.D.

^a See chapter 5 for details on the experimental procedure.

^b Required the addition of 1 equiv of PPh₃ to avoid exclusive formation of a directly reduced product **3.48**.

^c Ihara's protocol.

^d Refers to the selectivity of the second 5-*exo* radical cyclization.

^e N.D.: not determined; The selectivity was determined from a GC of the crude reaction mixture.

3.3.4 Cyclization of the Alkynyl Precursor **3.4**

We conducted the cyclization of substrate **3.4** using our standard reducing conditions of Bu₃SnH, AIBN in refluxing benzene (2 mM). The crude reaction mixture was purified by column chromatography to remove any tin by-products and then analyzed by GC and ¹H NMR spectroscopy. The ¹H NMR spectrum of this mixture showed no evidence of any tin containing impurities and all the necessary resonances for tricycles **3.19** were present. Most notably this mixture showed two resonances with chemical shifts of 5.17 and 4.99 ppm as shown in Figure 3-9. We attributed one of these resonances to the olefinic proton in compound **3.19_{syn}** and the other to the olefinic proton in tricycle **3.19_{anti}**. By integration, the ratio of these two peaks was

33/67 respectively. Interestingly GC analysis of the same mixture showed only a single peak with a retention time of 5.59 min, Figure 3-9, despite trying a number of different GC temperature profiles. Based on the NMR and the GC analysis we concluded that there were two products in this mixture in a 33/67 ratio that coincidentally eluted on the GC. At this point we were unable to definitively determine if **3.19_{syn}** or **3.19_{anti}** was the major isomer.

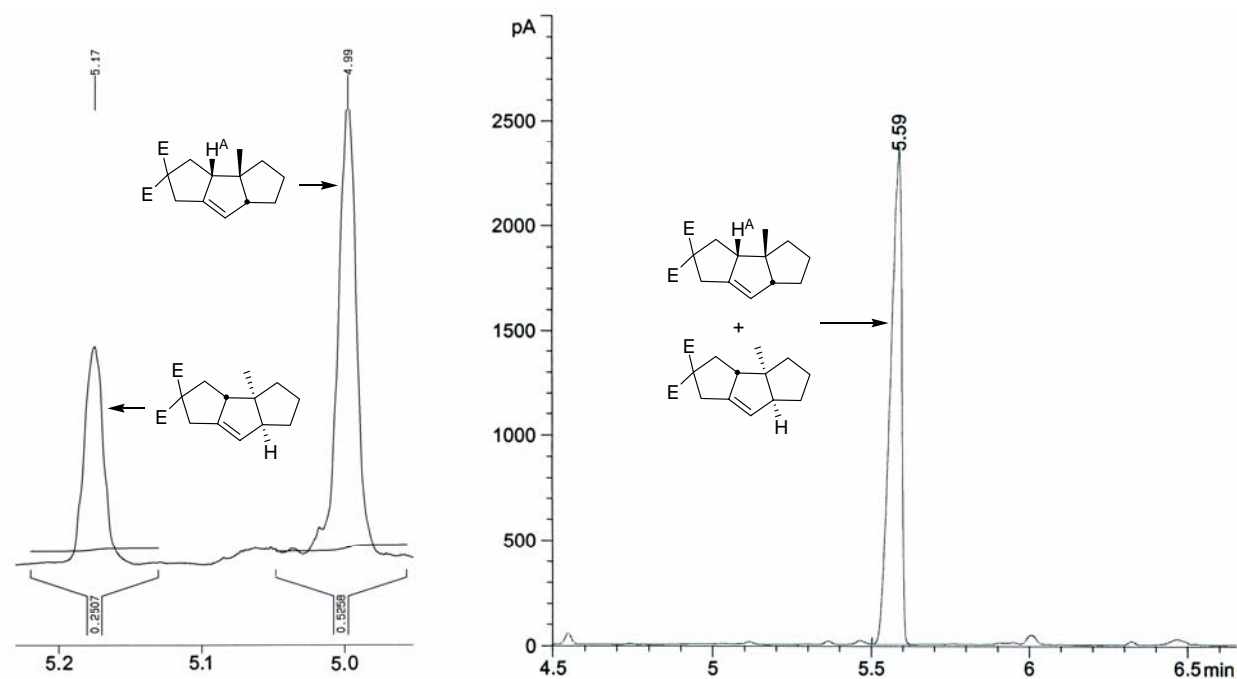


Figure 3-9: a) Left: Expansion of the olefinic region of the ^1H NMR spectrum of the cyclization mixture of precursor **3.4**. b) Right: GC chromatogram of the cyclization mixture of **3.4**. The GC injection was carried out under the same conditions as described for Figure 3-2.

We then subjected the cyclization mixture to a palladium-mediated hydrogenation in ethanol.⁴¹ GC analysis of the hydrogenation reaction showed rapid disappearance of the mixture peak at 5.59 min and appearance of two products with retention times of 5.73 and 5.92 min in a 67/33 ratio respectively, Figure 3-10. Purification of this mixture by filtration through Celite and concentration of the filtrate gave the two component mixture in 67% yield over both the cyclization and the hydrogenation step. Comparison of the retention times of these two products to the retention times of the four tricyclic products from the cyclization of the allyl precursor **3.3** showed that the major peak of the hydrogenation corresponded to the *cis-syn-cis* isomer **3.44** and that the minor peak corresponded to the *cis-anti-cis* isomer **3.45**.

We also performed the cyclization of **3.4** at 25 °C, Table 3-3 entry 2, which gave a 60/40 mixture of **3.19_{syn}** and **3.19_{anti}**. As expected, hydrogenation of this 60/40 mixture over palladium gave a 60/40 mixture of the *cis-syn-cis* triquinane **3.44** and the *cis-anti-cis* triquinane **3.45** in 65% yield over the two steps.

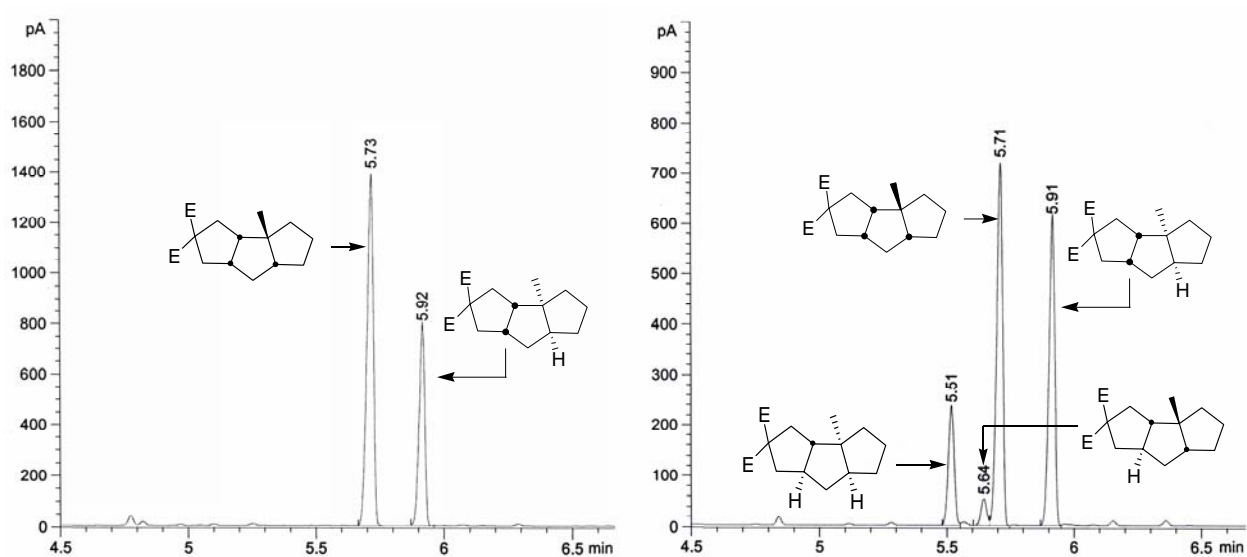
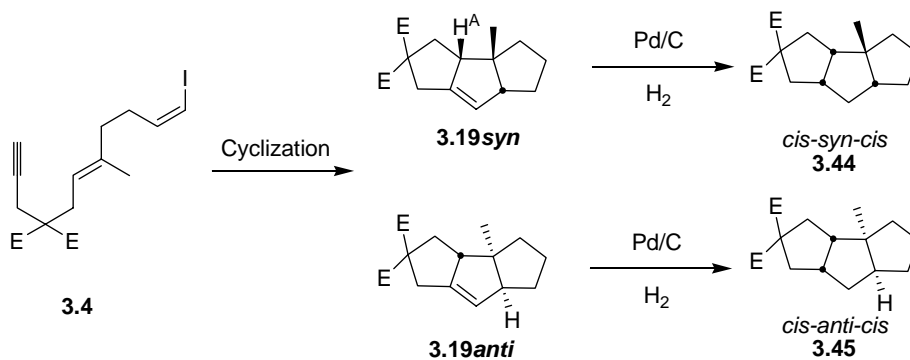


Figure 3-10: a) Left: GC chromatogram of the hydrogenation mixture and b) Right: GC chromatogram of the triquinane mixture from the cyclization of **3.3**. Both GC injections were carried out under the same conditions as described for Figure 3-2.

Table 3-3: Cyclization data for **3.4** and subsequent hydrogenation

Entry	Cyclization Method ^a	Reducing Agent	T (°C)	Cyclization % Composition by NMR		Hydrogenation % Composition by GC		Yield (%) ^b
				3.19_{syn}	3.19_{anti}	3.44	3.45	
1	A	Bu ₃ SnH	25	60	40	60	40	65
2	B	Bu ₃ SnH	80	66	34	66	34	67

^a See Chapter 5 for experimental procedures.

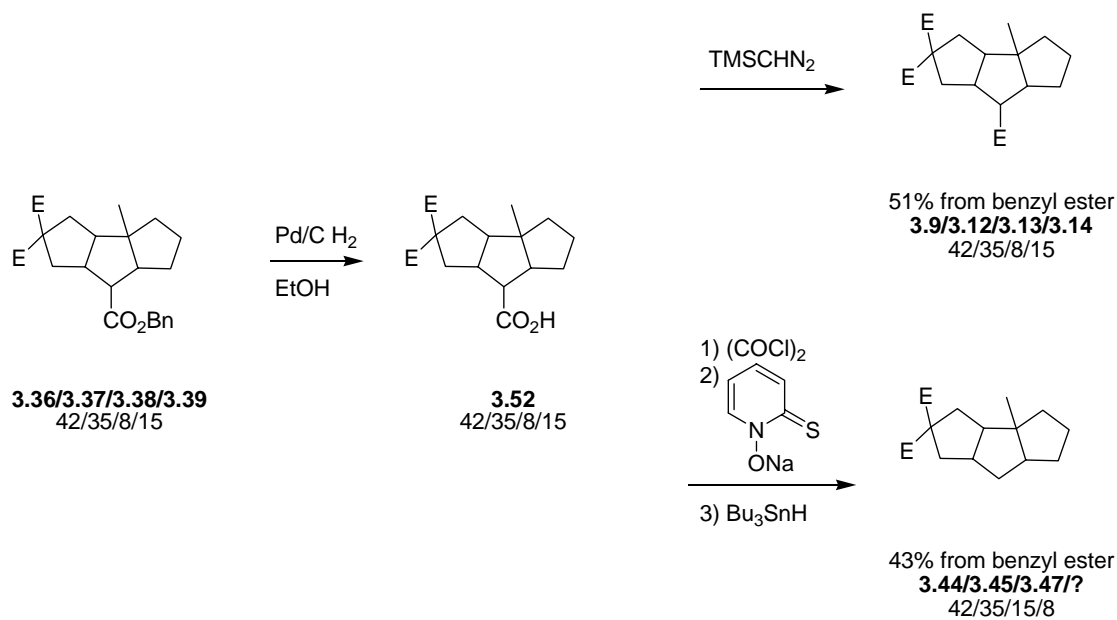
^b Refers to yield over both steps.

The cyclization of substrate **3.4** also showed very little variation in selectivity when carried out at different temperatures, but the clean hydrogenation reaction enabled us to make two conclusions. First, the major product of the radical cyclization of **3.4** is compound **3.19_{syn}** because we could establish that triquinane **3.44** was the major product of the hydrogenation. Second the hydrogenation of compound **3.19** occurs exclusively from the same face as H^A indicated in **3.19_{syn}**. If hydrogenation had occurred from the opposite face, then the *trans* substituted triquinanes **3.46** and **3.47** would have been formed, and these are not visible in the GC chromatogram from the hydrogenation reaction shown in Figure 3-10.

3.4 Stereochemical Relay Between Systems 1.65, 3.2 and 3.3

With the two major products in the cyclization of **1.65** firmly assigned and the minor products tentatively assigned, we relayed the assignments to the products of the cyclizations of **3.2** and **3.3**. This was accomplished by using the benzyl ester in triquinanes **3.36-3.39** as a handle as shown in Scheme 3-6. Treatment of a 42/35/8/15 mixture of benzyl triquinanes **3.36-3.39** with Pd/C under a hydrogen atmosphere in ethanol⁸³ gave the corresponding acids **3.52** as a mixture of four products, which was used without further purification. The acid mixture was

then then split into two portions, and one half was treated with TMSCHN₂ to give a mixture of products **3.9-3.12** in 51% yield from the benzyl triquinanes.⁶⁰ The other half was decarboxylated by using Barton's method²⁰ to give a mixture of tricycles **3.44-3.47** in 43% yield from tricycles **3.36-3.39**.



Scheme 3-6: Stereochemical relay experiments.

The transesterified mixture of triquinanes **3.9-3.12** exhibits 4 peaks upon GC analysis as shown in Figure 3-11. A GC co-injection of the transesterified triquinane mixture with the cyclization mixture obtained directly from **1.65** showed that the retention times of the four products in both mixtures were identical, Figure 3-11. This result confirms our initial assignments for the benzyl triquinanes **3.36-3.44**, because we were able to directly compare our firm assignments for **3.9** and **3.10** to the products arising from the cyclization of the benzyl ester precursor **3.2**.

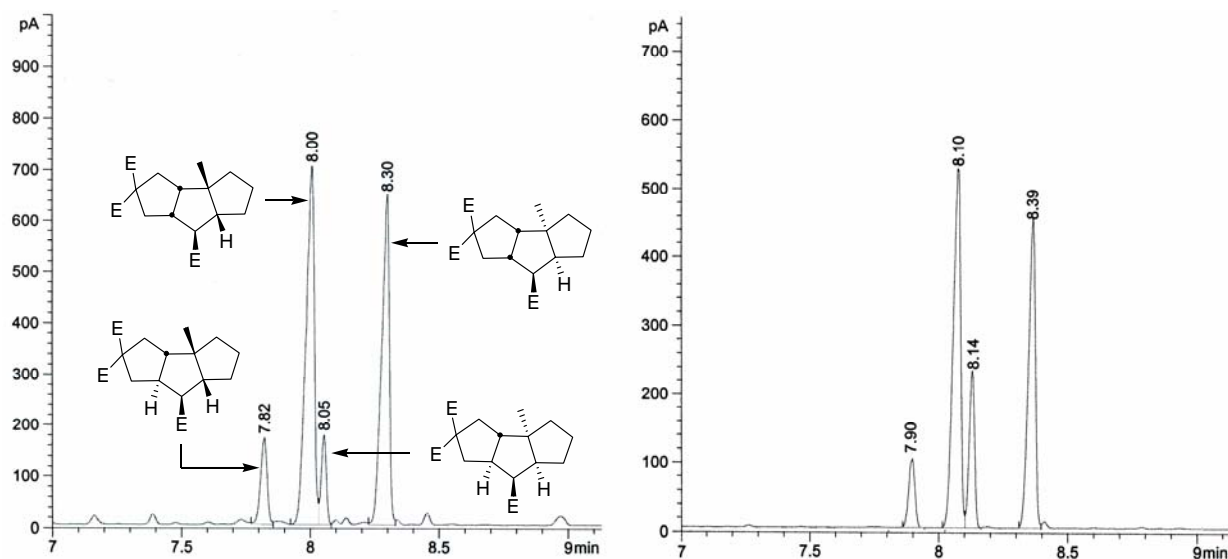


Figure 3-11: a) Left: GC chromatogram of the transesterified mixture **3.9-3.12** and b) Right: Co-injection of the transesterified mixture with the purified cyclization mixture of **1.65**. Both GC injections were carried out under the same conditions as described for Figure 3-2.

The mixture of tricycles from the decarboxylation experiment also showed 4 peaks upon GC analysis, Figure 3-12a. However a co-injection of the decarboxylation mixture with the original cyclization mixture from **3.4**, Figure 3-12b, showed a new product with a retention time of 4.02 min. So this experiment allowed us to confirm the assignments of the two major peaks as the *cis-syn-cis* and the *cis-anti-cis* triquinanes by direct comparison to our firm assignments of **3.9** and **3.10**. However, it only allows us to relay the assignment of *trans-anti-cis* compound **3.46**, because the other minor peak's retention time did not match to that of the cyclization mixture from **3.3**. We considered the possibility that the *trans-syn-cis* **3.39** isomer had epimerized under the decarboxylation conditions to give the new product. However we decided not to pursue this any further because our assignments for the minor products were only tentative and the new product was only present in small amounts (<10%).

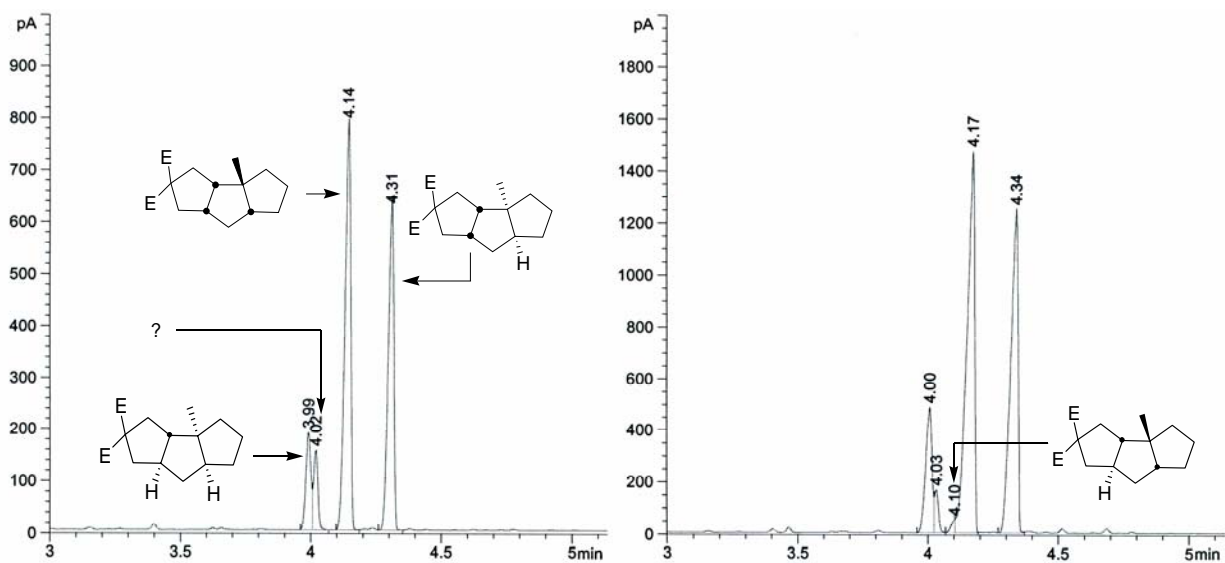


Figure 3-12: a) Left: GC chromatogram of the decarboxylated tricyclic mixture and b) Right: Co-injection of the decarboxylated mixture with the purified cyclization mixture of **3.3**. Both GC injections were carried out under the same conditions as described for Figure 3-2.

In addition to relaying our structural assignments, the decarboxylation experiments allowed us to confirm that the minor products in the cyclization of **1.65** were not epimers at the ester bearing stereocenter; if they were, then removal of the ester group would have given two products where four were clearly observed in the GC chromatogram in Figure 3-12. This observation also supports our conclusion that the minor products in the round trip cascade result from *trans* closure in the second cyclization.

3.5 Uncovering the Origin of the Temperature Effect

We were unable to reproduce the temperature effect that Ihara reports. Even in an exact repeat of his experiments, Table 3-1 entries 11 and 12, the selectivity only improves modestly to 86/14 from 77/23 *cis/trans* when running the reaction at 25 °C instead of 80 °C. This change in temperature however is reported to improve the ratio from 64/36 to 100/0.³⁸ We considered the possibility that this discrepancy did not arise from the way that the experiments were carried out, but in how the amounts of “other diastereomers” were quantified? The process of determining the product ratios was not detailed in the original publication, but Professor Ihara kindly explained his analysis and provided helpful additional data.

The top half of Figure 3-13 shows expansions of the methyl ester region of two separate ¹H NMR spectra that Ihara provided us. Figure 3-13a shows this region when the cyclization

was conducted at 80 °C while Figure 3-13b is representative of a ^1H NMR from a cyclization run at 25°C. Ihara assigned the singlet at 3.67 ppm to the *cis-cyn-cis* isomer **3.9** and the singlet at 3.66 ppm to the *cis-anti-cis* isomer **3.10**. We confirmed these assignments by using our enriched samples from the preparative GC experiments. Ihara then assigned the resonances around 3.68 ppm, highlighted by the boxes in Figure 3-13, as the other diastereomers and the reported product ratios then follow from integration. In comparing the NMR spectra in Figure 3-13a and Figure 3-13b, it is clear how Ihara concluded that this radical cascade cyclization was temperature dependent. However, it turns out that Ihara did not have all of the pieces needed to solve the assignment puzzle.

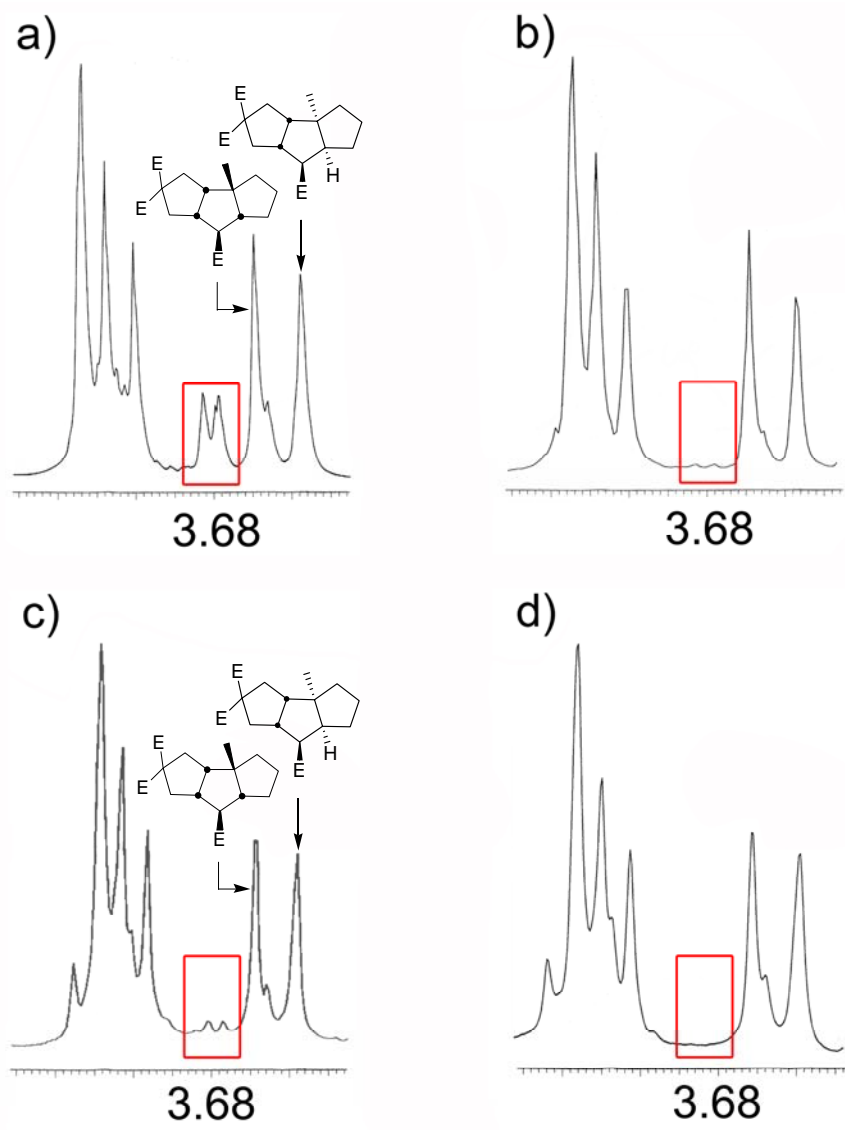


Figure 3-13: Comparison of methyl group resonances in ^1H NMR spectra (CDCl_3) of the reaction products of the cyclization of **1.65**. a) Ihara's spectrum, Bu_3SnH 80 $^\circ\text{C}$; b) Ihara's spectrum, Bu_3SnH 25 $^\circ\text{C}$; c) Our spectrum, Bu_3SnH 80 $^\circ\text{C}$, before *m*-CPBA treatment; d) Our spectrum, Bu_3SnH 80 $^\circ\text{C}$, after *m*-CPBA treatment; Spectra very similar to those shown in c) and d) were obtained when the cyclization was run at 25 $^\circ\text{C}$.

When carrying out the same NMR analysis but on samples from our 80 $^\circ\text{C}$ and 25 $^\circ\text{C}$ experiments, we observed about the same amount of resonances at 3.68 ppm in both cases as expected from the results of our GC analysis. However, if we examined the methyl ester region of our cyclization mixture before *m*-CPBA treatment, Figure 3-13c, and then again afterwards, Figure 3-13d, we noticed that the resonances at 3.68 ppm had disappeared. Accordingly, we conclude that the peaks at 3.68 ppm do not belong to other triquinane diastereomers, but rather to alkene-containing, prematurely reduced products that are removed by the *m*-CPBA oxidation.

Integration of the resonances at 3.68 ppm in Figure 3-10c also approximately matches the integration of the minor peaks in the GC chromatogram that are removed upon treatment with *m*-CPBA.

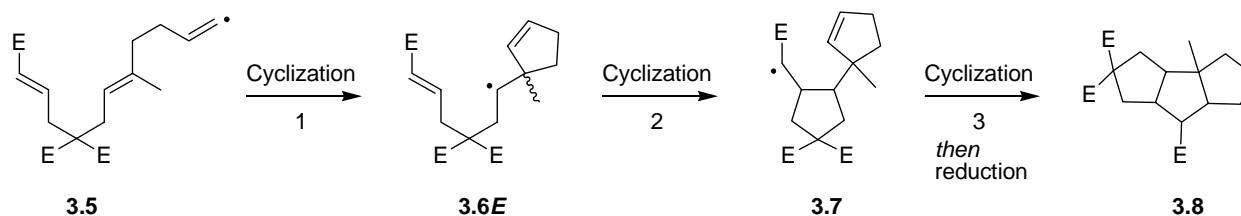
Having corrected the discrepancies in the analysis, we concluded that Ihara had not observed an improvement in the diastereoselectivity of the cyclization, but rather a decrease in the amount of premature reduction when the reaction was run at 25 °C instead of at 80 °C. However, our experiments consistently show that about the same amount of alkene-containing products are formed. At present it is unclear why the amount of prematurely reduced products differ in Ihara and our experiments. Nevertheless, the disappearance of the minor peaks in the GC and the NMR upon *m*-CPBA treatment support our conclusion that the resonances at 3.68 ppm are indeed from alkene containing products. While we have only tentatively assigned structures to the minor products, we have definitely shown that the “other diastereomers” do not have resonances at 3.68 ppm. The problem with using NMR integrations to determine the selectivity is that in the cyclization mixture of **1.65** there are two major products and at least five minor products, all of which have three non-equivalent methyl ester groups. This makes rigorous assignments in the OMe region of the ¹H NMR spectrum difficult. While the GC analysis is not complete, it is more accurate than the NMR analysis because we are able to classify each peak as tricyclic or not, and individually integrate it.

3.6 Transition State Analysis for **1.65** and **3.3**

We have demonstrated that the round-trip radical cyclization of substrates **1.65** and **3.1-3.3** gives two major triquinanes, the *cis-syn-cis* and the *cis-anti-cis* isomer, and two minor triquinanes namely the *trans-anti-cis* and the *trans-syn-cis* isomers. That the *cis* mode of cyclization accounts for 80% of the products in the second cyclization can be nicely rationalized using a Beckwith/Houk transition state analysis. This same model can also be used to explain why changing the geometry of the α,β -unsaturated ester from *E* (**1.65**) to *Z* (**3.1**) improves the selectivity of the second cyclization. While only the cyclization of compound **1.65** will be discussed, the same analysis applies analogously for the other two *E*-geometry α,β -unsaturated ester substrates **3.2** and **3.3**.

3.6.1 Transition State Analysis for the Cyclization of 1.65

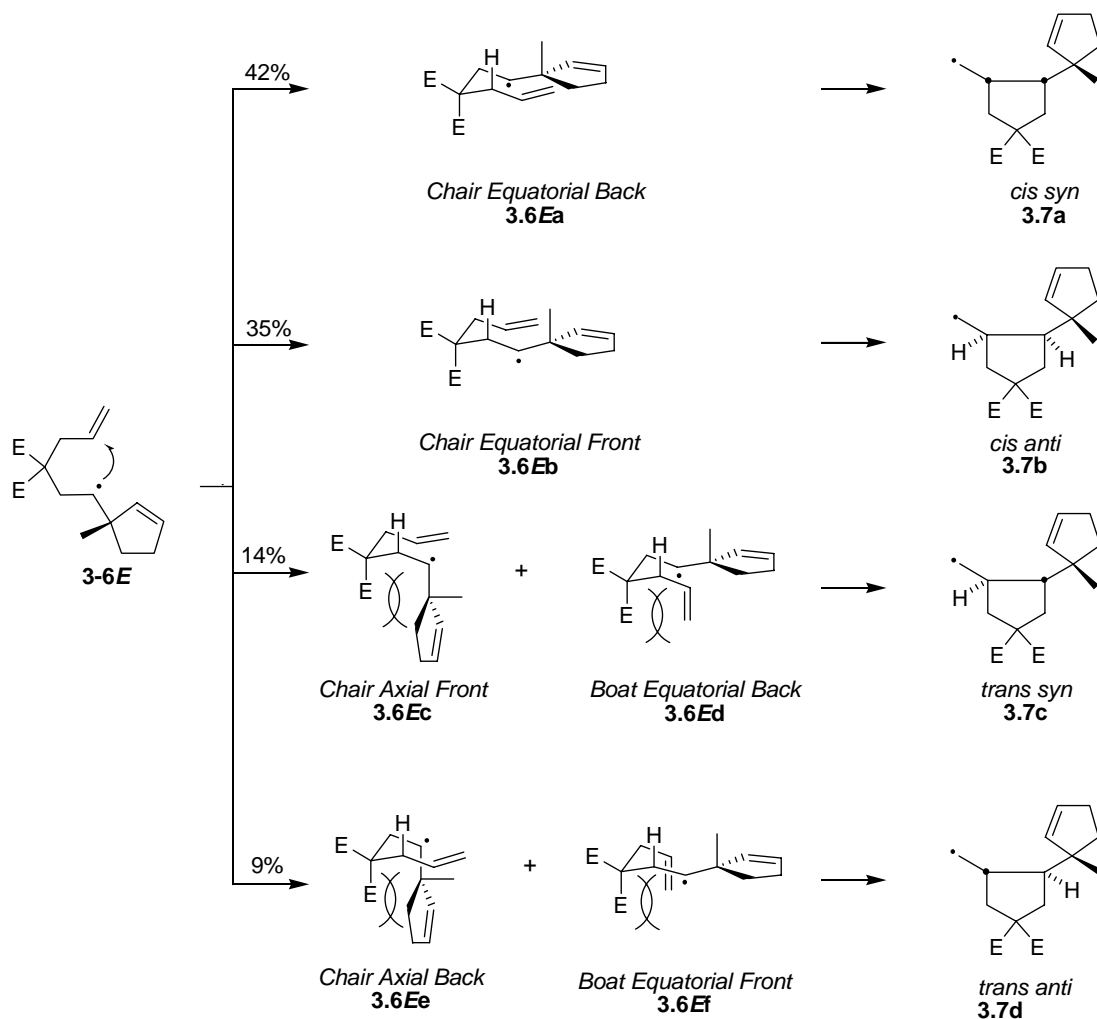
The transition state analysis for substrate **1.65** will be divided into two sections that will cover the second and third cyclizations in the cascade. The first cyclization merely gives a racemic mixture of compounds. The cascade cyclization is summarized in Scheme 3-7 starting with radical **3.5**, which cyclizes in a 5-*exo* fashion to give radical **3.6E**. A second 5-*exo* cyclization event gives radical **3.7** which then undergoes the third and final cyclization to give triquinanes **3.8** upon reduction.



Scheme 3-7: Summary of the round-trip radical cyclization.

In the second cyclization, radical **3.6E** cyclizes to give four bicyclic radicals **3.7Ea-d** as shown in Scheme 3-8. Four products arise because the adjacent stereocenter from the first cyclization makes 1,2 stereo-induction possible and two new stereocenters are established during the cyclization by placing the substituents either *cis* or *trans* to each other. The four product radicals are labeled either *cis* or *trans* based on the relationship of the ring substituents in the A ring and *syn* or *anti* based on the relationship between the methyl group and proton H^A, as shown in **3.7a**, Scheme 3-8.

These four products arise from eight transition states, but the two *axial boat* transition states will be ignored, leaving six to consider. Four of these transition states are chairs and the remaining two are boats. All six transition states are shown in Scheme 3-8 and are labeled either *chair* or *boat* depending on their conformation, *equatorial* or *axial* depending on the orientation of the group in the 1 position and *front* or *back* depending on the face of the olefin being attacked by the radical. As an example, transition state **3.6Ea** is named *chair-equatorial back* and inclusion of the *E* in the numbering is necessary to distinguish these transition states from the *Z*-unsaturated ester analogues to be discussed later.



Scheme 3-8: Transition states and products for the cyclization of radical **3.6E**.

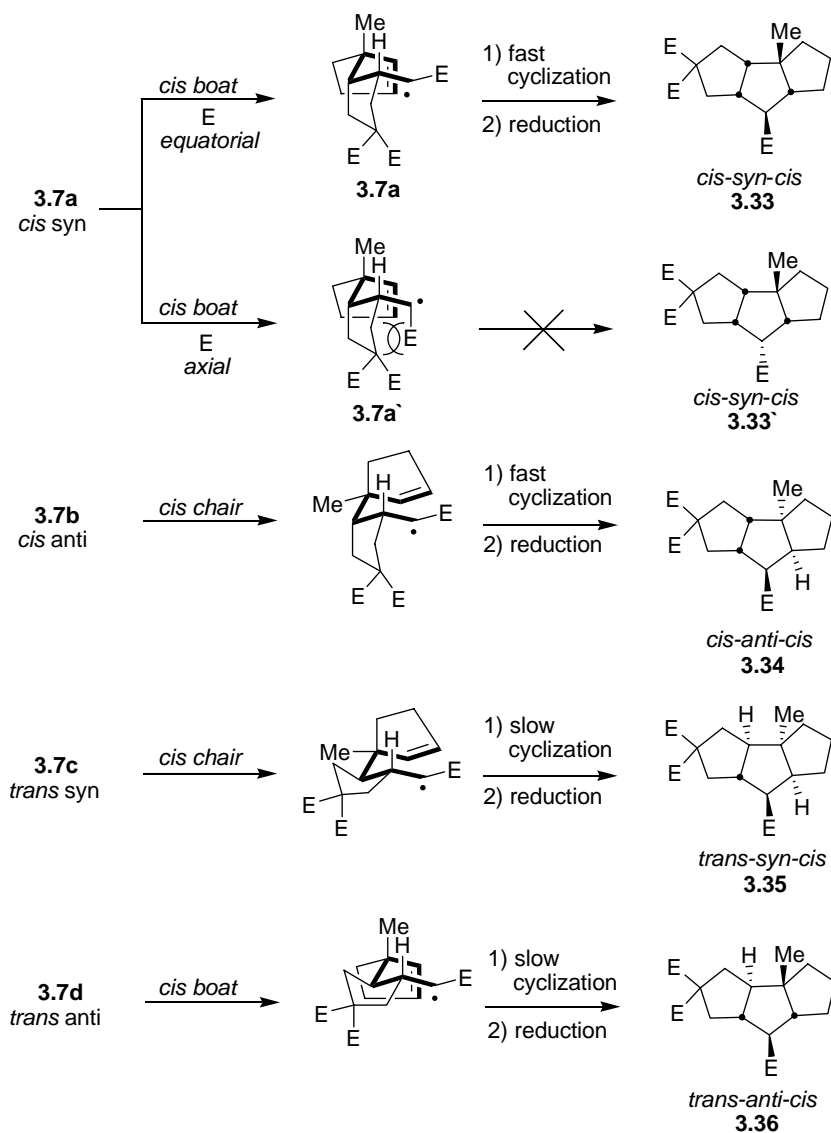
When radical **3.6E** adopts a *chair-equatorial* conformation with the olefin approaching the front face of the radical, transition state **3.6Ea** results and the ensuing 5-*exo* cyclization proceeds to give the *cis syn* product **3.7a**. Transition state **3.6Eb** also has a *chair-equatorial* conformation, but the olefin approaches the back face of the radical and so the cyclization gives the *cis anti* product **3.7b**. The *trans syn* product **3.7c** comes from transition states **3.6Ec** and **3.6Ed**. Likewise the final two transition states **3.6Ee** and **3.6Ef** both lead to the *trans anti* product radical **3.7d**. Four of these six transition states, **3.6Ec-f**, are disfavored by the 1,3 diaxial interactions that are indicated in Scheme 3-8. These interactions result in products **3.7c** and **3.7d** only making up 14% and 9% of the final cyclization mixture, respectively. Transition states

3.6Ea and **3.6Eb** have no axial like interactions and are therefore more favored. For this reason, products **3.7a** and **3.7b** make up 42% and 35% of the mixture of bicyclic radicals, respectively.

The cascade reaction is now poised to undergo the third and final 5-*exo* radical cyclization. This final cyclization, however, proceeds to give exclusively *cis* products because it forms a fused 5,5 ring system.³⁶ This greatly simplifies the analysis because there is only one possible transition state for each of the four radicals **3.7** that can give the 5,5 *cis* fused geometry as shown in Scheme 3-9.²⁶ In this final cyclization, the configuration of the ester stereocenter is also set and so in the transition state the ester group can be placed either equatorial or axial as shown in structures **3.7a** and **3.7a'**. Placing the ester group in the axial position induces a high energy 1,2 interaction with the adjacent ring and there is literature precedent that 1,2 substituted radicals give only a single product.⁸⁴ We assume that each bicyclic radical gives a single ester epimer and will therefore ignore the transition states with an axial ester group for the radicals **3.7b-d**.

In order to furnish a 5,5 *cis* fusion, *cis syn* radical **3.7a** must adopt a *cis boat* transition state which gives the *cis-syn-cis* tricycle **3.33** when the hexenyl radical cyclizes and is reduced. The *cis anti* radical **3.7b** must adopt a *cis chair* transition state in order to give the *cis* fusion, leading to the *cis-anti-cis* product **3.34** upon closure and reduction of the radical. Similarly, radicals **3.7c** and **3.7d** cyclize through a *cis chair* and a *cis boat* transition state, respectively, to give the *trans-syn-cis* **3.35** and the *trans-anti-cis* **3.36** tricycles.

The rate of the final cyclization is strongly influenced by the strain contained in the final product. The more strained the linear triquinane product is, the slower this final cyclization will be.³⁵ Therefore, the *cis* products from the second cyclization, radicals **3.7a** and **3.7b**, close faster to give the respective products whereas radicals **3.7c** and **3.7d** cyclize slower to give the more strained *trans* substituted triquinanes. This slow final step allows for a greater competition between cyclization and premature reduction to give bicyclic products. For that reason the *cis/trans* ratios that we report may be overstated in favor of *cis* selectivity because the bicyclic products that are removed during the *m*-CPBA workup will predominantly be from the *trans* closure in the second cyclization.

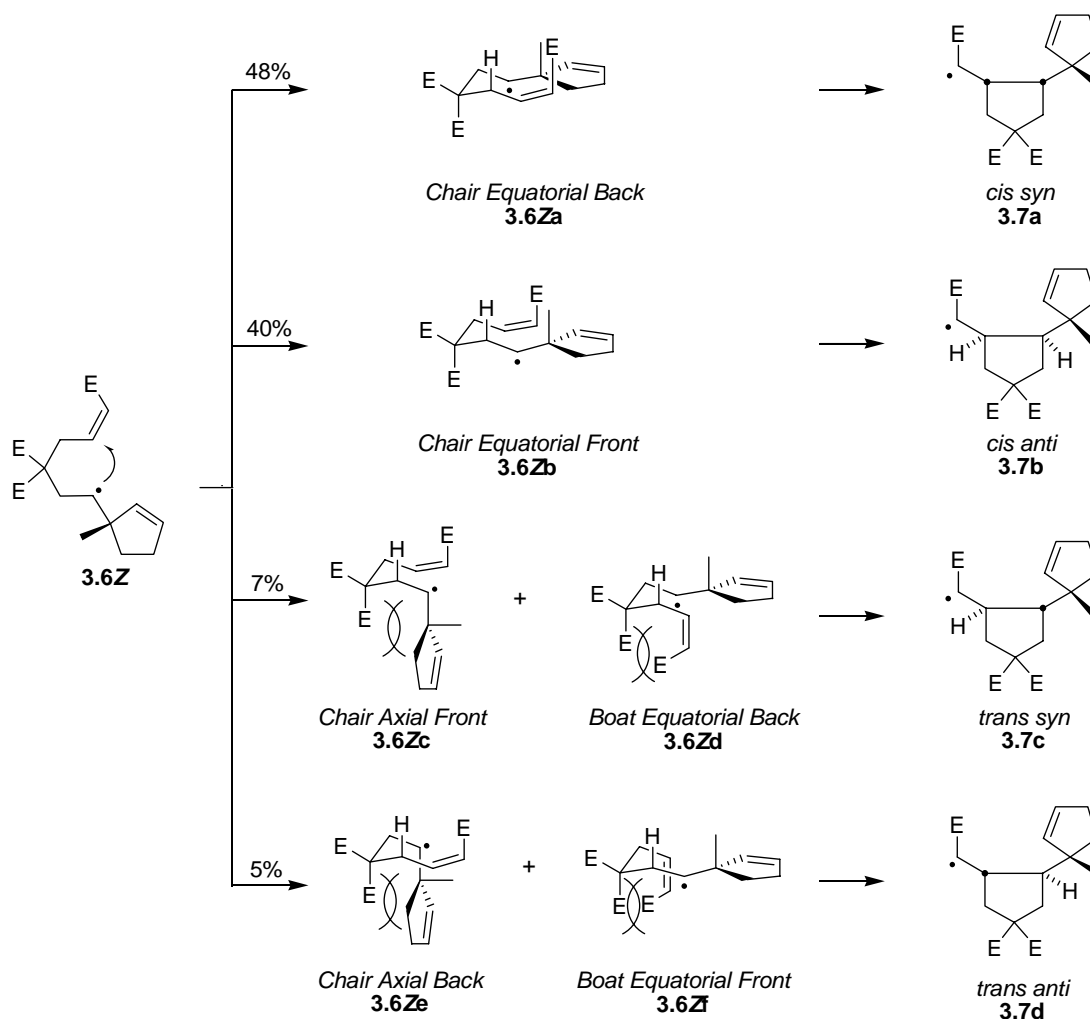


Scheme 3-9: Transition states and products for the cyclization of radical **3.6**.

3.6.2 Transition State Analysis for the Cyclization of **3.1**

From Table 3-1 Entries 2 and 6, we show that we can improve the selectivity for the second cyclization from 78/22 to 88/12 *cis/trans* by using the *Z* α,β -unsaturated ester cyclization precursor **3.1** instead of the *E* unsaturated ester precursor **1.65**. This improvement can be explained by revisiting the transition states for the second cyclization with the different geometry as shown in Scheme 3-10.⁷⁴ Similar to the analysis of substrate **1.65**, upon initiation and propagation vinyl iodide **3.1** is converted into a vinyl radical (not shown). This radical cyclizes to give cyclopentenyl radical **3.6Z**. Radical **3.6Z** can adopt six different transition states and

they are all shown in Scheme 3-10, again the two *boat axial* transition states are ignored. If the radical adopts a *chair equatorial* configuration with the radical approaching the back face of the olefin, transition state **3.6Za** results; this hexenyl radical then cyclizes to give *cis syn* product **3.7a**. Similarly the *cis anti* product **3.7b** arises from the *chair equatorial front* **3.6Zb** transition state. The *trans syn* product **3.7c** is produced when the hexenyl radical adopts either the *chair axial front* **3.6Zc** or the *boat equatorial back* **3.6Zd** transition state. Finally the *trans anti* product **3.7d** comes from transition states **3.6Ze** and **3.6Zf**.



Scheme 3-10: Transition state analysis for the second radical cyclization of vinyl iodide **3.1**.

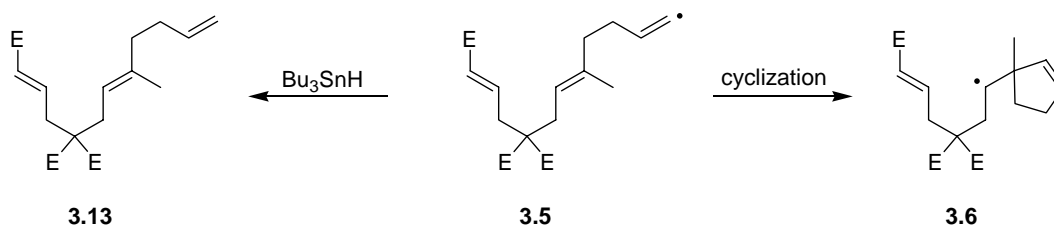
The improved selectivity in the cyclization can be attributed to the additional destabilizing interactions that the *Z*-unsaturated ester introduces into transition states **3.6Zd** and

3.6Zf. In comparison to the *E* analogues, the *Z* vinyl ester is forced back under the forming ring resulting in a collision with the malonate ester at position 3. This interaction significantly raises the energetic cost of accessing the boat transition states. The increased energetic cost causes a shift in the partitioning of the products towards **3.6Za** and **3.6Zb** and away from **3.6Zd** and **3.6Zf**. This new partitioning accounts for the 48/40/7/5 ratio of cyclization products **3.7a/b/c/d** that we observe in this cyclization as opposed to the 42/35/14/9 ratio that we found in the case of the *E* unsaturated ester cyclization. The products of the second cyclization are the same for the *Z* and the *E* olefin, so the transition state analysis for the third cyclization is the same as that shown in Scheme 3-9.

3.7 Kinetics of Cyclization

Under the standard cyclization conditions, the concentration of vinyl iodide **1.65** was 2 mM in benzene. If we increased this concentration to 10, 50 and 250 mM, we noticed that the amount of directly reduced product **3.13** increased at the expense of the tricycles. This indicates that the first cyclization of vinyl radical **3.5** to give radical **3.6** is the rate determining step of the entire cascade. Given that we can measure the amount of directly reduced product that is formed at the different reaction concentrations, we can estimate the rate constant of the first cyclization by using competition kinetics.⁸⁵

The competition in this case is between the reduction of **3.5** by Bu₃SnH to give **3.13** or intramolecular rearrangement (cyclization) to give radical **3.6** as shown in Scheme 3-11. Once the first cyclization occurs, the cascade proceeds rapidly through the remaining two cyclizations and reduction to give the tricyclic products. Plotting the ratio of the cyclized products (**3.9-3.12**) to directly reduced product **3.13** against the concentration of Bu₃SnH should give a straight line. The slope of this line is the ratio of the rate constants for reduction and rearrangement. The rate constants for the reduction of many types of radicals by Bu₃SnH are known.⁸⁶ Therefore we can readily calculate the rate of cyclization from the slope of the trend line.



Scheme 3-11: Rate determining step in the cyclization of **1.65**.

To determine the rate constant for the first cyclization at 25 °C, we performed four cyclizations at concentrations of 2, 10, 50, and 250 mM with respect to the cyclization precursor. This was done by dissolving vinyl iodide **1.65** (0.10 mmol), Et₃B (0.05 mmol), and Bu₃SnH (0.12 mmol) in the appropriate amount of benzene (2 mM = 50 mL, 10 mM = 10 mL, 50 mM = 2 mL and 250 mM = 0.4 mL). The reactions were stirred for 4 h, concentrated *in vacuo*, and subjected to a DBU workup to remove the tin by-products. Each reaction mixture was then analyzed by GC. The ratio of the reduced product to the cyclized products was determined by dividing the area of the peak known to come from **3.13** by the sum of the areas of the four tricyclic peaks **3.9-3.12**. This data is summarized in Table 3-4. In these experiments, the concentration of the reducing agent changes throughout the course of the reaction. For rate calculations, a good approximation of the reducing agent concentration is to use the amount of reaction solvent and the moles of reducing agent when 50% of the cyclization precursor has been consumed. Because we used 1.2 equiv of Bu₃SnH to 1.0 equiv of precursor, we used 0.7 equiv of reducing agent to calculate the concentration for a particular cyclization.

Table 3-4: Data for the cyclization of **1.65** at 25 °C at four different concentrations of reducing agent.

Concentration	Volume of Benzene (mL)	% of Reduced Product 3.13	% of Cyclized Products	Cyclized/Reduced	Concentration of Bu ₃ SnH
2	50	5	95	0.0526	0.0014
10	10	9	91	0.0989	0.0070
50	2	28	72	0.3889	0.0350
250	0.4	58	42	1.3809	0.1750

From this data, we plotted the cyclized/reduced ratio against the Bu₃SnH concentration to generate the plot shown in Figure 3-14. Linear regression analysis of these four data points generated a trend line that is also shown in Figure 3-14. The slope of this line is 7.6 and is equal to $k_{\text{red}}/k_{\text{cycl}}$. The rate of reduction (k_{red}) for a vinyl radical by Bu₃SnH at 25 °C has been reported

as $3.2 \cdot 10^8 \text{ M}^{-1}\text{s}^{-1}$. This rate constant was measured by laser flash photolysis and from this data the Arrhenius parameters were calculated.⁸⁷ Unfortunately, the rate measurements were carried out in pentane on a 1,1 substituted vinyl radical where our experiments involve a mono substituted vinyl radical in benzene, but we do not anticipate that either of these differences will affect the outcome of the calculations significantly. The rate constant calculation for the cyclization of **1.65** at 25 °C is shown in equation 1 and was found to be $4.2 \cdot 10^7 \text{ s}^{-1}$. This rate is reasonable because radical cyclizations often occur with rate constants on the order of 10^8 s^{-1} .

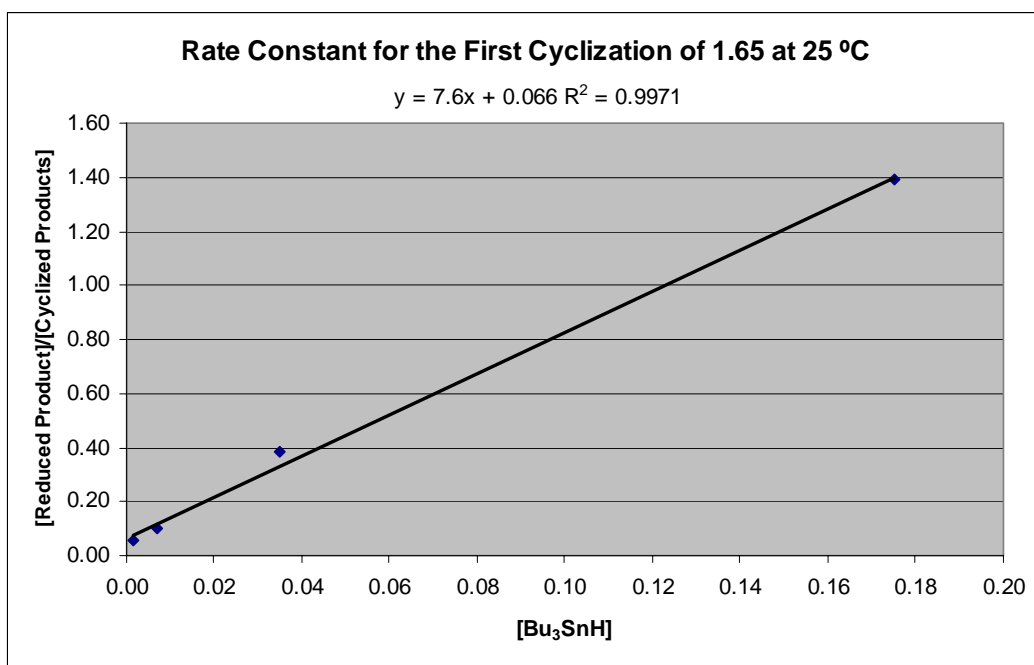


Figure 3-14: Plot used for determining the rate constant for the cyclization of **1.65** at 25 °C.

$$k_{cyclization,25^\circ\text{C}} = \frac{3.2 \cdot 10^8}{7.6} = 4.2 \cdot 10^7 \text{ s}^{-1} \quad (\text{eq. 1})$$

We then wanted to determine the rate constant for this cyclization at 80 °C and so repeated the cyclization experiments with **1.65**, but in refluxing benzene and with AIBN instead of Et₃B as the radical initiator. As before the four reactions we analyzed by GC and provided us with the necessary data shown in Table 3-5. Using this data we generated the plot shown in Figure 3-15 along with the calculated trend line.

Table 3-5: Data for the cyclization of **1.65** at 80 °C at four different concentrations of reducing agent.

Concentration	Volume of Benzene (mL)	% of Reduced Product 3.13	% of Cyclized Products	Cyclized/Reduced	Concentration of Bu ₃ SnH
2	50	7	93	0.0753	0.0014
10	10	6	94	0.0638	0.0070
50	2	14	86	0.1628	0.0350
250	0.4	31	69	0.4493	0.1750

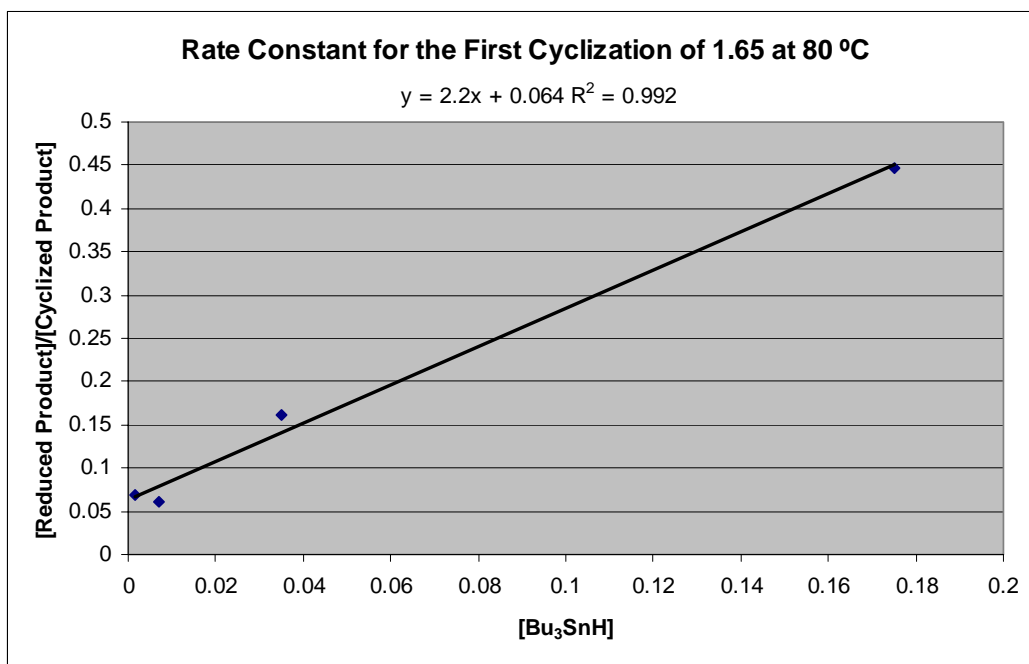


Figure 3-15: Plot used for determining the rate constant for the cyclization of **1.65** at 80 °C.

Using the reported Arrhenius parameters⁸⁷ we calculated the rate constant for the reduction of a vinyl radical by Bu₃SnH to be $5.1 \cdot 10^8 \text{ M}^{-1} \text{ s}^{-1}$. With the slope of the trend line and this rate constant we could calculate the rate constant for the radical cyclization at 80 °C as shown in equation 2.

$$k_{\text{cyclization},80^\circ\text{C}} = \frac{5.1 \cdot 10^8}{2.2} = 2.3 \cdot 10^8 \text{ s}^{-1} \quad (\text{eq. 2})$$

As expected, the cyclization at elevated temperatures is faster than it is at ambient temperature. However, the rate constant only increased by a factor of 5.5 even though the temperature increased by 60 °C. Using the normal rule of thumb that an increase of 10 °C doubles the rate of a reaction one expects an increase in rate constant of 64 times. Radical

reactions are less sensitive than ionic reactions to temperature and an increase of 5.5 times over 60 °C is in line with other cyclizations.⁴¹

3.8 Conclusions

The results presented in this chapter build upon the work presented in Chapter 2, where we showed that hexenyl radicals with large groups in the 1 position cyclize with an 80/20 *cis* preference. We have shown that this trend extends to relatively complex substrates such as **1.65**, **3.1**, **3.2**, and **3.3** with these cyclizations also proceeding with an 80/20 *cis* preference. This trend allowed Ihara to reduce the complexity of a round-trip radical cyclization to the point that two tricyclic products the *cis-syn-cis* and the *cis-anti-cis* isomer account for 80% of the products. We further increased the amount of these two products to 90% by changing the geometry of α,β -unsaturated ester from *E* to *Z*. Additionally we have shown that any increase in selectivity proposed by lowering the temperature is in fact an artifact of the analysis method.

Chapter 4 Conclusions

In this work we have presented a consistent picture of the stereoselectivity of hexenyl radical cyclizations with tertiary groups in the 1 position and a geminal malonate substitution in the 3 position. It has been demonstrated that such cyclizations proceed with moderate *cis* selectivity and that this selectivity is not affected by the nature of tertiary group, the presence of an ester on the radical acceptor or reaction temperature. Fortunately we have also shown that this stereochemical trend not only holds for simple substrates such as **2.4**, but also extends to relatively complex cascade cyclization precursors such as **1.65** and **2.10**.

The research presented and discussed in this thesis was in part initiated by a publication that reported a dramatic temperature effect for hexenyl radical cyclizations. This work though clearly shows that the reported temperature effect is an analytical oversight. None the less it is important to understand why these reactions do not exhibit a change in their selectivity upon changing the reaction temperature.

By examining a reaction coordinate diagram of the radical cyclizations, it is possible to find an underlying reason for the observed lack of a temperature effect. Using the cyclization of radical **2.2a** as an example, the Gibbs free energy diagram shown in Figure 4-1 can be drawn. Starting in the middle with hexenyl radical **2.2a** and heading to the left, the conformation approaches a local maximum at transition state **2.2aA**. By proceeding further to the left, radical **2.2aA** cyclizes and approaches the local minima of radical **4.1cis**. Once again starting in the middle and proceeding to the right a local maxima is reached corresponding to **2.2aB** and **2.2aC**. Both of these radicals then cyclize to give **4.1trans** shown in the resulting local minima.

In this analysis we are assuming, not unreasonably, that either cyclization is irreversible. This means that the product distribution is not going to depend on the free energy difference between the two product radicals **4.1cis** and **4.1trans**, but on the free energy difference of the respective transition states **2.2aA** and **2.2aB**, **2.2aC**. The energy difference in the transition state energies is represented by $\Delta\Delta G^\ddagger$.

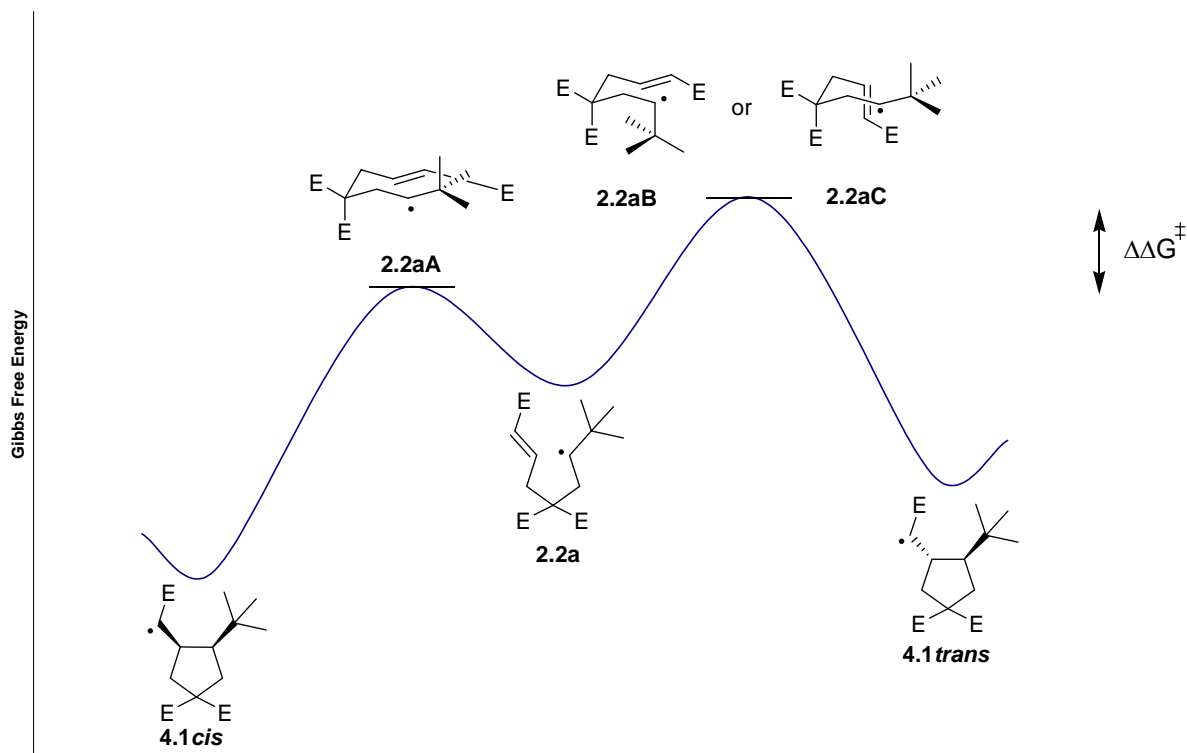


Figure 4-1: Reaction coordinate diagram for the cyclization of hexenyl radical **2.2a**.

Following from the Gibbs free energy equation, we can derive the following equation for $\Delta\Delta G^\ddagger$:

$$\Delta\Delta G^\ddagger = \Delta\Delta H^\ddagger - T\Delta\Delta S^\ddagger$$

The small temperature effect that is observed in all of the cyclizations indicates that the contribution from the $T\Delta\Delta S^\ddagger$ term to $\Delta\Delta G^\ddagger$ is very small. With the $T\Delta\Delta S^\ddagger$ term being very small, the free energy equation for the cyclization can be simplified to the following:

$$\Delta\Delta G^\ddagger = \Delta\Delta H^\ddagger$$

As the above equation indicates, the ratio of the final products depends only on the $\Delta\Delta H^\ddagger$ of the reaction. The $\Delta\Delta H^\ddagger$ of the cyclization is not entirely independent of the reaction temperature, but the relationship between the two is complicated and therefore not outright expressed in the equation. However the temperature dependence of $\Delta\Delta H^\ddagger$ is responsible for the minor temperature selectivity that was observed in the cyclization experiments.

This simplified free energy equation relies on $\Delta\Delta S^\ddagger$ being small and there are two situations that can allow for this 1) both ΔS^\ddagger terms for the separate cyclizations are zero or 2) both ΔS^\ddagger values are very close in value and thus the difference of the two is small. The more likely cause for the $\Delta\Delta S^\ddagger$ term being small is that the two individual values of ΔS^\ddagger are close. This is reasonable because in order to reach the two transition states about the same amount of bond rotation is necessary making the value of ΔS^\ddagger in both cases very close.

Additionally during the course of this work it was discovered that the *cis* and *trans* assignments for a key stereochemical literature benchmark were reversed. This is an important discovery that may have some crucial consequences in the planning of cascade cyclizations in the future. With this finding, however, we have further solidified the “1,2-*cis* selectivity” in cyclizations of 1-substituted hexenyl radicals as one of the most general stereochemical trends in radical cyclizations.

Chapter 5 Experimental Procedures

The experimental procedures chapter is broken up into four sections. Chapter 5.1 contains all of the general procedures that were used for all of the experiments reported here. Chapter 5.2 is a general description of how the various radical cyclization reactions were carried out. Chapter 5.3 and Chapter 5.4 cover the experimental procedures and compound characterization data for the chemistry discussed in chapters 2 and 3, respectively.

5.1 General Experimental

All reactions were performed under an atmosphere of argon unless the reaction solvent contained water. The reaction times reported were dictated by TLC analysis of the reaction mixture in comparison to the starting material. Reaction solvents were freshly dried either by distillation or passing through an activated alumina column. Methylene chloride was distilled from CaH₂ and toluene, benzene, diethyl ether and THF were distilled from Na/benzophenone. Solvents dried by activated alumina were done according to Pangborn, A.B.; Giardello, M. A.; Grubbs, R. H.; Rosen, R. K.; Timmers, F. J. *Organometallics* **1996** *15*, 1518-1520.

¹H and ¹³C NMR spectra were taken on a Bruker models Avance DPX 300 (300 MHz), Avance 300 (300 MHz), Avance DRX 500 (500 MHz), or an Avance 600 (600 MHz) NMR spectrometer. Chemical shifts are reported in parts per million (ppm) downfield relative to TMS using the residual solvent proton resonance of CDCl₃ (7.27 ppm) or central CDCl₃ carbon peak (77.0 ppm) as an internal standard. In reporting spectral data the format (δ) chemical shift (multiplicity, *J* values in Hz, integration) was used with the following abbreviations: s = singlet, br s = broad singlet, d = doublet, t = triplet, q = quartet, p = pentet, m = complex multiplet, dd = doublet of doublets, dt = doublet of triplets, dq = doublet of quartets, dm = doublet of multiplets, tt = triplet of triplets, tm = triplet of multiplets, ddd = doublet of doublet of doublets, ddt = doublet of doublet of triplets.

Infrared spectra were taken on a Mattson Genesis Series FTIR using thin film or neat deposition on NaCl plates. Peaks are reported in wavenumbers (cm⁻¹). Low and high resolution electronic impact mass spectra were obtained on a Micromass Inc, Autospec with an E-B-E geometry. Chemical ionization spectra were taken on the same instrument using methane as the carrier gas. All peaks reported are in units of *m/e*.

Gas chromatograms (GC) were run on an Agilent 6850 gas chromatograph equipped with HPCHEM enhanced integrator software. An HP-1 capillary methyl siloxane column of 30 m in length and 0.32 mm in diameter with a 0.25 μm film was used for all runs. GC data is reported with a retention time and % area of the total integrated area.

Thin layer chromatography was performed on silica gel 60 F₂₅₄ glass backed plates with a layer thickness of 0.25 mm manufactured by E. Merck. TLC visualization was performed by illumination with a 254 nm UV lamp or by staining with phosphomolybdic acid or permanganate solution and subsequent heating. Flash chromatography was performed on silica gel (230–400 mesh ASTM) purchased from Sorbtech or Bodman.

5.2 General Cyclization Procedures

Method A: General procedure for the radical cyclization reactions at fixed reducing agent concentrations at 25 °C temperature: To the cyclization precursor (0.1 mmol) in benzene (45 mL) was added the reducing agent (0.12 mmol) drop wise as a solution in benzene (5 mL). The reaction mixture was stirred and Et₃B (1.0M in hexanes, 0.05 mL, 0.05 mmol) was added. The mixture was stirred until GC analysis showed consumption of the starting material at which point the solvent was removed *in vacuo* to give the crude cyclization mixture.

Method B: Radical cyclization reactions at fixed reducing agent concentrations at 80 °C: To the cyclization precursor (0.1 mmol) in benzene (40 mL) was added AIBN (8.2 mg, 0.05 mmol) in benzene (5 mL). The reaction mixture was stirred and the reducing agent (0.12 mmol) was added drop wise as a solution in benzene (5 mL). The mixture was brought to reflux until GC analysis confirmed consumption of the starting material. The reaction was cooled to room temperature and the solvent was removed *in vacuo* to give the crude cyclization mixture.

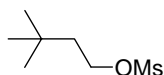
Method C: Radical cyclization reactions with syringe pump addition of the reducing agent at 25 °C: To the cyclization precursor (0.1 mmol) in benzene (50 mL) was added Et₃B (1.0M soln in hexanes, 0.05 mL, 0.05 mmol). The reaction mixture was stirred vigorously and the reducing agent (0.12 mmol in 5 mL of benzene) was added via syringe pump over 3 h. The reaction mixture was stirred until GC analysis confirmed consumption of the starting material.

The benzene was then removed by rotary evaporation *in vacuo* to yield the crude cyclization mixture.

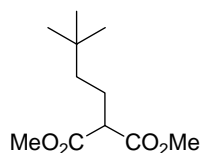
Method D: Radical cyclization reaction with syringe pump addition of the reducing agent at 80 °C: To the cyclization precursor (0.1 mmol) in benzene (45 mL) was added AIBN (8.2 mg, 0.05 mmol) as a solution in benzene (5 mL). The reaction mixture was stirred, brought to reflux and the reducing agent (0.12 mmol in 5 mL of benzene) was added via syringe pump through the condenser over 3 h. The reaction mixture was stirred until GC analysis confirmed consumption of the starting material. The reaction was allowed to cool to room temperature and the benzene was then removed by rotary evaporation *in vacuo* to yield the crude cyclization mixture.

5.3 Experimental Procedures and Characterization Data for Chapter 2

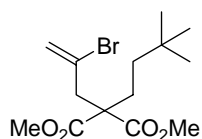
5.3.1 Synthesis of Cyclization Precursor 2.4



Methanesulfonic acid 3,3-dimethylbutyl ester (2.16): To a stirred solution of 3,3-dimethylbutanol (10.0 g, 97.9 mmol) in CH₂Cl₂ (500 mL) was added NEt₃ (28.3 mL, 202.7 mmol) and mesyl chloride (8.7 mL, 111.9 mmol) at room temperature. The resulting solution was stirred for 3 h and then diluted with water (10 mL). The layers were separated and the aqueous layer was extracted with CH₂Cl₂ (2 x 100 mL). The combined organic layers were washed with a satd aqueous solution of NaHCO₃ (200 mL). The combined organic layers were dried over MgSO₄, filtered and concentrated *in vacuo* to give 17.6 g of mesylate **2.16** (100%) as a dark brown oil that solidified upon cooling to -20 °C. The mesylate could be used in subsequent reactions without further purification: IR (thin film, CH₂Cl₂) 3059, 2985, 2962, 1423, 1357, 1335, 1259, 1174, 950 cm⁻¹; ¹H NMR (300 MHz, CDCl₃) δ 4.28 (t, *J* = 7.6 Hz, 2H), 3.00 (s, 3H), 1.69 (t, *J* = 7.4 Hz, 2H), 0.96 (s, 9H); ¹³C NMR (75 MHz, CDCl₃) δ 67.7, 42.1, 37.4, 29.7 29.4 (3C); MS *m/e* 181, 135, 133, 125, 124, 97, 85, 84, 69, 57; HRMS exact mass calcd for C₇H₁₇O₃S: 181.0898, found: 181.0906.



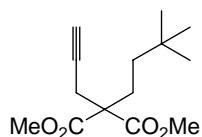
2-(3,3-Dimethylbutyl)malonic acid dimethyl ester (2.17): Mesylate **2.16** (18.4 g, 102.2 mmol) was dissolved in THF (250 mL) and then quickly poured into a stirred suspension of NaI (15.3 g, 102.2 mmol) in THF (500 mL). The reaction mixture was heated at reflux for 16 h at which point ^1H NMR analysis showed complete consumption of the mesylate and the reaction mixture was allowed to cool to room temperature. In a separate flask, dimethyl malonate (20.2 g, 153.3 mmol) was added drop wise to a suspension of NaH (95 % dry, 3.7 g, 153.3 mmol) in THF (350 mL) at 0 °C. Upon complete addition of the dimethyl malonate, the THF solution of 1-Iodo-3,3-dimethylbutane was cannulated into the reaction mixture. The resultant mixture was heated at reflux for 8 h, cooled to room temperature, quenched with water (300 mL) and extracted with ethyl acetate (3 x 250 mL). The combined organic layers were dried over MgSO_4 , filtered and concentrated *in vacuo* to give the title compound. Purification over silica gel eluting with hexanes/ethyl acetate (15/1) gave 11.4 g of **2.17** (52%) as a clear, pale yellow oil: IR (film, CH_2Cl_2) 2956, 1733, 1436, 1272, 1248, 1147 cm^{-1} ; ^1H NMR (300 MHz, CDCl_3) δ 3.70 (s, 6H), 3.25 (t, $J = 7.5$ Hz, 1H), 1.88–1.79 (m, 2H), 1.16–1.10 (m, 2H), 0.85 (s, 9H); ^{13}C NMR (75 MHz, CDCl_3) δ 169.8 (2C), 52.3 (2C), 52.2, 41.3, 30.2, 29.0 (3C), 24.2; MS m/e 217 ($\text{M}^+ + \text{H}$), 201, 185, 159, 132, 57; HRMS exact mass calcd for $\text{C}_{11}\text{H}_{21}\text{O}_4$ ($\text{M} + \text{H}$) $^+$ 217.1439, found 217.1444.



2-(2-Bromoallyl)-2-(3,3-dimethylbutyl)malonic acid dimethyl ester (2.4): To a stirred suspension of NaH (95% dry, 31 mg, 1.27 mmol) in THF (25 mL) cooled to 0 °C was added malonate **2.17** (250 mg, 1.16 mmol) drop wise. Upon complete addition of the malonate, 2,3-dibromopropene (Acros technical grade is 80% pure, 0.15 mL, 1.27 mmol) was added and the resulting mixture was stirred at room temperature for 16 h. The mixture was quenched with water (5 mL) and then extracted with ethyl acetate (3 x 10 mL). The combined organic layers

were dried over MgSO₄, filtered and concentrated *in vacuo* to give the title compound. Purification over silica gel eluting with hexanes/ethyl acetate (10/1) yielded 281 mg of malonate **2.4** (72%) as a brown solid: mp 50–51 °C; IR (film, CH₂Cl₂) 3050, 2986, 2957, 1733, 1422, 1272, 1254, 1172, 1152, 896 cm⁻¹; ¹H NMR (300 MHz, CDCl₃) δ 5.66 (dt, *J* = 0.8, 1.6 Hz, 1H), 5.59 (d, *J* = 1.7 Hz, 1H), 3.74 (s, 6H), 3.15 (d, *J* = 0.8 Hz, 2H), 2.03–1.97 (m, 2H), 1.05–0.99 (m, 2H), 0.89 (s, 9H); ¹³C NMR (75 MHz, CDCl₃) δ 171.1 (2C), 127.2, 121.7, 57.0, 52.6 (2C), 42.7, 37.5, 30.2, 29.2 (3C), 26.5; MS *m/e* 321 (M ⁸¹Br – Me)⁺, 319 (M ⁷⁹Br – Me)⁺, 305, 303, 279, 277, 255, 195, 171, 139, 69, 57; HRMS exact mass calcd for C₁₁H₂₀⁷⁹BrO₄ (M – Me)⁺ 319.0545, found 319.0558.

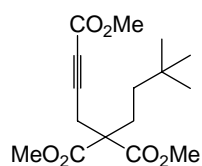
5.3.2 Synthesis of Cyclization Precursors 2.5a and 2.5b



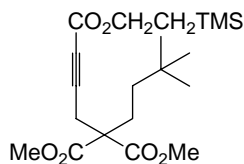
2-(3,3-Dimethylbutyl)-2-prop-2-ynylmalonic acid dimethyl ester (2.18): To a stirred suspension of NaH (95% dry, 1.22 g, 50.9 mmol) in THF (400 mL) cooled to 0 °C was added malonate **2.17** (10.0 g, 46.3 mmol) drop wise. Upon complete addition, propargyl bromide (80% solution in toluene, 7.6 mL, 50.9 mmol) was added and the resulting mixture was stirred at room temperature for 6 h. The reaction was quenched with water (50 mL) and then extracted with ethyl acetate (3 x 50 mL). The combined organic layers were dried over MgSO₄, filtered and concentrated *in vacuo* to give the title compound. Purification over silica gel eluting with hexanes/ethyl acetate (15/1) yielded 11.8 g of malonate **2.18** (95%) as a pale brown oil: IR (film, CH₂Cl₂) 3304, 2957, 1735, 1437, 1291, 1204 cm⁻¹; ¹H NMR (300 MHz, CDCl₃) δ 3.72 (s, 6H), 2.79 (d, *J* = 2.6 Hz, 2H), 2.05–1.98 (m, 3H), 1.03–0.97 (m, 2H), 0.87 (s, 9H); ¹³C NMR (75 MHz, CDCl₃) δ 170.7 (2C), 78.7, 71.2, 56.8, 52.6 (2C), 37.4, 30.1, 29.0 (3C), 27.0, 22.5; MS *m/e* 254, 239, 223, 197, 170, 139, 110, 69, 57; HRMS exact mass calcd for C₁₃H₁₉O₄ (M – Me)⁺ 239.1283, found 239.1282.

General Procedure for the synthesis of alkynes 2.19: To a stirred solution of malonate **2.18** in THF (2 mL/mmol of malonate) cooled to –78 °C was added BuLi (1.6 M in hexanes, 1.2 equiv

to the malonate) drop wise. The resulting solution was stirred at $-78\text{ }^{\circ}\text{C}$ for 2 h, at which point the respective chloroformate was added (2.0 equiv) and stirring was continued for an additional 2 h. The mixture was warmed to room temperature and stirred for 15 h, then the reaction was quenched with a satd aqueous solution of NH_4Cl (1 mL/mmol). After the addition of ethyl acetate (1 mL/mmol), the layers were separated and the aqueous phase was extracted with additional ethyl acetate (2 x 1 mL/mmol). The combined organic layers were washed with water (2 mL/mmol) and brine (2 mL/mmol), dried over MgSO_4 , filtered and concentrated *in vacuo* to give the crude compound. Purification over silica gel yielded the respective alkyne **2.19**.



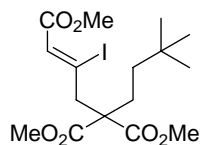
5-(3,3-Dimethylbutyl)-5-methoxycarbonylhex-2-ynedioic acid dimethyl ester (2.19a): Using alkyne **2.18** (2.0 g, 7.9 mmol), methyl chloroformate (1.21 mL, 15.7 mmol) and eluting the column with hexanes/ethyl acetate (15/1) yielded 1.6 g (64%) of the title compound **2.19a** as a clear pale yellow oil: IR (thin film, CH_2Cl_2) cm^{-1} 2957, 1736, 1715, 1435, 1275, 1174; ^1H NMR (300 MHz, CDCl_3) δ 3.70 (s, 6H), 3.68 (s, 3H), 2.91 (s, 2H), 2.01–1.95 (m, 2H), 1.0–0.94 (m, 2H), 0.84 (s, 9H); ^{13}C NMR (75 MHz, CDCl_3) δ 170.1 (2C), 153.5, 83.5, 75.0, 56.5, 52.7 (2C), 52.4, 37.3, 30.0, 28.9 (3C), 27.3, 22.6; MS *m/e* 297 ($\text{M} - \text{Me}$)⁺, 281, 255, 228, 221, 205, 196, 165, 164, 137; HRMS exact mass calcd for $\text{C}_{15}\text{H}_{21}\text{O}_6$ ($\text{M} - \text{Me}$)⁺ 297.1338, found 297.1341.



5-(3,3-Dimethyl-butyl)-5-methoxycarbonylhex-2-ynedioic acid 6-methyl ester 1-(2-trimethylsilyl)ethyl ester (2.19b): Using alkyne **2.18** (1.0 g, 3.9 mmol) and 2-(trimethylsilyl)ethyl chloroformate (1.4 g, 7.9 mmol), which was prepared immediately prior to use from 2-trimethylsilylethanol and phosgene.⁸⁸ The column was eluted with hexanes/ethyl acetate (15/1) to yield 0.97 g (62%) of the title compound **2.19b** as a clear yellow oil: IR (film, CH_2Cl_2) 2957, 1736, 1707, 1251, 1174, 734 cm^{-1} ; ^1H NMR (300 MHz, CDCl_3) δ 4.23–4.18 (m,

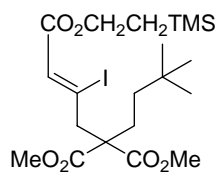
2H), 3.73 (s, 6H), 2.94 (s, 2H), 2.05–1.99 (m, 2H), 1.08–0.96 (m, 4H), 0.88 (s, 9H), 0.01 (s, 9H); ^{13}C NMR (75 MHz, CDCl_3) δ 170.2 (2C), 153.3, 82.8, 75.6, 64.2, 56.6, 52.8 (2C), 37.4, 30.1, 29.0 (3C), 27.3, 22.7, 17.0, –1.6 (3C); MS m/e 383 ($\text{M} - \text{Me}$) $^+$, 355, 229, 221, 205, 165, 89, 73, 57; HRMS exact mass calcd for $\text{C}_{19}\text{H}_{31}\text{O}_6\text{Si}$ ($\text{M} - \text{Me}$) $^+$ 383.1890, found 383.1885.

General Procedure for the hydroiodination of α,β -unsaturated esters 2.5: To alkyne **2.19** was added oven dried NaI (3.2 equiv) and glacial acetic acid (6.4 equiv). The resulting mixture was stirred at 115 °C until GC analysis revealed consumption of the starting material. The mixture was diluted with water (15 mL/mmol of alkyne) and ether (15 mL/mmol) and then K_2CO_3 was added until the formation of gas ceased. The layers were separated and the aqueous layer was extracted with ether (3 x 15 mL/mmol). The combined organic layers were washed with a 10% aqueous solution of $\text{Na}_2\text{S}_2\text{O}_3$ (10 mL/mmol) and water (10 mL/mmol), dried over MgSO_4 , filtered and concentrated by rotary evaporation *in vacuo* to give the desired compound. Purification over silica eluting with hexanes/ethyl acetate gave the respective vinyl iodide **2.5**.



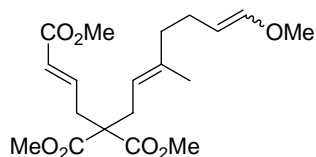
5-(3,3-Dimethylbutyl)-3-iodo-5-methoxycarbonylhex-2-enedioic acid dimethyl ester (2.5a):

Using alkyne **2.19a** (1.0 g, 3.2 mmol) and eluting the column with hexanes/ethyl acetate (15/1) yielded 0.52 g (37%) of the title compound as a pale yellow oil that solidified on cooling to –20 °C and liquefied again on warming to room temperature: IR (thin film, CH_2Cl_2) 3054, 2987, 1733, 1435, 1422, 1262, 1175, 896 cm^{-1} ; ^1H NMR (300 MHz, CDCl_3) δ 6.42 (s, 1H), 3.80 (s, 6H), 3.75 (s, 3H), 3.47 (s, 2H), 2.00–1.95 (m, 2H), 1.08–1.02 (m, 2H), 0.89 (s, 9H); ^{13}C NMR (75 MHz, CDCl_3) δ 170.7 (2C), 164.5, 128.8, 110.7, 57.8, 52.6 (2C), 51.7, 48.2, 37.5, 30.2, 29.1 (3C), 26.8; MS m/e 425 ($\text{M} - \text{Me}$) $^+$, 409, 393, 383, 377, 361, 349, 325, 313, 253; HRMS exact mass calcd for $\text{C}_{15}\text{H}_{22}\text{O}_5\text{I}$ ($\text{M} - \text{OMe}$) $^+$ 409.0512, found 409.0523.



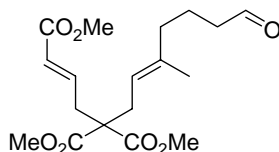
5-(3,3-Dimethylbutyl)-3-iodo-5-methoxycarbonylhex-2-enedioic acid 6-methyl ester 1-(2-trimethylsilyl ethyl) ester (2.5b): Using alkyne **2.19b** (1.3 g, 3.3 mmol) and eluting the column with hexanes/ethyl acetate (15/1) yielded 0.26 g (15%) of the title iodide as a dark yellow oil: IR (thin film, CH₂Cl₂) 2957, 1734, 1250, 1172, 861 cm⁻¹; ¹H NMR (300 MHz, CDCl₃) δ 6.37 (s, 1H), 4.27–4.20 (m, 2H), 3.75 (s, 6H), 3.46 (s, 2H), 2.00–1.94 (m, 2H), 1.07–0.99 (m, 4H), 0.88 (s, 9H), 0.03 (s, 9H); ¹³C NMR (75 MHz, CDCl₃) δ 170.8 (2C), 164.3, 129.4, 110.0, 63.0, 57.8, 52.7 (2C), 48.2, 37.6, 30.3, 29.2 (3C), 26.8, 17.2, –1.5 (3C); MS *m/e* 399 (M – I)⁺, 399, 73; HRMS exact mass calcd for C₂₀H₃₅O₆Si (M – I)⁺ 399.2203, found 399.2203. Acidification of the aqueous layer with 2N HCl and extraction with ethyl acetate yielded 0.32 g (23%) of 5-(3,3-dimethylbutyl)-3-iodo-5-methoxycarbonylhex-2-enedioic acid 6-methyl ester **2.20**. This acid could be used as such in a DCC mediated coupling with 2-trimethylsilyl ethanol to prepare more of precursor **2.5b**.

5.3.3 Synthesis of Cyclization Precursor 2.10



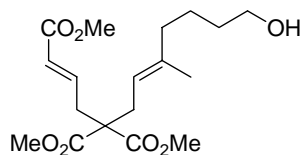
5-Methoxycarbonyl-5-(7-methoxy-3-methylhepta-2E,6E-dienyl)hex-2E-enedioic acid dimethyl ester (2.27): To stirred THF (213 mL) cooled to –78 °C was added diisopropylamine (3.11 mL, 17.9 mmol) and BuLi (1.6 M solution in hexanes, 11.54 mL, 18.5 mmol) and stirring was continued for 30 min. The resulting LDA solution was cannulated into a stirred suspension of methoxymethyl triphenylphosphonium chloride **2.26** (6.32 g, 18.5 mmol) in THF (213 mL) cooled to 0 °C. The dark red solution was stirred for 30 min, then aldehyde **3.26a** (3.0 g, 8.8 mmol) was cannulated in as a solution in THF (213 mL). The final suspension was stirred for 30 min at 0 °C, poured into a satd brine solution (750 mL) and extracted with methylene chloride (2

x 1200 mL). The combined organic layers were dried over anhydrous MgSO₄, filtered and concentrated *in vacuo* to give the title compound. Purification over silica gel eluting with hexanes/ethyl acetate (5/1) gave 1.6 g a 2:1 mixture of *E*:*Z* isomers of **2.27** (48%) as a clear, pale yellow oil. This compound was characterized as a mixture of both isomers: IR (thin film, CH₂Cl₂) 3049, 2985, 1731, 1423, 1280, 1249, 894 cm⁻¹; ¹H NMR (300 MHz, CDCl₃) Resonances attributed to the *E*-isomer: δ 5.85 (dt, *J* = 1.2, 15.5 Hz, 1H), 4.67 (dm, *J* = 12.6, 1H), 3.50 (s, 3H); Resonances attributed to the *Z*-isomer: δ 5.84 (dt, *J* = 1.2, 9.3 Hz, 1H), 4.27 (q, *J* = 7.0 Hz, 1H), 3.58 (s, 3H); Overlapping resonances: δ 6.79 (dt, *J* = 7.7, 15.5 Hz, 1H), 6.29 (d, *J* = 12.6 Hz, 1H), 4.95 (t, *J* = 7.4 Hz, 1H), 3.73 (s, 6H), 3.72 (s, 3H), 2.76 (dt, *J* = 1.2, 7.7 Hz, 2H), 2.63 (d, *J* = 7.5 Hz, 2H), 2.05–2.00 (m, 4H), 1.60 (s, 3H); ¹³C NMR (75 MHz, CDCl₃) Resonances attributed to the *E*-isomer: 146.9, 142.7, 139.0, 117.2, 101.6, 55.2, 40.7, 25.8, 15.8; Resonances attributed to the *Z* isomer: 145.9, 142.8, 139.4, 116.7, 105.4, 59.0, 39.4, 21.8, 15.7; Overlapping Resonances: δ 170.5 (2C), 165.8, 124.1, 57.2, 52.1 (2C), 51.0, 35.0, 31.1; MS *m/e* 368, 337, 336, 308, 304, 297, 71; HRMS exact mass calcd for C₁₉H₂₈O₇: 368.1835, found: 368.1836.

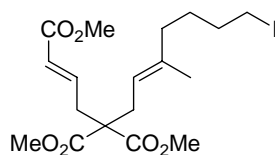


5-Methoxycarbonyl-5-(3-methyl-7-oxohept-2*E*-enyl)hex-2*E*-enedioic acid dimethyl ester (2.28**):** Enol ether **2.27** (1.9 g, 5.2 mmol) was dissolved in THF (220 mL) and a 9/1 (v/v) mixture of water and HCl (220 mL) was added. The resulting mixture was stirred at room temperature for 2 h, poured into a satd NaHCO₃ solution (600 mL) and extracted with CH₂Cl₂ (3 x 600 mL). The combined organic layers were dried over anhydrous MgSO₄, filtered and concentrated *in vacuo* to give the title compound. Purification over silica gel eluting with hexanes/ethyl acetate (5/1) gave 1.10 g of **2.28** (57%) as a clear, colorless oil: IR (thin film, CH₂Cl₂) 3057, 2986, 2952, 2845, 2727, 1726, 1660, 1441, 1288, 1205, 1040, 984 cm⁻¹; ¹H NMR (300 MHz, CDCl₃) δ 9.73 (t, *J* = 1.6 Hz, 1H), 6.74 (dt, *J* = 7.7, 15.5 Hz, 1H), 5.82 (dt, *J* = 1.3, 15.5 Hz, 1H), 4.94 (tq, *J* = 1.1, 7.5 Hz, 1H), 3.69 (s, 6H), 3.68 (s, 3H), 2.72 (dd, *J* = 1.3, 7.7 Hz, 2H), 2.59 (d, *J* = 7.4 Hz, 2H), 2.35 (td, *J* = 1.6, 7.3 Hz, 2H), 1.99 (t, *J* = 7.4 Hz, 2H), 1.68 (p, *J* = 7.4 Hz, 2H), 1.56 (d, *J* = 1.1 Hz, 3H); ¹³C NMR (75 MHz, CDCl₃) δ 202.2, 170.7 (2C), 166.1, 142.8, 138.9, 124.5, 118.0,

57.4, 52.5 (2C), 51.4, 42.9, 38.9, 35.3, 31.3, 20.0, 15.9; APCI: Mass calcd for C₁₈H₂₆O₇Na (M + Na)⁺: 377.2, found 377.1; Mass calcd for C₁₈H₂₈O₇K (M + K)⁺: 393.1, found 393.0.

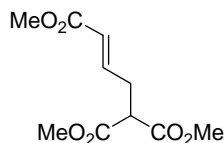


5-(7-Hydroxy-3-methylhept-2E-enyl)-5-methoxycarbonylhex-2E-enedioic acid dimethyl ester (2.29): Aldehyde **2.28** (0.041 g, 0.1 mmol) was dissolved in absolute methanol (10 mL) and cooled to 0 °C. Sodium borohydride powder (0.017 g, 0.5 mmol) was added to the stirred solution and the flask was stoppered. After 14 h the reaction mixture was poured into distilled water (30 mL), acidified with 1M hydrochloric acid (10 mL) and extracted with ethyl acetate (3 x 20 mL). The combined organic layers were dried over MgSO₄, filtered and concentrated *in vacuo* to give the title compound. Purification over silica gel eluting with hexanes/ethyl acetate (2/1) gave 0.032 g of **2.29** (79%) as a clear, colorless oil: IR (thin film, CH₂Cl₂) 3612, 3063, 2953, 2863, 1722, 1660, 1439, 1287, 1197, 1060, 1038, 984 cm⁻¹; ¹H NMR (300 MHz, CDCl₃) δ 6.73 (dt, *J* = 7.8, 15.5 Hz, 1H), 5.79 (dt, *J* = 1.2, 15.5 Hz, 1H), 4.90 (tq, *J* = 1.0, 7.5 Hz, 1H), 3.67 (s, 6H), 3.66 (s, 3H), 3.56 (t, *J* = 6.2 Hz, 2H), 2.69 (dd, *J* = 1.2, 7.7 Hz, 2H), 2.57 (d, *J* = 7.4, 2H), 2.17 (br s, 1H), 1.95 (t, *J* = 6.6 Hz, 2H), 1.53 (d, *J* = 1.0 Hz, 3H), 1.47–1.35 (m, 4H); ¹³C NMR (75 MHz, CDCl₃) δ 170.8 (2C), 166.2, 142.9, 139.8, 124.4, 116.9, 62.4, 57.4, 52.3 (2C), 51.4, 39.4, 35.2, 31.9, 31.2, 23.7, 15.9; APCI: Mass calculated for C₁₈H₂₈O₇Na (M + Na)⁺: 379.2, found: 379.1; Mass calculated for C₁₈H₂₈O₇K (M + K)⁺: 395.2, found: 395.1.

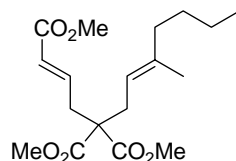


5-(7-Iodo-3-methylhept-2E-enyl)-5-methoxycarbonylhex-2E-enedioic acid dimethyl ester (2.10): Triphenylphosphine (0.147 g, 0.6 mmol) and imidazole (0.030 g, 0.4 mmol) were added to CH₂Cl₂ (5 mL) and the solution was stirred. The mixture was cooled to 0 °C and then iodine (0.111 g, 0.4 mmol) was added. The resulting mixture was stirred for 15 min and alcohol **2.29** (0.10 g, 0.3 mmol) was added. The reaction mixture was stirred for 1h, poured into a satd

aqueous solution of Na₂S₂O₃ (3 mL) and extracted with ethyl acetate (3 x 5 mL). The combined organic layers were dried over anhydrous MgSO₄, filtered and concentrated *in vacuo* to give the title compound. Purification over silica gel eluting with hexanes/ethyl acetate (5/1) gave 0.111 g of iodide **2.10** (85%) as a clear, brown oil: IR (thin film, CH₂Cl₂) 3058, 2985, 2953, 1730, 1437, 1281, 1250, 1173, 894 cm⁻¹; ¹H NMR (300 MHz, CDCl₃) δ 6.76 (dt, *J* = 7.6, 15.6 Hz, 1H), 5.83 (d, *J* = 15.5 Hz, 1H), 4.93 (t, *J* = 7.4 Hz, 1H), 3.70 (s, 6H), 3.69 (s, 3H), 3.16 (t, *J* = 6.9 Hz, 2H), 2.73 (d, *J* = 7.7 Hz, 2H), 2.60 (d, *J* = 7.4 Hz, 2H), 1.98 (t, *J* = 7.4 Hz, 2H), 1.74 (tt, *J* = 6.9, 7.5 Hz, 2H), 1.57 (s, 3H), 1.46 (tt, *J* = 7.1, 7.8 Hz, 2H); ¹³C NMR (75 MHz, CDCl₃) δ 170.8 (2C), 166.1, 142.9, 139.3, 124.5, 117.4, 57.4, 52.5 (2C), 51.5, 38.6, 35.3, 32.7, 31.3, 28.5, 16.0, 6.7; MS *m/e* 466, 435, 434, 406, 374, 335, 303, 230, 198, 166, 145, 109, 67, 59, 54; HRMS exact mass calcd for C₁₈H₂₇IO₆ 466.0852, found: 466.0875.



(E)-trimethylbut-3-ene-1,1,4-tricarboxylate (2.30): Dimethyl malonate (0.95 mL, 7.5 mmol) was added drop wise to a stirred suspension of NaH (95 % dry, 0.18 g, 7.5 mmol) in anhydrous THF (30 mL) at 0 °C. After complete addition, (*E*)-methyl-4-crotonate **3.23a** (0.69 mL, 5.0 mmol) was added to the mixture drop wise. After 16 h the resulting mixture was poured into a mixture of H₂O (10 mL) and ethyl acetate (100 mL). After separation of the layers, the aqueous layer was extracted with ethyl acetate (3 x 5 mL) and the combined organic layers were dried over anhydrous MgSO₄. Filtration and solvent evaporation *in vacuo* gave the title compound. Purification by flash chromatography on silica gel eluting with hexanes/ethyl acetate (8/1) gave 0.68 g of **2.30** (59%) as a clear, pale yellow oil: IR (film, CHCl₃) 2955, 2925, 2855, 1735, 1731, 1438, 1378, 1341, 1274, 1243, 1216, 1156, 1094, 1041, 929, 909, 888 cm⁻¹; ¹H NMR (300 MHz, CDCl₃) δ 6.81 (dt, *J* = 7.1, 15.6 Hz, 1H), 5.83 (dt, *J* = 1.5, 15.6 Hz, 1H), 3.68 (s, 6H), 3.65 (s, 3H), 3.47 (t, *J* = 7.4 Hz, 1H), 2.72 (app dt, *J* = 1.5, 7.2 Hz, 1H); ¹³C NMR (75 MHz, CDCl₃) δ 168.5 (2C), 166.1, 143.7, 123.4, 52.5 (2C), 51.3, 50.2, 30.9; MS *m/e* 230, 215, 199, 198, 167, 166, 139, 111, 59 HRMS exact mass calcd for C₁₀H₁₄O₆ 230.0790, found 230.0800.

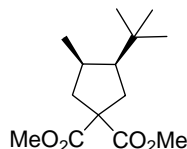


5-Methoxycarbonyl-5-(3-methylhept-2E-enyl)hex-2E-enedioic acid dimethyl ester (2.13):

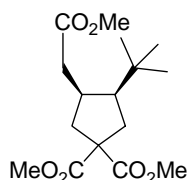
To a solution of PBr_3 (0.03 mL, 0.33 mmol) and pyridine (0.01 mL) in petroleum ether (2.6 mL) at $-10\text{ }^\circ\text{C}$, was added, drop wise, a solution of alcohol **2.31** (0.10 g, 0.78 mmol) in petroleum ether (0.4 mL). The resulting reaction mixture was stirred at $0\text{ }^\circ\text{C}$ for 1.5 h. The reaction was then quenched with an ice/water mixture (2 mL) and the layers were separated. The aqueous layer was extracted with ether (3 x 10 mL) and the combined organic layers were washed with 2 N HCl (3 mL), satd NaHCO_3 (2 x 5 mL), brine (5 mL) and dried over MgSO_4 . The organic layer was filtered and carefully concentrated *in vacuo*. The resulting allyl bromide was used without further purification in the alkylation of malonate **2.30**.

To a stirred suspension of NaH (95% dry, 0.011 g, 0.48 mmol) in THF (3 mL) was added, drop wise malonate **2.30** (0.100 g, 0.43 mmol) over 5 min. To this was added allyl bromide 110 (0.083 g, 0.43 mmol) and the reaction mixture was stirred for 16 h. The mixture was then poured into a mixture of water (2 mL) and ethyl acetate (2 mL). The layers were separated and the aqueous layer was extracted with ethyl acetate (3 x 5 mL). The combined organic layers were dried over MgSO_4 , filtered and concentrated *in vacuo* to give the title compound. Purification over silica gel eluting with hexanes/ethyl acetate (5/1) yielded 0.115 g of malonate **2.13** as a clear pale yellow oil (79%): IR (film, CH_2Cl_2) 3057, 2987, 1731, 1422, 1280, 1248, 1172, 894 cm^{-1} ; ^1H NMR (300MHz, CDCl_3) δ 6.75 (dt, $J = 7.8, 15.5$ Hz, 1H), 5.81 (dt, $J = 1.1, 15.5$ Hz, 1H), 4.90 (dt, $J = 1.0, 7.4$ Hz, 1H), 3.69 (s, 6H), 3.68 (s, 3H), 2.72 (dd, $J = 1.1, 7.8$ Hz, 2H), 2.58 (d, $J = 7.4$ Hz, 2H), 1.93 (t, $J = 7.5$ Hz, 2H), 1.54 (d, $J = 1.0$ Hz, 3H), 1.35–1.16 (m, 4H), 0.85 (t, $J = 7.2$ Hz, 3H); ^{13}C NMR (75 MHz, CDCl_3) δ 170.9 (2C), 166.2, 143.0, 140.3, 124.4, 116.6, 57.5, 52.4 (2C), 51.4, 39.5, 35.3, 31.4, 30.0, 22.2, 16.1, 13.8; MS *m/e* 340, 309, 280, 248, 230, 209, 198, 177, 166, 145, 135, 121, 111, 79, 69; HRMS exact mass calcd for $\text{C}_{18}\text{H}_{28}\text{O}_6$: 340.1886, found: 340.1889.

5.3.4 Cyclization Reactions of Precursors 2.4, 2.5a,b and 2.10

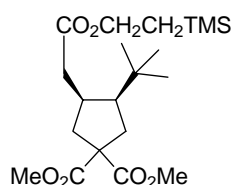


3-*tert*-Butyl-4-methylcyclopentane-1,1-dicarboxylic acid dimethyl ester (2.7): Subjecting precursor **2.4** (33 mg, 0.1 mmol) to the cyclization conditions described for method B for 3 h and purification of the crude reaction mixture by column chromatography eluting with hexanes/ethyl acetate (10/1) after eluting with five column volumes of hexanes, yielded 14 mg (50 %) of a 75/25 *cis/trans* mixture of the title compound **2.7**. The NMR data reported is that of the major *cis* isomer, the minor *trans* isomer was independently synthesized and the data is reported subsequently: IR (film, CH₂Cl₂) 2956, 1730, 1276, 1246, 1201 cm⁻¹; ¹H NMR (500 MHz, CDCl₃) δ 3.74 (s, 3H), 3.72 (s, 3H), 2.40 (dd, *J* = 7.2, 13.8 Hz, 1H), 2.28 (m, 2H), 2.16 (t, *J* = 13.4 Hz, 1H), 2.06 (d, *J* = 13.8 Hz, 1H), 1.74 (dt, *J* = 6.2, 13.5 Hz, 1H), 0.96 (s, 9H), 0.91 (d, *J* = 7.2 Hz, 3H); ¹³C NMR (125 MHz, CDCl₃) δ 173.9, 173.8, 57.7, 53.5, 52.7 (2C), 42.6, 35.6, 33.0, 31.8, 29.1 (3C), 17.1; MS *m/e* 257 (M + H)⁺, 241, 225, 201, 181, 169, 145, 113, 57; HRMS exact mass calcd for C₁₄H₂₄O₄ 256.1675, found 256.1668.

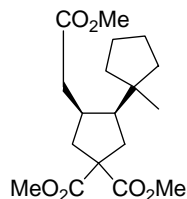


3-*tert*-Butyl-4-methoxycarbonylmethyl-cyclopentane-1,1-dicarboxylic acid dimethyl ester (2.8a): Subjecting precursor **2.5a** (44 mg, 0.1 mmol) to the cyclization conditions outlined in method B for 1.5 h and purification of the crude reaction mixture by column chromatography eluting with hexanes/ethyl acetate (15/1) after five column volumes of hexanes, yielded 16 mg (52%) of a 78/22 *cis/trans* isomeric mixture of the title compound **2.8a**. These two products were inseparable and so characterization was performed on the mixture: IR (film, CH₂Cl₂) 3054, 2987, 1730, 1439, 1262, 1175, 896 cm⁻¹; ¹H NMR (500 MHz, CDCl₃) resonances assigned to the *cis* isomer δ 3.74 (s, 3H), 3.72 (s, 3H), 3.68 (s, 3H), 2.64–2.60 (m, 1H), 2.52 (dd, *J* = 3.6, 15.2 Hz, 1H), 2.38 (dd, *J* = 6.9, 14.3 Hz, 1H), 2.34 (dd, *J* = 6.6, 13.4 Hz, 1H), 2.21 (d, *J* = 14.7 Hz,

2H), 2.10 (t, $J = 13.5$ Hz, 1H), 1.83 (dt, $J = 6.1, 13.7$ Hz, 1H), 0.97 (s, 9H); resonances assigned to the *trans* isomer δ 3.74 (s, 3H), 3.71 (s, 3H), 3.67 (s, 3H), 1.92 (dd, $J = 10.9, 13.3$ Hz, 1H), 0.90 (s, 9H), the remaining resonances are insufficiently resolved from those of the *cis* isomer to be reported. ^{13}C NMR (125 MHz, CDCl_3) resonances assigned to the *cis* isomer δ 173.5, 173.4, 173.3, 57.5, 53.3, 52.7 (2C), 51.5, 39.4, 37.8, 34.6, 33.6, 31.6, 29.1 (3C); resonances assigned to the *trans* isomer 54.4, 52.6, 41.5, 40.1, 36.6, 35.9, 32.7, 27.8 (3C), 25.1, the remaining resonances are insufficiently resolved from those of the *cis* isomer to be reported. MS m/e 283 ($\text{M} - \text{MeO}$) $^+$; HRMS exact mass calcd for $\text{C}_{15}\text{H}_{23}\text{O}_5$ ($\text{M} - \text{MeO}$) $^+$ 283.1545, found 283.1559.

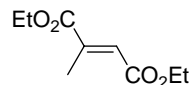


3-*tert*-Butyl-4-(2-trimethylsilanylethoxycarbonylmethyl)cyclopentane-1,1-dicarboxylic acid dimethyl ester (2.5b): Subjecting precursor **2.5b** (53 mg, 0.1 mmol) to the cyclization conditions outlined in method B for 1.5 h and purification of the crude reaction mixture by column chromatography eluting with hexanes/ethyl acetate (15/1) after five column volumes of hexanes yielded 27 mg (67 %) of a 77/23 *cis/trans* isomeric mixture of the title compound **2.8b**. These two products were inseparable and so characterization was performed on the mixture: IR (film, CH_2Cl_2) 2972, 1734, 1250, 1172, 861 cm^{-1} ; ^1H NMR (500 MHz, CDCl_3) resonances assigned to the *cis* isomer δ 4.20–4.15 (m, 2H), 3.75 (s, 3H), 3.74 (s, 3H), 2.64–2.62 (m, 1H), 2.50 (dd, $J = 3.4, 15.0$ Hz, 1H), 2.41 (dd, $J = 6.6, 14.6$ Hz, 1H), 2.33 (dd, $J = 6.5, 13.4$ Hz, 1H), 2.23 (d, $J = 14.6$ Hz, 1H), 2.19–2.08 (m, 2H), 1.83 (dt, $J = 6.2, 13.6$ Hz, 1H), 1.02–0.94 (m, 11 H), 0.06 (s, 9H); resonances assigned to the *trans* isomer: δ 3.76 (s, 3H), 3.72 (s, 3H), 1.92 (dd, $J = 11.0, 12.1$ Hz, 1H), 0.90–0.87 (m, 11H), the remaining resonances are insufficiently resolved from those of the *cis* isomer to be reported; ^{13}C NMR (125 MHz, CDCl_3) resonances assigned to the *cis* isomer δ 173.5, 173.4, 173.1, 62.5, 57.5, 53.2, 52.8 (2C), 39.3, 37.7, 35.0, 33.6, 31.6, 29.1 (3C), 17.4, -1.6 (3C); resonances assigned to the *trans* isomer δ 62.4, 52.6, 52.5, 42.4, 40.0, 32.6, 27.5 (3C), the remaining resonances are insufficiently resolved from those of the *cis* isomer to be reported; MS m/e 400, 343, 241, 185, 73, 57; HRMS exact mass calcd for $\text{C}_{20}\text{H}_{35}\text{O}_6\text{Si}$ ($\text{M} - \text{H}$) $^+$ 399.2203, found 399.2224.



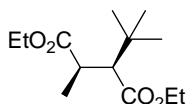
5-Methoxycarbonylmethyl-1'-methyl-bicyclo[2.2.1]heptane-3,3-dicarboxylic acid dimethyl ester (2.12): Subjecting precursor **2.10** (0.28 g, 0.6 mmol) to the cyclization conditions outlined in method B for 4 h and purification of the crude reaction mixture by column chromatography eluting with hexanes/ethyl acetate (8/1) after five column volumes of hexanes, yielded 0.12 g (60 %) of a 80/20 *cis/trans* isomeric mixture of the title compound **2.12** as a pale opaque yellow oil. These two products were inseparable and so characterization was performed on the mixture: IR (thin film, CH₂Cl₂) 3058, 2987, 2958, 1732, 1437, 1279, 1254, 1173, 894 cm⁻¹; ¹H NMR (500 MHz, CD₃OD) resonances assigned to the *cis* isomer δ 3.72 (s, 3H), 3.70 (s, 3H), 3.66 (s, 3H), 2.61–2.58 (m, 1H), 2.40 (dd, *J* = 7.1, 14.4 Hz, 1H), 2.40 (dd, *J* = 2.7, 15.0 Hz, 1H), 2.31 (dd, *J* = 6.1, 12.9 Hz, 1H), 2.19 (dd, *J* = 12.5, 15.3 Hz, 1H), 2.19 (dd, *J* = 2.7, 15.0 Hz, 1H), 2.08 (t, *J* = 13.3 Hz, 1H), 2.02 (ddd, *J* = 6.2, 6.2, 13.4 Hz, 1H), 1.64–1.54 (m, 4H), 1.37–1.31 (m, 2H), 1.27–1.22 (m, 2H), 0.97 (s, 3H); resonances assigned to the *trans* isomer δ 1.91–1.85 (m, 1H), 1.73–1.68 (m, 4H), 0.80 (s, 3H), the remaining resonances are insufficiently resolved from those of the *cis* isomer to be reported; ¹³C NMR (125 MHz, CD₃OD) resonances assigned to the *cis* isomer δ 175.2, 174.8, 174.6, 59.0, 53.9, 53.3 (2C), 52.0, 43.8, 41.4, 40.1, 39.1, 37.7, 35.7, 34.9, 27.0, 26.6, 25.3; *trans* isomer δ 59.8, 53.3 (2C), 41.3, 41.2, 39.8, 38.3, 25.2, the remaining resonances are insufficiently resolved from those of the *cis* isomer to be reported; MS *m/e* 340, 309, 267, 248, 207, 185, 145, 83; HRMS exact mass calcd for C₁₈H₂₈O₆ 340.1886, found 340.1894.

5.3.5 Synthesis of 2.7*trans*



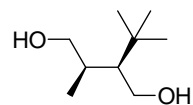
(E)-2-Methyl-but-2-enedioic acid diethyl ester (2.33): To mesaconic acid (5.20 g, 40 mmol) was added ethanol (40 mL) and concentrated H₂SO₄ (0.5 mL). The resulting mixture was stirred and slowly brought to reflux and maintained there for 16 h. After cooling, the reaction mixture

was concentrated by *in vacuo* and the residue was taken up in water (20 mL) and extracted with ethyl acetate (3 x 20 mL). The combined organic layers were washed with water (20 mL), 2M NaOH (20 mL) and then dried over MgSO₄. The organic layers were filtered and concentrated *in vacuo* to give 6.0 g of the title compound **2.33** (81%) as a pale yellow oil. The product was analytically pure and used without further purification: IR (film, CH₂Cl₂) 2984, 1721, 1650, 1447, 1367, 1260, 1112, 1040 cm⁻¹; ¹H NMR (300 MHz, CDCl₃) δ 6.76 (q, *J* = 1.5 Hz, 1H), 4.27–4.17 (m, 4H), 2.27 (d, *J* = 1.4 Hz, 3H), 1.33–1.27 (m, 6H); ¹³C NMR (75 MHz, CDCl₃) δ 167.1, 165.9, 143.7, 126.6, 61.5, 60.5, 14.2, 14.1, 14.0; MS *m/e* 186, 141, 140, 113, 112, 84, 68; HRMS exact mass calcd for C₉H₁₄O₄ 186.0892, found 186.0884.

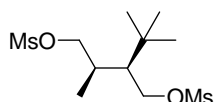


2-tert-Butyl-3-methylsuccinic acid diethyl ester (2.34): To a suspension of vitamin B_{12a} (0.50 g, 0.36 mmol) in DMF (48 mL) was added activated zinc (5.33 g, 81.6 mmol) and the resulting mixture was stirred vigorously under argon. Zinc activation was carried out by washing the zinc powder with 2N HCl (2 x 30 mL), water (2 x 30 mL), EtOH (2 x 30 mL), Et₂O (2 x 30 mL) and finally drying the solid *in vacuo*. After 15 min, a degassed solution of *t*-BuBr (8.30 mL, 72.0 mmol), alkene **2.33** (1.33 g, 7.2 mmol) and Et₃N (14.9 mL, 103.2 mmol) in DMF (24 mL) was added. The resulting suspension was stirred for 12 h at room temperature during which the reaction turned from dark red to dark green accompanied by the evolution of a large amount of heat. After consumption of the alkene, the reaction was quenched with water (90 mL). This suspension was filtered and 2N HCl (30 mL) was added. The reaction mixture was then extracted with Et₂O (3 x 300 mL) and the combined organic layers were washed with water (60 mL) and dried over MgSO₄. The organic layers were filtered and concentrated *in vacuo* to give the title compound. Purification over silica gel eluting with hexanes/ethyl acetate (15/1) gave 0.805 g of diester **2.34** (46%) as a clear, colorless oil: IR (thin film, CH₂Cl₂) 2978, 1736, 1466, 1370, 1151, 1030 cm⁻¹; ¹H NMR (300 MHz, CDCl₃) δ 4.03–3.96 (m, 4H), 2.78 (app quint, *J* = 7.2 Hz, 1H), 2.30 (d, *J* = 7.6 Hz, 1H), 1.22 (d, *J* = 7.1 Hz, 3H), 1.18–1.12 (m, 6H), 0.94 (s, 9H); ¹³C NMR (75 MHz, CDCl₃) δ 175.6, 173.6, 60.2, 59.7, 58.2, 39.7, 33.0, 28.5 (3C), 19.0, 14.0,

13.8; MS m/e 199 ($M - OEt$)⁺, 188, 142, 115, 83, 69, 57; HRMS exact mass calcd for C₁₁H₁₉O₃ ($M - OEt$)⁺ 199.1334, found: 199.1340.

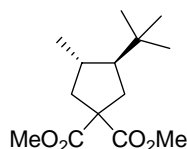


2-tert-Butyl-3-methylbutane-1,4-diol (2.35): To a stirred solution of diester **2.34** (0.71 g, 2.91 mmol) in THF (40 mL) was added LiAlH₄ (0.40 g, 10.6 mmol) in small portions over 10 min. The suspension was stirred at room temperature for 12 h at which point ethyl acetate (10 mL) was added slowly followed by 1M H₂SO₄ to decompose the excess hydride. Ether (20 mL) was added to the reaction mixture and after separation of the two phases, the aqueous layer was extracted with ether (2 x 20 mL). The combined organic layers were washed with brine (20 mL), dried over MgSO₄, filtered and concentrated *in vacuo* to give the title compound. Purification over silica gel eluting with hexanes/ethyl acetate (1/1) gave 0.45 g of diol **2.35** (96%) as a clear colorless oil: IR (thin film, neat) 3299, 2960, 1471, 1396, 1367, 1040 cm⁻¹; ¹H NMR (300 MHz, CDCl₃) δ 3.93–3.81 (m, 3H), 3.69 (dd, $J = 5.0, 11.3$ Hz, 1H), 2.84 (br s, 2H), 2.08–1.99 (m, 1H), 1.32–1.27 (m, 1H), 1.13 (d, $J = 7.2$ Hz, 3H), 0.97 (s, 9H); ¹³C NMR (75 MHz, CDCl₃) δ 64.4, 60.4, 54.3, 33.8, 33.4, 28.5 (3C), 20.3; MS m/e 142 ($M - H_2O$)⁺, 112, 109, 97, 73, 61, 57; HRMS exact mass calcd for C₉H₁₈O ($M - H_2O$)⁺: 142.1357, found: 142.1360.



Methanesulfonic acid 3-methanesulfonyloxymethyl-2,4,4-trimethyl-pentyl ester (2.35): To a stirred solution of diol **2.35** (0.45 g, 2.79 mmol) in CH₂Cl₂ (30 mL) was added Et₃N (1.61 mL, 11.56 mmol) and mesyl chloride (0.49 mL, 6.37 mmol). The reaction was stirred for 20 h at which point the reaction was diluted with CH₂Cl₂ and washed with water (30 mL). The layers were separated and the aqueous layer was extracted with CH₂Cl₂ (2 x 30 mL). The combined organic layer were washed with satd NaHCO₃, dried over MgSO₄, filtered and concentrated to give the title compound. Purification over silica gel eluting with hexanes/ethyl acetate (3/2) gave 0.61 g of *bis*-mesylate **2.36** (69%) as flaky white solid: mp 71–74 °C, IR (thin film, neat) 3027, 2967, 1475, 1334, 1171, 944, 735 cm⁻¹; ¹H NMR (300 MHz, CDCl₃) δ 4.39–4.33 (m, 2H), 4.24

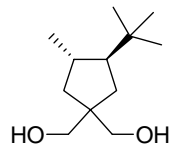
(dd, $J = 7.7, 10.2$ Hz, 1H), 4.06 (dd, $J = 8.5, 9.0$ Hz, 1H), 2.99 (s, 3H), 2.97 (s, 3H), 2.41–2.30 (m, 1H), 1.57–1.54 (m, 1H), 1.07 (d, $J = 7.1$ Hz, 3H), 0.97 (s, 9H); ^{13}C NMR (75 MHz, CDCl_3) δ 72.4, 67.8, 51.5, 37.4, 37.2, 33.7, 32.3, 28.5 (3C), 19.4; MS m/e 221 ($\text{M} - \text{OMs}$) $^+$, 205, 193, 175, 164, 109, 79, 68, 57; HRMS exact mass calcd for $\text{C}_{10}\text{H}_{21}\text{O}_3\text{S}$ ($\text{M} - \text{OMs}$) $^+$ 221.1211, found: 221.1206.



***trans*-3-*tert*-Butyl-4-methylcyclopentane-1,1-dicarboxylic acid dimethyl ester (2.7*trans*):** To a solution of *bis*-mesylate **2.36** (0.173 g, 0.55 mmol) in acetone (2.7 mL) was added oven dried NaI (0.414 g, 2.76 mmol). The resulting solution was stirred and refluxed for 16 h at which point silica gel was added to the reaction and concentrated *in vacuo*. The solid was loaded onto a short column of silica gel and eluted with hexanes/ethyl acetate (5/1). The first eluting fraction was the *bis*-iodide **2.37** which was used as such in the following step.

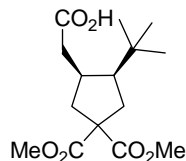
To a suspension of NaH (95%, 0.074 g, 3.1 mmol) in THF (20 mL) was added dimethyl malonate (0.44 mg, 3.3 mmol) drop wise as a solution in THF (20 mL). The resulting solution was stirred for 1 h at which point the *bis*-iodide **2.37** was added as a solution in THF (1 mL). The resulting mixture was refluxed for 10 h during which time a fine white precipitate formed. Additional dimethyl malonate anion (10 equiv at a time, 43.3 mmol total) were added until complete consumption of the alkylating agent was observed. The reaction was quenched by the addition of water (10 mL) and after separation of the layers, the aqueous layers were extracted with ethyl acetate (3 x 10 mL). The combined organic layers were dried over MgSO_4 , filtered and concentrated *in vacuo* to give the title compound. Purification over silica gel eluting with hexanes/ethyl acetate (15/1) gave 0.059 g of malonate **2.7*trans*** (69%, based on the mesylate **2.35**) as a clear pale yellow oil: IR (thin film, CH_2Cl_2) 2958, 2931, 1730, 1257 cm^{-1} ; ^1H NMR (500 MHz, CDCl_3) δ 3.73 (s, 3H), 3.71 (s, 3H), 2.47 (dd, $J = 8.2, 13.5$ Hz, 1H), 2.42 (dd, $J = 8.2, 13.0$ Hz, 1H), 1.99–1.85 (m, 3H), 1.51 (app q, $J = 8.3$ Hz, 1H), 1.00 (d, $J = 6.6$ Hz, 3H), 0.88 (s, 9H); ^{13}C NMR (125 MHz, CDCl_3) δ 173.3, 173.0, 58.7, 56.4, 52.6 (2C), 43.3, 37.3, 34.6, 32.5, 28.0 (3C), 22.3; MS m/e 257, 241, 225, 145, 57; HRMS exact mass calcd for $\text{C}_{14}\text{H}_{24}\text{O}_4$: 256.1675, found: 256.1668.

5.3.6 Synthesis of Diol 2.43



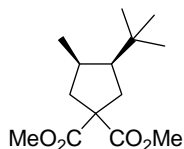
(3-*tert*-Butyl-1-hydroxymethyl-4-methylcyclopentyl)methanol (2.43): To a solution of malonate **2.7trans** (0.059 g, 0.23 mmol) in THF (3.0 mL) was added, in small portions, LiAlH₄ (0.032 g, 0.83 mmol). The resulting suspension was stirred for 6 h at which point ethyl acetate (1 mL) and 1M H₂SO₄ was added to quench any excess hydride. The reaction mixture was extracted with ether (3 x 10 mL), the combined organic layers were washed with brine (10 mL), dried over MgSO₄, filtered and concentrated *in vacuo* to give the title compound. Purification over silica gel eluting with hexanes/ethyl acetate (1/5 followed by 1/1) gave 0.32 g of diol **2.43** (69%) as a crystalline white solid. Crystals suitable for x-ray diffraction analysis were grown by slow diffusion of hexanes into a solution of diol **2.43** in ethyl acetate: mp 87–89 °C, IR (thin film, CH₂Cl₂) 3354, 2940 cm⁻¹; ¹H NMR (500 MHz, CDCl₃) δ 3.65–3.53 (m, 4H), 2.91 (br s, 2H), 1.88–1.79 (m, 1H), 1.71 (dd, *J* = 8.0, 13.1 Hz, 1H), 1.64 (dd, *J* = 8.0, 13.3 Hz, 1H), 1.40 (app q, *J* = 9.7 Hz, 1H), 1.27–1.18 (m, 1H), 1.10 (dd, *J* = 9.1, 13.1 Hz, 1H), 1.06 (d, *J* = 6.6 Hz, 3H), 0.90 (s, 9H); ¹³C NMR (125 MHz, CDCl₃) δ 71.0, 70.9, 56.0, 45.5, 42.0, 35.1, 34.6, 32.3, 28.3 (3C), 22.3; ESI 223 (M + Na)⁺; HRMS ESI exact mass calcd for C₁₂H₂₄O₂Na (M + Na)⁺: 223.1674, found: 223.1692.

5.3.7 Monocyclic Relay Experiments

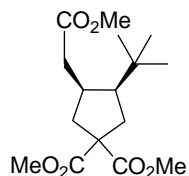


3-*tert*-Butyl-4-carboxymethylcyclopentane-1,1-dicarboxylic acid dimethyl ester (2.44): To a 77/23 *cis/trans* mixture of **2.8b** (23 mg, 0.057 mmol) in THF (1.0 mL), was added a solution of *p*-toluenesulfonic acid (24 mg, 0.13 mmol) and TBAF (1.0M solution in THF, 0.40 mL, 0.40 mmol). The resulting mixture was stirred for 12 h at room temperature at which point the reaction was diluted with ethyl acetate (5 mL) and washed with water (5 x 2 mL). The organic

layer was dried over anhydrous MgSO_4 , filtered and concentrated *in vacuo* to give 16 mg the title acid **2.44** (94%). ^1H NMR analysis showed complete loss of the ethyl TMS group and the acid was used as such without further purification or characterization.



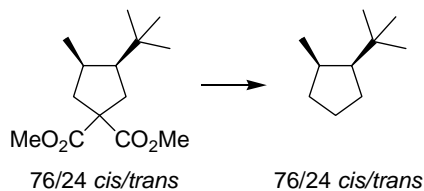
3-tert-Butyl-4-methylcyclopentane-1,1-dicarboxylic acid dimethyl ester (2.7'): A 77/23 *cis/trans* mixture of acid **2.44** (16 mg, 0.06 mmol) was taken up in benzene (0.3 mL) and treated with oxallyl chloride (0.05 mL, 0.57 mmol) and DMF (1 drop). The resulting solution was stirred at room temperature for 2 h and then concentrated *in vacuo*. The crude reaction mixture was re-dissolved in benzene and concentrated *in vacuo* again. The crude acid chloride was taken up in benzene (0.3 mL) and added to a suspension of 2-mercaptopyridine-1-oxide sodium salt (11 mg, 0.07 mmol) and DMAP (2 mg, 0.01 mmol) in benzene (0.6 mL). The reaction was heated at reflux for 20 min. The heat source was removed and a solution of AIBN (10 mg, 0.06 mmol) and Bu_3SnH (0.05 mL, 0.18 mmol) in benzene (0.3 mL) was added. The reaction was once again brought to reflux for 15 h, cooled, concentrated *in vacuo* and directly purified by column chromatography over silica gel eluting with hexanes/ethyl acetate (20/1) after four column volumes of hexanes to yield 11 mg (68 % from **2.8b**) of a 77/23 *cis/trans* mixture of the title malonate **2.7'** as a pale yellow oil. Spectral data for this mixture were identical to that previously synthesized.



3-tert-Butyl-4-methoxycarbonylmethylcyclopentane-1,1-dicarboxylic acid dimethyl ester (2.8a'): To a 77/23 *cis/trans* mixture of acid **2.44** (5 mg, 0.020 mmol) in benzene (0.1 mL) and methanol (0.03 mL) was added TMS diazomethane (2.0M solution in hexanes, 0.02 mL, 0.04 mmol). The resulting solution was stirred for 1 h, concentrated *in vacuo* and purified by column chromatography over silica gel eluting with hexanes/ethyl acetate (15/1) to give 4 mg (77% from

2.8b) of a 77/23 *cis/trans* mixture of malonate **2.8a'** as a pale yellow oil. Spectral data for this mixture was identical to that previously synthesized

5.3.8 Full Decarboxylation Experiments

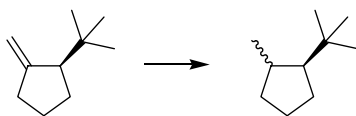


1-tert-Butyl-2-methyl-cyclopentane 2.45: To a 76/24 *cis/trans* mixture of malonate **2.7** (61 mg, 0.24 mmol) in MeOH (1 mL) and H₂O (1 mL) was added solid KOH (6 mg, 1.11 mmol) and the resulting mixture was stirred at room temperature for 16 h. The mixture was diluted with water and acidified to pH 1 with 2M HCl. The aqueous layer was then extracted with CH₂Cl₂ (3 x 5 mL) and the combined organic layers were dried over anhydrous Na₂SO₄, filtered and concentrated *in vacuo* to yield the corresponding malonic acid as a white solid which was used as such. The crude malonic acid was taken up in water (5 mL) and subjected to microwave irradiation at 200 °C for 20 min. The reaction vessel was allowed to cool and the reaction mixture was acidified to pH 1, extracted with CH₂Cl₂ (3 x 5 mL) and dried over Na₂SO₄. Filtration and concentration *in vacuo*, gave 12 mg of a mono-acid **2.46** (28 %) as a colorless oil. Acid **2.46** is a mixture of diastereomers, and so it was not characterized and used as such in the following reaction.

A mixture of the acids **2.46** (12 mg, 0.06 mmol) was taken up in C₆D₆ (0.3 mL) and treated with oxallyl chloride (0.05 mL, 0.57 mmol) and DMF (1 drop). The resulting solution was stirred at room temperature for 2 h and then concentrated *in vacuo*. The crude reaction mixture was then re-dissolved in C₆D₆ and concentrated *in vacuo* again. The crude acid chloride was taken up in C₆D₆ (0.3 mL) and added to a suspension of 2-mercaptopyridine-1-oxide sodium salt (11 mg, 0.07 mmol) and DMAP (2 mg, 0.01 mmol) in C₆D₆ (1.0 mL). The reaction was then brought to reflux and allowed to do so for 20 min. The heat source was then removed and a solution of AIBN (10 mg, 0.06 mmol) and Ph₃SnH (63 mg, 0.18 mmol) in C₆D₆ (0.3 mL) was added. The reaction was once again brought to reflux for 15 h and then cooled. Due to the

volatility of the products **2.45**, the GC and NMR analyses were carried out as this crude solution in C₆D₆.

5.3.9 Hydrogenation Experiments



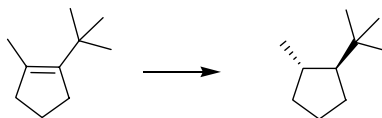
1-*tert*-Butyl-2-methylcyclopentane **2.45**

*General Procedure for the hydrogenation of olefin **2.50** using a metal hydrogenation catalyst:*

To a solution of alkene **2.50** (50 mg, 0.36 mmol) in ethanol (1.0 mL) was added the metal catalyst (0.036 mmol, either Pd/C, Pt/C, or Raney Nickel in water). The flask was fitted with a three way stopcock with one outlet to a hydrogen balloon and the other to an aspirator vacuum. The mixture was stirred vigorously and evacuated until the suspension bubbled at which point it was released to the hydrogen balloon. The purging of the reaction mixture with hydrogen was repeated an additional two times. After stirring for 12 h under the hydrogen atmosphere, the mixture was filtered through a 2 μ m filter. Due to the volatility of the products **2.45**, the GC analysis was carried out on this crude mixture as a solution in ethanol.

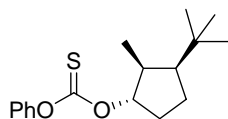
*Procedure for the hydrogenation of **2.50** using diimide as the reducing agent:*

To solution of alkene **2.50** (10 mg, 0.07 mmol) in absolute ethanol (0.5 mL) was added anhydrous hydrazine (0.22 mL, 7.0 mmol) and anhydrous copper sulfate (11 mg, 0.7 mmol). The flask was fitted with a cold finger and the suspensions was stirred for 15 min at room temperature and then at 70 °C for 16 h. Additional hydrazine and copper sulfate was added as needed until complete consumption of the starting material was observed by GC. The mixture was filtered through a 2 μ m filter and analyzed by GC without further purification as a solution in ethanol.

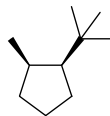


***trans*-1-*tert*-Butyl-2-methylcyclopentane (2.45):** To a solution of alkene **2.51** (50 mg, 0.36 mmol) in ethyl acetate (0.75 mL) was added Pd/C (10% by weight, 12 mg). The flask was fitted with a three way stopcock with one outlet to a hydrogen balloon and the other to an aspirator vacuum. The mixture was stirred vigorously and evacuated until the suspension bubbled at which point it was released to the hydrogen balloon. The purging of the reaction mixture with hydrogen was repeated an additional two times. After stirring for 12 h under the hydrogen atmosphere, the mixture was filtered through a 2 μ m filter. Due to the volatility of the products **2.45**, the GC analysis was carried out on this crude mixture as a solution in ethyl acetate.

5.3.10 Deoxygenation Experiments

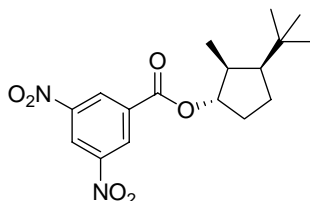


Thiocarbonic acid *O*-(3-*tert*-butyl-2-methylcyclopentyl) ester *O*-phenyl ester (S20): Cyclopentanol **2.58** (0.050 g, 0.32 mmol) was dissolved in CH₂Cl₂ (1.5 mL) to which was added phenylchlorothionoformate (0.05 mL, 0.35 mmol) and pyridine (0.10 mL, 1.18 mmol). The resulting mixture was stirred for 16 h at which point it was poured into water and extracted with ethyl acetate (2 x 15 mL). The combined organic layers were washed with 10 % HCl (4 x 2 mL) and satd NaHCO₃ (5 mL), dried over MgSO₄, filtered and concentrated *in vacuo* to give the title compound. Purification by column chromatography over silica gel eluting with hexanes/ethyl acetate (25/1) gave 0.080 g of thionoformate **2.61** (86%) as a clear colorless oil: IR (thin film, CH₂Cl₂) 2975, 1180, 1040, 960 cm⁻¹; ¹H NMR (300 MHz, CDCl₃) δ 7.59–7.53 (m, 2H), 7.45–7.43 (m, 1H), 7.29–7.25 (m, 2H), 5.36 (dm, *J* = 6.3 Hz, 1H), 2.60–2.56 (m, 1H), 2.44–2.38 (m, 1H), 2.20–1.90 (m, 2H), 1.84–1.69 (m, 2H), 1.14–1.10 (m, 12H); ¹³C NMR (75 MHz, CDCl₃) δ 194.3, 153.4, 129.4 (2C), 126.4, 122.0 (2C), 94.0, 51.2, 41.9, 31.8, 29.2 (3C), 29.1, 22.1, 13.7; MS *m/e* 139 (M – PhOC(S)O)⁺, 138, 123, 94, 81, 69, 57; HRMS exact mass calcd for C₁₀H₁₉(M – PhOC(S)O)⁺ 139.1487, found 139.1487.



cis-1-tert-Butyl-2-methylcyclopentane (2.45): To a solution of thionoformate **2.61** (50 mg, 0.17 mmol) in hexanes (2 mL) was added a solution of AIBN (3 mg, 0.03 mmol) and Bu₃SnH (0.05 mL, 0.19 mmol) in hexanes (1.3 mL). The resulting solution was refluxed for 16 h and the reaction was cooled. Due to the volatility of the products **2.45**, the GC analysis was carried out on this crude mixture as a solution in hexanes.

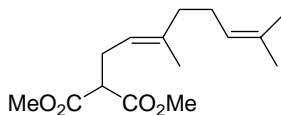
5.3.11 Synthesis of 2.62



(1R,2R,3R)-3-tert-Butyl-2-methylcyclopentyl-3,5-dinitrobenzoate (2.62): Cyclopentanol **2.58** (52 mg, 0.33 mmol) was diluted with CH₂Cl₂ (2 mL) and to this solution was added *m*-dinitrobenzoyl chloride (114 mg, 0.50 mmol). The stirred solution was then cooled to 0 °C and DMAP (60 mg, 0.50 mmol) was added drop wise as a solution in CH₂Cl₂ (1 mL). The reaction temperature was maintained at 0 °C for 1.5 h and then warmed to room temperature for an additional 1.5 h. The mixture was then diluted with CH₂Cl₂ (5 mL) and washed with 1M HCl (5 mL) and water (5 mL). The organic layers was dried over MgSO₄, filtered and concentrated *in vacuo* to give the title compound. Purification over silica gel eluting with hexanes/ethyl acetate (1/7) gave 116 mg of ester **2.62** (99%) as a crystalline white solid. Crystals suitable for x-ray diffraction analysis were grown by slow evaporation of methanol from a solution of title compound: mp 54–56 °C, IR (thin film, CH₂Cl₂) 2940, 1720, 1310, 895, 710 cm⁻¹; ¹H NMR (300 MHz, CDCl₃) δ 9.22–9.20 (m, 1H), 9.12–9.11 (m, 2H), 5.08 (br d, *J* = 6.5 Hz, 1H), 2.37–2.27 (m, 2H), 2.05–1.96 (m, 1H), 1.89–1.78 (m, 2H), 1.72–1.57 (m, 1H), 1.01 (d, *J* = 6.9 Hz, 3H), 1.00 (s, 9H); ¹³C NMR (75 MHz, CDCl₃) δ 162.2, 148.7, 134.6, 129.3 (2C), 122.1(2C), 86.6, 51.6, 42.4, 31.8, 29.4 (3C), 29.3, 22.3, 14.1; MS *m/e* 350, 293, 278, 212, 195, 149, 123, 81, 57; HRMS exact mass calcd for C₁₇H₂₂N₂O₆ 350.1478, found 350.1485.

5.4 Experimental Procedures and Characterization Data for Chapter 3

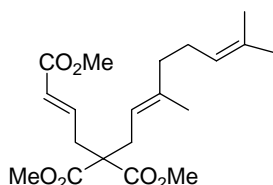
5.4.1 Synthesis of Cyclization Precursors 1.65, 3.2 and 3.3



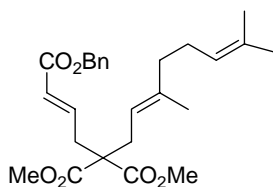
2-(3,7-Dimethylocta-2E,6-dienyl)malonic acid dimethyl ester (3.22): Dimethyl malonate (21.1 mL, 184 mmol) was added via syringe pump over 30 min to a stirred suspension of NaH (95 % dry, 4.4 g, 184 mmol) in anhydrous THF (500 mL) at 0 °C. After addition, the flask was protected from light with aluminum foil and geranyl bromide (24.4 mL, 122 mmol) was added via syringe pump over 1 h to the mixture. After 16 h the resulting mixture was poured into a mixture of water (250 mL) and ethyl acetate (250 mL). After separation of the layers, the aqueous layer was extracted with ethyl acetate (3 x 250 mL) and the combined organic layers were dried over anhydrous MgSO₄. Filtration and solvent evaporation *in vacuo* gave the title compound. Purification by flash chromatography on silica gel eluting with hexanes/ethyl acetate (15/1) gave 27.5 g of **3.22** (83%) as a clear, pale yellow oil: IR (film, CH₂Cl₂) 2955, 2925, 2855, 1731, 1438, 1378, 1341, 1274, 1243, 1216, 1156, 1094, 1041, 929, 909, 888 cm⁻¹; ¹H NMR (300 MHz, CDCl₃) δ 5.09–5.06 (m, 2H), 3.74 (s, 6H), 3.39 (t, *J* = 7.7 Hz, 1H), 2.63 (t, *J* = 7.4 Hz, 2H), 2.07–2.02 (m, 4H), 1.70 (s, 3H), 1.66 (s, 3H), 1.61 (s, 3H); ¹³C NMR (75 MHz, CDCl₃) δ 169.4 (2C), 138.5, 131.3, 123.8, 119.3, 52.3 (2C), 51.7, 39.5, 27.4, 26.4, 25.5, 17.5, 15.8; MS *m/e* 268, 225, 199, 139, 121, 107, 93, 79, 69, 59; HRMS exact mass calcd for C₁₅H₂₄O₄ 268.1675, found 268.1683.

General Procedure for the Alkylation of 3.22: Alkylated malonate **3.22** was added via syringe pump over 30 min to a stirred suspension of NaH (95% dry, 1.1 equiv) in anhydrous THF (150 mL per gram of NaH) at 0 °C. Upon complete addition, the respective alkylating agent, **3.23**, was added via syringe pump over 1 h to the mixture. After 16 h the mixture was poured into a mixture of water (150 mL per gram of NaH) and ethyl acetate (50 mL per gram of NaH). After separation of the layers, the aqueous layer was extracted with ethyl acetate (3 x 130 mL per gram NaH) and the combined organic layers were dried over anhydrous MgSO₄. Filtration and solvent

evaporation *in vacuo* gave the bis-alkylated product. Purification by flash chromatography on silica gel yielded the title compound.

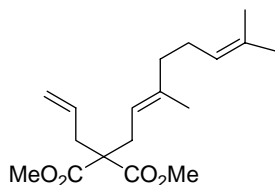


5-(3,7-Dimethylocta-2E,6-dienyl)-5-methoxycarbonylhex-2E-enedioic acid dimethyl ester (3.24a): Alkylating **3.22** (23.0 g, 85.7 mmol) with (*E*)-methyl-4-bromocrotonate **3.23a** (11.9 mL, 100.8 mmol, sample available from Aldrich is only 85 % pure and so this represents 1.0 equiv of the crotonate) and eluting the column with hexanes/ethyl acetate (5/1) yielded 27.3 g of **3.24a** (87%) as a clear, pale yellow oil: IR (thin film, CHCl₃) 2954, 2925, 2853, 1732, 1659, 1438, 1377, 1342, 1283, 1214, 1175, 1101, 1062, 1041 cm⁻¹; ¹H NMR (300 MHz, CDCl₃) δ 6.79 (dt, *J* = 7.7, 15.5 Hz, 1H), 5.85 (dt, *J* = 1.4, 15.5 Hz, 1H), 5.07–5.03 (m, 1H), 4.94 (dt, *J* = 1.2, 7.5 Hz, 1H), 3.73 (s, 6H), 3.71 (s, 3H) 2.76 (dd, *J* = 1.4, 7.7 Hz, 2H), 2.63 (d, *J* = 7.4 Hz, 2H), 2.07–1.99 (m, 4H), 1.69 (d, *J* = 1.0 Hz, 3H), 1.60 (br s, 6H); ¹³C NMR (75 MHz, CDCl₃) δ 170.9 (2C), 166.2, 143.1, 139.9, 131.6, 124.5, 123.9, 117.0, 57.6, 52.5 (2C), 51.5, 39.9, 35.3, 31.4, 26.4, 25.6, 17.6, 16.2; MS *m/e* 367 (M + H)⁺, 334, 319, 306, 284, 265, 246, 237, 205, 177, 166, 145, 135, 117, 109, 91, 82, 69, 59; HRMS exact mass calcd for C₂₀H₃₁O₆ (M + H)⁺: 367.2121, found 367.2134.



5-(3,7-Dimethylocta-2E,6-dienyl)-5-methoxycarbonylhex-2E-enedioic acid 1-benzyl ester 6-dimethyl ester (3.24b): Alkylating **3.22** (2.8 g, 10.3 mmol) with 4-bromobut-2E-enoic acid benzyl ester **3.23b**⁸⁹ (2.6 g, 10.3 mmol) and eluting the column with hexanes/ethyl acetate (10/1) yielded 3.9 g of **3.24b** (86%) as a clear, pale, brown oil: IR (neat) 2952, 2852, 1730, 1657, 1436, 1378, 1277, 1212, 1164, 983, 735 cm⁻¹; ¹H NMR (300 MHz, CDCl₃) δ 7.41–7.31 (m, 5H), 6.85 (dt, *J* = 7.7, 15.5 Hz, 1H), 5.90 (dt, *J* = 1.3, 15.5 Hz, 1H), 5.18 (s, 2H), 5.07–5.03 (m, 1H), 4.94 (tq, *J* = 1.1, 7.4 Hz, 1H), 3.73 (s, 6H), 2.77 (dd, *J* = 1.3, 7.7 Hz, 2H), 2.64 (d, *J* = 7.4 Hz, 2H),

2.07–1.99 (m, 4H), 1.68 (d, $J = 1.0$ Hz, 3H), 1.59 (s, 6H); ^{13}C NMR (75 MHz, CDCl_3) δ 170.9 (2C), 165.6, 143.5, 139.9, 136.0, 131.6, 128.5 (2C), 128.1 (3C), 124.5, 123.9, 117.0, 66.1, 57.6, 52.5 (2C), 39.8, 35.3, 31.4, 26.4, 25.6, 17.7, 16.2; MS m/e 443 ($\text{M} + \text{H}$) $^+$, 351, 157, 135, 109, 91, 69; HRMS exact mass calcd for $\text{C}_{26}\text{H}_{34}\text{O}_6$: 442.2355, found: 442.2348.

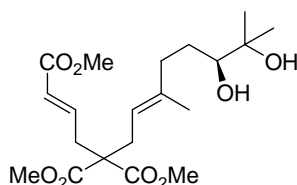


2-Allyl-2-(3,7-dimethylocta-2E,6-dienyl)malonic acid dimethyl ester (3.24c): Alkylating **3.22** (4.0 g, 14.9 mmol) with allyl bromide **3.23c** (1.3 mL, 15.0 mmol) and eluting the column with hexanes/ethyl acetate (15/1) yielded 4.2 g of **3.24c** (92%) as a clear pale, yellow oil: IR (thin film, CH_2Cl_2) 3056, 2985, 1731, 1435, 1273, 1249, 1225 cm^{-1} ; ^1H NMR (300 MHz, CDCl_3) δ 5.68–5.54 (m, 1H), 5.06–5.00 (m, 3H), 4.92 (dq, $J = 1.3, 7.5$ Hz, 1H), 3.66 (s, 6H), 2.58 (dm, $J = 7.4$ Hz, 4H), 2.03–1.94 (m, 4H), 1.64 (d, $J = 1.4$ Hz, 3H), 1.58–1.55 (m, 6H); ^{13}C NMR (75 MHz, CDCl_3) δ 171.4 (2C), 139.1, 132.6, 131.3, 123.9, 118.7, 117.5, 57.8, 52.1 (2C), 39.8, 36.8, 30.9, 26.4, 25.5, 17.5, 16.0; MS m/e 308, 293, 277, 179, 147, 119, 105, 91, 79, 69, 59; HRMS exact mass calcd for $\text{C}_{18}\text{H}_{28}\text{O}_4$: 308.1988, found 308.1991.

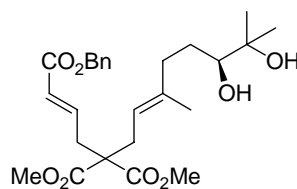
General Procedure for the Selective Dihydroxylation of the bis-Alkylated Malonates 3.25:

To a mixture of *t*-BuOH (5 mL per mmol of olefin) and water (5 mL per mmol of olefin), was added AD-Mix α (1.4 g per mmol of olefin). The mixture was stirred vigorously and $\text{CH}_3\text{SO}_2\text{NH}_2$ (0.095 g per mmol of olefin) was added. The entire mixture was cooled to 0 $^\circ\text{C}$ and the *bis*-alkylated malonate **3.24**, was added. The mixture was vigorously stirred for 14 h. Sodium sulfite (1.5 g per mmol of olefin) was added and the mixture was warmed to room temperature and stirred for 1 h. Ethyl acetate (10 mL per mmol of olefin) was added to the mixture and after separation of the layers, the aqueous layer was extracted with ethyl acetate (3 x 5 mL per mmol of olefin). The combined organic layers were then washed with 2N KOH (5 mL per mmol of olefin) and dried over anhydrous MgSO_4 . Filtration and solvent evaporation *in vacuo* yielded the respective diol. Purification was carried out by flash chromatography on silica

gel eluting with hexanes/ethyl acetate to recover any unreacted alkene starting material and then pure ethyl acetate to obtain the product.

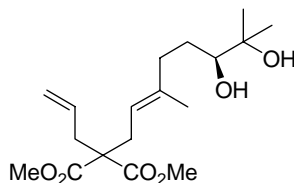


5-(6,7-Dihydroxy-3,7-dimethyloct-2E-enyl)-5-methoxycarbonylhex-2E-enedioic acid dimethyl ester (3.25a): Using malonate **3.24a** (19.5 g, 53.2 mmol), and eluting the column with hexanes/ethyl acetate (3/1) yielded 19.7 g (92%) of the title diol **3.25a** as a thick pale yellow oil: IR (thin film, CHCl₃) 3553, 2985, 2955, 1743, 1659, 1439, 1374, 1261, 1044, 984 cm⁻¹; ¹H NMR (300 MHz, CDCl₃) δ 6.80 (dt, *J* = 7.6, 15.5 Hz, 1H), 5.87 (dt, *J* = 1.4, 15.5 Hz, 1H), 5.05 (t, *J* = 7.3 Hz, 1H), 3.74 (s, 6H), 3.73 (s, 3H), 3.31 (dd, *J* = 2.0, 10.4 Hz, 1H), 3.00 (br s, 1H), 2.69 (br s, 1H), 2.77 (dd, *J* = 1.6, 6.5 Hz, 2H), 2.64 (d, *J* = 7.4 Hz, 2H), 2.30–2.22 (m, 1H), 2.14–2.06 (m, 1H), 1.62 (s, 3H), 1.62–1.56 (m, 1H) 1.42–1.27 (m, 1H), 1.26 (s, 3H), 1.20 (s, 3H); ¹³C NMR (75 MHz, CDCl₃) δ 171.8 (2C), 166.2, 142.9, 139.8, 124.3, 117.3, 77.2, 72.7, 57.4, 52.4 (2C), 51.3, 36.7, 35.2, 31.3, 29.4, 26.1, 23.1, 15.9; MS *m/e* 382 (M – H₂O)⁺, 351, 299, 291, 277, 267, 265, 264, 263, 259, 219, 198, 166, 93, 81, 71, 59; HRMS exact mass calcd for C₂₀H₃₀O₇: (M – H₂O)⁺ 382.1992, found: 382.1997.



5-(6,7-Dihydroxy-3,7-dimethyloct-2E-enyl)-5-methoxycarbonylhex-2E-enedioic acid 1-benzyl ester 6-methyl ester (3.25b): Using malonate **3.24b** (3.85 g, 8.7 mmol), and eluting the column with hexanes/ethyl acetate (5/1) yielded 3.6 g (87%) of diol **3.25b** as a thick yellow oil: IR (neat) 3472, 2955, 1730, 1657, 1438, 1379, 1274, 1168, 1075, 735 cm⁻¹; ¹H NMR (300 MHz, CDCl₃) δ 7.40–7.32 (m, 5H), 6.84 (dt, *J* = 7.7, 15.5 Hz, 1H), 5.91 (dt, *J* = 1.2, 15.5 Hz, 1H), 5.17 (s, 2H), 5.05 (tq, *J* = 1.0, 7.5 Hz, 1H), 3.73 (s, 6H), 3.30 (dd, *J* = 2.0, 10.3 Hz, 1H), 2.78 (dd, *J* = 1.2, 7.7 Hz, 2H), 2.64 (d, *J* = 7.4 Hz, 2H), 2.28–2.21 (m, 1H), 2.22 (br s, 1H), 2.15–2.07 (m, 1H), 1.99 (br s, 1H), 1.61 (d, *J* = 1.0 Hz, 3H), 1.45–1.32 (m, 2H), 1.20 (s, 3H), 1.16 (s, 3H); ¹³C

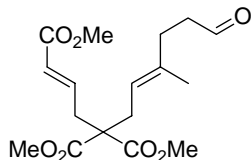
NMR (75 MHz, CDCl₃) δ 170.9 (2C), 165.6, 143.4, 139.6, 135.9, 128.4 (2C), 128.1 (3C), 124.5, 117.6, 77.6, 72.9, 66.1, 57.5, 52.5 (2C), 36.8, 35.4, 31.5, 29.4, 26.2, 23.3, 16.1; MS *m/e* 458 (M – H₂O)⁺, 430, 375, 215, 191, 121, 91, 71 59; HRMS exact mass calcd for C₂₆H₃₄O₇ (M – H₂O)⁺ 458.2305, found 458.2316.



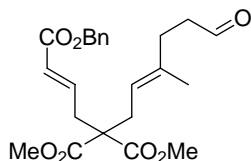
2-Allyl-2-(6,7-dihydroxy-3,7-dimethyloct-2E-enyl)malonic acid dimethyl ester (3.25c):

Using malonate **3.24c** (2.0 g, 6.5 mmol), and eluting the column with hexanes/ethyl acetate (3/1) yielded 2.1 g (93%) of the **3.25c** as a dark yellow oil: IR (thin film, neat) 3445, 2954, 1729, 1439, 1384, 1291, 1228, 1146, 1075, 921, 735 cm⁻¹; ¹H NMR (300 MHz, CDCl₃) δ 5.69–5.55 (m, 1H), 5.09–4.99 (m, 3H), 3.68 (s, 6H), 3.27 (d, *J* = 10.2 Hz, 1H), 2.59 (d, *J* = 7.0 Hz, 4H), 2.59 (br s, 1H), 2.42 (br s, 1H), 2.26–2.16 (m, 1H), 2.11–2.01 (m, 1H), 1.59 (s, 3H), 1.59–1.49 (m, 1H), 1.39–1.34 (m, 1H), 1.17 (s, 3H), 1.13 (s, 3H); ¹³C NMR (75 MHz, CDCl₃) δ 171.5 (2C), 139.0, 132.3, 119.0, 117.9, 77.5, 72.9, 57.8, 52.3 (2C), 36.8 (2C), 30.8, 29.4, 26.1, 23.2, 16.0; MS *m/e* 324 (M – H₂O)⁺, 251, 241, 219, 179, 172, 161, 153, 141, 140, 108, 93, 81, 71, 67, 59; HRMS exact mass calcd for C₁₈H₂₈O₅ (M – H₂O)⁺ 324.1937, found 324.1942.

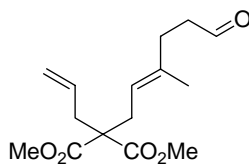
General Procedure for the Diol Cleavage of 3.25: A 3/1 (v/v) mixture of THF and water (5 mL per mmol of diol) was added to the diol **3.25** and the resulting mixture was stirred vigorously until the solution was homogeneous. NaIO₄ (1.0 equiv) was added in small portions over 30 min. The flask was stoppered and the mixture was stirred for 17 h during which time a white solid precipitated. The reaction mixture was poured into water (6 mL per mmol of diol) and Et₂O (6 mL per mmol of diol). After separation of the layers, the aqueous layer was extracted with Et₂O (3 x 7 mL per mmol of diol) and the combined organic layers were dried over anhydrous MgSO₄. Filtration and solvent evaporation *in vacuo* followed by purification by flash chromatography on silica gel.



5-Methoxycarbonyl-5-(3-methyl-6-oxohex-2E-enyl)hex-2E-enedioic acid dimethyl ester (3.26a): Using diol **3.25a** (19.7 g, 49 mmol) and eluting the column with hexanes/ethyl acetate (3/1) yielded 15.7 g (94%) of the title aldehyde **3.25a** as a clear, pale yellow oil: IR (thin film, CH₂Cl₂) 2996, 2954, 2845, 2729, 1731, 1659, 1437, 1278, 1171, 1068, 1043, 986 cm⁻¹; ¹H NMR (300 MHz, CDCl₃) δ 9.76 (t, *J* = 1.7 Hz, 1H), 6.77 (dt, *J* = 7.6, 15.5 Hz, 1H), 5.85 (dt, *J* = 1.4, 15.5 Hz, 1H), 5.01 (t, *J* = 7.4 Hz, 1H), 3.73 (s, 6H), 3.72 (s, 3H), 2.74 (dd, *J* = 1.4, 7.7 Hz, 2H), 2.62 (d, *J* = 7.4 Hz, 2H), 2.53 (tm, *J* = 7.2 Hz, 2H), 2.34 (t, *J* = 7.2 Hz, 2H), 1.60 (s, 3H); ¹³C NMR (75 MHz, CDCl₃) δ 201.7, 170.6 (2C), 166.0, 142.6, 137.8, 124.4, 118.0, 57.2, 52.4 (2C), 51.3, 41.8, 35.2, 31.7, 31.2, 16.1; MS *m/e* 341 (M + H)⁺, 291, 263, 249, 241, 177, 166, 111, 107, 93, 81, 59; HRMS exact mass calcd for C₁₇H₂₄O₇: 340.1522, found: 340.1535.



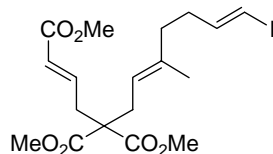
5-Methoxycarbonyl-5-(3-methyl-6-oxohex-2E-enyl)hex-2E-enedioic acid 1-benzyl ester 6-methyl ester (3.26b): Using diol **3.25b** (3.6 g, 7.5 mmol) and eluting the column with hexanes/ethyl acetate (3/1) yielded 2.8 g (89%) of the title aldehyde **3.26b** as a clear dark yellow oil: IR (thin film, CH₂Cl₂) 3057, 2986, 1730, 1436, 1423, 1281, 1250, 1170 cm⁻¹; ¹H NMR (300 MHz, CDCl₃) δ 9.67 (t, *J* = 1.5 Hz, 1H), 7.29–7.32 (m, 5H), 6.78 (dt, *J* = 7.7, 15.5 Hz, 1H), 5.86 (dt, *J* = 1.3, 15.5 Hz, 1H), 5.12 (s, 2H), 4.97 (dq, *J* = 1.3, 7.5 Hz, 1H), 3.67 (s, 6H), 2.71 (dd, *J* = 1.3, 7.8 Hz, 2H), 2.58 (d, *J* = 7.5 Hz, 2H), 2.45 (dt, *J* = 1.5, 7.5 Hz, 2H), 2.27 (t, *J* = 7.5 Hz, 2H), 1.56 (d, *J* = 1.0 Hz, 3H); ¹³C NMR (75 MHz, CDCl₃) δ 201.7, 170.5 (2C), 165.3, 143.1, 137.7, 135.7, 128.3 (2C), 128.0, 127.9 (2C), 124.4, 117.9, 65.9, 57.2, 52.4 (2C), 41.8, 35.2, 31.7, 31.2, 16.1; APCI: Mass calcd for C₂₃H₂₈O₇Na (M + Na)⁺: 439.2, found 439.1; Mass calcd for C₂₃H₂₈O₇K (M + K)⁺: 455.2, found: 455.1.



2-Allyl-2-(3-methyl-6-oxohex-2-enyl)malonic acid dimethyl ester (3.26c): Using diol **3.25c** (3.9 g, 11.3 mmol) and eluting the column with hexanes/ethyl acetate (3/1) yielded 2.8 g (93%) of the title aldehyde **3.26c** as a clear, pale yellow oil: IR (thin film, CH₂Cl₂) 3057, 2986, 2954, 2859, 1729, 1437, 1274, 1223 cm⁻¹; ¹H NMR (300 MHz, CDCl₃) δ 9.73 (t, *J* = 1.8 Hz, 1H), 5.69–5.56 (m, 1H), 5.10–4.99 (m, 3H), 3.70 (s, 6H), 2.60 (dm, *J* = 7.4 Hz, 4H), 2.49 (tm, *J* = 7.8 Hz, 2H), 2.32 (t, *J* = 7.7 Hz, 2H), 1.61 (s, 3H); ¹³C NMR (75 MHz, CDCl₃) δ 202.0, 171.3 (2C), 137.3, 132.4, 119.0, 118.7, 57.7, 52.3 (2C), 42.1, 38.7, 37.0, 32.0, 30.9, 16.2; MS *m/e* 241 (M – C₃H₅)⁺, 209, 179, 177, 165, 139, 119, 108, 93, 81, 77, 59; HRMS exact mass calcd for C₁₂H₁₇O₅ (M – C₃H₇)⁺: 241.1076, found: 241.1076.

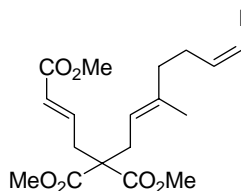
General Procedure for the Synthesis of the Vinyl Iodides From Aldehydes 3.26: To a stirred suspension of (iodomethyl)triphenylphosphonium iodide **3.27** (2.0 equiv) in THF (2.0 mL per mmol of Wittig salt) was added NaHMDS (2.0 equiv of a 1M solution in THF). The resulting suspension was stirred at room temperature for 30 min during which time it turned to a clear dark red solution. The mixture was cooled to –78 °C and to this was added the aldehyde (1.0 equiv) in THF (2.0 mL per mmol of aldehyde). The reaction was removed from the cold bath and warmed to room temperature and stirred for 1 h. The crude reaction mixture was then filtered through a short column of silica gel eluting with ether. Solvent evaporation and purification over silica gel yielded the respective vinyl iodide in a 6/1 *Z/E* ratio.

5-(7-Iodo-3-methylhepta-2*E*,6*Z*-dienyl)-5-methoxycarbonylhex-2*E*-enedioic acid dimethyl ester (1.65): Using aldehyde **3.26a** (10.0 g, 29.4 mmol) and eluting the column with hexanes/ethyl acetate (10/1) yielded 5.5 g (41%) of iodide **1.65** as a light brown oil. On a small scale, the *E* and the *Z* were separated with the *E*-isomer eluting first:



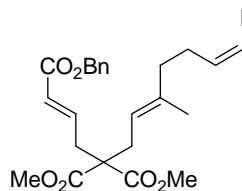
E-isomer

IR (thin film, CH₂Cl₂) 3055, 2986, 1422, 1731, 1422, 1267, 896 cm⁻¹; ¹H NMR (300 MHz, CDCl₃) δ 6.77 (dt, *J* = 7.7, 15.5 Hz, 1H), 6.45 (dt, *J* = 7.1, 14.4 Hz, 1H), 6.00 (dt, *J* = 1.3, 14.4 Hz, 1H), 5.84 (dt, *J* = 1.2, 15.5 Hz, 1H), 4.96 (tq, 1.2, 7.5 Hz, 1H), 3.73 (s, 6H), 3.71 (s, 3H), 2.75 (dd, *J* = 1.2, 7.7 Hz, 2H), 2.62 (d, *J* = 7.3 Hz, 2H), 2.24–2.07 (m, 4H), 1.58 (d, *J* = 1.2 Hz, 3H); ¹³C NMR (75 MHz, CDCl₃) δ 170.9 (2C), 166.2, 145.7, 142.9, 138.5, 124.6, 118.1, 74.9, 57.4, 52.6 (2C), 51.5, 38.5, 35.3, 34.3, 31.4, 16.2; MS *m/e* 464, 433, 404, 365, 333, 277, 245, 205, 198, 167, 145, 107, 91, 79, 59; HRMS exact mass calcd for C₁₈H₂₆IO₆ (M + H)⁺ 465.0774, found 465.0766.

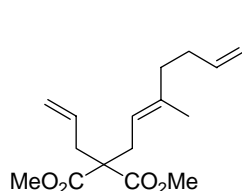


Z-isomer

IR (thin film, CH₂Cl₂) 3048, 2964, 2928, 2860, 1732, 1437, 1280, 1252 cm⁻¹; ¹H NMR (300 MHz, CDCl₃) δ 6.79 (dt, *J* = 7.7, 15.5 Hz, 1H), 6.21 (dt, *J* = 1.2, 7.3 Hz, 1H), 6.11 (dt, *J* = 6.4, 7.2 Hz, 1H), 5.86 (dt, *J* = 1.2, 15.5 Hz, 1H), 4.99 (tq, 1.4, 7.4 Hz, 1H), 3.74 (s, 6H), 3.73 (s, 3H), 2.76 (dd, *J* = 1.2, 7.7 Hz, 2H), 2.64 (d, *J* = 7.4 Hz, 2H), 2.24 (ddt, *J* = 1.2, 6.7, 6.7 Hz, 2H), 2.12 (t, *J* = 6.7 Hz, 2H), 1.64 (d, *J* = 1.4 Hz, 3H); ¹³C NMR (75 MHz, CDCl₃) δ 170.8 (2C), 166.2, 142.9, 140.5, 138.8, 124.6, 117.9, 82.7, 57.5, 52.6 (2C), 51.5, 37.8, 35.4, 33.0, 31.4, 16.2; MS *m/e* 464, 432, 400, 365, 333, 305, 277, 237, 217, 205, 177, 166, 145, 107, 91, 79, 59; HRMS exact mass calcd for C₁₈H₂₆IO₆ (M + H)⁺ 465.0774, found 465.0762.

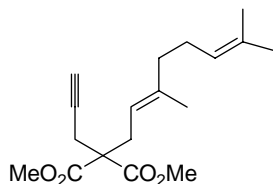


5-(7-Iodo-3-methyl-hepta-2E,6Z-dienyl)-5-methoxycarbonylhex-2E-enedioic acid 1-benzyl ester 6-methyl ester (3.2): Using aldehyde **3.26b** (0.015 g, 0.36 mmol) and eluting the column with hexanes/ethyl acetate (10/1) yielded 0.073 g (39%) of the title iodide **3.2** as a clear, light brown oil: IR (thin film, CH₂Cl₂) 3057, 2986, 1732, 1422, 1278, 1249, 895 cm⁻¹; ¹H NMR (300 MHz, CDCl₃) δ 7.37–7.31 (m, 5H), 6.83 (dt, *J* = 7.7, 15.5 Hz, 1H), 6.20 (dm, *J* = 7.3 Hz, 1H), 6.10 (dt, *J* = 6.7, 7.1 Hz, 1H), 5.91 (dm, *J* = 15.5 Hz, 1H), 5.17 (s, 2H), 4.97 (dq, *J* = 1.2, 7.4 Hz, 1H), 3.72 (s, 6H), 2.76 (d, *J* = 7.7 Hz, 2H), 2.63 (d, *J* = 7.4 Hz, 2H), 2.21 (dt, *J* = 6.5, 7.1 Hz, 2H), 2.11 (t, *J* = 7.1 Hz, 2H), 1.62 (d, *J* = 1.2 Hz, 3H); ¹³C NMR (75 MHz, CDCl₃) δ 170.8 (2C), 165.6, 143.3, 140.5, 138.8, 135.9, 128.5 (2C), 128.2, 128.1 (2C), 124.6, 117.8, 82.7, 66.1, 57.4, 52.6 (2C), 37.8, 35.3, 33.0, 31.4, 16.1; MS *m/e* 509 (M – MeOH)⁺, 481, 449, 431, 403, 333, 233 167, 91; HRMS exact mass calcd for C₂₃H₂₆IO₅ (M – MeOH)⁺ 509.0825, found 509.0831.



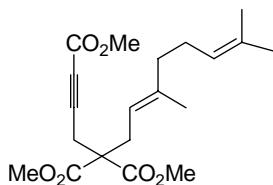
2-Allyl-2-(7-iodo-3-methylhepta-2E,6Z-dienyl)malonic acid dimethyl ester (3.3): Using aldehyde **3.26c** (2.8 g, 9.8 mmol) and eluting the column with hexanes/ethyl acetate (20/1) yielded 2.3 g (57%) of the title iodide **18** as a dark yellow oil: IR (thin film, CH₂Cl₂) 3058, 2975, 2933, 2869, 1732, 1438, 1276, 1224 cm⁻¹; ¹H NMR (300 MHz, CDCl₃) δ 6.18 (dt, *J* = 1.3, 7.3 Hz, 1H), 6.09 (dt, *J* = 6.5, 7.3 Hz, 1H), 5.70–5.56 (m, 1H), 5.07 (dm, *J* = 14.1 Hz, 2H), 4.98 (dq, *J* = 1.1, 7.5 Hz, 1H), 3.71 (s, 6H), 2.61 (d, *J* = 7.4 Hz, 4H), 2.22 (ddt, *J* = 6.8, 6.8, 1.1 Hz, 2H), 2.11 (t, *J* = 6.9, 2H), 1.63 (d, *J* = 1.1, 3H); ¹³C NMR (75 MHz, CDCl₃) δ 171.3 (2C), 140.5, 138.1, 132.4, 119.0, 118.4, 82.6, 57.7, 52.3 (2C), 37.8, 36.8, 33.0, 30.9, 16.0; ¹³C NMR resonances attributed to the *E* isomer: 152.3, 145.7, 137.8, 137.5, 74.8, 38.4, 38.4, 34.4, 31.5, 22.6, 14.1 MS *m/e* 406, 375, 365, 333, 179, 167, 119, 107, 91, 79, 59; HRMS exact mass calcd for C₁₆H₂₃IO₄: 406.0641, found 406.0645.

5.4.2 Synthesis of Cyclization Precursor 3.1



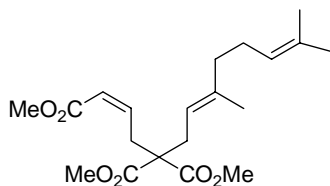
2-(3,7-Dimethylocta-2E,6-dienyl)-2-(prop-2-ynyl)malonate (**3.29**):

Malonate **3.22** was added via syringe pump over 30 min to a stirred suspension of NaH (95% dry, 0.095g, 3.52 mmol) in anhydrous THF (28 mL) at 0 °C. Upon complete addition, propargyl bromide (80% solution in toluene, 0.43 mL, 3.9 mmol) was added drop wise to the mixture. After 16 h the reaction mixture was poured into water (10 mL) and ethyl acetate (10 mL). After separation of the layers, the aqueous layer was extracted with ethyl acetate (3 x 10 mL) and the combined organic layers were dried over anhydrous MgSO₄, filtration and solvent evaporation *in vacuo* gave the title compound. Purification by flash chromatography on silica gel eluting the column with hexanes/ethyl acetate (5/1) yielded 0.84 g of **3.29** (78%) as a clear, pale, brown oil: IR (neat) 3292, 2954, 2926, 2856, 1740, 1437, 1291, 1223, 1056, 734 cm⁻¹; ¹H NMR (300 MHz, CDCl₃) δ 5.03–4.99 (m, 1H), 4.87 (t, *J* = 7.4 Hz, 1H), 3.75 (s, 6H), 2.78–2.74 (m, 4H), 2.04–1.98 (m, 5H), 1.66 (s, 3H), 1.62 (s, 3H), 1.57 (s, 3H); ¹³C NMR (75 MHz, CDCl₃) δ 170.2 (2C), 140.3, 131.4, 123.9, 117.0, 79.2, 71.1, 57.1, 52.5 (2C), 39.8, 30.5, 26.3, 25.5, 22.3, 17.5, 16.0; MS *m/e* 306, 291, 275, 237, 203, 177, 145, 117, 69; HRMS exact mass calcd for C₁₈H₂₆O₄: 306.1831, found: 306.1817.



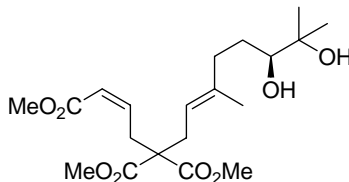
Trimethyl 7,11-dimethyldodeca-6E,10-dien-1-yne-1,4,4-tricarboxylate (3.30): To a stirred solution of malonate **3.29** (0.84 g, 2.8 mmol) in THF (6 mL) cooled to -78 °C was added BuLi (1.6M soln in hexanes, 2.6 mL, 3.30 mmol) drop wise. The resulting solution was stirred at -78 °C for 2 h, at which point methyl chloroformate (0.42 mL, 5.5 mmol) was added and stirring was continued for an additional 2 h. The mixture was warmed to room temperature and stirred for 15 h, then the reaction was quenched with a saturated aqueous solution of NH₄Cl (3 mL). After the

addition of ethyl acetate (3 mL), the layers were separated and the aqueous layer was extracted with additional ethyl acetate (2 x 3 mL). The combined organic layers were washed with water (6 mL) and brine (6 mL), dried over MgSO₄, filtered and concentrated *in vacuo* to give the crude compound. Purification over silica gel eluting the column with hexanes/ethyl acetate (15/1) to recover the starting material and changing to hexanes/ethyl acetate (10/1) to isolate the product yielded 0.36 g of alkyne **3.30** (28%) as a pale yellow oil: IR (neat) 2955, 2917, 1740, 1720, 1436, 1322, 1257, 1222, 1079 cm⁻¹; ¹H NMR (300 MHz, CDCl₃) δ 5.05–5.01 (m, 1H), 4.88 (t, *J* = 7.7 Hz, 1H), 3.75 (s, 9H), 2.93 (s, 2H), 2.80 (d, *J* = 7.6 Hz, 2H), 2.07–2.01 (m, 4H), 1.69 (s, 3H), 1.65 (s, 3H), 1.60 (s, 3H); ¹³C NMR (75 MHz, CDCl₃) δ 169.7 (2C), 153.4, 140.7, 131.4, 123.7, 116.5, 83.5, 74.9, 56.6, 52.6 (2C), 52.3, 39.7, 30.7, 26.1, 25.4, 22.4, 17.4, 15.9; MS *m/e* 332 (M – MeOH)⁺, 317, 304, 289, 273, 203, 175, 145, 109, 69; HRMS exact mass calcd for C₁₉H₂₄O₅ (M – MeOH)⁺: 332.1623, found: 332.1609.



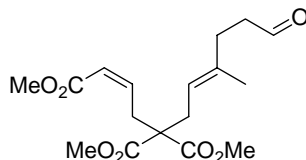
5-(3,7-Dimethylocta-2E,6-dienyl)-5-methoxycarbonylhex-2Z-enedioic acid dimethyl ester (3.31): To a solution of alkyne **3.30** (0.34 g, 0.92 mmol) and quinoline (0.34 mL, 2.85 mmol) in hexanes (26 mL) was added Lindlar's catalyst (0.17 g). The suspension was stirred and the flask was fitted with a three way stopcock with one outlet to a hydrogen balloon and the other to a vacuum pump. The mixture was stirred vigorously and evacuated until the suspension bubbled at which point it was released to the hydrogen balloon. The purging of the reaction mixture with hydrogen was repeated an additional two times. After stirring for 12 h under the hydrogen atmosphere, the mixture was filtered through celite, washing with an additional hexanes (15 mL). The filtrate was concentrated *in vacuo* to give the title compound and purified over silica gel eluting the column with hexanes/ethyl acetate (10/1) to give 0.28 g of *Z*-alkene **3.31** (83%) as a clear pale yellow oil: IR (neat) 2953, 2923, 2856, 1736, 1649, 1438, 1288, 1206, 1174, 1078 cm⁻¹; ¹H NMR (300 MHz, CDCl₃) δ 6.20 (dt, *J* = 7.2, 11.6 Hz, 1H), 5.86 (dt, *J* = 1.8, 11.6 Hz, 1H), 5.02–4.94 (m, 2H), 3.68 (s, 3H), 3.67 (s, 6H), 3.22 (dd, *J* = 1.7, 7.2 Hz, 2H), 2.61 (d, *J* = 7.5 Hz, 2H), 2.02–1.95 (m, 4H), 1.64 (s, 3H), 1.56 (s, 6H); ¹³C NMR (75 MHz, CDCl₃) δ 171.2 (2C),

166.2, 144.0, 139.6, 131.4, 123.9, 121.5, 117.3, 57.5, 52.3 (2C), 51.0, 39.8, 32.1 (2C), 26.4, 25.5, 17.5, 16.1; MS m/e 389 (M + Na)⁺, 276; HRMS exact mass calcd for C₂₀H₃₀O₆Na (M + Na)⁺: 389.1940, found: 389.1924.

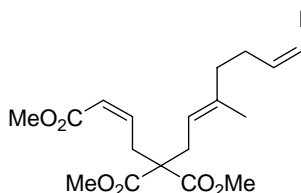


5-(6,7-Dihydroxy-3,7-dimethyloct-2E-enyl)-5-methoxycarbonylhex-2Z-enedioic acid

dimethyl ester (3.31): To a mixture of *t*-BuOH (3.8 mL) and water (3.8 mL), was added AD-Mix α (1.06 g). The mixture was stirred vigorously and CH₃SO₂NH₂ (0.072 g, 0.76 mmol) was added. The entire mixture was cooled to 0 °C and malonate **3.31** (0.28 g, 0.76 mmol) was added and the mixture was vigorously stirred for 14 h. Sodium sulfite (1.14 g) was added and the mixture was warmed to room temperature and stirred for 1 h. Ethyl acetate (1 mL) was added to the mixture and after separation of the layers, the aqueous layer was extracted with ethyl acetate (3 x 5 mL). The combined organic layers were then washed with 2N KOH (5 mL) and dried over anhydrous MgSO₄. Filtration and solvent evaporation *in vacuo* yielded the title compound. Purification was carried out by flash chromatography on silica gel eluting with hexanes/ethyl acetate (10/1) yielded 0.27 g (89%) of diol **3.32** as a thick yellow oil: IR (neat) 3530, 2954, 1735, 1720, 1648, 1438, 1325, 1290, 1209, 1080 cm⁻¹; ¹H NMR (300 MHz, CDCl₃) δ 6.17 (dt, J = 7.4, 11.6 Hz, 1H), 5.89 (dt, J = 1.9, 11.6 Hz, 1H), 5.07 (t, J = 7.2 Hz, 1H), 3.73 (s, 3H), 3.72 (s, 6H), 3.37 (dd, J = 1.6, 7.6 Hz, 2H), 3.20 (dd, J = 1.8, 6.6 Hz, 1H), 2.64 (d, J = 7.7 Hz, 2H), 2.53 (br d, J = 7.7 Hz, 1H), 2.26 (br s, 1H), 2.19–2.14 (m, 2H), 1.66–1.56 (m, 1H), 1.59 (s, 3H), 1.47–1.34 (m, 1H), 1.20 (s, 3H), 1.19 (s, 3H); ¹³C NMR (75 MHz, CDCl₃) δ 171.3 (2C), 166.4, 144.1, 139.3, 121.4, 117.9, 76.9, 72.8, 57.4, 52.4 (2C), 51.1, 36.4, 32.0, 31.9, 28.9, 25.7, 23.4, 15.8; MS m/e 423 (M + Na)⁺; HRMS exact mass calcd for C₂₀H₃₂O₈Na (M + Na)⁺ 423.1995, found 423.1992.



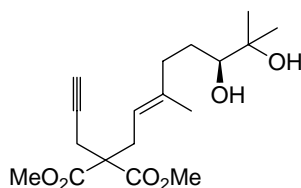
5-Methoxycarbonyl-5-(3-methyl-6-oxohex-2E-enyl)hex-2Z-enedioic acid dimethyl ester (3.33): THF (3mL) and water (1 mL) was added to the diol **3.32** (0.27 g, 0.69 mmol) and the resulting mixture was stirred vigorously until the solution was homogeneous. NaIO₄ (0.15 g, 0.69 mmol) was added in small portions over 30 min. The flask was stoppered and the mixture was stirred for 17 h during which time a white solid precipitated. The reaction mixture was poured into water (5 mL) and Et₂O (5 mL). After separation of the layers, the aqueous layer was extracted with Et₂O (3 x 5 mL) and the combined organic layers were dried over anhydrous MgSO₄. Filtration and solvent evaporation *in vacuo* provided the title compound. Purification over silica gel eluting with hexanes/ethyl acetate (3/1) yielded 0.20 g (85%) of aldehyde **3.33** as a clear, pale yellow oil: IR (neat) 2954, 1732, 1650, 1438, 1412, 1289, 1207, 816 cm⁻¹; ¹H NMR (300 MHz, CDCl₃) δ 9.27 (t, *J* = 1.6 Hz, 1H), 6.16 (dt, *J* = 7.2, 11.6 Hz, 1H), 5.87 (dt, *J* = 1.7, 11.6 Hz, 1H), 5.07 (t, *J* = 7.6 Hz, 1H), 3.72 (s, 9H), 3.25 (dd, *J* = 1.8, 7.2 Hz, 2H), 2.63 (d, *J* = 7.4 Hz, 2H), 2.51 (td, *J* = 1.4, 7.7 Hz, 2H), 2.31 (t, *J* = 7.5 Hz, 2H), 1.62 (s, 3H); ¹³C NMR (75 MHz, CDCl₃) δ 201.8, 171.0 (2C), 166.1, 143.6, 137.6, 121.6, 118.4, 57.3, 52.3 (2C), 50.9, 41.9, 32.0, 31.9, 31.7, 16.1; MS *m/e* 363 (M + Na)⁺; HRMS exact mass calcd for C₁₇H₂₄O₇Na: 363.1420, found: 363.1413.



5-(7-Iodo-3-methylhepta-2E,6Z-dienyl)-5-methoxycarbonylhex-2Z-enedioic acid dimethyl ester (3.1): To a stirred suspension of (iodomethyl)triphenylphosphonium iodide **3.27** (0.63 g, 1.18 mmol) in THF (2.5 mL) was added NaHMDS (1M solution in THF, 1.18 mL, 1.18 mmol). The resulting suspension was stirred at room temperature for 30 min during which time it turned to a clear dark red solution. The mixture was cooled to -78 °C and to this was added the aldehyde **3.33** (0.20 g, 0.59 mmol) in THF (1 mL). The reaction was removed from the cold

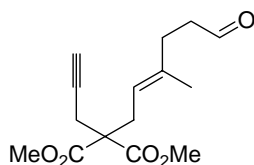
bath, warmed to room temperature and stirred for 1 h. The crude reaction mixture was then filtered through a short column of silica gel eluting with ether. Solvent evaporation and purification over silica gel eluting with hexanes/ethyl acetate (8/1 to 6/1) yielded 0.10 g (37%) of iodide **3.1** as a clear, light brown oil: IR (neat) 2951, 1732, 1650, 1438, 1287, 1207, 1174; ^1H NMR (300 MHz, CDCl_3) δ 6.23–6.08 (m, 3H), 5.87 (dt, $J = 1.7, 11.7$ Hz, 1H), 5.04 (t, $J = 7.6$ Hz, 1H), 3.73 (s, 3H), 3.72 (s, 6H), 3.27 (dd, $J = 1.7, 7.1$ Hz, 2H), 2.66 (d, $J = 7.6$ Hz, 2H), 2.26–2.19 (m, 2H), 2.11 (t, $J = 7.1$ Hz, 2H), 1.63 (s, 3H); ^{13}C NMR (75 MHz, CDCl_3) δ 171.2 (2C), 166.2, 143.9, 140.5, 138.5, 121.7, 118.3, 82.5, 57.5, 52.4 (2C), 51.1, 37.9, 33.0, 32.2 (2C), 16.1; MS m/e 433 ($\text{M} - \text{MeO}$) $^+$, 404, 373, 365, 333, 205, 173, 167, 145, 117, 91, 79, 59; HRMS exact mass calcd for $\text{C}_{17}\text{H}_{22}\text{IO}_5$ ($\text{M}^+ - \text{MeO}$) $^+$ 433.0512, found 433.0492.

5.4.3 Synthesis of Precursor 3.4.

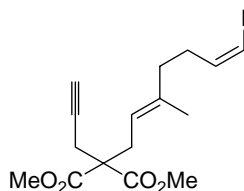


2-(6S,7-Dihydroxy-3,7-dimethyloct-2E-enyl)-2-prop-2-ynylmalonic acid dimethyl ester (3.34): To a mixture of *t*-BuOH (20 mL) and water (20 mL), was added AD-Mix α (5.64 g). The mixture was stirred vigorously and $\text{CH}_3\text{SO}_2\text{NH}_2$ (0.38 g, 4.03 mmol) was added. The entire mixture was cooled to 0 °C and malonate **3.31** (1.23g, 4.03 mmol) was added and the mixture was vigorously stirred for 14 h. Sodium sulfite (6.05 g) was added and the mixture was warmed to room temperature and stirred for 1 h. Ethyl acetate (10 mL) was added to the mixture and after separation of the layers, the aqueous layer was extracted with ethyl acetate (3 x 10 mL). The combined organic layers were then washed with 2N KOH (10 mL) and dried over anhydrous MgSO_4 . Filtration and solvent evaporation *in vacuo* yielded the title compound. Purification was carried out by flash chromatography on silica gel eluting with hexanes/ethyl acetate (15/1 to 1/1 to 2/1) yielded 1.24 g (90%) of diol **3.34** as a clear pale yellow oil: IR (thin film) 3434, 3291, 2955, 1732, 1436, 1385, 1294, 1225, 1072 cm^{-1} ; ^1H NMR (300 MHz, CDCl_3) δ 4.93 (t, $J = 7.6$ Hz, 1H), 3.68 (s, 6H), 3.23 (br d, $J = 9.9$ Hz, 1H), 2.73 (d, $J = 8.7$ Hz, 2H), 2.71 (d, $J = 2.6$ Hz, 2H), 2.21–2.15 (m, 1H), 2.07–2.01 (m, 1H), 1.98 (t, $J = 2.4$ Hz, 1H), 1.60 (s, 3H), 1.55–1.45 (m, 1H), 1.39–1.29 (m, 1H), 1.13 (s, 3H), 1.09 (s, 3H); ^{13}C NMR (75 MHz, CDCl_3) δ 170.4 (2C),

140.2, 117.3, 78.9, 77.5, 72.9, 71.3, 57.0, 52.6 (2C), 36.8, 30.5, 29.4, 26.1, 23.1, 22.4, 15.9; MS m/e 363 ($M + Na$)⁺; HRMS exact mass calcd for C₁₈H₂₈O₆Na ($M + Na$)⁺ 363.1784, found 363.1762.



2-(3-Methyl-6-oxohex-2E-enyl)-2-prop-2-ynylmalonic acid dimethyl ester (3.35): THF (15 mL) and water (5 mL) was added to the diol **3.33** (1.11 g, 3.27 mmol) and the resulting mixture was stirred vigorously until the solution was homogeneous. NaIO₄ (0.77 g, 3.6 mmol) was added in small portions over 30 min. The flask was stoppered and the mixture was stirred for 17 h during which time a white solid precipitated. The reaction mixture was poured into water (15 mL) and Et₂O (15 mL). After separation of the layers, the aqueous layer was extracted with Et₂O (3 x 15 mL) and the combined organic layers were dried over anhydrous MgSO₄. Filtration and solvent evaporation *in vacuo* provided the title compound. Purification over silica gel eluting with hexanes/ethyl acetate (3/1) yielded 0.90 g (97%) of aldehyde **3.35** as a clear, colorless oil: IR (thin film) 3282, 2955, 2817, 1736, 1436, 1322, 1291, 120, 1057 cm⁻¹; ¹H NMR (300 MHz, CDCl₃) δ: 9.69 (s, 1H), 4.93 (t, $J = 7.5$ Hz, 1H), 3.69 (s, 6H), 2.74 (d, $J = 8.0$ Hz, 2H), 2.71 (d, $J = 2.2$ Hz, 2H), 2.47 (t, $J = 7.1$ Hz, 2H), 2.28 (t, $J = 7.3$ Hz, 2H), 1.98 (t, $J = 2.5$ Hz, 1H), 1.62 (s, 3H); ¹³C NMR (75 MHz, CDCl₃) δ 201.8, 170.1, 138.4, 118.1, 78.9, 71.3, 56.9, 52.6 (2C), 41.9, 31.9, 30.5, 22.5, 16.2; MS m/e 303 ($M + Na$)⁺; HRMS exact mass calcd for C₁₅H₂₀O₅Na ($M + Na$)⁺ 303.1193, found 303.1208.

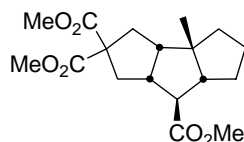


2-(7-Iodo-3-methylhepta-2E,6Z-dienyl)-2-prop-2-ynylmalonic acid dimethyl ester (3.4): To a stirred suspension of (iodomethyl)triphenylphosphonium iodide **3.27** (1.70 g, 1.60 mmol) in THF (7 mL) was added NaHMDS (1M solution in THF, 3.20 mL, 3.20 mmol). The resulting suspension was stirred at room temperature for 30 min during which time it turned to a clear dark

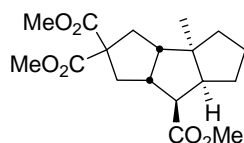
red solution. The mixture was cooled to $-78\text{ }^{\circ}\text{C}$ and to this was added aldehyde **3.35** (0.44 g, 1.60 mmol) in THF (1 mL). The reaction was removed from the cold bath, warmed to room temperature and stirred for 1 h. The crude reaction mixture was then filtered through a short column of silica gel eluting with ether. Solvent evaporation and purification over silica gel eluting the column with hexanes/ethyl acetate (15/1) provided 0.37g, after recycling the mixed fractions once, of vinyl iodide **3.4** (57%) as a dark brown oil: IR (thin film) 3295, 2995, 2951, 2849, 1737, 1435, 1321, 1290, 1202, 1056 cm^{-1} ; ^1H NMR (300 MHz, CDCl_3) δ 6.21 (dt, $J = 1.2, 7.3$ Hz, 1H), 6.11 (dt, $J = 6.7, 7.1$ Hz, 1H), 4.95 (tq, $J = 1.2, 7.7$ Hz, 1H), 3.76 (s, 6H), 2.81 (d, $J = 8.0$ Hz, 2H), 2.79 (d, $J = 2.7$ Hz, 2H), 2.24 (ddt, $J = 1.4, 6.1, 7.7$ Hz, 2H), 2.12 (t, $J = 6.9$ Hz, 2H), 2.02 (t, $J = 2.6$ Hz, 1H), 1.75 (s, 3H); ^{13}C NMR (75 MHz, CDCl_3) δ 170.2 (2C), 140.4, 139.2, 117.8, 82.6, 79.0, 71.3, 56.9, 52.6 (2C), 37.8, 32.9, 30.5, 22.4, 16.0; MS m/e 427 ($\text{M} + \text{Na}$) $^+$; HRMS exact mass calcd for $\text{C}_{16}\text{H}_{21}\text{O}_4\text{INa}$ ($\text{M} + \text{Na}$) $^+$ 427.0382, found 427.0370.

5.4.4 Cyclization Reactions with Precursors **1.65**, **3.1**, **3.3** and **3.4**

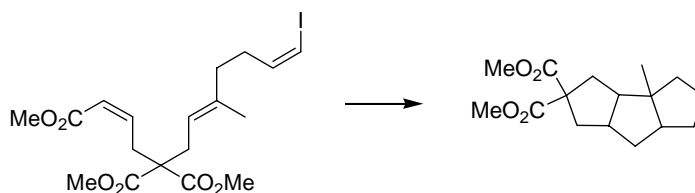
3 β -Methyldecahydrocyclopenta[α]pentalene-2,2,7-tricarboxylic acid trimethyl ester (3.9 and 3.10): Cyclization of precursor **1.65** (0.05 g, 0.1 mmol) was carried according to method B. The reducing agent used was Bu_3SnH and the mixture was refluxed for 4 h. The crude reaction mixture which was subjected to a DBU⁸¹ workup and subsequent column chromatography over silica gel eluting with hexanes/ethyl acetate (15/1) after 6 column volumes of hexanes to give 24 mg of a tin free cyclization mixture. This mixture was taken up in CH_2Cl_2 (15 mL) and cooled to $0\text{ }^{\circ}\text{C}$. The mixture was then vigorously stirred and *m*-CPBA (0.017 g, 0.1 mmol) was added. The reaction was stirred for 14 h and quenched with NaHCO_3 (15 mL) and extracted with ethyl acetate (3 x 15 mL). The combined organic layers were dried over MgSO_4 , filtered and concentrated *in vacuo*. The resulting oil was purified by column chromatography eluting with hexanes/ethyl acetate (15/1) to yield 0.018 g (52%) of a mixture of four isomeric tricyclic products **3.9/3.10/3.11/3.12** in a 47/39/6/8 ratio as determined by GC analysis. This mixture was then further purified by preparative GC which isolated the two major tricycles from the cyclization as pale yellow oils:



1st eluting on the GC *cis-syn-cis* isomer **3.9**: IR (film, CH₂Cl₂) 3054, 2964, 2928, 2860, 1728, 1440, 1275, 1256 cm⁻¹; ¹H NMR (600 MHz, CDCl₃) δ 3.74 (s, 3H), 3.73 (s, 3H), 3.68 (s, 3H), 2.89–2.86 (m, 1H), 2.57 (dd, *J* = 8.2, 14.0 Hz, 1H), 2.43–2.32 (m, 3H), 2.27 (t, *J* = 10.1 Hz, 1H), 2.05 (dd, *J* = 5.6, 14.0 Hz, 1H), 2.00 (t, *J* = 10.7 Hz, 1H), 1.77–1.68 (m, 4H), 1.21–1.26 (m, 2H) 1.09 (s, 3H) ; ¹³C NMR (150 MHz, CDCl₃) δ 175.8, 172.6, 172.5, 62.7, 59.8, 56.7, 54.8, 52.8, 52.7, 51.7 (2C), 48.4, 38.8, 36.3, 36.1, 30.0, 29.7 26.0; MS *m/e* 338, 320, 306, 278, 246, 218, 145, 67, 59 ; HRMS exact mass calcd for C₁₈H₂₆O₆ 338.1729, found 338.1713.



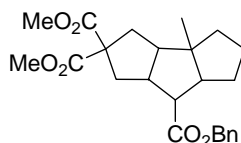
2nd eluting on the GC *cis-anti-cis* isomer **3.10**: IR (film, CH₂Cl₂) 3055, 2968, 2930, 2858, 1730, 1440, 1275, 1256 cm⁻¹; ¹H NMR (500 MHz, CDCl₃) δ 3.73 (s, 3H), 3.72 (s, 3H), 3.67 (s, 3H), 2.97–2.91 (m, 1H), 2.82 (dd, *J* = 8.4, 11.2 Hz, 1H), 2.64 (dd, *J* = 7.9, 14.5 Hz, 1H), 2.34–2.29 (m, 2H), 2.24 (dt, *J* = 7.5, 12.5 Hz, 1H), 2.05–2.00 (m, 2H) 1.77–1.74 (m, 4H), 1.26–1.24 (m, 2H), 1.09 (s, 3H); MS *m/e* 338, 320, 306, 278, 246, 218, 145, 67, 59 ; HRMS exact mass calcd for C₁₈H₂₆O₆ 338.1729, found 338.1713.



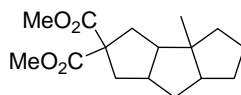
3β-Methyldecahydrocyclopenta[α]pentalene-2,2,7-tricarboxylic acid trimethyl ester 3.44/3.45/3.46.3.47: Cyclization of precursor **3.1** (0.05 g, 0.1 mmol) according to method B using Bu₃SnH as the reducing agent for 4 h gave a crude reaction mixture. Column chromatography over silica gel eluting with hexanes/ethyl acetate (15/1) after 6 column volumes of hexanes to give 29 mg of a tin free cyclization mixture. This mixture was taken up in CH₂Cl₂ (15 mL) and cooled to 0 °C. The mixture was then vigorously stirred and *m*-CPBA (0.021 g,

0.09 mmol) was added. The reaction was stirred for 14 h and quenched with NaHCO₃ (15 mL) and extracted with ethyl acetate (3 x 15 mL). The combined organic layers were dried over MgSO₄, filtered and concentrated *in vacuo*. The resulting oil was purified by column chromatography eluting with hexanes/ethyl acetate (15/1) to yield 0.021 g (62%) of a mixture of four isomeric tricyclic products **3.9/3.10/3.11/3.12** in a 51/40/8/1 ratio as determined by GC analysis.

3 β -Methyldecahydrocyclopenta[α]pentalene-2,2,7-tricarboxylic acid trimethyl ester

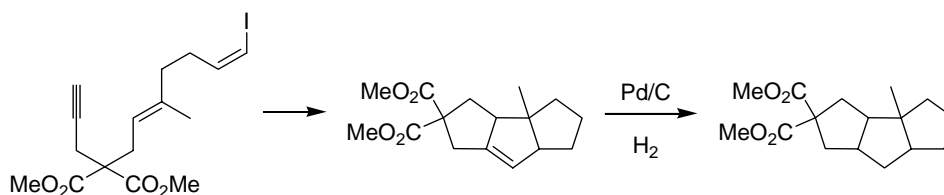


3 β -Methyldecahydrocyclopenta[α]pentalene-2,2,7-tricarboxylic acid 7-benzyl ester 2,2-dimethyl ester (3.36/3.37/3.38/3.39): Cyclization of precursor **3.2** (66 mg, 0.12 mmol) was carried out according to method B. Bu₃SnH was used as the reducing agent in benzene (60 mL). The solution was refluxed for 4 h and the crude reaction mixture which was subjected to a DBU workup. Subsequent column chromatography over silica gel eluting with hexanes/ethyl acetate (15/1) after 6 column volumes of hexanes gave 35 mg of a tin-free cyclization mixture. This mixture was then taken up in CH₂Cl₂ (15 mL) and cooled to 0 °C. The reaction was then vigorously stirred and *m*-CPBA (0.017 g, 0.1 mmol) was added. The reaction was stirred for 14 h and quenched with NaHCO₃ (15 mL) and extracted with ethyl acetate (3 x 15 mL). The combined organic layers were dried over MgSO₄, filtered and concentrated *in vacuo*. The resulting oil was purified by column chromatography eluting with hexanes/ethyl acetate (15/1) to yield 25 mg (50% from **3.2**) of a mixture of four isomeric tricyclic products **3.36/3.37/3.38/3.39** in a 47/37/7/8 ratio as determined by GC.



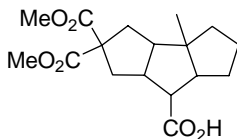
3 β -Methyldecahydrocyclopenta[α]pentalene-2,2-dicarboxylic acid dimethyl ester (3.44/3.45/3.46/3.47): Cyclization of precursor **3.3** (50 mg, 0.12 mmol) was carried out according to method D using Bu₃SnH as the reducing agent with a total of 60 mL of benzene.

The reaction was refluxed for 4 h and the crude reaction mixture which was subjected to a DBU workup. Subsequent column chromatography over silica gel eluting with hexanes/ethyl acetate (20/1) after 6 column volumes hexanes to give a tin-free cyclization mixture. This mixture was then taken up in CH₂Cl₂ (15 mL) and cooled to 0 °C. The reaction was then vigorously stirred and *m*-CPBA (0.017g, 0.1 mmol) was added. The reaction was stirred for 14 h and quenched with NaHCO₃ (15 mL) and extracted with ethyl acetate (3 x 15 mL). The combined organic layers were dried over MgSO₄, filtered and concentrated *in vacuo*. The resulting oil was purified by column chromatography eluting with hexanes/ethyl acetate (20/1) to yield 17 mg (52% from **3.3**) of a mixture of four isomeric tricyclic products **3.44/3.45/3.46/3.47** in a 42/38/14/6 ratio as determined by GC analysis.



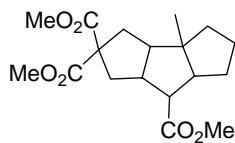
3β-Methyldecahydrocyclopenta[α]pentalene-2,2-dicarboxylic acid dimethyl ester (3.44/3.45): Cyclization of precursor **3.4** (40 mg, 0.10 mmol) was carried out according to method B using Bu₃SnH as the reducing agent with a total of 50 mL of benzene. The resulting solution was refluxed for 4 h. The crude reaction mixture was subjected to a DBU workup. Subsequent column chromatography over silica gel eluting with hexanes/ethyl acetate (20/1) after 6 column volumes hexanes to give 19 mg (70%) of a tin-free cyclization mixture. This mixture was then taken up in ethanol (1.0 mL) and to this solution was added Pd/C (10% by weight, 15 mg). The flask was fitted with a three way stopcock with one outlet to a hydrogen balloon and the other to an aspirator vacuum. The mixture was stirred vigorously and evacuated until the suspension bubbled at which point it was released to the hydrogen balloon. The purging of the reaction mixture with hydrogen was repeated an additional two times. After stirring for 12 h under the hydrogen atmosphere, the mixture was concentrated *in vacuo*. The resulting oil was purified by column chromatography over silica gel eluting with hexanes/ethyl acetate (20/1) to give 18 mg (93%) of a 67/34 mixture of tricycles **3.44** and **3.45**.

5.4.5 Tricyclic Relay Experiments

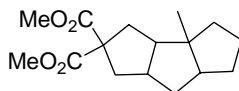


3β-Methyldecahydrocyclopenta[α]pentalene-2,2,7-tricarboxylic acid dimethyl ester (3.52):

To a 42/35/8/15 mixture of **3.36/3.37/3.38/3.39** (25 mg, 0.06 mmol) in ethyl acetate (5 mL) was added Pd/C (10 wt% on carbon, 20 mg). The flask was fitted with a three way stopcock with one outlet to a hydrogen balloon and the other to an aspirator vacuum. The mixture was stirred vigorously and evacuated until the suspension bubbled at which point it was released to the hydrogen balloon. The purging of the reaction mixture with hydrogen was repeated an additional two times. After stirring for 12 h under the hydrogen atmosphere, the mixture was filtered through celite, washing with an additional 15 mL of ethyl acetate. The solvent was removed *in vacuo* to give 19 mg (99%) of the title acid which was used as such in the following reaction.



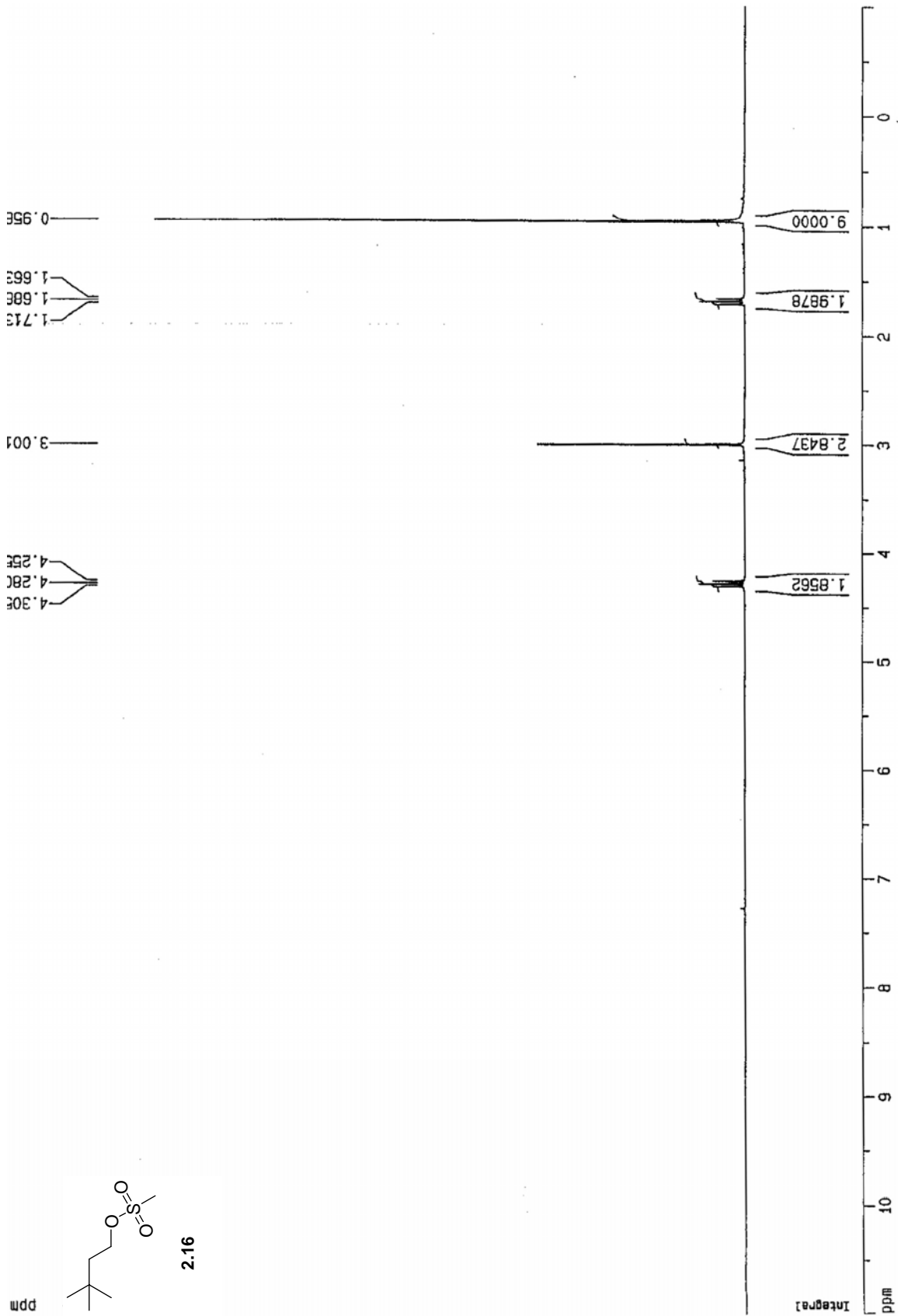
3β-Methyl-decahydro-cyclopenta[α]pentalene-2,2,7-tricarboxylic acid trimethyl ester: To a 42/35/6/15 diastereomeric mixture of acid **3.52** (10 mg, 0.030 mmol) in benzene (0.2 mL) and methanol (0.06 mL) was added TMSCHN₂ (0.02 mL, 2.0 M solution in hexanes, 0.04 mmol). The resulting solution was stirred for 1 h, concentrated *in vacuo* and purified by column chromatography over silica gel eluting with hexanes/ethyl acetate (15/1) to give 13 mg of the title tricycles **3.9/3.10/3.11/3.12** (51% from the benzyl ester mixture **3.36/3.37/3.38/3.39**) as a pale yellow oil. Spectral data for this mixture was identical to that previously synthesized.

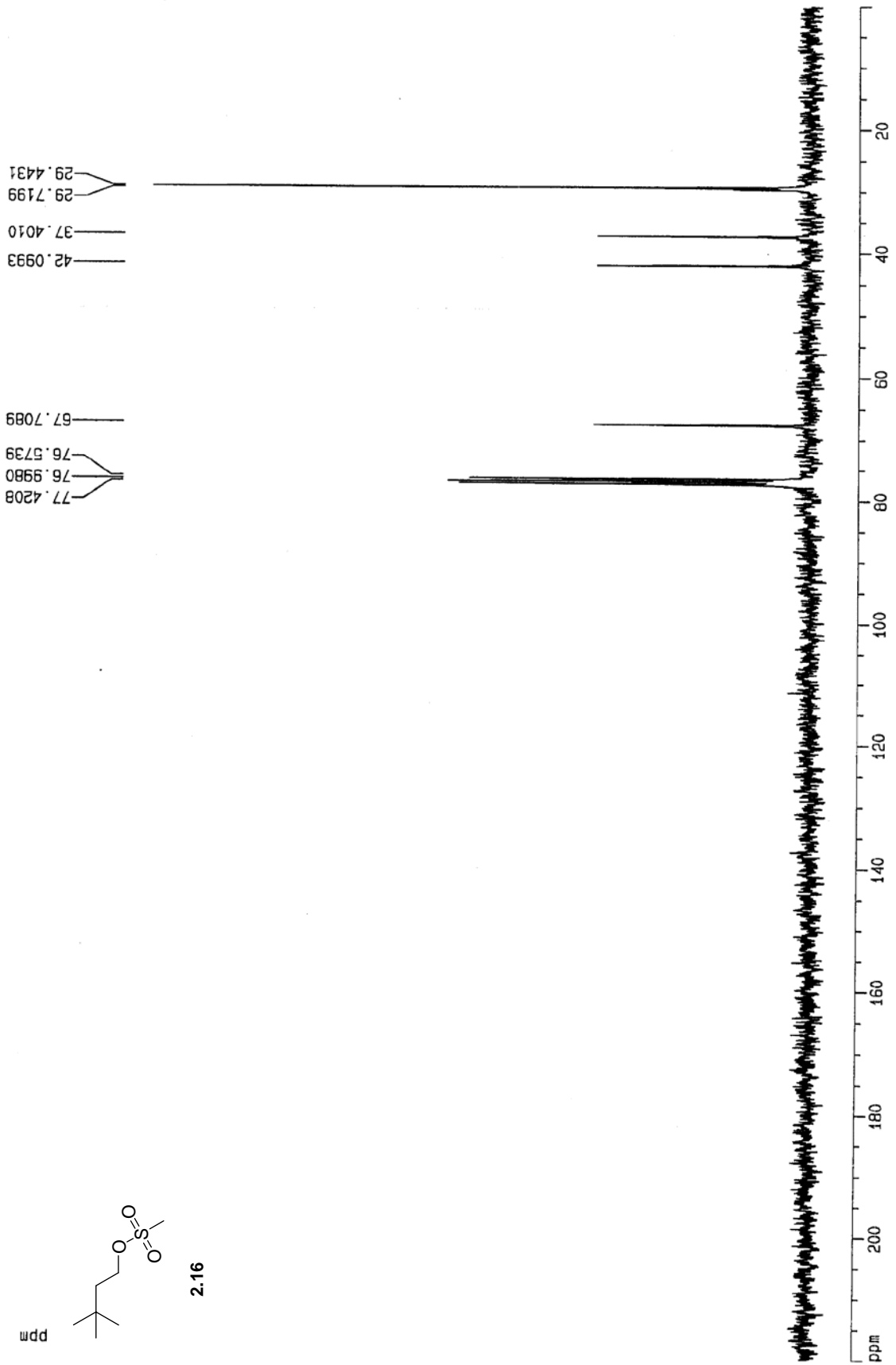


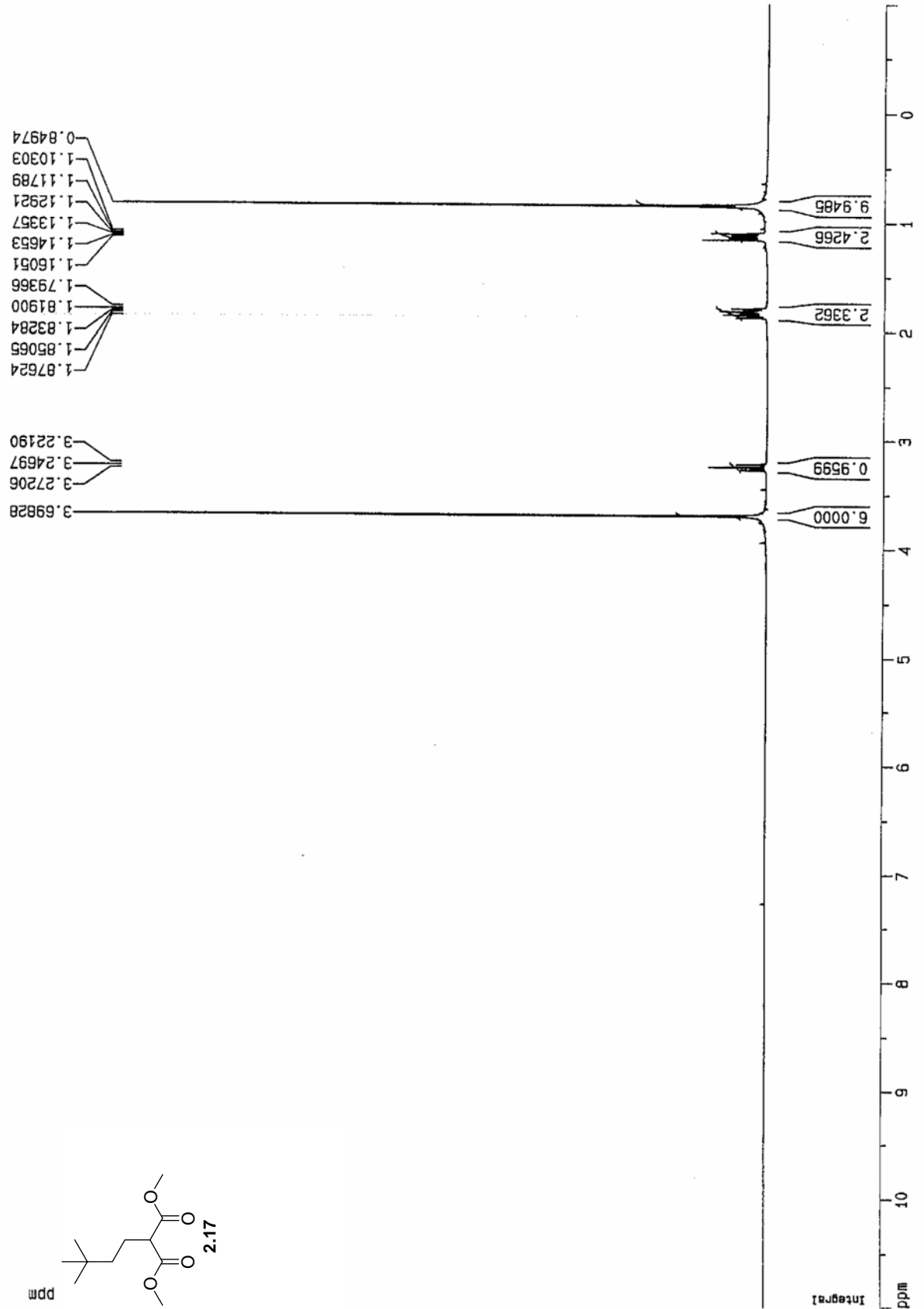
3β-Methyldecahydrocyclopenta[α]pentalene-2,2-dicarboxylic acid dimethyl ester 3.44/3.45/3.47/?: A 42/35/6/15 diastereomeric mixture of acid **S19** (19 mg, 0.06 mmol) was

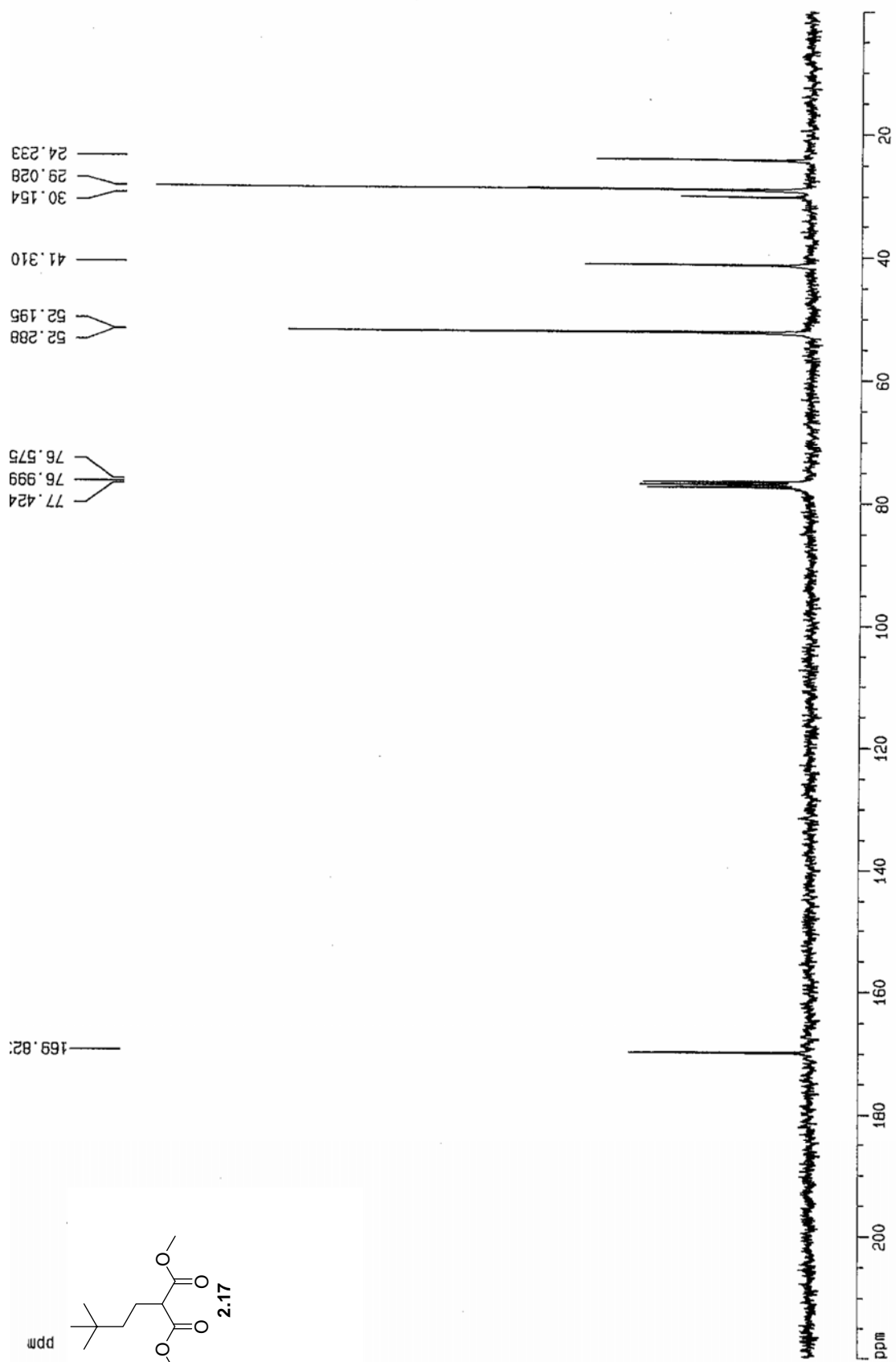
taken up in benzene (0.4 mL) and treated with oxallyl chloride (0.06 mL, 0.69 mmol) and DMF (1 drop). The resulting solution was stirred at room temperature for 2 h and then concentrated *in vacuo*. The crude reaction mixture was then re-dissolved in benzene and concentrated *in vacuo* again. The crude acid chloride was taken up in benzene (0.3 mL) and added to a suspension of 2-mercaptopyridine-1-oxide sodium salt (11 mg, 0.07 mmol) and DMAP (2 mg, 0.01 mmol) in benzene (0.6 mL). The reaction was brought to reflux and allowed to do so for 20 min. The heat source was removed and a solution of AIBN (10 mg, 0.06 mmol) and Bu₃SnH (0.05 mL, 0.18 mmol) in benzene (0.3 mL) was added. The reaction was once again brought to reflux and kept there for 15 h, cooled, concentrated *in vacuo* and directly purified by column chromatography over silica gel eluting with hexanes/ethyl acetate (20/1) after five column volumes of hexanes to yield 7 mg of the title tricycles **3.44/3.45/3.47/?** (43% from the benzyl ester mixture **3.36/3.37/3.38/3.39**) as a pale yellow oil. It was only possible to match the retention times of three of the four products upon comparison to the authentically cyclized material. Unfortunately the identity of the fourth product in the decarboxylation remains unknown.

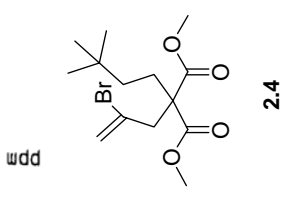
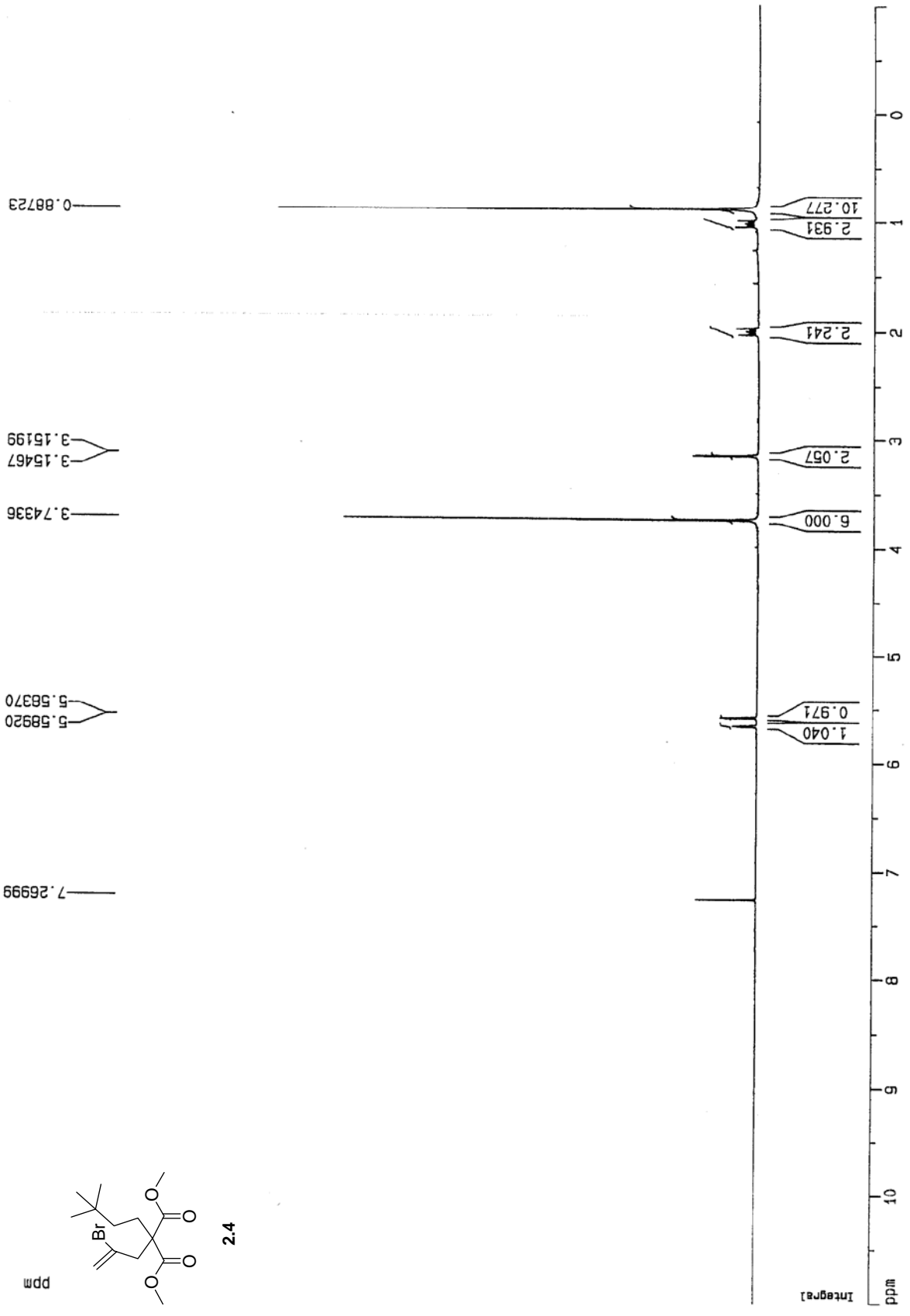
APPENDIX A: Spectra

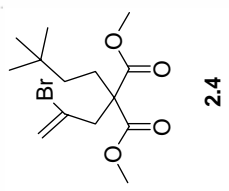
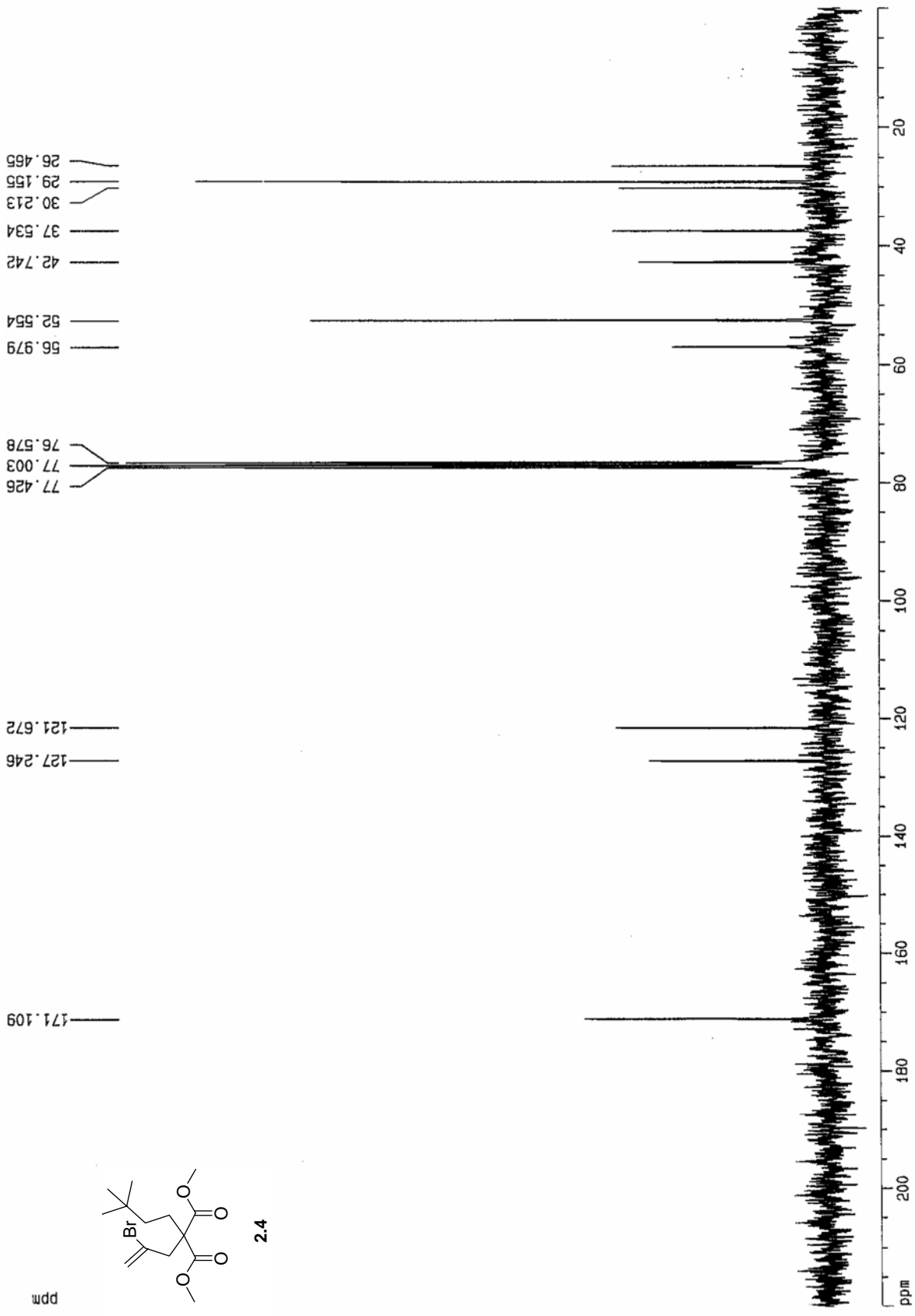




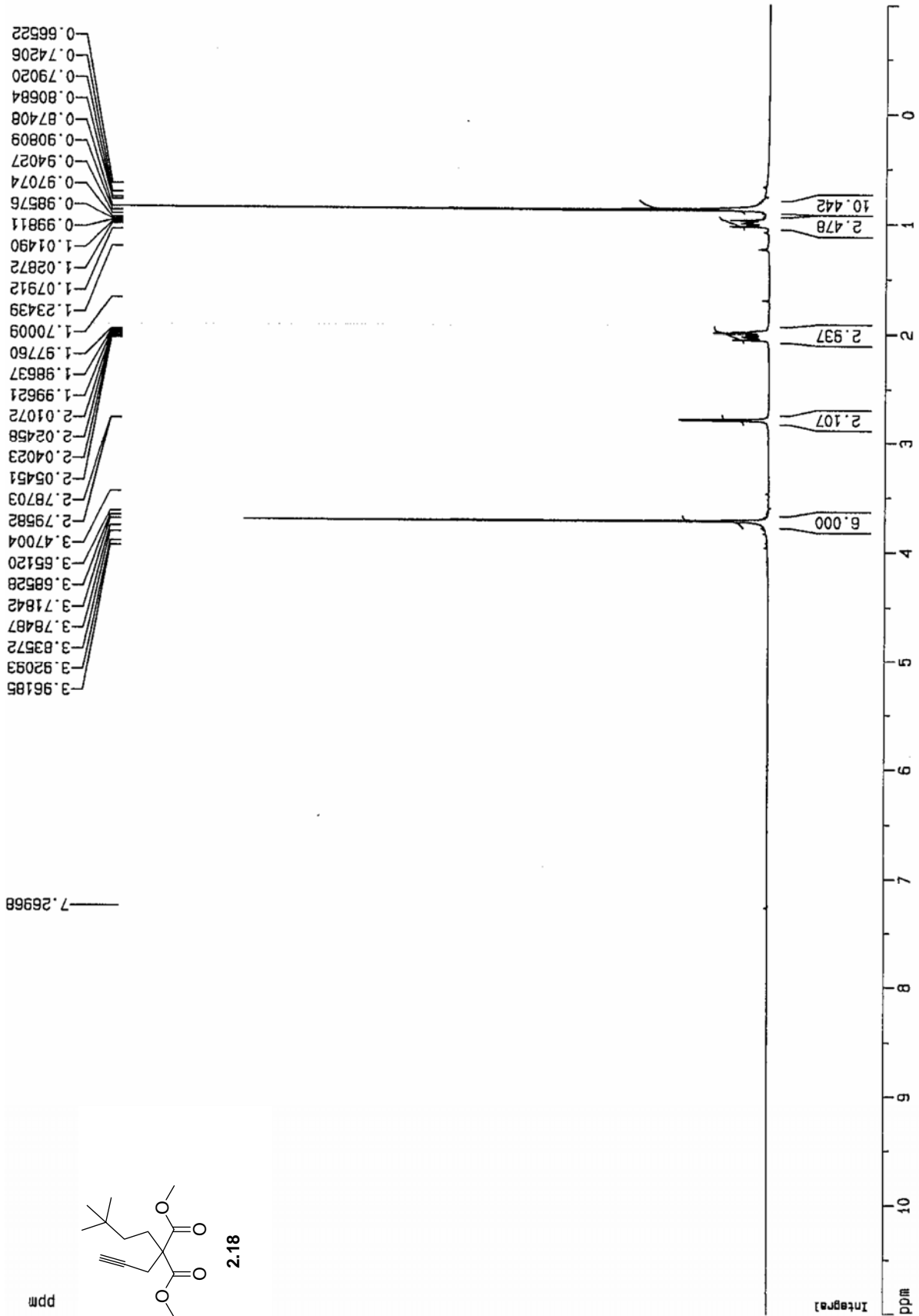


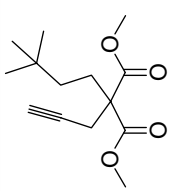
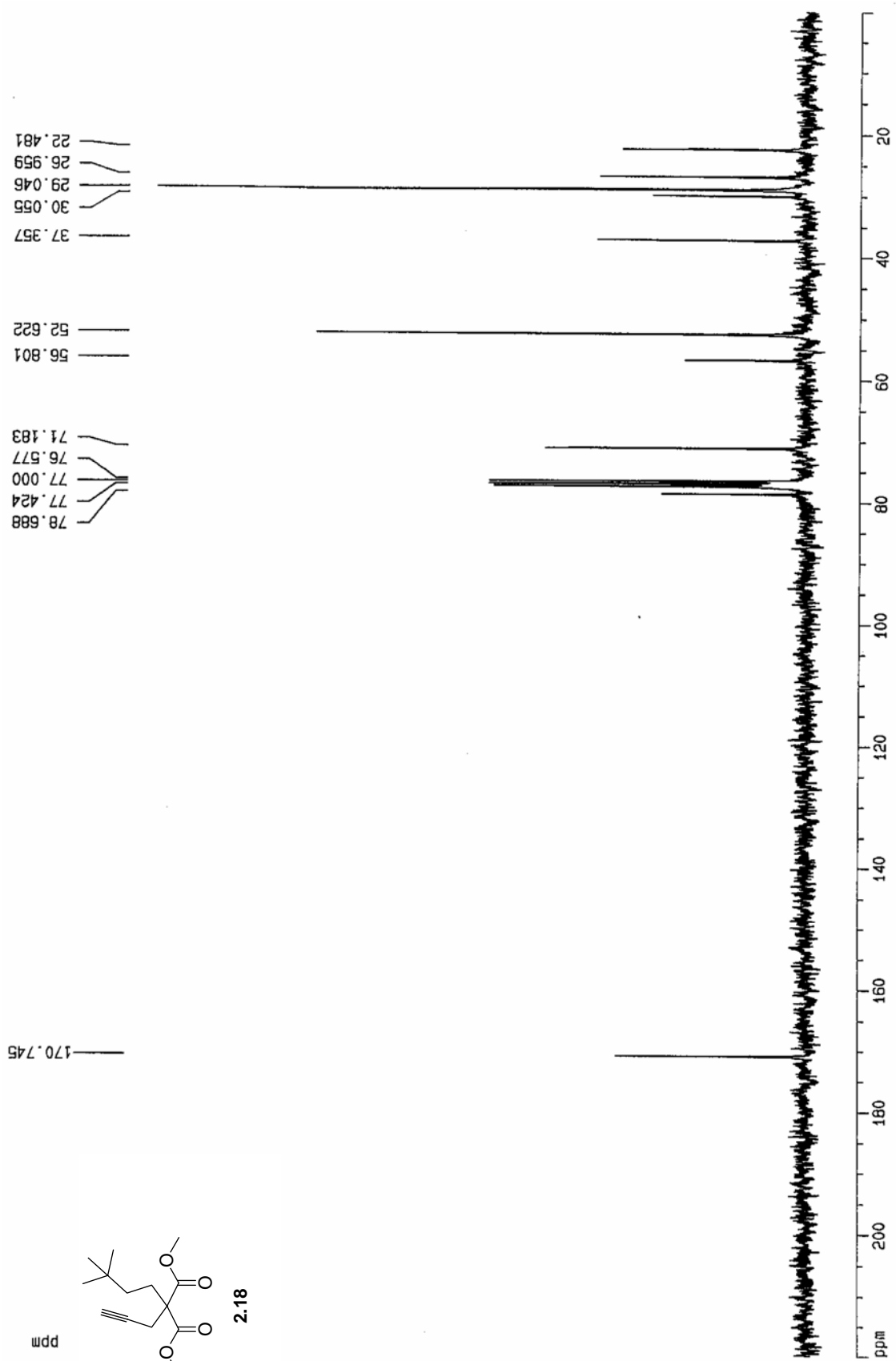






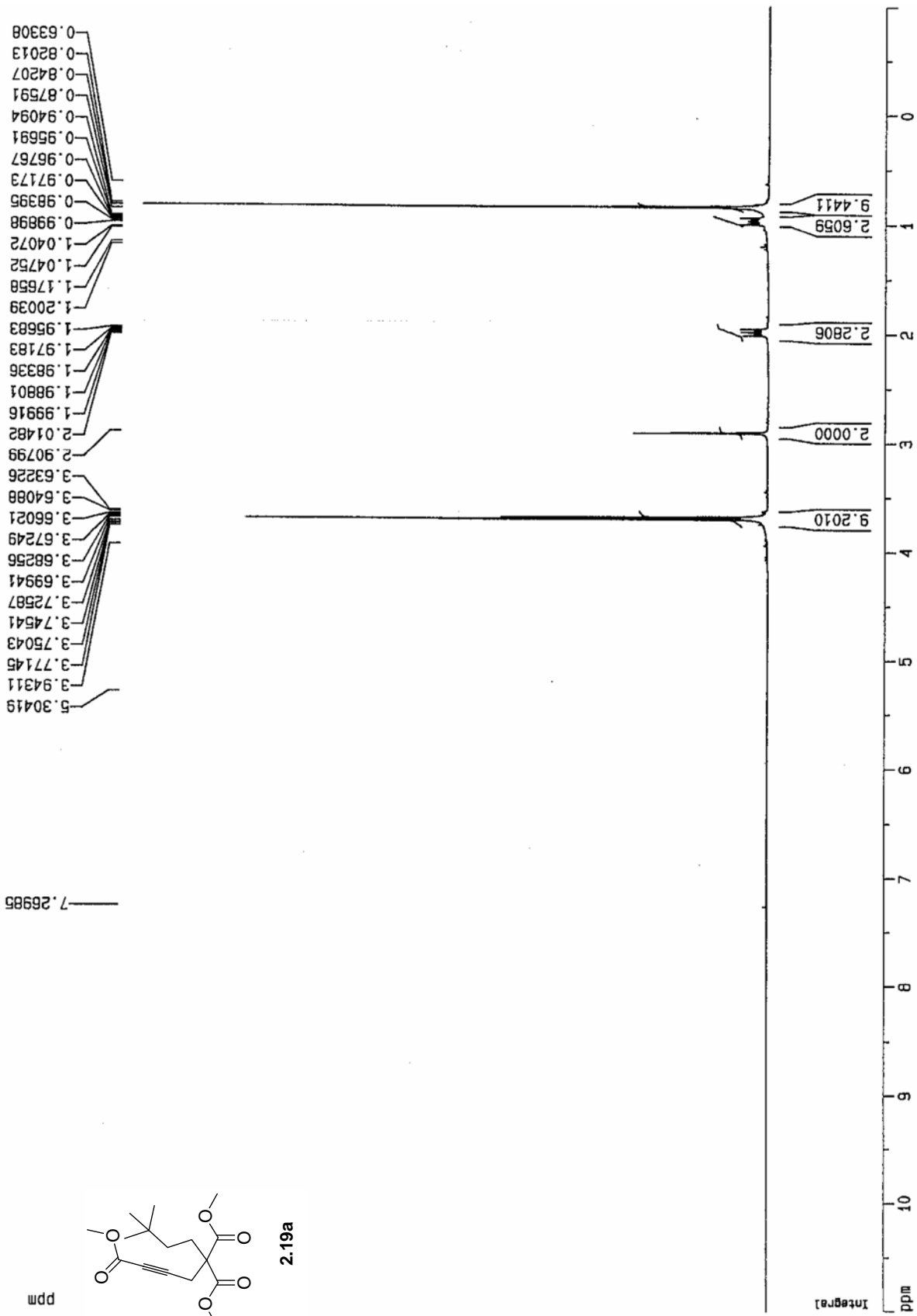
ppm

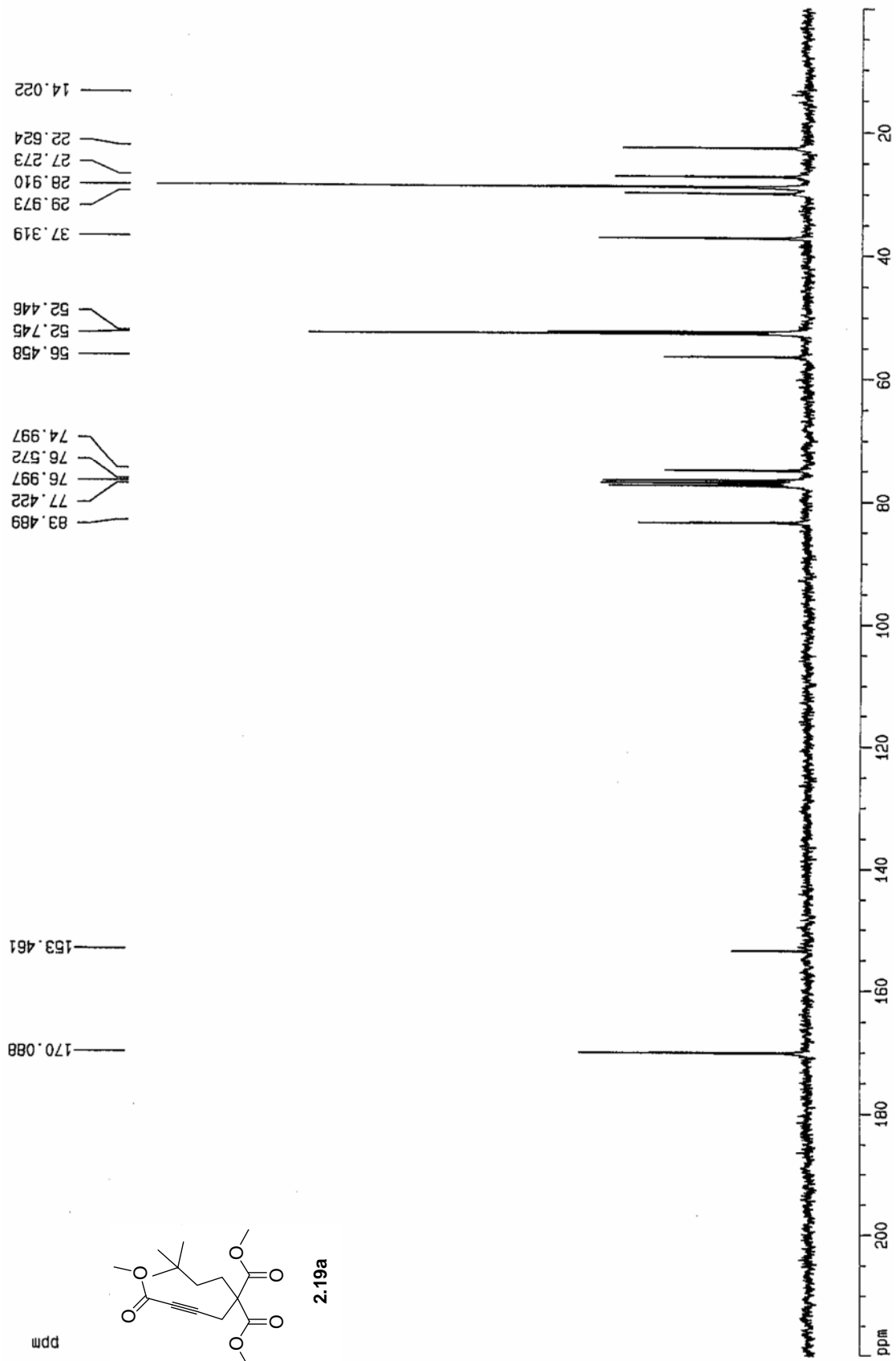


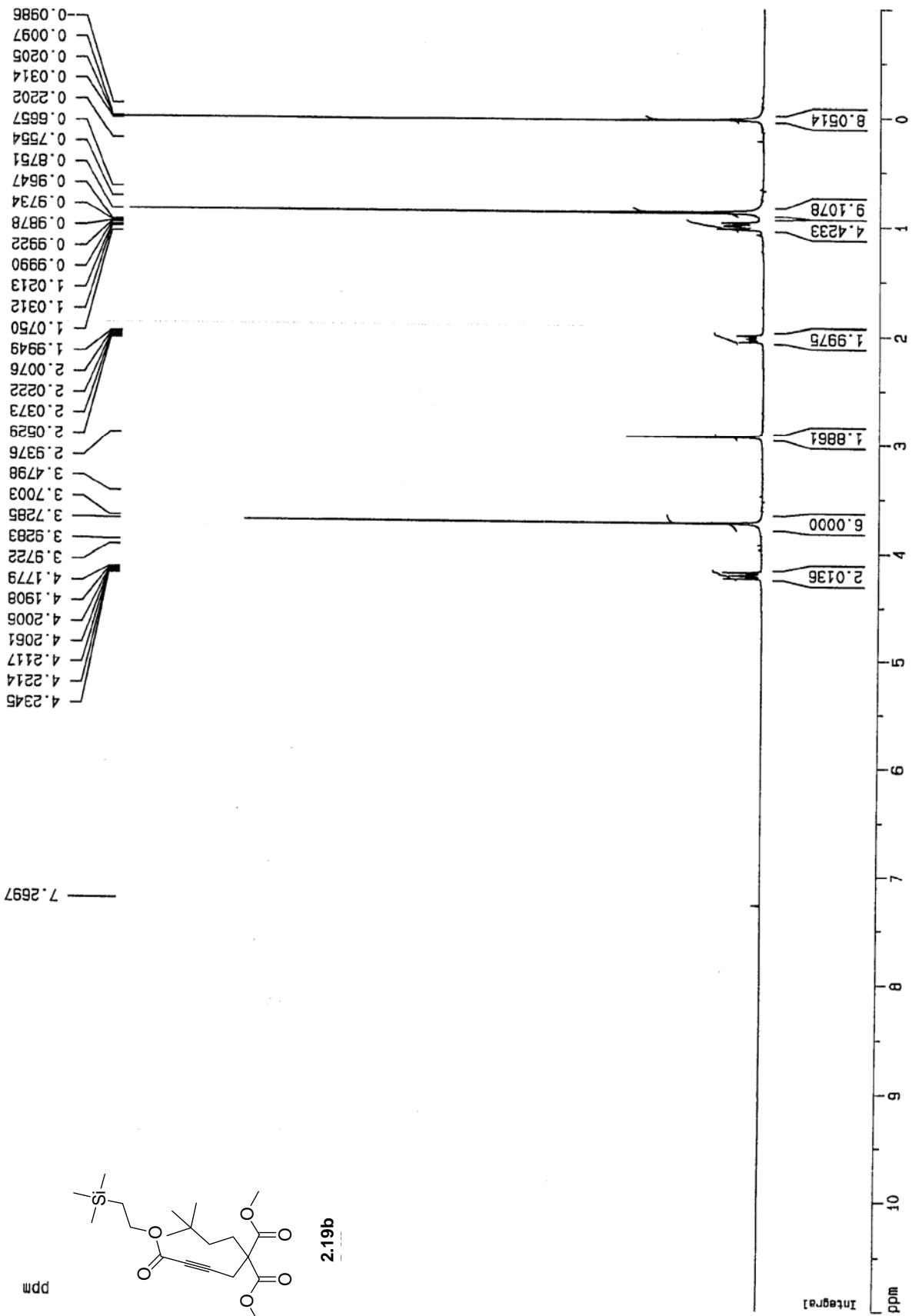


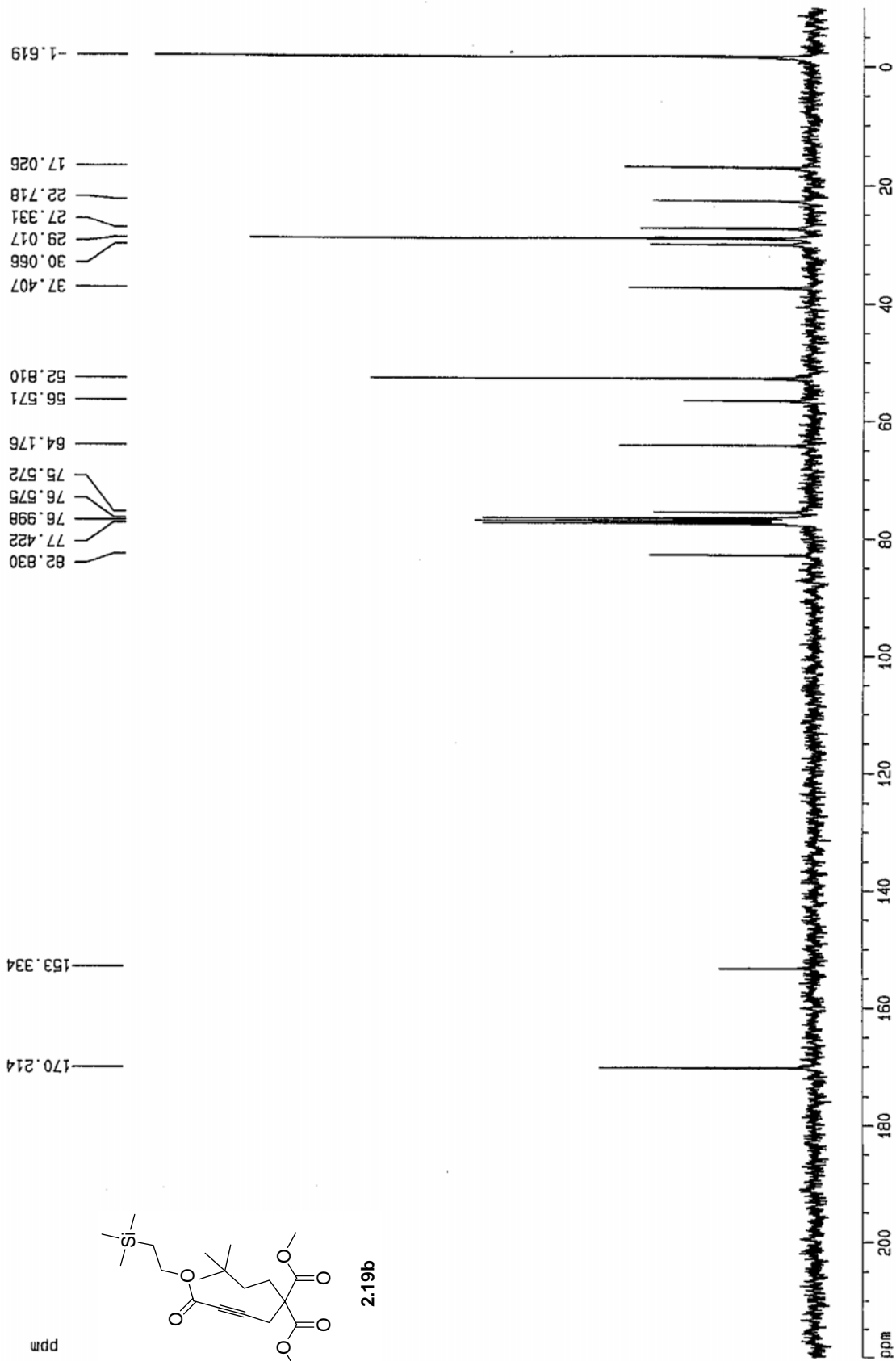
2.18

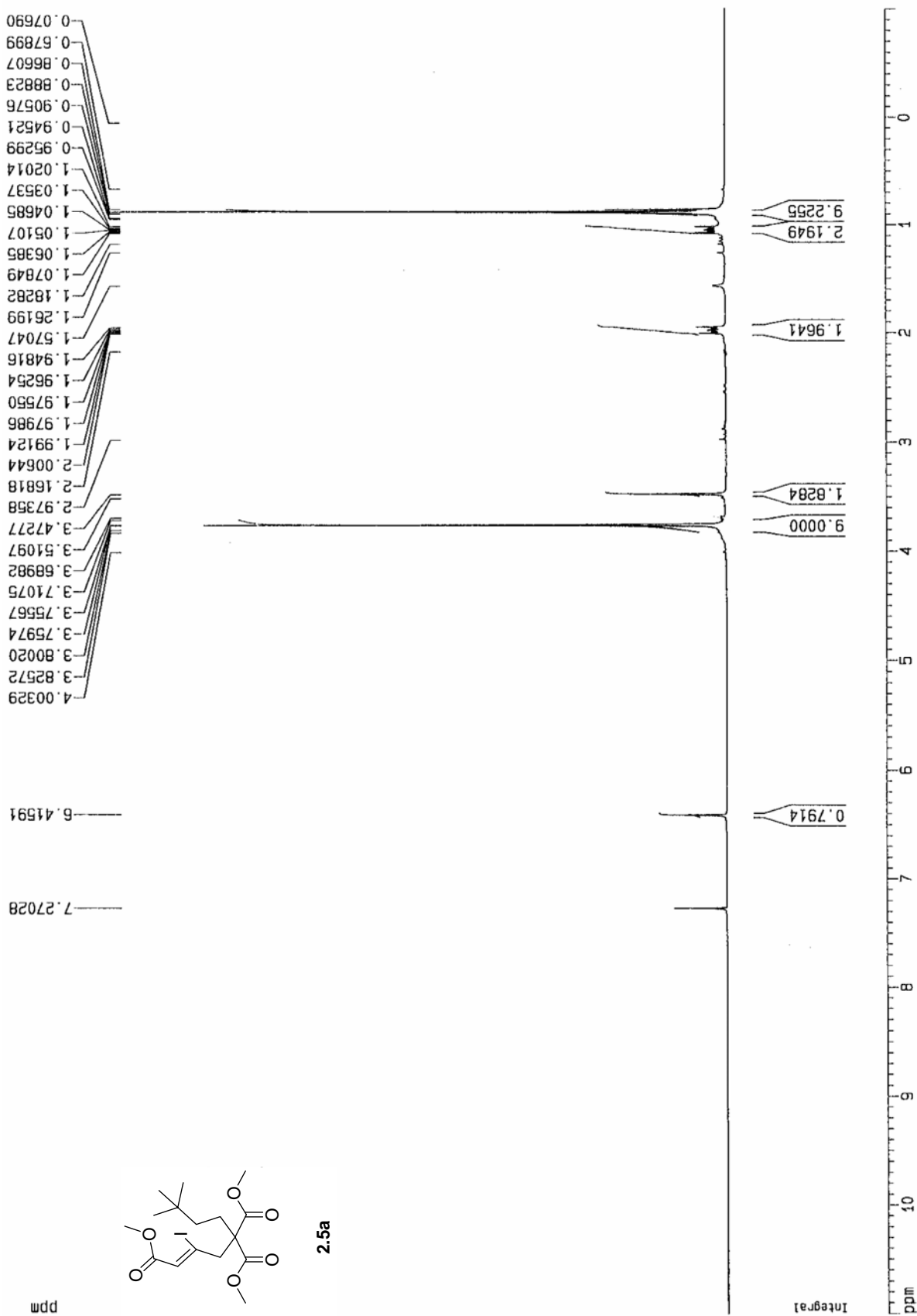
ppm









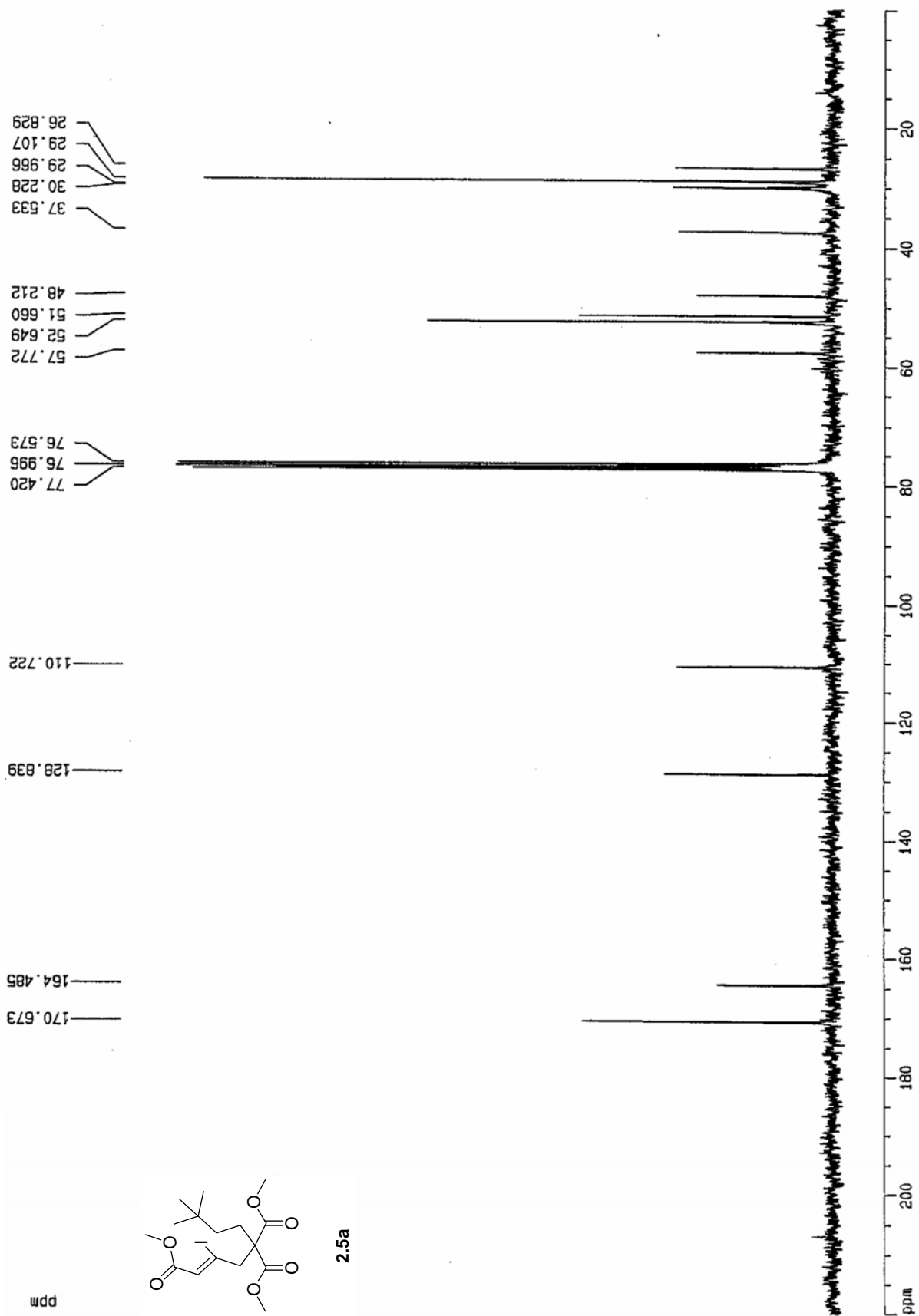


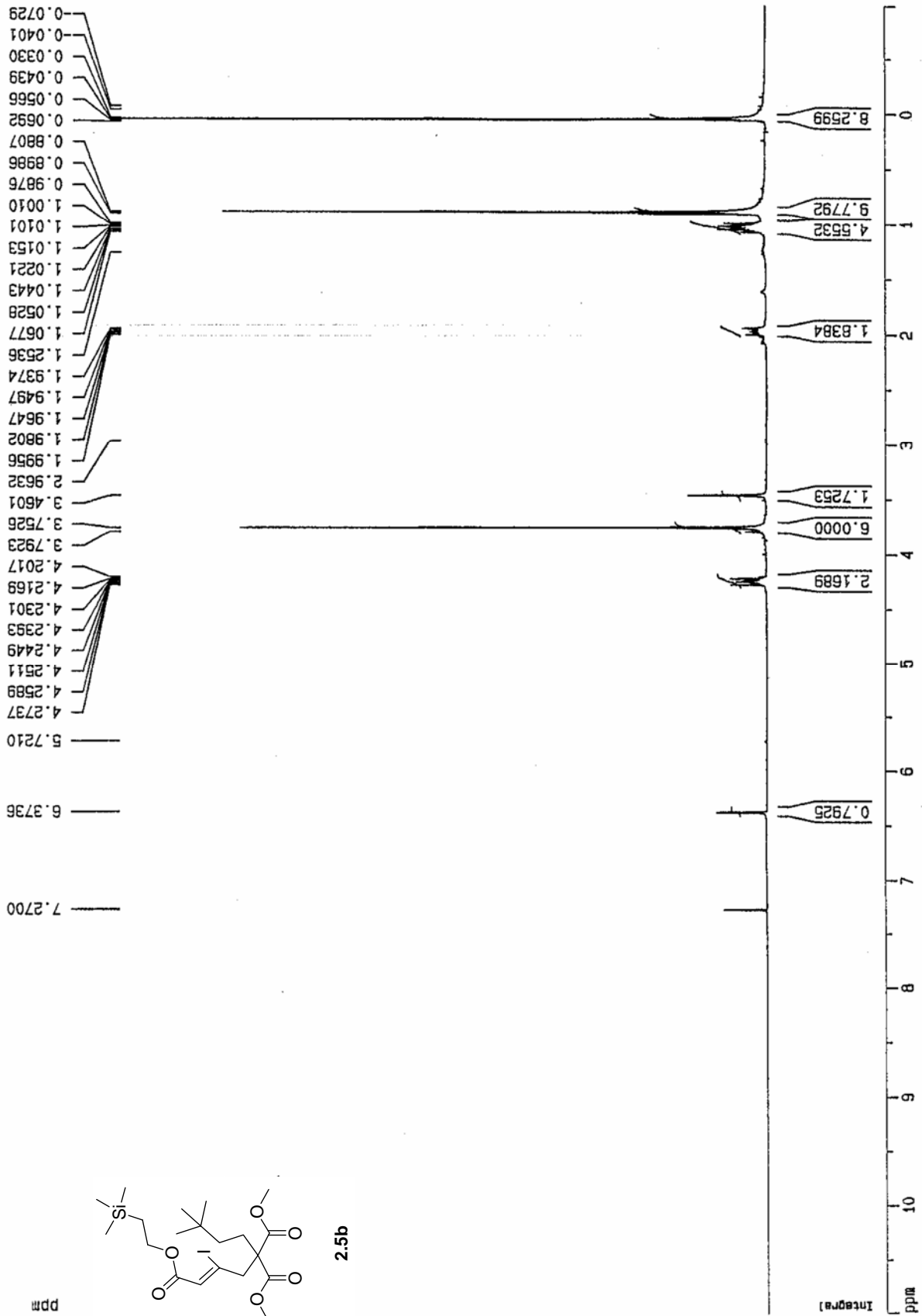
2.5a

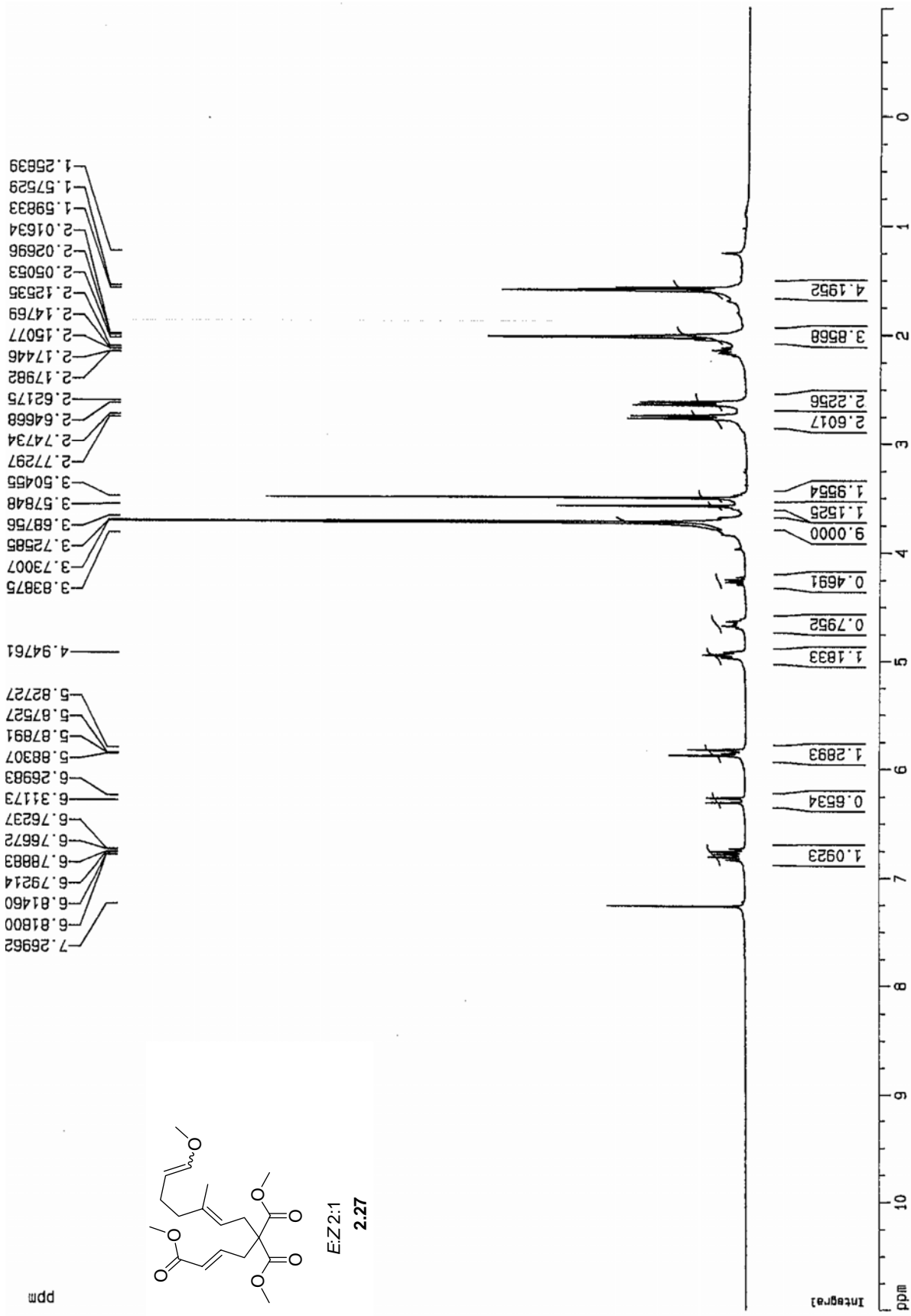
ppm

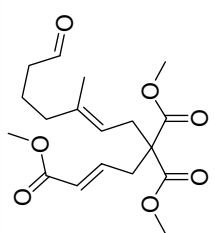
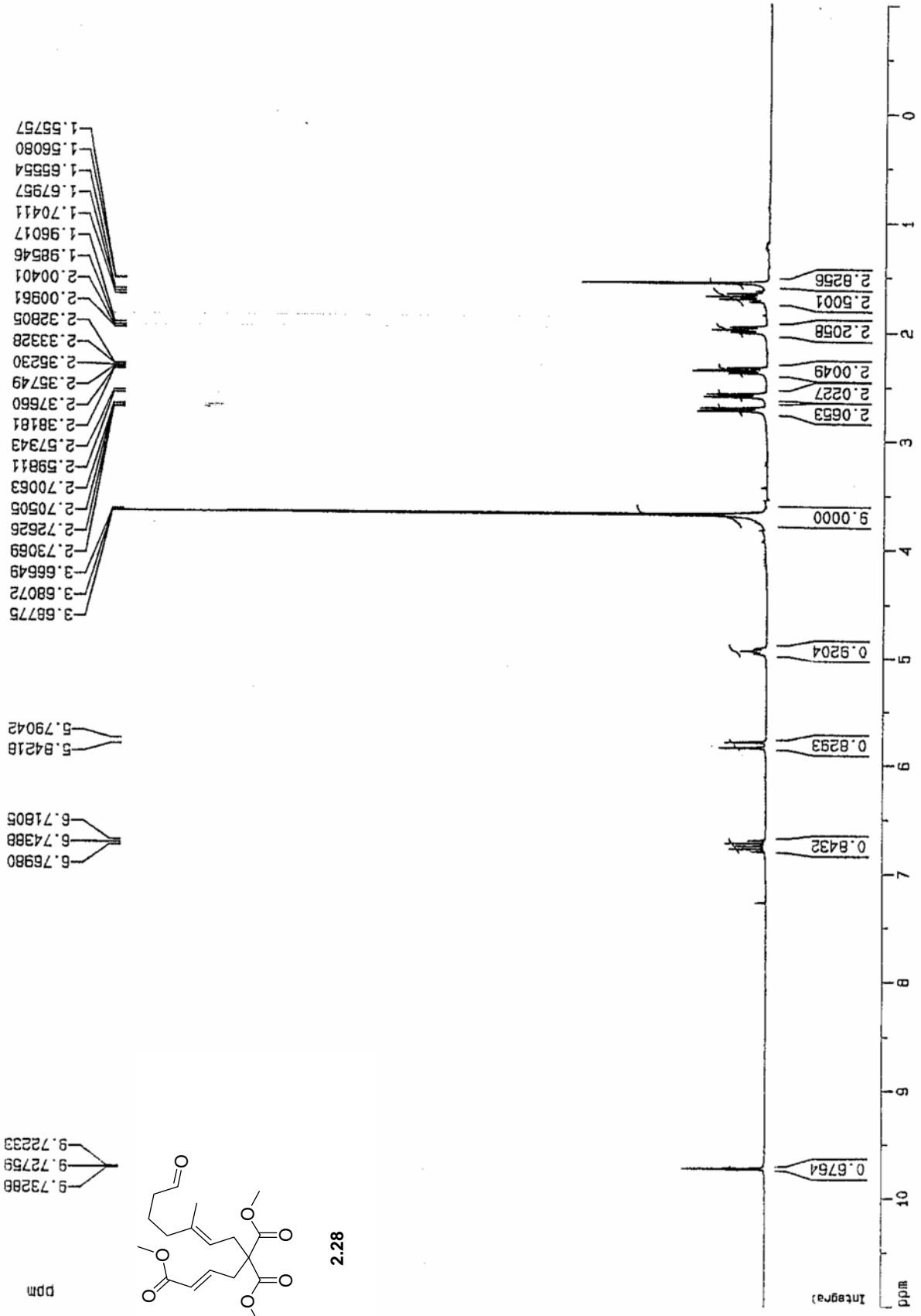
Integral

ppm

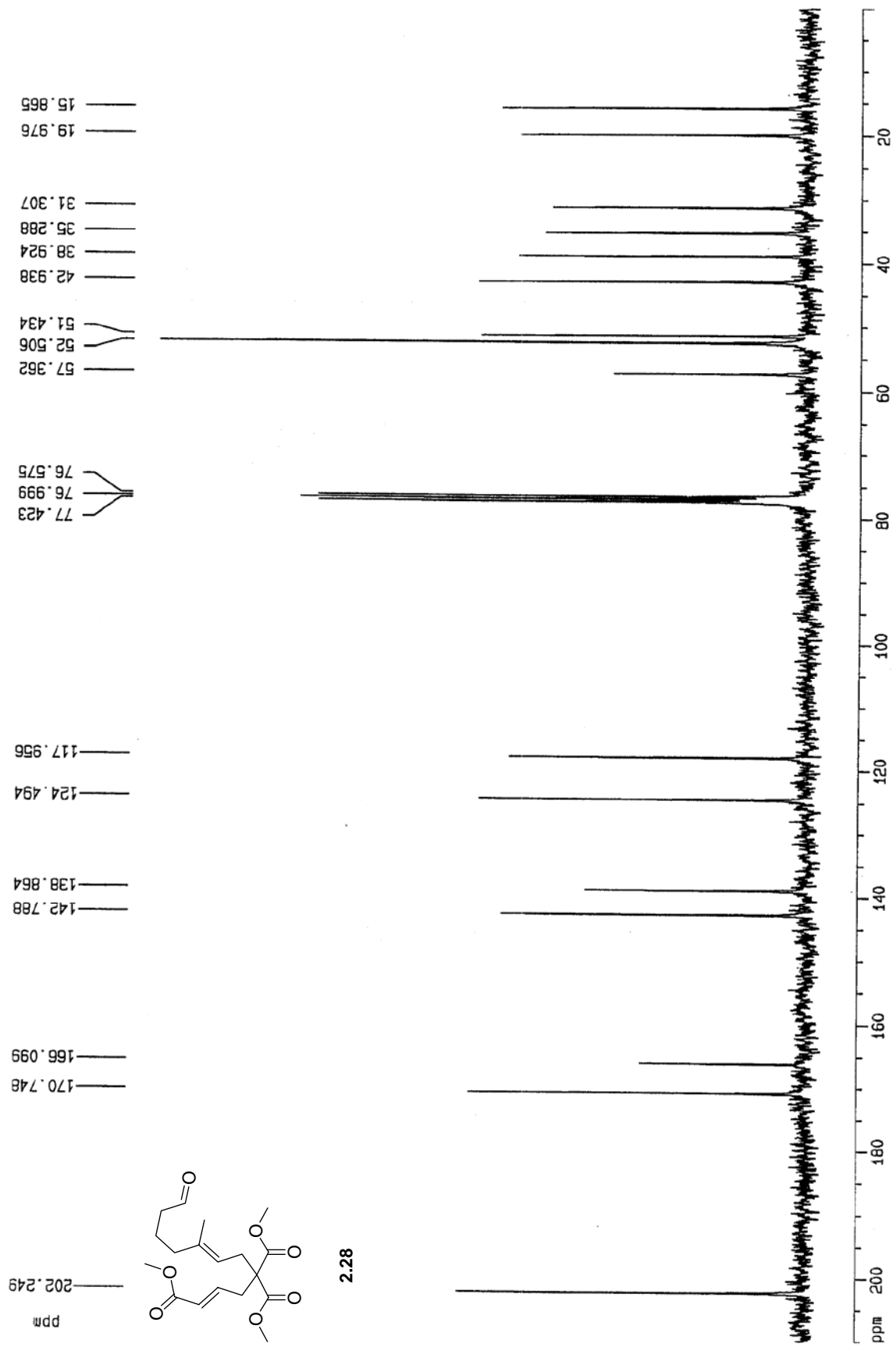


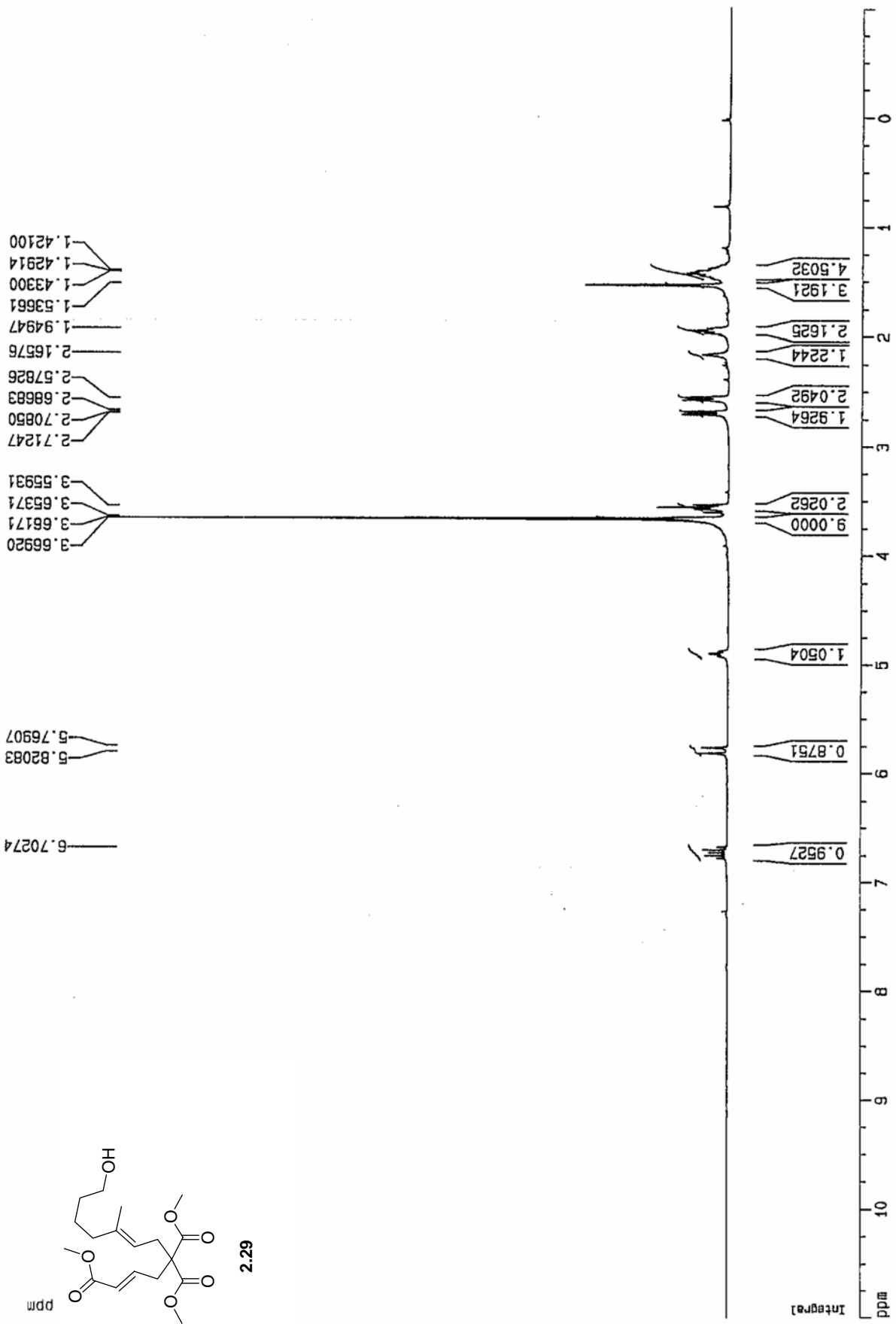


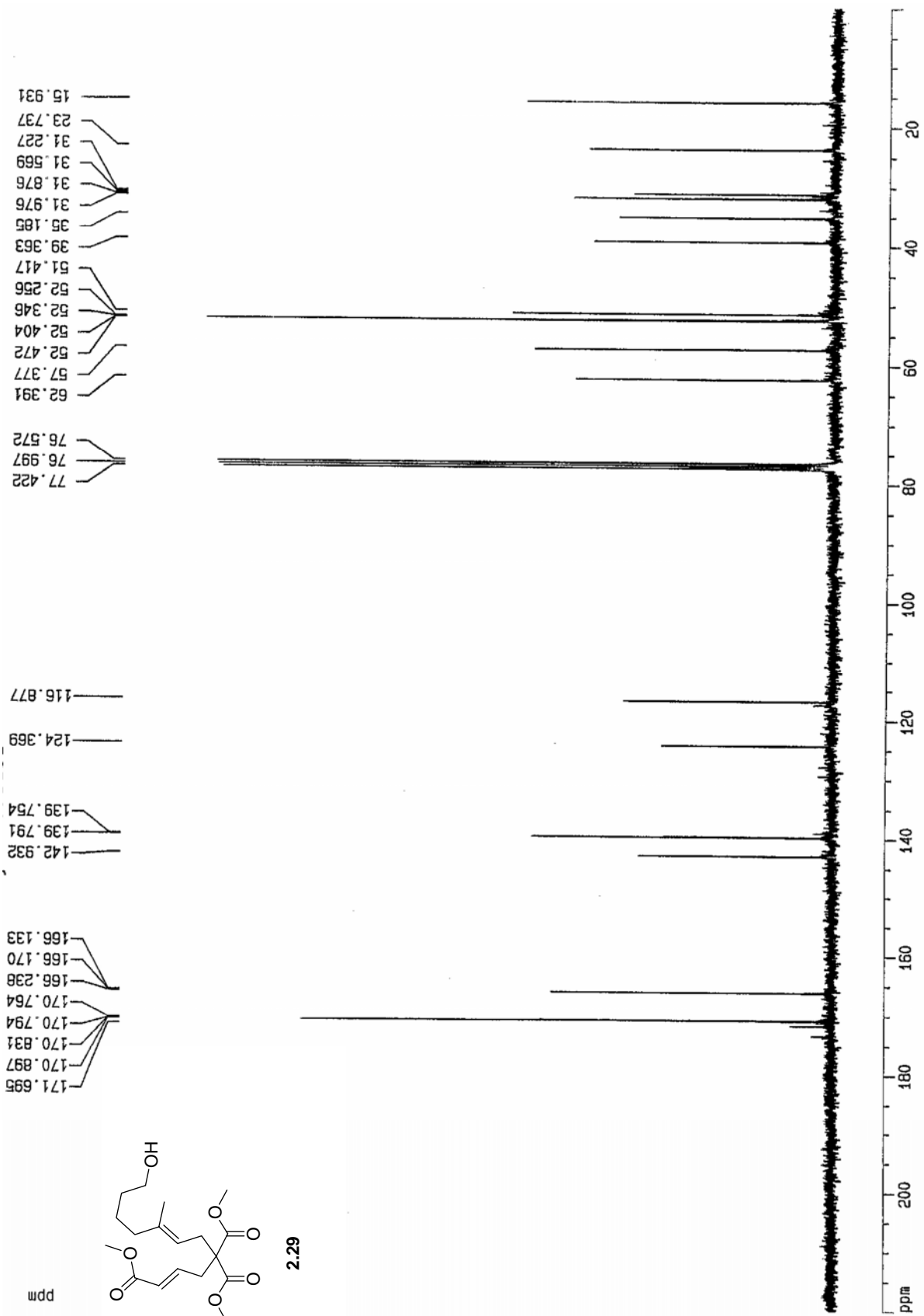


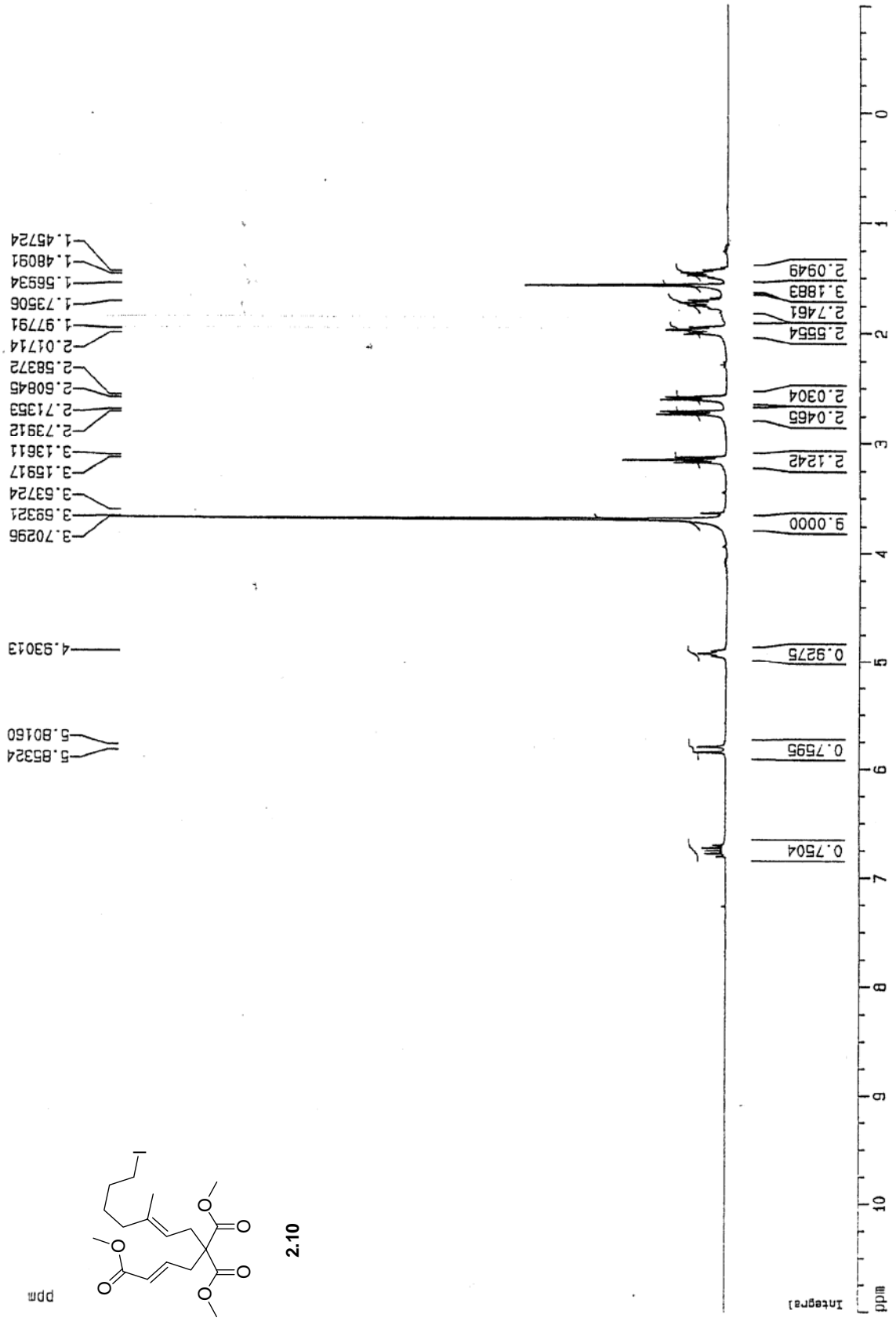


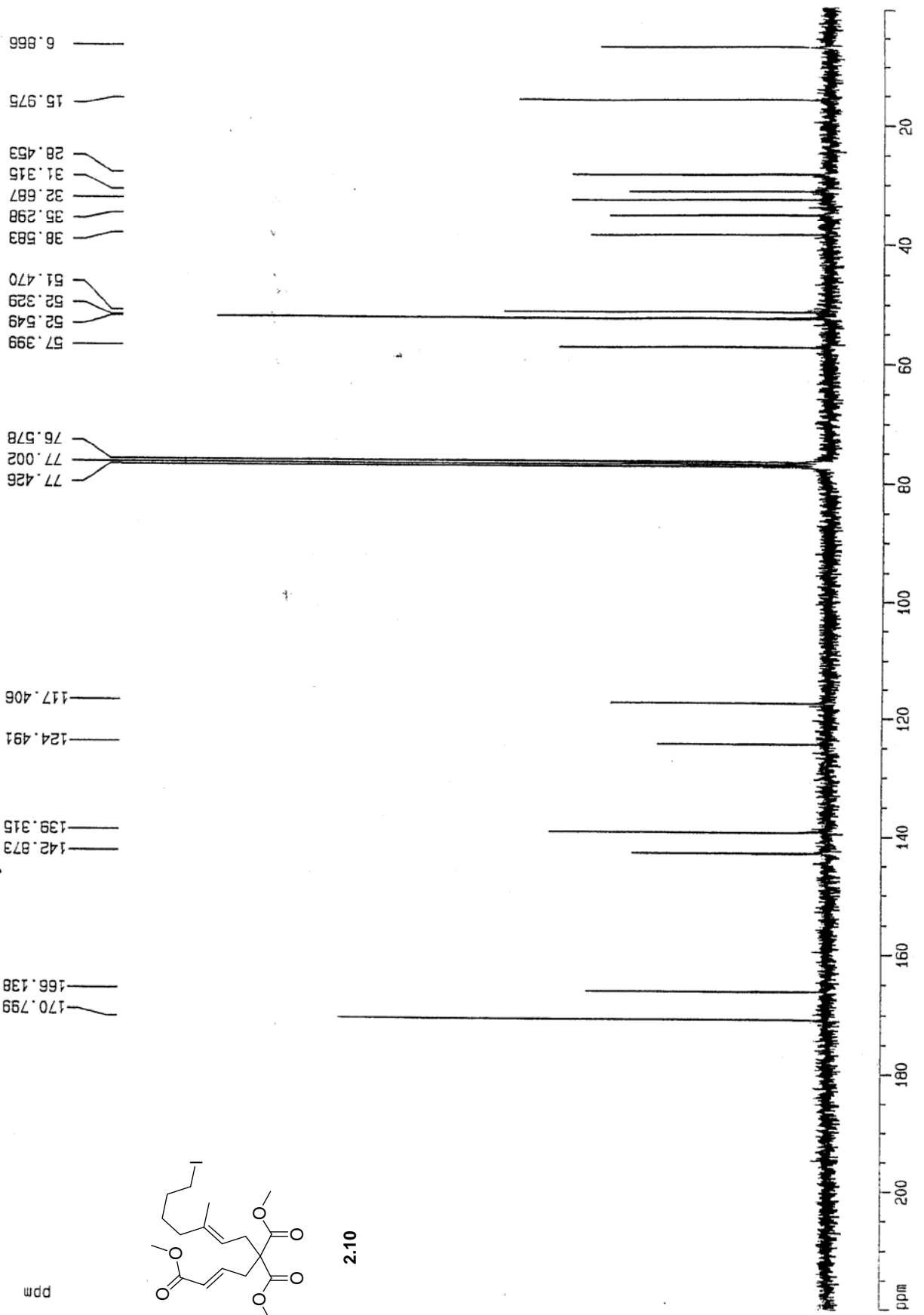
ppm
9.73288
9.72759
9.72233

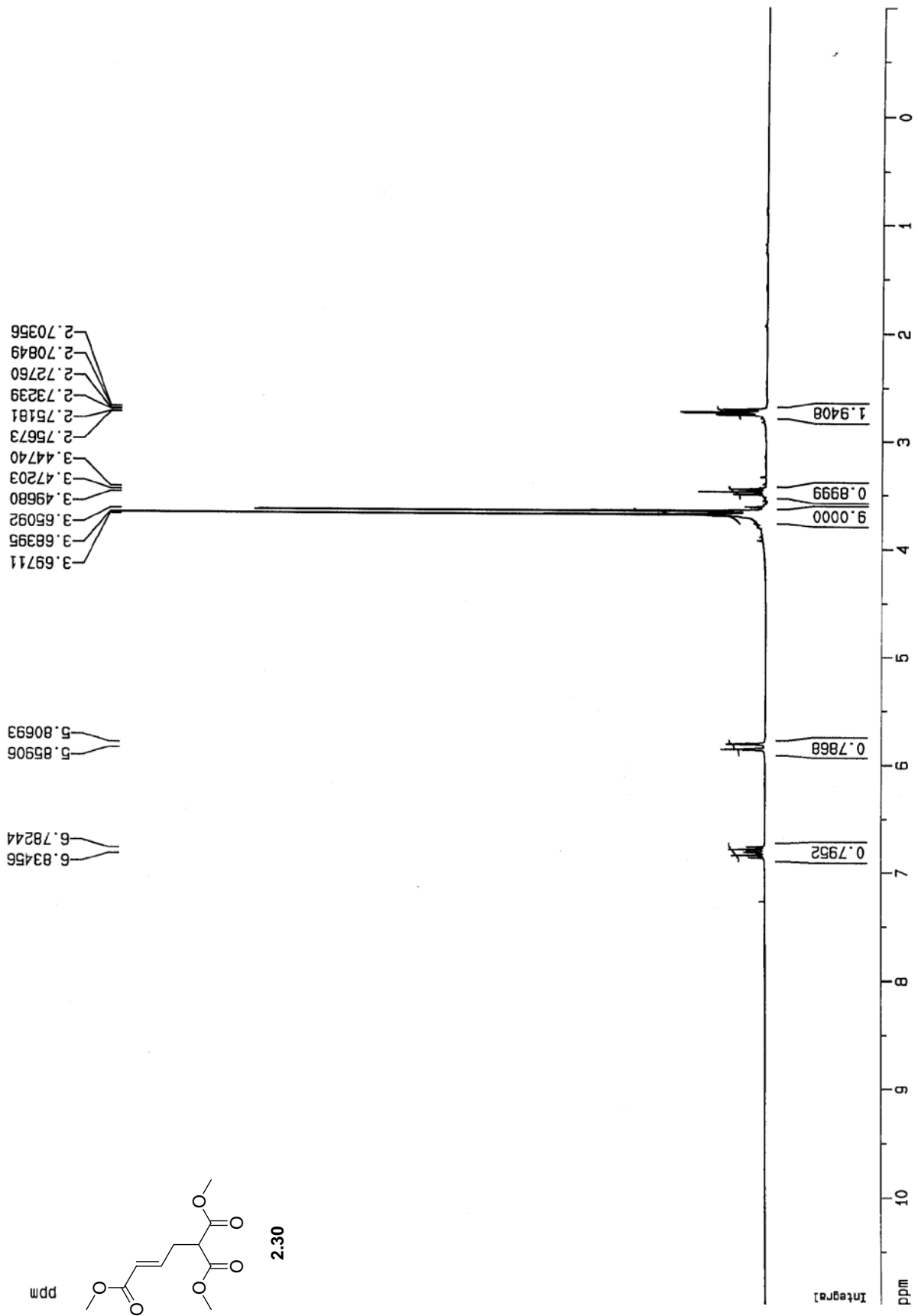


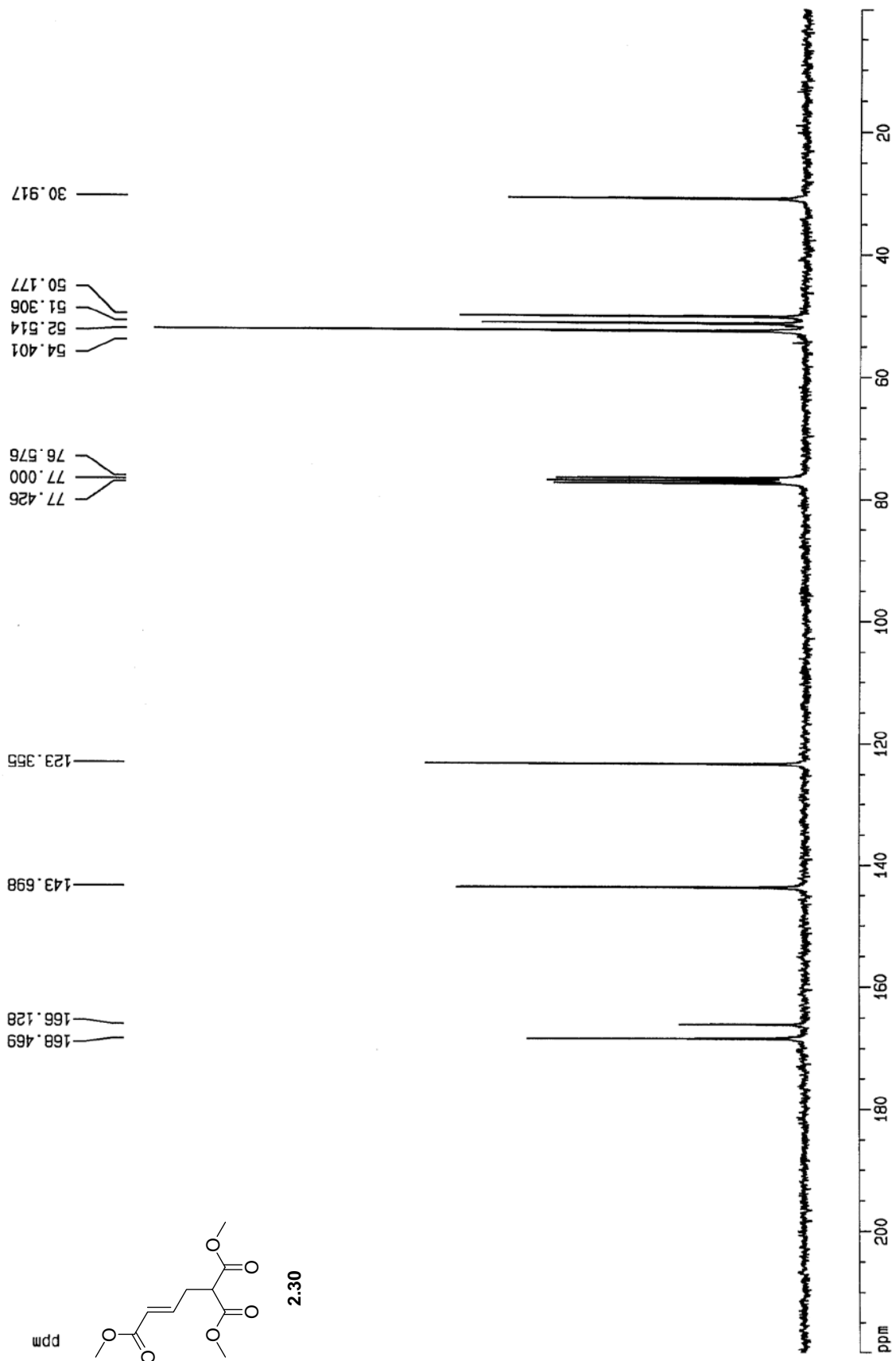




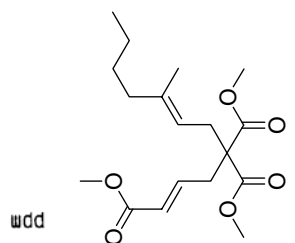




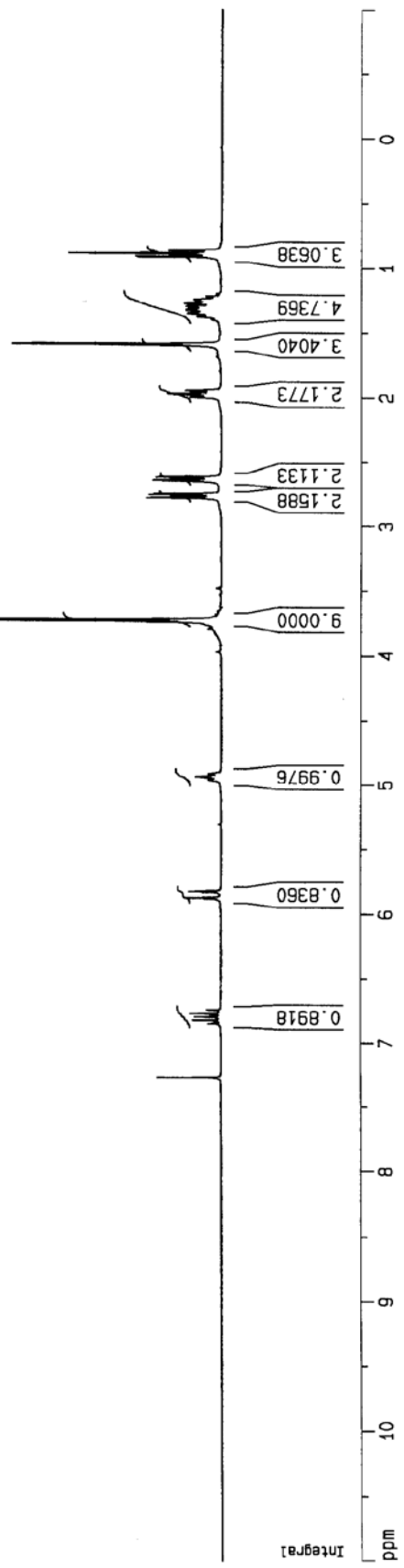




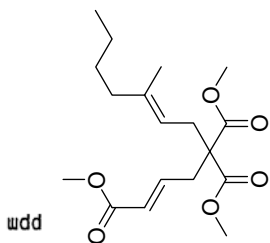
0.86752
 0.89133
 0.91482
 1.24956
 1.25750
 1.27300
 1.29597
 1.32010
 1.32381
 1.33672
 1.34557
 1.35089
 1.37532
 1.58884
 1.59099
 1.94978
 1.97479
 1.99783
 2.61570
 2.64052
 2.74543
 2.74966
 2.77110
 2.77531
 3.47895
 3.53175
 3.65994
 3.68444
 3.72852
 3.79493
 3.97183
 4.91327
 4.93436
 4.93833
 4.95933
 5.30760
 5.82567
 5.82966
 5.87744
 6.74376
 6.76951
 6.79525
 6.82125
 6.84683
 7.27000



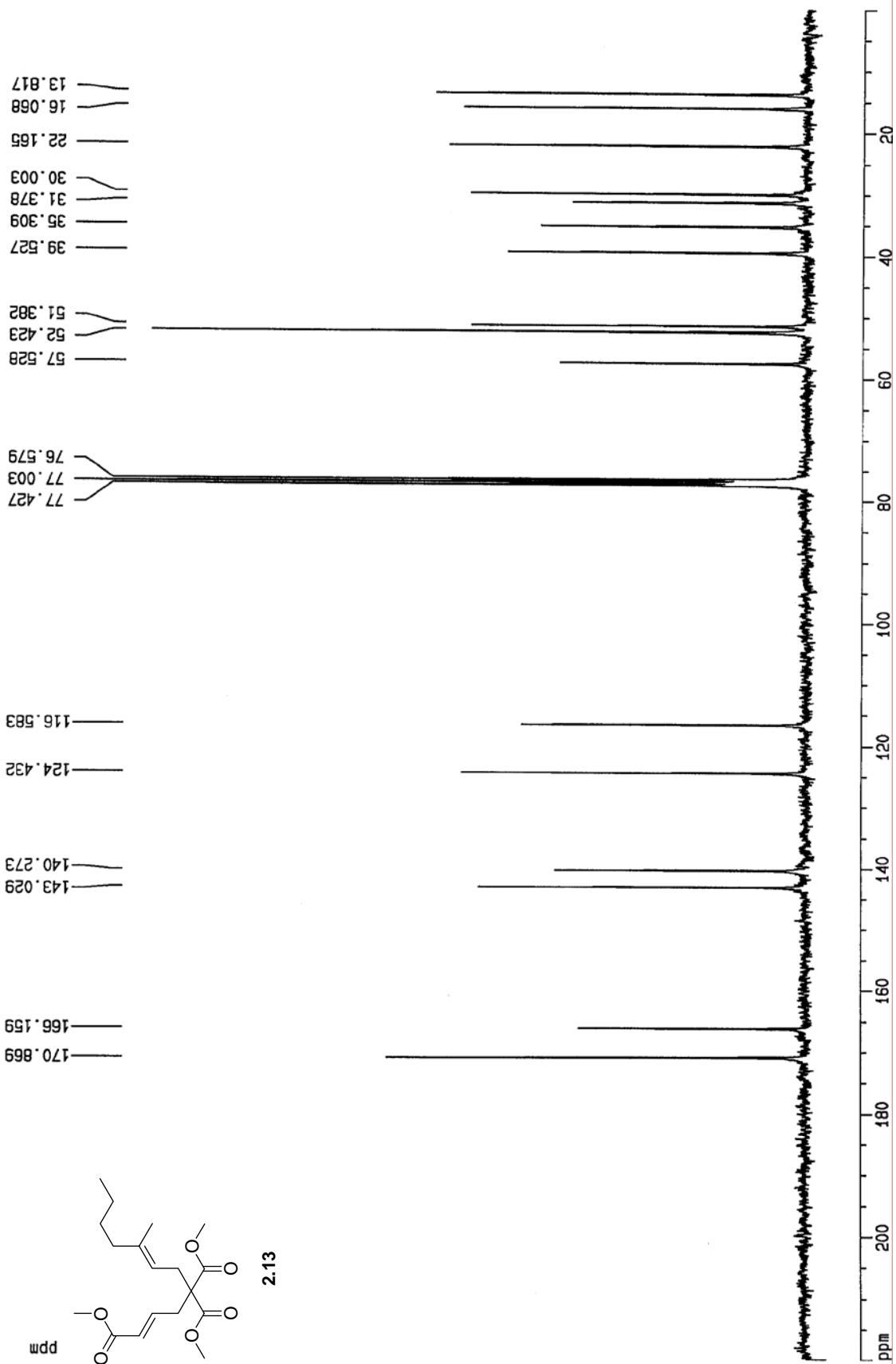
2.13



13.817
 16.068
 22.165
 30.003
 31.378
 35.309
 39.527
 51.382
 52.423
 57.528
 76.579
 77.003
 77.427
 116.583
 124.432
 140.273
 143.029
 166.159
 170.869



2.13

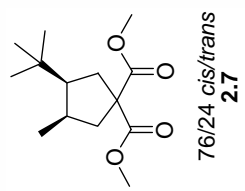
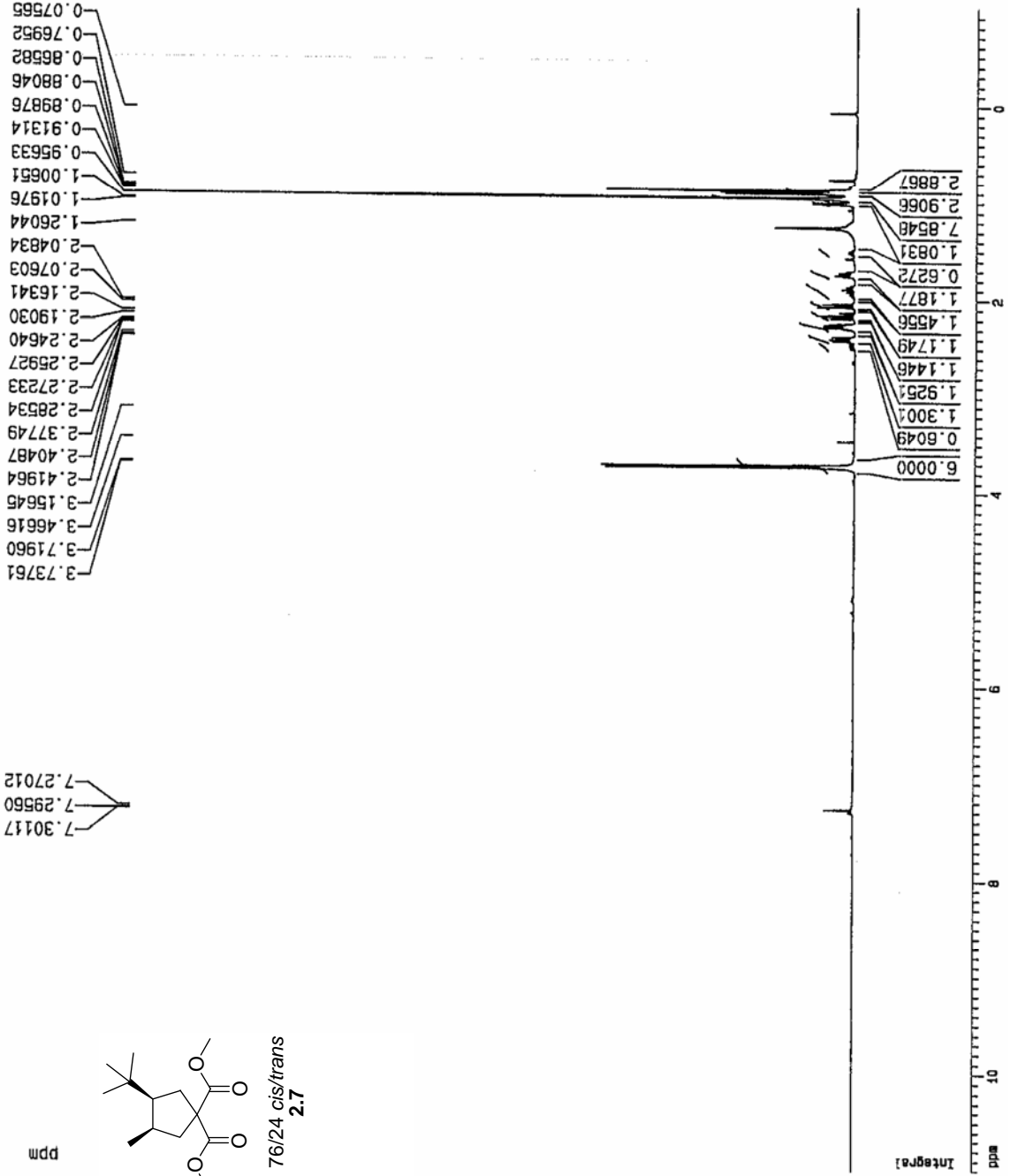


EXPNO 1
 PROCNO 1

F2 - Acquisition Parameters
 Date_ 500000
 Time 12.16
 INSTRUM spect
 PROBHD 5 mm TXI 13C
 PULPROG zg
 TD 32768
 SOLVENT CDC13
 NS 16
 DS 0
 SWH 7507.507 Hz
 FIDRES 0.229111 Hz
 AQ 2.1823988 sec
 RG 45.3
 DK 66.600 usec
 DE 6.00 usec
 TE 290.0 K
 D1 1.0000000 sec
 P1 11.00 usec
 DE 6.00 usec
 SF01 500.1330008 MHz
 NUC1 1H
 PL1 0.00 dB

F2 - Processing parameters
 SI 32768
 SF 500.1300233 MHz
 WDM EM
 SSB 0
 LB 0.40 Hz
 GB 0
 PC 1.00

1D NMR plot parameters
 CX 20.00 cm
 F1P 11.000 ppm
 F1 5501.43 Hz
 F2P -1.000 ppm
 F2 -500.13 Hz
 PPMCM 0.60000 ppm/cm
 HZCM 300.07803 Hz/cm



ppm

EXPNO 1
PROCNO 1

F2 - Acquisition Parameters

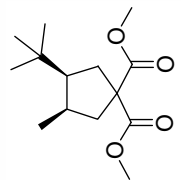
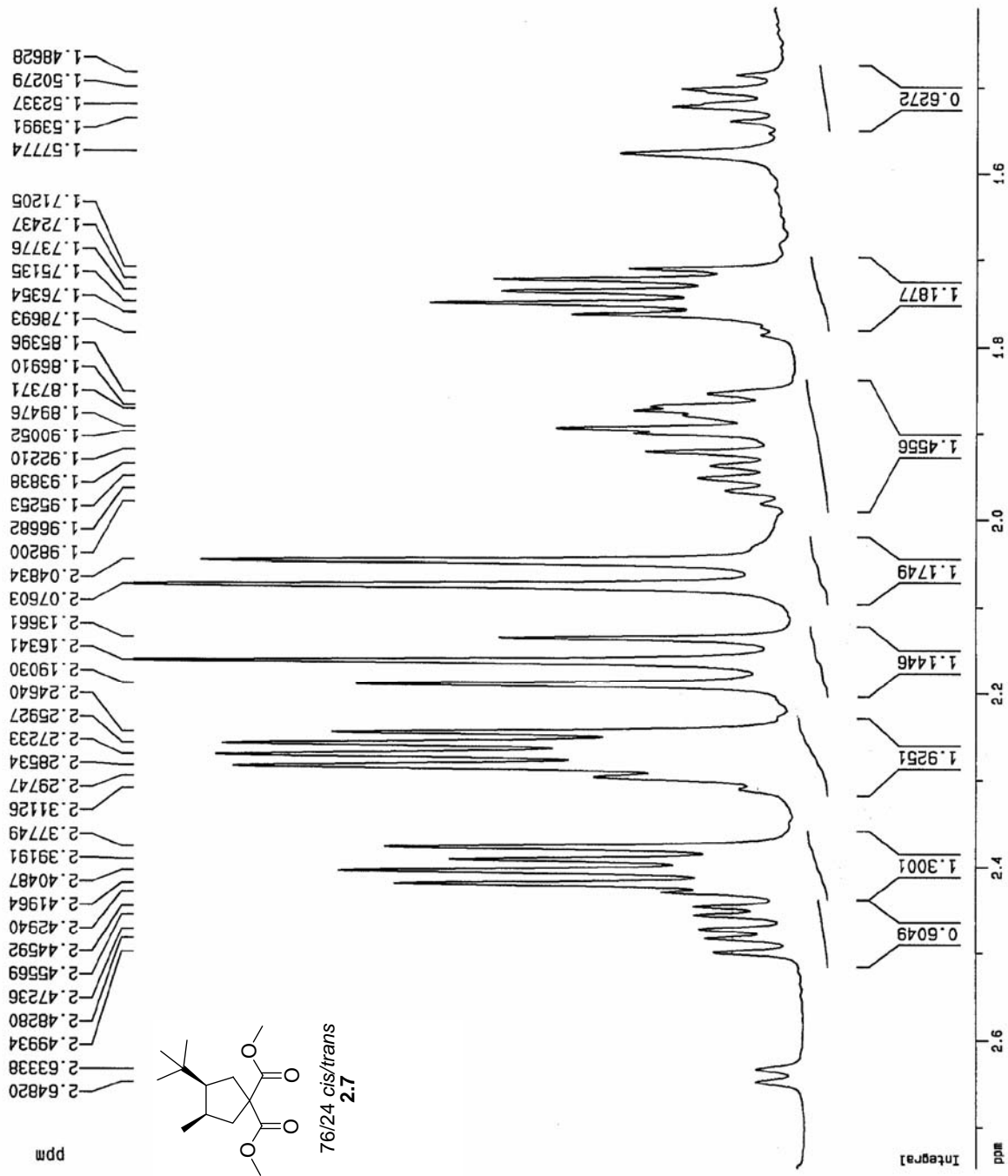
Date_ 500000
Time 12.16
INSTRUM spect
PROBHD 5 mm TXI 13C
PULPROG zg
TD 32768
SOLVENT CDCl3
NS 16
DS 0
SMH 7507.507 Hz
FIDRES 0.229111 Hz
AQ 2.1823988 sec
RG 45.3
DW 66.500 usec
DE 6.00 usec
TE 290.0 K
D1 1.0000000 sec
DE 11.00 usec
DE 6.00 usec
SF01 500.1330008 MHz
NUC1 1H
PL1 0.00 dB

F2 - Processing parameters

SI 32768
SF 500.1300233 MHz
WDW EM
SSB 0
LB 0.40 Hz
GB 0
PC 1.00

1D NMR plot parameters

CX 20.00 cm
F1P 2.748 ppm
F1 1374.47 Hz
F2P 1.409 ppm
F2 704.45 Hz
PPMCM 0.06698 ppm/cm
HZCM 33.50040 Hz/cm



PROCNO 1

F2 - Acquisition Parameters

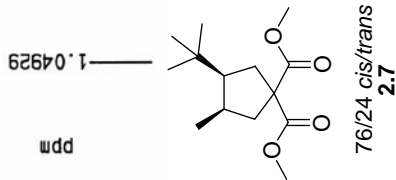
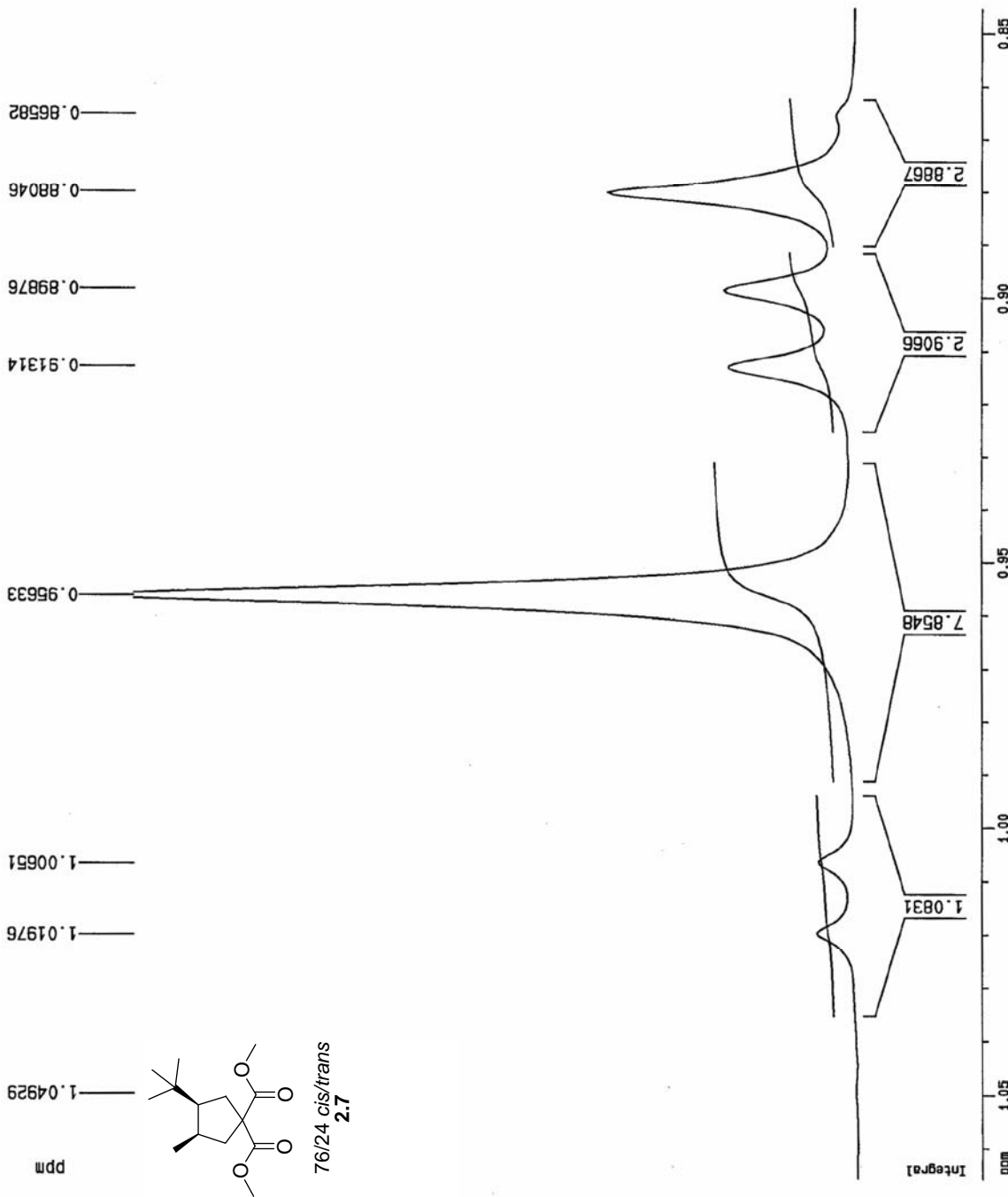
Date_ 500000
Time 12.16
INSTRUM spect
PROBHD 5 mm TXI 13C
PULPROG zg
TD 32768
SOLVENT CDC13
NS 16
DS 0
SWH 7507.507 Hz
FIDRES 0.229111 Hz
AQ 2.1823988 sec
RG 45.3
DW 66.600 usec
DE 6.00 usec
TE 290.0 K
D1 1.0000000 sec
P1 11.00 usec
DE 6.00 usec
SF01 500.1330008 MHz
NUC1 1H
PL1 0.00 dB

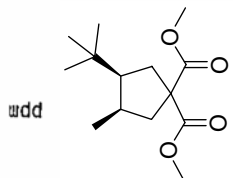
F2 - Processing parameters

SI 32768
SF 500.1300233 MHz
WDW EM
SSB 0
LB 0.40 Hz
GB 0
PC 1.00

1D NMR plot parameters

CX 20.00 cm
F1P 1.066 ppm
F1 533.00 Hz
F2P 0.845 ppm
F2 422.83 Hz
PPMCM 0.01101 ppm/cm
HZCM 5.50861 Hz/cm





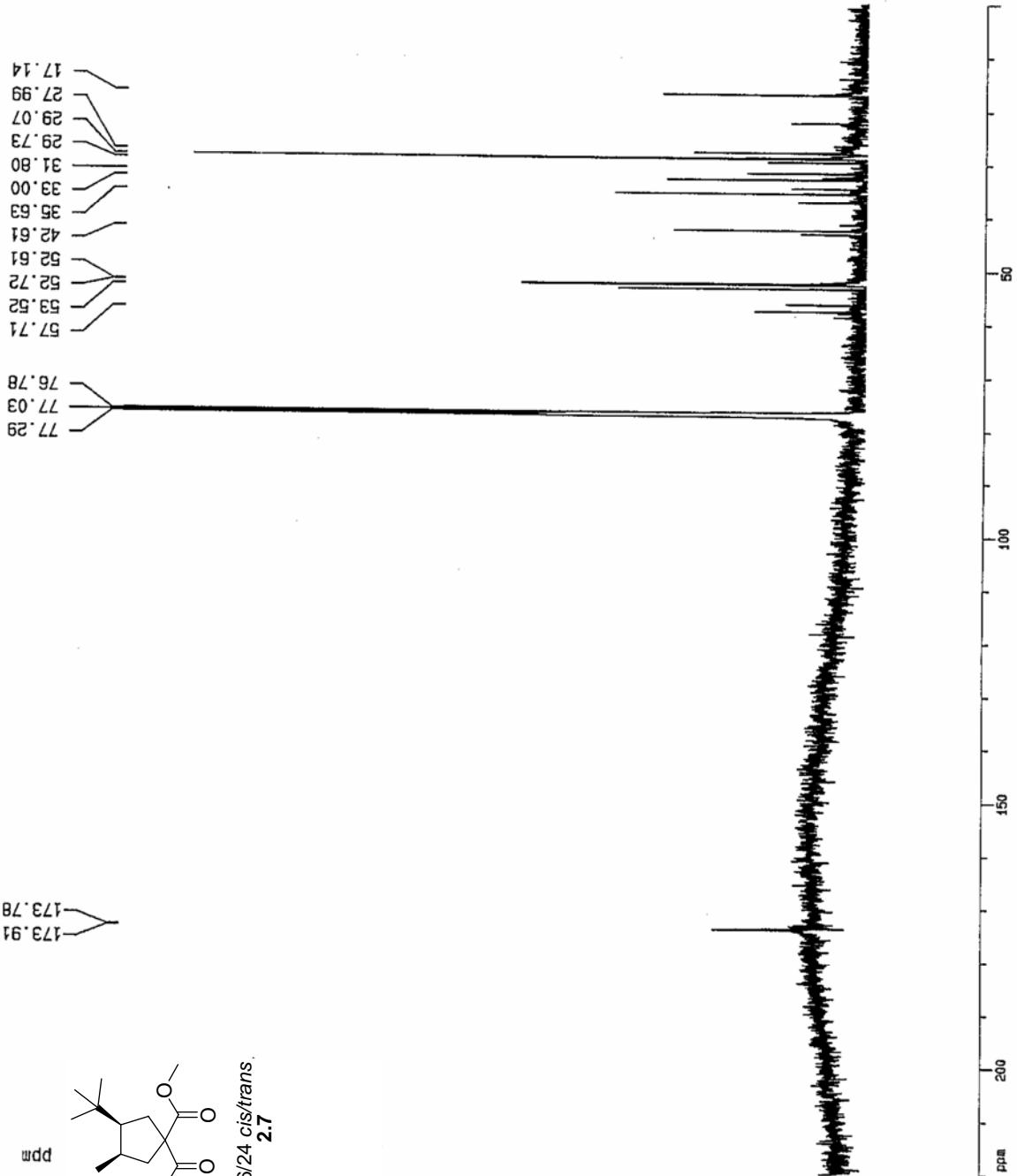
173.91
173.78

77.29
77.03
76.78
57.71
59.52
52.72
52.61
42.61
38.63
39.00
31.80
29.73
29.07
27.99
17.14

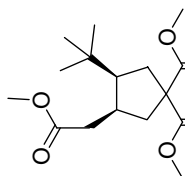
F2 - Acquisition Parameters
 Date_ 500000
 Time 9.57
 INSTRUM spect
 PROBHD 5 mm TXI 13C
 PULPROG c13winoe
 TD 32768
 SOLVENT CDCl3
 NS 8531
 DS 2
 SWH 32679.738 Hz
 FIDRES 0.997306 Hz
 AQ 0.5014004 sec
 RG 32768
 DW 15.300 usec
 DE 6.00 usec
 TE 290.0 K
 D3 0.00100000 sec
 PL12 6.00 dB
 D1 6.00000000 sec
 CPDPRG2 waltz16
 PCPD2 100.00 usec
 SF02 500.1330008 MHz
 NUC2 1H
 PL2 120.00 dB
 P1 17.00 usec
 DE 6.00 usec
 SF01 125.7715724 MHz
 NUC1 13C
 PL1 0.00 dB

F2 - Processing parameters
 SI 8192
 SF 125.7577921 MHz
 WDW EM
 SSB 0
 LB 4.00 Hz
 GB 0
 PC 1.00

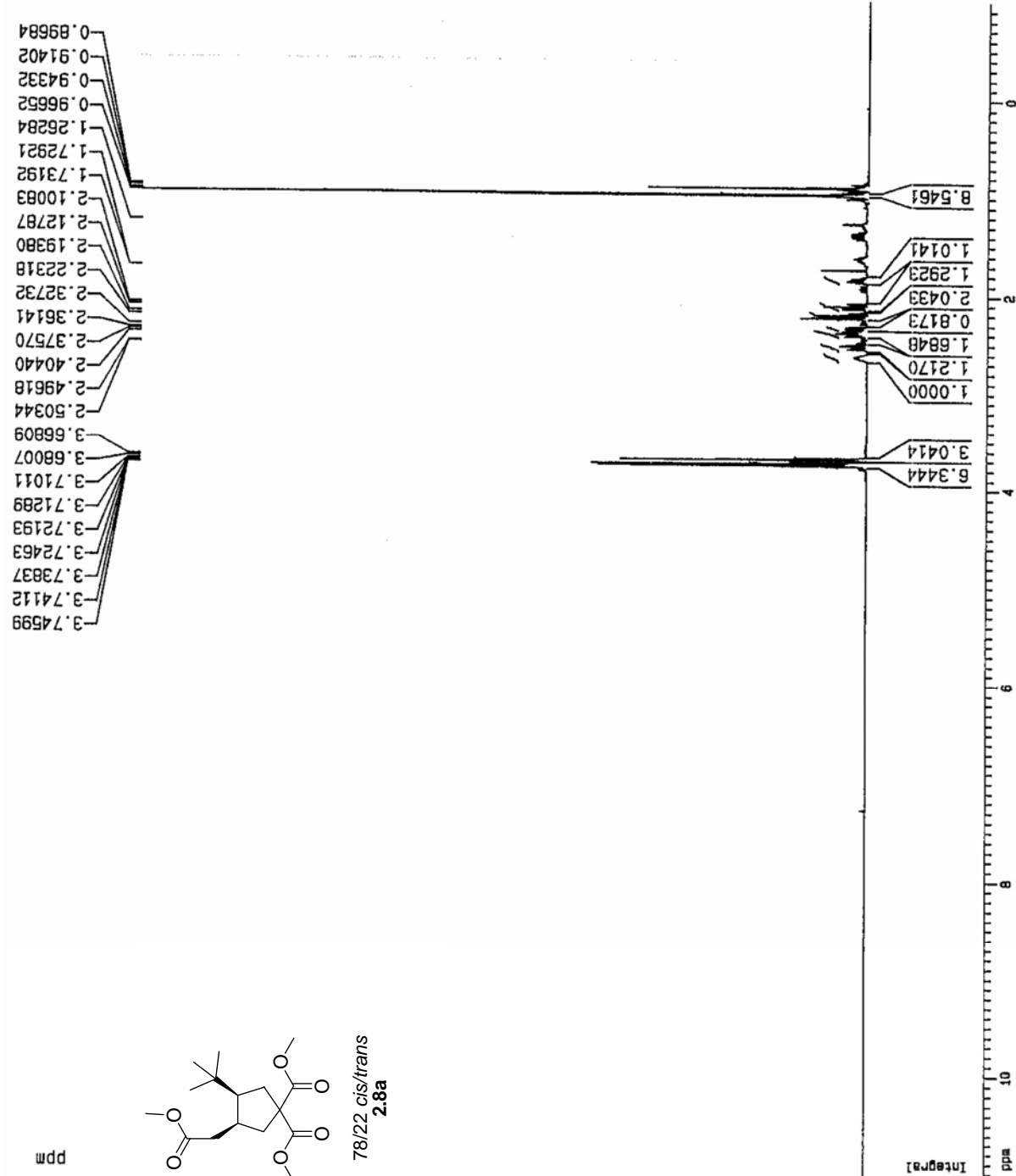
1D NMR plot parameters
 EX 20.00 cm
 F1P 220.000 ppm
 F1 27666.71 Hz
 F2P 0.000 ppm
 F2 0.00 Hz
 PPMCH 11.00000 ppm/cm
 HZCM 1383.33569 Hz/cm



ppm



78/22 cis/trans
2.8a



PROCNO 1

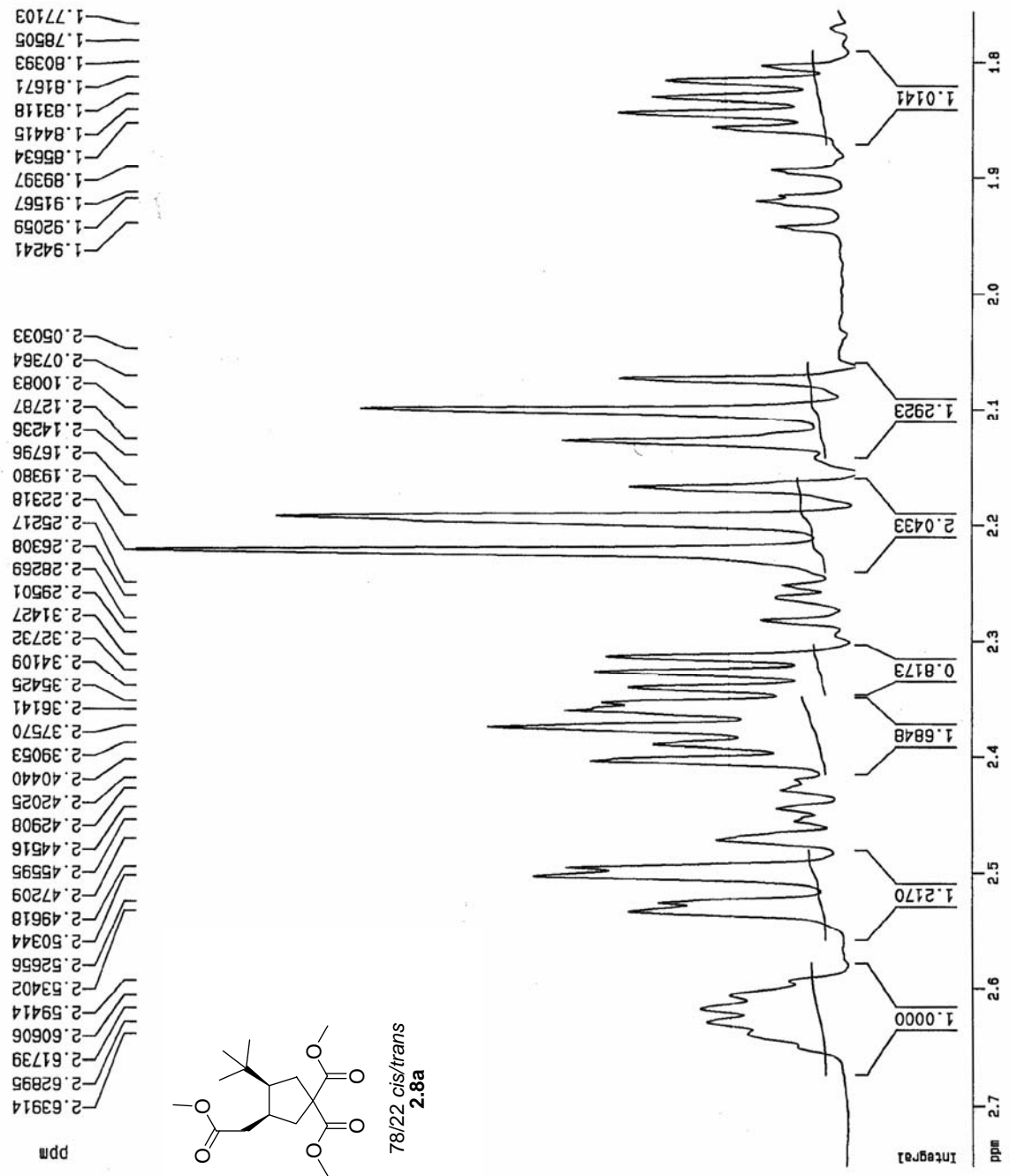
F2 - Acquisition Parameters

Date_ 500000
Time 12.23
INSTRUM spect
PROBHD 5 mm TXI 13C
PULPROG zg
TD 32768
SOLVENT CDC13
NS 16
DS 0
SWH 7507.507 Hz
FIDRES 0.229111 Hz
AQ 2.1823988 sec
RG 35.9
DM 66.600 usec
DE 6.00 usec
TE 290.0 K
D1 1.0000000 sec
P1 10.60 usec
DE 6.00 usec
SF01 500.1330008 MHz
NUC1 1H
PL1 0.00 dB

F2 - Processing parameters

SI 32768
SF 500.1300222 MHz
WDW EM
SSB 0
LB 0.40 Hz
GB 0
PC 1.00

XHPNU 1
 PROCNO 1
 F2 - Acquisition Parameters
 Date_ 500000
 Time 12.23
 INSTRUM spect
 PROBH0 5 mm TXI 13C
 PULPROG zg
 TD 32768
 SOLVENT CDCl3
 NS 16
 DS 0
 SWH 7507.507 Hz
 FIDRES 0.229111 Hz
 AQ 2.1823988 sec
 RG 35.9
 DW 66.600 usec
 DE 6.00 usec
 TE 290.0 K
 D1 1.0000000 sec
 P1 10.60 usec
 DE 6.00 usec
 SF01 500.1330008 MHz
 NUC1 1H
 PL1 0.00 dB
 F2 - Processing parameters
 SI 32768
 SF 500.1300222 MHz
 MDW EM
 SSB 0
 LB 0.40 Hz
 GB 0
 PC 1.00
 1D NMR plot parameters
 CX 20.00 cm
 F1P 2.753 ppm
 F1 1376.82 Hz
 F2P 1.756 ppm
 F2 878.15 Hz
 PPMCM 0.04985 ppm/cm
 HZCM 24.93336 Hz/cm



F2 - Acquisition Parameters

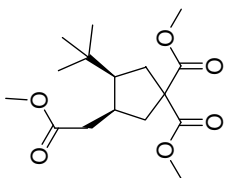
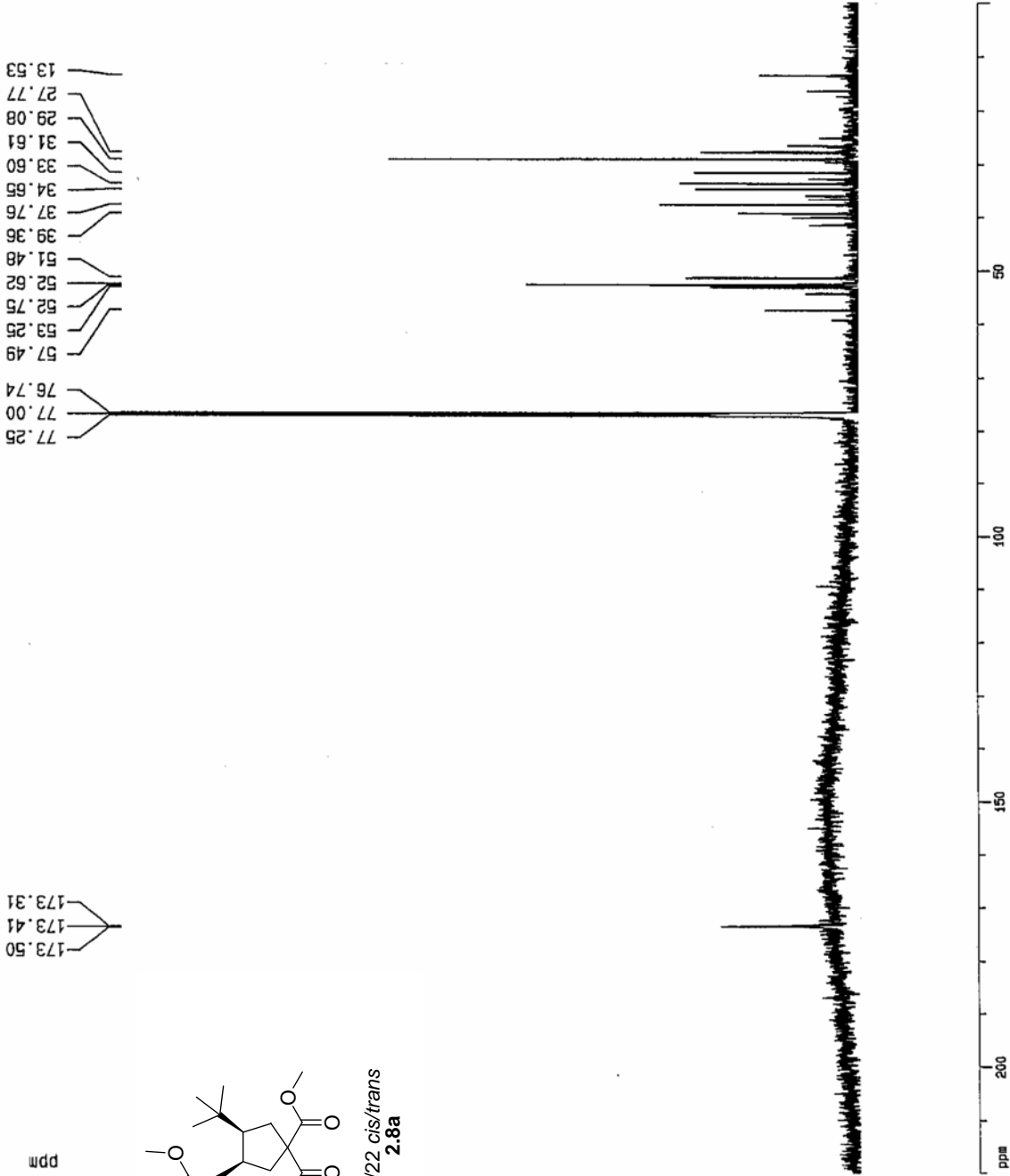
Date_ 500000
 Time 8.49
 INSTRUM spect
 PROBHD 5 mm TXI 13C
 PULPROG c13wznoe
 TD 32768
 SOLVENT D2O
 NS 3562
 DS 0
 SWH 32679.738 Hz
 FIDRES 0.997306 Hz
 AQ 0.5014004 sec
 RG 32768
 DW 15.300 usec
 DE 6.00 usec
 TE 290.0 K
 D3 0.00100000 sec
 PL12 6.00 dB
 D1 8.00000000 sec
 CPDPRG2 waltz16
 PCPD2 100.00 usec
 SF02 500.1330008 MHz
 NUC2 1H
 PL2 120.00 dB
 P1 21.60 usec
 DE 6.00 usec
 SF01 125.7715724 MHz
 NUC1 13C
 PL1 0.00 dB

F2 - Processing parameters

SI 8192
 SF 125.7577961 MHz
 WDW EM
 SSB 0
 LB 4.00 Hz
 GB 0
 PC 1.00

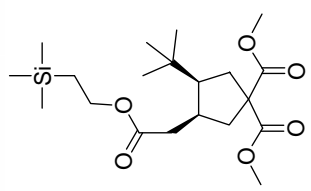
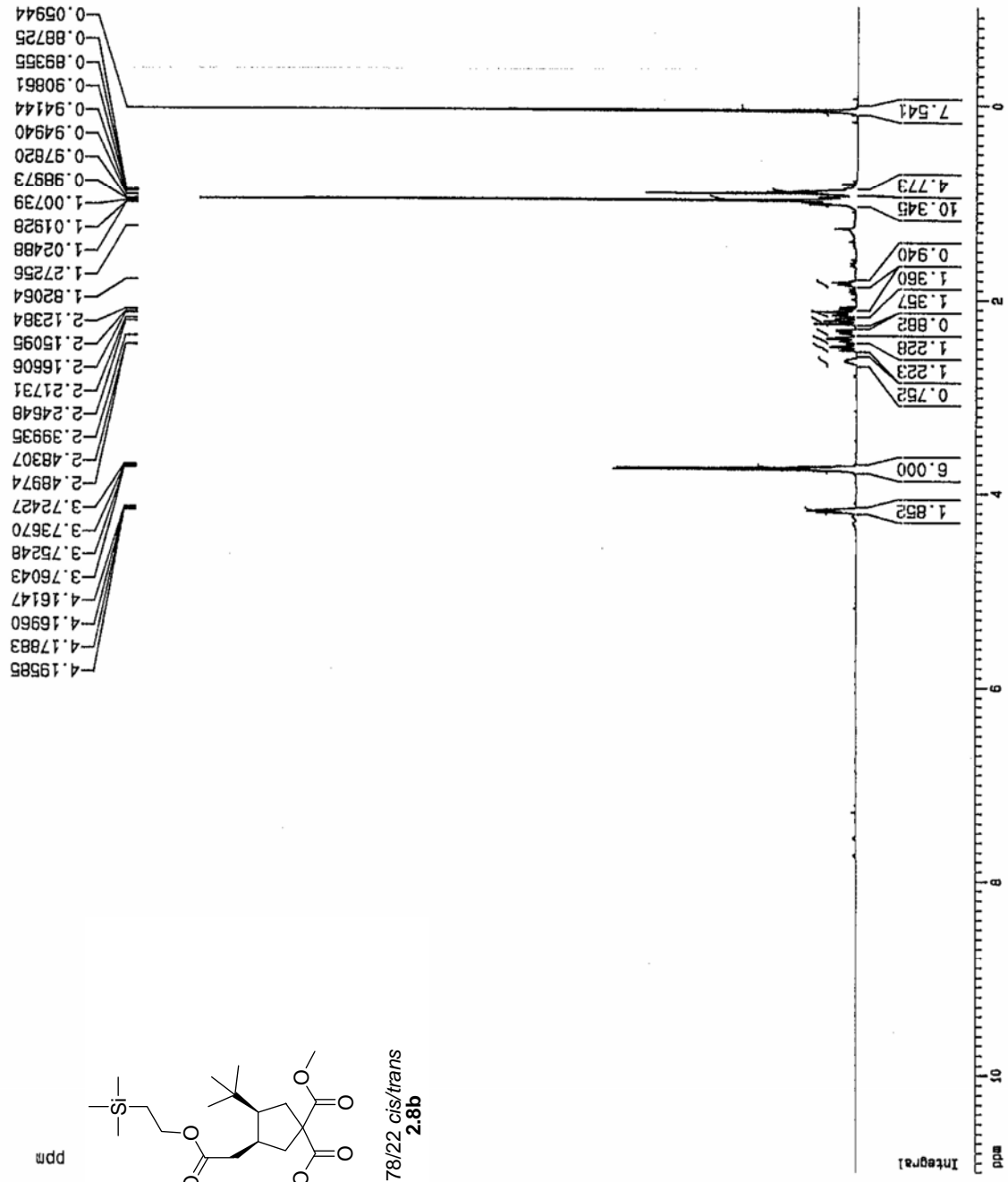
1D NMR plot parameters

CX 20.00 cm
 F1P 220.000 ppm
 F1 27666.71 Hz
 F2P 0.000 ppm
 F2 0.00 Hz
 PPMCM 11.00000 ppm/cm
 HZCM 1363.33562 Hz/cm

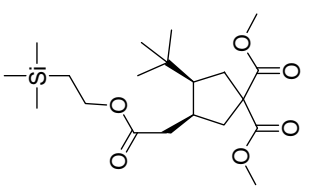


78/22 cis/trans
2.8a

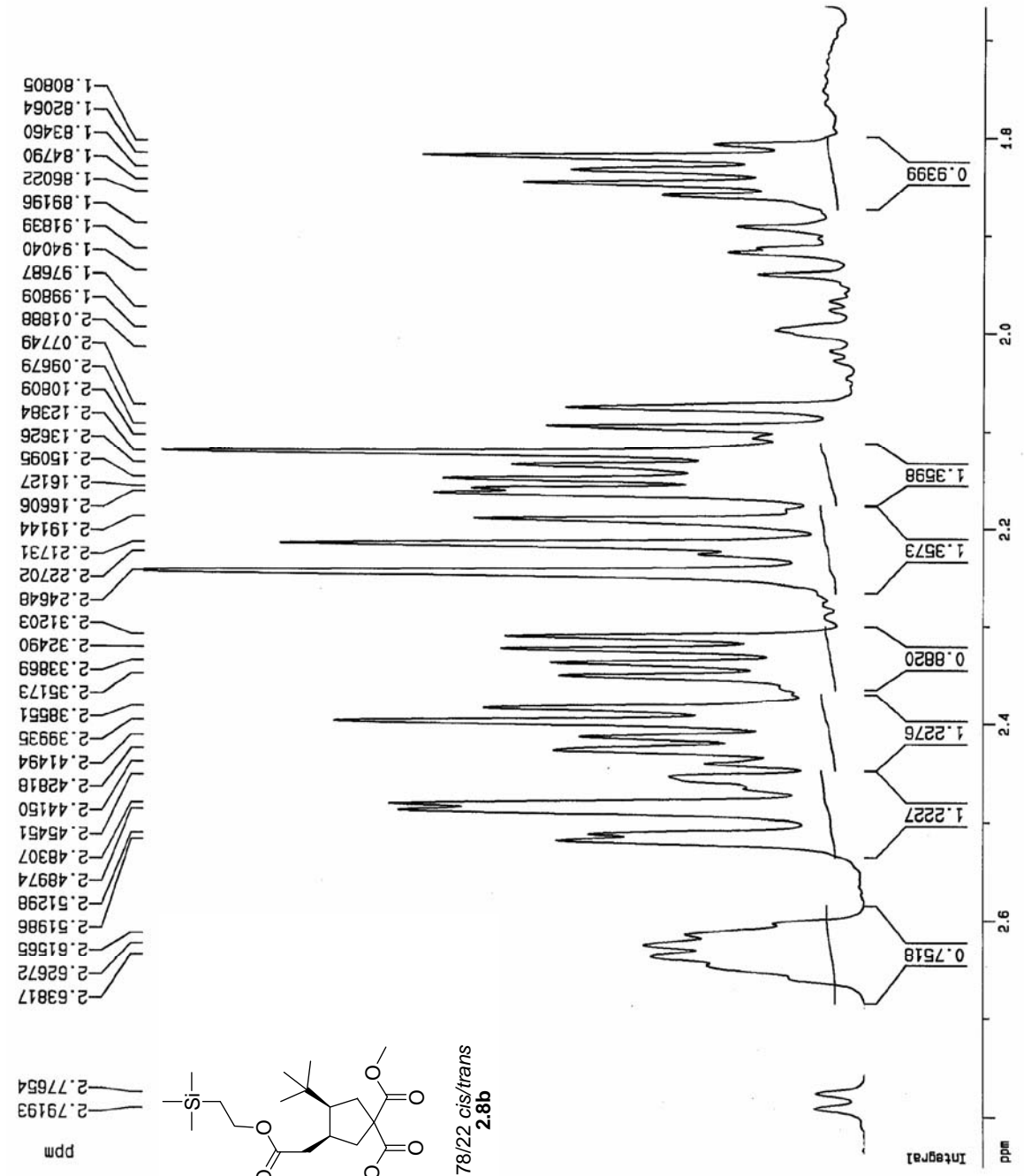
L41111
 PROCNO 1
 F2 - Acquisition Parameters
 Date_ 500000
 Time 18.38
 INSTRUM spect
 PROBHD 5 mm TXI 13C
 PULPROG zg
 TD 32768
 SOLVENT CDCl3
 NS 16
 DS 0
 SWH 7507.507 Hz
 FIDRES 0.229111 Hz
 AQ 2.1823988 sec
 RG 25.4
 DK 66.600 usec
 DE 6.00 usec
 TE 290.0 K
 D1 1.0000000 sec
 P1 10.60 usec
 DE 6.00 usec
 SF01 500.1330008 MHz
 NUC1 1H
 PL1 0.00 dB
 F2 - Processing parameters
 SI 32768
 SF 500.1300141 MHz
 WDW EM
 SSB 0
 LB 0.40 Hz
 GB 0
 PC 1.00
 1D NMR plot parameters
 CX 20.00 cm
 F1P 11.000 ppm
 F1 5501.43 Hz
 F2P -1.000 ppm
 F2 -500.13 Hz
 PPMCM 0.60000 ppm/cm
 HZCM 300.07800 Hz/cm



2.77654
2.79193
ppm



78/22 cis/trans
2.8b



CAINU 1
PROCNO 1

F2 - Acquisition Parameters

Date_ 500000
Time 18.38
INSTRUM spect
PROBHD 5 mm TXI 13C
PULPROG zg
TD 32768
SOLVENT CDCl3
NS 16
DS 0
SMH 7507.507 Hz
FIDRES 0.229111 Hz
AQ 2.1823988 sec
RG 25.4
DM 66.600 usec
DE 6.00 usec
TE 290.0 K
D1 1.0000000 sec
P1 10.60 usec
DE 6.00 usec
SF01 500.1330008 MHz
NUC1 1H
PL1 0.00 dB

F2 - Processing parameters

SI 32768
SF 500.1300141 MHz
WDW EM
SSB 0
LB 0.40 Hz
GB 0
PC 1.00

1D NMR plot parameters

CX 20.00 cm
F1P 2.851 ppm
F1 1425.90 Hz
F2P 1.666 ppm
F2 833.43 Hz
PPMCH 0.05923 ppm/cm
HZCM 29.62326 Hz/cm

EXPNO 1
PROCNO 1

F2 - Acquisition Parameters

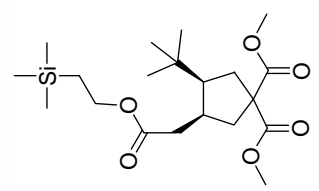
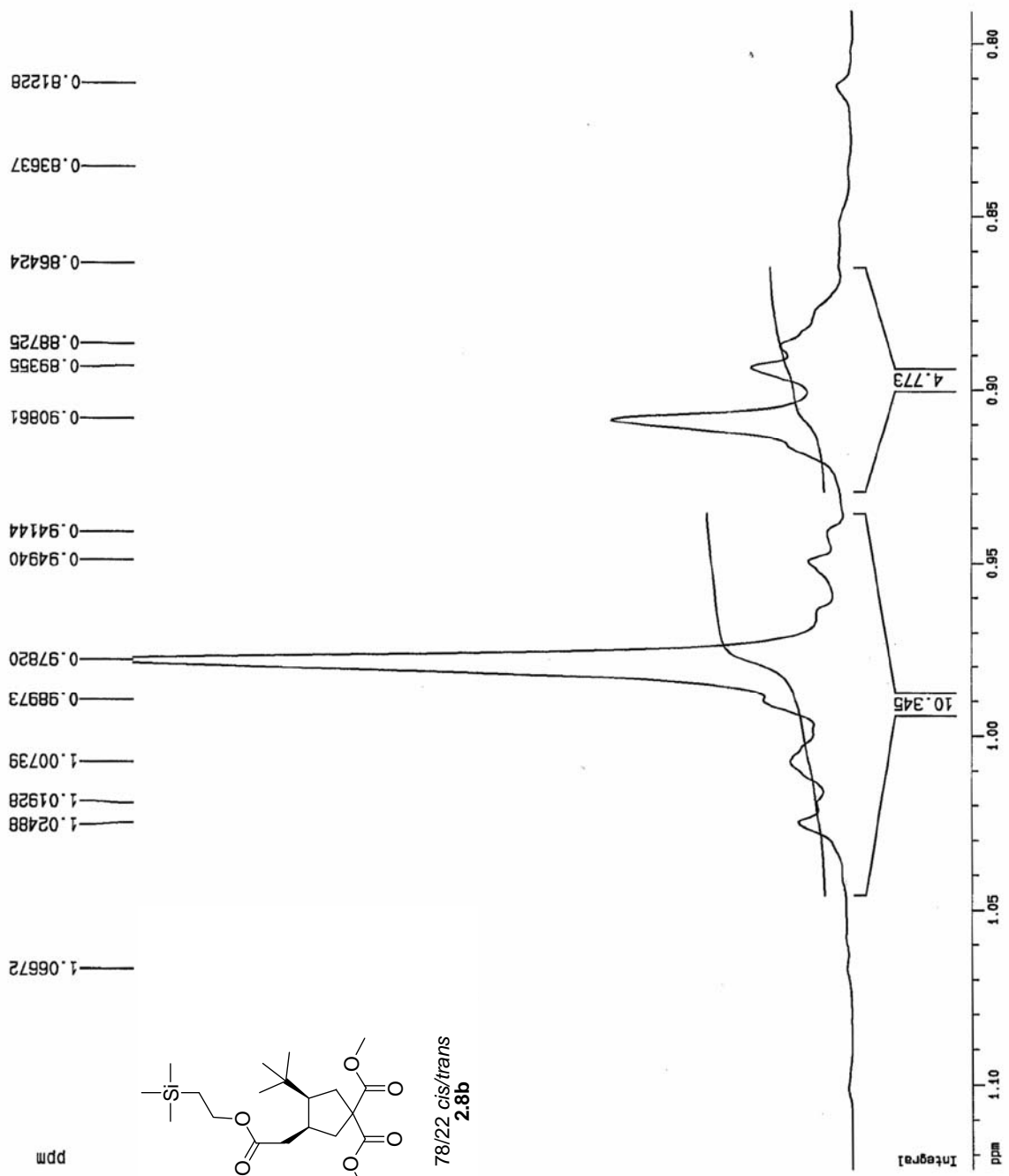
Date_ 500000
Time 18.38
INSTRUM spect
PROBHD 5 mm TXI 13C
PULPROG zg
TD 32768
SOLVENT CDC13
NS 16
DS 0
SMH 7507.507 Hz
FIDRES 0.229111 Hz
AQ 2.1823988 sec
RG 25.4
DM 66.600 usec
DE 6.00 usec
TE 290.0 K
D1 1.0000000 sec
P1 10.60 usec
DE 6.00 usec
SF01 500.1330008 MHz
NUC1 1H
PL1 0.00 dB

F2 - Processing parameters

SI 32768
SF 500.1300141 MHz
WDW EM
SSB 0
LB 0.40 Hz
GB 0
PC 1.00

1D NMR plot parameters

CX 20.00 cm
F1P 1.124 ppm
F1 562.28 Hz
F2P 0.791 ppm
F2 395.40 Hz
PRMCM 0.01668 ppm/cm
HZCM 8.34438 Hz/cm



78/22 cis/trans
2.8b

F2 - Acquisition Parameters

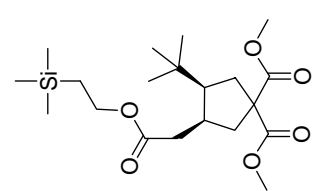
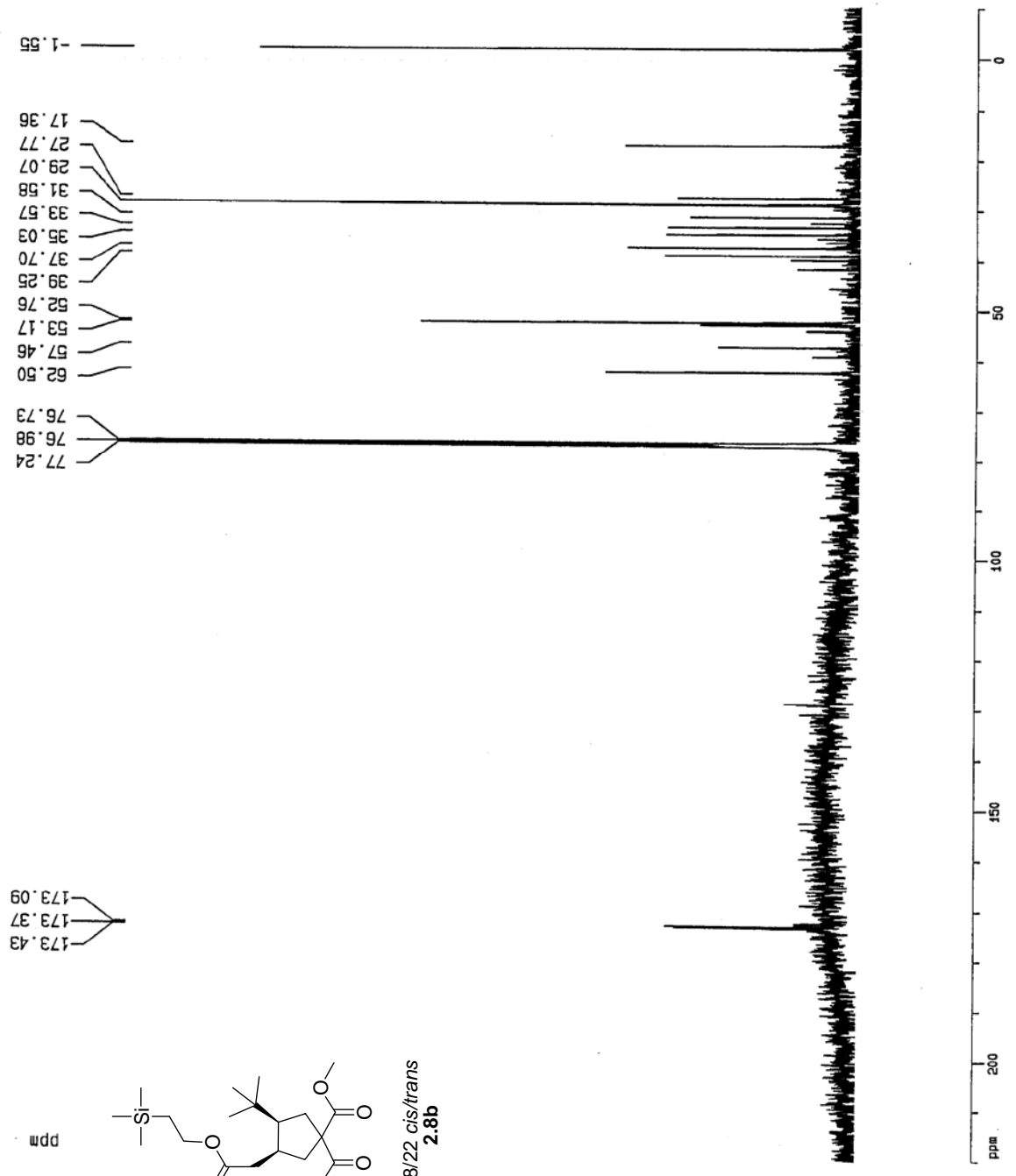
Date_ 500000
 Time 5.48
 INSTRUM spect
 PROBHD 5 mm TXI 13C
 PULPROG c13wzorde
 TD 32768
 SOLVENT CDCl3
 NS 1473
 DS 0
 SWH 32679.738 Hz
 FIDRES 0.997306 Hz
 AQ 0.5014004 sec
 RG 32768
 DW 15.300 usec
 DE 6.00 usec
 TE 290.0 K
 D3 0.00100000 sec
 PL12 6.00 dB
 D1 8.00000000 sec
 CPDPRG2 waltz16
 PCPD2 100.00 usec
 SF02 500.133008 MHz
 NUC2 1H
 PL2 120.00 dB
 P1 21.60 usec
 DE 6.00 usec
 SF01 125.7715724 MHz
 NUC1 13C
 PL1 0.00 dB

F2 - Processing parameters

SI 8192
 SF 125.7578000 MHz
 WDW EM
 SSB 0
 LB 4.00 Hz
 GB 0
 PC 1.00

1D NMR plot parameters

CX 20.00 cm
 F1P 220.000 ppm
 F1 27666.71 Hz
 F2P -10.000 ppm
 F2 -1257.58 Hz
 PPMCM 11.50000 ppm/cm
 HZCM 1446.21472 Hz/cm



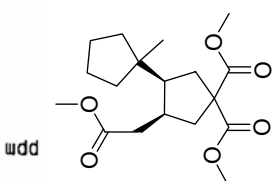
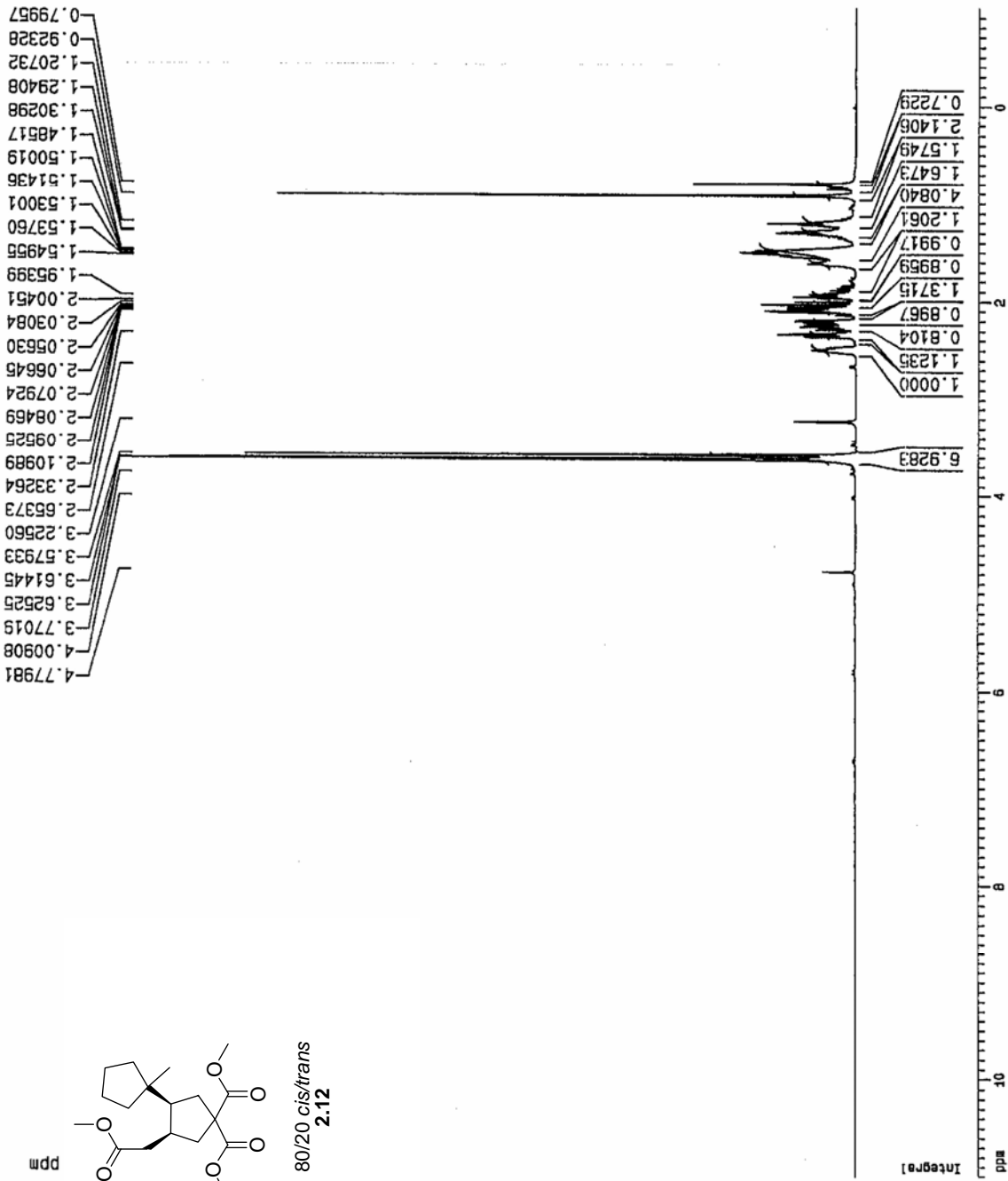
78/22 cis/trans
 2.8b

EXPNO 1
 PROCNO 1

F2 - Acquisition Parameters
 Date_ 500000
 Time 17.51
 INSTRUM spect
 PROBHD 5 mm TXI 13C
 PULPROG zg
 TD 32768
 SOLVENT MeOH
 NS 16
 DS 0
 SMH 7507.507 Hz
 FIDRES 0.229111 Hz
 AQ 2.1823988 sec
 RG 16
 DW 66.600 usec
 DE 6.00 usec
 TE 290.0 K
 D1 1.00000000 sec
 P1 11.00 usec
 DE 6.00 usec
 SF01 500.1330008 MHz
 NUC1 1H
 PL1 0.00 dB

F2 - Processing parameters
 SI 32768
 SF 500.1300532 MHz
 WDW EM
 SSB 0
 LB 0.40 Hz
 GB 0
 PC 1.00

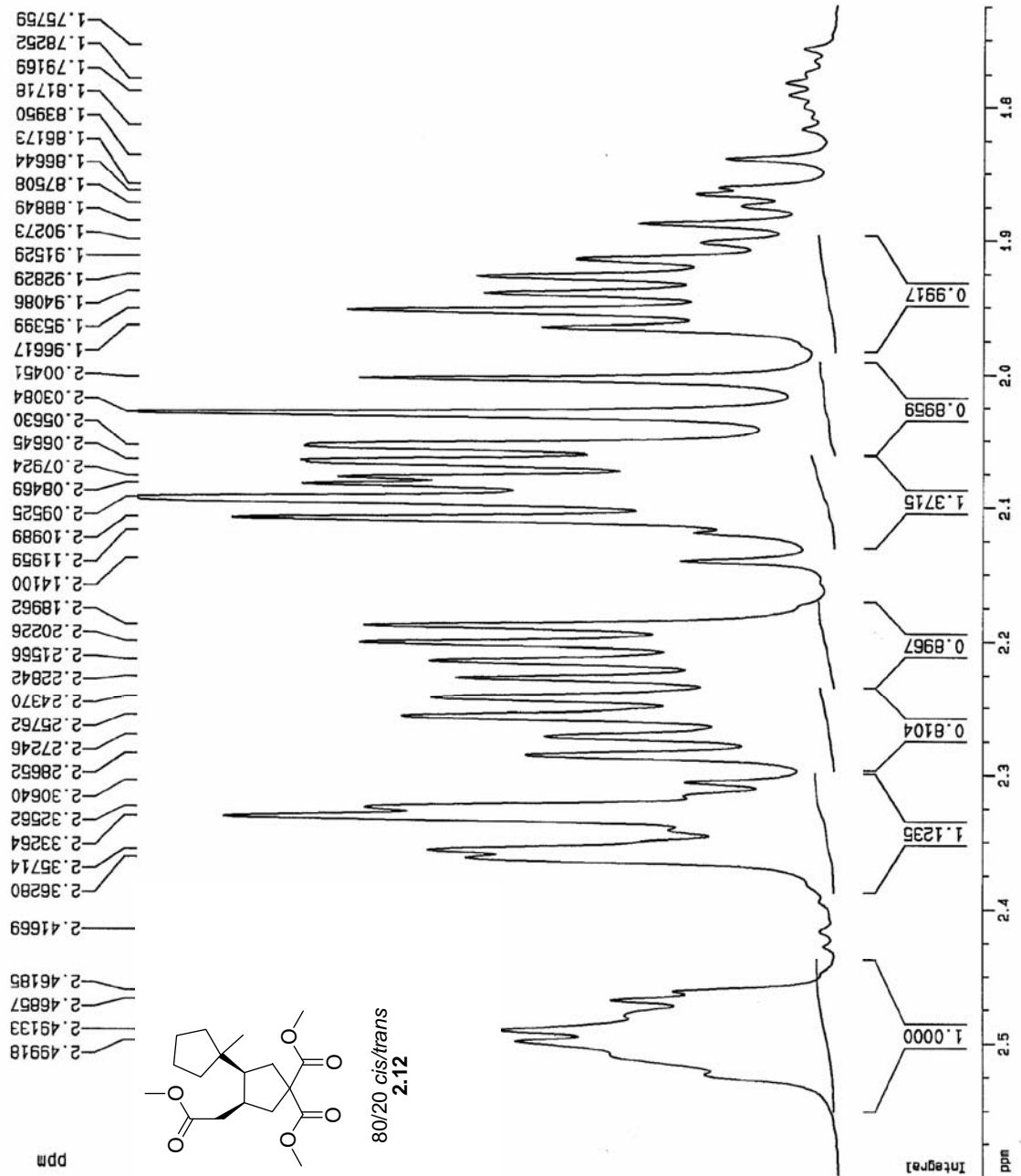
1D NMR plot parameters
 CX 20.00 cm
 F1P 11.000 ppm
 F1 5501.43 Hz
 F2P -1.000 ppm
 F2 -500.13 Hz
 PPMCM 0.60000 ppm/cm
 HZCM 300.07803 Hz/cm



```

EXPNO 1
PROCNO 1
F2 - Acquisition Parameters
Date_ 500000
Time 17.51
INSTRUM spect
PROBHD 5 mm TXI 13C
PULPROG zg
TD 32768
SOLVENT MeOH
NS 16
DS 0
SWH 7507.507 Hz
FIDRES 0.229111 Hz
AQ 2.1823988 sec
RG 16
DM 66.600 usec
DE 6.00 usec
TE 290.0 K
D1 1.0000000 sec
P1 11.00 usec
DE 6.00 usec
SF01 500.1330008 MHz
NUC1 1H
PL1 0.00 dB
F2 - Processing parameters
SI 32768
SF 500.1300532 MHz
WDW EM
SSB 0
LB 0.40 Hz
GB 0
PC 1.00
1D NMR plot parameters
CX 20.00 cm
F1P 2.599 ppm
F1 1299.70 Hz
F2P 1.725 ppm
F2 862.51 Hz
PPMCM 0.04371 ppm/cm
HZCM 21.85944 Hz/cm

```



NAME jt217-2
 EXPNO 1
 PROCNO 1

F2 - Acquisition Parameters

Date_ 500000
 Time 17.51
 INSTRUM spect
 PROBHD 5 mm TXI 13C
 PULPROG zg
 TD 32768
 SOLVENT MeOH
 NS 16
 DS 0

SMH 7507.507 Hz
 FIDRES 0.229111 Hz
 AQ 2.1823988 sec
 RG 16

DW 66.600 usec
 DE 6.00 usec
 TE 290.0 K

D1 1.0000000 sec
 P1 11.00 usec
 DE 6.00 usec

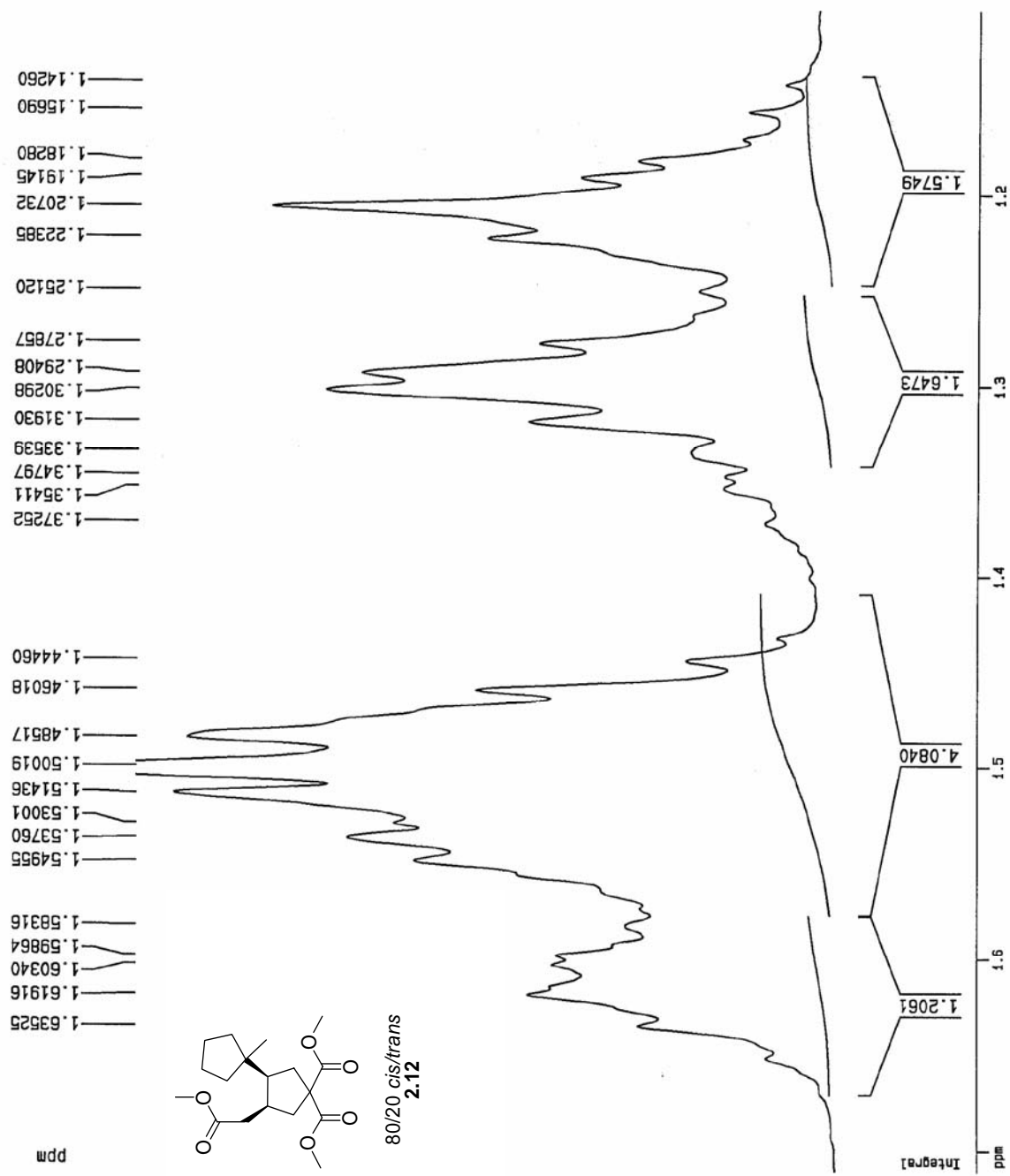
SF01 500.1330008 MHz
 NUC1 1H
 PL1 0.00 dB

F2 - Processing parameters

SI 32768
 SF 500.1300532 MHz
 MDW EM
 SSB 0
 LB 0.40 Hz
 GB 0
 PC 1.00

1D NMR plot parameters

CX 20.00 cm
 F1P 1.711 ppm
 F1 855.67 Hz
 F2P 1.104 ppm
 F2 552.02 Hz
 PPMCM 0.03036 ppm/cm
 HZCM 15.18245 Hz/cm



EXPNO 1
 PROCNO 1

F2 - Acquisition Parameters

Date_ 500000
 Time 17.51
 INSTRUM spect
 PROBHD 5 mm TXI 13C
 PULPROG zg
 TD 32768
 SOLVENT MeOH
 NS 16
 DS 0
 SWH 7507.507 Hz
 FIDRES 0.229111 Hz
 AQ 2.1823988 sec
 RG 16
 DW 66.600 usec
 DE 6.00 usec
 TE 290.0 K
 D1 1.0000000 sec
 P1 11.00 usec
 DE 6.00 usec
 SF01 500.1330008 MHz
 NUC1 1H
 PL1 0.00 dB

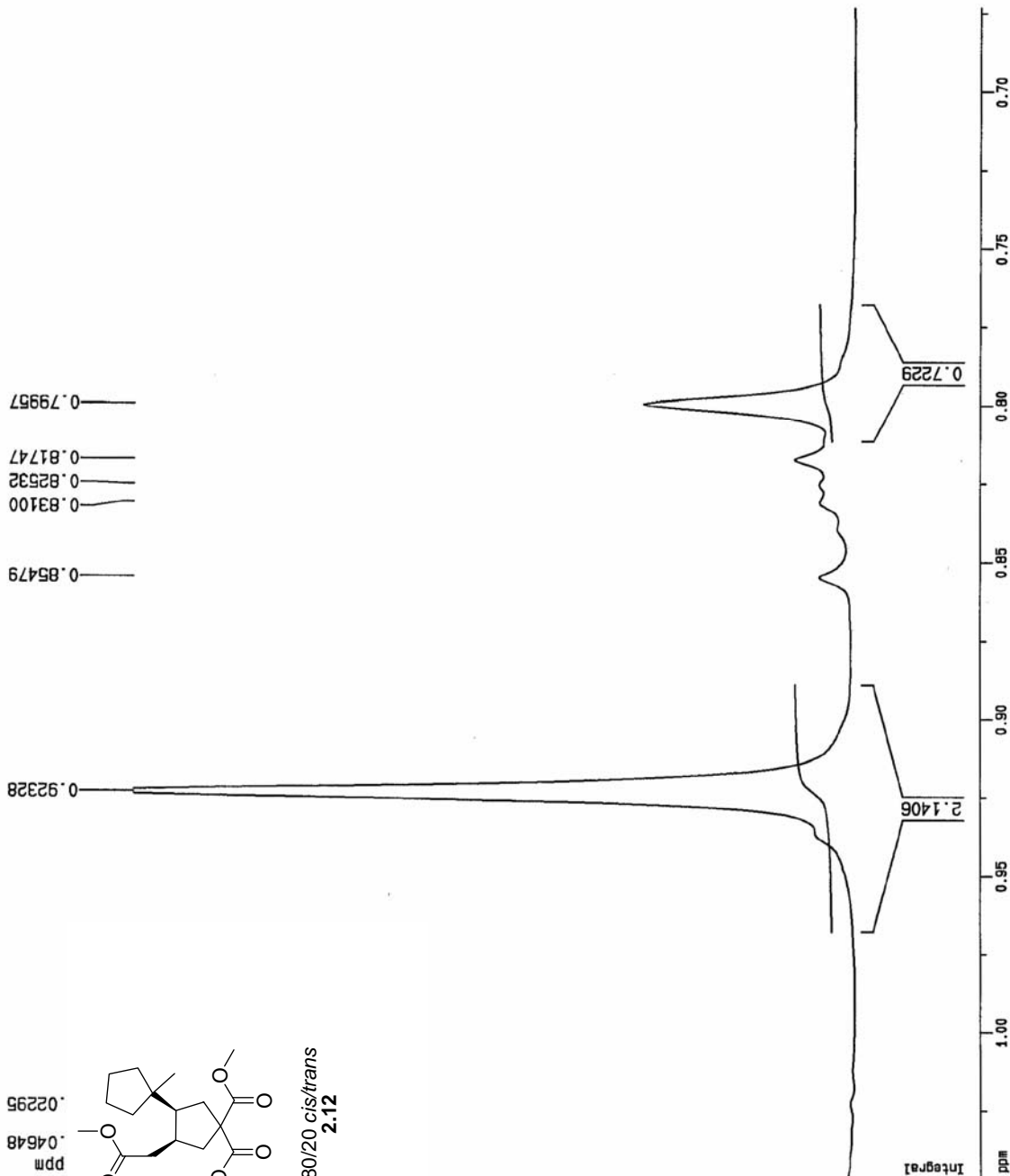
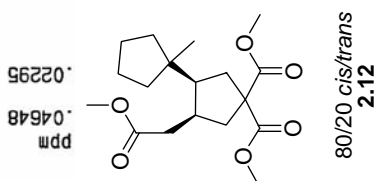
F2 - Processing parameters

SI 32768
 SF 500.1300532 MHz
 WDW EM
 SSB 0
 LB 0.40 Hz
 GB 0
 PC 1.00

1D NMR plot parameters

CX 20.00 cm
 F1P 1.046 ppm
 F1 523.38 Hz
 F2P 0.673 ppm
 F2 336.66 Hz
 PPMCM 0.01867 ppm/cm
 HZCM 9.33559 Hz/cm

0.92328
 0.85479
 0.83100
 0.82532
 0.81747
 0.79957



F2 - Acquisition Parameters

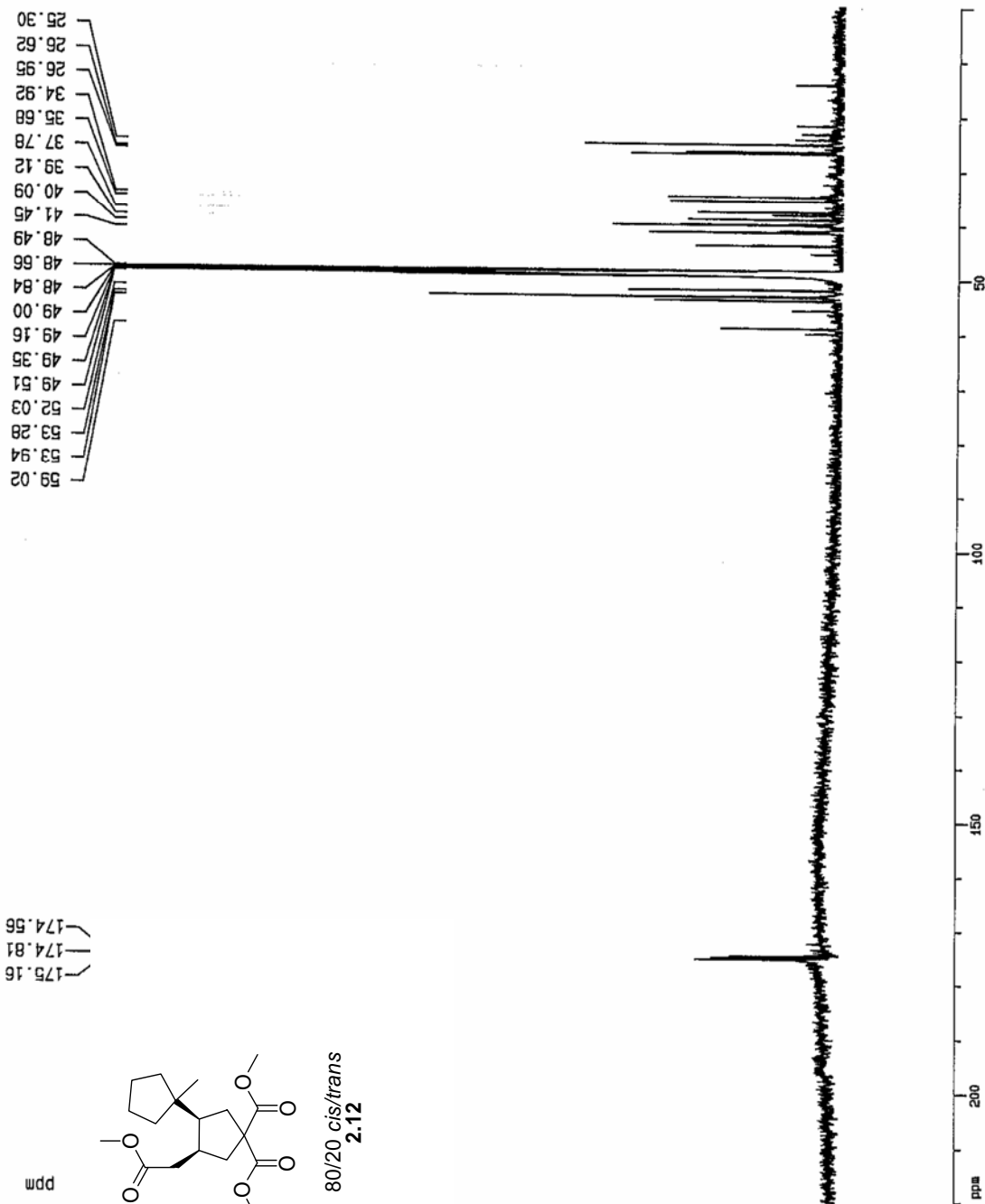
Date_	500000
Time	18.11
INSTRUM	spect
PROBHD	5 mm TXI 13C
PULPROG	c13wprose
TD	32768
SOLVENT	CDCl3
NS	2538
DS	0
SWH	32679.738 Hz
FIDRES	0.997306 Hz
AQ	0.5014004 sec
RG	18390.4
DW	15.300 usec
DE	6.00 usec
TE	290.0 K
D3	0.00100000 sec
PL12	6.00 dB
D1	8.00000000 sec
CPDPRG2	waltz16
PCPD2	100.00 usec
SFO2	500.1330008 MHz
NUC2	1H
PL2	120.00 dB
P1	21.60 usec
DE	6.00 usec
SFO1	125.7715724 MHz
NUC1	13C
PL1	0.00 dB

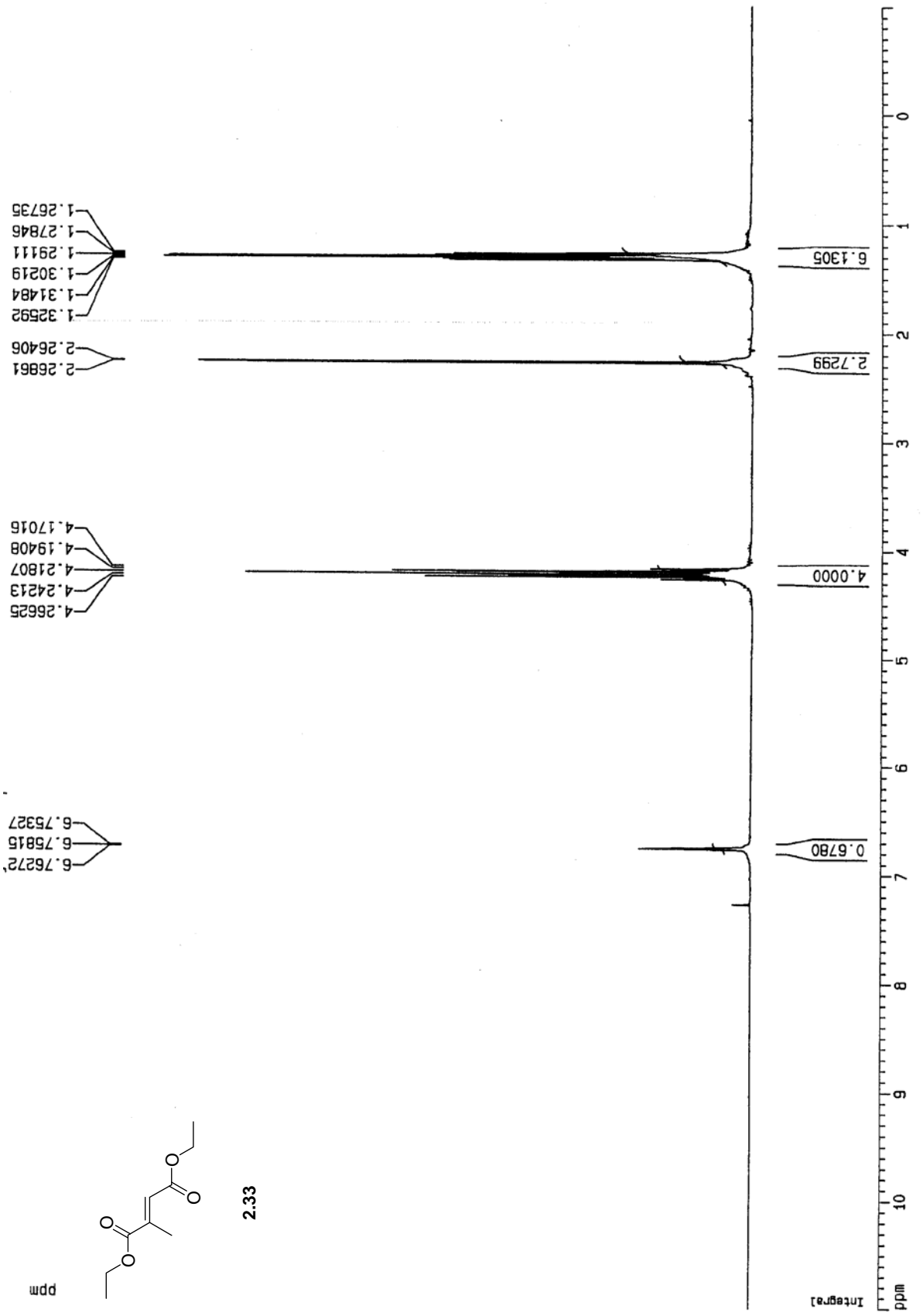
F2 - Processing parameters

SI	8192
SF	125.7575153 MHz
NDM	EM
SSB	0
LB	4.00 Hz
GB	0
PC	1.00

1D NMR plot parameters

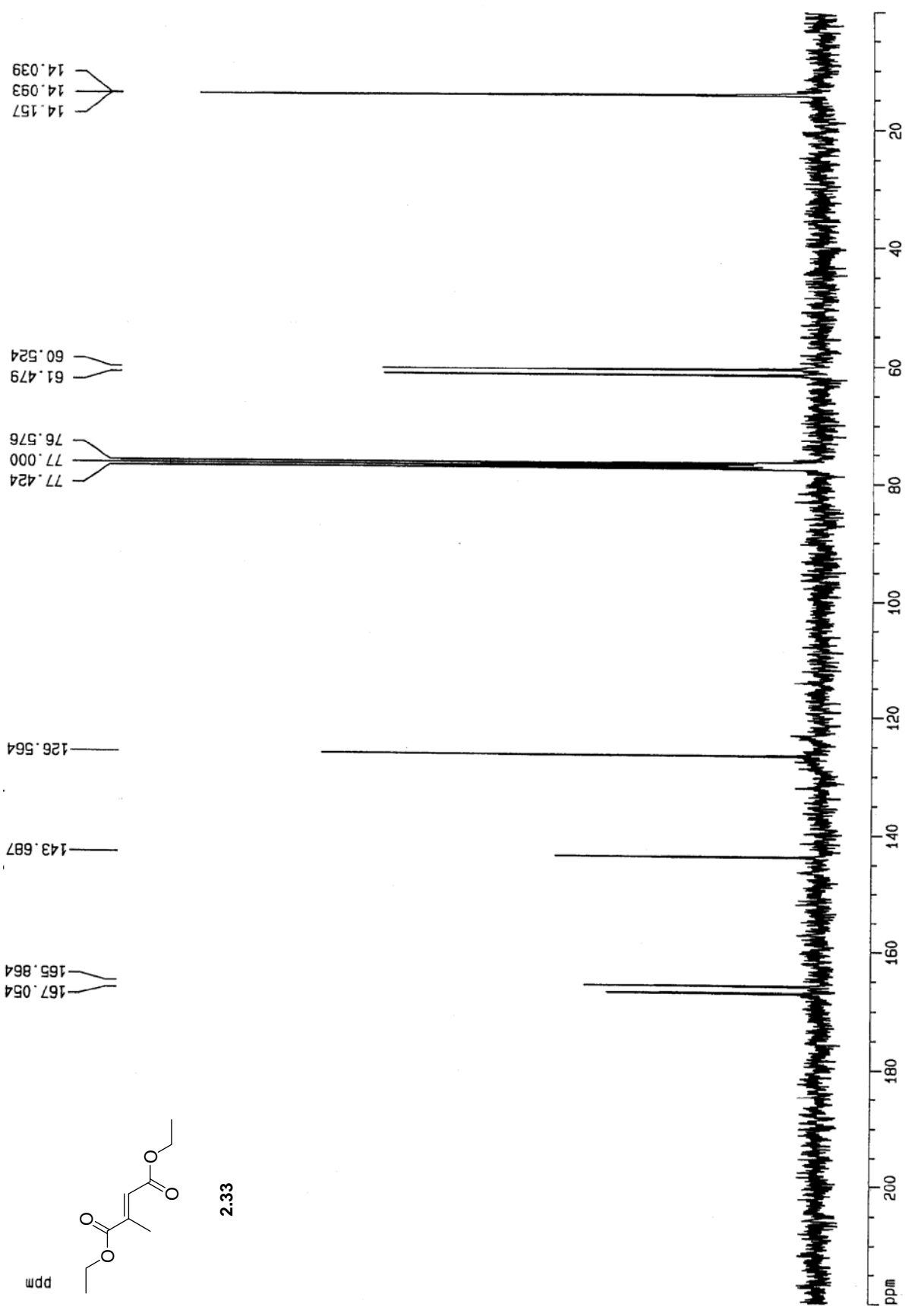
CX	20.00 cm
F1P	220.000 ppm
F1	27666.68 Hz
F2P	0.000 ppm
F2	0.00 Hz
PPHOM	11.00000 ppm/cm
HZCM	1383.33374 Hz/cm





2.33

ppm



14.157
14.093
14.039

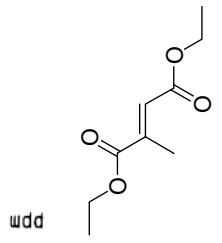
60.524
61.479

76.576
77.000
77.424

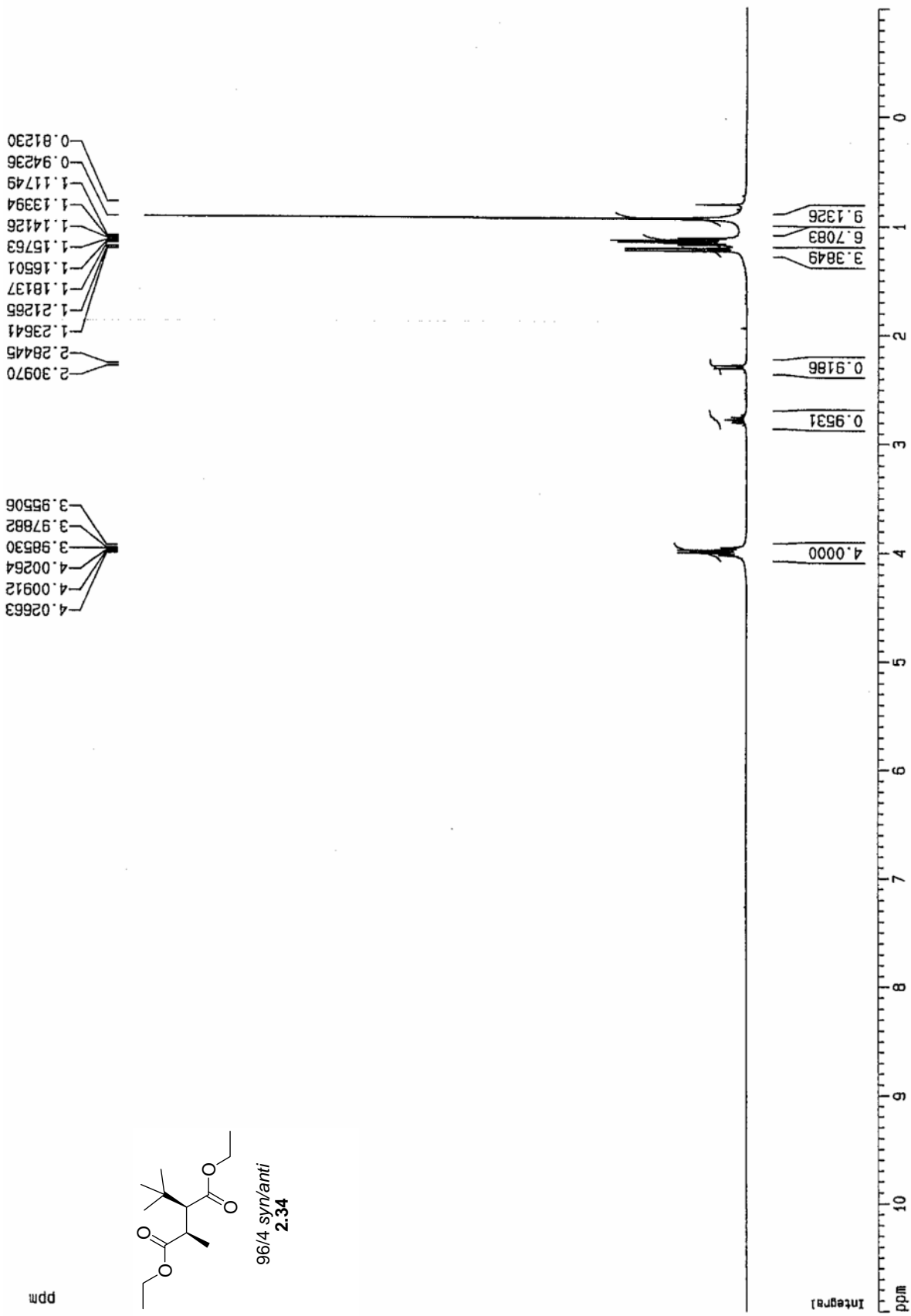
126.564

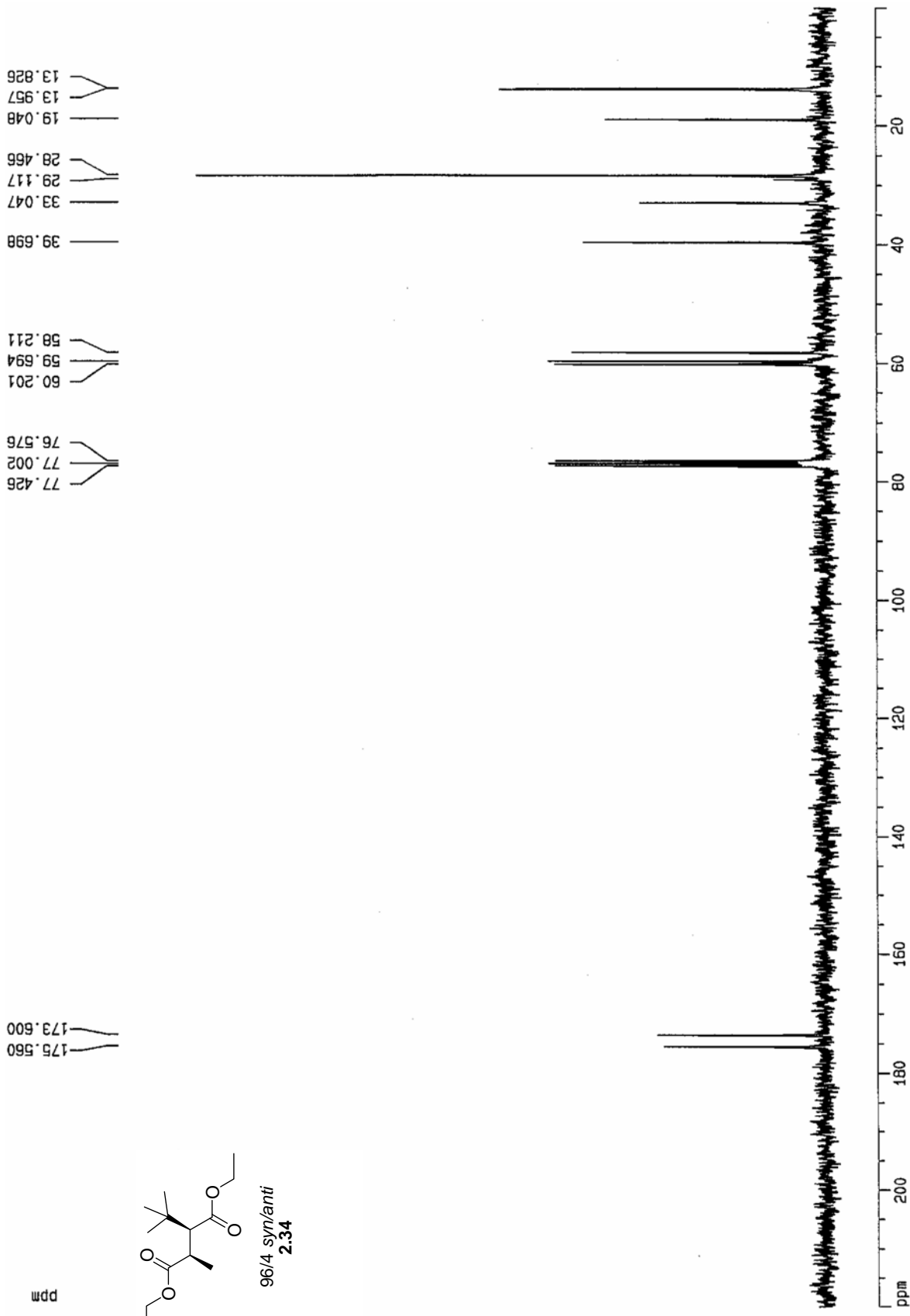
143.687

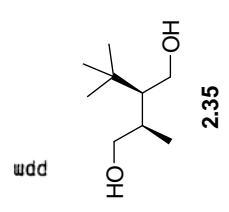
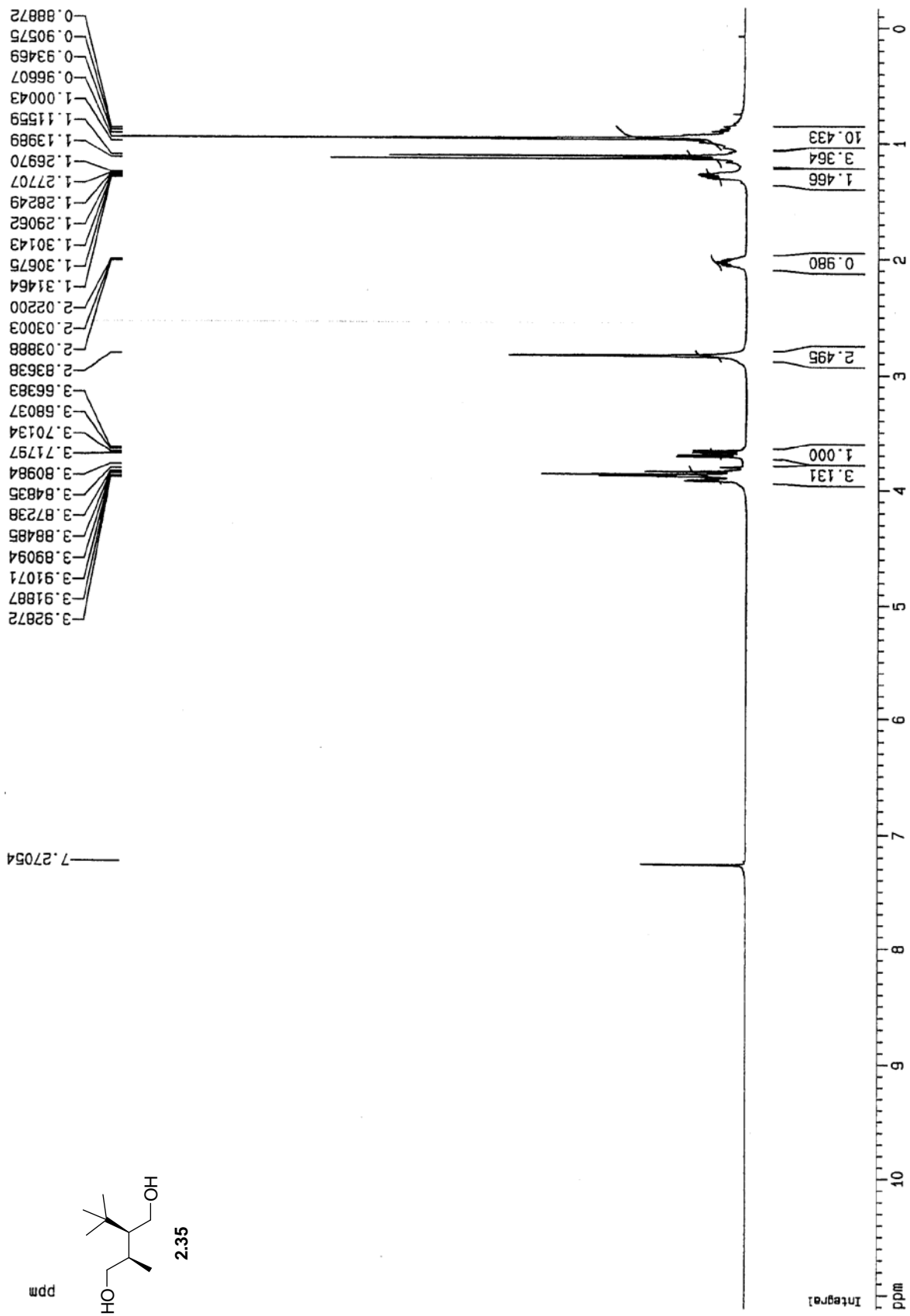
165.864
167.054

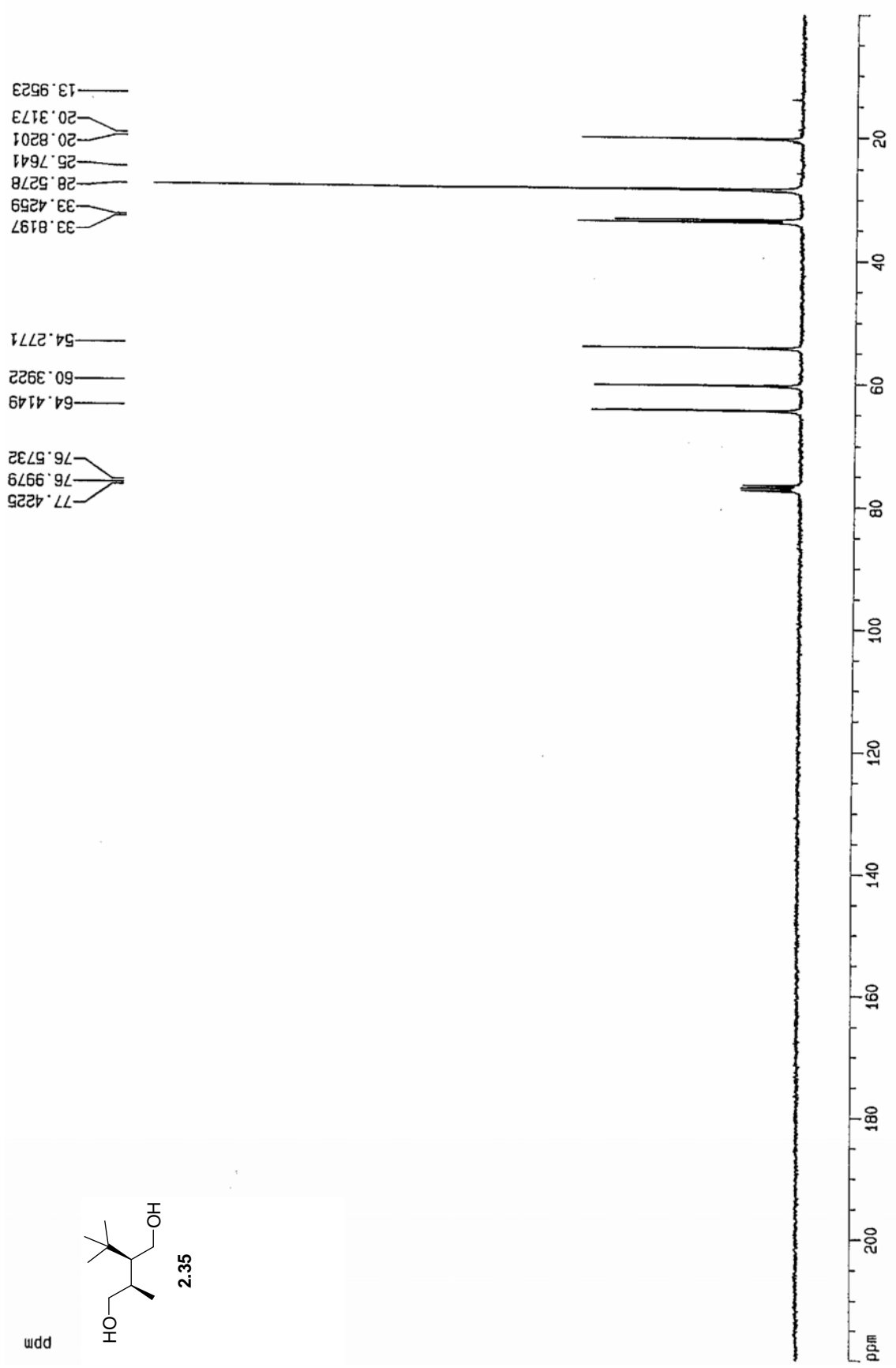


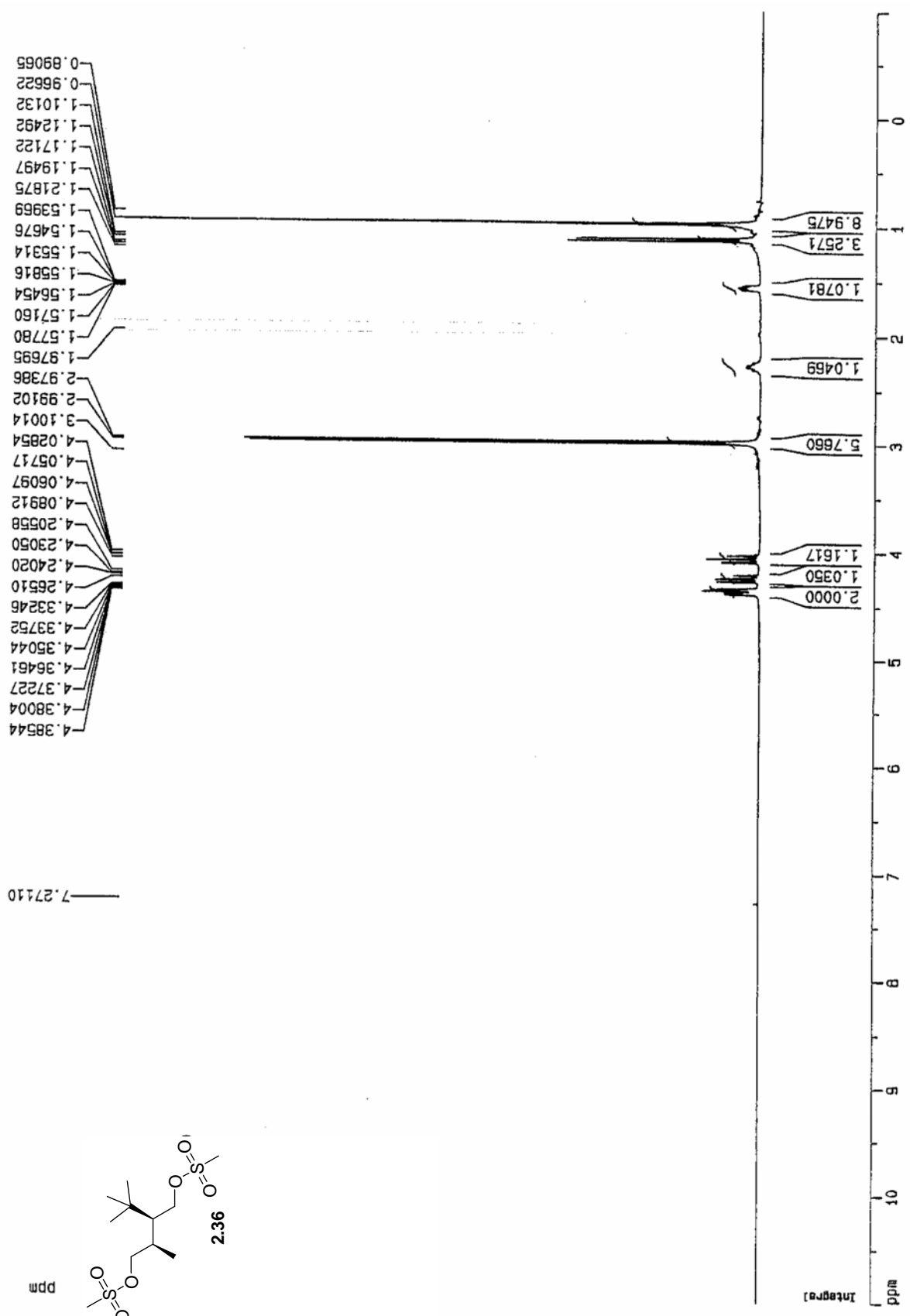
2.33

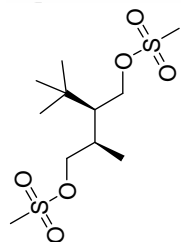




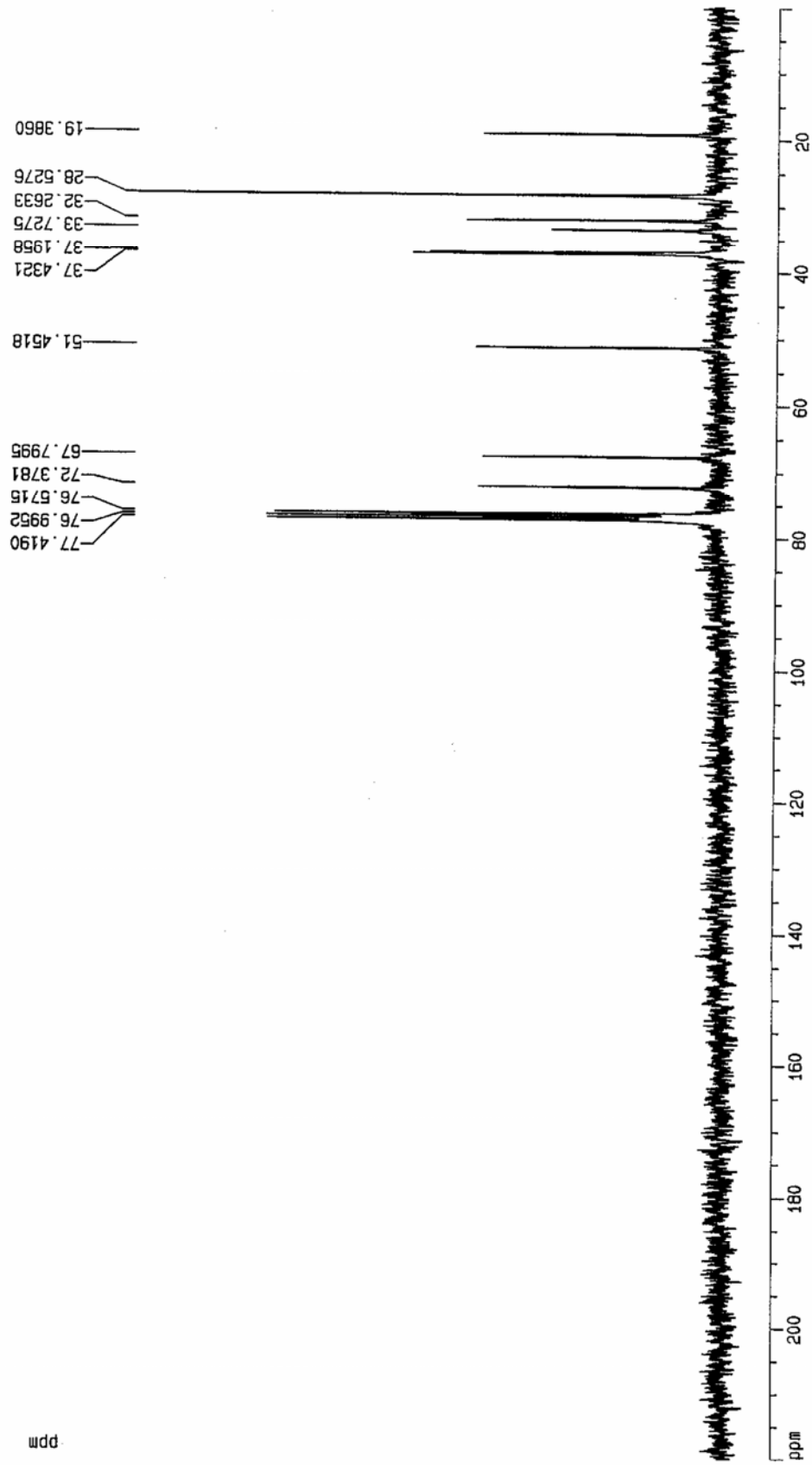








2.36

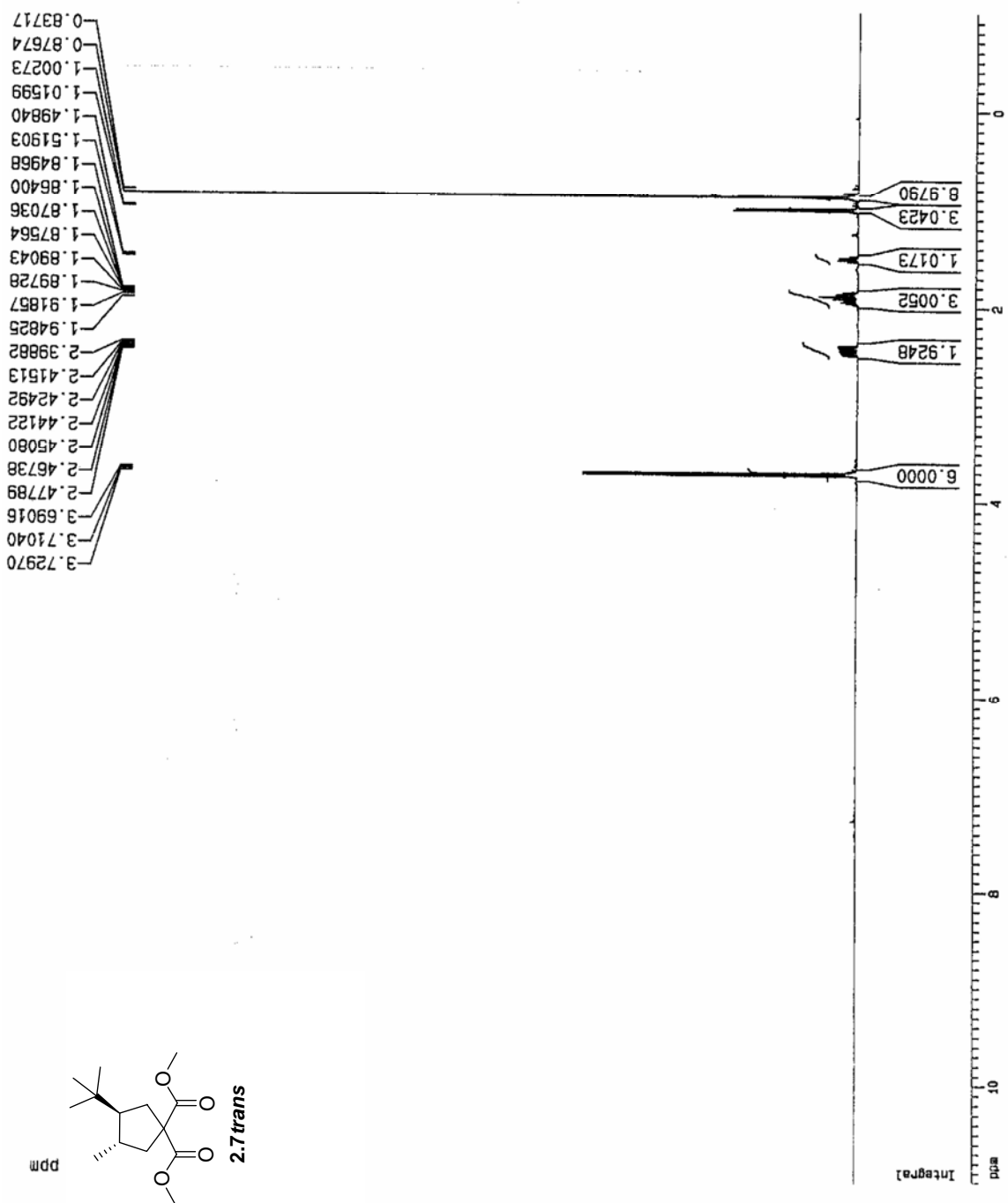


PROCNO 1

F2 - Acquisition Parameters
 Date_ 500000
 Time 11.10
 INSTRUM spect
 PROBHD 5 mm TXI 13C
 PULPROG zg
 TD 32768
 SOLVENT CDCl3
 NS 1
 DS 0
 SWH 7507.507 Hz
 FIDRES 0.229111 Hz
 AQ 2.1823988 sec
 RG 32
 DM 66.600 usec
 DE 6.00 usec
 TE 290.0 K
 D1 1.0000000 sec
 P1 16.00 usec
 DE 6.00 usec
 SF01 500.1330008 MHz
 NUC1 1H
 PL1 0.00 dB

F2 - Processing parameters
 SI 32768
 SF 500.1300238 MHz
 WDW EM
 SSB 0
 LB 0.40 Hz
 GB 0
 PC 1.00

1D NMR plot parameters
 CX 20.00 cm
 F1P 11.000 ppm
 F1 5501.43 Hz
 F2P -1.000 ppm
 F2 -500.13 Hz
 PPMCM 0.60000 ppm/cm
 HZCM 300.07803 Hz/cm



F2 - Acquisition Parameters

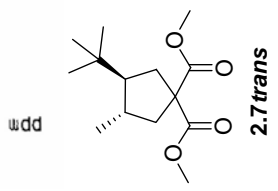
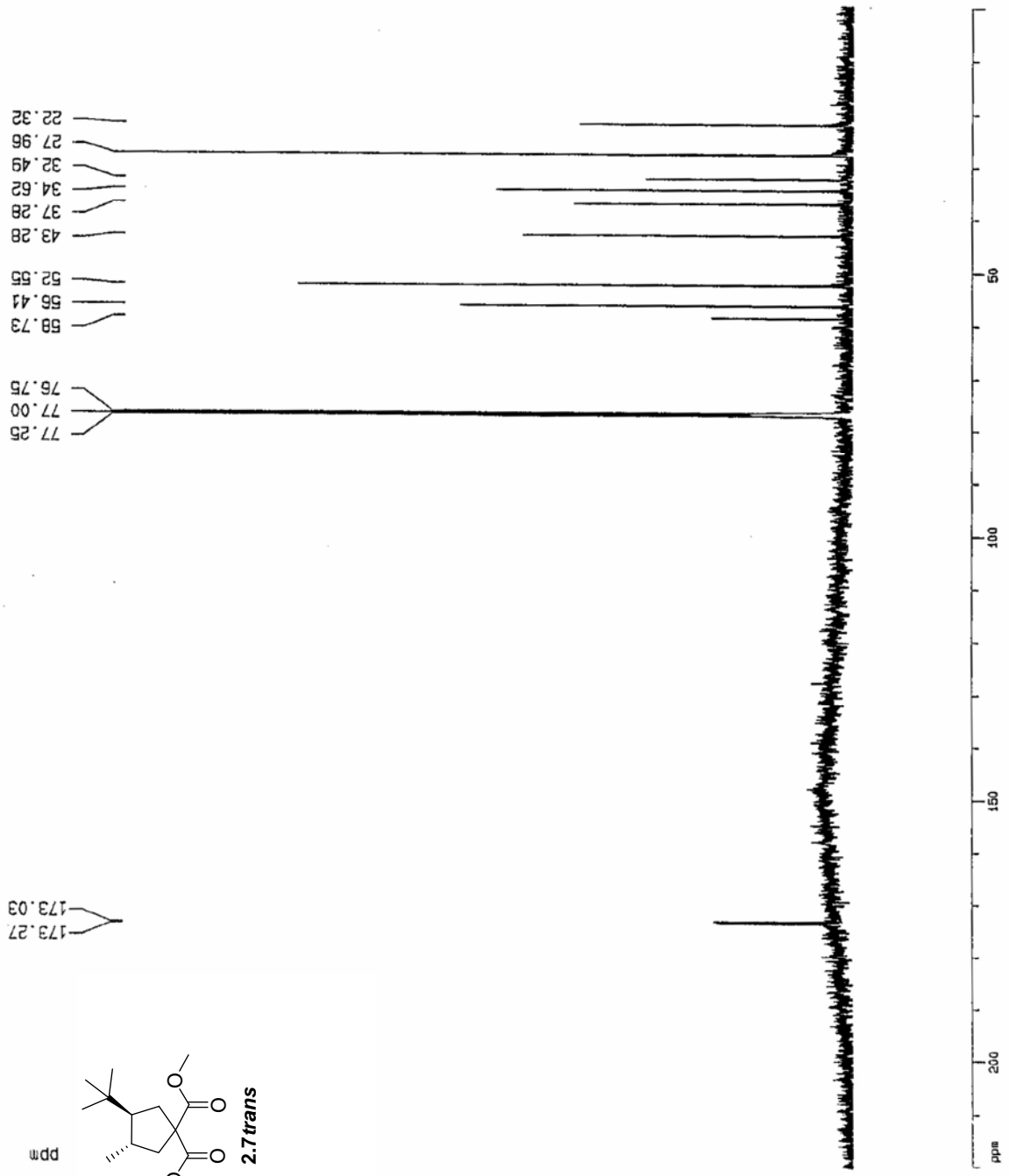
Date_ 500000
 Time 0.22
 INSTRUM spect
 PROBHD 5 mm TXI 13C
 PULPROG zgpg30
 TD 32768
 SOLVENT CDCl3
 NS 2874
 DS 0
 SWH 32679.738 Hz
 FIDRES 0.997306 Hz
 AQ 0.5014004 sec
 RG 32768
 DM 15.300 usec
 DE 6.00 usec
 TE 290.0 K
 D3 0.00100000 sec
 PL12 6.00 dB
 D1 8.00000000 sec
 CPDPRG2 waltz16
 PCPD2 100.00 usec
 SF02 500.1330008 MHz
 NU2 1H
 PL2 120.00 dB
 P1 21.60 usec
 DE 6.00 usec
 SF01 125.7715724 MHz
 NU1 13C
 PL1 0.00 dB

F2 - Processing parameters

SI 8192
 SF 125.7577961 MHz
 WDW EM
 SSB 0
 LB 4.00 Hz
 GB 0
 PC 1.00

1D NMR plot parameters

CX 20.00 cm
 F1P 220.000 ppm
 F1 27666.71 Hz
 F2P 0.000 ppm
 F2 0.00 Hz
 PPMCM 11.00000 ppm/cm
 HZCM 1383.33562 Hz/cm

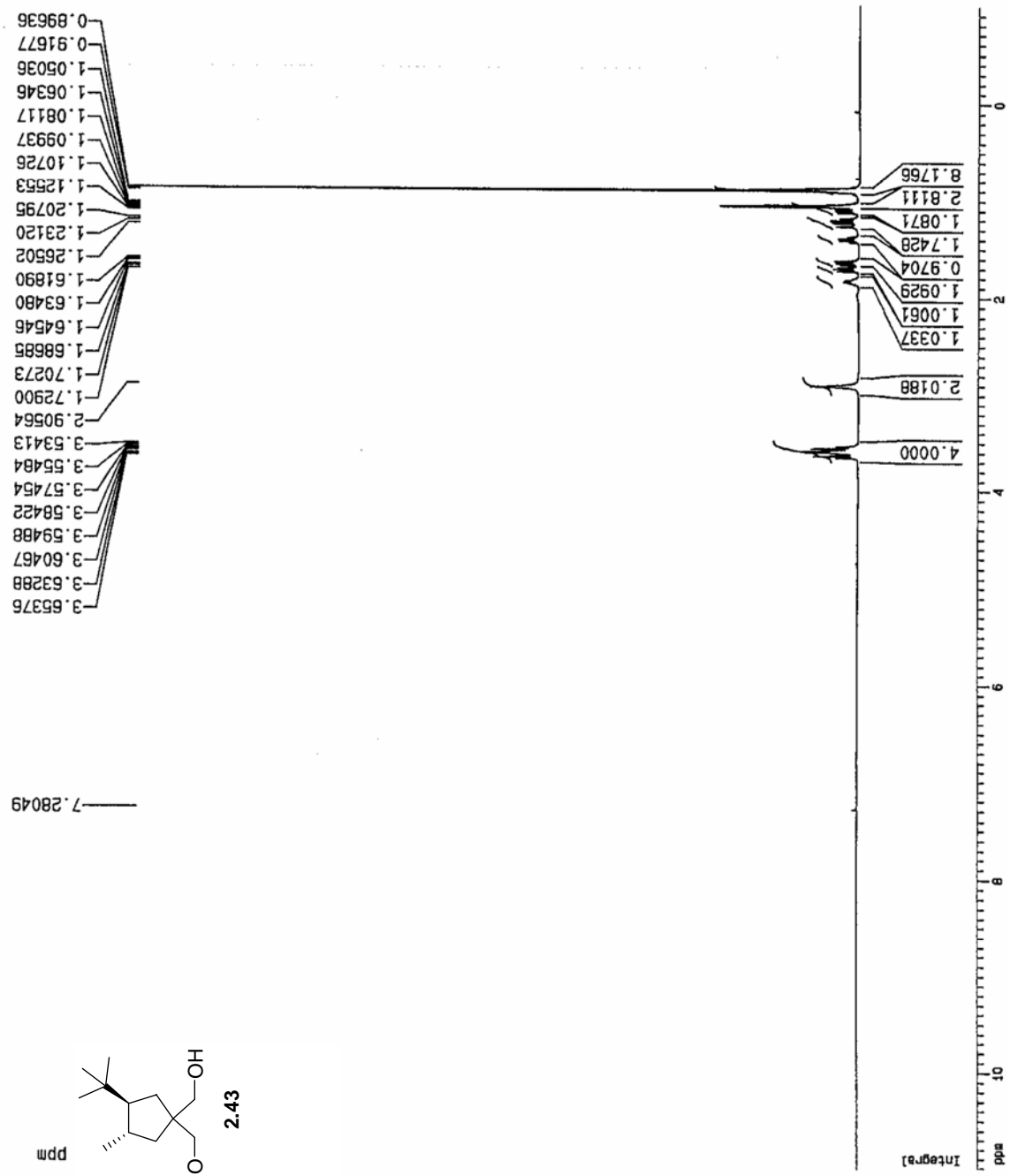


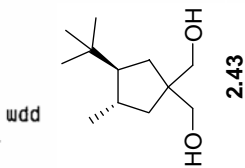
EXPNO 1
 PROCNO 1

F2 - Acquisition Parameters
 Date_ 500000
 Time 16.30
 INSTRUM spect
 PROBHD 5 mm TXI 13C
 PULPROG zg
 TD 32768
 SOLVENT CDCl3
 NS 16
 DS 0
 SMH 7507.507 Hz
 FIDRES 0.229111 Hz
 AQ 2.1823988 sec
 RG 71.8
 DM 66.600 usec
 DE 6.00 usec
 TE 290.0 K
 D1 1.0000000 sec
 P1 10.60 usec
 DE 6.00 usec
 SFO1 500.1330008 MHz
 NUCL1 1H
 PL1 0.00 dB

F2 - Processing parameters
 SI 32768
 SF 500.1300185 MHz
 MDW EM
 SSB 0
 LB 0.40 Hz
 GB 0
 PC 1.00

1D NMR plot parameters
 CX 20.00 cm
 F1P 11.000 ppm
 F1 5501.43 Hz
 F2P -1.000 ppm
 F2 -500.13 Hz
 PPMCH 0.60000 ppm/cm
 HZCM 300.07800 Hz/cm





F2 - Acquisition Parameters

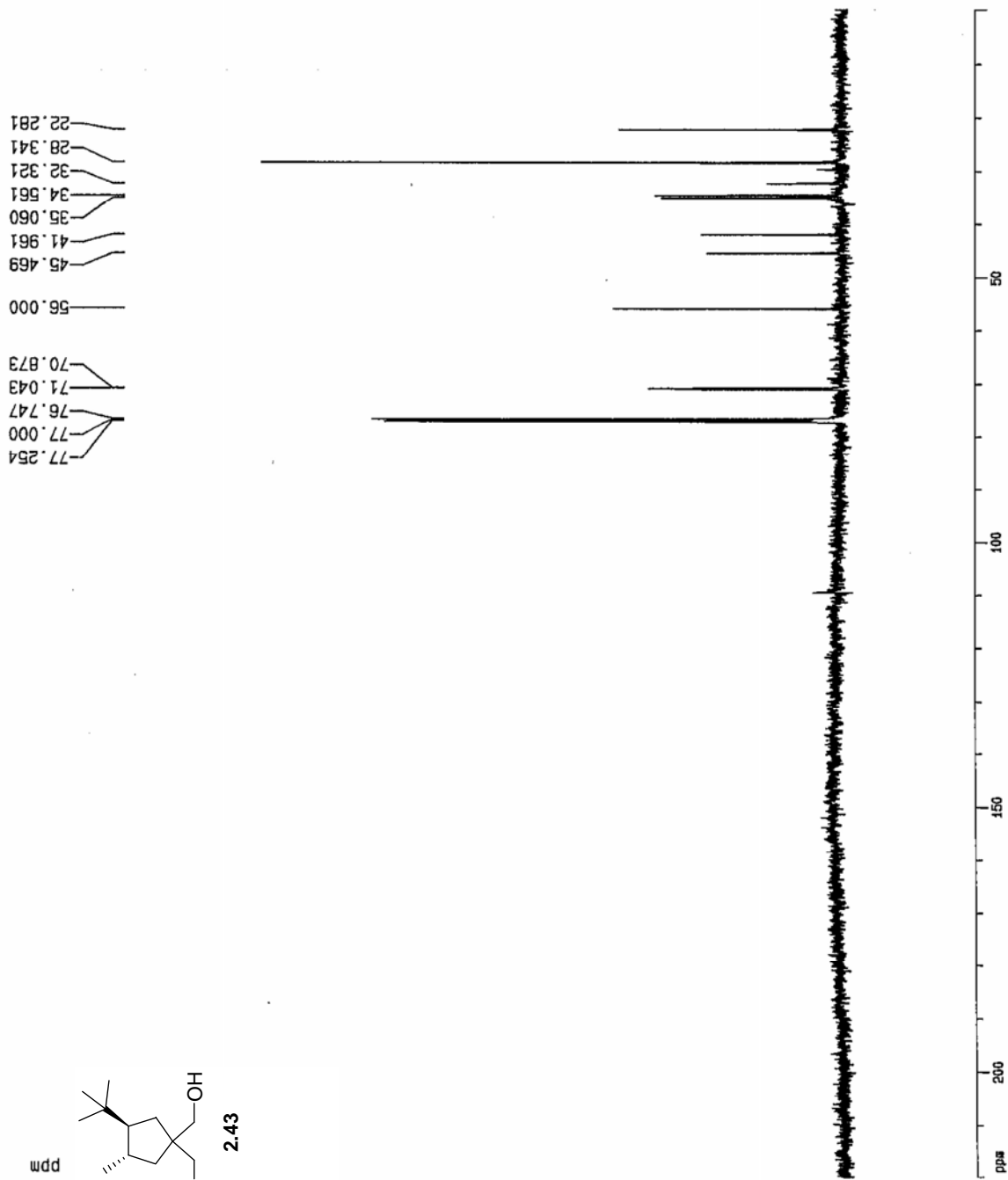
Date_ 500000
 Time_ 16.36
 INSTRUM spect
 PROBHD 5 mm TXI 13C
 PULPROG c13wznoe
 TD 32768
 SOLVENT COCL3
 NS 551
 DS 0
 SMH 32679.738 Hz
 FIDRES 0.997306 Hz
 AQ 0.5014004 sec
 RG 32768
 CW 15.300 usec
 DE 6.00 usec
 TE 290.0 K
 D3 0.00100000 sec
 PL12 6.00 dB
 D1 8.00000000 sec
 CPDPRG2 waltz16
 PCPD2 100.00 usec
 SF02 500.1330008 MHz
 NUC2 1H
 PL2 120.00 dB
 P1 21.60 usec
 DE 6.00 usec
 SF01 125.7715724 MHz
 NUC1 13C
 PL1 0.00 dB

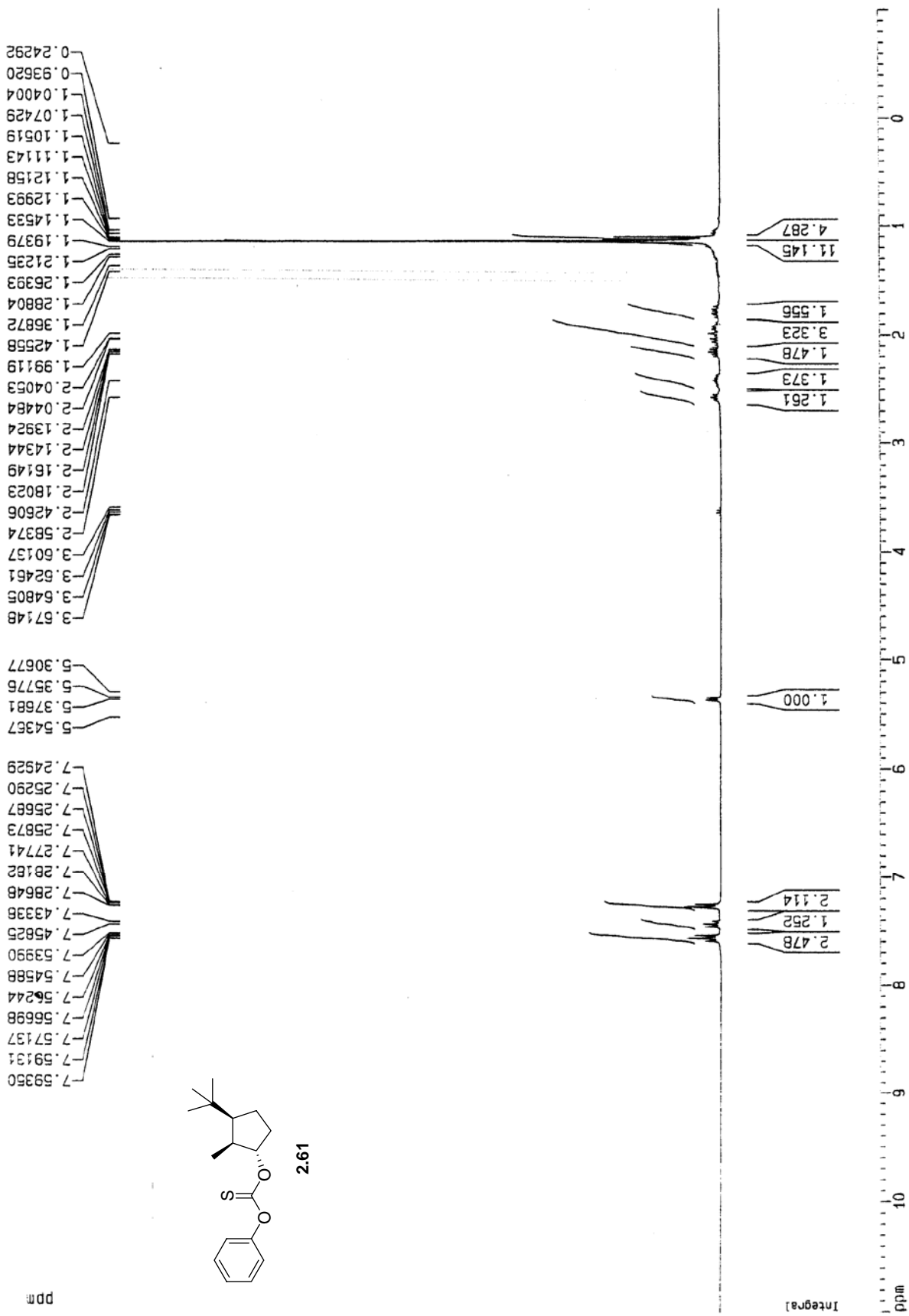
F2 - Processing parameters

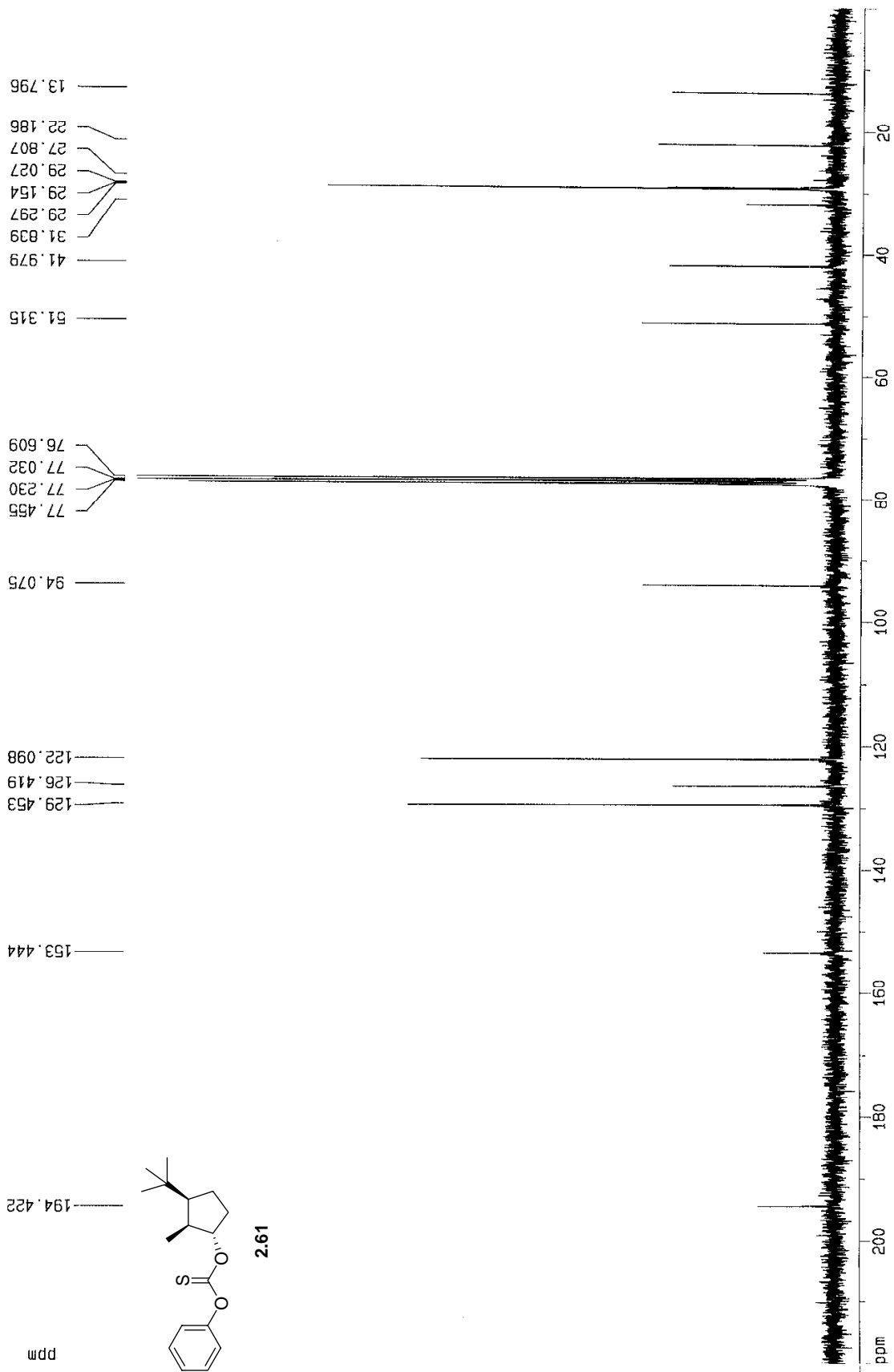
SI 8192
 SF 125.7577951 MHz
 WDW EM
 SSB 0
 LB 4.00 Hz
 GB 0
 PC 1.00

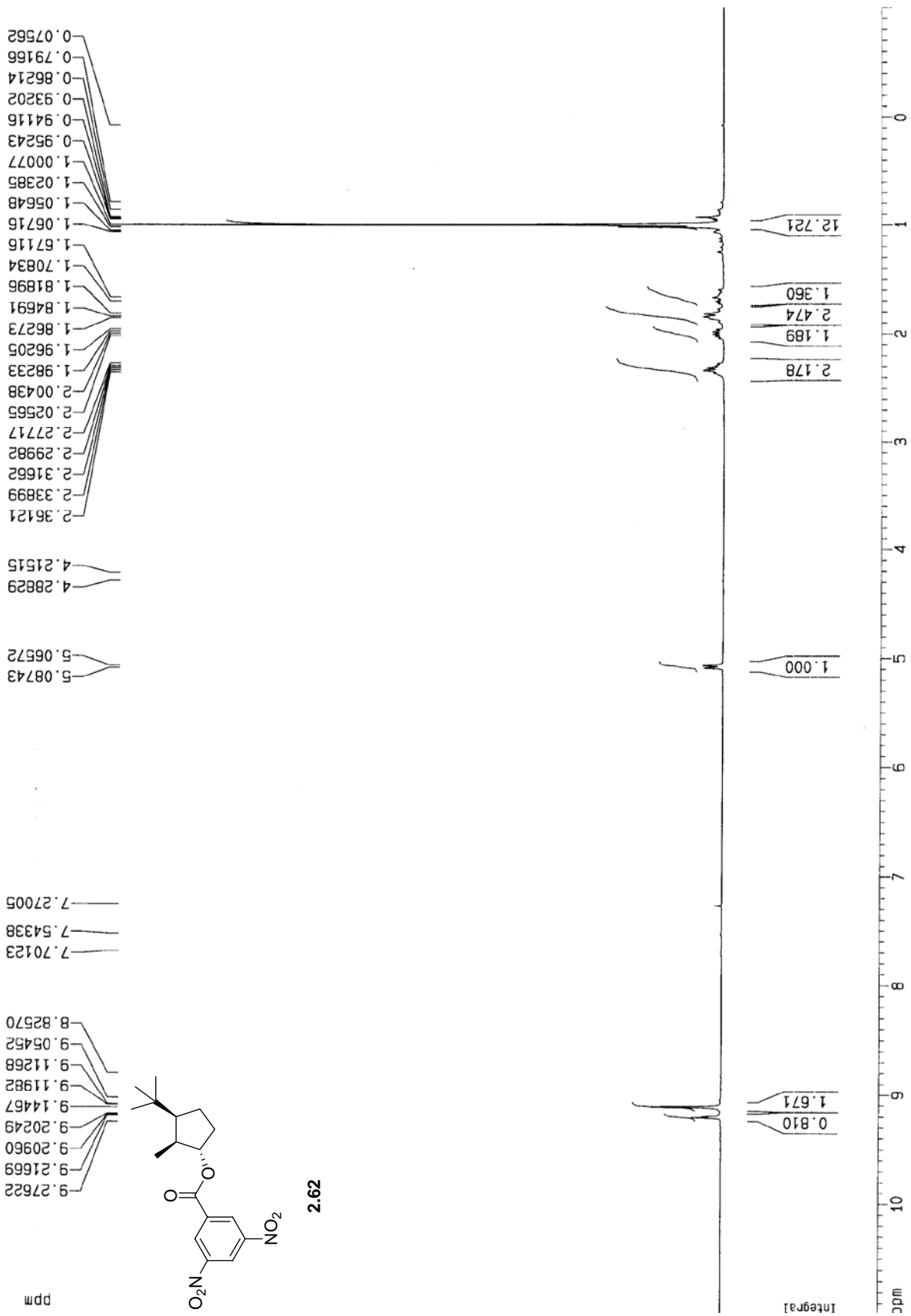
1D NMR plot parameters

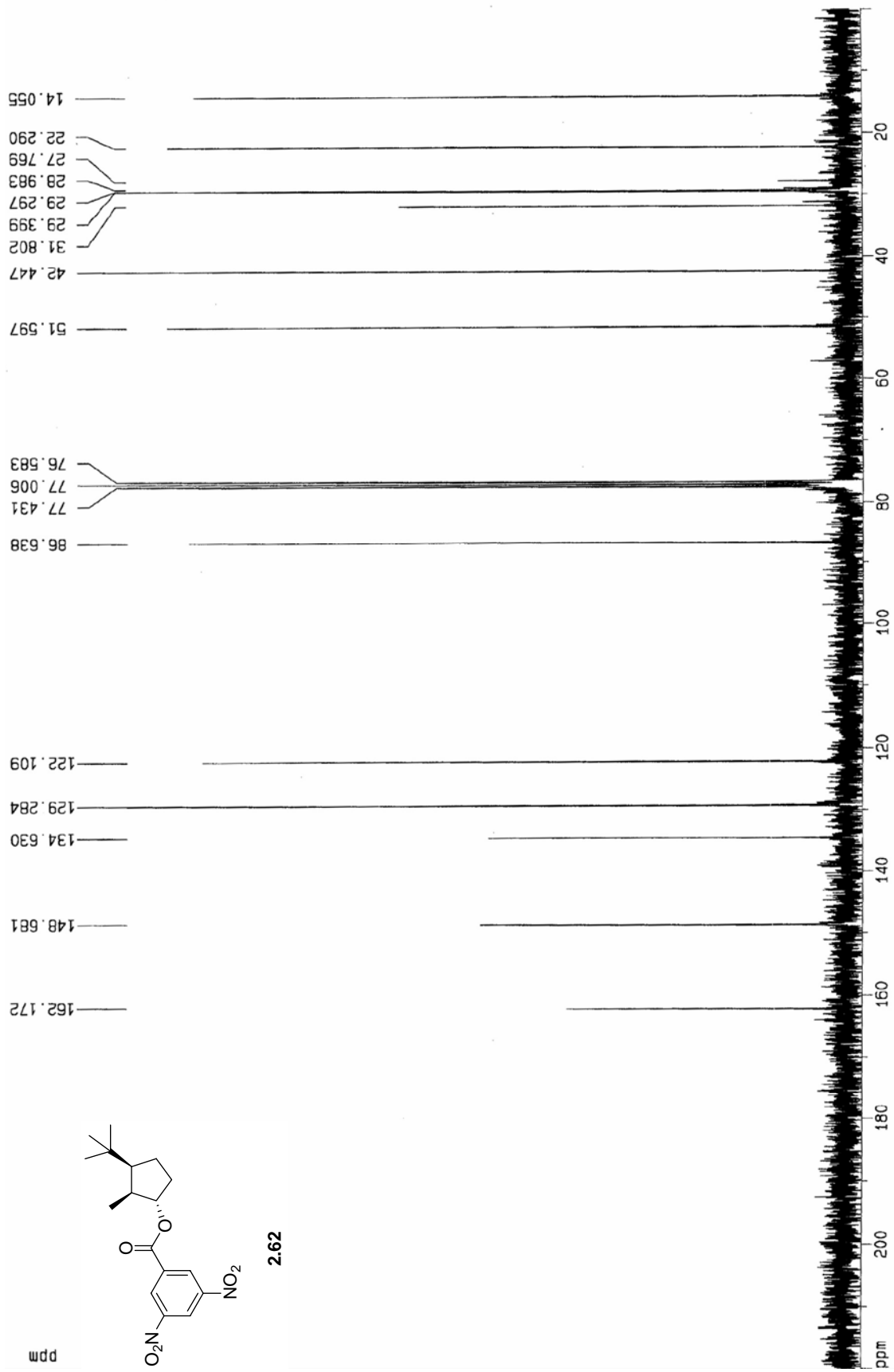
CX 20.00 cm
 F1P 220.000 ppm
 F1 27666.71 Hz
 F2P 0.000 ppm
 F2 0.00 Hz
 PPMCM 11.00000 ppm/cm
 HZCM 1363.33582 Hz/cm

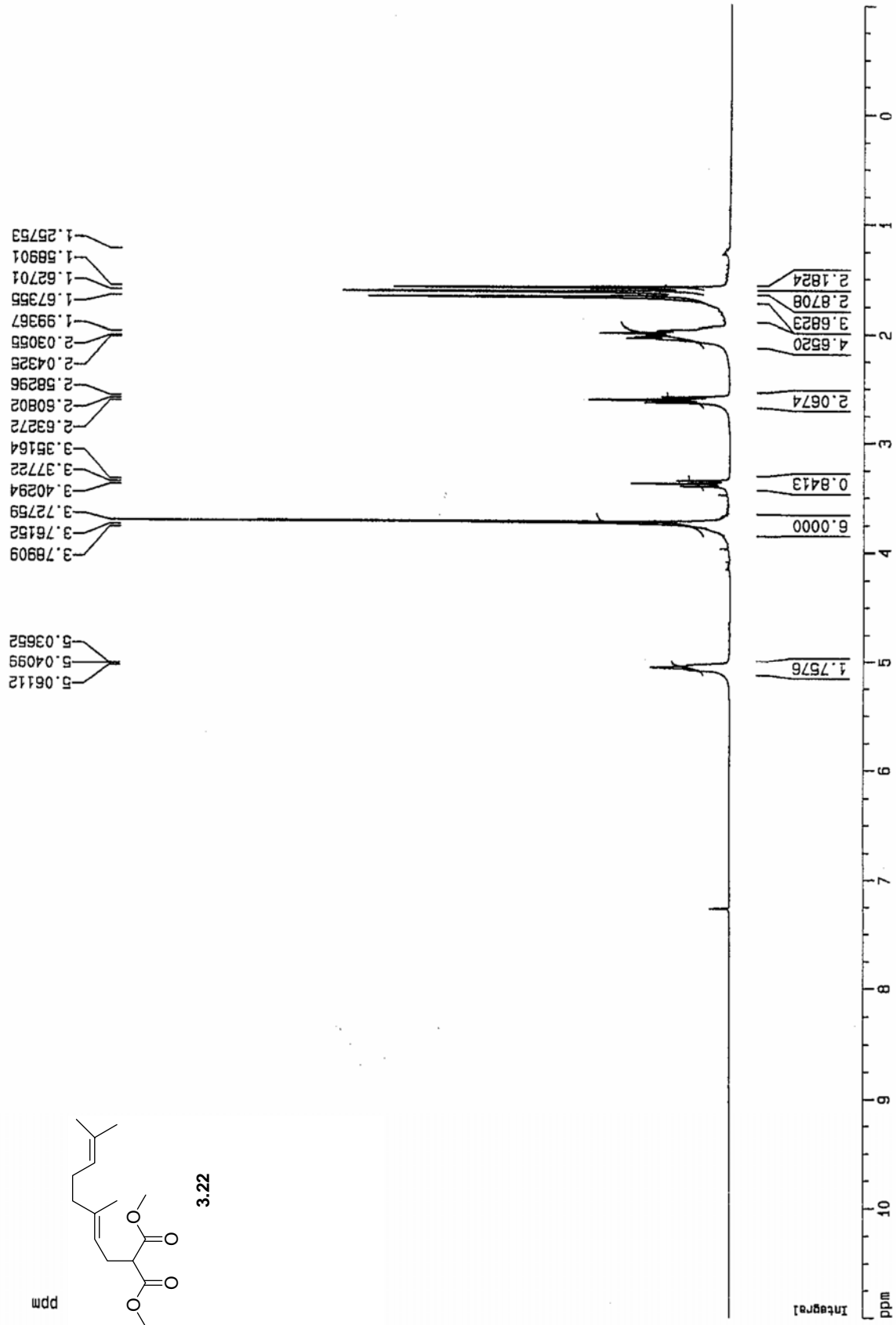


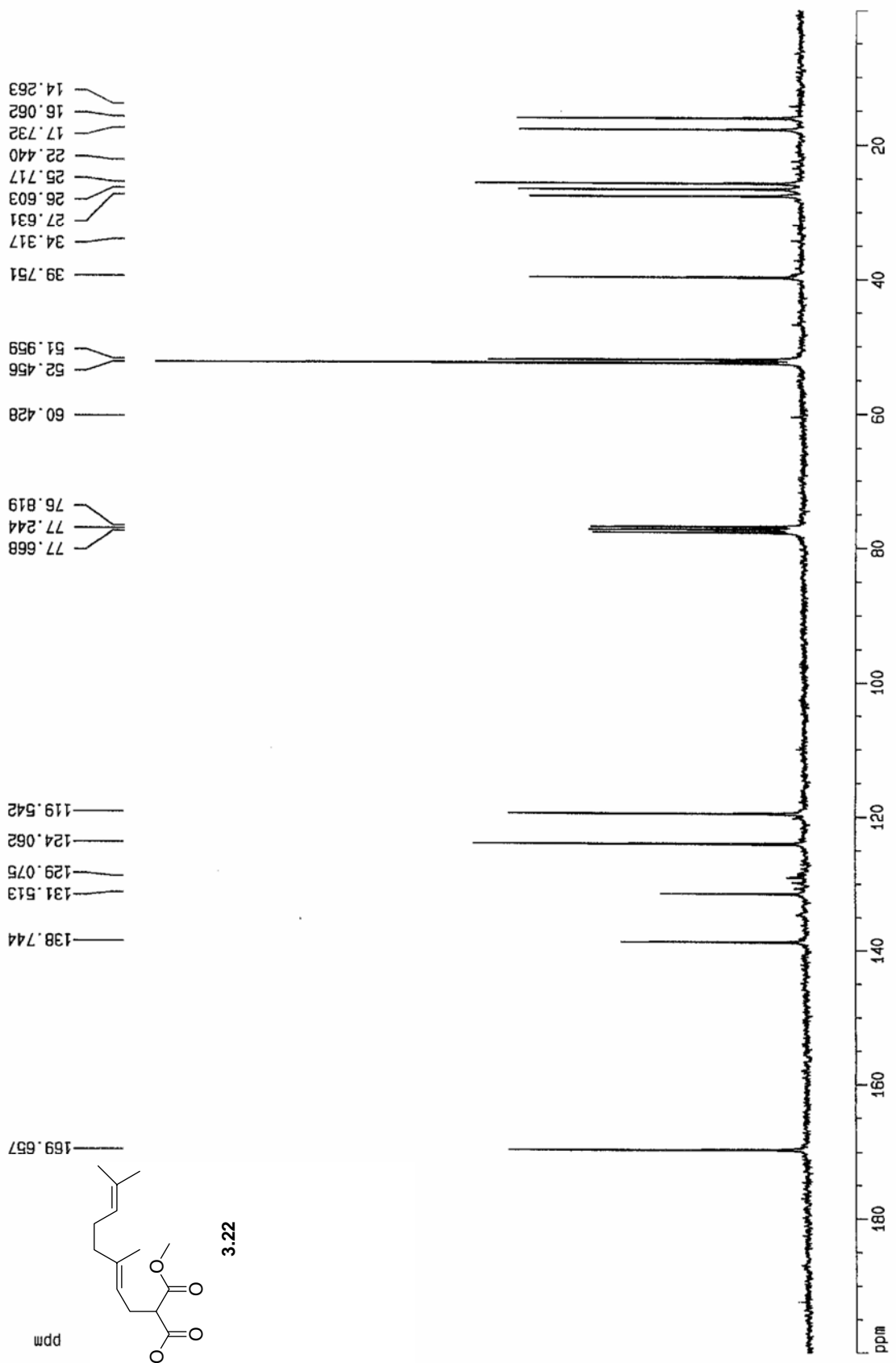


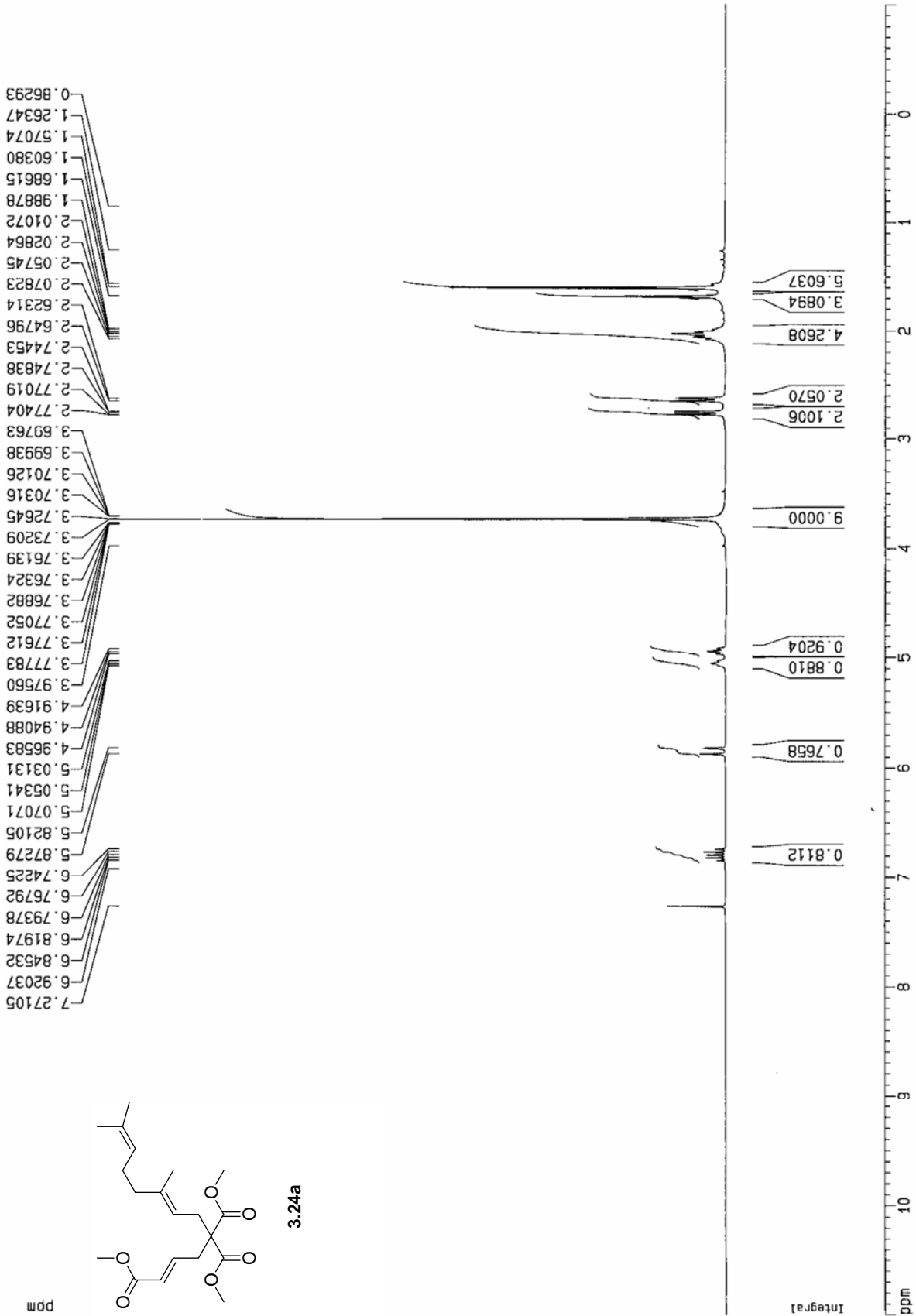


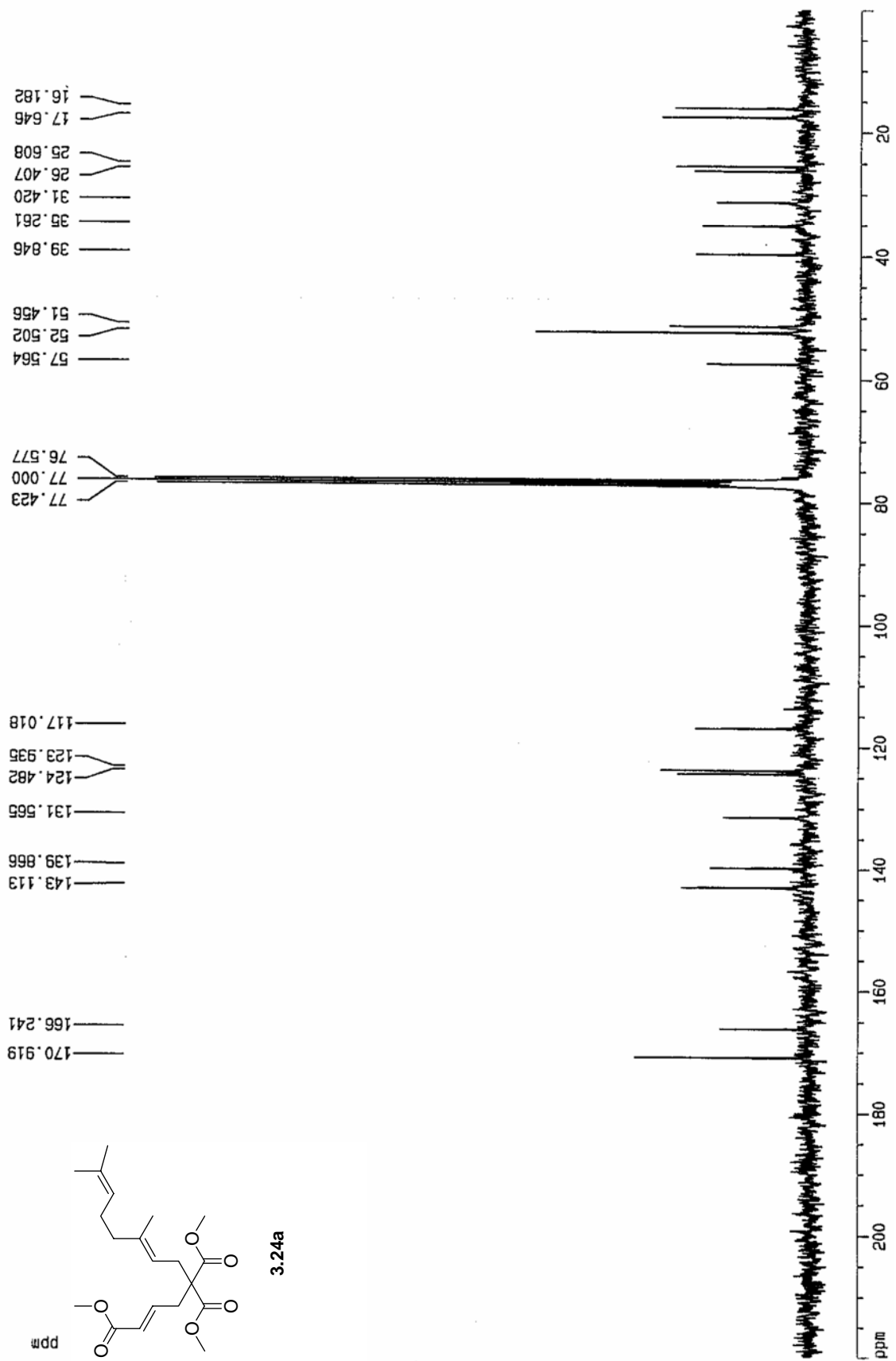


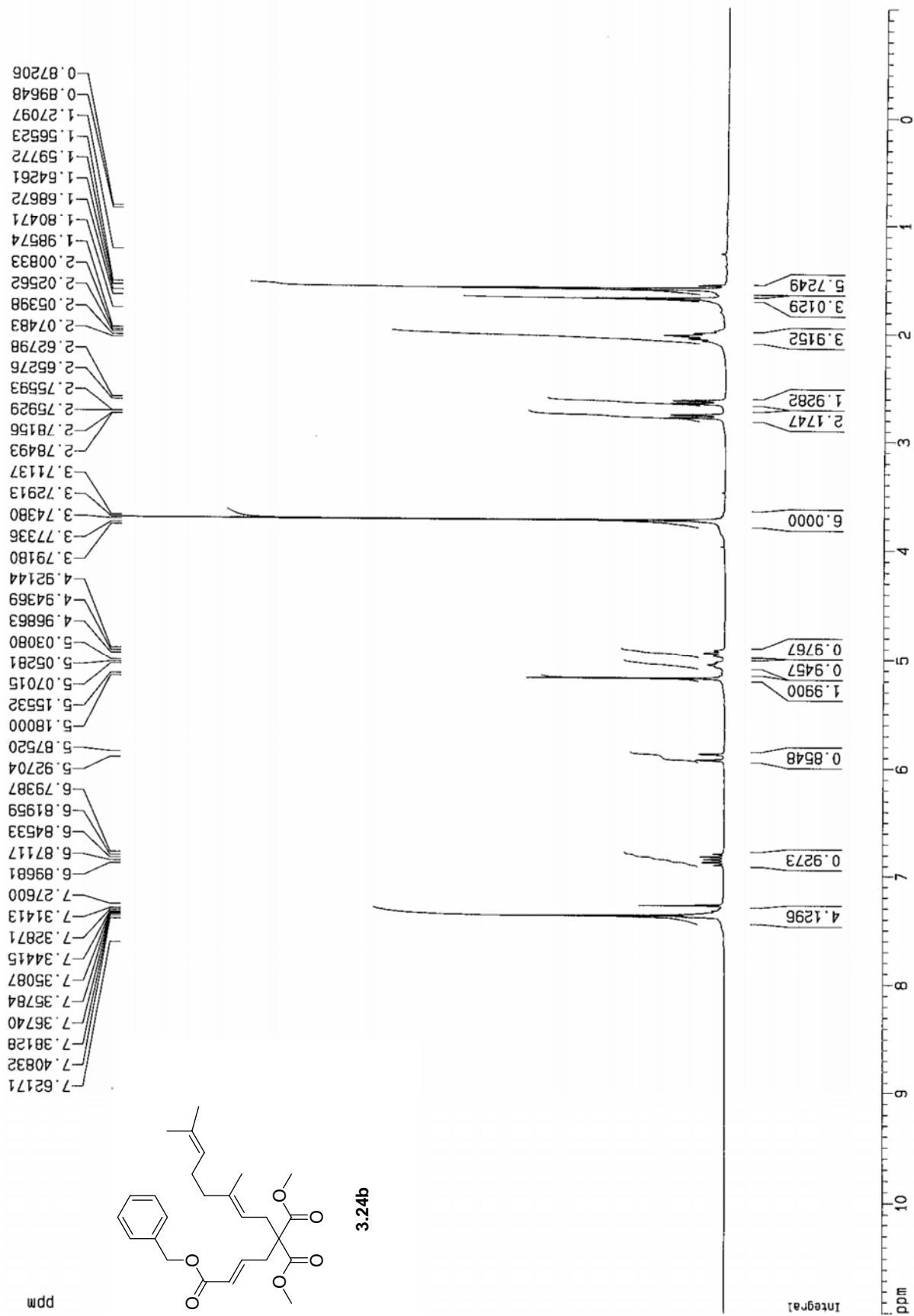


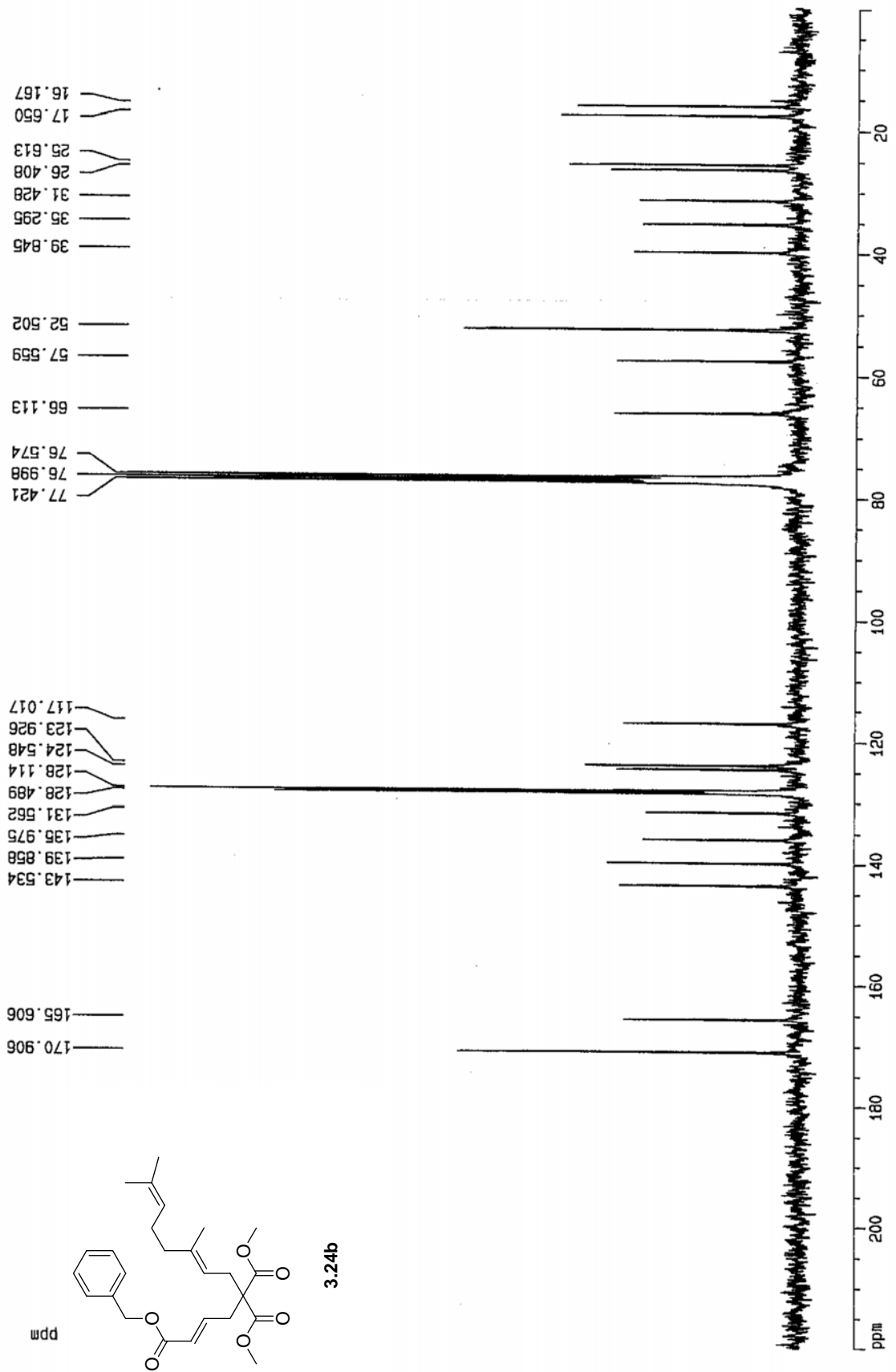


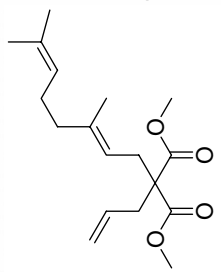
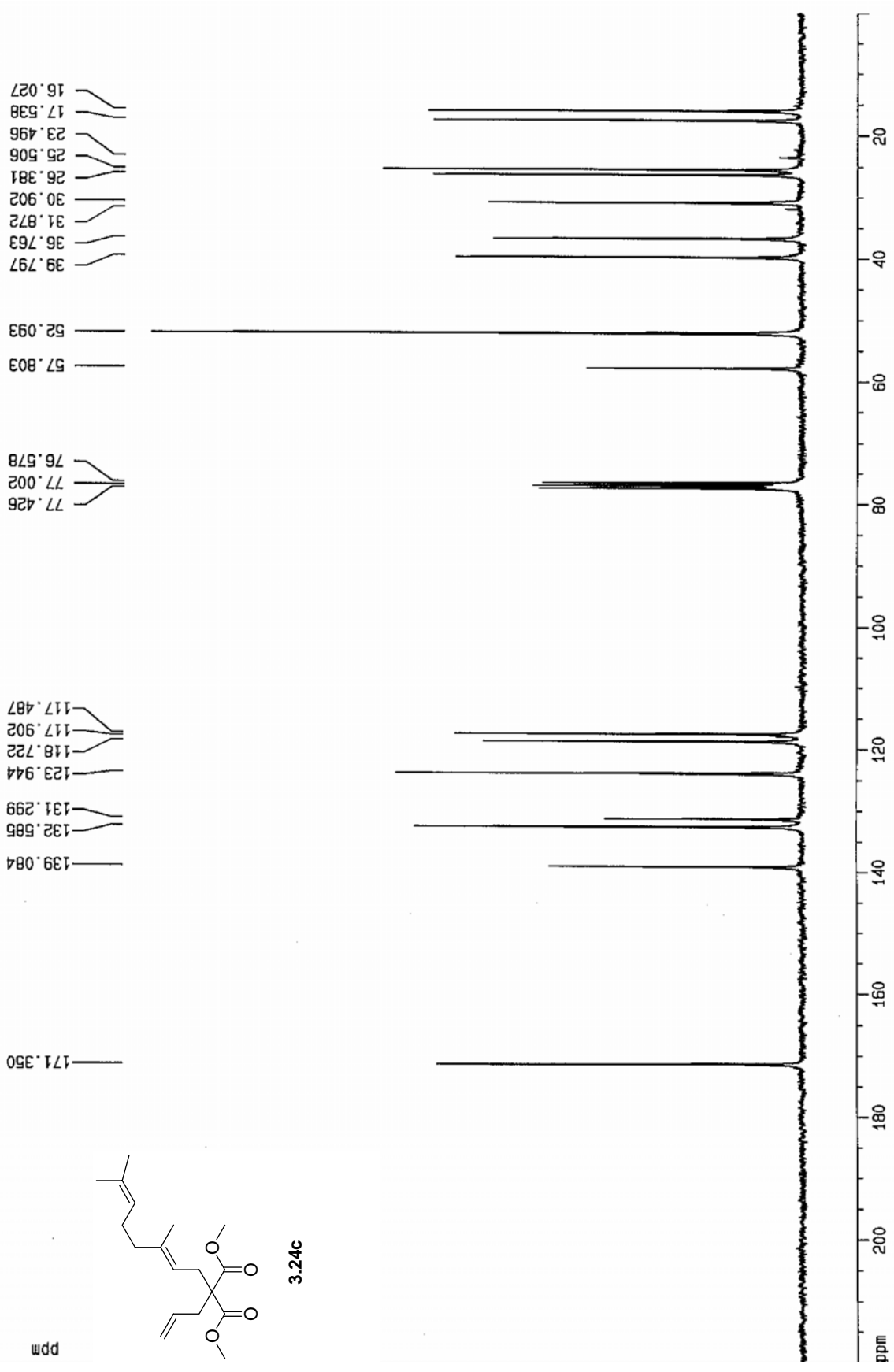






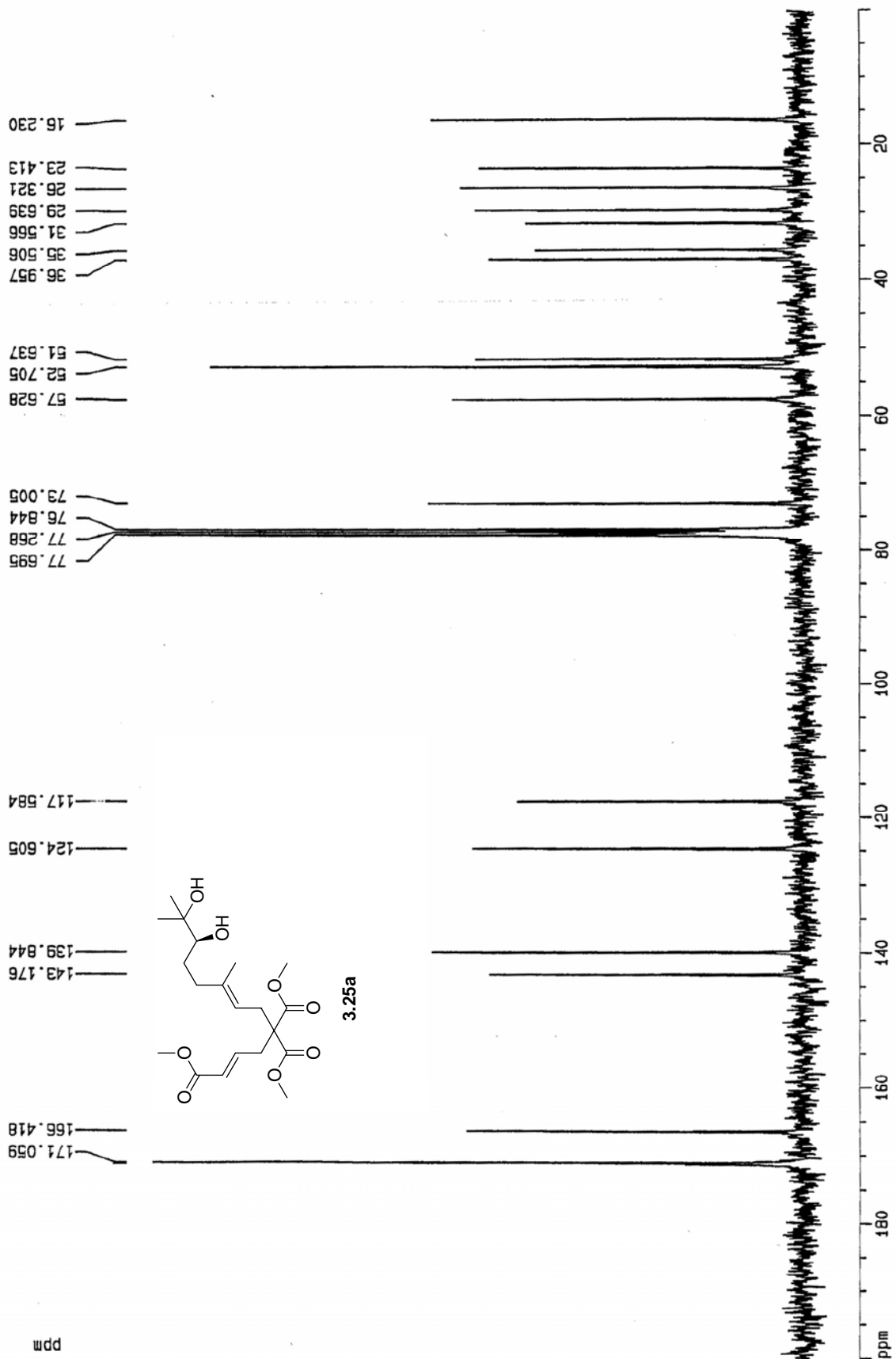


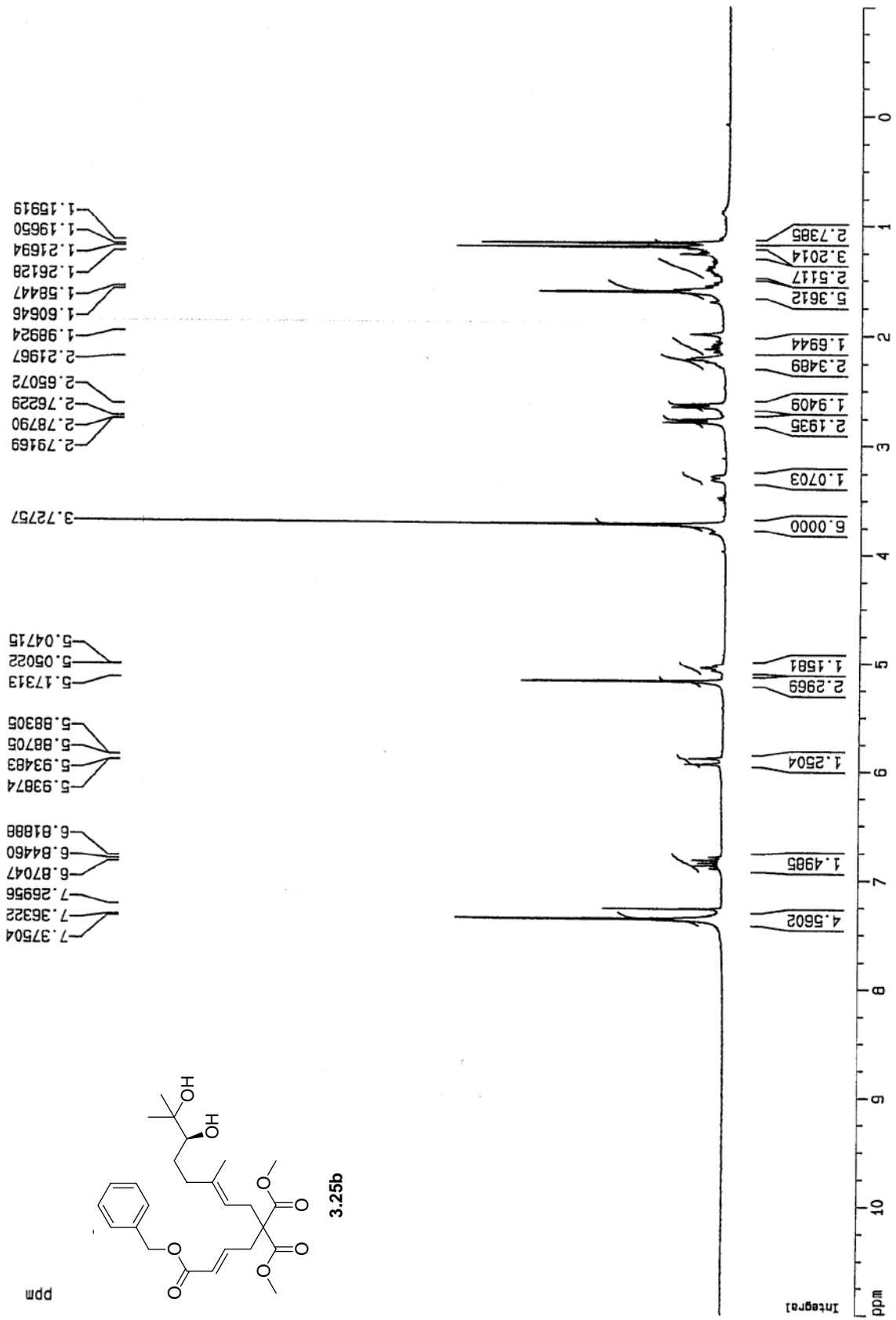


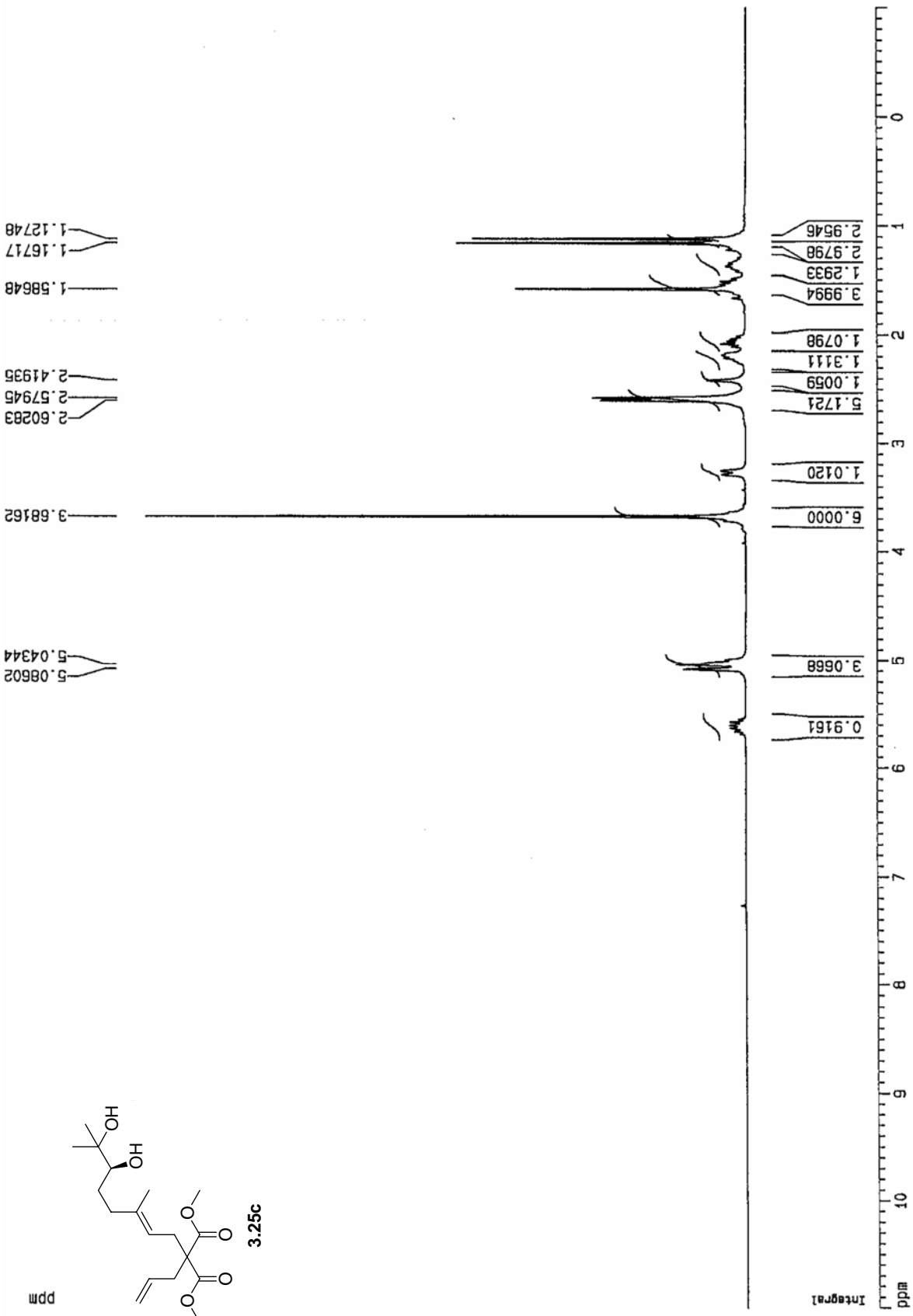


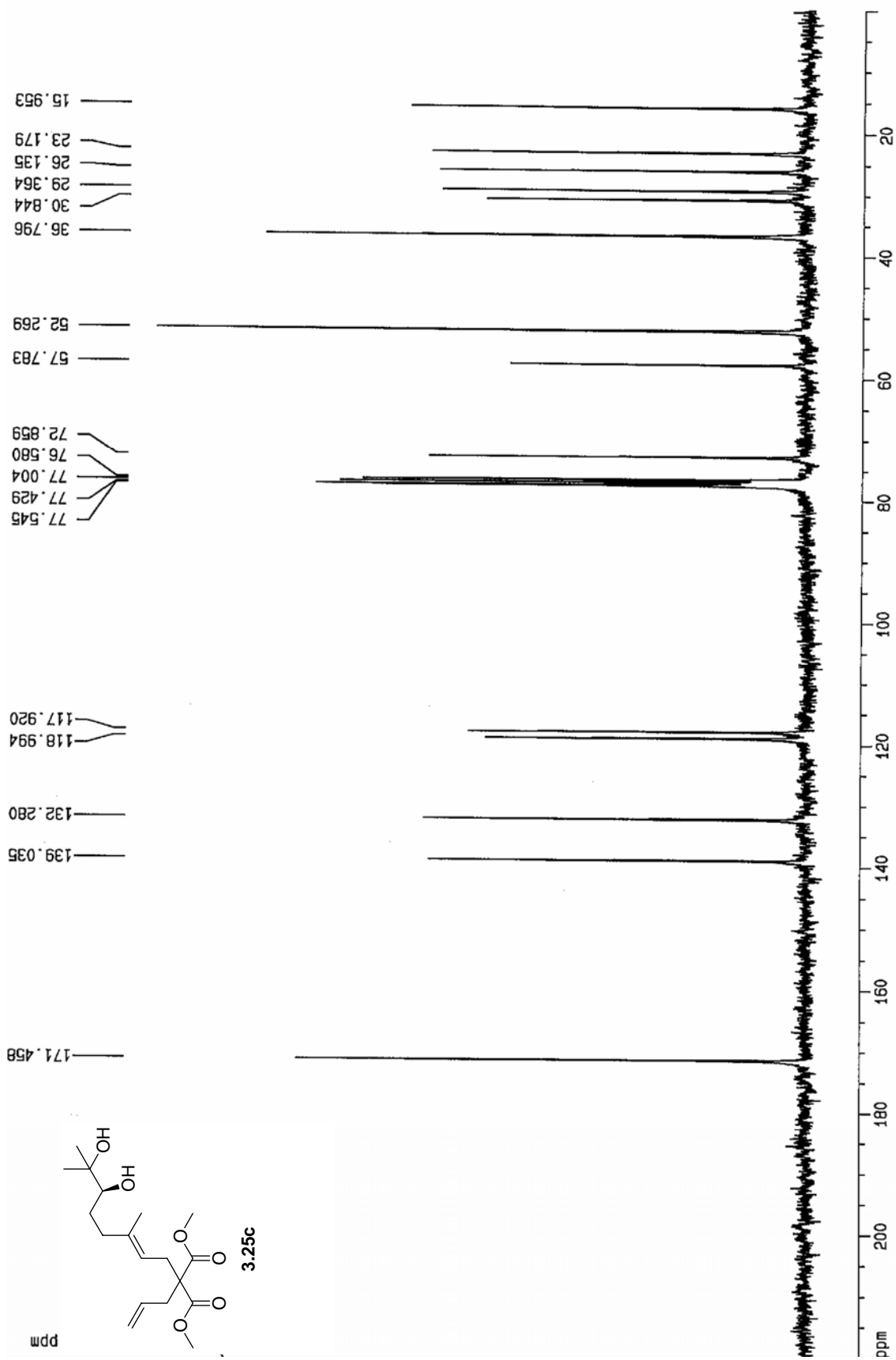
3.24c

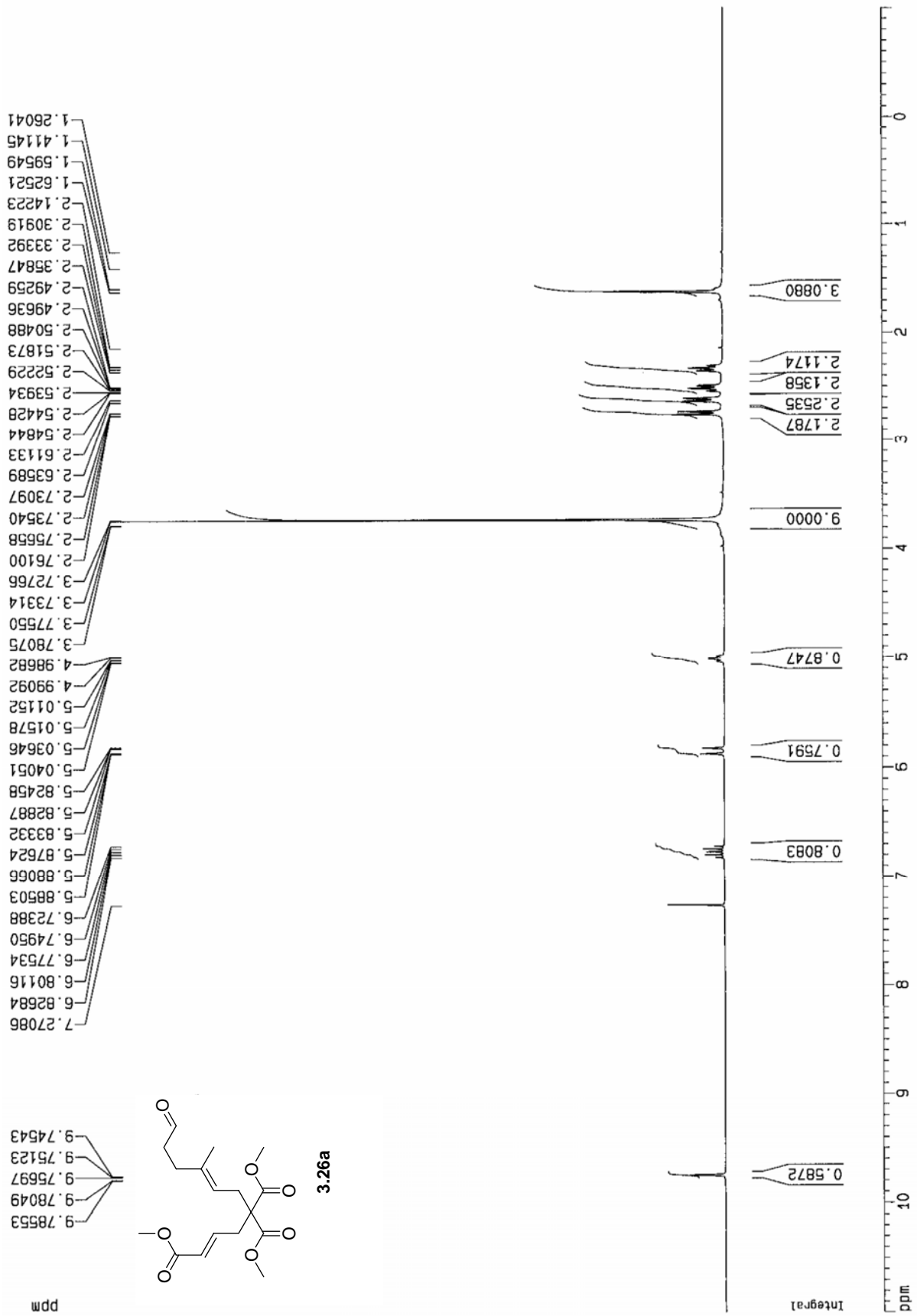
ppm

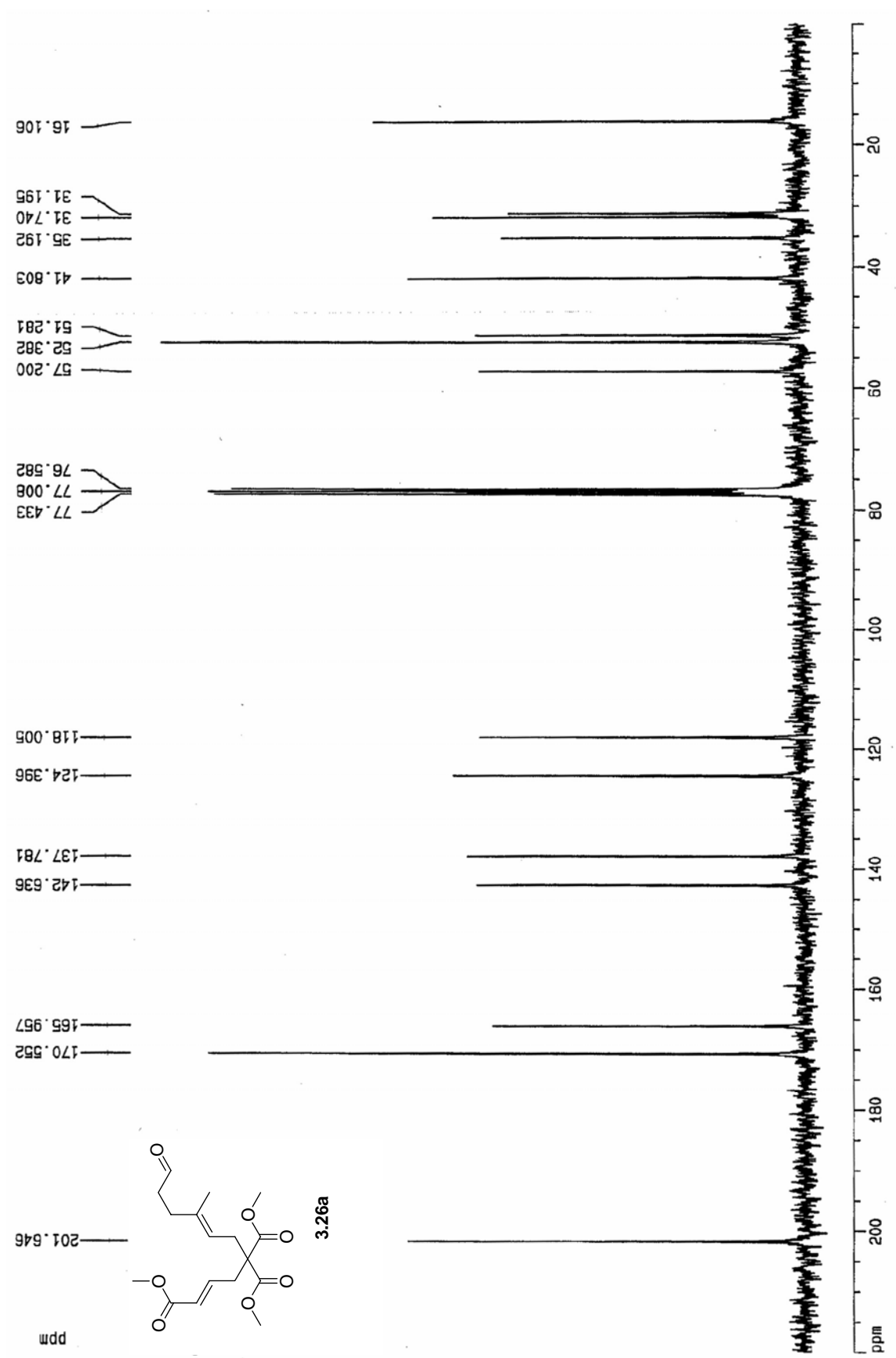


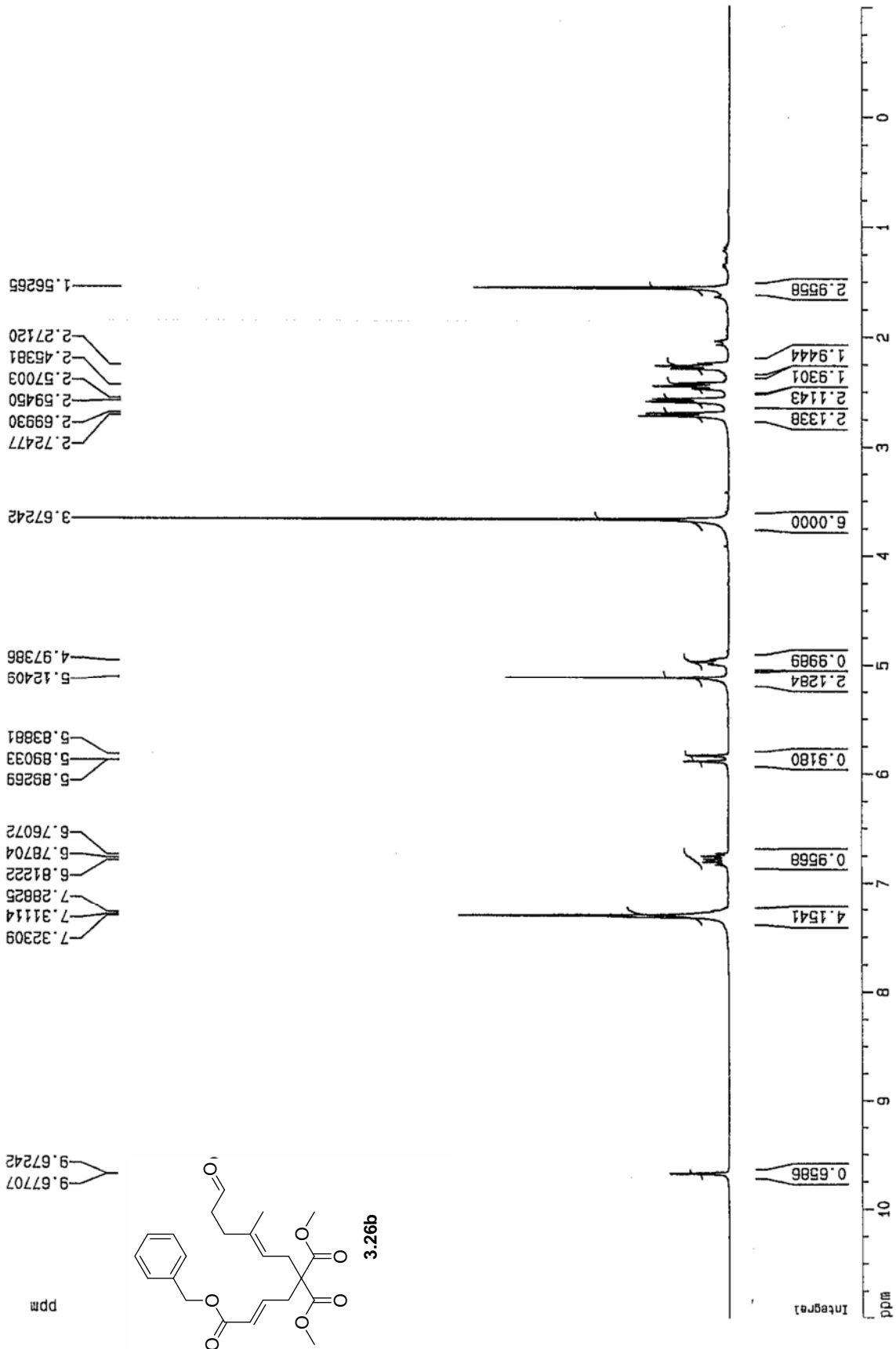


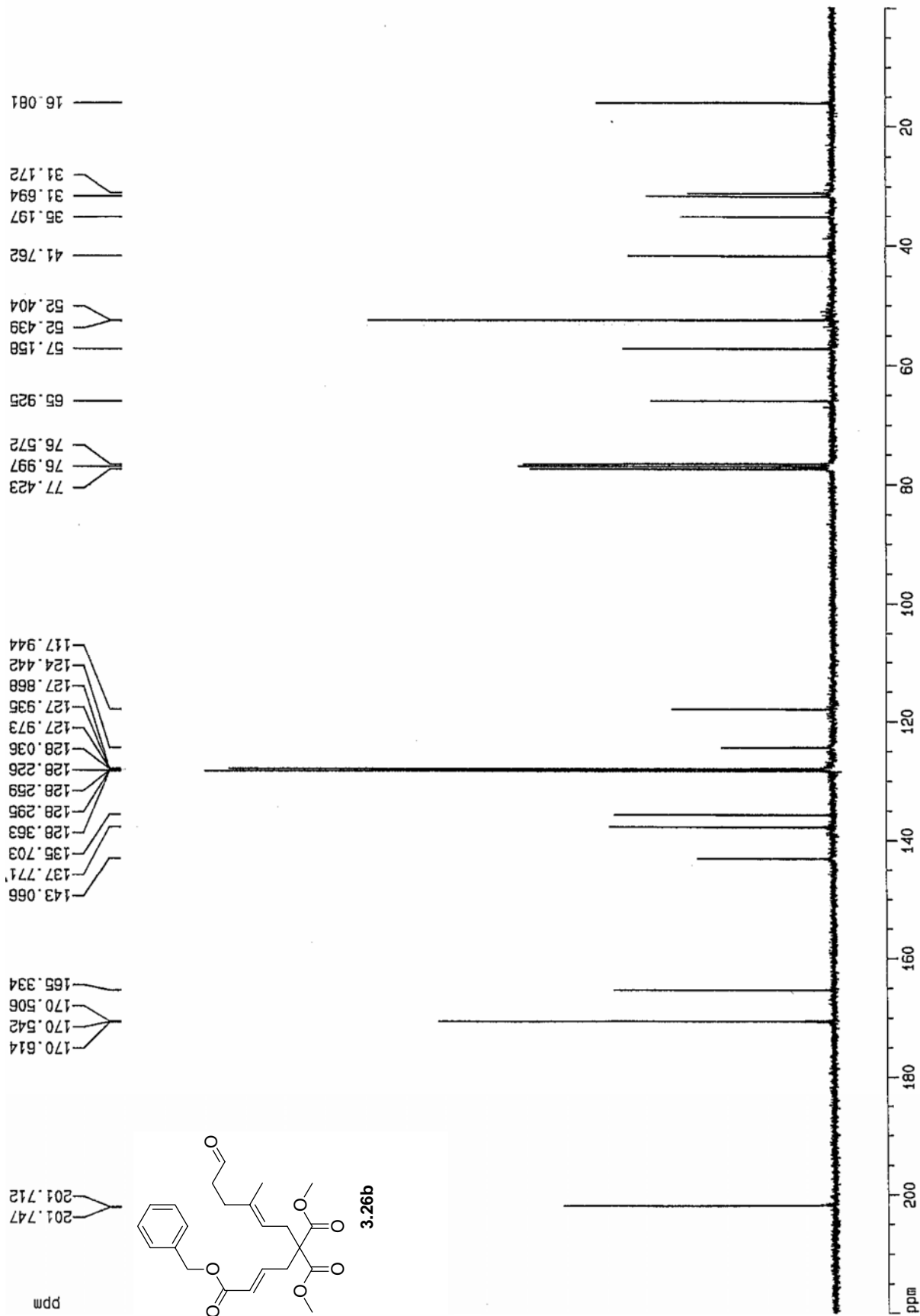


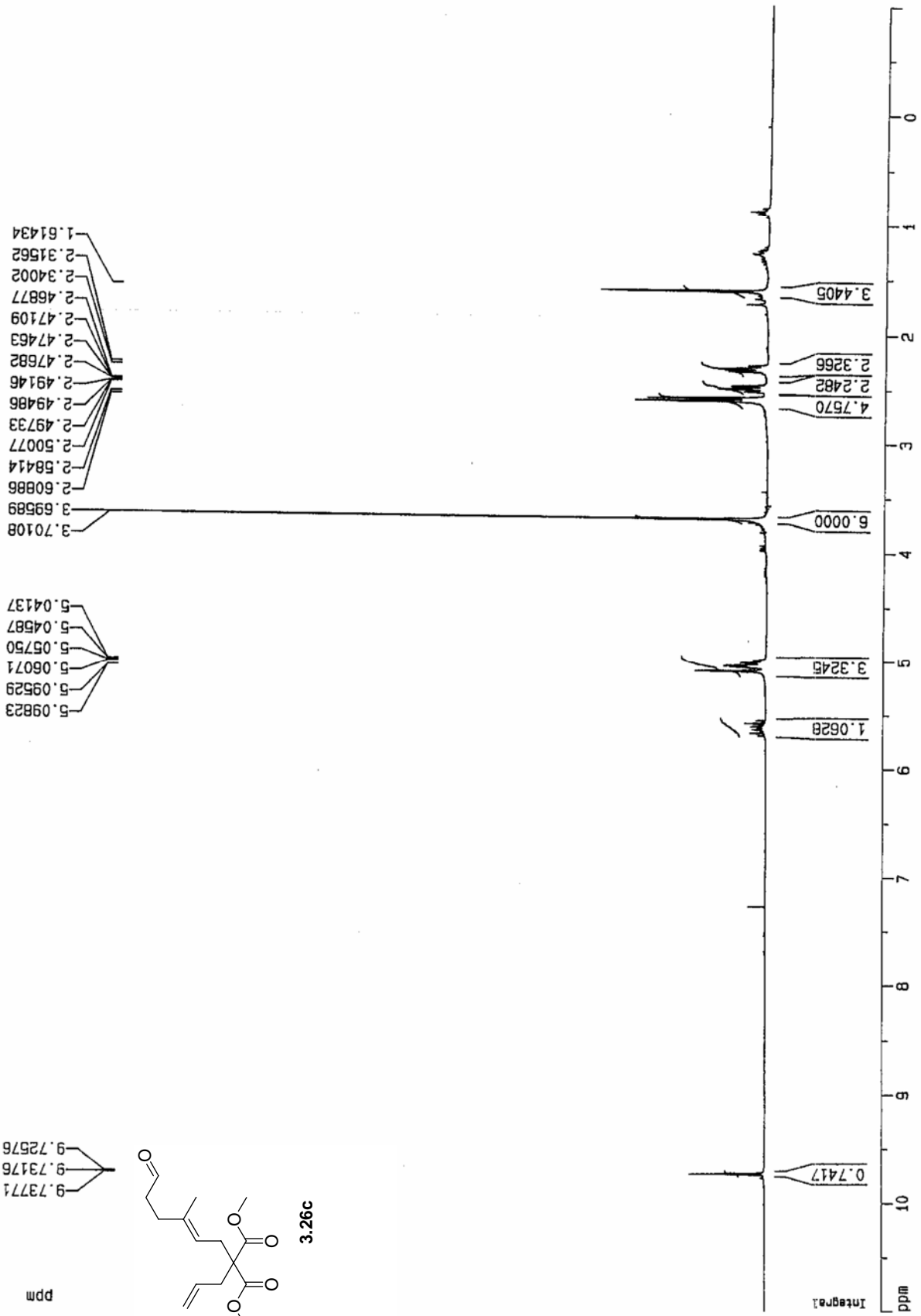


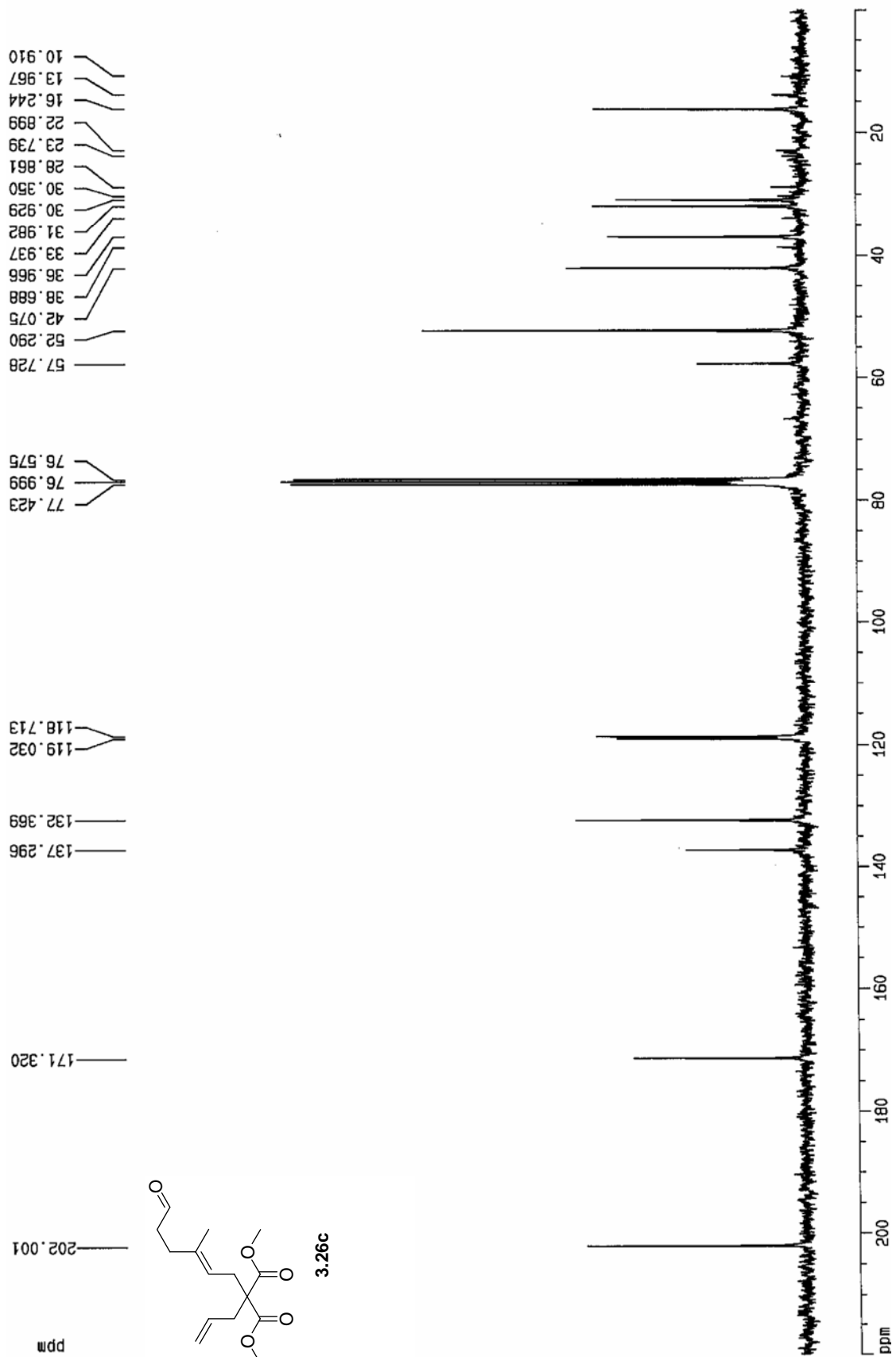


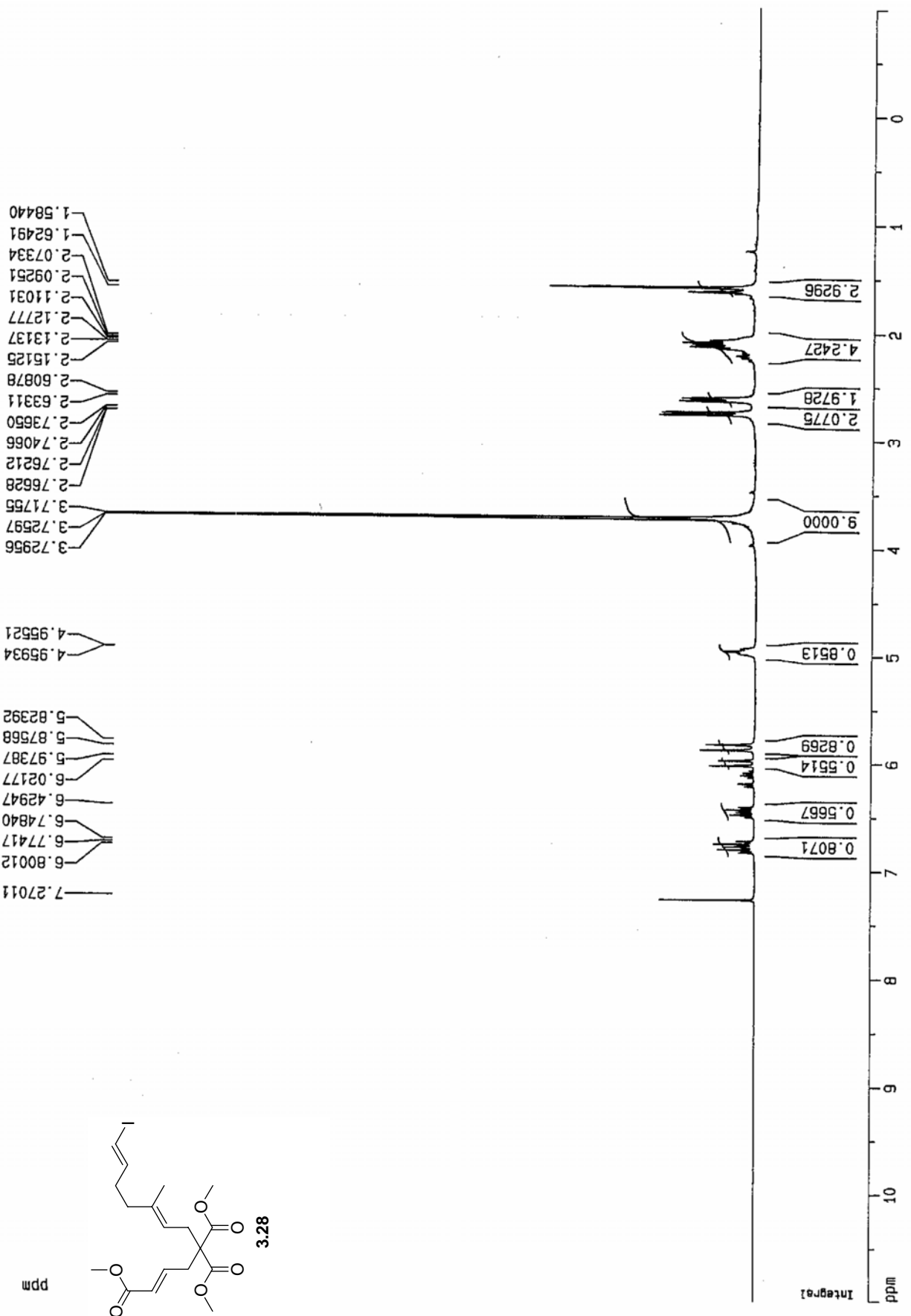


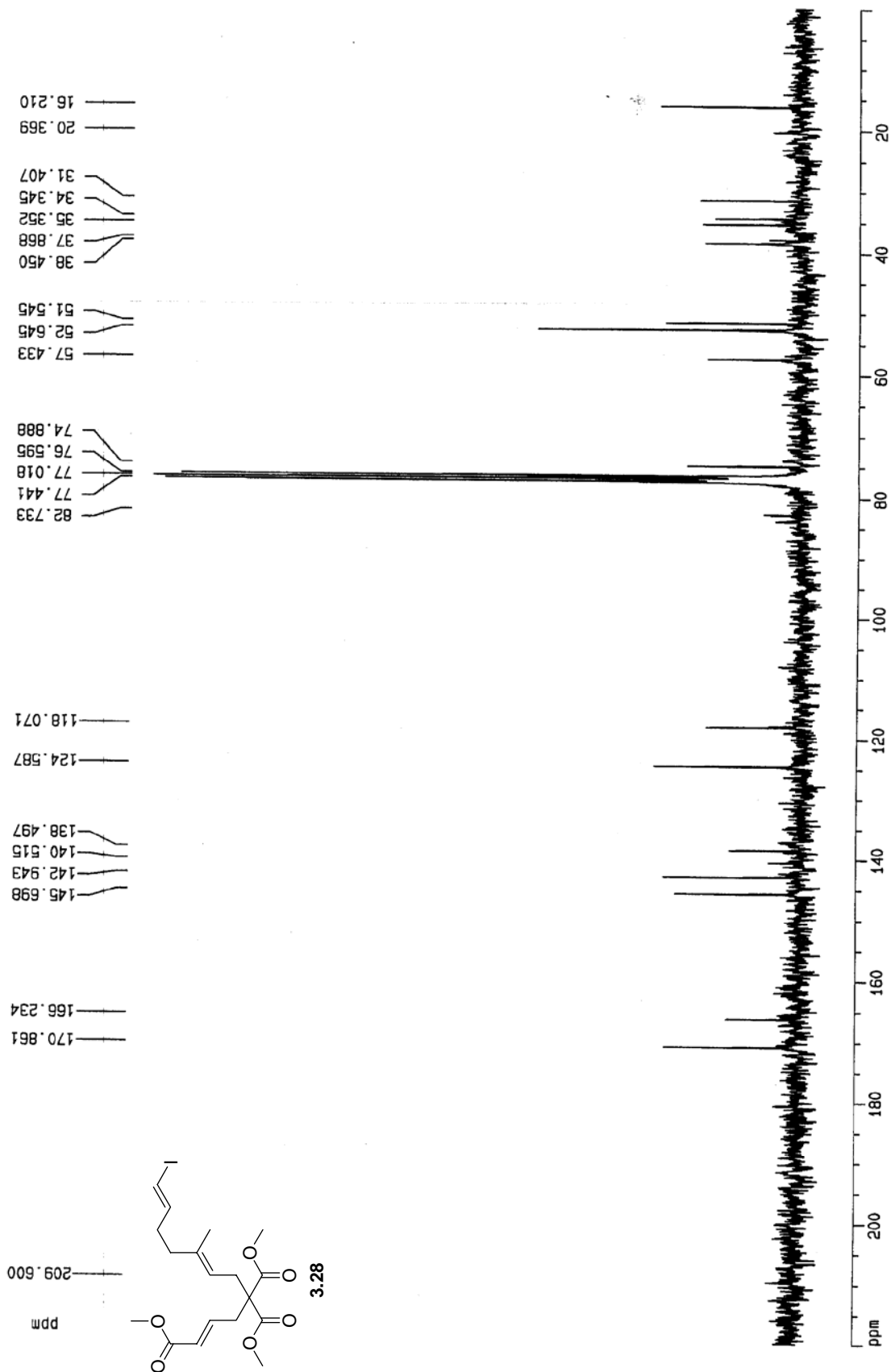


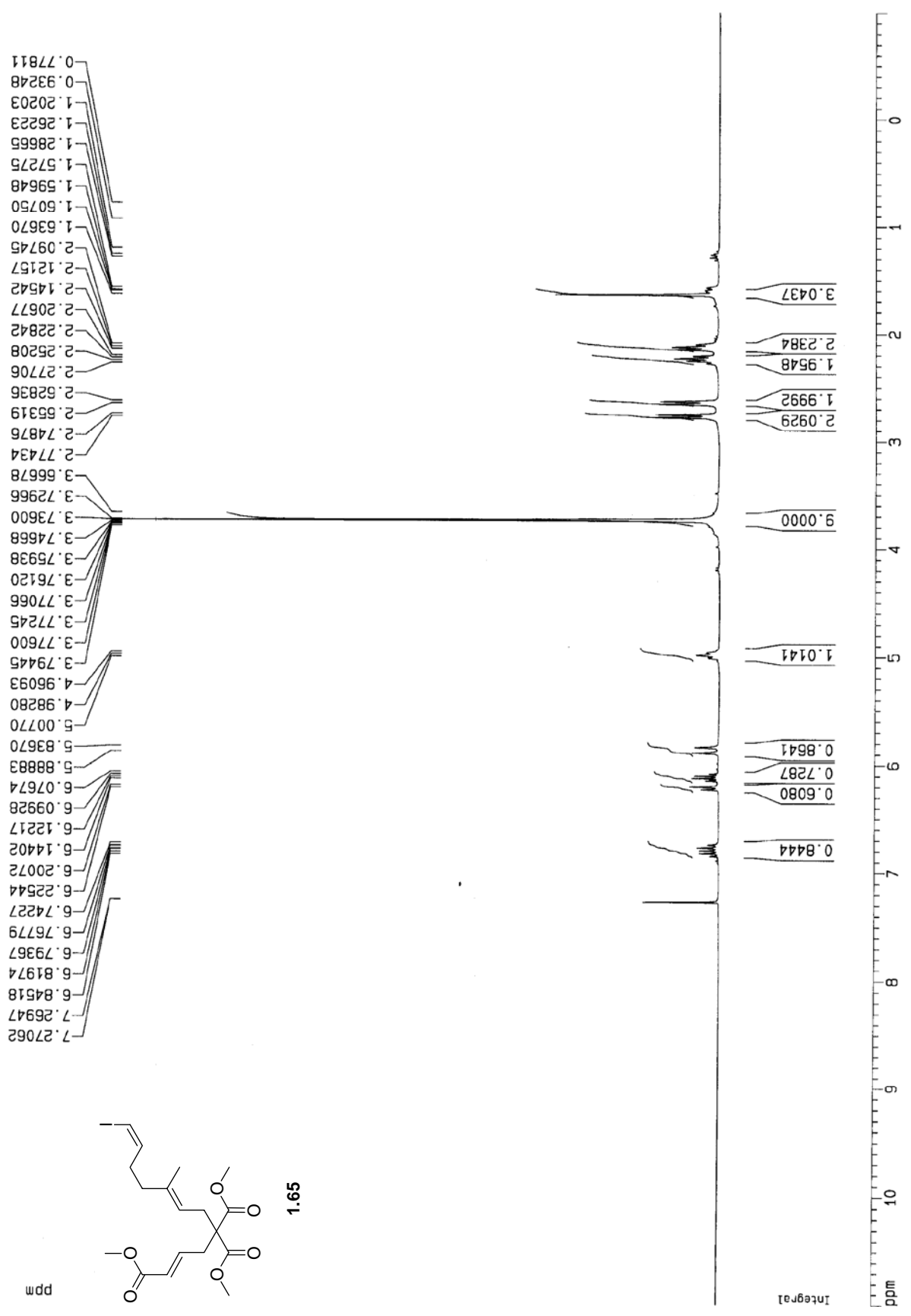


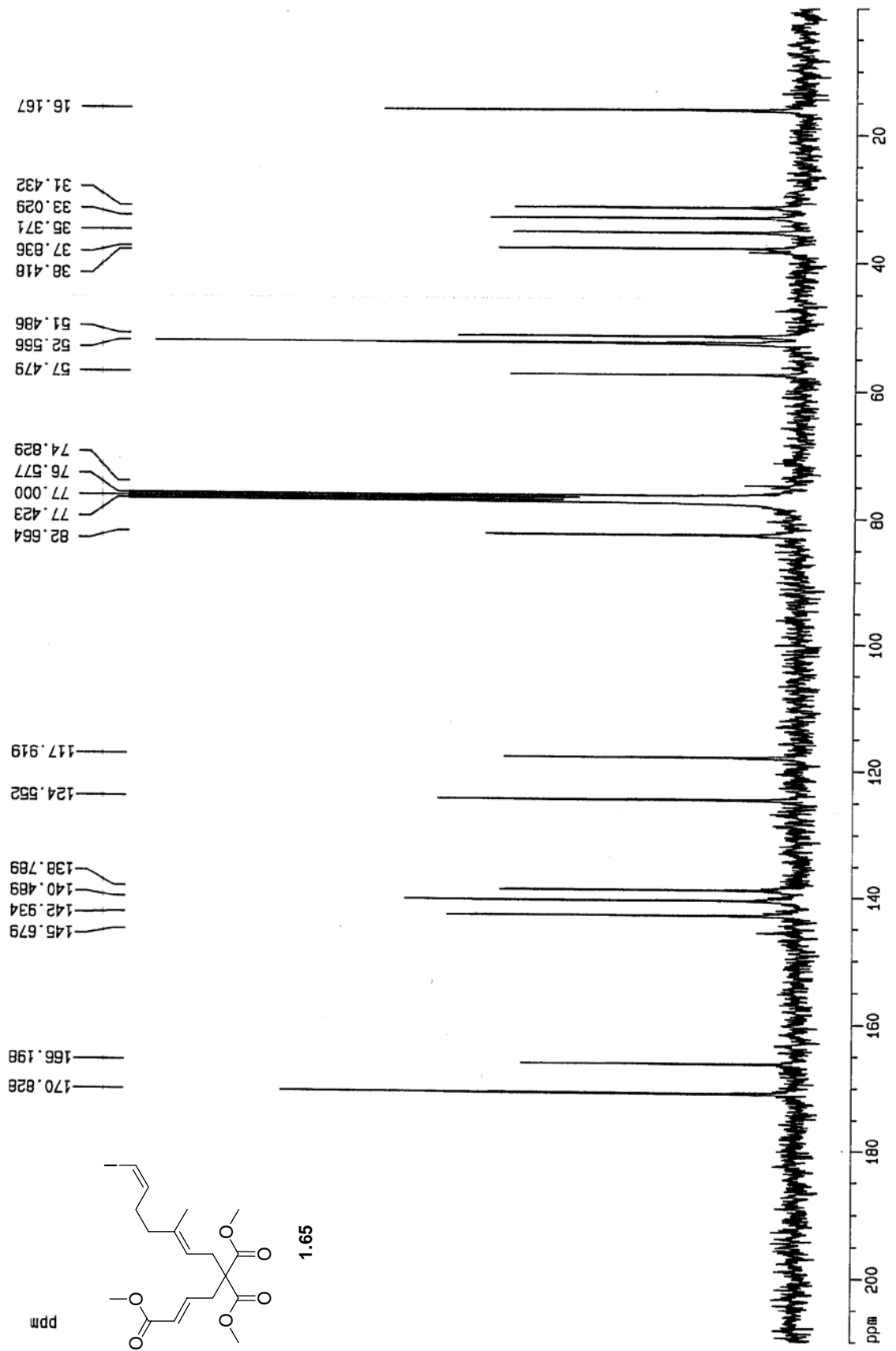


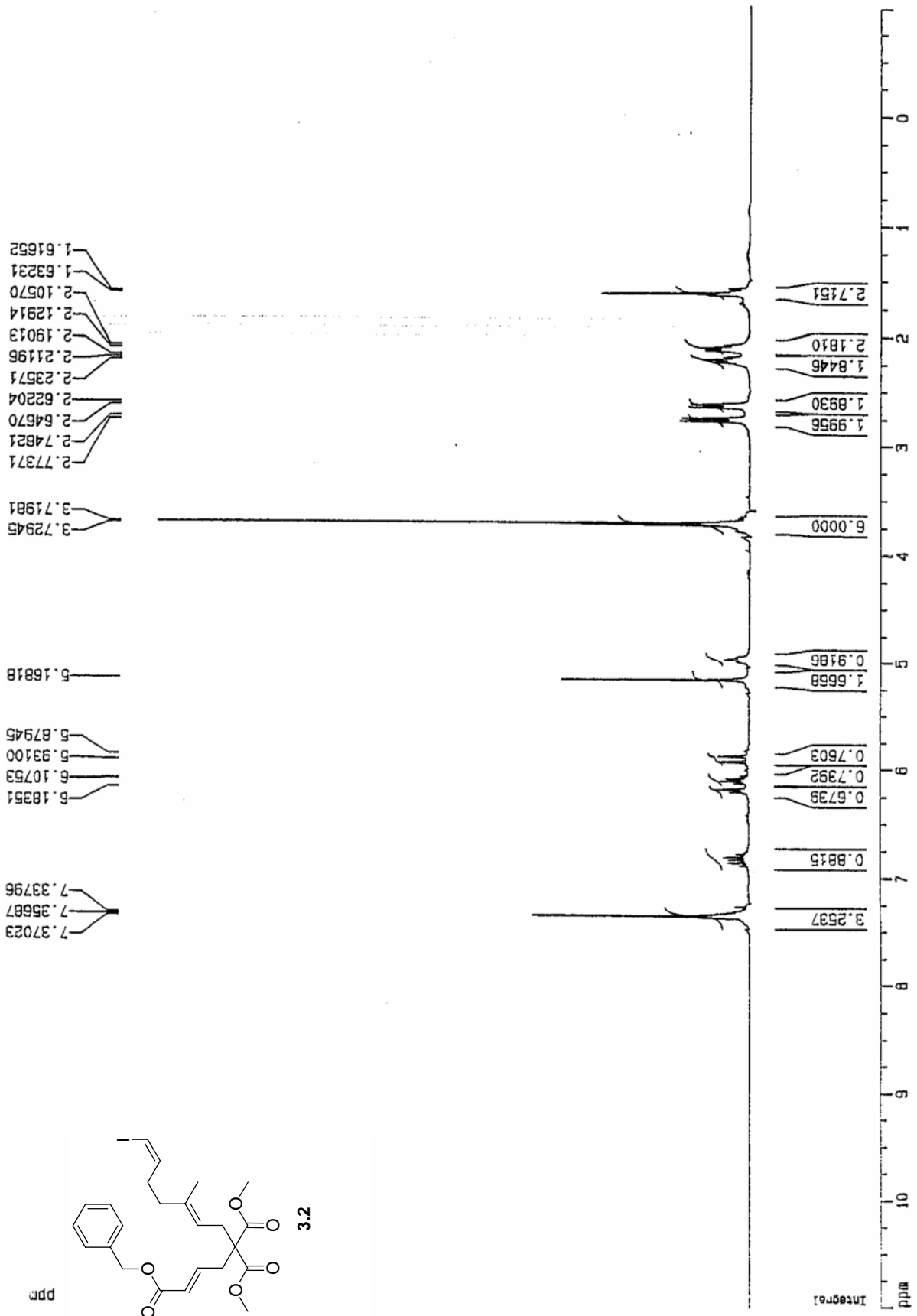


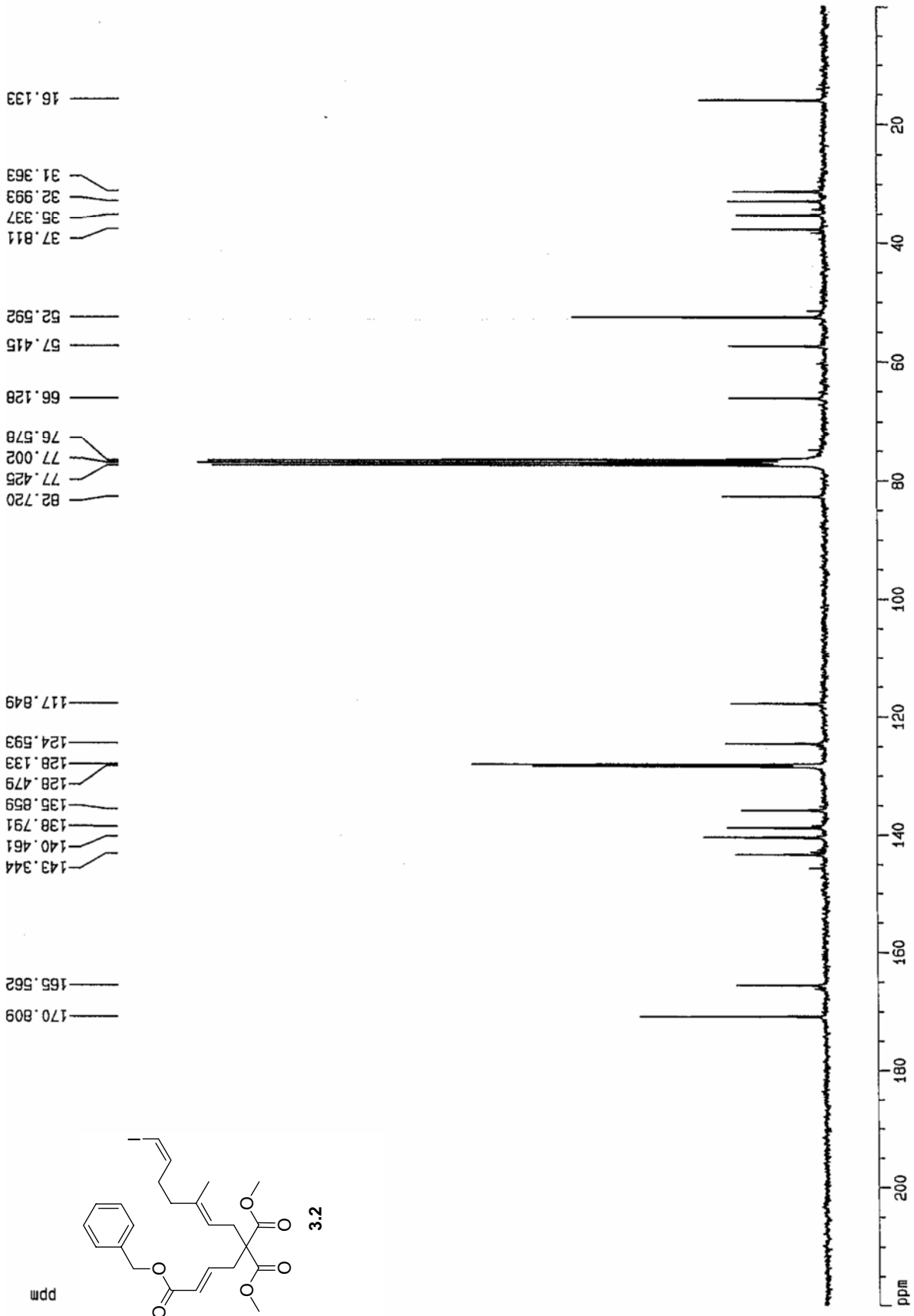


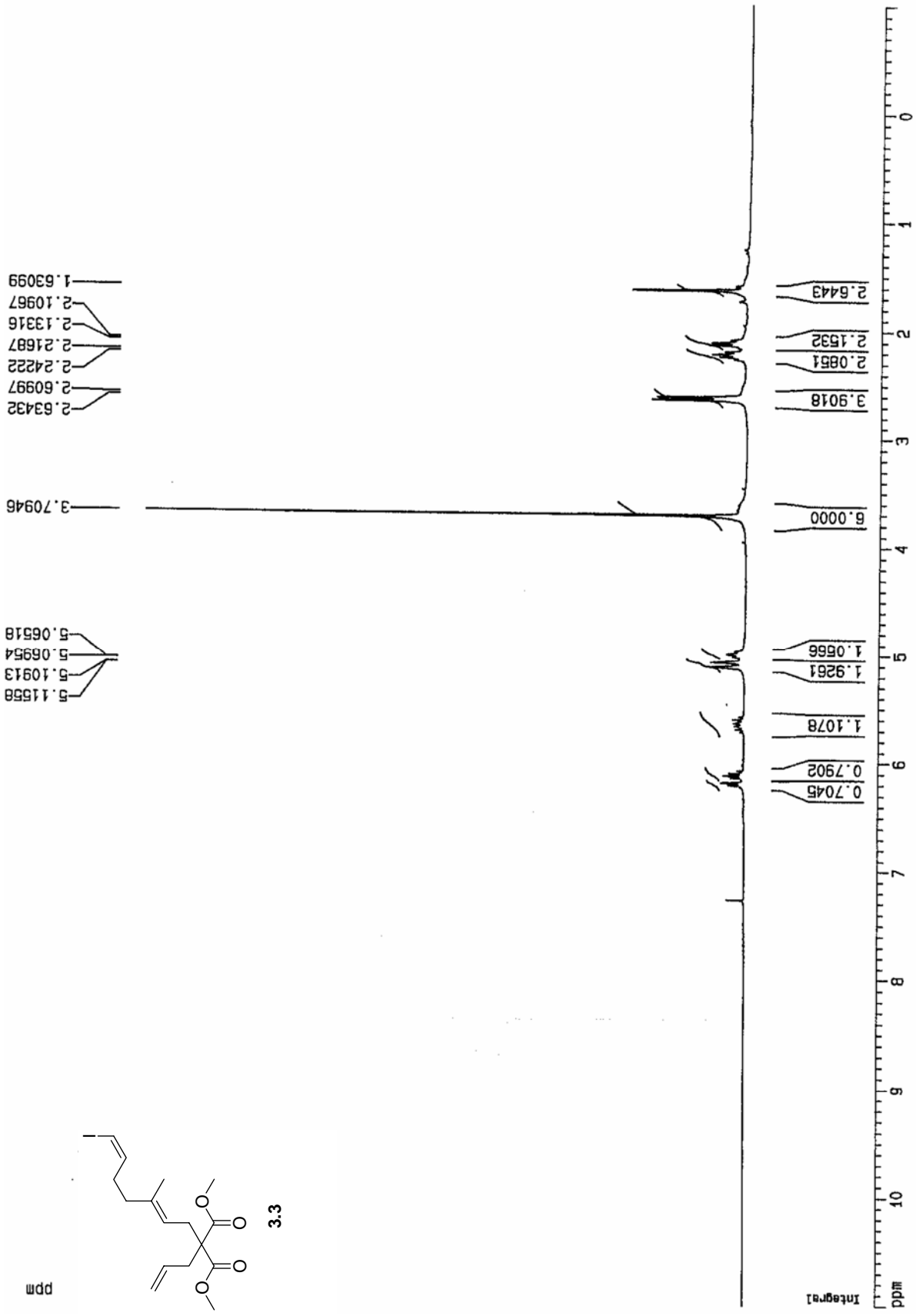


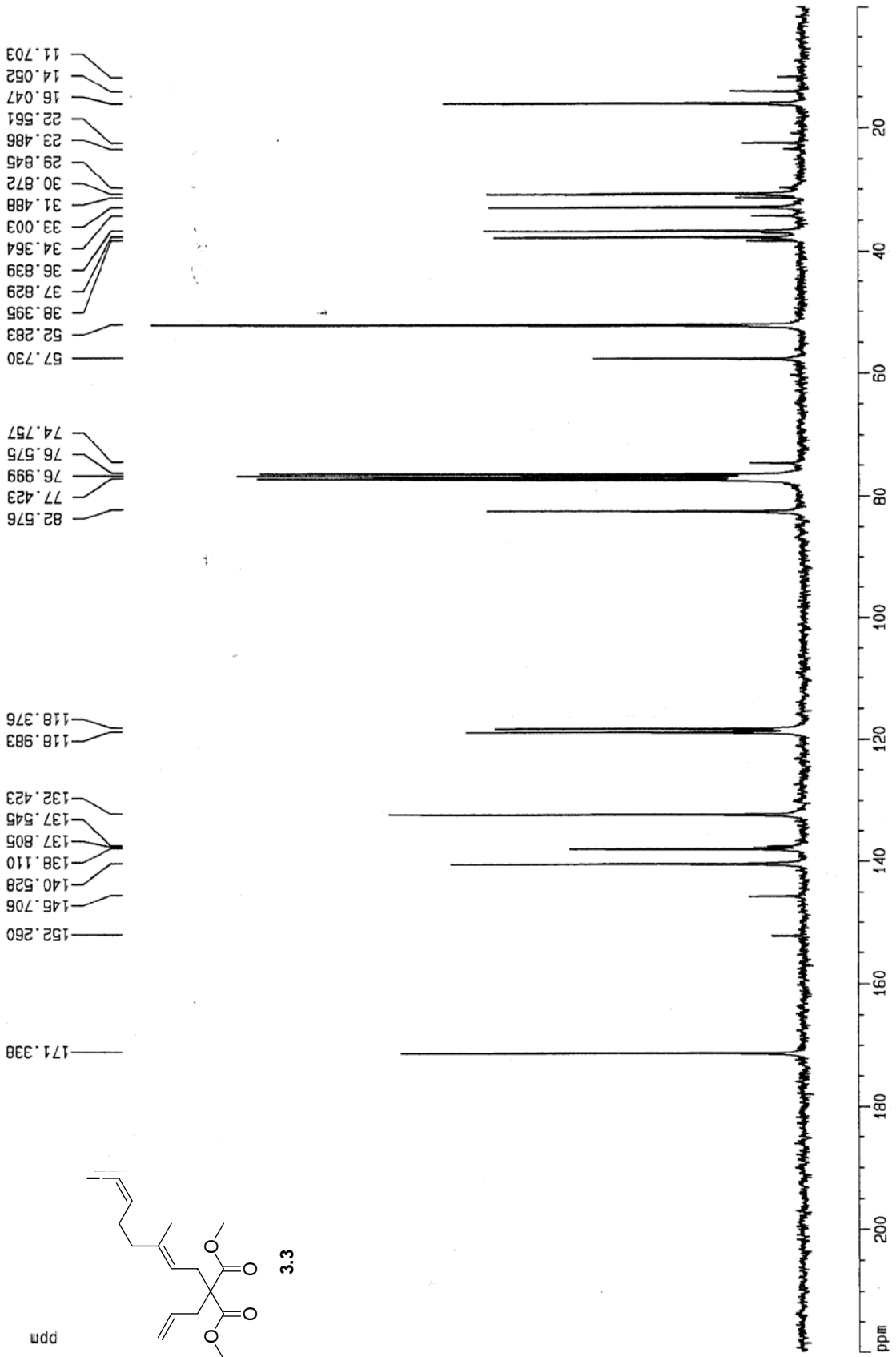




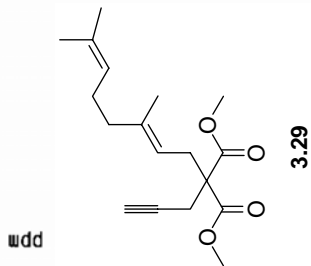
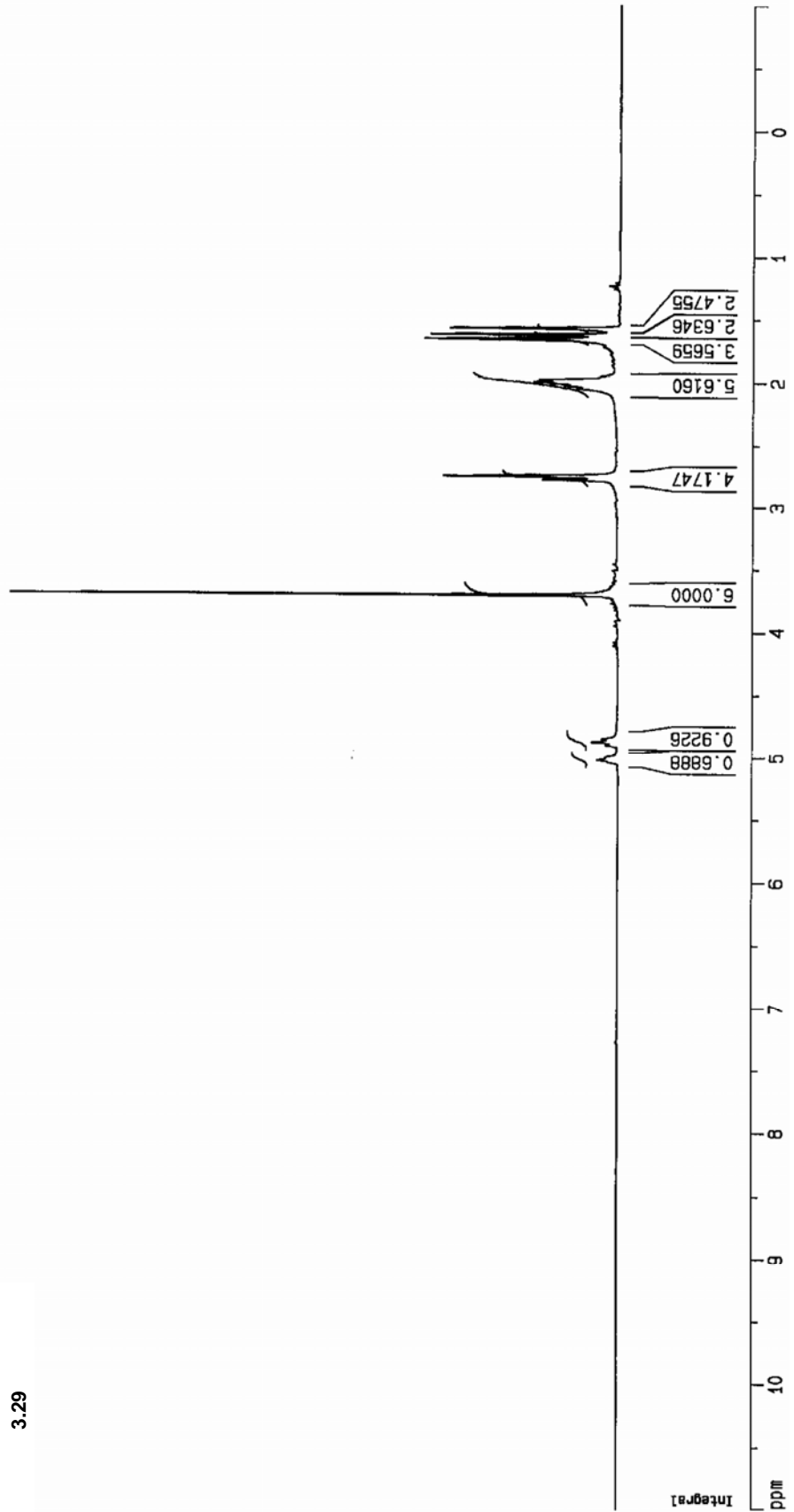


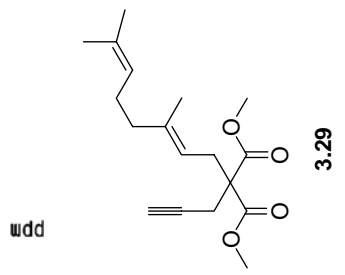
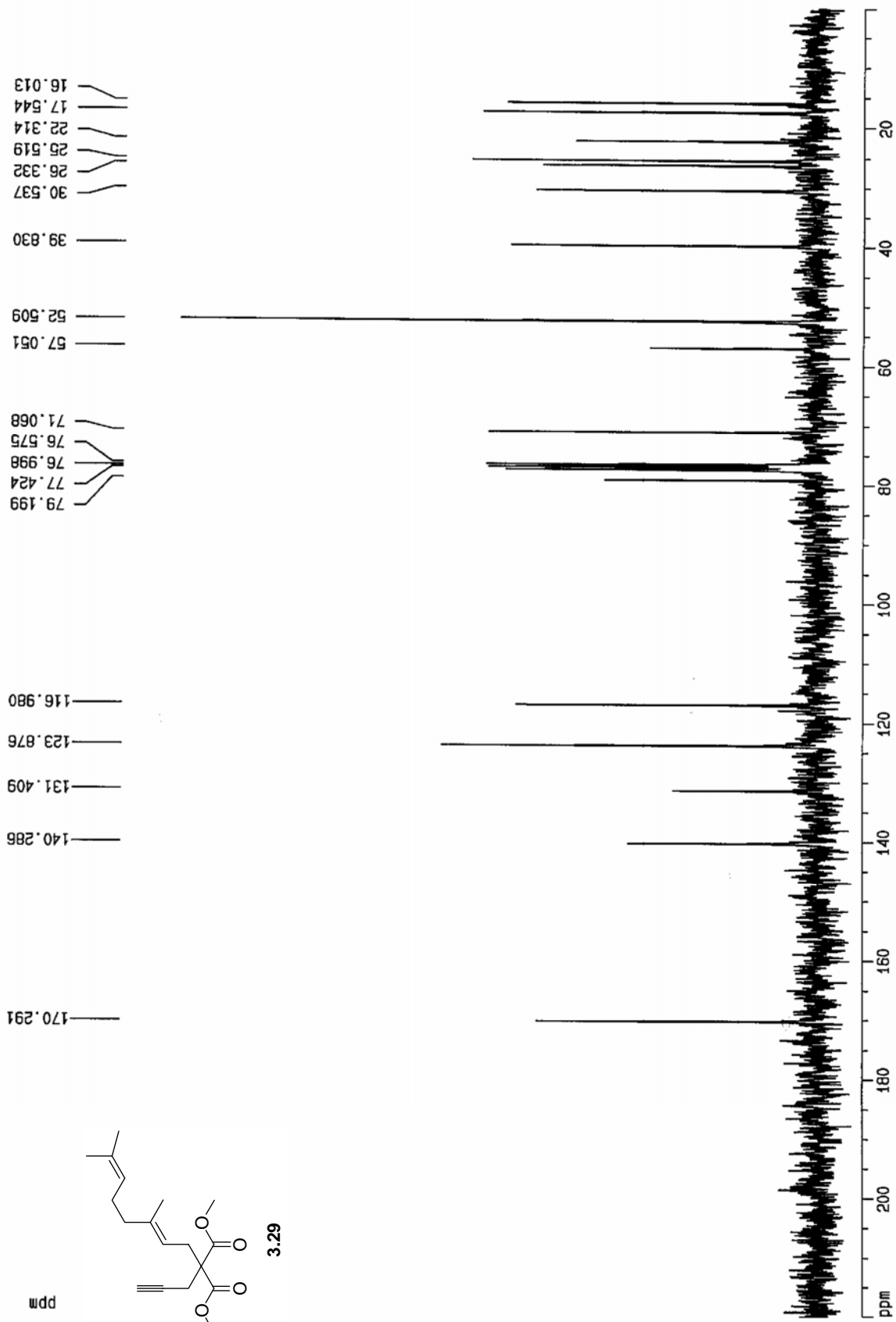


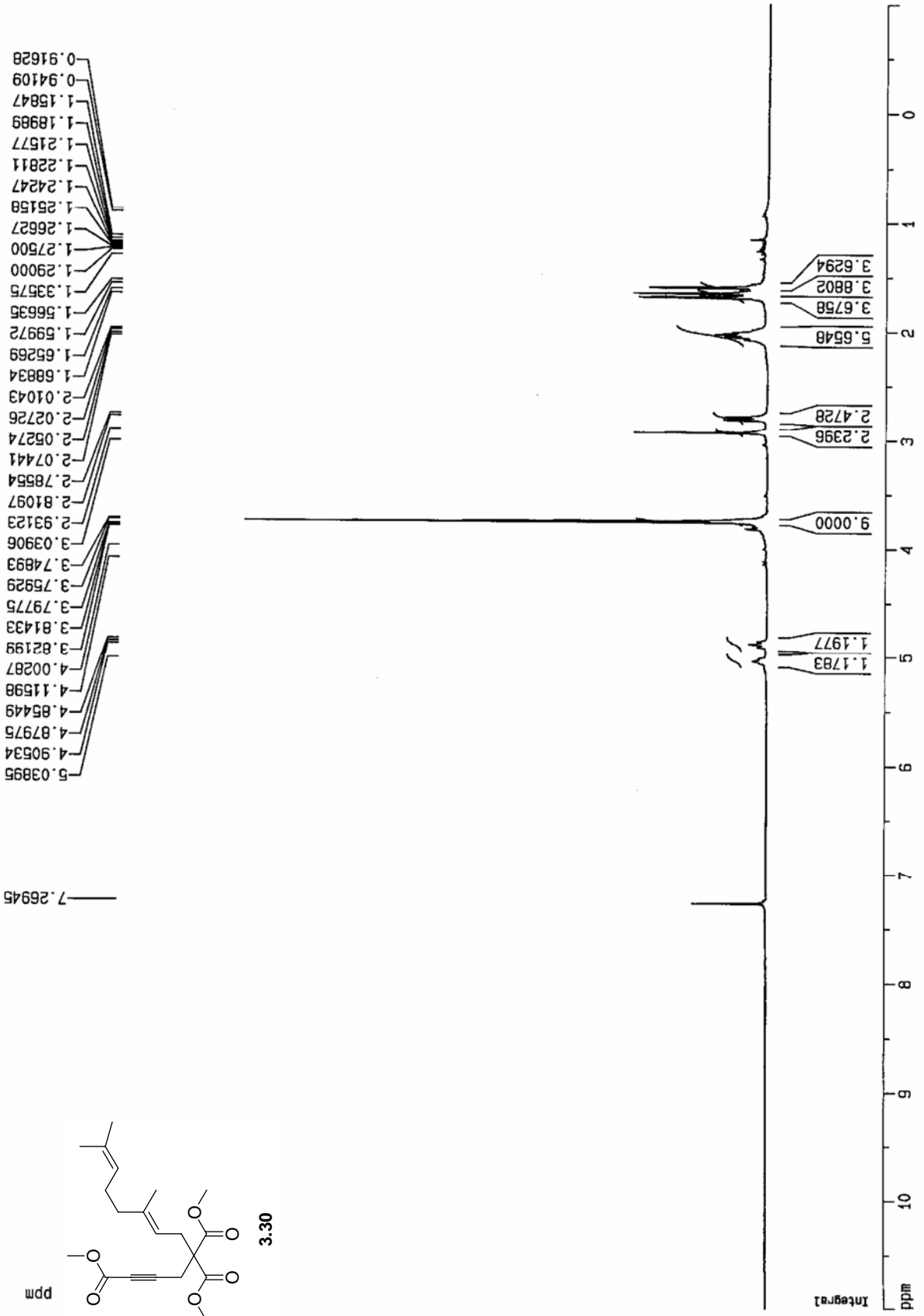


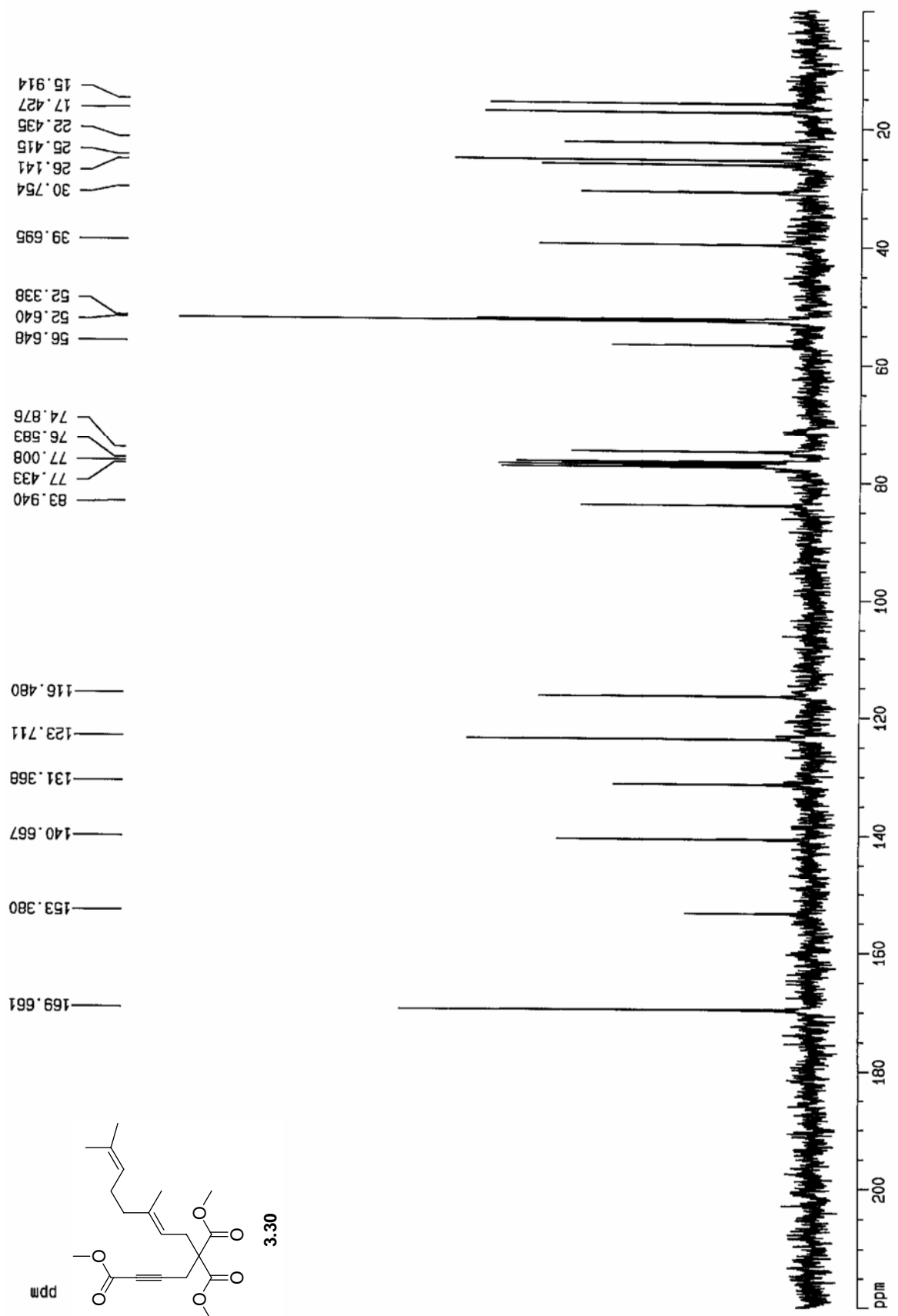


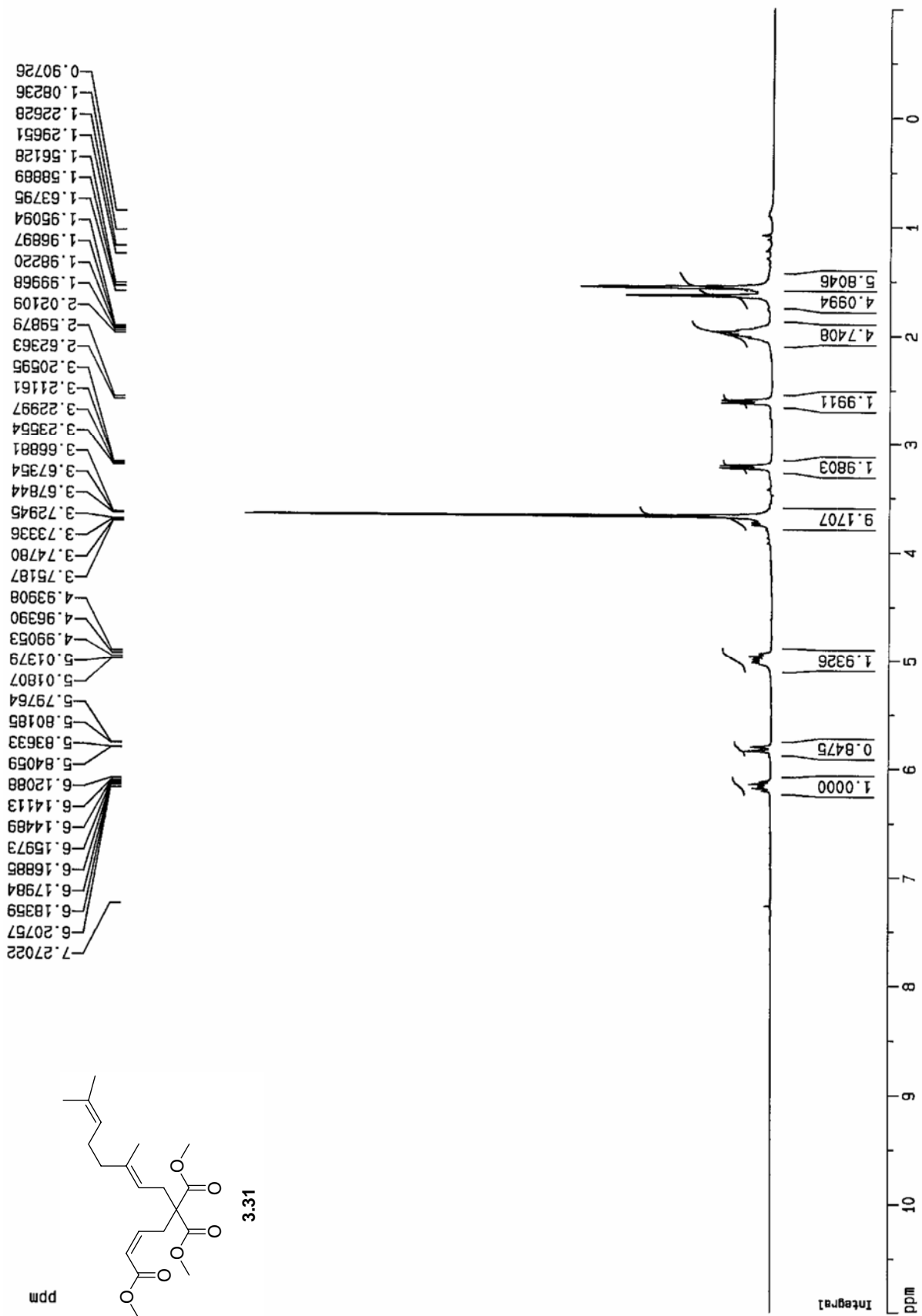
1.20527
 1.22912
 1.25277
 1.56981
 1.62224
 1.65755
 1.71891
 1.77710
 1.83000
 1.86491
 1.97860
 1.99376
 2.00975
 2.02511
 2.04664
 2.74292
 2.75108
 2.77814
 3.45560
 3.50532
 3.57747
 3.60382
 3.70382
 3.74288
 3.76867
 3.79964
 3.94714
 4.07739
 4.10119
 4.84768
 4.87292
 4.89753
 5.01604

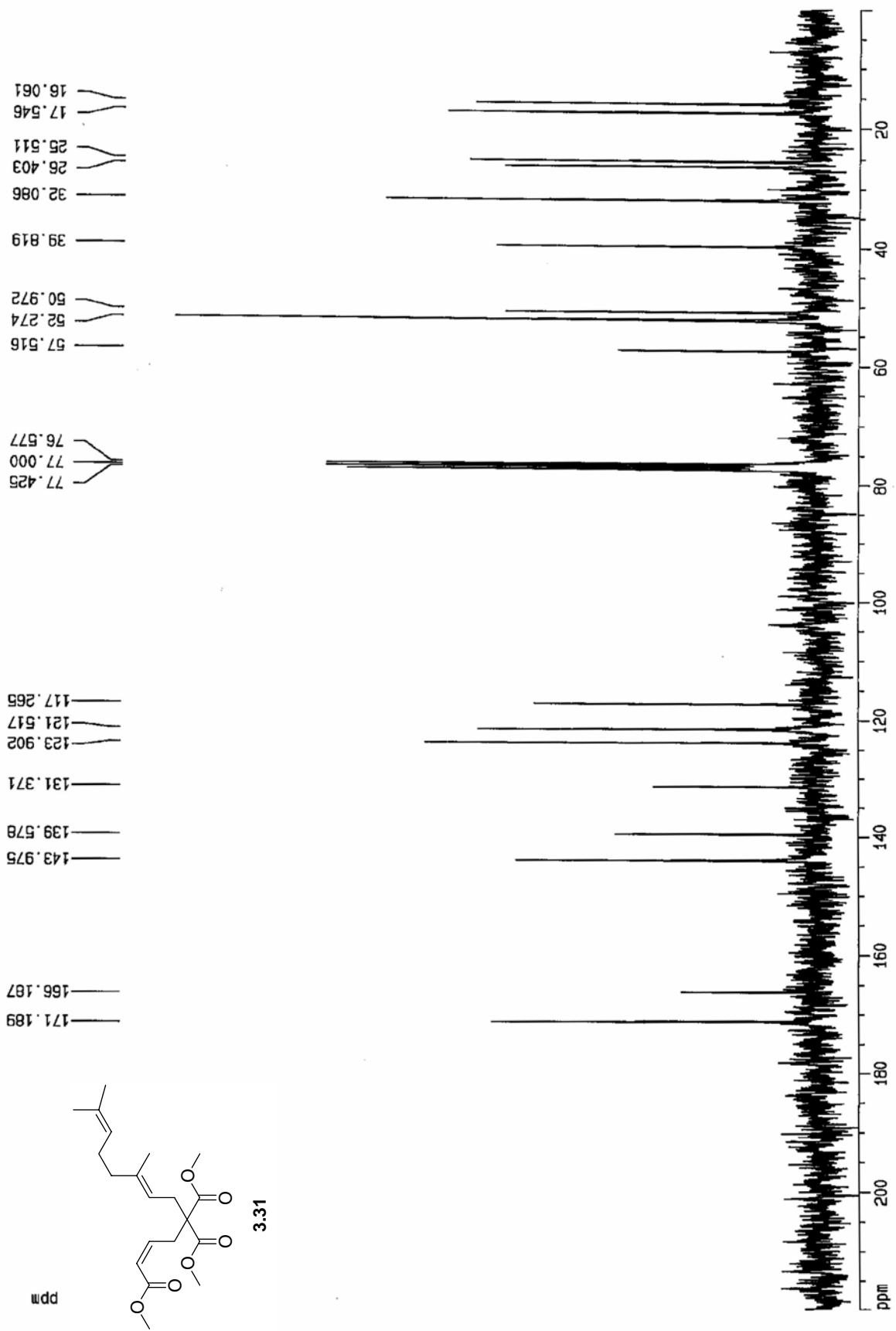


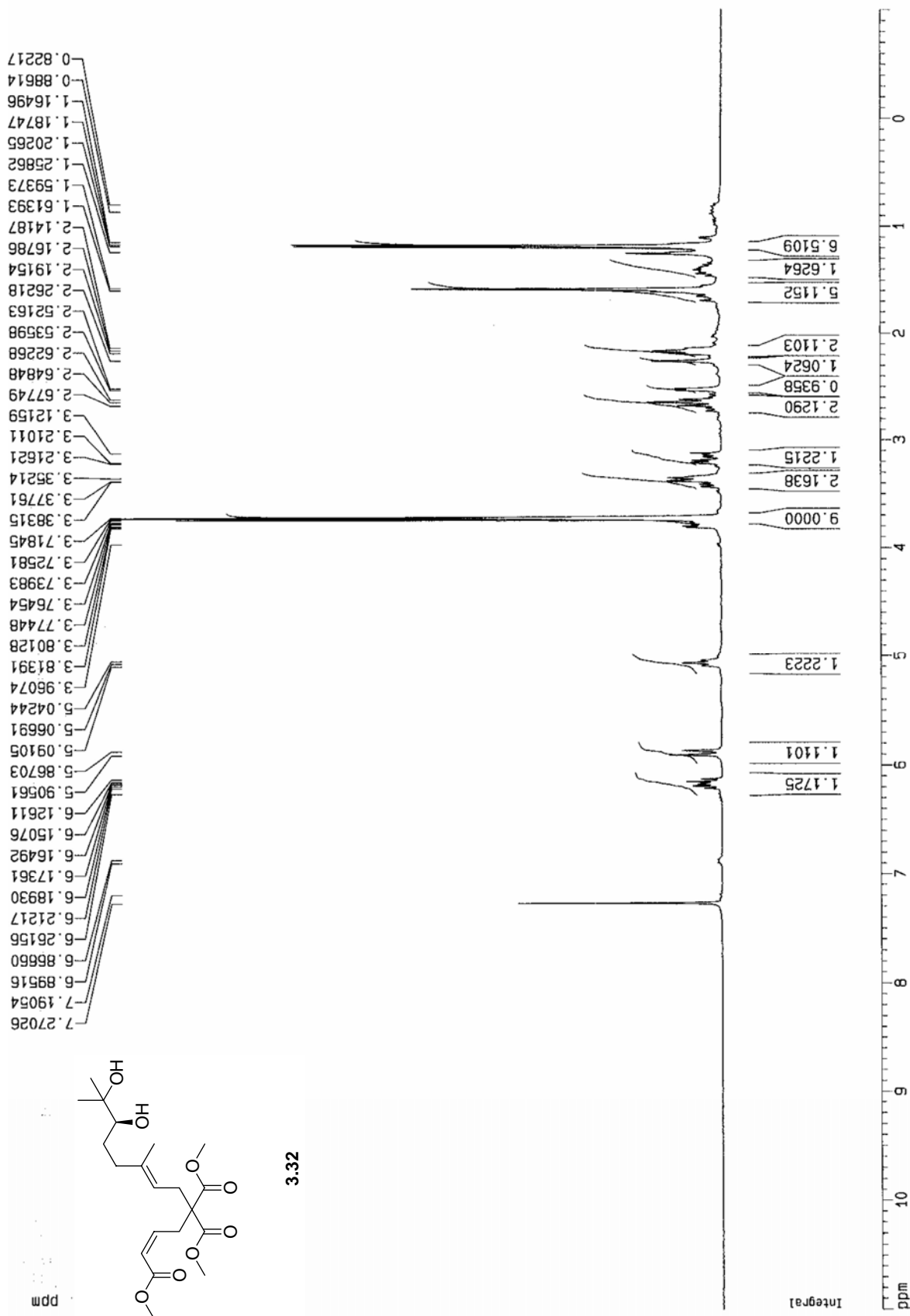


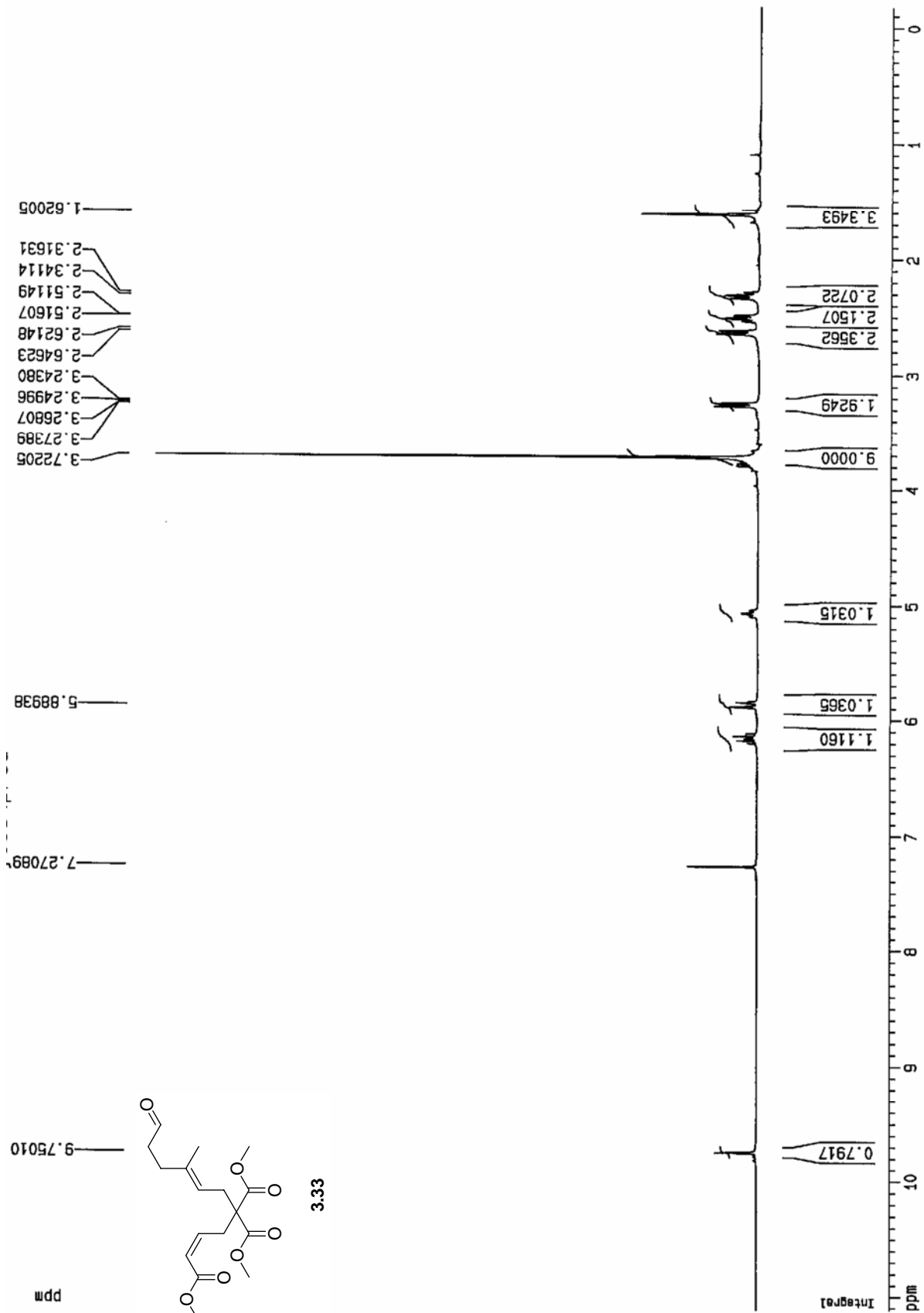


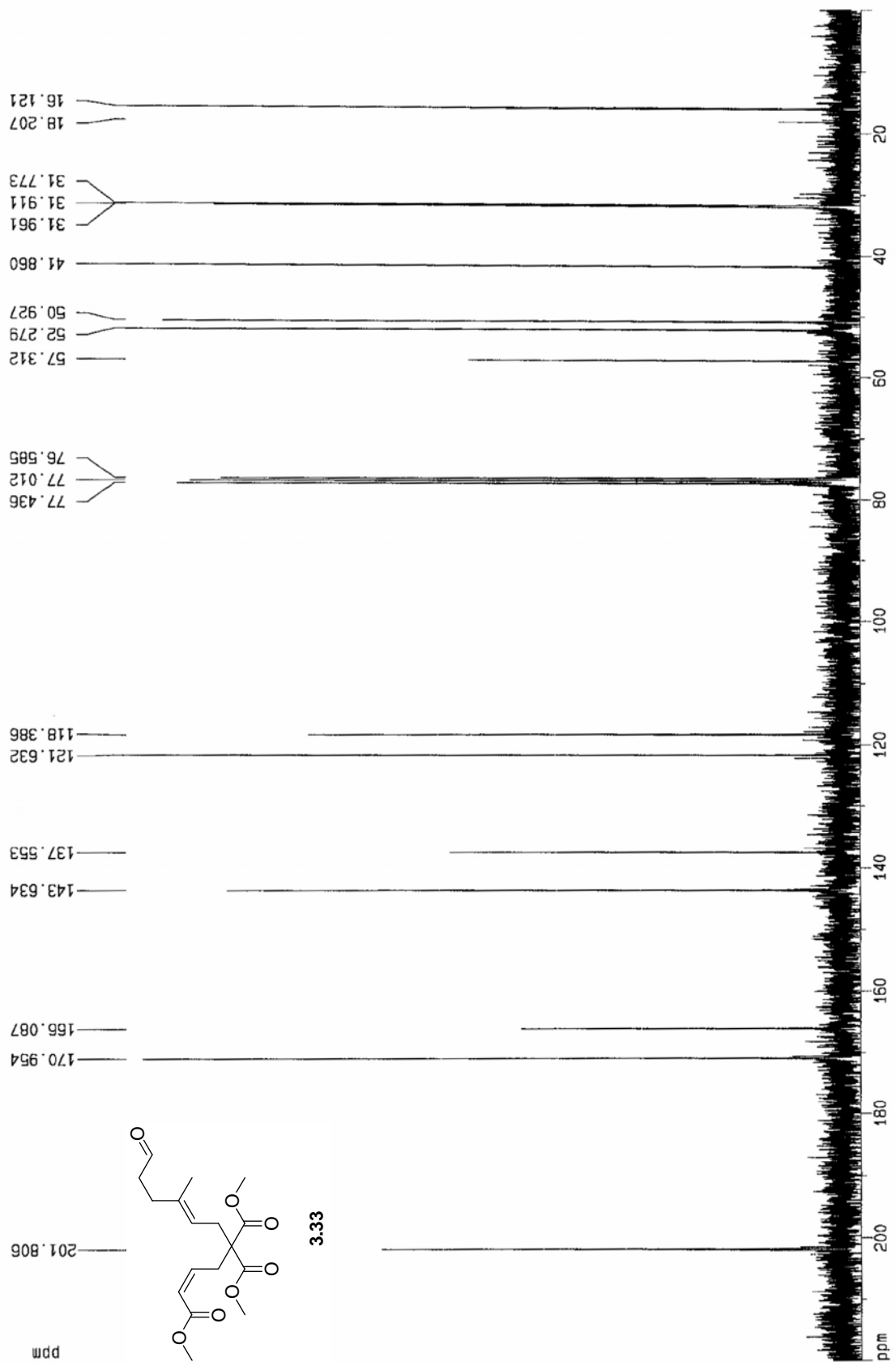


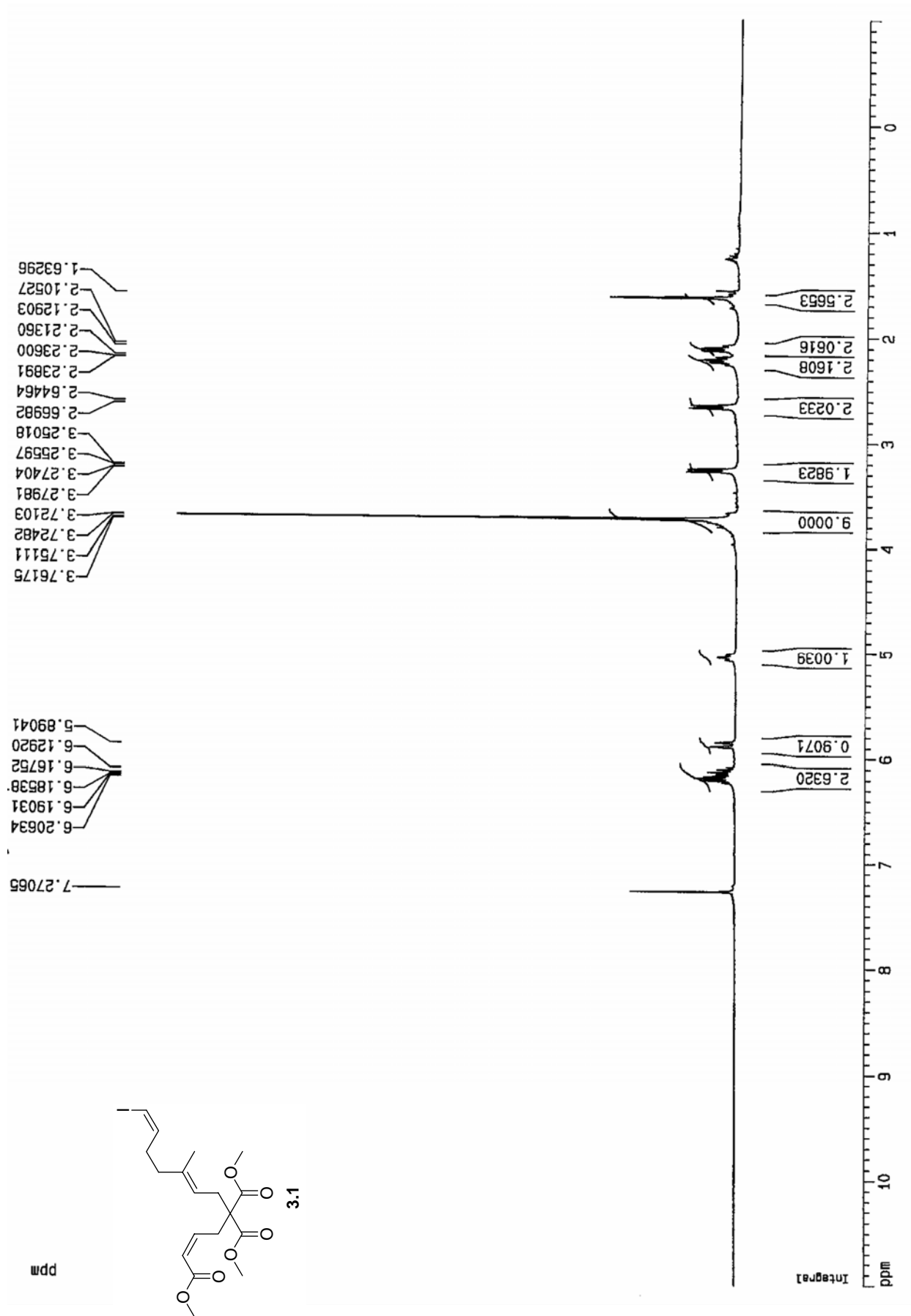


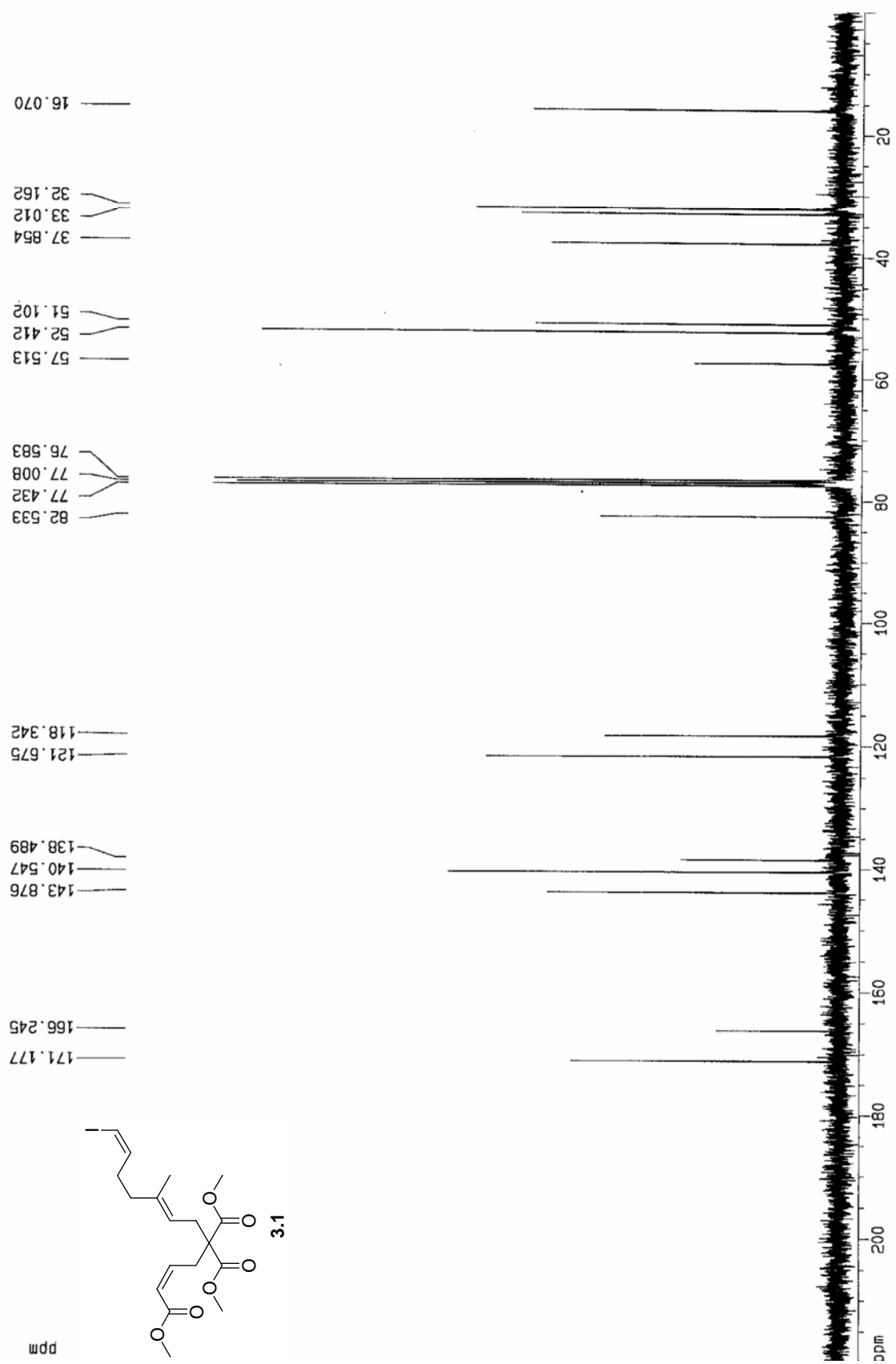


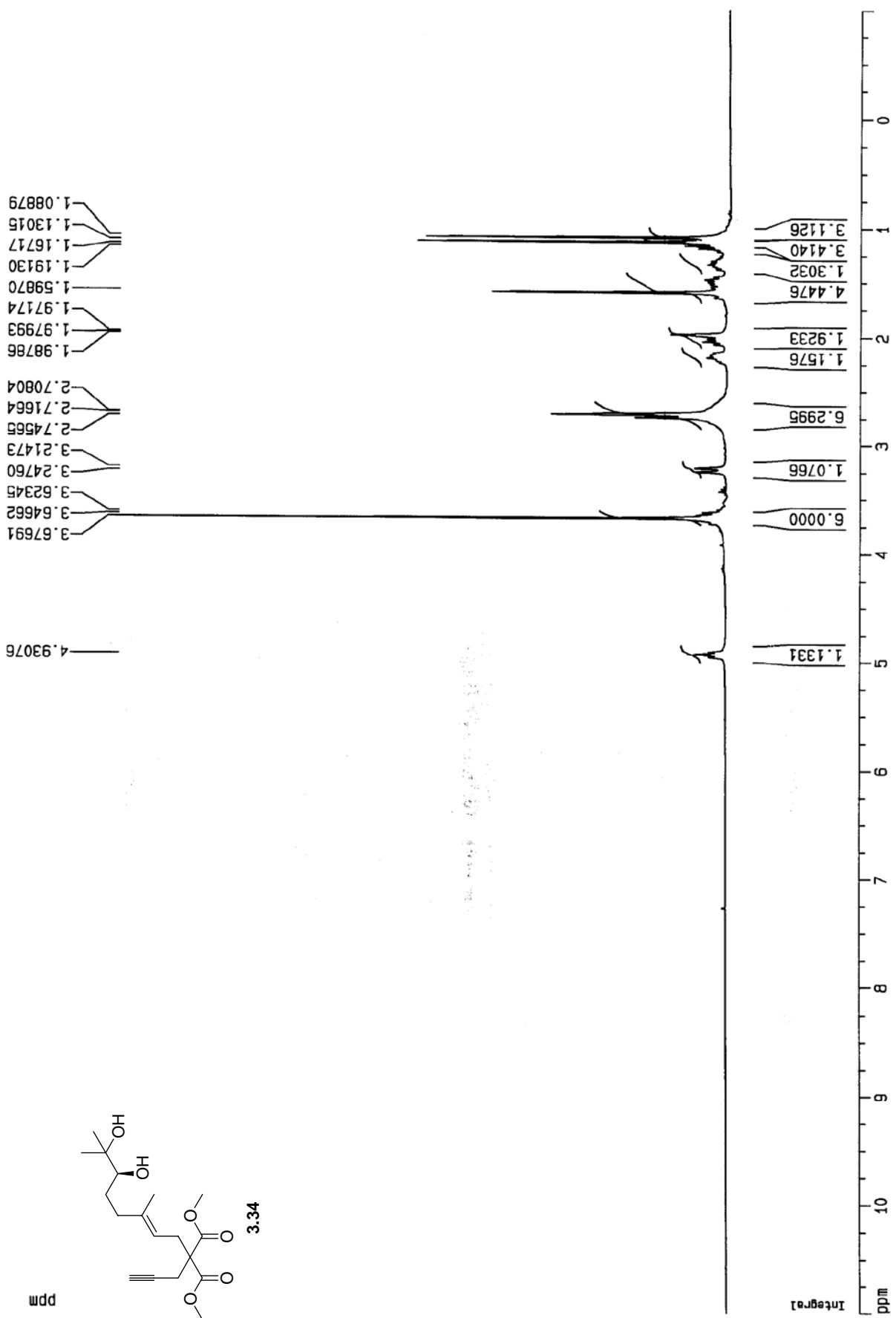






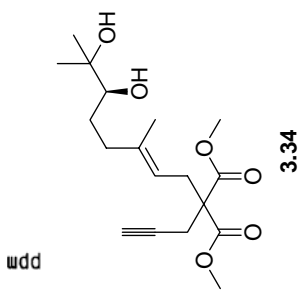




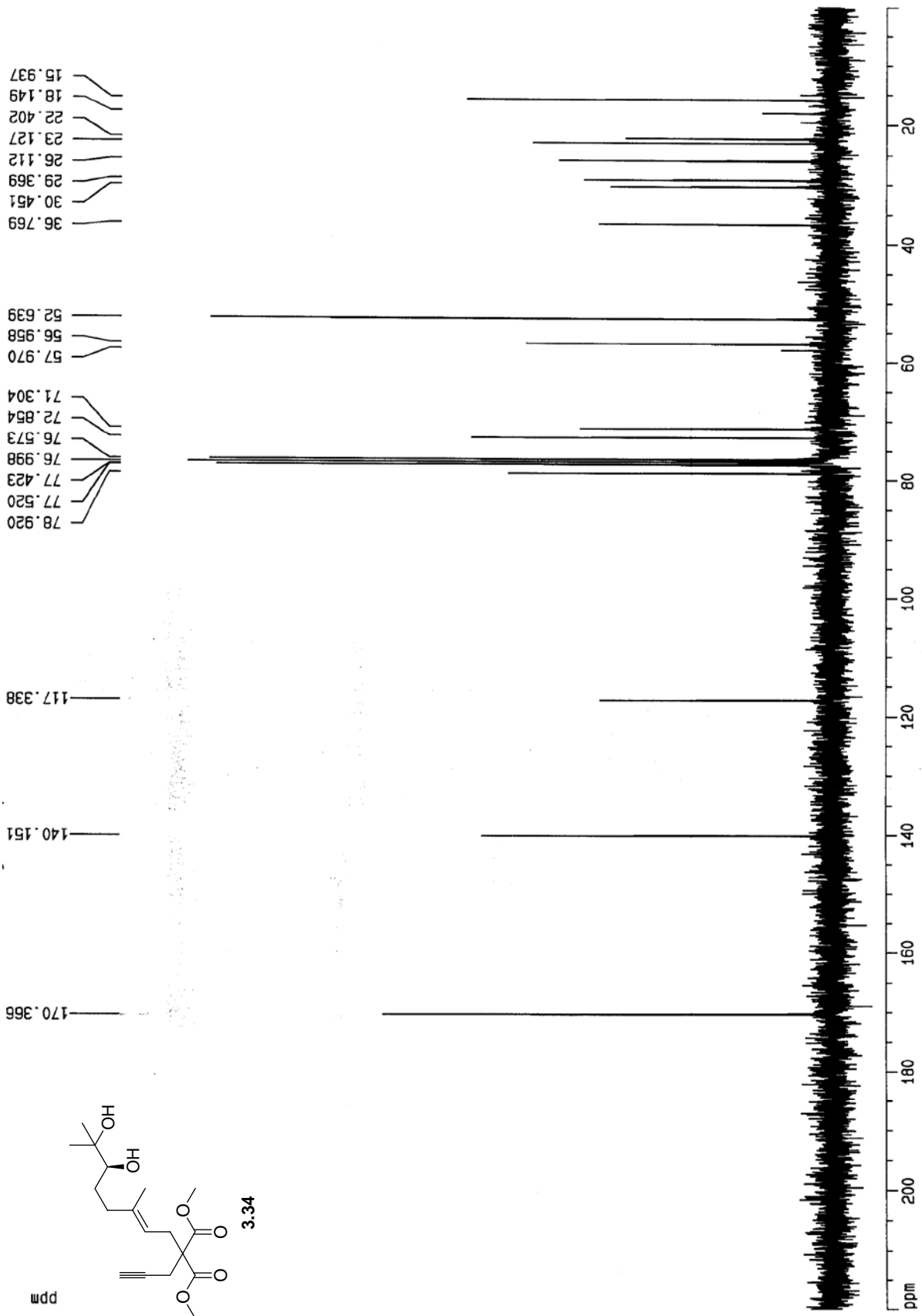


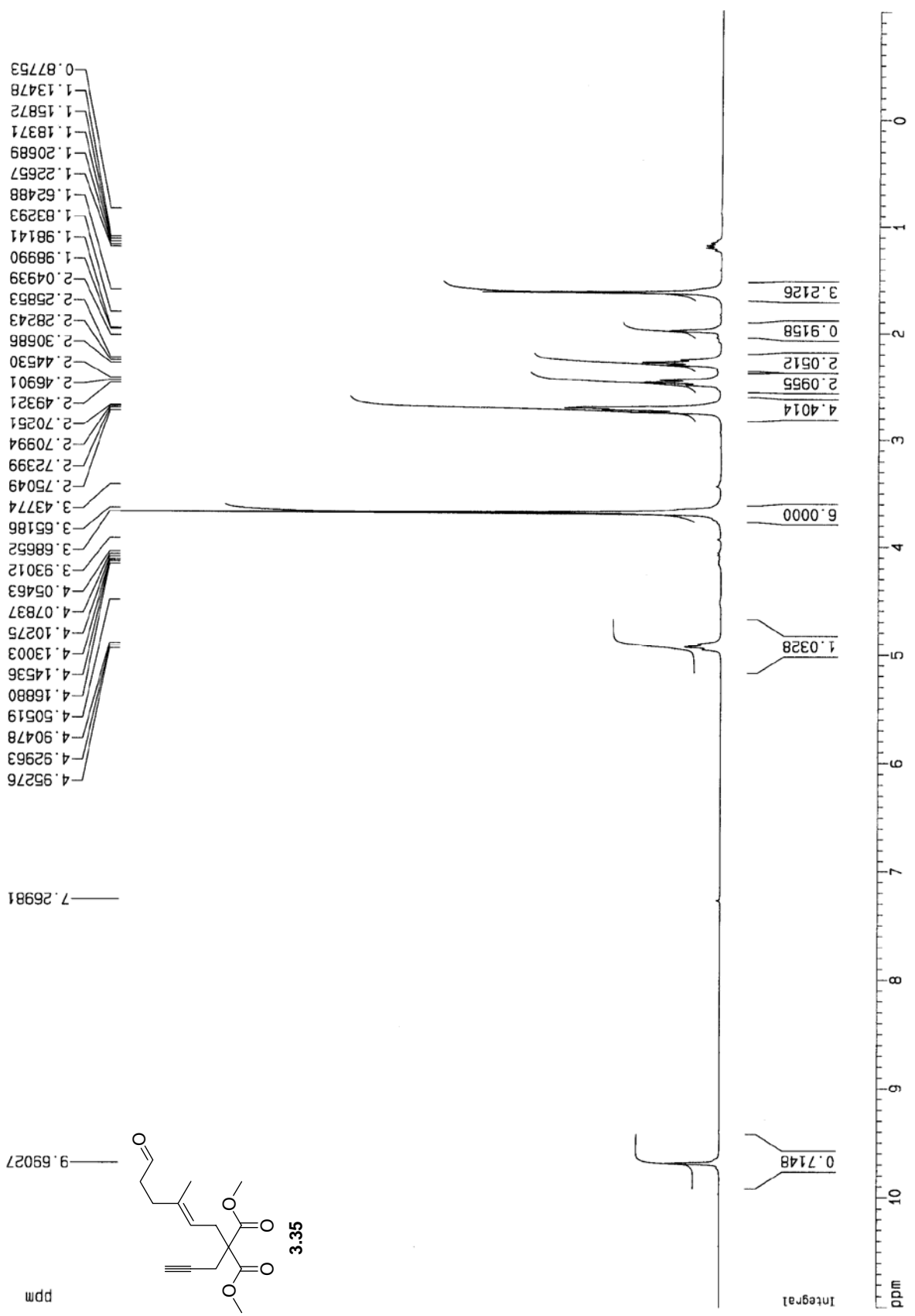
15.937
 18.149
 22.402
 23.127
 26.112
 29.369
 30.451
 36.769
 52.639
 56.958
 57.970
 71.304
 72.854
 76.573
 76.998
 77.423
 77.520
 78.920

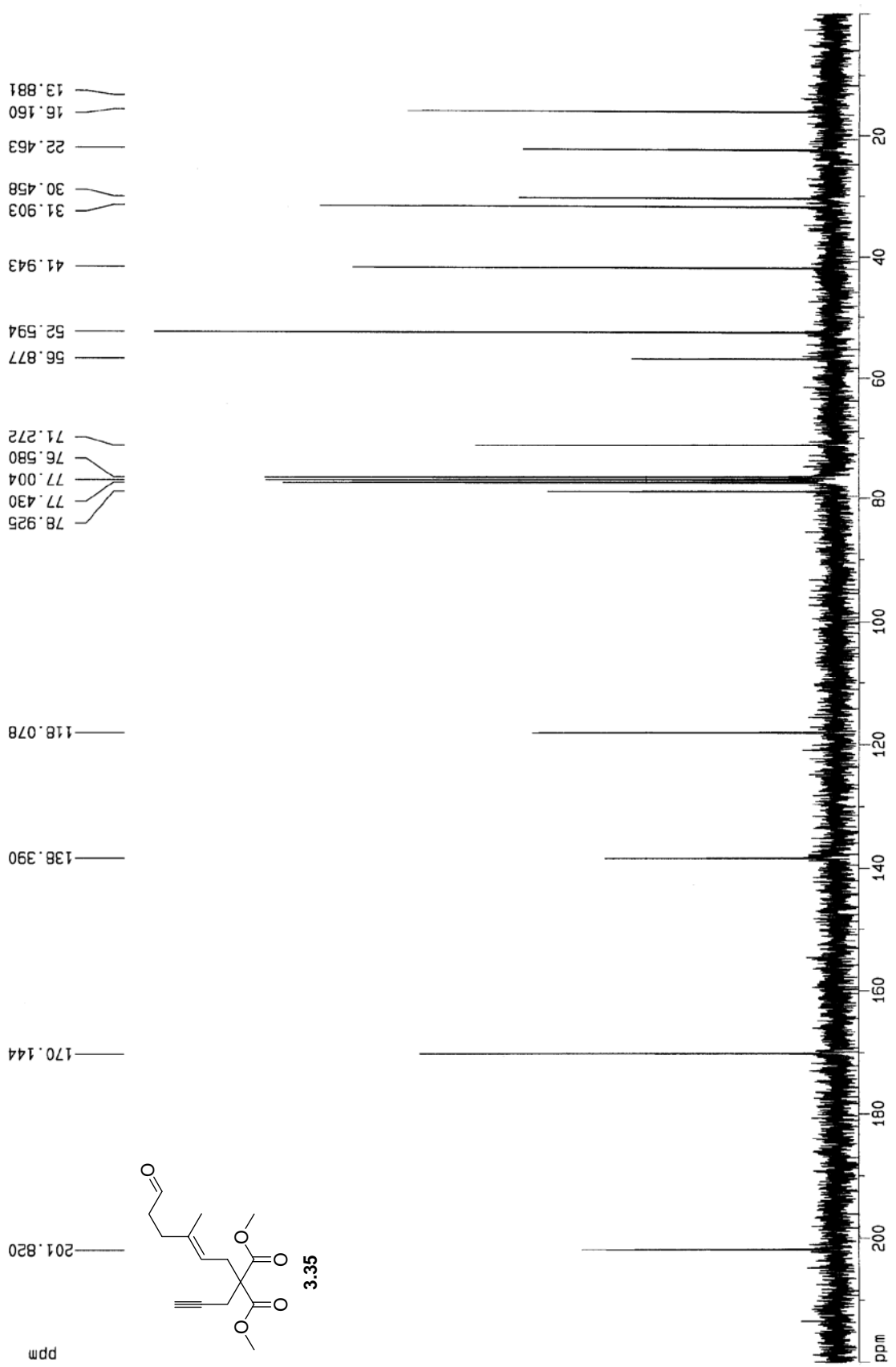
117.338
 140.151
 170.366

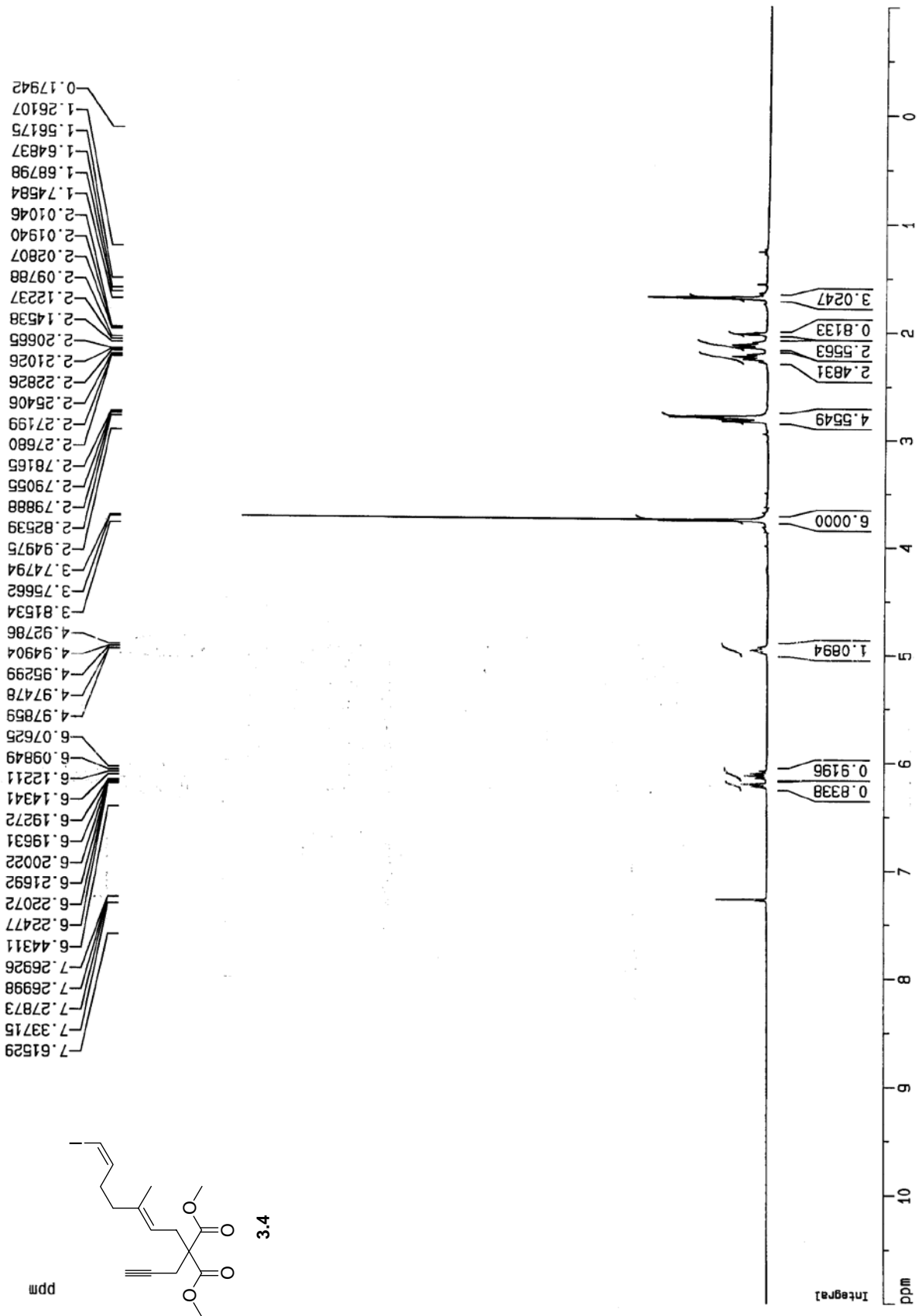


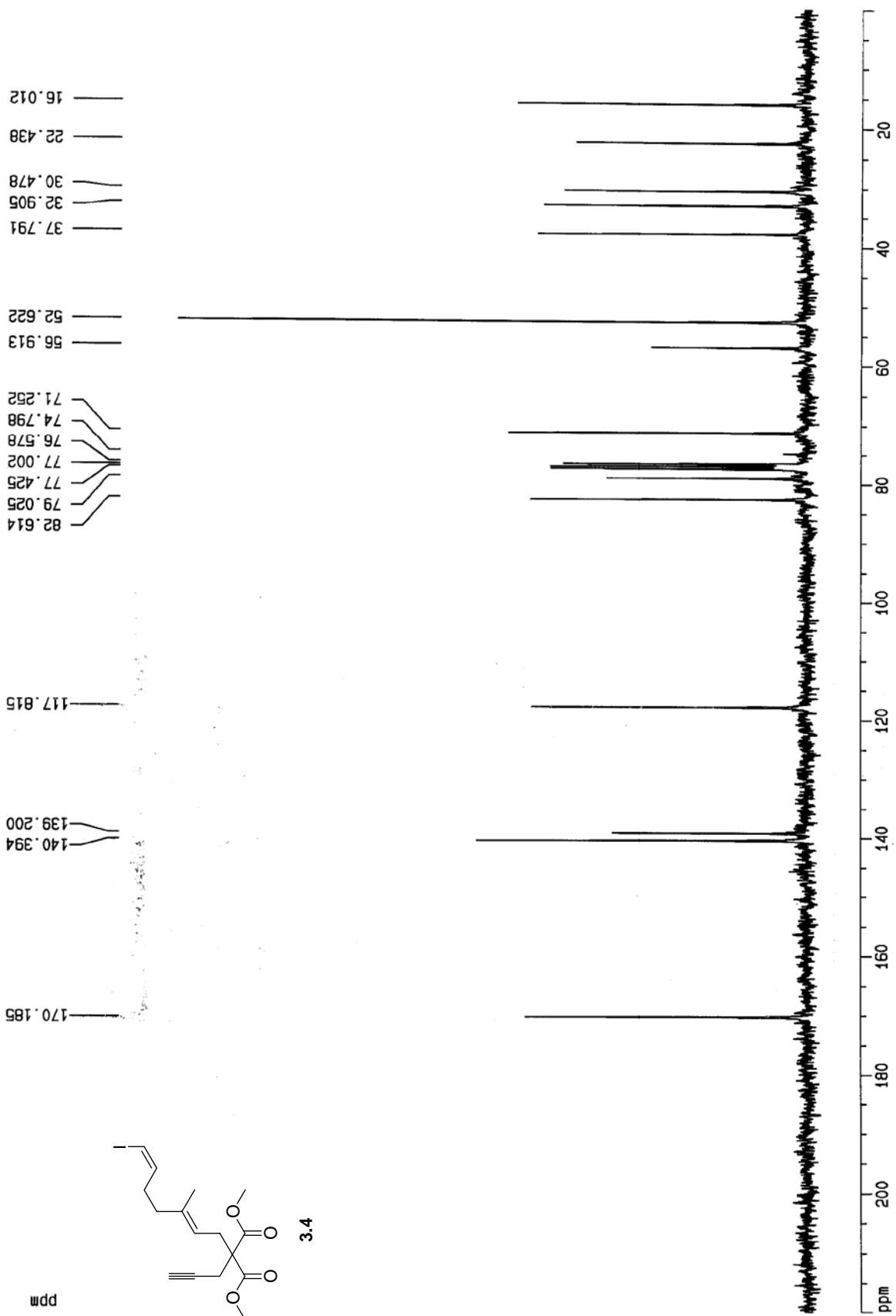
ppm









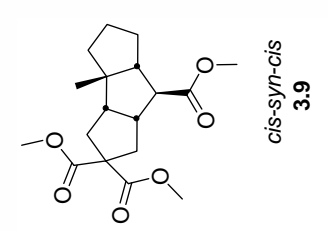
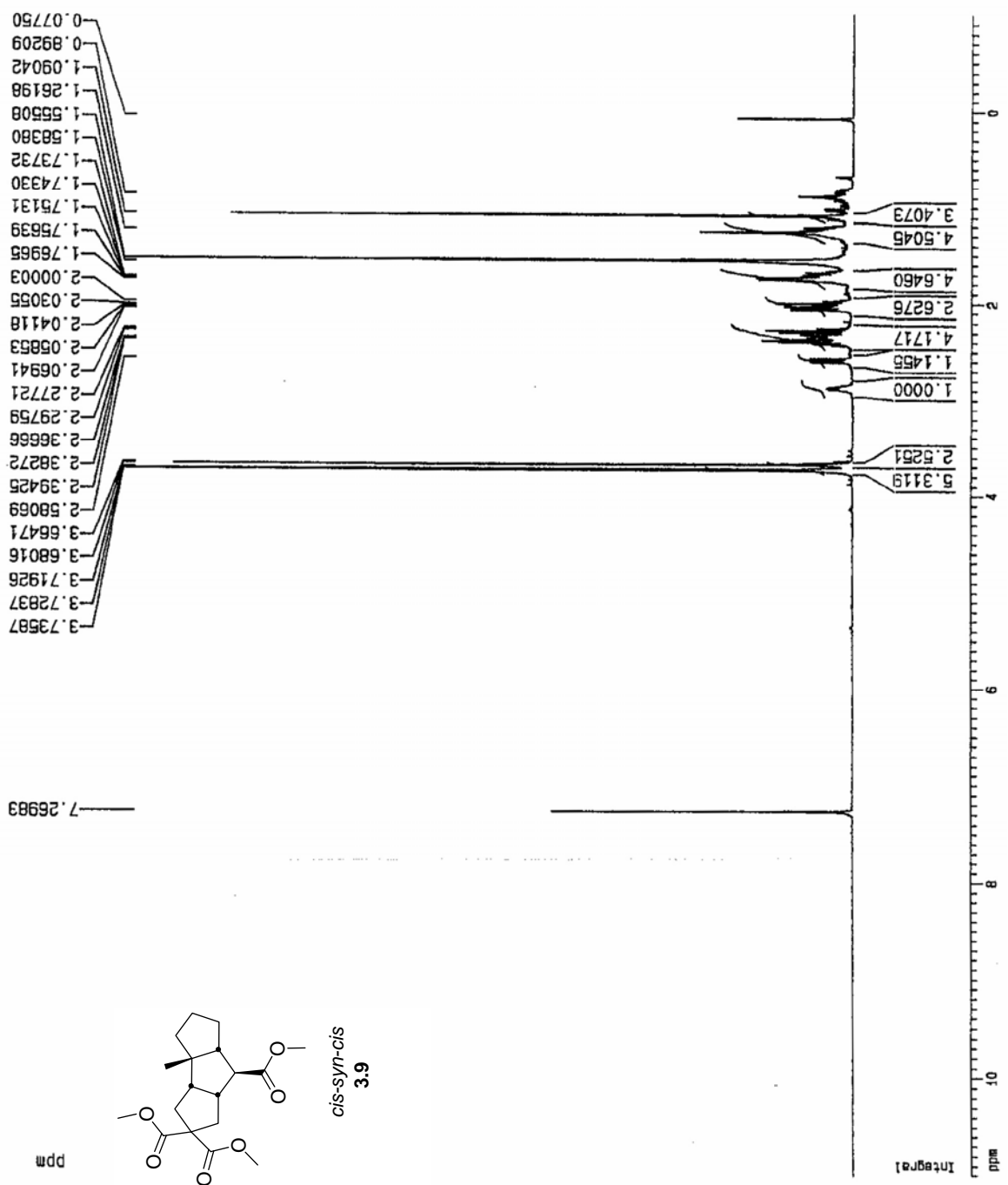


EXPNO 1
 PROCNO 1

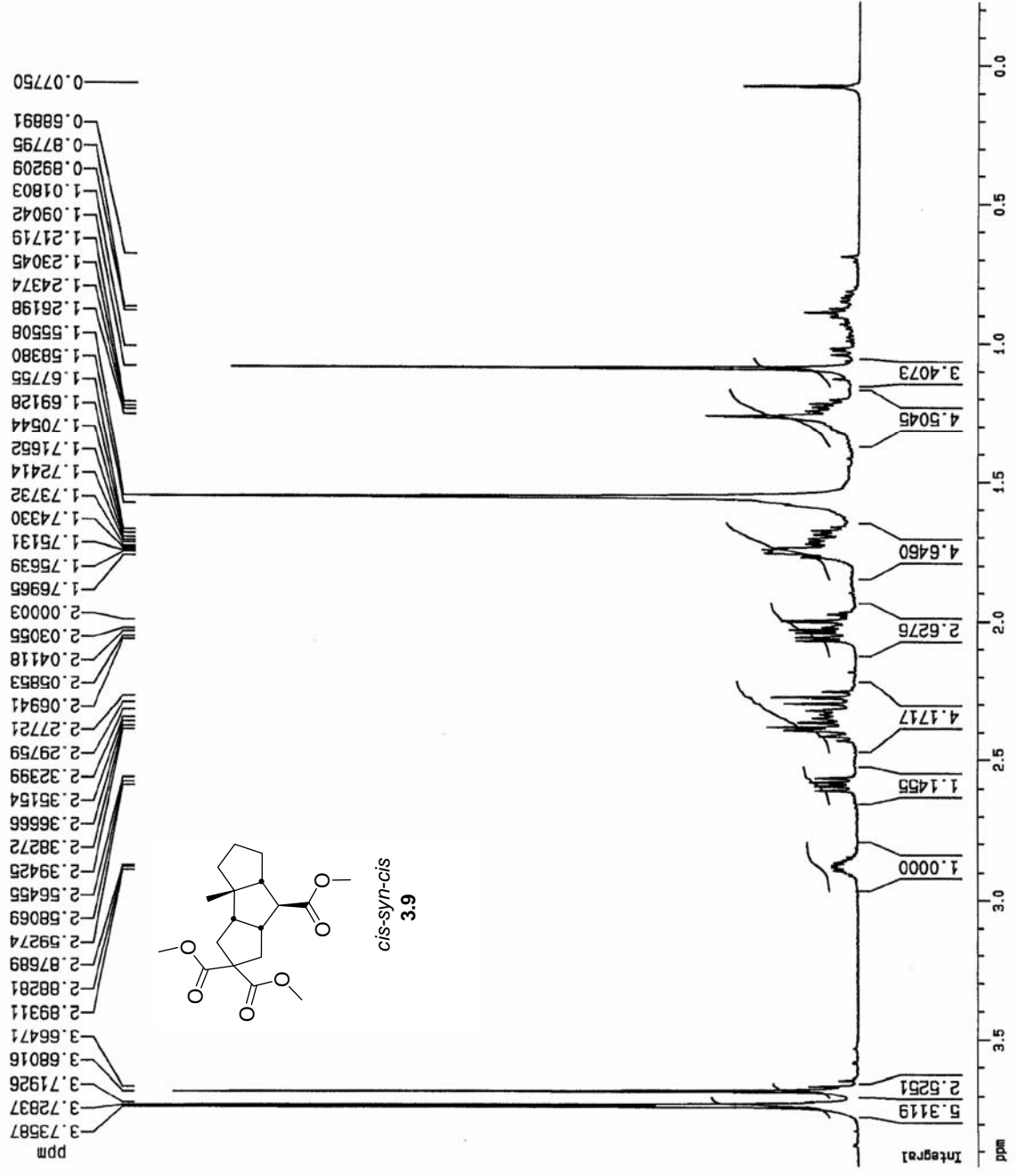
F2 - Acquisition Parameters
 Date_ 500000
 Time 19.06
 INSTRUM spect
 PROBHD 5 mm TXI 13C
 PULPROG zg
 TD 32768
 SOLVENT CDCl3
 NS 16
 DS 0
 SWH 7507.507 Hz
 FIDRES 0.229111 Hz
 AQ 2.1823988 sec
 RG 456.1
 DM 66.600 usec
 DE 6.00 usec
 TE 290.0 K
 D1 1.00000000 sec
 P1 10.50 usec
 DE 6.00 usec
 SF01 500.1330008 MHz
 NUC1 1H
 PL1 0.00 dB

F2 - Processing parameters
 SI 32768
 SF 500.1300238 MHz
 WDW EM
 SSB 0
 LB 0.40 Hz
 GB 0
 PC 1.00

1D NMR plot parameters
 CX 20.00 cm
 F1F 11.000 ppm
 F1 5504.43 Hz
 F2F -1.000 ppm
 F2 -500.13 Hz
 PPHCM 0.60000 ppm/cm
 HZCM 300.07803 Hz/cm



EXPTNO 1
 PROCNO 1
 F2 - Acquisition Parameters
 Date_ 500000
 Time 19.06
 INSTRUM spect
 PROBHD 5 mm TXI 13C
 PULPROG zg
 TD 32768
 SOLVENT CDC13
 NS 16
 DS 0
 SWH 7507.507 Hz
 FIDRES 0.229111 Hz
 AQ 2.1823988 sec
 RG 456.1
 DM 66.600 usec
 DE 6.00 usec
 TE 290.0 K
 D1 1.0000000 sec
 P1 10.60 usec
 DE 6.00 usec
 SF01 500.1330008 MHz
 NUC1 1H
 PL1 0.00 dB
 F2 - Processing parameters
 SI 32768
 SF 500.1300238 MHz
 MDW EM
 SSB 0
 LB 0.40 Hz
 GB 0
 PC 1.00
 1D NMR plot parameters
 CX 20.00 cm
 F1P 3.952 ppm
 F1 1976.60 Hz
 F2P -0.226 ppm
 F2 -112.93 Hz
 PPMCM 0.20890 ppm/cm
 HZCM 104.47655 Hz/cm



F2 - Acquisition Parameters

Date_ 20030616
 Time 7.54
 INSTRUM spect
 PROBHD 5 mm TBJ 4H/
 PULPROG c13wznoe
 TD 65536
 SOLVENT CDCl3
 NS 55331
 DS 0
 SWH 37878.789 Hz
 FIDRES 0.577984 Hz
 AQ 0.9651252 sec
 RG 32768
 DW 13.200 usec
 DE 6.00 usec
 TE 290.0 K
 D1 8.0000000 sec
 D3 0.00100000 sec

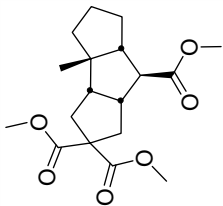
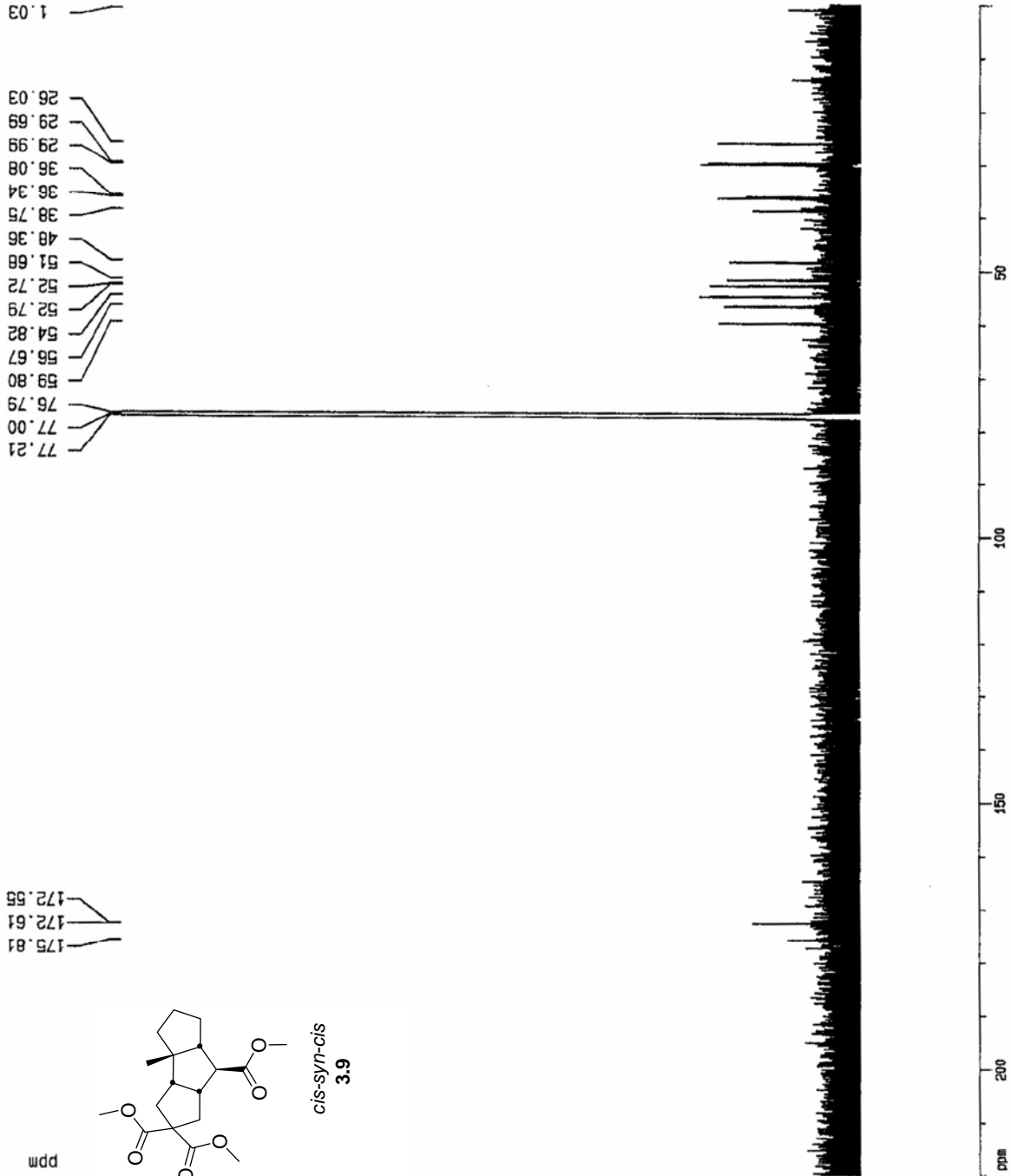
===== CHANNEL f1 =====
 NUC1 13C
 P1 13.50 usec
 PL1 0.00 dB
 SFO1 151.0953827 MHz

===== CHANNEL f2 =====
 CPDPRG2 waltz16
 NUC2 1H
 PCD2 100.00 usec
 PL2 0.00 dB
 PL12 12.00 dB
 SFO2 500.8336050 MHz

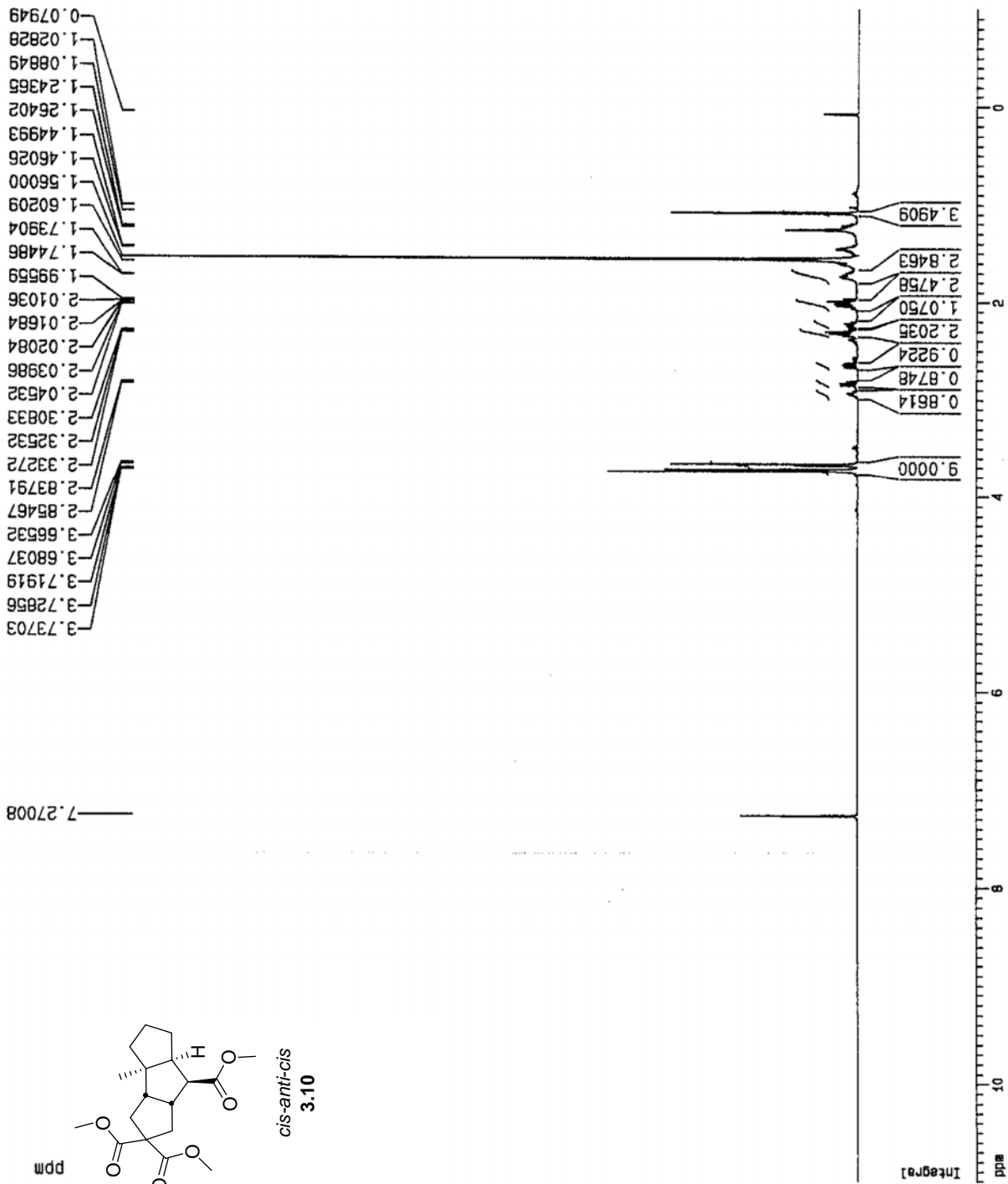
F2 - Processing parameters

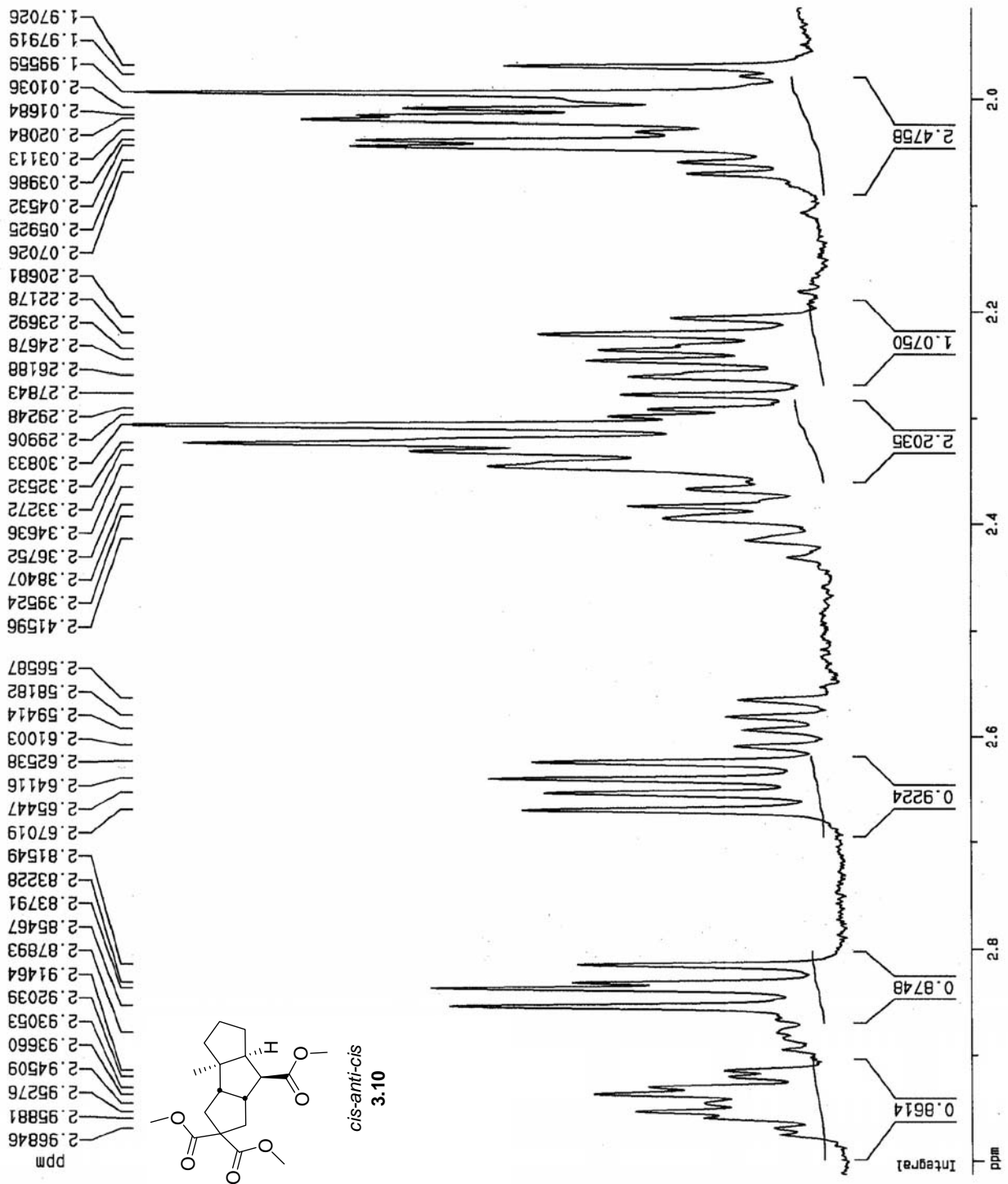
SI 65536
 SF 151.0788327 MHz
 WDW EM
 SSB 0
 LB 1.00 Hz
 GB 0
 PC 1.00

ID NMR plot parameters
 CX 20.00 cm
 F1P 220.000 ppm
 F1 33237.34 Hz
 F2P 0.000 ppm
 F2 0.00 Hz
 PPMCM 11.00000 ppm/cm
 HZCM 1661.86707 Hz/cm



cis-syn-cis
3.9





APPENDIX B: Crystallographic Data Tables

This information is also available in CIF format from the *J. Am. Chem. Soc.* Webpage at:
http://pubs3.acs.org/acs/journals/supporting_information.page?in_manuscript=ja042595u
Reference: Tripp, J. C.; Schiesser, C. H; Curran, D. P *J. Am. Chem. Soc.* **2005**, *127*, 5518-5527

Crystallographic Tables for Diol 2.43

Table 1. Crystal data and structure refinement for jt0527.

Identification code	jt0527	
Empirical formula	C ₁₂ H ₂₄ O ₂	
Formula weight	200.31	
Temperature	295(2) K	
Wavelength	0.71073 Å	
Crystal system	Monoclinic	
Space group	P2(1)/c	
Unit cell dimensions	a = 17.543(3) Å	α = 90°.
	b = 6.1234(10) Å	β = 105.708(4)°.
	c = 12.0521(19) Å	γ = 90°.
Volume	1246.3(3) Å ³	
Z	4	
Density (calculated)	1.068 Mg/m ³	
Absorption coefficient	0.070 mm ⁻¹	
F(000)	448	
Crystal size	0.03 x 0.03 x 0.18 mm ³	
Theta range for data collection	2.41 to 24.99°.	
Index ranges	-20 ≤ h ≤ 20, -7 ≤ k ≤ 7, -14 ≤ l ≤ 14	
Reflections collected	9457	
Independent reflections	2188 [R(int) = 0.1757]	
Completeness to theta = 24.99°	100.0 %	
Absorption correction	None	
Refinement method	Full-matrix least-squares on F ²	
Data / restraints / parameters	2188 / 0 / 128	
Goodness-of-fit on F ²	1.127	
Final R indices [I > 2σ(I)]	R1 = 0.1611, wR2 = 0.3250	
R indices (all data)	R1 = 0.2559, wR2 = 0.3685	
Extinction coefficient	0.000(4)	
Largest diff. peak and hole	0.330 and -0.284 e.Å ⁻³	

Table 2. Atomic coordinates ($\times 10^4$) and equivalent isotropic displacement parameters ($\text{\AA}^2 \times 10^3$) for jt0527. $U(\text{eq})$ is defined as one third of the trace of the orthogonalized U^{ij} tensor.

	x	y	z	$U(\text{eq})$
C(1)	3622(4)	3413(10)	10412(5)	31(2)
O(1)	4326(3)	116(8)	11279(5)	69(2)
O(2)	4568(4)	5841(8)	11700(5)	77(2)
C(2)	2805(4)	2332(14)	10242(8)	67(3)
C(3)	2210(4)	3519(14)	9243(8)	61(3)
C(4)	2621(5)	5444(16)	9007(8)	70(3)
C(5)	3488(4)	4975(12)	9386(6)	43(2)
C(6)	4247(5)	1728(12)	10419(7)	55(2)
C(7)	3842(5)	4672(13)	11525(7)	57(2)
C(8)	2373(5)	6624(17)	7872(7)	78(3)
C(9)	1359(4)	3428(11)	9301(6)	37(2)
C(10)	774(5)	4496(19)	8296(9)	96(4)
C(11)	1116(6)	1093(17)	9358(14)	151(7)
C(12)	1269(7)	4610(30)	10362(11)	129(5)

Table 3. Bond lengths [Å] and angles [°] for jt0527.

C(1)-C(6)	1.504(9)
C(1)-C(7)	1.504(10)
C(1)-C(5)	1.531(9)
C(1)-C(2)	1.541(9)
O(1)-C(6)	1.411(9)
O(2)-C(7)	1.425(10)
C(2)-C(3)	1.545(10)
C(3)-C(4)	1.450(11)
C(3)-C(9)	1.514(10)
C(4)-C(5)	1.493(10)
C(4)-C(8)	1.503(11)
C(9)-C(11)	1.498(12)
C(9)-C(10)	1.509(11)
C(9)-C(12)	1.514(13)
C(6)-C(1)-C(7)	109.6(6)
C(6)-C(1)-C(5)	112.6(6)
C(7)-C(1)-C(5)	110.3(6)
C(6)-C(1)-C(2)	110.9(6)
C(7)-C(1)-C(2)	110.1(7)
C(5)-C(1)-C(2)	103.1(5)
C(1)-C(2)-C(3)	108.0(6)
C(4)-C(3)-C(9)	126.0(7)
C(4)-C(3)-C(2)	105.6(6)
C(9)-C(3)-C(2)	114.4(7)
C(3)-C(4)-C(5)	107.6(7)
C(3)-C(4)-C(8)	122.2(8)
C(5)-C(4)-C(8)	113.0(7)
C(4)-C(5)-C(1)	106.8(5)
O(1)-C(6)-C(1)	114.2(7)
O(2)-C(7)-C(1)	113.1(6)
C(11)-C(9)-C(10)	108.1(8)
C(11)-C(9)-C(12)	108.7(10)
C(10)-C(9)-C(12)	105.5(8)

C(11)-C(9)-C(3)	109.5(7)
C(10)-C(9)-C(3)	114.3(7)
C(12)-C(9)-C(3)	110.5(7)

Symmetry transformations used to generate equivalent atoms:

Table 4. Anisotropic displacement parameters ($\text{\AA}^2 \times 10^3$) for jt0527. The anisotropic displacement factor exponent takes the form: $-2\pi^2 [h^2 a^{*2} U^{11} + \dots + 2 h k a^* b^* U^{12}]$

	U ¹¹	U ²²	U ³³	U ²³	U ¹³	U ¹²
C(1)	33(4)	30(4)	33(4)	-8(3)	17(3)	3(3)
O(1)	66(4)	30(3)	85(4)	-5(3)	-24(3)	8(3)
O(2)	92(5)	35(3)	70(4)	-1(3)	-40(3)	-2(3)
C(2)	32(4)	63(6)	99(7)	48(5)	3(4)	-3(4)
C(3)	36(5)	57(5)	79(6)	34(5)	-4(4)	3(4)
C(4)	56(6)	85(7)	62(6)	42(5)	2(4)	-13(5)
C(5)	39(4)	47(5)	48(5)	0(4)	21(3)	-10(4)
C(6)	55(5)	33(4)	61(5)	-9(4)	-12(4)	10(4)
C(7)	77(6)	43(5)	57(5)	18(4)	28(5)	33(5)
C(8)	76(7)	90(7)	62(6)	34(6)	11(5)	-3(6)
C(9)	29(4)	33(4)	42(4)	-3(3)	-1(3)	0(3)
C(10)	48(6)	117(9)	110(9)	27(7)	-2(6)	16(6)
C(11)	55(7)	59(7)	290(19)	22(9)	-35(9)	-23(5)
C(12)	80(8)	200(16)	120(10)	-24(10)	50(8)	48(9)

Table 5. Hydrogen coordinates ($\times 10^4$) and isotropic displacement parameters ($\text{\AA}^2 \times 10^{-3}$) for jt0527.

	x	y	z	U(eq)
H(1A)	4673	481	11854	103
H(2C)	4864	5522	12330	116
H(2A)	2637	2448	10943	81
H(2B)	2833	797	10059	81
H(3A)	2201	2580	8582	74
H(4A)	2541	6523	9566	84
H(5A)	3785	6314	9612	52
H(5B)	3659	4305	8765	52
H(6A)	4122	1018	9672	66
H(6B)	4752	2463	10527	66
H(7A)	3422	5697	11530	68
H(7B)	3887	3665	12161	68
H(8A)	1812	6865	7665	116
H(8B)	2508	5757	7288	116
H(8C)	2642	8002	7937	116
H(10A)	794	3789	7593	144
H(10B)	905	6012	8263	144
H(10C)	250	4367	8391	144
H(11A)	1163	334	8682	226
H(11B)	577	1035	9396	226
H(11C)	1453	416	10031	226
H(12A)	726	4546	10382	194
H(12B)	1426	6104	10338	194
H(12C)	1597	3918	11040	194

Crystallographic Tables for Cyclopentane 2.62

Table 1. Crystal data and structure refinement for trip104.

Identification code	trip104	
Empirical formula	C ₁₇ H ₂₂ N ₂ O ₆	
Formula weight	350.37	
Temperature	295(2) K	
Wavelength	0.71073 Å	
Crystal system	Monoclinic	
Space group	P2(1)/c	
Unit cell dimensions	a = 20.881(10) Å	α = 90°.
	b = 8.843(4) Å	β = 92.772(10)°.
	c = 10.102(5) Å	γ = 90°.
Volume	1863.1(15) Å ³	
Z	4	
Density (calculated)	1.249 Mg/m ³	
Absorption coefficient	0.095 mm ⁻¹	
F(000)	744	
Crystal size	0.03 x 0.07 x 0.16 mm ³	
Theta range for data collection	1.95 to 23.99°.	
Index ranges	-23 ≤ h ≤ 23, -10 ≤ k ≤ 10, -11 ≤ l ≤ 11	
Reflections collected	12308	
Independent reflections	2912 [R(int) = 0.0930]	
Completeness to theta = 23.99°	99.7 %	
Absorption correction	Sadabs	
Refinement method	Full-matrix least-squares on F ²	
Data / restraints / parameters	2912 / 0 / 227	
Goodness-of-fit on F ²	1.120	
Final R indices [I > 2σ(I)]	R1 = 0.1581, wR2 = 0.4022	
R indices (all data)	R1 = 0.1802, wR2 = 0.4141	
Extinction coefficient	0.013(5)	
Largest diff. peak and hole	0.357 and -0.365 e.Å ⁻³	

Table 2. Atomic coordinates ($\times 10^4$) and equivalent isotropic displacement parameters ($\text{\AA}^2 \times 10^3$) for trip104. $U(\text{eq})$ is defined as one third of the trace of the orthogonalized U^{ij} tensor.

	x	y	z	$U(\text{eq})$
C(1)	1644(4)	5165(8)	8413(7)	54(2)
N(1)	1838(5)	6527(8)	6348(8)	77(2)
O(1)	2409(4)	6528(11)	6664(8)	122(3)
C(2)	1387(4)	5749(8)	7238(8)	60(2)
N(2)	-330(4)	4716(9)	7243(8)	76(2)
O(2)	1605(4)	7114(9)	5338(7)	103(2)
C(3)	746(5)	5613(8)	6819(8)	65(2)
O(3)	-528(4)	5396(10)	6230(7)	107(3)
C(4)	367(4)	4845(9)	7654(8)	62(2)
O(4)	-676(3)	3953(8)	7945(9)	102(2)
O(5)	1139(3)	2895(8)	11188(6)	86(2)
C(5)	592(4)	4232(9)	8830(8)	64(2)
O(6)	2098(3)	3946(7)	10760(5)	72(2)
C(6)	1231(4)	4388(8)	9221(8)	58(2)
C(7)	1475(4)	3662(9)	10510(8)	62(2)
C(8)	2407(5)	3267(11)	11969(9)	79(3)
C(9)	3135(5)	3324(12)	11800(9)	87(3)
C(10)	3285(4)	4930(11)	12277(8)	74(2)
C(11)	2881(5)	5087(14)	13506(11)	96(3)
C(12)	2267(5)	4182(13)	13163(9)	93(3)
C(13)	3472(7)	2021(16)	12545(13)	128(5)
C(14)	3995(5)	5548(16)	12400(12)	102(4)
C(15)	4368(6)	4970(20)	13656(14)	149(6)
C(16)	3957(7)	7280(20)	12494(19)	164(7)
C(17)	4358(6)	5150(20)	11182(13)	135(5)

Table 3. Bond lengths [Å] and angles [°] for trip104.

C(1)-C(2)	1.378(11)
C(1)-C(6)	1.398(10)
N(1)-O(2)	1.225(10)
N(1)-O(1)	1.220(11)
N(1)-C(2)	1.500(11)
C(2)-C(3)	1.390(12)
N(2)-O(4)	1.237(10)
N(2)-O(3)	1.240(10)
N(2)-C(4)	1.498(11)
C(3)-C(4)	1.366(11)
C(4)-C(5)	1.368(12)
O(5)-C(7)	1.212(9)
C(5)-C(6)	1.381(12)
O(6)-C(7)	1.335(10)
O(6)-C(8)	1.481(10)
C(6)-C(7)	1.518(11)
C(8)-C(12)	1.493(13)
C(8)-C(9)	1.538(14)
C(9)-C(10)	1.528(14)
C(9)-C(13)	1.530(15)
C(10)-C(11)	1.541(13)
C(10)-C(14)	1.579(14)
C(11)-C(12)	1.538(15)
C(14)-C(15)	1.544(17)
C(14)-C(16)	1.54(2)
C(14)-C(17)	1.518(17)
C(2)-C(1)-C(6)	117.5(8)
O(2)-N(1)-O(1)	124.1(8)
O(2)-N(1)-C(2)	117.3(9)
O(1)-N(1)-C(2)	118.5(8)
C(3)-C(2)-C(1)	124.0(7)
C(3)-C(2)-N(1)	118.7(8)
C(1)-C(2)-N(1)	117.3(8)
O(4)-N(2)-O(3)	123.9(9)

O(4)-N(2)-C(4)	117.9(8)
O(3)-N(2)-C(4)	118.2(8)
C(4)-C(3)-C(2)	115.7(8)
C(5)-C(4)-C(3)	123.2(9)
C(5)-C(4)-N(2)	119.9(8)
C(3)-C(4)-N(2)	116.8(8)
C(4)-C(5)-C(6)	119.7(8)
C(7)-O(6)-C(8)	117.5(6)
C(5)-C(6)-C(1)	119.8(7)
C(5)-C(6)-C(7)	118.9(7)
C(1)-C(6)-C(7)	121.2(8)
O(5)-C(7)-O(6)	125.7(8)
O(5)-C(7)-C(6)	122.8(8)
O(6)-C(7)-C(6)	111.5(7)
O(6)-C(8)-C(12)	110.6(8)
O(6)-C(8)-C(9)	106.8(7)
C(12)-C(8)-C(9)	107.8(8)
C(10)-C(9)-C(13)	117.5(9)
C(10)-C(9)-C(8)	100.6(8)
C(13)-C(9)-C(8)	110.8(10)
C(9)-C(10)-C(11)	103.0(8)
C(9)-C(10)-C(14)	121.6(9)
C(11)-C(10)-C(14)	117.0(8)
C(12)-C(11)-C(10)	104.8(8)
C(8)-C(12)-C(11)	105.7(8)
C(15)-C(14)-C(16)	107.8(12)
C(15)-C(14)-C(17)	109.7(10)
C(16)-C(14)-C(17)	108.2(13)
C(15)-C(14)-C(10)	112.6(11)
C(16)-C(14)-C(10)	107.4(9)
C(17)-C(14)-C(10)	111.1(10)

Symmetry transformations used to generate equivalent atoms:

Table 4. Anisotropic displacement parameters ($\text{\AA}^2 \times 10^3$) for trip104. The anisotropic displacement factor exponent takes the form: $-2\pi^2 [h^2 a^{*2} U^{11} + \dots + 2 h k a^* b^* U^{12}]$

	U ¹¹	U ²²	U ³³	U ²³	U ¹³	U ¹²
C(1)	68(5)	47(4)	47(4)	-2(3)	3(3)	-2(3)
N(1)	106(6)	62(4)	64(5)	15(4)	27(5)	-4(4)
O(1)	105(6)	162(8)	102(6)	26(6)	23(5)	-37(6)
C(2)	91(6)	39(4)	52(4)	-2(3)	18(4)	0(4)
N(2)	77(5)	80(5)	70(5)	-7(4)	-1(4)	-2(4)
O(2)	132(6)	101(5)	78(5)	41(4)	27(4)	1(4)
C(3)	98(7)	42(4)	56(5)	0(4)	3(4)	10(4)
O(3)	104(5)	148(7)	66(4)	5(5)	-14(4)	13(5)
C(4)	86(6)	46(4)	56(5)	-8(4)	8(4)	-9(4)
O(4)	85(5)	80(5)	140(7)	6(5)	1(4)	-20(4)
O(5)	107(5)	88(5)	64(4)	21(3)	2(3)	-31(4)
C(5)	83(6)	49(4)	62(5)	-8(4)	9(4)	-9(4)
O(6)	87(4)	73(4)	54(3)	17(3)	3(3)	-10(3)
C(6)	82(6)	35(4)	59(5)	-3(3)	8(4)	-5(4)
C(7)	88(6)	49(4)	49(4)	4(4)	4(4)	-9(4)
C(8)	103(7)	69(5)	63(5)	11(4)	-2(5)	-8(5)
C(9)	100(7)	102(8)	60(5)	-6(5)	10(5)	19(6)
C(10)	86(6)	83(6)	52(5)	3(4)	1(4)	9(5)
C(11)	76(6)	115(9)	97(8)	-24(7)	4(5)	5(6)
C(12)	106(8)	117(8)	58(5)	10(5)	26(5)	-6(6)
C(13)	158(12)	123(10)	99(9)	-3(8)	-12(8)	48(9)
C(14)	56(6)	142(11)	109(9)	-1(8)	1(5)	8(6)
C(15)	85(8)	238(18)	119(10)	-23(12)	-43(7)	15(10)
C(16)	122(11)	162(15)	207(18)	-22(13)	-20(11)	-71(11)
C(17)	86(8)	222(17)	99(9)	4(10)	14(7)	-3(9)

Table 5. Hydrogen coordinates ($\times 10^4$) and isotropic displacement parameters ($\text{\AA}^2 \times 10^{-3}$) for trip104.

	x	y	z	U(eq)
H(1A)	2077	5285	8658	65
H(3A)	586	6020	6022	78
H(5A)	315	3713	9364	77
H(8A)	2264	2220	12076	95
H(9A)	3218	3248	10856	105
H(10A)	3069	5583	11610	88
H(11A)	3108	4672	14285	115
H(11B)	2782	6140	13671	115
H(12A)	2164	3528	13894	111
H(12B)	1908	4857	12972	111
H(13A)	3924	2070	12419	191
H(13B)	3306	1075	12211	191
H(13C)	3397	2099	13473	191
H(15A)	4415	3889	13604	223
H(15B)	4137	5222	14424	223
H(15C)	4784	5429	13721	223
H(16A)	3732	7674	11716	247
H(16B)	4383	7696	12560	247
H(16C)	3733	7560	13265	247
H(17A)	4386	4067	11103	203
H(17B)	4782	5567	11265	203
H(17C)	4137	5553	10406	203

APPENDIX C: Gaussian Entry Archives

Chair-Equatorial 2.63

MP2/6-311G**

```
1\1\CHEMCLUSTER-KNET10\FTS\UMP2-FC\6-311G(d,p)\C10H19(2)\CARLHS\02-Au
g-2004\1\#\MP2/6-311G** OPT=(GRAD,TS,READFC,NOEIGENTEST) GEOM=CHECKPOI
NT GUESS=READ\tert-butylhexenyl cyclization TS - cis-
chair\0,2\C\C,1,cc2\C,2,cc3,1,ccc3\C,2,cc4,3,ccc4,1,dih4,0\C,4,cc5,2,cc
c5,3,dih5,0\C,5,cc6,4,ccc6,2,dih6,0\C,1,cc7,2,ccc7,3,dih7,0\C,7,cc8,1,
ccc8,2,dih8,0\C,7,cc9,1,ccc9,2,dih9,0\C,7,cc10,1,ccc10,2,dih10,0\H,3,h
c11,2,hcc11,1,dih11,0\H,3,hc12,2,hcc12,1,dih12,0\H,2,hc13,3,hcc13,1,di
h13,0\H,4,hc14,2,hcc14,3,dih14,0\H,4,hc15,2,hcc15,3,dih15,0\H,5,hc16,4
,hcc16,2,dih16,0\H,5,hc17,4,hcc17,2,dih17,0\H,6,hc18,5,hcc18,4,dih18,0
\H,6,hc19,5,hcc19,4,dih19,0\H,1,hc20,2,hcc20,3,dih20,0\H,8,hc21,7,hcc2
1,1,dih21,0\H,8,hc22,7,hcc22,1,dih22,0\H,8,hc23,7,hcc23,1,dih23,0\H,9,
hc24,7,hcc24,1,dih24,0\H,9,hc25,7,hcc25,1,dih25,0\H,9,hc26,7,hcc26,1,d
ih26,0\H,10,hc27,7,hcc27,1,dih27,0\H,10,hc28,7,hcc28,1,dih28,0\H,10,hc
29,7,hcc29,1,dih29,0\cc2=2.23130145\cc3=1.35415345\ccc3=112.7423977\c
c4=1.51320502\ccc4=121.4241114\dih4=-108.46798016\cc5=1.52777801\ccc5=
111.54232961\dih5=143.88990796\cc6=1.52877233\ccc6=106.6214492\dih6=-5
0.98797842\cc7=1.51446232\ccc7=117.73488834\dih7=8.08202027\cc8=1.5329
9087\ccc8=109.61799984\dih8=62.22181059\cc9=1.53321172\ccc9=112.846155
89\dih9=-60.11515709\cc10=1.5439221\ccc10=107.88144764\dih10=180.05498
936\hc11=1.0857062\hcc11=120.89741815\dih11=91.95806395\hc12=1.0840303
7\hcc12=121.74735051\dih12=-84.89704689\hc13=1.08871807\hcc13=117.5253
057\dih13=98.24779899\hc14=1.09731452\hcc14=108.61718477\dih14=23.0845
1232\hc15=1.09726528\hcc15=108.84266146\dih15=-93.41728639\hc16=1.0978
8678\hcc16=109.62848552\dih16=67.22576476\hc17=1.09558027\hcc17=111.49
85315\dih17=-173.72414384\hc18=1.09647503\hcc18=109.21159303\dih18=-66
.61606031\hc19=1.10075155\hcc19=110.74876685\dih19=175.46229368\hc20=1
.09491077\hcc20=93.88959245\dih20=125.41027979\hc21=1.09636202\hcc21=1
10.51415928\dih21=56.8069876\hc22=1.0962788\hcc22=110.47156357\dih22=1
76.381635\hc23=1.09267951\hcc23=110.71737498\dih23=-63.46598964\hc24=1
.09631811\hcc24=109.67093195\dih24=180.07916674\hc25=1.09471427\hcc25=
111.56847531\dih25=-60.84104151\hc26=1.09250246\hcc26=110.81176554\dih
26=60.2923637\hc27=1.09587441\hcc27=110.80054251\dih27=-57.05652135\hc
28=1.09503954\hcc28=111.07333148\dih28=63.50422447\hc29=1.09707765\hcc
29=110.0499719\dih29=-176.78694613\Version=x86-Linux-G03RevB.04\State
=2-A\HF=-389.7517918\MP2=-391.2306445\PUHF=-389.7696929\PMP2-0=-391.24
59873\S2=0.985458\S2-1=0.916574\S2A=0.759351\RMSD=9.997e-09\RMSF=1.643
e-05\Dipole=-0.2152658,0.0776339,-0.1370106\PG=C01 [X(C10H19)]\@
```

BHLYP/6-311G**

```
1\1\CHEMCLUSTER-KNET6\FTS\UBHandHLYP\6-311G(d,p)\C10H19(2)\CARLHS\01-
Aug-2004\1\#\BHANDHLYP/6-311G** OPT=(GRAD,TS,READFC,NOEIGENTEST)
GEOM=
```

CHECKPOINT GUESS=READ\\tert-butylhexenyl cyclization TS – cis-chair\\0,2\C\C,1,cc2\C,2,cc3,1,ccc3\C,2,cc4,3,ccc4,1,dih4,0\C,4,cc5,2,ccc5,3,dih5,0\C,5,cc6,4,ccc6,2,dih6,0\C,1,cc7,2,ccc7,3,dih7,0\C,7,cc8,1,ccc8,2,dih8,0\C,7,cc9,1,ccc9,2,dih9,0\C,7,cc10,1,ccc10,2,dih10,0\H,3,hc11,2,hcc11,1,dih11,0\H,3,hc12,2,hcc12,1,dih12,0\H,2,hc13,3,hcc13,1,dih13,0\H,4,hc14,2,hcc14,3,dih14,0\H,4,hc15,2,hcc15,3,dih15,0\H,5,hc16,4,hcc16,2,dih16,0\H,5,hc17,4,hcc17,2,dih17,0\H,6,hc18,5,hcc18,4,dih18,0\H,6,hc19,5,hcc19,4,dih19,0\H,1,hc20,2,hcc20,3,dih20,0\H,8,hc21,7,hcc21,1,dih21,0\H,8,hc22,7,hcc22,1,dih22,0\H,8,hc23,7,hcc23,1,dih23,0\H,9,hc24,7,hcc24,1,dih24,0\H,9,hc25,7,hcc25,1,dih25,0\H,9,hc26,7,hcc26,1,dih26,0\H,10,hc27,7,hcc27,1,dih27,0\H,10,hc28,7,hcc28,1,dih28,0\H,10,hc29,7,hcc29,1,dih29,0\\cc2=2.18980902\cc3=1.3715969\ccc3=114.37364303\cc4=1.50861935\ccc4=120.87578639\dih4=-110.9506488\cc5=1.52076581\ccc5=111.12389872\dih5=145.96464548\cc6=1.52169203\ccc6=106.96349563\dih6=-49.07723611\cc7=1.5160304\ccc7=118.58845899\dih7=7.50248107\cc8=1.52986357\ccc8=109.62957635\dih8=61.79511898\cc9=1.52989408\ccc9=112.87440884\dih9=-60.34736733\cc10=1.5401404\ccc10=108.13847792\dih10=179.56303948\hc11=1.07745946\hcc11=121.15997353\dih11=91.45977918\hc12=1.0757411\hcc12=121.69043203\dih12=-84.42550948\hc13=1.07953342\hcc13=116.30387118\dih13=101.15942865\hc14=1.08850793\hcc14=108.90523875\dih14=25.15508669\hc15=1.0882826\hcc15=109.43287508\dih15=-91.21515944\hc16=1.08936107\hcc16=109.76927984\dih16=69.65964497\hc17=1.08644602\hcc17=111.58333984\dih17=-171.90122655\hc18=1.08750715\hcc18=109.24535301\dih18=-69.12688364\hc19=1.09104962\hcc19=110.678553\dih19=173.65727029\hc20=1.08404219\hcc20=93.79336904\dih20=124.46520616\hc21=1.08734555\hcc21=110.91672108\dih21=56.6765741\hcc22=1.08703221\hcc22=110.65027198\dih22=176.19484392\hc23=1.08386556\hcc23=111.23281461\dih23=-63.71290354\hc24=1.08707274\hcc24=110.01174788\dih24=180.10896868\hc25=1.08569679\hcc25=111.86450092\dih25=-60.7314473\hc26=1.08381936\hcc26=111.12519539\dih26=60.3801219\hc27=1.08688529\hcc27=111.17583977\dih27=-57.37389428\hc28=1.08591976\hcc28=111.4550709\dih28=63.26242061\hc29=1.08761393\hcc29=110.29696532\dih29=-177.03295816\\Version=x86-Linux-G03Rev B.04\State=2-A\HF=-392.2550652\S2=0.826565\S2-1=0.\S2A=0.750781\RMSE=3.822e-09\RMSF=3.426e-05\Dipole=-0.193569,0.0619395,-0.1447944\PG=C01 [X(C10H19)]\\@

BHLYP/cc-pVDZ**

1\1\ CHEMCLUSTER-KNET12\Freq\UBHandHLYP\CC-pVDZ\C10H19(2)\CARLHS\14-Aug-2004\1\#\BHANDHLYP/CC-PVDZ FREQ=NORAMAN GEOM=CHECKPOINT GUESS=READ\\tert-butylhexenyl cyclization TS – cis-chair\\0,2\C\C,1,cc2\C,2,cc3,1,ccc3\C,2,cc4,3,ccc4,1,dih4,0\C,4,cc5,2,ccc5,3,dih5,0\C,5,cc6,4,ccc6,2,dih6,0\C,1,cc7,2,ccc7,3,dih7,0\C,7,cc8,1,ccc8,2,dih8,0\C,7,cc9,1,ccc9,2,dih9,0\C,7,cc10,1,ccc10,2,dih10,0\H,3,hc11,2,hcc11,1,dih11,0\H,3,hc12,2,hcc12,1,dih12,0\H,2,hc13,3,hcc13,1,dih13,0\H,4,hc14,2,hcc14,3,dih14,0\H,4,hc15,2,hcc15,3,dih15,0\H,5,hc16,4,hcc16,2,dih16,0\H,5,

hc17,4,hcc17,2,dih17,0\H,6,hc18,5,hcc18,4,dih18,0\H,6,hc19,5,hcc19,4,dih19,0\H,1,hc20,2,hcc20,3,dih20,0\H,8,hc21,7,hcc21,1,dih21,0\H,8,hc22,7,hcc22,1,dih22,0\H,8,hc23,7,hcc23,1,dih23,0\H,9,hc24,7,hcc24,1,dih24,0\H,9,hc25,7,hcc25,1,dih25,0\H,9,hc26,7,hcc26,1,dih26,0\H,10,hc27,7,hcc27,1,dih27,0\H,10,hc28,7,hcc28,1,dih28,0\H,10,hc29,7,hcc29,1,dih29,0\cc2=2.20068464\cc3=1.37547601\ccc3=114.37446391\cc4=1.50900893\ccc4=120.97873046\dih4=-110.81181334\cc5=1.52066768\ccc5=111.2234901\dih5=145.83273699\cc6=1.52137448\ccc6=107.03986682\dih6=-49.18576988\cc7=1.51816537\ccc7=118.75281191\dih7=7.5896219\cc8=1.52997948\ccc8=109.59158598\dih8=61.94484213\cc9=1.53011403\ccc9=112.83574252\dih9=-60.16158761\cc10=1.53987154\ccc10=108.12905139\dih10=179.73350758\hc11=1.08589859\hcc11=121.10230691\dih11=91.42148828\hc12=1.08407336\hcc12=121.60171274\dih12=-84.09836749\hc13=1.08742645\hcc13=116.31659485\dih13=100.90858643\hc14=1.09629306\hcc14=108.88497727\dih14=24.89969451\hc15=1.09605671\hcc15=109.4559421\dih15=-91.35911964\hc16=1.09734029\hcc16=109.74283934\dih16=69.58601799\hc17=1.09407498\hcc17=111.60810851\dih17=-172.11356145\hc18=1.09521543\hcc18=109.28455103\dih18=-68.85617307\hc19=1.09863416\hcc19=110.65811687\dih19=174.04389363\hc20=1.09185711\hcc20=93.81045763\dih20=124.60696411\hc21=1.09501691\hcc21=110.97889257\dih21=56.63197867\hc22=1.09468629\hcc22=110.71551889\dih22=176.16862005\hc23=1.09170969\hcc23=111.28170286\dih23=-63.72453032\hc24=1.09477168\hcc24=110.0911908\dih24=180.22511811\hc25=1.09351294\hcc25=111.89738814\dih25=-60.63567935\hc26=1.09169417\hcc26=111.1870977\dih26=60.4650933\hc27=1.09470607\hcc27=111.23767922\dih27=-57.33777891\hc28=1.09377617\hcc28=111.51367511\dih28=63.28897445\hc29=1.09539511\hcc29=110.37582343\dih29=-177.01070724\Version=x86-Linux-G03RevB.04\State=2-A\HF=-392.1708576\S2=0.828984\S2-1=0.\S2A=0.750818\RMSD=3.535e-09\RMSF=2.365e-05\Dipole=-0.1899796,0.0590236,-0.1305518\

BHLYP/aug-cc-pVDZ**

1\1\ CHEMCLUSTER-KNET3\FTS\UBHandHLYP\Aug-CC-pVDZ\C10H19(2)\CARLHS\03-Aug-2004\1\#\BHANDHLYP/AUG-CC-PVDZ OPT=(GRAD,TS,READFC,NOEIGENTEST) GE

OM=CHECKPOINT GUESS=READ\tert-butylhexenyl cyclization TS - cis-chair\0,2\C\C,1,cc2\C,2,cc3,1,ccc3\C,2,cc4,3,ccc4,1,dih4,0\C,4,cc5,2,ccc5,3,dih5,0\C,5,cc6,4,ccc6,2,dih6,0\C,1,cc7,2,ccc7,3,dih7,0\C,7,cc8,1,ccc8,2,dih8,0\C,7,cc9,1,ccc9,2,dih9,0\C,7,cc10,1,ccc10,2,dih10,0\H,3,hc11,2,hcc11,1,dih11,0\H,3,hc12,2,hcc12,1,dih12,0\H,2,hc13,3,hcc13,1,dih13,0\H,4,hc14,2,hcc14,3,dih14,0\H,4,hc15,2,hcc15,3,dih15,0\H,5,hc16,4,hcc16,2,dih16,0\H,5,hc17,4,hcc17,2,dih17,0\H,6,hc18,5,hcc18,4,dih18,0\H,6,hc19,5,hcc19,4,dih19,0\H,1,hc20,2,hcc20,3,dih20,0\H,8,hc21,7,hcc21,1,dih21,0\H,8,hc22,7,hcc22,1,dih22,0\H,8,hc23,7,hcc23,1,dih23,0\H,9,hc24,7,hcc24,1,dih24,0\H,9,hc25,7,hcc25,1,dih25,0\H,9,hc26,7,hcc26,1,dih26,0\H,10,hc27,7,hcc27,1,dih27,0\H,10,hc28,7,hcc28,1,dih28,0\H,10,hc29,7,hcc29,1,dih29,0\cc2=2.2013806\cc3=1.37477796\ccc3=114.33475674\cc4=1.50877124\ccc4=121.12138395\dih4=-110.82474415\cc5=1.52

134789\ccc5=111.17136022\dih5=146.23720626\cc6=1.52206432\ccc6=107.045
04144\dih6=-49.42666386\cc7=1.516194\ccc7=118.67998711\dih7=6.82618093
\ccc8=1.52966757\ccc8=109.633904\dih8=62.0969781\cc9=1.52978098\ccc9=11
2.83789334\dih9=-60.04108981\cc10=1.53994435\ccc10=108.00802518\dih10=
179.92619976\hc11=1.08296019\hcc11=121.19192786\dih11=91.63194717\hc12
=1.08121954\hcc12=121.62035651\dih12=-84.1027383\hc13=1.08441534\hcc13
=116.28731858\dih13=100.61376244\hc14=1.09316569\hcc14=108.8802551\dih
14=25.36345068\hc15=1.09310921\hcc15=109.36862097\dih15=-91.04180604\h
c16=1.09408592\hcc16=109.79306619\dih16=69.44265945\hc17=1.09143084\h
c17=111.49502111\dih17=-172.07614068\hc18=1.09189342\hcc18=109.2299583
3\dih18=-69.1163097\hc19=1.09578226\hcc19=110.65512481\dih19=173.64644
95\hc20=1.08845844\hcc20=93.64224174\dih20=123.85134468\hc21=1.0919831
8\hcc21=110.89999136\dih21=56.67577126\hc22=1.09176131\hcc22=110.65567
714\dih22=176.22055014\hc23=1.08862824\hcc23=111.17612976\dih23=-63.68
808463\hc24=1.09168135\hcc24=109.9938943\dih24=180.20916108\hc25=1.090
25299\hcc25=111.8293364\dih25=-60.65597949\hc26=1.08841849\hcc26=111.0
8047117\dih26=60.48551125\hc27=1.09169648\hcc27=111.14756787\dih27=-57
.25396732\hc28=1.09064023\hcc28=111.41061907\dih28=63.37478045\hc29=1.
0924174\hcc29=110.2939663\dih29=-176.92991653\\Version=x86-Linux-G03Re
vB.04\State=2-A\HF=-392.1932547\S2=0.82603\S2-1=0.\S2A=0.750785\RMSE=9
.356e-09\RMSE=2.754e-05\Dipole=-0.2050929,0.0638116,-0.1851088\PG=C01
[X(C10H19)]\@

Chair-Axial 2.64

MP2/6-311G**

1\1\ CHEMCLUSTER-KNET15\FTS\UMP2-FC\6-311G(d,p)\C10H19(2)\CARLHS\06-Au
g-2004\1\#MP2/6-311G** OPT=(GRAD,TS,READFC,NOEIGENTEST,NOFREEZE) GEOM
=CHECKPOINT GUESS=READ\tert-butylhexenyl cyclization TS – trans-chair\0,2
\C\C,1,r\C,2,cc3,1,ccc3\C,1,cc4,2,ccc4,3,dih4,0\C,1,cc5,2,ccc5,3,dih5,
0\C,2,cc6,3,ccc6,1,dih6,0\C,6,cc7,2,ccc7,3,dih7,0\C,5,cc8,1,ccc8,2,dih
8,0\C,5,cc9,1,ccc9,2,dih9,0\C,5,cc10,1,ccc10,2,dih10,0\H,1,hc11,2,hcc1
1,3,dih11,0\H,2,hc12,3,hcc12,1,dih12,0\H,3,hc13,2,hcc13,1,dih13,0\H,3,
hc14,2,hcc14,1,dih14,0\H,6,hc15,2,hcc15,3,dih15,0\H,6,hc16,2,hcc16,3,d
ih16,0\H,7,hc17,6,hcc17,2,dih17,0\H,7,hc18,6,hcc18,2,dih18,0\H,4,hc19,
1,hcc19,2,dih19,0\H,4,hc20,1,hcc20,2,dih20,0\H,8,hc21,5,hcc21,1,dih21,
0\H,8,hc22,5,hcc22,1,dih22,0\H,8,hc23,5,hcc23,1,dih23,0\H,9,hc24,5,hcc
24,1,dih24,0\H,9,hc25,5,hcc25,1,dih25,0\H,9,hc26,5,hcc26,1,dih26,0\H,1
0,hc27,5,hcc27,1,dih27,0\H,10,hc28,5,hcc28,1,dih28,0\H,10,hc29,5,hcc29
,1,dih29,0\ccc3=1.34890722\ccc3=107.44204204\cc4=1.50996816\ccc4=95.91
557786\dih4=131.94134094\cc5=1.51608875\ccc5=111.01404046\dih5=-101.83
22809\cc6=1.51054744\ccc6=123.01489062\dih6=104.43082934\cc7=1.5267461
7\ccc7=110.80886702\dih7=-144.95793032\cc8=1.53428606\ccc8=109.9521439
8\dih8=56.16543746\cc9=1.54392464\ccc9=107.78320612\dih9=173.78775113\
cc10=1.53334129\ccc10=113.05666197\dih10=-66.49021682\hc11=1.09015652\

hcc11=97.62152633\dih11=15.31506518\hc12=1.08872742\hcc12=118.04415959
\dih12=-98.54617943\hc13=1.08415827\hcc13=121.51824849\dih13=85.664078
76\hc14=1.08594246\hcc14=120.88592585\dih14=-89.11128026\hc15=1.097207
97\hcc15=109.09717063\dih15=-23.58195977\hc16=1.09756839\hcc16=108.825
31497\dih16=93.3183526\hc17=1.09575815\hcc17=109.22088653\dih17=-65.23
710066\hc18=1.09625417\hcc18=111.64520224\dih18=176.0782263\hc19=1.096
64698\hcc19=109.42392035\dih19=-97.29076098\hc20=1.09910825\hcc20=111.
58382689\dih20=144.56886215\hc21=1.09571381\hcc21=110.57425628\dih21=5
3.00794463\hc22=1.09390036\hcc22=111.40895306\dih22=-67.2033059\hc23=1
.09637841\hcc23=110.25311656\dih23=172.71967937\hc24=1.0952939\hcc24=1
10.53929886\dih24=-59.42123919\hc25=1.09713807\hcc25=110.24117161\dih2
5=-179.16838565\hc26=1.09506139\hcc26=111.16087036\dih26=60.95441681\h
c27=1.09448923\hcc27=111.68079023\dih27=62.50337708\hc28=1.09492659\h
c28=111.55892852\dih28=-58.86538291\hc29=1.09608359\hcc29=109.67914503
\dih29=-178.10544681\rc=2.2523784\Version=x86-Linux-G03RevB.04\State=2
-A\HF=-389.7512035\MP2=-391.2302372\PUHF=-389.7688341\PMP2-0=-391.2453
975\S2=0.986243\S2-1=0.918453\S2A=0.759553\RMSD=5.098e-09\RMSF=1.931e-
05\Dipole=-0.1831039,-0.0624719,-0.1898693\PG=C01 [X(C10H19)]\@

BHLYP/6-311G**

1\1\ CHEMCLUSTER-KNET15\FTS\UBHandHLYP\6-311G(d,p)\C10H19(2)\CARLHS\04
-Aug-2004\1\#BHANDHLYP/6-311G**

OPT=(GRAD,TS,READFC,NOEIGENTEST,NOFRE

EZE) GEOM=CHECKPOINT GUESS=READ\tert-butylhexenyl cyclization TS - trans-

chair\0,2\C\C,1,r\C,2,cc3,1,ccc3\C,1,cc4,2,ccc4,3,dih4,0\C,1,cc5,2,ccc
5,3,dih5,0\C,2,cc6,3,ccc6,1,dih6,0\C,6,cc7,2,ccc7,3,dih7,0\C,5,cc8,1,c
cc8,2,dih8,0\C,5,cc9,1,ccc9,2,dih9,0\C,5,cc10,1,ccc10,2,dih10,0\H,1,hc
11,2,hcc11,3,dih11,0\H,2,hc12,3,hcc12,1,dih12,0\H,3,hc13,2,hcc13,1,dih
13,0\H,3,hc14,2,hcc14,1,dih14,0\H,6,hc15,2,hcc15,3,dih15,0\H,6,hc16,2,
hcc16,3,dih16,0\H,7,hc17,6,hcc17,2,dih17,0\H,7,hc18,6,hcc18,2,dih18,0\
H,4,hc19,1,hcc19,2,dih19,0\H,4,hc20,1,hcc20,2,dih20,0\H,8,hc21,5,hcc21
,1,dih21,0\H,8,hc22,5,hcc22,1,dih22,0\H,8,hc23,5,hcc23,1,dih23,0\H,9,h
c24,5,hcc24,1,dih24,0\H,9,hc25,5,hcc25,1,dih25,0\H,9,hc26,5,hcc26,1,di
h26,0\H,10,hc27,5,hcc27,1,dih27,0\H,10,hc28,5,hcc28,1,dih28,0\H,10,hc2
9,5,hcc29,1,dih29,0\cc3=1.36613271\ccc3=108.89181693\cc4=1.50787495\c
cc4=95.87969317\dih4=131.8357007\cc5=1.51801567\ccc5=112.50212773\dih5
=-101.13333295\cc6=1.50554646\ccc6=122.254848\dih6=106.661246\cc7=1.51
932859\ccc7=110.59451562\dih7=-146.25028487\cc8=1.53041295\ccc8=109.93
04782\dih8=56.7173932\cc9=1.53988732\ccc9=107.86156008\dih9=174.325408
9\cc10=1.53027571\ccc10=113.08896224\dih10=-65.76957742\hc11=1.0798712
4\hcc11=97.68550336\dih11=16.07882666\hc12=1.07932476\hcc12=117.017114
2\dih12=-101.55909409\hc13=1.07589835\hcc13=121.56323232\dih13=85.5814
0725\hc14=1.07775244\hcc14=121.07990372\dih14=-88.55116729\hc15=1.0885
3554\hcc15=109.25934102\dih15=-24.91938201\hc16=1.08872729\hcc16=109.4
0139985\dih16=91.7027809\hc17=1.08755448\hcc17=109.41598213\dih17=-67.
71970814\hc18=1.08695632\hcc18=111.64949783\dih18=174.0971418\hc19=1.0

8752148\hcc19=109.23077226\dih19=-98.23447398\hc20=1.08911538\hcc20=111.6332388\dih20=144.34570438\hc21=1.08667225\hcc21=110.95094442\dih21=53.9448954\hc22=1.08491996\hcc22=111.63049554\dih22=-66.31072567\hc23=1.08709988\hcc23=110.55968766\dih23=173.62034678\hc24=1.08643814\hcc24=110.93081668\dih24=-59.10728813\hc25=1.08775183\hcc25=110.50965068\dih25=-178.81063225\hc26=1.0859887\hcc26=111.54188069\dih26=61.30240912\hc27=1.08547635\hcc27=111.83826201\dih27=62.55552809\hc28=1.08583806\hcc28=111.78834289\dih28=-58.6849458\hc29=1.086846\hcc29=110.07306514\dih29=-177.98493858\r=2.21508175\\Version=x86-Linux-G03RevB.04\State=2-A\HF=-392.254233\S2=0.827342\S2-1=0.\S2A=0.750801\RMSD=4.128e-09\RMSF=3.484e-05\Dipole=-0.1604153,-0.0553529,-0.1899717\PG=C01 [X(C10H19)]\

@

BHLYP/cc-pVDZ**

1\1\ CHEMCLUSTER-KNET10\FTS\UBHandHLYP\CC-pVDZ\C10H19(2)\CARLHS\04-Aug-2004\1\#\BHANDHLYP\CC-PVDZ

OPT=(GRAD,TS,READFC,NOEIGENTEST,NOFREEZE)

GEOM=CHECKPOINT GUESS=READ\\tert-butylhexenyl cyclization TS – trans-chair\

\0,2\C\C,1,r\C,2,cc3,1,ccc3\C,1,cc4,2,ccc4,3,dih4,0\C,1,cc5,2,ccc5,3,dih5,0\C,2,cc6,3,ccc6,1,dih6,0\C,6,cc7,2,ccc7,3,dih7,0\C,5,cc8,1,ccc8,2,dih8,0\C,5,cc9,1,ccc9,2,dih9,0\C,5,cc10,1,ccc10,2,dih10,0\H,1,hc11,2,hcc11,3,dih11,0\H,2,hc12,3,hcc12,1,dih12,0\H,3,hc13,2,hcc13,1,dih13,0\H,3,hc14,2,hcc14,1,dih14,0\H,6,hc15,2,hcc15,3,dih15,0\H,6,hc16,2,hcc16,3,dih16,0\H,7,hc17,6,hcc17,2,dih17,0\H,7,hc18,6,hcc18,2,dih18,0\H,4,hc19,1,hcc19,2,dih19,0\H,4,hc20,1,hcc20,2,dih20,0\H,8,hc21,5,hcc21,1,dih21,0\H,8,hc22,5,hcc22,1,dih22,0\H,8,hc23,5,hcc23,1,dih23,0\H,9,hc24,5,hcc24,1,dih24,0\H,9,hc25,5,hcc25,1,dih25,0\H,9,hc26,5,hcc26,1,dih26,0\H,10,hc27,5,hcc27,1,dih27,0\H,10,hc28,5,hcc28,1,dih28,0\H,10,hc29,5,hcc29,1,dih29,0\ccc3=1.37011297\ccc3=108.90481014\cc4=1.50894533\ccc4=95.64269156\dih4=131.78088718\cc5=1.52048079\ccc5=112.59561408\dih5=-101.18340512\cc6=1.50608757\ccc6=122.38691401\dih6=106.56716002\cc7=1.51918326\ccc7=110.63114776\dih7=-146.21654729\cc8=1.53063844\ccc8=109.87679375\dih8=56.87647606\cc9=1.53969946\ccc9=107.82342746\dih9=174.46378802\cc10=1.53057445\ccc10=113.13489497\dih10=-65.59599361\hc11=1.08797696\hcc11=97.8824794\dih11=16.05767877\hc12=1.08736003\hcc12=117.01970432\dih12=-101.30511883\hc13=1.08421018\hcc13=121.45743664\dih13=85.43887994\hc14=1.08613109\hcc14=121.0334271\dih14=-88.51926369\hc15=1.09632373\hcc15=109.28388404\dih15=-24.77266028\hc16=1.0964919\hcc16=109.43286452\dih16=91.77983749\hc17=1.09561897\hcc17=109.38146679\dih17=-67.47420773\hc18=1.09466628\hcc18=111.6871235\dih18=174.5086607\hc19=1.09515205\hcc19=109.21553442\dih19=-97.99107741\hc20=1.09684128\hcc20=111.65872133\dih20=144.66529559\hc21=1.09437639\hcc21=111.01818541\dih21=53.8428716\hc22=1.09273085\hcc22=111.67596005\dih22=-66.40122213\hc23=1.09478244\hcc23=110.62049693\dih23=173.53540696\hc24=1.09424508\hcc24=111.00145946\dih24=-59.1167499\hc25=1.09554277\hcc25=110.59245726\dih25=-178.84611555\hc26=1.0938461\hcc26=111.57109767\dih26=61.27537281

\hc27=1.09332199\hcc27=111.89104021\dih27=62.51703983\hc28=1.09360476\
hcc28=111.85697736\dih28=-58.75591281\hc29=1.0946261\hcc29=110.1421353
5\dih29=-178.03493756\r=2.22501266\\Version=x86-Linux-G03RevB.04\State
=2-A\HF=-392.1698217\S2=0.829603\S2-1=0.\S2A=0.750836\RMSD=6.320e-09\R
MSF=3.410e-05\Dipole=-0.1704833,-0.0420482,-0.181867\PG=C01 [X(C10H19)
J]\@

BHLYP/aug-cc-pVDZ**

1\1\ CHEMCLUSTER-KNET5\FTS\UBHandHLYP\Aug-CC-pVDZ\C10H19(2)\CARLHS\06-
Aug-2004\1\#\BHANDHLYP/AUG-CC-PVDZ

OPT=(GRAD,TS,READFC,NOEIGENTEST,NOF

REEZE) GEOM=CHECKPOINT GUESS=READ\\tert-butylhexenyl cyclization TS – trans-

chair\0,2\C\C,1,r\C,2,cc3,1,ccc3\C,1,cc4,2,ccc4,3,dih4,0\C,1,cc5,2,c
cc5,3,dih5,0\C,2,cc6,3,ccc6,1,dih6,0\C,6,cc7,2,ccc7,3,dih7,0\C,5,cc8,1
,ccc8,2,dih8,0\C,5,cc9,1,ccc9,2,dih9,0\C,5,cc10,1,ccc10,2,dih10,0\H,1,
hc11,2,hcc11,3,dih11,0\H,2,hc12,3,hcc12,1,dih12,0\H,3,hc13,2,hcc13,1,d
ih13,0\H,3,hc14,2,hcc14,1,dih14,0\H,6,hc15,2,hcc15,3,dih15,0\H,6,hc16,
2,hcc16,3,dih16,0\H,7,hc17,6,hcc17,2,dih17,0\H,7,hc18,6,hcc18,2,dih18,
0\H,4,hc19,1,hcc19,2,dih19,0\H,4,hc20,1,hcc20,2,dih20,0\H,8,hc21,5,hcc
21,1,dih21,0\H,8,hc22,5,hcc22,1,dih22,0\H,8,hc23,5,hcc23,1,dih23,0\H,9
,hc24,5,hcc24,1,dih24,0\H,9,hc25,5,hcc25,1,dih25,0\H,9,hc26,5,hcc26,1,
dih26,0\H,10,hc27,5,hcc27,1,dih27,0\H,10,hc28,5,hcc28,1,dih28,0\H,10,h
c29,5,hcc29,1,dih29,0\\ccc3=1.36926002\ccc3=108.78493003\cc4=1.50806779
\ccc4=95.69589617\dih4=131.77754915\cc5=1.51800038\ccc5=112.30480767\d
ih5=-101.3351738\cc6=1.50592155\ccc6=122.45455936\dih6=106.46378541\cc
7=1.52005294\cc7=110.69558507\dih7=-145.96234949\cc8=1.53038627\ccc8=
109.9235212\dih8=56.76417681\cc9=1.53983682\ccc9=107.76660229\dih9=174
.43979841\cc10=1.53024691\ccc10=113.05374651\dih10=-65.71514296\hc11=1
.08452481\hcc11=97.61802365\dih11=15.91335688\hc12=1.08411142\hcc12=11
7.05786115\dih12=-100.87208373\hc13=1.08150299\hcc13=121.5301691\dih13
=85.35814594\hc14=1.08331115\hcc14=121.13608298\dih14=-89.24397539\hc1
5=1.09328365\hcc15=109.21201812\dih15=-24.57266588\hc16=1.09359872\hcc
16=109.34671053\dih16=92.08048247\hc17=1.09224757\hcc17=109.42435924\d
ih17=-67.69231422\hc18=1.09196606\hcc18=111.53545716\dih18=174.1440086
2\hc19=1.09232928\hcc19=109.22461477\dih19=-98.11135887\hc20=1.0939948
5\hcc20=111.59375837\dih20=144.44337692\hc21=1.09145003\hcc21=110.9515
9273\dih21=53.9242196\hc22=1.08973697\hcc22=111.63057345\dih22=-66.387
07832\hc23=1.09189601\hcc23=110.53007629\dih23=173.59217802\hc24=1.091
3256\hcc24=110.91526032\dih24=-59.01454536\hc25=1.09267773\hcc25=110.5
1854175\dih25=-178.75589541\hc26=1.09088414\hcc26=111.4866036\dih26=61
.3724741\hc27=1.09015977\hcc27=111.83580051\dih27=62.57973545\hc28=1.0
9051654\hcc28=111.76894498\dih28=-58.71854565\hc29=1.09152583\hcc29=11
0.0505674\dih29=-177.97033792\r=2.22744449\\Version=x86-Linux-G03RevB.
04\State=2-A\HF=-392.1926802\S2=0.825479\S2-1=0.\S2A=0.750786\RMSD=2.9
97e-09\RMSF=5.710e-05\Dipole=-0.1907371,-0.0558838,-0.2300665\PG=C01 [
X(C10H19)]\@

Boat-Equatorial 2.65

MP2/6-311G**

```
1\1\ CHEMCLUSTER-KNET9\FTS\UMP2-FC\6-311G(d,p)\C10H19(2)\CARLHS\16-Aug
-2004\1\1\#MP2/6-311G** OPT=(GRAD,TS,READFC,NOEIGENTEST,NOFREEZE) GEOM=
CHECKPOINT GUESS=READ\tert-butylhexenyl cyclization TS - cis-
boat\0,2\C\C,1,r\C,2,cc3,1,ccc3\C,1,cc4,2,ccc4,3,dih4,0\C,1,cc5,2,cc
c5,3,dih5,0\C,2,cc6,3,ccc6,1,dih6,0\C,5,cc7,1,ccc7,2,dih7,0\C,5,cc8,1,
ccc8,2,dih8,0\C,5,cc9,1,ccc9,2,dih9,0\C,6,cc10,2,ccc10,3,dih10,0\H,6,h
c11,2,hcc11,3,dih11,0\H,6,hc12,2,hcc12,3,dih12,0\H,10,hc13,6,hcc13,2,d
ih13,0\H,10,hc14,6,hcc14,2,dih14,0\H,4,hc15,1,hcc15,2,dih15,0\H,4,hc16
,1,hcc16,2,dih16,0\H,1,hc17,2,hcc17,3,dih17,0\H,2,hc18,3,hcc18,1,dih18
,0\H,3,hc19,2,hcc19,1,dih19,0\H,3,hc20,2,hcc20,1,dih20,0\H,7,hc21,5,hc
c21,1,dih21,0\H,7,hc22,5,hcc22,1,dih22,0\H,7,hc23,5,hcc23,1,dih23,0\H,
8,hc24,5,hcc24,1,dih24,0\H,8,hc25,5,hcc25,1,dih25,0\H,8,hc26,5,hcc26,1
,dih26,0\H,9,hc27,5,hcc27,1,dih27,0\H,9,hc28,5,hcc28,1,dih28,0\H,9,hc2
9,5,hcc29,1,dih29,0\ccc3=1.35224449\ccc3=112.82513106\cc4=1.5137957\cc
c4=97.79702417\dih4=104.19953797\cc5=1.51400574\ccc5=115.22867385\dih5
=-24.72806115\cc6=1.51964755\ccc6=120.63008741\dih6=103.04254185\cc7=1
.54446267\ccc7=107.90791771\dih7=-174.19918634\cc8=1.53319876\ccc8=109
.92350379\dih8=-56.57248442\cc9=1.53291426\ccc9=112.47787036\dih9=65.9
8443815\cc10=1.52840616\ccc10=109.27871294\dih10=-73.54535009\hc11=1.0
9535201\hcc11=109.75845184\dih11=48.81747254\hc12=1.09666292\hcc12=109
.81650451\dih12=166.85054758\hc13=1.0960629\hcc13=109.2093382\dih13=58
.84389973\hc14=1.09640364\hcc14=112.07165962\dih14=-181.78498198\hc15=
1.09761877\hcc15=109.58663594\dih15=108.0073912\hc16=1.09596684\hcc16=
111.39472595\dih16=-133.72705595\hc17=1.09294742\hcc17=92.84642316\dih
17=-140.71270288\hc18=1.08732227\hcc18=117.63478497\dih18=-99.60832256
\hc19=1.08381046\hcc19=121.77403593\dih19=86.99548197\hc20=1.08618024\
hcc20=121.14137157\dih20=-90.17283118\hc21=1.09565594\hcc21=110.690701
12\dih21=58.80023711\hc22=1.09711619\hcc22=110.0452391\dih22=178.47622
409\hc23=1.09493655\hcc23=111.25405042\dih23=-61.74394249\hc24=1.09638
607\hcc24=110.50983305\dih24=-56.06455616\hc25=1.09245415\hcc25=110.92
909428\dih25=64.33522043\hc26=1.09628317\hcc26=110.39783036\dih26=-175
.51983698\hc27=1.09521915\hcc27=111.52416228\dih27=58.34117305\hc28=1.
09632043\hcc28=109.7932722\dih28=-182.47192178\hc29=1.0926933\hcc29=11
0.83810814\dih29=-62.60809855\r=2.2296369\Version=x86-Linux-G03RevB.0
4\State=2-A\HF=-389.7462302\MP2=-391.227236\PUHF=-389.7641956\PMP2-0=-
391.2426793\S2=0.989811\S2-1=0.920841\S2A=0.759828\RMSD=3.592e-09\RMSF
=6.341e-06\Dipole=-0.1600088,-0.0875349,-0.1531037\PG=C01 [X(C10H19)]\
\@
```

BHLYP/6-311G**

```
1\1\ CHEMCLUSTER-KNET23\FTS\UBHandHLYP\6-311G(d,p)\C10H19(2)\CARLHS\14
```


-Aug-2004\1\#BHANDHLYP/6-311G**

OPT=(GRAD,TS,READFC,NOEIGENTEST,NOFRE

EZE) GEOM=CHECKPOINT GUESS=READ\\tert-butylhexenyl cyclization TS - cis-

boat\0,2\C\C,1,r\C,2,cc3,1,ccc3\C,1,cc4,2,ccc4,3,dih4,0\C,

1,cc5,2,ccc5,3,dih5,0\C,2,cc6,3,ccc6,1,dih6,0\C,5,cc7,1,ccc7,2,dih7,0\

C,5,cc8,1,ccc8,2,dih8,0\C,5,cc9,1,ccc9,2,dih9,0\C,6,cc10,2,ccc10,3,dih

10,0\H,6,hc11,2,hcc11,3,dih11,0\H,6,hc12,2,hcc12,3,dih12,0\H,10,hc13,6

,hcc13,2,dih13,0\H,10,hc14,6,hcc14,2,dih14,0\H,4,hc15,1,hcc15,2,dih15,

0\H,4,hc16,1,hcc16,2,dih16,0\H,1,hc17,2,hcc17,3,dih17,0\H,2,hc18,3,hcc

18,1,dih18,0\H,3,hc19,2,hcc19,1,dih19,0\H,3,hc20,2,hcc20,1,dih20,0\H,7

,hc21,5,hcc21,1,dih21,0\H,7,hc22,5,hcc22,1,dih22,0\H,7,hc23,5,hcc23,1,

dih23,0\H,8,hc24,5,hcc24,1,dih24,0\H,8,hc25,5,hcc25,1,dih25,0\H,8,hc26

,5,hcc26,1,dih26,0\H,9,hc27,5,hcc27,1,dih27,0\H,9,hc28,5,hcc28,1,dih28

,0\H,9,hc29,5,hcc29,1,dih29,0\cc3=1.37050066\ccc3=113.79747867\cc4=1.

51147399\ccc4=97.59051265\dih4=107.23177038\cc5=1.51621879\ccc5=116.73

756391\dih5=-22.72996832\cc6=1.51449396\ccc6=120.30145306\dih6=105.991

53168\cc7=1.5405595\ccc7=108.04878479\dih7=-174.31741015\cc8=1.5299008

1\ccc8=109.88729305\dih8=-56.76419143\cc9=1.52952382\ccc9=112.62181692

\dih9=65.66830842\cc10=1.52076443\ccc10=109.55954931\dih10=-78.7725318

4\hc11=1.08661566\hcc11=110.15824871\dih11=43.86330518\hc12=1.08779927

\hcc12=109.65313765\dih12=161.29652493\hc13=1.08783026\hcc13=109.31304

609\dih13=63.13981155\hc14=1.08712428\hcc14=111.88632129\dih14=-178.35

569373\hc15=1.08844896\hcc15=109.3297329\dih15=107.73689409\hc16=1.086

46348\hcc16=111.5147249\dih16=-134.75736282\hc17=1.08221365\hcc17=93.1

0115177\dih17=-138.51464318\hc18=1.07794303\hcc18=116.48418874\dih18=-

102.78558313\hc19=1.07551994\hcc19=121.68693479\dih19=86.16188515\hc20

=1.07779873\hcc20=121.40215317\dih20=-89.92486808\hc21=1.08668446\hcc2

1=111.07822809\dih21=58.69493106\hc22=1.08770368\hcc22=110.30057543\di

h22=178.32426944\hc23=1.08588696\hcc23=111.65457761\dih23=-61.90977263

\hc24=1.08728071\hcc24=110.90195534\dih24=-55.96053876\hc25=1.08366094

\hcc25=111.38921382\dih25=64.50844895\hc26=1.08705995\hcc26=110.610117

27\dih26=-175.38682258\hc27=1.0861201\hcc27=111.73663919\dih27=58.3153

0769\hc28=1.08704358\hcc28=110.17650821\dih28=-182.41556137\hc29=1.083

73001\hcc29=111.11188263\dih29=-62.55137814\r=2.19475749\\Version=x86-

Linux-G03RevB.04\State=2-A\HF=-392.2503205\S2=0.828687\S2-1=0.\S2A=0.7

50823\RMSD=3.986e-09\RMSF=2.527e-05\Dipole=-0.1507661,-0.0734521,-0.15

04174\PG=C01 [X(C10H19)]\@

BHLYP/cc-pVDZ**

1\1\CHEMCLUSTER-KNET9\FTS\UBHandHLYP\CC-pVDZ\C10H19(2)\CARLHS\14-Aug-

2004\1\#BHANDHLYP/CC-PVDZ

OPT=(GRAD,TS,READFC,NOEIGENTEST,NOFREEZE) G

EOM=CHECKPOINT GUESS=READ\\tert-butylhexenyl cyclization TS - cis-

boat\0,2\C\C,1,r\C,2,cc3,1,ccc3\C,1,cc4,2,ccc4,3,dih4,0\C,1,cc5,

2,ccc5,3,dih5,0\C,2,cc6,3,ccc6,1,dih6,0\C,5,cc7,1,ccc7,2,dih7,0\C,5,cc

8,1,ccc8,2,dih8,0\C,5,cc9,1,ccc9,2,dih9,0\C,6,cc10,2,ccc10,3,dih10,0\H

,6,hc11,2,hcc11,3,dih11,0\H,6,hc12,2,hcc12,3,dih12,0\H,10,hc13,6,hcc13,2,dih13,0\H,10,hc14,6,hcc14,2,dih14,0\H,4,hc15,1,hcc15,2,dih15,0\H,4,hc16,1,hcc16,2,dih16,0\H,1,hc17,2,hcc17,3,dih17,0\H,2,hc18,3,hcc18,1,dih18,0\H,3,hc19,2,hcc19,1,dih19,0\H,3,hc20,2,hcc20,1,dih20,0\H,7,hc21,5,hcc21,1,dih21,0\H,7,hc22,5,hcc22,1,dih22,0\H,7,hc23,5,hcc23,1,dih23,0\H,8,hc24,5,hcc24,1,dih24,0\H,8,hc25,5,hcc25,1,dih25,0\H,8,hc26,5,hcc26,1,dih26,0\H,9,hc27,5,hcc27,1,dih27,0\H,9,hc28,5,hcc28,1,dih28,0\H,9,hc29,5,hcc29,1,dih29,0\ccc3=1.37504145\ccc3=113.99995159\cc4=1.51240575\ccc4=97.26672238\dih4=108.81591049\cc5=1.5189221\ccc5=116.82900248\dih5=-20.94780926\cc6=1.51538722\ccc6=120.30788331\dih6=106.33919609\cc7=1.54039425\ccc7=108.02487332\dih7=-174.64509006\cc8=1.53007499\ccc8=109.8706231\dih8=-57.12696696\cc9=1.52984816\ccc9=112.60338535\dih9=65.3305536\cc10=1.52057858\ccc10=109.64519824\dih10=-79.9432809\hc11=1.09451229\hcc11=110.19758001\dih11=42.68298921\hc12=1.09548687\hcc12=109.68225213\dih12=160.05755546\hc13=1.09602456\hcc13=109.23961493\dih13=63.04075781\hc14=1.09492693\hcc14=111.93538267\dih14=-178.57217636\hc15=1.09605324\hcc15=109.34176894\dih15=106.14178138\hc16=1.0943927\hcc16=111.5554334\dih16=-136.39121725\hc17=1.08997905\hcc17=93.38217985\dih17=-136.82521665\hc18=1.08576656\hcc18=116.42013053\dih18=-102.40382962\hc19=1.08385773\hcc19=121.62353854\dih19=85.47761808\hc20=1.08630782\hcc20=121.34145178\dih20=-90.22982422\hc21=1.09452289\hcc21=111.14905291\dih21=58.53891362\hc22=1.09550546\hcc22=110.36490454\dih22=178.17641932\hc23=1.09373289\hcc23=111.70944126\dih23=-62.07518803\hc24=1.09498852\hcc24=110.95399713\dih24=-56.01855398\hc25=1.0913913\hcc25=111.46388253\dih25=64.43823227\hc26=1.09475291\hcc26=110.65237217\dih26=-175.43331138\hc27=1.09397691\hcc27=111.75395743\dih27=58.26993959\hc28=1.09479787\hcc28=110.25497207\dih28=-182.5001224\hc29=1.09169878\hcc29=111.1835274\dih29=-62.60434908\rr=2.20496082\\Version=x86-Linux-G03RevB.04\State=2-A\HF=-392.1657503\S2=0.831417\S2-1=0.\S2A=0.750864\RMSD=6.642e-09\RMSF=2.946e-05\Dipole=-0.1464813,-0.0686936,-0.1377149\PG=C01 [X(C10H19)]\@

BHLYP/aug-cc-pVDZ**

1\1\CHEMCLUSTER-KNET10\FTS\UBHandHLYP\Aug-CC-pVDZ\C10H19(2)\CARLHS\15-Aug-2004\1\#BHANDHLYP/AUG-CC-PVDZ
 OPT=(GRAD,TS,READFC,NOEIGENTEST,NO
 FREEZE) GEOM=CHECKPOINT GUESS=READ\tert-butylhexenyl cyclization TS – cis-boat\0,2\C\C,1,r\C,2,cc3,1,ccc3\C,1,cc4,2,ccc4,3,dih4,0\C,1,cc5,2,ccc5,3,dih5,0\C,2,cc6,3,ccc6,1,dih6,0\C,5,cc7,1,ccc7,2,dih7,0\C,5,cc8,1,ccc8,2,dih8,0\C,5,cc9,1,ccc9,2,dih9,0\C,6,cc10,2,ccc10,3,dih10,0\H,6,hc11,2,hcc11,3,dih11,0\H,6,hc12,2,hcc12,3,dih12,0\H,10,hc13,6,hcc13,2,dih13,0\H,10,hc14,6,hcc14,2,dih14,0\H,4,hc15,1,hcc15,2,dih15,0\H,4,hc16,1,hcc16,2,dih16,0\H,1,hc17,2,hcc17,3,dih17,0\H,2,hc18,3,hcc18,1,dih18,0\H,3,hc19,2,hcc19,1,dih19,0\H,3,hc20,2,hcc20,1,dih20,0\H,7,hc21,5,hcc21,1,dih21,0\H,7,hc22,5,hcc22,1,dih22,0\H,7,hc23,5,hcc23,1,dih23,0\H,8,hc24,5,hcc24,1,dih24,0\H,8,hc25,5,hcc25,1,dih25,0\H,8,h

c26,5,hcc26,1,dih26,0\H,9,hc27,5,hcc27,1,dih27,0\H,9,hc28,5,hcc28,1,dih28,0\H,9,hc29,5,hcc29,1,dih29,0\cc3=1.37402574\ccc3=113.87593374\cc4=1.51200556\ccc4=97.4340559\dih4=108.13191798\cc5=1.51660469\ccc5=116.77797056\dih5=-21.67397666\cc6=1.51518919\ccc6=120.42570988\dih6=106.08356066\cc7=1.54049882\ccc7=107.94797469\dih7=-174.467631\cc8=1.52984948\ccc8=109.89686694\dih8=-56.85983159\cc9=1.5294977\ccc9=112.55888049\dih9=65.59062397\cc10=1.52143108\ccc10=109.68890292\dih10=-79.33831637\hc11=1.0915815\hcc11=110.15342938\dih11=43.21339865\hc12=1.0926738\hcc12=109.60428294\dih12=160.71933429\hc13=1.09251718\hcc13=109.31790168\dih13=63.1071743\hc14=1.09198899\hcc14=111.77553826\dih14=-178.36211703\hc15=1.09312014\hcc15=109.31380967\dih15=106.92134179\hc16=1.09116735\hcc16=111.49389728\dih16=-135.52413751\hc17=1.08684935\hcc17=93.05322393\dih17=-137.51806274\hc18=1.0829572\hcc18=116.48135489\dih18=-102.17209876\hc19=1.08097812\hcc19=121.67608339\dih19=85.60627095\hc20=1.0832582\hcc20=121.40046024\dih20=-90.34033869\hc21=1.09149982\hcc21=111.04669045\dih21=58.54899804\hc22=1.09252771\hcc22=110.29967039\dih22=178.19807903\hc23=1.09066293\hcc23=111.61939415\dih23=-62.04246958\hc24=1.09194341\hcc24=110.8820588\dih24=-56.08261956\hc25=1.0883129\hcc25=111.37997526\dih25=64.39441858\hc26=1.09179341\hcc26=110.58904215\dih26=-175.50034032\hc27=1.09065608\hcc27=111.69803441\dih27=58.42754007\hc28=1.09162123\hcc28=110.13893422\dih28=-182.37691673\hc29=1.0885025\hcc29=111.11538765\dih29=-62.52197086\r=2.20455032\Version=x86-Linux-G03RevB.04\State=2-A\HF=-392.188454\S2=0.828205\S2-1=0.\S2A=0.750826\RMSD=4.170e-09\RMSF=2.510e-05\Dipole=-0.163207,-0.0765512,-0.1894014\PG=C01 [X(C10H19)]\@

Boat-Axial 2.66

MP2/6-311G**

1\1\CHEMCLUSTER-KNET19\FTS\UMP2-FC\6-311G(d,p)\C10H19(2)\CARLHS\02-Au-g-2004\1\#\MP2/6-311G** OPT=(GRAD,TS,READFC,NOEIGENTEST) GEOM=CHECKPOINT GUESS=READ\tert-butylhexenyl cyclization TS – trans-boat\0,2\C\C,1,cc2\C,2,cc3,1,ccc3\C,2,cc4,3,ccc4,1,dih4,0\C,4,cc5,2,ccc5,3,dih5,0\C,5,cc6,4,ccc6,2,dih6,0\C,1,cc7,2,ccc7,3,dih7,0\C,7,cc8,1,ccc8,2,dih8,0\C,7,cc9,1,ccc9,2,dih9,0\C,7,cc10,1,ccc10,2,dih10,0\H,2,hc11,3,hcc11,1,dih11,0\H,4,hc12,2,hcc12,3,dih12,0\H,4,hc13,2,hcc13,3,dih13,0\H,5,hc14,4,hcc14,2,dih14,0\H,5,hc15,4,hcc15,2,dih15,0\H,6,hc16,5,hcc16,4,dih16,0\H,6,hc17,5,hcc17,4,dih17,0\H,1,hc18,2,hcc18,3,dih18,0\H,8,hc19,7,hcc19,1,dih19,0\H,8,hc20,7,hcc20,1,dih20,0\H,8,hc21,7,hcc21,1,dih21,0\H,9,hc22,7,hcc22,1,dih22,0\H,9,hc23,7,hcc23,1,dih23,0\H,9,hc24,7,hcc24,1,dih24,0\H,10,hc25,7,hcc25,1,dih25,0\H,10,hc26,7,hcc26,1,dih26,0\H,10,hc27,7,hcc27,1,dih27,0\H,3,hc28,2,hcc28,1,dih28,0\H,3,hc29,2,hcc29,1,dih29,0\cc2=2.25659832\cc3=1.34895166\ccc3=107.02691502\cc4=1.51901739\ccc4=121.74201524\dih4=103.09788398\cc5=1.53180873\ccc5=110.30757685\dih5=-80.42437246\cc6=1.53164837\ccc6=106.83900156\dih6=-55.27

475912\cc7=1.51449576\ccc7=112.21379516\dih7=-110.67232656\cc8=1.53387
207\ccc8=109.44889912\dih8=62.04628842\cc9=1.54309826\ccc9=108.0547117
2\dih9=180.10144335\cc10=1.53426125\ccc10=112.94154435\dih10=-59.99359
788\hc11=1.08598981\hcc11=117.82563868\dih11=-97.30940377\hc12=1.09522
797\hcc12=109.76858977\dih12=42.15068438\hc13=1.09668314\hcc13=109.483
53496\dih13=159.82388844\hc14=1.09640883\hcc14=111.69604549\dih14=-177
.78009398\hc15=1.09690978\hcc15=109.19746865\dih15=63.08368404\hc16=1.
10044265\hcc16=110.41919634\dih16=173.38703567\hc17=1.09605528\hcc17=1
08.83637527\dih17=-69.1696954\hc18=1.09208274\hcc18=96.63008868\dih18=
7.01010245\hc19=1.09580394\hcc19=110.52375562\dih19=55.15229023\hc20=1
.09450516\hcc20=111.22322794\dih20=-64.88757014\hc21=1.0962669\hcc21=1
10.46044094\dih21=174.91688554\hc22=1.09551581\hcc22=110.61402078\dih2
2=-58.46711747\hc23=1.09727173\hcc23=110.33156589\dih23=-178.32874895\
hc24=1.09530619\hcc24=110.91066315\dih24=61.81707061\hc25=1.09467869\
cc25=111.6580968\dih25=59.05021599\hc26=1.09419575\hcc26=111.73759732\
dih26=-62.33330192\hc27=1.09602211\hcc27=109.65372476\dih27=178.520651
7\hc28=1.08433881\hcc28=121.43201697\dih28=83.81428976\hc29=1.08640341
\hcc29=121.13455865\dih29=-91.28508483\Version=x86-Linux-G03RevB.04\S
tate=2-A\HF=-389.7507696\MP2=-391.2289001\PUHF=-389.7686184\PMP2-0=-39
1.2442993\S2=0.993739\S2-1=0.925212\S2A=0.759982\RMSD=6.793e-09\RMSF=1
.898e-05\Dipole=-0.155251,-0.0821864,-0.2269171\PG=C01 [X(C10H19)]\@

BHLYP/6-311G**

1\1\ CHEMCLUSTER-KNET18\FTS\UBHandHLYP\6-311G(d,p)\C10H19(2)\CARLHS\31
-Jul-2004\1\#\BHANDHLYP\6-311G** OPT=(GRAD,TS,READFC,NOEIGENTEST) GEOM
=CHECKPOINT GUESS=READ\tert-butylhexenyl cyclization TS - trans-
boat\0,2\C,C,1,cc2\C,2,cc3,1,ccc3\C,2,cc4,3,ccc4,1,dih4,0\C,4,cc5,2
,ccc5,3,dih5,0\C,5,cc6,4,ccc6,2,dih6,0\C,1,cc7,2,ccc7,3,dih7,0\C,7,cc8
,1,ccc8,2,dih8,0\C,7,cc9,1,ccc9,2,dih9,0\C,7,cc10,1,ccc10,2,dih10,0\H,
2,hc11,3,hcc11,1,dih11,0\H,4,hc12,2,hcc12,3,dih12,0\H,4,hc13,2,hcc13,3
,dih13,0\H,5,hc14,4,hcc14,2,dih14,0\H,5,hc15,4,hcc15,2,dih15,0\H,6,hc1
6,5,hcc16,4,dih16,0\H,6,hc17,5,hcc17,4,dih17,0\H,1,hc18,2,hcc18,3,dih1
8,0\H,8,hc19,7,hcc19,1,dih19,0\H,8,hc20,7,hcc20,1,dih20,0\H,8,hc21,7,h
cc21,1,dih21,0\H,9,hc22,7,hcc22,1,dih22,0\H,9,hc23,7,hcc23,1,dih23,0\H
,9,hc24,7,hcc24,1,dih24,0\H,10,hc25,7,hcc25,1,dih25,0\H,10,hc26,7,hcc2
6,1,dih26,0\H,10,hc27,7,hcc27,1,dih27,0\H,3,hc28,2,hcc28,1,dih28,0\H,3
,hc29,2,hcc29,1,dih29,0\cc2=2.21648427\cc3=1.36724792\ccc3=108.210793
04\cc4=1.51514506\ccc4=121.35137602\dih4=106.15996936\cc5=1.52543303\c
cc5=110.94705455\dih5=-89.56169143\cc6=1.52224326\ccc6=107.44534088\di
h6=-49.22031746\cc7=1.516014\ccc7=114.02859259\dih7=-102.95459182\cc8=
1.53036636\ccc8=109.46445388\dih8=60.39683611\cc9=1.53938139\ccc9=108.
21394147\dih9=178.38995045\cc10=1.53066777\ccc10=112.99981021\dih10=-6
1.43431059\hc11=1.07708278\hcc11=116.85190145\dih11=-100.41749808\hc12
=1.08625184\hcc12=110.02266833\dih12=33.33567678\hc13=1.08764941\hcc13
=109.23958067\dih13=150.25931304\hc14=1.0871008\hcc14=111.51435362\dih
14=-172.13505401\hc15=1.08874705\hcc15=109.43702825\dih15=69.55470015\

hc16=1.0913568\hcc16=110.41757097\dih16=173.97581227\hc17=1.08719569\h
cc17=109.1699296\dih17=-68.98581923\hc18=1.08207522\hcc18=96.38193818\
dih18=14.69203902\hc19=1.08674836\hcc19=110.96300677\dih19=55.25483347\
\hc20=1.08529723\hcc20=111.41239937\dih20=-64.86056463\hc21=1.08699252\
\hcc21=110.6631118\dih21=175.03539167\hc22=1.08662186\hcc22=110.997551
48\dih22=-58.29812885\hc23=1.08783013\hcc23=110.55035936\dih23=-178.05
268258\hc24=1.08614468\hcc24=111.3457055\dih24=62.09987692\hc25=1.0857
0186\hcc25=111.79486535\dih25=59.55558717\hc26=1.08529331\hcc26=112.00
234755\dih26=-61.75456085\hc27=1.08679716\hcc27=109.99044652\dih27=178
.97704939\hc28=1.07607876\hcc28=121.49179015\dih28=83.08861257\hc29=1.
07809709\hcc29=121.27946444\dih29=-91.21468588\Version=x86-Linux-G03R
evB.04\State=2-A\HF=-392.2533513\S2=0.830085\S2-1=0.\S2A=0.750839\RMSD
=4.888e-09\RMSF=4.032e-05\Dipole=-0.1458086,-0.0732846,-0.2209501\PG=C
01 [X(C10H19)]\@

BHLYP/cc-pVDZ**

1\1\ CHEMCLUSTER-KNET2\FTS\UBHandHLYP\CC-pVDZ\C10H19(2)\CARLHS\31-Jul-
2004\1\#\BHANDHLYP/CC-PVDZ OPT=(GRAD,TS,READFC,NOEIGENTEST)
GEOM=CHECK

POINT GUESS=READ\tert-butylhexenyl cyclization TS – trans-boat
\0,2\C,C,1,cc2\C,2,cc3,1,ccc3\C,2,cc4,3,ccc4,1,dih4,0\C,4,cc5,2,ccc5,
3,dih5,0\C,5,cc6,4,ccc6,2,dih6,0\C,1,cc7,2,ccc7,3,dih7,0\C,7,cc8,1,ccc
8,2,dih8,0\C,7,cc9,1,ccc9,2,dih9,0\C,7,cc10,1,ccc10,2,dih10,0\H,2,hc11
,3,hcc11,1,dih11,0\H,4,hc12,2,hcc12,3,dih12,0\H,4,hc13,2,hcc13,3,dih13
,0\H,5,hc14,4,hcc14,2,dih14,0\H,5,hc15,4,hcc15,2,dih15,0\H,6,hc16,5,hc
c16,4,dih16,0\H,6,hc17,5,hcc17,4,dih17,0\H,1,hc18,2,hcc18,3,dih18,0\H,
8,hc19,7,hcc19,1,dih19,0\H,8,hc20,7,hcc20,1,dih20,0\H,8,hc21,7,hcc21,1
,dih21,0\H,9,hc22,7,hcc22,1,dih22,0\H,9,hc23,7,hcc23,1,dih23,0\H,9,hc2
4,7,hcc24,1,dih24,0\H,10,hc25,7,hcc25,1,dih25,0\H,10,hc26,7,hcc26,1,di
h26,0\H,10,hc27,7,hcc27,1,dih27,0\H,3,hc28,2,hcc28,1,dih28,0\H,3,hc29,
2,hcc29,1,dih29,0\cc2=2.22575546\cc3=1.3713579\ccc3=108.35810927\cc4=
1.51593068\ccc4=121.44241105\dih4=106.18630213\cc5=1.52528629\ccc5=111
.08942606\dih5=-90.23759849\cc6=1.52178298\ccc6=107.51944909\dih6=-49.
03414276\cc7=1.51812216\ccc7=114.20231011\dih7=-102.16536299\cc8=1.530
53419\ccc8=109.45035325\dih8=60.37023691\cc9=1.53917734\ccc9=108.18869
303\dih9=178.38437032\cc10=1.53086102\ccc10=112.95965454\dih10=-61.442
07537\hc11=1.08512312\hcc11=116.85357109\dih11=-100.03157984\hc12=1.09
406195\hcc12=110.05954385\dih12=32.66457634\hc13=1.09526898\hcc13=109.
21291613\dih13=149.50497066\hc14=1.09476109\hcc14=111.54472002\dih14=-
172.10367346\hc15=1.09678172\hcc15=109.40688408\dih15=69.70867987\hc16
=1.09901018\hcc16=110.41147883\dih16=174.5777847\hc17=1.09492832\hcc17
=109.24471824\dih17=-68.48086924\hc18=1.09017527\hcc18=96.51700527\dih
18=15.57012957\hc19=1.09443678\hcc19=111.03181137\dih19=55.09289728\hc
20=1.09307819\hcc20=111.44536712\dih20=-64.99253221\hc21=1.0946565\hcc
21=110.7306465\dih21=174.90383563\hc22=1.09442262\hcc22=111.06022238\
ih22=-58.33231877\hc23=1.09561705\hcc23=110.63332475\dih23=-178.107998

89\hc24=1.09400171\hcc24=111.39345288\dih24=62.04267154\hc25=1.0936106
1\hcc25=111.83541988\dih25=59.51772316\hc26=1.09315473\hcc26=112.05229
776\dih26=-61.79622792\hc27=1.09453387\hcc27=110.07737882\dih27=178.93
554691\hc28=1.08440577\hcc28=121.39347928\dih28=82.7779569\hc29=1.0865
3287\hcc29=121.23555646\dih29=-91.30551424\\Version=x86-Linux-G03RevB.
04\State=2-A\HF=-392.1689515\S2=0.83238\S2-1=0.\S2A=0.750874\RMSD=4.59
3e-09\RMSF=2.962e-05\Dipole=-0.1542421,-0.0608861,-0.2123918\PG=C01 [X
(C10H19)]\@

BHLYP/aug-cc-pVDZ**

1\1\ CHEMCLUSTER-KNET4FTS\UBHandHLYP\Aug-CC-pVDZ\C10H19(2)\CARLHS\03-
Aug-20041\#\BHANDHLYP/AUG-CC-PVDZ OPT=(GRAD,TS,READFC,NOEIGENTEST)
GE

OM=CHECKPOINT GUESS=READ\\tert-butylhexenyl cyclization TS - trans-
boat\0,2\C\C,1,cc2\C,2,cc3,1,ccc3\C,2,cc4,3,ccc4,1,dih4,0\C,4,cc5
,2,ccc5,3,dih5,0\C,5,cc6,4,ccc6,2,dih6,0\C,1,cc7,2,ccc7,3,dih7,0\C,7,c
c8,1,ccc8,2,dih8,0\C,7,cc9,1,ccc9,2,dih9,0\C,7,cc10,1,ccc10,2,dih10,0\
H,2,hc11,3,hcc11,1,dih11,0\H,4,hc12,2,hcc12,3,dih12,0\H,4,hc13,2,hcc13
,3,dih13,0\H,5,hc14,4,hcc14,2,dih14,0\H,5,hc15,4,hcc15,2,dih15,0\H,6,h
c16,5,hcc16,4,dih16,0\H,6,hc17,5,hcc17,4,dih17,0\H,1,hc18,2,hcc18,3,di
h18,0\H,8,hc19,7,hcc19,1,dih19,0\H,8,hc20,7,hcc20,1,dih20,0\H,8,hc21,7
,hcc21,1,dih21,0\H,9,hc22,7,hcc22,1,dih22,0\H,9,hc23,7,hcc23,1,dih23,0
\H,9,hc24,7,hcc24,1,dih24,0\H,10,hc25,7,hcc25,1,dih25,0\H,10,hc26,7,hc
c26,1,dih26,0\H,10,hc27,7,hcc27,1,dih27,0\H,3,hc28,2,hcc28,1,dih28,0\H
,3,hc29,2,hcc29,1,dih29,0\cc2=2.22844872\cc3=1.37024625\ccc3=108.1762
5624\cc4=1.51525369\ccc4=121.54255695\dih4=106.03459671\cc5=1.52616072
\ccc5=110.9902288\dih5=-89.37002416\cc6=1.52268342\ccc6=107.55848564\d
ih6=-49.42955169\cc7=1.51596358\ccc7=113.831247\dih7=-103.10140477\cc8
=1.53034168\ccc8=109.46337874\dih8=60.39812741\cc9=1.53916686\ccc9=108
.07891847\dih9=178.43207997\cc10=1.53055369\ccc10=112.97031141\dih10=-
61.44476246\hc11=1.0818605\hcc11=116.90399475\dih11=-99.55763654\hc12=
1.09118613\hcc12=110.01350007\dih12=33.41757095\hc13=1.09252993\hcc13=
109.20344923\dih13=150.4673218\hc14=1.09204039\hcc14=111.43134707\dih1
4=-172.22346405\hc15=1.0934356\hcc15=109.44081669\dih15=69.42355441\hc
16=1.09621828\hcc16=110.38018894\dih16=174.11847228\hc17=1.09153322\hc
c17=109.1605509\dih17=-68.80077168\hc18=1.08644569\hcc18=96.32089446\d
ih18=14.59897986\hc19=1.09141998\hcc19=110.95431596\dih19=55.0304344\h
c20=1.09005645\hcc20=111.40939328\dih20=-65.12343846\hc21=1.09171344\h
cc21=110.63594009\dih21=174.81241157\hc22=1.09144318\hcc22=110.9597631
9\dih22=-58.34025084\hc23=1.09266659\hcc23=110.54920473\dih23=-178.115
41793\hc24=1.09088635\hcc24=111.29134424\dih24=62.03920538\hc25=1.0903
8741\hcc25=111.77763209\dih25=59.18661222\hc26=1.08999784\hcc26=111.94
874809\dih26=-62.14477371\hc27=1.09146289\hcc27=109.98092986\dih27=178
.62039038\hc28=1.08160924\hcc28=121.48444933\dih28=82.61523051\hc29=1.
083566\hcc29=121.3309882\dih29=-92.00215831\\Version=x86-Linux-G03RevB
.04\State=2-A\HF=-392.1916733\S2=0.828235\S2-1=0.\S2A=0.750824\RMSD=5.

832e-10\RMSF=3.612e-05\Dipole=-0.1748551,-0.0745232,-0.2597575\PG=C01
[X(C10H19)]\@

APPENDIX D: The Dioxin and Silicon-Tethered Cyclization Precursor

Appendix D: Other Model Systems

Although we were disappointed that the temperature related improvement reported by Ihara turned out to be non-existent,³⁸ we still wanted to focus on the synthesis of linear triquinanes by way of a cascade radical cyclization. It is clear from our work and that of others that the lack of selectivity arises in the second of the three cyclizations in the cascade and so our efforts focused on improving the selectivity of this step. With this in mind we designed two general types of cyclization precursor shown in Figure D-1. Both of these substrates are designed to undergo three consecutive 5-*exo* radical cyclizations to give the linear triquinane as before. However the second hexenyl radical is tethered by either the dioxin or the silicon bridge. We reasoned that by installing this removable tether, we may be able to lock the hexenyl radical of the second cyclization into a particular geometry. Hopefully the locking effect of the tether would force the cyclization to proceed more selectively.

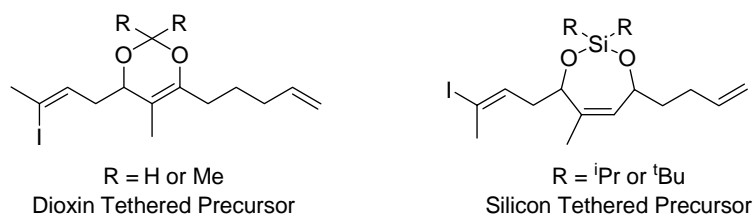
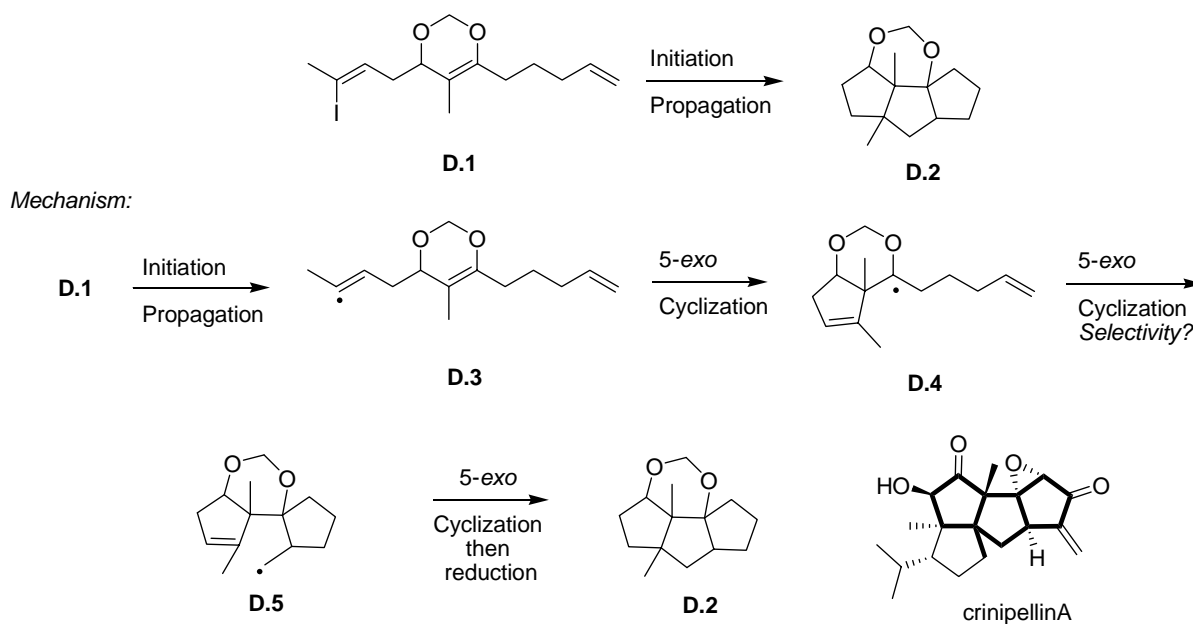


Figure D-1: Two new classes of cyclization precursor.

D.1: Cyclization Mechanisms

The mechanism for the cascade of the dioxin system is shown in Scheme D-1. In a typical reductive cyclization of iodide **D.1**, the three consecutive cyclizations should give linear triquinanes **D.2**. The cascade cyclization is initiated by iodine abstraction from **D.1** to give vinyl radical **D.3**. Cyclization of **D.3** gives bicyclic radical **D.4**. This key second hexenyl radical is interesting because it not only contains the *t*-butyl like group in the 1 position that we have studied previously, but it also has an oxo substituent in the 1 position. We have shown that the *t*-butyl group should induce *cis* selectivity in the cyclization, but the oxo group is reported to impart *trans* selectivity. Therefore it is fundamentally interesting to see what the result will be of this competition in the cyclization of **D.4** to give radical **D.5**. Finally, compound **D.5** can undergo the third and final radical cyclization to complete the round-trip cyclization and give

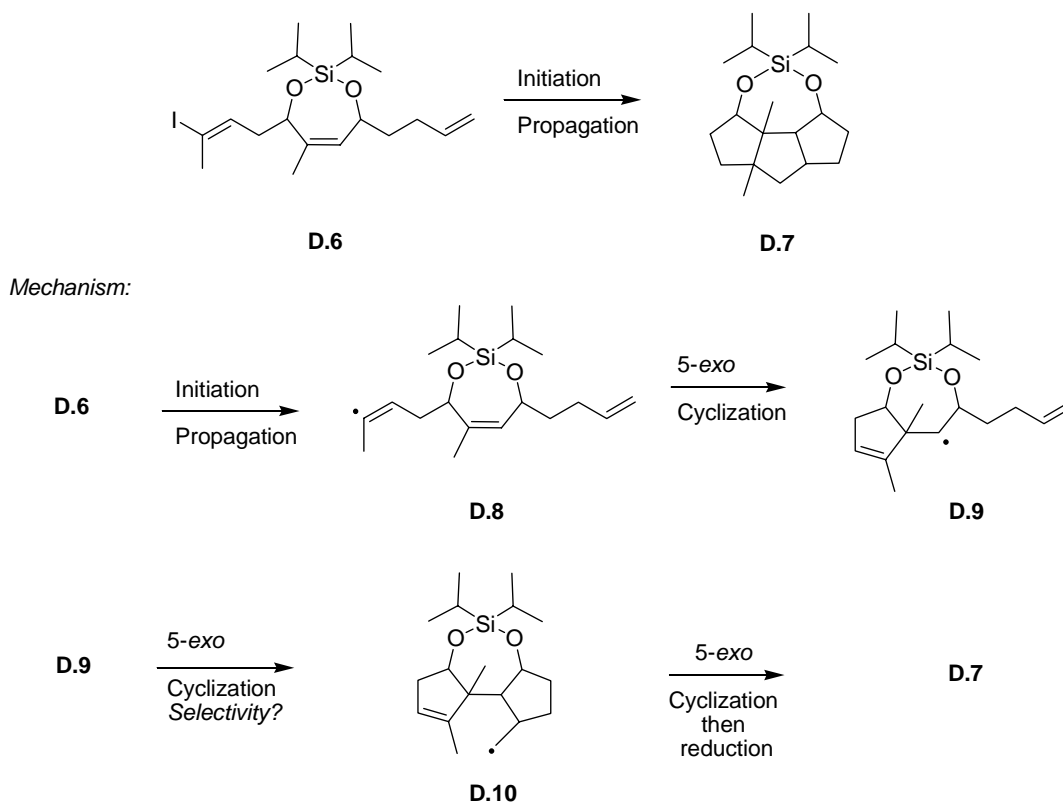
linear triquinane **D.2** upon reduction. Compound **D.5** should cyclize selectively to give a single linear triquinane because a 5,5 fused system is being formed. When we compare the final triquinane products of the cascade to crinipellin A, linear triquinane portion highlighted, we see some key structural similarities. The two oxygens in **D.2** match the positioning of two of the oxygens in crinipellin A. Furthermore we notice that the two methyl groups in **D.2** nicely match with a methyl group and an alkyl group in crinipellin A. For these reasons, the cyclization of the dioxin precursor could be an efficient approach to the crinipellin skeleton and **D.1** serves as a good model system to study to what extent this is true.



Scheme D-1: Mechanism for the cyclization of vinyl iodide **D.1**.

The cyclization cascade for silicon tethered vinyl iodide **D.6** is similar to that of the dioxin tether and is shown in Scheme D-2. The cyclization of iodide **D.6** is expected to give triquinanes **D.7**. In a typical cyclization sequence, abstraction of iodine from **D.6** gives vinyl radical **D.8**. Radical **D.8** can then cyclize to give the key second hexenyl radical **D.9**. Hexenyl radical **D.9** also has a *t*-butyl like group in the 1 position, but in contrast to the dioxin precursor **D.9** has an *oxo* group in the 2 position. It is difficult to assess what affect this *oxo* substitution will have on the selectivity of the cyclization because it is highly dependent on the nature and

substitution pattern of the chain.⁹⁰ After 5-*exo* cyclization of radical **D.9**, tricyclic radical **D.10** is formed. Reduction of **D.10** gives the desired tricyclic products **D.7**.



Scheme D-2: Mechanism for the cyclization of vinyl iodide **D.6**.

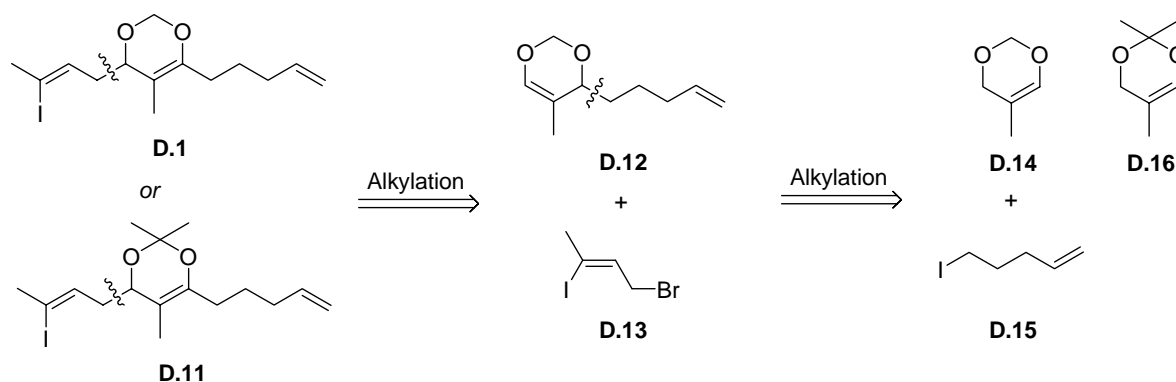
D.2: Synthesis of the Dioxin Precursor

We approached the synthesis of the dioxin precursor **D.1** in two separate ways. The first approach involved two sequential alkylations of a dioxin ring whereas the second approach employed a methylenation of a suitably functionalized β -hydroxy acid.

D.2.1: First Retrosynthetic Analysis of Vinyl Iodide **D.1**

Our first retrosynthesis for precursor **D.1** is shown in Scheme D-3. We reasoned that the requisite vinyl iodide precursor could be synthesized using Funk's conditions⁹¹ for the alkylation of dioxin **D.12** with known allylic bromide **D.13**.⁴⁶ Using the same alkylation strategy, **D.11** can be assembled from known dioxin **D.14** and alkyl iodide **D.15**. Should we opt for the dimethyl

variant of the precursor **D.11**, then the same retrosynthetic analysis is applicable leading back to dioxin **D.16**.



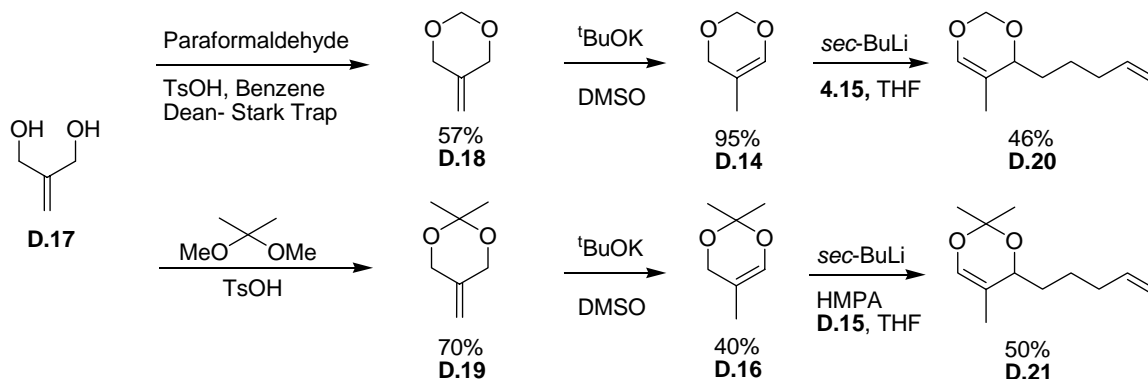
Scheme D-3: Retrosynthetic analysis of cyclization precursors **D.1** or **D.11**.

D.2.2: Progress Towards the Synthesis of **D.1** and **D.11** by the Alkylation Route

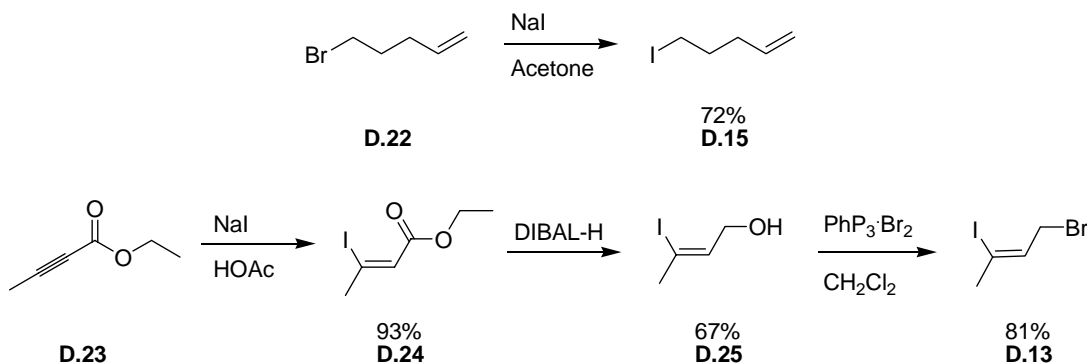
The requisite dioxins were prepared according to known procedures starting from 2-methylene-1,3-propanediol **D.17**.⁹² Treatment of this diol with paraformaldehyde and TsOH in benzene readily gave dioxane **D.18** in 57% yield. Similarly treatment of **D.17** with TsOH in neat 2,2-dimethoxypropane gave dimethyl dioxane **D.19** in 70% yield. The *exo*-methylene group in **D.18** and **D.19** was then isomerized to the internal alkene by *t*-BuOK to give the desired dioxins **D.14** and **D.16** in 95% and 40% yield respectively.

The necessary iodopentene alkylating agent **D.15** was synthesized⁹³ in 72% yield by a Finkelstein reaction on bromide **D.22** with NaI. The allylic bromide was synthesized by the three-step procedure outlined in Scheme D-4 starting from alkynoate **D.23**. Treatment of **D.23** with NaI in refluxing acetic acid gave vinyl iodide **D.24** in 93% yield. The ester was then reduced to the allylic alcohol using DIBAL-H in hexanes to give iodoalcohol **D.25** in 67% yield. Finally the alcohol was converted to the corresponding bromide **D.13** using *in situ* generated $\text{Ph}_3\text{P}\cdot\text{Br}_2$ complex in 81% yield.

The first alkylation reaction was carried out by treating dioxin **D.14** with 1.2 equiv of *sec*-BuLi at -78°C . The resulting metalated species was then quenched with iodide **D.15** to give dioxin **D.20** in 46% yield. Using the same conditions for the alkylation of dioxin **D.16** proved to be unsuccessful, but addition of HMPA as a co-solvent during the metalation enabled compound **D.21** to be isolated in 50% yield.



Synthesis of Alkylating Agents

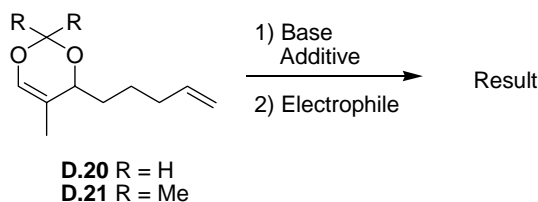


Scheme D-4: Synthesis of alkylated dioxins **D.20** and **D.21**.

Having successfully carried out the first alkylation of the dioxins, we next turned our attention to the second alkylation as shown in Table D-1. Unfortunately the alkylation conditions that were developed for the first alkylation step did work in this case resulting in the recovery of the starting material (Entry 1). Alkylating agent **D.13** is known to be somewhat unstable and so tried the same set of conditions with allyl bromide, entries 3, 4, and 5, with no more success. We further verified that vinyl iodide **4.13** was not the culprit by using it to alkylate dimethyl malonate (not shown). This reaction smoothly afforded the desired product in 75% yield proving that the alkylating agent was not the problem. We then proceeded to vary the base used for the deprotonation to *tert*-BuLi or *tert*-BuOK, entries 4, 5, 7, and 8 without any success. Addition of HMPA as a co-solvent, entries 2, 3, and 4, and variation of the reaction temperature, entries 3, 4, 5, and 8 also did not allow any desirable product to be isolated. At this point we suspected that the dioxin was simply not being metalated and tested for this by trying to quench the reactions with D₂O, entries 6 and 9, but we were unable to detect any deuterium incorporation. The two deuterium experiments confirm our suspicions and it is not entirely

surprising because vinyl ethers of this type are known to be difficult to metalate.⁹⁴ With no encouraging results, we abandoned this approach to the dioxin precursors.

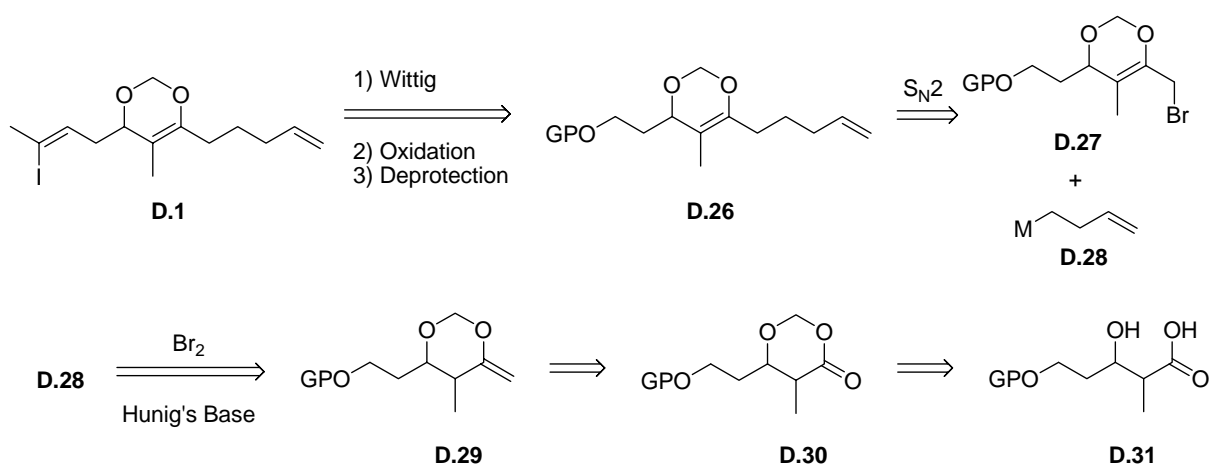
Table D-1: Attempted alkylations of dioxins **D.20** and **D.21**.



Entry	Dioxin	Base	Electrophile	T (°C)	Additive	Result
1	D.20	<i>sec</i> -BuLi	D.13	-78	-	Recovered starting material
2	D.20	<i>sec</i> -BuLi	D.13	-78	HMPA	Recovered starting material
3	D.20	<i>sec</i> -BuLi	Allyl bromide	-65	HMPA	Recovered starting material
4	D.20	<i>tert</i> -BuLi	Allyl bromide	-65	HMPA	Decomposition
5	D.20	<i>tert</i> -BuOK	Allyl bromide	20	-	Recovered starting material
6	D.20	<i>sec</i> -BuLi	D ₂ O	-78	-	No D incorporation
7	D.20	<i>tert</i> -BuLi	D.13	-78	-	Recovered starting material
8	D.21	<i>tert</i> -BuOK	D.13	20	-	Recovered starting material
9	D.21	<i>sec</i> -BuLi	D ₂ O	-78	-	No D incorporation

D.2.3: Second Retrosynthetic Analysis of Vinyl Iodide **D.1**

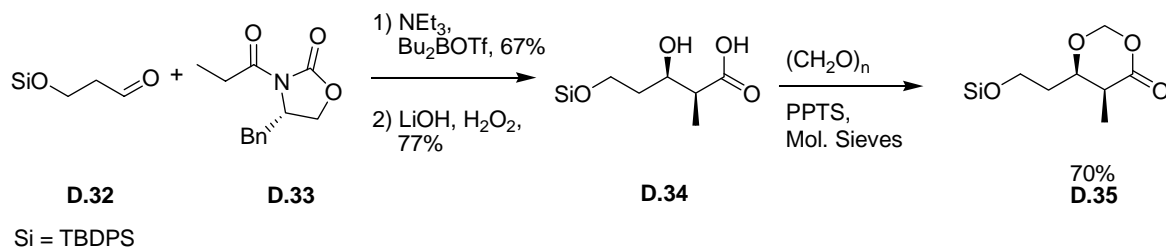
Our second retrosynthetic analysis for the dioxin precursors is outlined in Scheme D-5. We envisioned installing the vinyl iodide through a Wittig olefination in the final step. We unmasked the necessary aldehyde for the Wittig reaction by an oxidation and a deprotection leading back to protected alcohol **D.26**. The other side chain is installed using an S_N2 displacement of allylic bromide **D.27** with a suitably metalated four carbon alkene building block **D.28**. We saw compound **D.27** coming from a bromination of *exo*-methylene compound **D.29**⁹⁵ which in turn was synthesized by methylenation of lactone **D.30**. Finally lactone **D.30** can be formed by treating β-hydroxy acid **D.31** with paraformaldehyde and a number of such acids are known in the literature.



Scheme D-5: Second retrosynthetic analysis for dioxin **D.1**.

D.2.4: Progress Towards the Synthesis of **D.1** by the β -Hydroxy Acid Route

Some of the steps in our retrosynthetic analysis place heavy demands upon the protecting group and so we chose to use a TBDPS group. Therefore we synthesized known β -hydroxy acid **D.34** shown in Scheme 4-6. This acid is a known compound⁹⁶ and is readily constructed through an Evans aldol between aldehyde **D.32** and propiolated Evans' auxiliary **D.33** in 67% yield as shown in Scheme D-6. Hydrolysis of the chiral auxiliary using LiOOH gave the desired β -hydroxy acid **D.34** in 77% yield. Treatment of the acid with paraformaldehyde and catalytic PPTS provided us with the desired lactone **D.35** in 70% yield.⁹⁷



Scheme D-6: Synthesis of lactone **D.35**.

With the desired lactone in hand we proceeded to examine the methylenation reaction to form **D.29** shown in Scheme 4-7. Unfortunately treatment of lactone **D.35** using either the Tebbe or Petasis reagent resulted in decomposition of the starting material. In a related experiment, we treated known lactone **D.36** with the Petasis reagent and were able to isolate enol

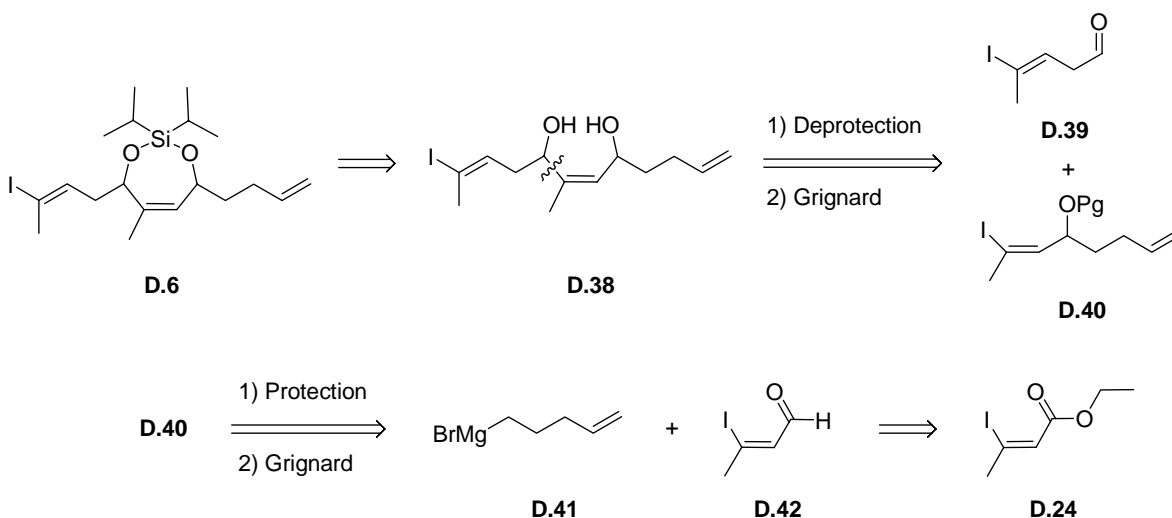
ether **D.37** in 65% yield. The success of the methyleneation for lactone **D.36**⁹⁶ and its failure for **D.35** indicated to us that our lactone was unstable to the reaction conditions. At this point we decided to focus our efforts on the silicon tethered precursor **D.6**.



Scheme D-7: Methylenation attempts on lactone **D.35** and methylenation of lactone **D.36**.

D.3: Synthesis of the Silicon Tethered Precursor **D.6**

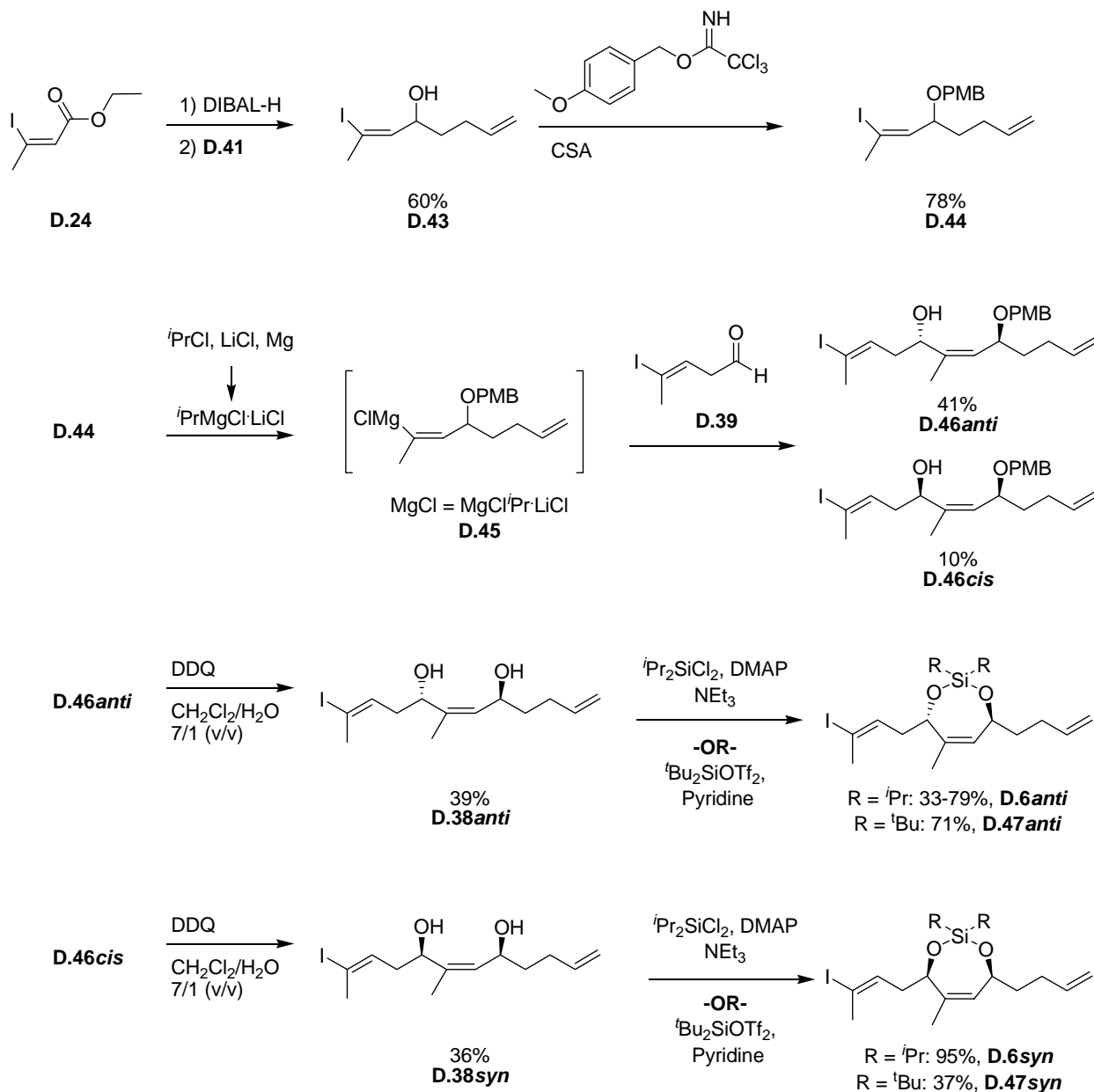
Our retrosynthetic analysis for vinyl iodide **D.6** is shown in Scheme **D-8**. Based on some other work that we had done with the diisopropyl silicon tethers we knew that this functionality can be unstable and so we envisioned installing it in the last step which leads back to diol **D.38**. Diol **D.38** can be assembled through a Grignard reaction between known aldehyde **D.39**⁹⁸ and vinyl iodide **D.40**. Iodide **D.40** can be synthesized through a coupling reaction between Grignard reagent **D.41** and aldehyde **D.42**.⁹⁹ Aldehyde **D.42** was constructed by a DIBAL-H reduction of ester **4.24**.⁹⁹



Scheme D-8: Retrosynthetic analysis for vinyl iodide **D.6**.

D.3.1: Forward Synthesis of the Silicon Tethered Precursor D.6

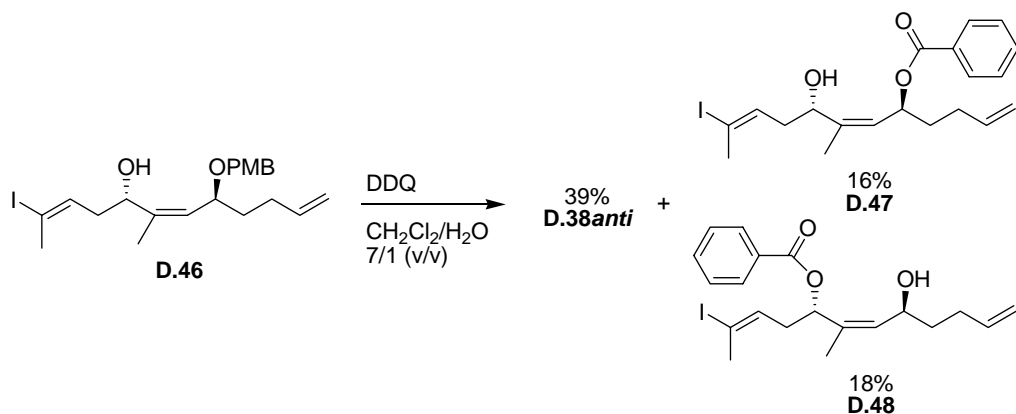
Our synthesis of a silicon tethered vinyl iodide **4.6** and other related precursors is shown in Scheme 4-9. Treatment of iodoester **D.24** with 1 equiv of DIBAL-H gave aldehyde **D.42**, Scheme D-8, which was not isolated, but was immediately treated with butenyl Grignard reagent **D.41** to give alcohol **D.42** in 60% yield. PMB protection of the secondary alcohol with PMB-trichloroacetimidate gave vinyl iodide **D.44**.¹⁰⁰ Conversion of iodide **D.44** to the corresponding Grignard reagent **D.45** was accomplished using Knochel's protocol¹⁰¹ and then quenched with aldehyde **D.39**. As expected this reaction produced two diastereomers **D.46anti** and **D.46syn** in 41% and 10% yield respectively. DDQ deprotection of allylic PMB ethers **D.46anti** and **D.46syn** yielded diols **D.38anti** and **D.38syn** in 39% and 36% respectively. Finally installation of the silicon tether was accomplished by treating diol **D.38anti** with ^tPr₂SiCl₂, DMAP and Et₃N.¹⁰² The final tethering reaction was very clean, but the yields were quite variable ranging from 33% to 79% with 60% being the most reproducible yield. Inexplicably the tethering reaction of **D.38syn** consistently gave a 95% yield under the same reaction conditions. Similarly if diol **D.38anti** was treated with ^tBu₂SiOTf₂ in the presence of pyridine, we could isolate di-*t*-butyl tethered compound **D.47anti** in 71% yield. Subjecting diol **D.38syn** to the same conditions gave silicon tethered compound **D.47syn** albeit in 37% yield, where mono silylated products made up the remainder of the recovered material.



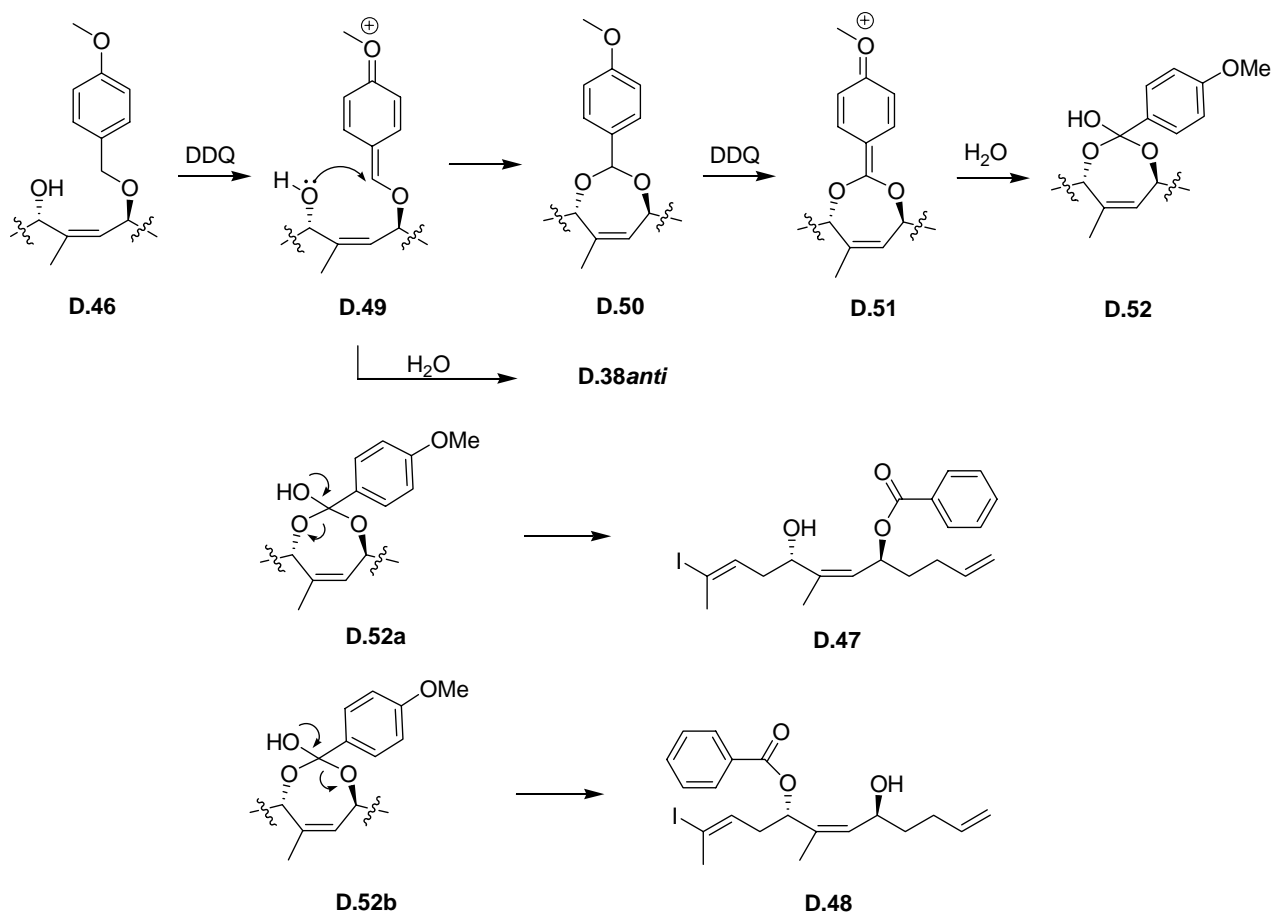
Scheme D-9: Synthesis of silicon tethered precursor **D.6**.

The yield of the DDQ protection of **D.46anti/syn** to give diols **D.38** suffered from a side reaction as shown in Scheme D-10 in which esters **D.47** and **D.48** were isolated in addition to the desired diol. In Scheme D.11 we propose a mechanism for the formation of **D.47** and **D.48**. Treatment of PMB ether **D.46** with DDQ leads to oxo-carbenium ion **D.49**. Ion **D.49** can then be attacked by water to give the desired diol **D.38anti**. However the oxo-carbenium ion can also be attacked by the free alcohol in the 4 position to give acetal **D.50**. Acetal **D.50** is then oxidized by DDQ to give another oxo-carbenium ion **D.51** which is attacked by water to give compound

D.52. Compound **D.52** can then collapse in one of two ways either by the pathway shown in **D.52a** to give ester **D.47** or according to the path in **D.52b** to give the other regio-isomer **D.48**.

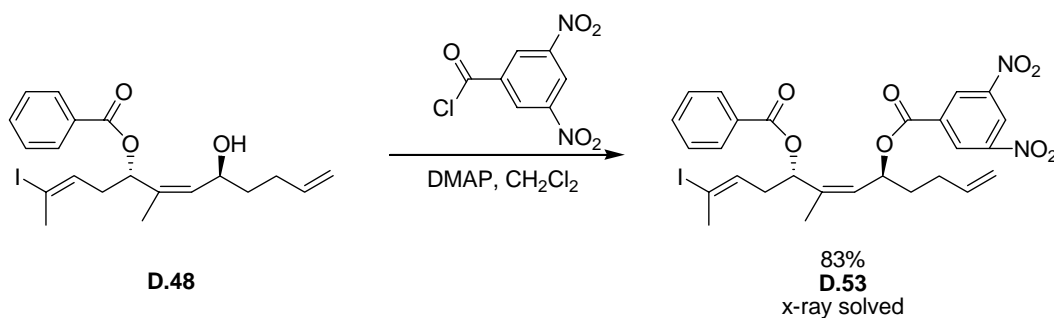


Scheme 4-10: Side reaction in the deprotection of PMB ether **D.46**.



Scheme 4-11: Mechanism for the formation of esters **D.47** and **D.48**.

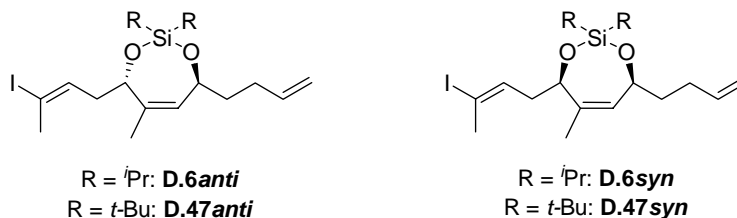
To ascertain the major isomer from the Knochel coupling reaction **D.44**→**D.46**, we derivatized ester **D.48** with *bis m*-nitrobenzoylchloride as shown in Scheme D-11 to give ester **D.53**. The solid that resulted from this reaction was taken up in THF and a single crystal, suitable for x-ray diffraction analysis, was grown by slow evaporation of this solution. When the crystal structure was solved we were able to conclude that the major product had the *anti* configuration. This allowed us to rigorously assign the configurations of all of the cyclization precursors.



Scheme D-12: Derivatization of alcohol **D.48** in order to obtain an x-ray crystal structure.

D.4: Cyclization Results of the Silicon Tethered Precursors

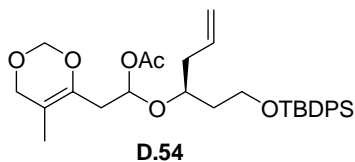
With the desired silicon tethered precursors in hand and their relative stereochemistry firmly assigned, we subjected them to various radical cyclization conditions which are summarized in Table D-2. Using our standard conditions, Entry 1 (Bu_3SnH , AIBN, 2mM and 80°C), we observed rapid consumption of the starting material by GC, but the appearance of numerous peaks with no major product(s) being observed. We made similar observations when we ran the same reaction at room temperature with Et_3B as the initiator Entry 2. Changing the hydride source to $(\text{TMS})_3\text{SiH}$ also did not alter the outcome of the reaction Entries 3 and 4. We next moved to the **D.6syn** isomer, but similarly disappointing results were obtained with either Bu_3SnH entry 5 or $(\text{TMS})_3\text{SiH}$ entry 6 as the reducing agent. We also attempted a cyclization with a $\text{Bu}_3\text{SnCl}/\text{NaCNBH}_3$ system entry 7, but to no avail. At this point we thought that maybe the isopropyl tether was unstable to the reaction conditions and so we opted for the more stable di-*t*-butyl silicon tether, entries 8, 9 and 10, but the results were similar to those from other cyclization attempts.

Table 4-2: Cyclization results for precursors **D.6anti/syn** and **D.47syn/anti**.

Entry	Precursor	Reducing Agent	T (°C)	Initiator	Concentration (mM)	Results
1	D.6anti	Bu ₃ SnH	80	AIBN	2	Decomposition
2	D.6anti	Bu ₃ SnH	25	Et ₃ B	2	Decomposition
3	D.6anti	(TMS) ₃ SiH	25	Et ₃ B	2	Decomposition
4	D.6anti	(TMS) ₃ SiH	25	Et ₃ B	4	Decomposition
5	D.6syn	Bu ₃ SnH	80	AIBN	2	Decomposition
6	D.6syn	(TMS) ₃ SiH	80	AIBN	2	Decomposition
7	D.6syn	Bu ₃ SnCl, NaCNBH ₃	80	AIBN	5	Decomposition
8	D.47anti	Bu ₃ SnH	80	AIBN	2	Decomposition
9	D.47anti	Bu ₃ SnH	25	Et ₃ B	2	Decomposition
10	D.47syn	Bu ₃ SnH	80	AIBN	2	Decomposition

D.5: Conclusions and Outlook

It is unfortunate that at present our results with either of these precursors are not more encouraging. These two precursor however remain incredibly attractive due to their potential to allow the second cyclization cascade to proceed more selectively. For the dioxin tether, the problems lie with synthesis of the precursor, but recent work by Rychnovsky and Dalgard describes another possible route to this compound. They recently reported¹⁰³ the synthesis of compound **D.54**, and suitable modifications should allow for a synthesis of **D.1**.



The problems with the silicon tethered radical cyclizations rest with finding reductive conditions that are compatible with the substrate. Radical cyclizations with similar silicon tethers have been reported¹⁰⁴ and so the anticipated cascade should be possible. With a facile synthesis of the precursors already developed it should be possible to find suitable conditions to effect the tricyclization and study the effect that tethering has on the second cyclization.

BIBLIOGRAPHY

- ¹ Perkins, J. M. *Radical Chemistry: The Fundamentals*; Oxford Science Publications: Oxford, United Kingdom, 2000; Chapter 1, pp 1-7.
- ² Gomberg, M. J. *Am. Chem. Soc.* **1900**, *22*, 757-771.
- ³ a) Carey, F. A.; Sundberg, R. J. *Advanced Organic Chemistry*; Kluwer Academic/Plenum Publishers: New York, New York, United States of America, 2000; 4th Edition, Part A, Chapter 12, pp 663-734. b) Lowry, T. H.; Richardson, K. S. *Mechanism and Theory in Organic Chemistry*; Harper & Row: United States of America, 1987; 3rd Edition, Chapter 9, pp 737-809.
- ⁴ a) Jasperse, C. P.; Curran, D. P.; Fevig, T. L. *Chem. Rev.* **1991**, *91*, 1237-1286 b) Curran, D. P.; Sisko, J.; Yeske, P. E.; Liu, H. *Pure & Appl. Chem.* **1993**, *65*, 1153-1159.
- ⁵ a) Comprehensive review of the use of radicals in synthesis: *Radicals in Organic Synthesis*; Renard, P., Sibi, M., Eds.; Wiley-VCH: Weinheim, 2001; Vol. 2 Applications. b) Curran, D. P. In *Comprehensive Organic Synthesis*; Trost, B. M., Fleming, I., Eds.; Pergamon: Oxford, United Kingdom, 1991; Vol. 4, pp 715-831. e) Giese, B. *Radicals in Organic Synthesis: Formation of Carbon-Carbon Bonds*; Pergamon Press: New York, New York, United States of America, 1986 d) Curran, D. P., *Synthesis*, **1988**, *6*, 417-439. e) Curran, D. P. *Synthesis* **1988**, *6*, 489-513. f) Barton, D. H. R.; Motherwell, W. B. *Pure Appl. Chem.* **1981**, *53*, 15-31. g) Barton, D. H. R. *Aldrichchimica Acta*, **1990**, *23*, 3-10.
- ⁶ Solomons, T. W. G., *Organic Chemistry*; John Wiley & Sons, Inc.: New York, New York, United States of America, 1996; 6th Edition, Chapter 9, Table 9.1, pp 370.
- ⁷ Kita, Y, Matsugi, M. In *Radicals in Organic Synthesis*; Renard, P., Sibi, M., Eds.; Wiley-VCH: Weinheim, Germany 2001; Vol. 1 Basic Principles, Chapter 1.1, pp 1-10.
- ⁸ Yorimitsu, H., Oshima, K. In *Radicals in Organic Synthesis*; Renard, P., Sibi, M., Eds.; Wiley-VCH: Weinheim, Germany 2001; Vol. 1 Basic Principles, Chapter 1.2, pp 11-27.
- ⁹ Chatgililoglu, C. In *Radicals in Organic Synthesis*; Renard, P., Sibi, M., Eds.; Wiley-VCH: Weinheim, Germany 2001; Vol. 1 Basic Principles, Chapter 1.3, pp 28-49.
- ¹⁰ Beckwith, A. L. J.; Easton, C. J.; Serelis, A. K. *J. Chem. Soc., Chem. Commun.* **1980**, 482-483.
- ¹¹ Stork, G.; Sher, P. M. *J. Am. Chem. Soc.* **1986**, *108*, 303-304.
- ¹² Giese, B.; González-Gómez, J. A., Witzel, T. *Angew. Chem., Int. Ed. Engl.* **1984**, *23*, 69-70.
- ¹³ Wayner, D. D. M.; Griller, D. In *Advances in Free Radical Chemistry*; Tanner, D. D., Ed; JAI Press Inc.: Greenwich, Connecticut, United States of America, 1990; Chapter 4, pp159-192.
- ¹⁴ Barton, D. H. R. *Pure Appl. Chem.* **1968**, *16*, 1-15.
- ¹⁵ Wolff, M. E. *Chem. Rev.* **1963**, *63*, 55-64.
- ¹⁶ Lopez, J. C.; Alonso, R.; Fraser-Reid, B. *J. Am. Chem. Soc.* **1989**, *111*, 6471-6473.

- ¹⁷ a) Curran, D. P.; Dooseop, K.; Hong, T. Shen, W. *J. Am. Chem. Soc.* **1988**, *110*, 5900-5902., b) Curran, D. P.; Shen, W. *J. Am. Chem. Soc.* **1993**, *115*, 6051-6059.
- ¹⁸ Dorigo, A. E.; Houk, K. N. *J. Am. Chem. Soc.* **1987**, *109*, 2195-2197.
- ¹⁹ Beckwith, A. L. J.; Ingold, K. U. In *Rearrangements in Ground and Excited States*; deMayo, P. Ed.; Academic Press, New York, New York, United States of America, 1980, Vol. 1, pp 162-283.
- ²⁰ Barton, D. H. R.; Crich, D.; Motherwell, W. B. *Tetrahedron* **1985**, *41*, 3901-3924.
- ²¹ Walling, C.; Cioffari, A. *J. Am. Chem. Soc.* **1972**, *1972*, 6059-6064.
- ²² Curran, D. P.; Chang, C-T. *J. Org. Chem.* **1989**, *54*, 3140-3157.
- ²³ a) Beckwith, A. L. J.; Easton, C. J.; Lawrence, T.; Serelis, A. K. *Aust. J. Chem.* **1983**, *36*, 545-565. b) Beckwith, A. L. J.; Lawrence, T.; Serelis, A. K. *J. Chem. Soc., Chem. Commun.* **1980**, 484-485. c) Beckwith, A. L. J.; Schiesser, C. H. *Tetrahedron. Lett.* **1985**, *26*, 373-376. d) Spellmeyer, D. C.; Houk, K. N. *J. Org. Chem.* **1987**, *52*, 959-974.
- ²⁴ Allinger, N. L.; Miller, M. A.; Van Catledge, F. A.; Hirsch, J. A. *J. Am. Chem. Soc.* **1967**, *89*, 4345-4357.
- ²⁵ RajanBabu, T. V. *Acc. Chem. Res.* **1991**, *24*, 139-145.
- ²⁶ For a detailed review on the stereochemistry of 5-*exo* hexenyl radical cyclizations: Curran, D. P.; Porter, N. A.; Giese, B. *Stereochemistry of Radical Reactions: Concepts, Guidelines and Synthetic Applications*; VCH: Weinheim, Germany, 1996; Chapter 2, pp 23-115.
- ²⁷ Tietze, L. F. *Chem Rev.* **1996**, *96*, 115-136.
- ²⁸ a) Dhimane, A. L.; Fensterbank, L.; Malacria, M. In *Radicals in Organic Synthesis*; Renard, P., Sibi, M., Eds.; Wiley-VCH: Weinheim, Germany 2001; Vol. 2 Applications, Chapter 4.4, pp 350-382. b) Aïssa, C.; Delouvrie, B.; Dhimané, A.-L., Fensterbank, L.; Malacria, M. *Pure Appl. Chem.* **2000**, *72*, 1605-1613. c) Dhimané, A.-L.; Malacria, M. In *Strategies and Tactics in Organic Synthesis*; Harmata, M., Ed.; Elsevier Ltd.: London, United Kingdom 2004; Vol. 5, Chapter 6, pp 153-179.
- ²⁹ a) Schwartz, E. C.; Curran, D. P. *J. Am. Chem. Soc.* **1990**, *112*, 9272-9284. b) Curran, D. P.; Sisko, J.; Balog, A.; Sonoda, N.; Nagahara, K.; Ryu I. *J. Chem. Soc., Perkin Trans. I* **1998**, 1591-1594. c) Balog, A.; Ph. D. Thesis, University of Pittsburgh, 1996. d) Haney, B.; Ph. D. Thesis, University of Pittsburgh, 2000.
- ³⁰ Curran, D. P.; Rakiewicz, D. M. *J. Am. Chem. Soc.* **1985**, *107*, 1448-1449.
- ³¹ Curran, D. P.; Chen, M-H. *Tetrahedron Lett.* **1985**, *26*, 4991-4994.
- ³² Fevig, T. L.; Elliot, R. L.; Curran, D. P. *J. Am. Chem. Soc.* **1988**, *110*, 5064-5067.
- ³³ Haney, B. P.; Curran D. P. *J. Org. Chem.* **2000**, *65*, 2007-2013.
- ³⁴ Beckwith, A. L. J.; Roberts, D. H.; Schiesser, C. L.; Wallner, A. *Tetrahedron Lett.* **1985**, *26*, 3349-3352.
- ³⁵ Curran, D. P.; Sun, S. *Aust. J. Chem.* **1995**, *48*, 261-267.
- ³⁶ a) Giese, B.; Kopping, B.; Göbel, T.; Dickhaut, J.; Thoma, G.; Kulicke, K. J.; Trach, F. In *Organic Reactions*; Paquette, L. A., Ed., John Wiley & Sons, Inc.; **1996**; New York, New York, United States of America, Volume 48, Chapter 2, pp 301-856. b) Wolf, S.; Agosta, W. C. *J. Chem. Res., Synop.* **1981**, 78-79. c) Mohammed, A. Y.; Clive, D. L. J. *J. Chem. Soc. Comm.* **1986**, 588-589.

-
- ³⁷ Devin, P.; Fensterbank, L.; Malacria, M. *J. Org. Chem.* **1998**, *63*, 6764-6765.
- ³⁸ Takasu, K.; Maiti, S.; Katsumata, A.; Ihara, M. *Tetrahedron Lett.* **2001**, *42*, 2157-2160.
- ³⁹ Jung, M. E. *Synlett* **1999**, 843-849.
- ⁴⁰ a) Curran, D.P.; Shen, W. *J. Am. Chem. Soc.* **1993**, *115*, 6051-6059. b) Robertson, J.; Pillai, J.; Lush, R. K. *Chem. Soc. Rev.* **2001**, *30*, 94-103. c) Beaufile, F.; Dénès, F.; Renaud, P. *Org. Lett.* **2004**, *6*, 2563-2566.
- ⁴¹ Beckwith, A. L. J.; Cliff, M. D.; Schiesser, C. H. *Tetrahedron* **1992**, *48*, 4641-4648.
- ⁴² Boger, D. L.; Turnbull, P. *J. Org. Chem.* **1998**, *63*, 8004-8011.
- ⁴³ Bailey, W. F.; Gagnier, R. P.; Patricia, J. J. *J. Org. Chem.* **1984**, *49*, 2098-2107.
- ⁴⁴ Ma, S.; Xu, B.; Ni, B. *J. Org. Chem.* **2000**, *65*, 8532-8543.
- ⁴⁵ Qin, D.-G.; Zha, H.-Y.; Yao, Z.-J. *J. Org. Chem.* **2002**, *67*, 1038-1040.
- ⁴⁶ Piers, E.; Harrison, C. L.; Zetina-Rocha, C. *Org. Lett.* **2001**, *21*, 3245-3247.
- ⁴⁷ Fleming, I.; Ghosh, S. K. *J. Chem. Soc., Perkin 1* **1998**, 2733-2748.
- ⁴⁸ Ma, S.; Lu, X.; Li, Z. *J. Org. Chem.* **1992**, *57*, 709-713.
- ⁴⁹ The barrier to inversion of the vinyl radical has been calculated to be 3.3 kcal/mol and interconverting at $4 \cdot 10^{10} \text{ s}^{-1}$ @ 300 K. See, Galli, C.; Guarnieri, A.; Koch, H.; Mencarelli, P.; Rappoport, Z. *J. Org. Chem.* **1997**, *62*, 4072-4077.
- ⁵⁰ Paquette, L. A.; Bulman-Page, P. C.; Pansegrau, P. D.; Wiedeman, P. E. *J. Org. Chem.* **1988**, *53*, 1450-1460.
- ⁵¹ Chaikin, S. W.; Brown, W. G. *J. Am. Chem. Soc.* **1949**, *71*, 122-125.
- ⁵² Marshall, J. A.; Cleary, D. G. *J. Org. Chem.* **1986**, *51*, 858-863.
- ⁵³ Martin, R.; Islas, G.; Moyano, A.; Pericas, M. A.; Riera, A. *Tetrahedron*, **2001**, *57*, 6367-6374.
- ⁵⁴ Haynes, R. K.; Katsifis, A. G.; Vonwiller, S. C.; Hambley, T. W. *J. Am. Chem. Soc.* **1988**, *110*, 5423-5433.
- ⁵⁵ This is a known compound, but the spectral data is not reported CAS # 2418-31-7.
- ⁵⁶ Erdmann, P.; Schäfer, J.; Springer, R.; Zeitz, H.-G.; Giese, B. *Helv. Chim. Acta* **1992**, *75*, 638-644.
- ⁵⁷ Romero, J. M. L.; Sapmaz, S.; Fensterbank, L.; Malacria, M. *Eur. J. Org. Chem.* **2001**, 767-773.
- ⁵⁸ Canonne, P.; Plamondon, J. *Can. J. Chem.* **1989**, *67*, 555-564.
- ⁵⁹ Hanessian, S.; Huynh, H. K.; Reddy, G. V.; Duthaler, R. O.; Katopodis, A.; Streiff, M. B.; Kinzy, W.; Oehrlein, R. *Tetrahedron* **2001**, *57*, 3281-3290.
- ⁶⁰ Hashimoto, N.; Aoyama, T.; Shioiri, T. *Chem. Pharm. Bull.* **1981**, *29*, 1475-1478.
- ⁶¹ Grunewald, G. L.; Ye, Q. *J. Org. Chem.* **1988**, *53*, 4021-4026.
- ⁶² Zara, C. L.; Jin, T.; Giguere, R. J. *Synth. Comm.* **2000**, *30*, 2099-2104.

-
- ⁶³ Molander, G.; Winterfeld, J. *J. Organomet. Chem.* **1996**, *524*, 275-279.
- ⁶⁴ Chan, K.-K.; Cohen, N.; De Noble, J. P.; Specian, A. C., Jr.; Saucy, G. *J. Org. Chem.* **1976**, *41*, 3497-3505.
- ⁶⁵ Reetz, M. T.; Maier, W. F.; Chatziiosifadis, I.; Giannis, Heimbach, H.; Löwe, U. *Chem. Ber* **1980**, *113*, 3741-3757.
- ⁶⁶ Hupe, E.; Denisenko, D.; Knochel, P. *Tetrahedron* **2003**, *59*, 9187-9198.
- ⁶⁷ Siegel, S. In *Comprehensive Organic Synthesis*; Trost, B. M., Fleming, I., Eds.; Pergamon Press: Oxford, U.K., 1991; Vol. 8, pp 417-442.
- ⁶⁸ Mitsui, S.; Shionoya, M.; Gohke, K.; Watanabe, F.; Imazizumi, S.; Senda, Y. *J. Catal.* **1975**, *40*, 372-378.
- ⁶⁹ a) Rylander, P. *Catalytic Hydrogenation in Organic Syntheses*; Academic Press, London, United Kingdom, 1979; Chapter 3, pp 31-63. b) Rylander, P. N. *Hydrogenation Methods*; Academic Press, London, United Kingdom, 1985 Chapter 2, pp 29-52
- ⁷⁰ Dandapani, S; Ph. D. Thesis, University of Pittsburgh, 2003.
- ⁷¹ Claridge, T. D. W. *High-Resolution NMR Techniques in Organic Chemistry*; Pergamon, Amsterdam, The Netherlands, 1999, Chapter 8 pp 277-339.
- ⁷² Barton, D.H.R.; McCombie, S.W. *J. Chem. Soc., Perkin 1* **1975**, 1574-1585.
- ⁷³ Frisch, M. J.; Trucks, G. W.; Schlegel, H. B.; Scuseria, G. E.; Robb, M. A.; Cheeseman, J. R.; Montgomery, J. A., Jr.; Vreven, T.; Kudin, K. N.; Burant, J. C.; Millam, J. M.; Iyengar, S. S.; Tomasi, J.; Barone, V.; Mennucci, B.; Cossi, M.; Scalmani, G.; Rega, N.; Petersson, G. A.; Nakatsuji, H.; Hada, M.; Ehara, M.; Toyota, K.; Fukuda, R.; Hasegawa, J.; Ishida, M.; Nakajima, T.; Honda, Y.; Kitao, O.; Nakai, H.; Klene, M.; Li, X.; Knox, J. E.; Hratchian, H. P.; Cross, J. B.; Adamo, C.; Jaramillo, J.; Gomperts, R.; Stratmann, R. E.; Yazyev, O.; Austin, A. J.; Cammi, R.; Pomelli, C.; Ochterski, J. W.; Ayala, P. Y.; Morokuma, K.; Voth, G. A.; Salvador, P.; Dannenberg, J. J.; Zakrzewski, V. G.; Dapprich, S.; Daniels, A. D.; Strain, M. C.; Farkas, O.; Malick, D. K.; Rabuck, A. D.; Raghavachari, K.; Foresman, J. B.; Ortiz, J. V.; Cui, Q.; Baboul, A. G.; Clifford, S.; Cioslowski, J.; Stefanov, B. B.; Liu, G.; Liashenko, A.; Piskorz, P.; Komaromi, I.; Martin, R. L.; Fox, D. J.; Keith, T.; Al-Laham, M. A.; Peng, C. Y.; Nanayakkara, A.; Challacombe, M.; Gill, P. M. W.; Johnson, B.; Chen, W.; Wong, M. W.; Gonzalez, C.; Pople, J. A. *Gaussian 03*, revision B.05; Gaussian, Inc.: Pittsburgh, PA, 2003.
- ⁷⁴ Wilcox, C. S.; Thomasco, L. M. *J. Org. Chem.* **1985**, *50*, 546-547.
- ⁷⁵ Kolb, H. C.; VanNieuwenhze, M. S.; Sharpless, K. B. *Chem. Rev.* **1994**, *94*, 2483-2547.
- ⁷⁶ Kodama, M.; Shiobara, Y.; Sumitomo, H.; Mitani, K.; Ueno, K. *Chem. Pharm. Bull.* **1987**, *35*, 4039-4042.
- ⁷⁷ Seyfrehth, D.; Heeren, J. K.; Singh G.; Grim, S. O.; Hughes, W. B. *J. Organomet. Chem.* **1966**, *5*, 267-274.
- ⁷⁸ Stork, G.; Zhao, K. *Tetrahedron Lett.* **1989**, *30*, 2173-2174.
- ⁷⁹ Panek, J. S.; Liu, P. *J. Am. Chem. Soc.* **2000**, *122*, 11090-11097.
- ⁸⁰ Hu, S.-G.; Hu, T.-S.; Wu, Y.-L. *Org. & Biomol. Chem.* **2004**, *2*, 2305-2310.
- ⁸¹ Curran, D. P.; Chang, C.-T. *J. Org. Chem.* **1989**, *54*, 3140-3157.
- ⁸² Hung, D. T.; Nerenberg, J. B.; Schreiber, S. L. *J. Am. Chem. Soc.* **1996**, *118*, 11054-11080.

-
- ⁸³ Helms, A.; Heiler, D.; McLendon, G. *J. Am. Chem. Soc.* **1992**, *114*, 6227-6238.
- ⁸⁴ a) Curran, D. P.; Seong, C. M. *Tetrahedron* **1992**, *48*, 2157-2174. b) Curran, D. P.; Seong, C. M. *Tetrahedron* **1992**, *48*, 2175-2190
- ⁸⁵ Newcomb, M. *Tetrahedron* **1993**, *49*, 1151-1176.
- ⁸⁶ Chatgililoglu, C.; Newcomb, M. In *Advances in Organometallic Chemistry*; West, R.; Hill, A. F. Eds.; Academic Press, London, United Kingdom, 1999, Vol. 44, pp 67-109.
- ⁸⁷ Johnston, L. J.; Luszytk, J.; Wayner, D. D. M.; Abeywickreyma, A. N.; Beckwith, A. L. J.; Scaiano, J. C.; Ingold, K. U. *J. Am. Chem. Soc.* **1985**, *107*, 4594-4596.
- ⁸⁸ Shute, R. E.; Rich, D. H. *Synthesis* **1987**, 346-349.
- ⁸⁹ Sun, G.; Savle, P. S.; Gandour, R. D.; Bhaird, N. N.; Ramsay, R. R.; Fronczek, F. R. *J. Org. Chem.* **1995**, *60*, 6688-6695.
- ⁹⁰ a) Ueno, Y.; Chino, K.; Watanabe, M.; Moriya, O.; Okawara, M. *J. Am. Chem. Soc.* **1982**, *104*, 5564-5566. b) Stork, G.; Mook, R. Jr.; Biller, S. A.; Rychnovsky, S. D. *J. Am. Chem. Soc.* **1983**, *105*, 3741-3742.
- ⁹¹ a) Funk, R. L.; Bolton, G. L. *Tetrahedron Lett.* **1988**, *29*, 1111-1114 b) personal e-mail communications with the authors.
- ⁹² a) Wattenbach, C.; Maurer, M.; Frauenrath, H. *Synlett*, **1999**, 303-306. b) Frauenrath, H.; Kaulard, M.; *Synlett*, **1994**, 517-518. c) personal e-mail communication with the author.
- ⁹³ Padwa, A.; Kamigata, N. *J. Am. Chem. Soc.* **1977**, *99*, 1871-1880.
- ⁹⁴ Boeckman, R. K. Jr; Bruza, K. J. *Tetrahedron*, **1981**, *37*, 3997-4006.
- ⁹⁵ Greshock, T. J.; Funk, R. L. *J. Am. Chem. Soc.* **2002**, *124*, 754-755
- ⁹⁶ Smith, A. B., III; Minbiole, K. P.; Verhoest, P. R.; Schelhaas, M. *J. Am. Chem. Soc.* **2001**, *123*, 10942-10953
- ⁹⁷ Zimmermann, J.; Seebach, D.; Ha, T.-K. *Helvetica. Chim. Acta* **1988**, *71*, 1143-1155.
- ⁹⁸ Commeiras, L.; Santelli, M.; Parrain, J.-L. *Org. Lett.* **2001**, *3*, 1713-1715.
- ⁹⁹ Marek, I.; Meyer, C.; Normant, J.-F. *Organic Syntheses* **1997**, *74*, 194-204.
- ¹⁰⁰ Toshima, K.; Jyojima, T.; Miyamoto, N.; Katohno, M.; Nakata, M. Matsumura, S. *J. Org. Chem.* **2001**, *66*, 1708-1715.
- ¹⁰¹ Ren, H; Krasovskiy, A, Knochel, P. *Org. Lett.* **2004**, *6*, 4215-4217.
- ¹⁰² Petit, M.; Chouraqui, G.; Aubert, C.; Malacria, M. *Org. Lett* **2003**, *5*, 2037-2040.
- ¹⁰³ Dalgard, J. E.; Rychnovsky, S. D. *Org. Lett.* **2005**, *7*, 1589-1591.
- ¹⁰⁴ Hutchinson, J. H.; Daynard, T. S.; Gillard, J. W. *Tetrahedron Letters*, **1991**, *32*, 573-576.